МЕЖДУНАРОДНЫЙ НАУЧНЫЙ ЖУРНАЛ

АЛЬТЕРНАТИВНАЯ ЭНЕРГЕТИКА И ЭКОЛОГИЯ

ISSN 1608-8298

№6 2008

ISJAEE № 6(62) 2008

ISSN 1608-8298

Выходит ежемесячно
Издается с июля 2000 г.

Международный научный журнал
«Альтернативная энергетика и экология»

РЕДАКЦИОННАЯ КОЛЛЕГИЯ

Журнал зарегистрирован Международным центром ЮНЕСКО в 2000 г. (название: "Al'ternativnaâ ènergetika i ècologiâ", краткое название: "Al'tern. ènerg. ècol."), ISSN 1608-8298.

Тематика журнала одобрена Международной ассоциацией водородной энергетики (МАВЭ) и Международным центром развития водородной энергетики Департамента по вопросам промышленного развития ООН (UNIDO-ICHET).

Журнал включен в "Перечень периодических научных и научно-технических изданий, выпускаемых в РФ, рекомендованных для публикации основных результатов диссертаций на соискание ученой степени кандидата наук" ВАК.

Награды журнала: Медаль Рентгена (2007 г.), Диплом Фонда им. В.И. Вернадского и Комитета по экологии Государственной Думы ФС РФ (2007 г.), Премия "Российский Энергетический Олимп – 2008".

Журнал включен в Реферативный журнал и Базы данных ВИНИТИ.

Журнал включен в каталоги: "Роспечать" (индекс 20487), Объединенный каталог "Пресса России. Российские и зарубежные газеты и журналы" (индекс 41935), "Интерпочта-2003", "Артос-ГАЛ", "Деловая пресса", "Экспресс", "Ермак-Пресс", "Пресс-инфо", "Южно-уральская почта", Красносельское агентство "Союзпечать".

Полные электронные версии статей представлены на сайте Научной электронной библиотеки http://e-library.ru, на сайте Международного научного журнала "Альтернативная энергетика и экология" http://isjaee.hydrogen.ru, а также на сайте Международного научного и образовательного портала "Водород" http://www.hydrogen.ru.

Журнал зарегистрирован в Федеральной службе по надзору за соблюдением законодательства в сфере массовых коммуникаций и охране культурного наследия (свидетельство ПИ № ФС77-21881) от 14 сентября 2005 г.

ISJAEE
International Scientific Journal for Alternative Energy and Ecology
№ 6(62) 2008
ISSN 1608-8298
Monthly
Found in july 2000

EDITORIAL BOARD

The journal is registered in UNESCO in ISSN International Centre in 2000 (key title: "Al'ternativnaâ ènergetika i èkologiâ", abbreviated key title: "Al'tern. ènerg. èkol."), ISSN 1608-8298.

The subjects of the journal are approved by International Association for Hydrogen Energy (IAHE).

The journal has been included into the "List of scientific and technical periodicals in Russian Federation and recommended to publish main results of the candidate of science dissertation" of All-Russian Certifying Commission.

The journal has been included into catalogues: "Rospechat'" (20487), Joined catalogue "Press of Russia. Russian and foreign newspapers and journals" (41935), "Interpochta-2003", "Artos-GAL", "Business press", "Express", "Ermak-Press", "Press-Info", "Yuzhno-Ural'skaya pochta", Krasnosel'skoe agency "Soyuzpechat'".

Journal awards: Röntgen Medal (2007), Award of V.I. Vernadskyi fund and RF State Committee for Ecology (2007). The Premium "Russian Energetic Olympus – 2008".

The journal has been included into the abstract journal and data base VINITI. Information on the journal is annually published in the international reverence system of periodical of current issues "Ulrich's Periodicals Directory".

Full version of papers has been presented at Scientific electronic library http://e-library.ru, web-site of International Scientific Journal for Alternative Energy and Ecology http://isjaee.hydrogen.ru, and International Information and Education Portal "Hydrogen" http://www.hydrogen.ru.

The journal has been registered at Russian Federal Service on Supervision of Observance of the Legislation in Sphere of Mass Communications and Protection of a Cultural Heritage (Certificate PI No FC77-21881) September 14, 2005.

ISJAEE

MATHEMATICS
CHEMISTRY
PHYSICS
BIOLOGY
BIOCHEMISTRY
ELECTROCHEMISTRY

THERMODYNAMICS
HYDRAULICS
CATALYSIS
CRYOGENICS
MECHANICS
NANOTECHNOLOGIES

IN THIS ISSUE

СПЕЦИАЛЬНЫЙ ВЫПУСК, ПОСВЯЩЕННЫЙ АЛЬТЕРНАТИВНОЙ ЭНЕРГЕТИКЕ ФРАНЦИИ И ФРАНКОГОВОРЯЩИХ СТРАН

СОДЕРЖАНИЕ

На 1-й стр. обложки: Поле гелиостатов Темис для проекта «Pegas».

Учредитель, издатель и редакция
Научно-технический центр "ТАТА"
Генеральный директор А.Л. Гусев
E-mail: gusev@hydrogen.ru
Почтовый адрес:
607183, Россия, Нижегородская обл.,
Саров, а/я 687, НТЦ "ТАТА"
Тел.: 8 (83130) 63107, 97472, факс: 8 (83130) 63107
Моб. тел.: +7-962-50-77-914
http://www.hydrogen.ru

Основной партнер
Институт водородной экономики
Генеральный директор А.Л. Гусев
E-mail: gusev@hydrogen.ru
Почтовый адрес:
607183, Россия, Нижегородская обл., Саров, а/я 683
Тел.: 8 (83130) 91846, 90708, факс: 8 (83130) 63107
Моб. тел.: +7-961-63-99-126
http://www.hydrogen.ru

Журнал печатается на сертифицированной экологически чистой бумаге KYM LUX (ISO 9001, ISO 14001, OHSAS 18001, SMS 1003-1)

THIS SPECIAL ISSUE IS DEVOTED TO ALTERNATIVE ENERGY OF FRANCE AND FRENCH SPEAKING COUNTRIES

CONTENTS

Basic problems of energy and renewable energy

Application of helium and special materials in vehicles

Legislative basis

Energy and ecology

Information

1st page of cover: Field of heliostats Themis for PEGASE project.

Founder and publisher
Scientific Technical Centre "TATA"
General manager A.L. Gusev
E-mail: gusev@hydrogen.ru
607183, Russia, Nizhni Novgorod region, Sarov, P.O.B. 687, STC "TATA"
Ph.: +7(83130)63107,97472, fax:+7(83130) 63107
Cell phone: +7-962-50-77-914
http://www.hydrogen.ru

General cooperation
Institute for Hydrogen Economy
General manager A.L. Gusev
E-mail: gusev@hydrogen.ru
607183, Russia, Nizhni Novgorod region, Sarov, P.O.B. 683
Ph.: +7(83130)91846, 90708, fax:+7(83130) 63107
Cell phone: +7-961-63-99-126
http://www.hydrogen.ru

MODELING OF THE THERMAL TRANSFERS IN AN ENCLOSURE OF THE TROMBE WALL TYPE

A. Mezrhab, M. Rabhi*

Faculté des Sciences, Département de Physique, Laboratoire de Mécanique & Energétique, 60000 Oujda, Maroc.
*Corresponding author: mezrhab@fso.ump.ma

Received: 26 Nov 2007; accepted: 16 Jan 2008

The heat transfer by natural convection and thermal radiation between the two compartments of an enclosure filled of air and divided by a vertical partition wall are studied numerically. The air is aspired in the cavity from the bottom, then it is heated and pushed into the ventilation openings at the top. This two-dimensional configuration is a simplified representation of the solar system with ventilated wall Trombe. We show that the radiative exchanges reduce the temperature differences between the surfaces and increase the average Nusselt number as well as the air flow through the openings. The increase in the dimensionless width of the opening promotes the heat transfer within the cavity.

Keywords: solar buildings, natural convection, thermal radiation, partition, average Nusselt number

Ahmed Mezrhab

Organization(s): Mohamed 1 University, Professor.
Education: Conservatoire National des Arts et Métiers (CNAM) − Paris (1992-1994), Mohamed 1 University, Faculty of Sciences, Department of Physics, Oujda, Morocco (1995–2008).
Experience: Direction of research of Renault (Paris), research engineer (1990-1992). Conservatoire National des Arts et Métiers (CNAM)-Paris, Former researcher (1992-1994). Society Distal − Paris, Engineer (1994-1995). University Mohamed 1, Professor (1995-2008).
Main range of scientific interests: heat transfer, fluid flow, renewable energy, solar energy, numerical computations.
Publications: 26 papers in international scientific journals, 90 communications in congress, reviewer for several international scientific journals.

Mohammed Rabhi

Organization(s): Mohamed 1 University, Philosophy Doctor.
Education: Mohamed 1 University, Faculty of Sciences, Department of Physics, Oujda, Morocco.
Main range of scientific interests: Renewable Energy, Numerical modeling, heat transfer.
Publications: 2 papers in international scientific journals, 10 communications in congress.

Nomenclature

d – thickness of the partition wall, (m)
D – dimensionless thickness of the partition wall ($D = d/L$)
g – gravity acceleration, ($m \cdot s^{-2}$)
k – thermal conductivity, ($W \cdot m^{-1} \cdot K^{-1}$)
L – width of the cavity, (m)
l – distance between the low opening and the bottom adiabatic wall, (m)
l_0 – width of the opening, (m)
L_0 – dimensionless width of the opening, l_0/L
l_p – length of the partition wall, (m)
s – distance between the hot wall and the partition wall, (m)
S – dimensionless distance between the hot wall and the partition wall, $S = s/L$
Nr – radiation number, $\sigma T_c^4/(k_a \Delta T/L)$
Nu – Nusselt number
p – pressure, (Pa)
P – dimensionless pressure, $(p + \rho_o g y)L^2/\rho_o \alpha^2$
Pr – Prandtl number, ν/α
Q – dimensionless air flow crossing the openings
q_r – net radiative flux density, ($W \cdot m^{-2}$)

Qr – dimensionless net radiative flux density, $q_r/\sigma T_h^4$
Ra – Rayleigh number, $g\beta(T_h - T_c)L^3/\nu\alpha$
R_k – thermal conductivity ratio, k_w/k_a
T – temperature, (K)
T_h – temperature of the hot wall
T_c – temperature of the cold wall
T_0 – average temperature, $(T_h + T_c)/2$, (K)
u, v – velocity components, (m·s^{-1})
U, V – dimensionless velocity components $U = uL/\alpha$, $V = vL/\alpha$
x, y – coordinates, (m)
X, Y – dimensionless coordinates ($X = x/L$, $Y = y/L$)

Greek letters

ΔT – maximal temperature difference, $T_h - T_c$, (K)
α – thermal diffusivity of fluid, (m^2·s^{-1})
β – volumetric expansion coefficient, (K^{-1})
λ – dynamic viscosity ratio, μ_w/μ_a
μ – dynamic viscosity, (Kg·m^{-1}·s^{-1})
ν – kinematic viscosity of fluid, (m^2·s^{-1})
ρ_0 – density of the fluid with T_0, (kg·m^{-3})
θ – dimensionless temperature, $(T - T_0)/(T_h - T_c)$
σ – Stefan–Boltzmann constant, (W·m^{-2}·K^{-4})
ε – emissivity of a radiative surface

Indices and exponents

a – air
h – hot
c – cold
w – wall
o – opening

Introduction

Several numerical and experimental studies were carried out on the heat transfer by natural convection and thermal radiation in partitioned rectangular cavities [1-2]. This interest is due to the various industrial applications that these geometries reflect in several problems of engineering. Among this work, one quotes in particular that of Mezrhab et al. [1] who studied the interaction natural convection - radiation in a vertical enclosure blocked by a solid block. They showed that the thermal radiation has a great influence on the pace of the isotherms and streamlines, then increases the average Nusselt number considerably. They have also found that the effect of the thermal conductivity of the solid block is more pronounced in combined mode than in pure natural convection. Mezrhab et al. [2] analyzed the effect of the thermal radiation on the heat transfer and the air flow within an enclosure containing a solid block generating heat. They found that the thermal radiation reduces the maximum temperature in the enclosure, because of radiative fluxes lost by the side bordering solid block. An experimental and numerical study concerning the effect of a partition placed at the medium of a rectangular enclosure was carried out by Nakamura and Asko [3]. They concluded that emissivities of the walls opposite influence considerably the heat transfer by convection.

Among technologies, search and studies carried out in simple enclosure of geometry, several works was interested in the study of the thermal behavior of the solar systems of the type wall Trombe and its alternatives. Tadrari et al. [4] studied numerically the coupled heat transfer by conduction, natural convection and radiation in a vertical rectangular enclosure delimited by a glass and a massive wall absorbing a solar flux. They noted that for ΔT=10K, there is a critique value (Rac) of Ra about 1.7×10^8 for which the flow change direction. They have also shown that more than 75% of the total heat transfer in the enclosure is through radiation. Buzzoni et al. [5] presented a numerical solution to the problem of natural convection in the case of heating buildings by a passive solar system, which is a variant of the system Trombe-Michel. Gan [6] studied the Trombe walls for use in the cooling of buildings in summer conditions. He pointed to a study which showed that the computer code developed by CFD (Computational Fluid Dynamics) can be used for predicting the movement of the air flow and buoyant in the fences with the geometry of Trombe wall. Borgers and Akbari [7] studied numerically turbulent convective flow free in a Trombe wall. They then developed correlations to estimate the performance of Trombe walls. Ong [8] proposed a simple mathematical model of a solar chimney, the physical model is similar to the Trombe wall. Awbi and Gan [9] used a CFD programs to simulate air flow and heat transfer in a Trombe wall.

In our work, the results are obtained by using the real data of the solar systems with passive wall. We study the effect of two openings located meadows of the hot wall, one in bottom and the other in top of the enclosure (Fig. 1) on the heat transfer within an enclosure differentially heated. One holds account of the coupling between thermal conduction through the walls, the exchanges by natural convection in and between the compartments and the exchanges by radiation between radiative surfaces constituting the enclosure.

The principal objective of this work is to analyse the influence of the radiative exchanges on the average Nusselt number and the air flow through the openings.

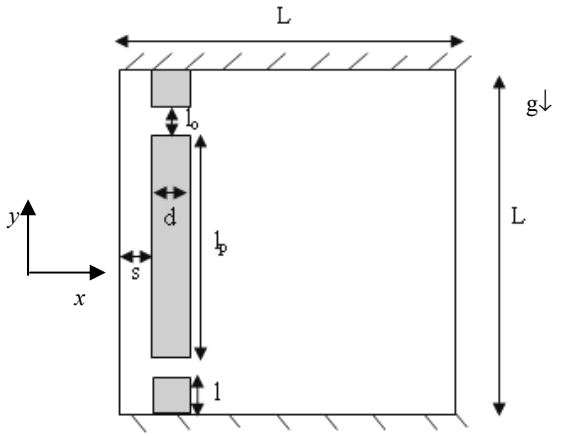

Fig. 1. *Studied configuration*

Mathematical formulation and numerical procedure

We assume that the geometry is two-dimensional, the flow is laminar, the radiative surfaces are diffuse gray and the physical properties of the air, except its density, are constants at the average temperature T_o. Only solid surfaces take part in the radiation exchange. The horizontal walls of the enclosure are adiabatic, while the vertical walls left and right-hand side are respectively hot and cold.

The dimensionless equations controlling the heat transfer and the flow in the enclosure are written in the dimensionless form:

$$\frac{\partial U}{\partial X}+\frac{\partial V}{\partial Y}=0 \qquad (1)$$

$$U\frac{\partial U}{\partial X}+V\frac{\partial U}{\partial Y}=-\frac{\partial P}{\partial X}+\lambda Pr\left(\frac{\partial^2 U}{\partial X^2}+\frac{\partial^2 U}{\partial Y^2}\right) \qquad (2)$$

$$U\frac{\partial V}{\partial X}+V\frac{\partial V}{\partial Y}=-\frac{\partial P}{\partial Y}+\lambda Pr\left(\frac{\partial^2 V}{\partial X^2}+\frac{\partial^2 V}{\partial Y^2}\right)+RaPr\theta \qquad (3)$$

$$U\frac{\partial \theta}{\partial X}+V\frac{\partial \theta}{\partial Y}=R_k\left(\frac{\partial^2 \theta}{\partial X^2}+\frac{\partial^2 \theta}{\partial Y^2}\right) \qquad (4)$$

with: $\lambda = 1$, $R_k = 1$ in the fluid area and $\lambda = \infty$, $R_k = k_w/k_a$ in the solid; k_a, k_w are thermal conductivities of the air and the wall, respectively.

The boundary conditions are: on the walls of the enclosure: $U = V = 0$; for $X = 0$, $0 \le Y \le 1$: $\theta = 0.5$ and for $X = 1$, $0 \le Y \le 1$: $\theta = -0.5$.

Along the partition wall: $R_k\frac{\partial \theta_w}{\partial n}=\frac{\partial \theta_a}{\partial n}-NrQr$; on the adiabatic walls: $0=\frac{\partial \theta_a}{\partial Y}-NrQr$, n: normal direction on the radiative surface considered.

The equations (1-4) are discretized using the method of finite volumes. The coupling pressure-velocity is treated using the algorithm SIMPLER. The view factors, with screening effects, were determined by using the methods of the boundary element and Monte Carlo [2]. The equations, of the algebraic system, obtained were solved by the method of the conjugate gradients.

After study, we found that the grid 60×60, irregular and fine near the enclosure walls and the faces of the partition wall, gives a good compromise between the precision of the results and the computing time.

When one takes into account the thermal radiation, the average temperature T_0 is fixed at 290 K. In order to respect the validity of the Boussinesq approximation, the maximal temperature difference ΔT is chosen lower or equal to 15 K. The Prandtl number was fixed at $Pr = 0.71$. R_k is fixed to 50 in all calculations, whereas the Rayleigh number Ra and the dimensionless width L_0 of the opening were varied from 10^3 to 10^7 and 0 to 0.2, respectively. The ends high and low of the central partition wall are located at the same distance of adiabatic walls and its height is fixed at $0.6L$. Consequently, the increase in widths of the two openings causes the reduction in widths L of the walls (top and bottom), respectively attached to the adiabatic walls. The distance between the hot wall and the partition wall, and the thickness of the partition wall were fixed respectively to $S = 0.05$ and $D = 0.15$.

Our objective in this work, is to study the effects of the thermal radiation, the Rayleigh number and the opening width on the average Nusselt number and the air flow through the openings.

$$Nu=\int_0^1\left(-\frac{\partial \theta}{\partial X}\bigg|_{X=0,Y}+NrQr(X=0,Y)\right)dY$$

and the dimensionless air flow through the openings:

$$Q=-\int_{l/L}^{0.2}U(X=S,Y)dY=\int_{0.8}^{(0.8+L_0)}U(X=S,Y)dY.$$

The comparison between the results obtained in pure natural convection and natural convection combined with the thermal radiation makes it possible to highlight the influence of the thermal radiation.

Results and discussion

Fig. 2 presents the isotherms and streamlines obtained for $Ra = 10^6$, $0 \le L_0 \le 0.2$ and $\varepsilon = 0$. For the comparison, the case of the empty enclosure (without partition) is also presented in this study. It is noted that the fluid circulates in the clockwise direction and is mono-cellular owing to the position of the isothermal walls (hot and cold). Indeed, the fluid goes up along the hot wall and goes down along the cold wall. At the center of the enclosure, one attends a thermal stratification of the temperature under the effect of the buoyancy forces. Also, the isotherms are dense in the vicinity of the hot wall and the vicinity of the left wall of the partition, like those of the cold wall of the right face of the partition wall.

The isotherms and streamlines corresponding to $Ra = 10^6$ and $0 \le L_0 \le 0.2$ are presented in Fig. 3 for $\varepsilon = 1$. We note that the radiative exchanges bring closer the temperatures the hot wall and the left face of the partition wall, like those of the cold wall and the right face of the partition wall. The slope of the isotherms close to the adiabatic walls is due to the importance of radiative fluxes. Along the cold wall, the variations in temperature are clearly less important in the upper part than in the low part of the enclosure. Indeed, the difference between the average temperatures of the air in the left and right parts of the enclosure rises under the effect of the radiation.

The average convective Nusselt number is more important when the radiation exchange is taken into account. Furthermore, we observe also the increase of the air flow through the openings.

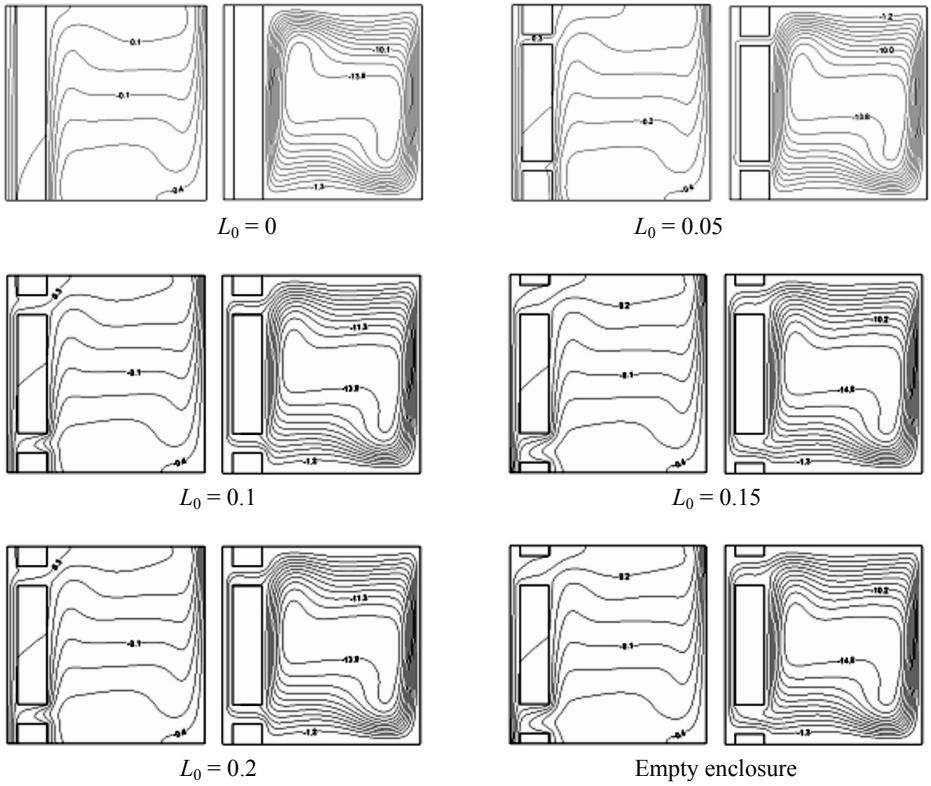

Fig. 2. *Isotherms and streamlines for Ra = 10^6, $\varepsilon = 0$ and $0 \le L_0 \le 0.2$*

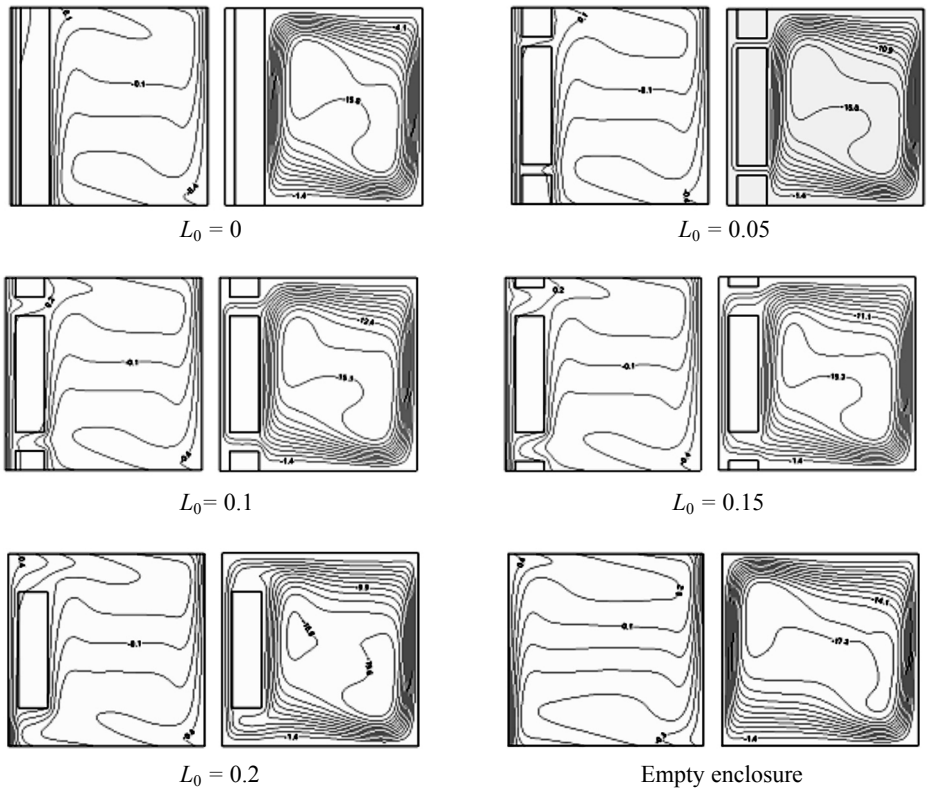

Fig. 3. *Isotherms and streamlines for Ra = 10^6, $\varepsilon = 1$ and $0 \le L_0 \le 0.2$*

Average Nusselt number and air flow crossing the openings

The average Nusselt number and the air flow increase with the opening width, in presence ($\varepsilon = 1$) or in absence ($\varepsilon = 0$) of the radiation, as it is indicated in Fig. 4 and 5, respectively.

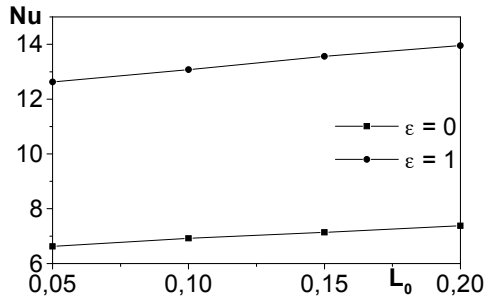

***Fig. 4**. Average Nusselt number according to L_0 for $Ra=10^6$*

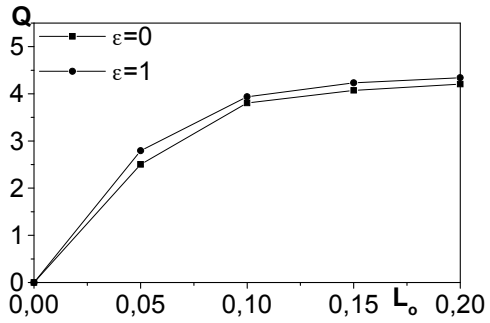

***Fig. 5.** Air flow according to L_o for $Ra= 10^6$*

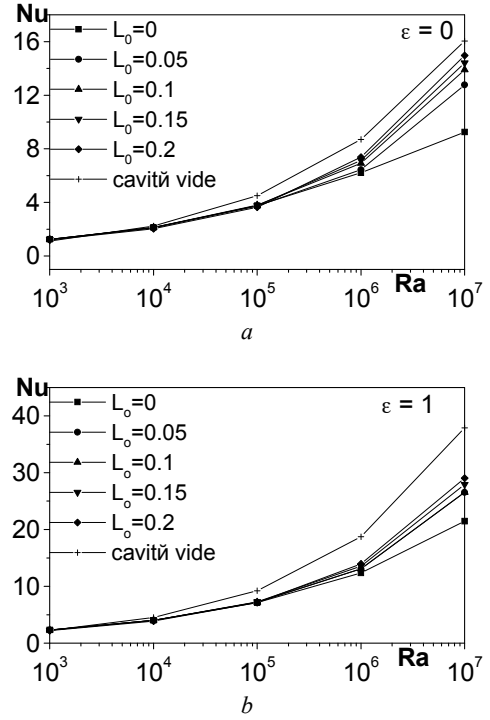

***Fig. 6**. Variation of the average Nusselt number according to Ra: (a) $\varepsilon = 0$ and (b) $\varepsilon = 1$*

The influence of the opening on the average Nusselt number is negligible until $Ra = 10^5$ (Fig. 6 and 7) because, the air circulation being weak, the heat transfer is done mainly by conduction and radiation. We note an increase in Nu and Q with L_0, particularly for large Rayleigh number and in presence of the radiation exchange. The variation of the air flow according to L_0 is presented on figure 5 for $Ra = 10^6$. It is clear that the air flow increases with the increase in the width opening L_0 and also in presence of the thermal radiation. For $Ra \leq 10^5$ (Fig. 7) (mode of conduction and transition), the flow is low, even if it increases under the influence of the radiation.

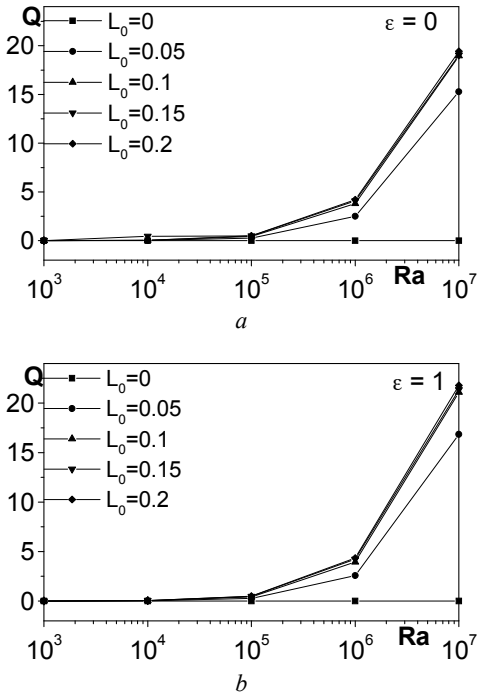

***Fig. 7.** Variation of the air flow through the openings according to Ra: (a) $\varepsilon = 0$ and (b) $\varepsilon = 1$*

Conclusion

Numerical simulations carried out on the coupling between the natural convection and the thermal radiation in a partitioned enclosure lead to the following conclusions: (i) the streamlines and the isotherms are considerably affected by the presence of the partition wall, (ii) the thermal radiation standardizes the temperatures in the two parts of the enclosure and increases the difference between their average temperatures, (iii) the air flow through the openings increases under the thermal radiation effect, (iv) the thermal radiation contributes to an increase in the heat transfer, mainly for larger values Ra, (v) the heat transfer is minimum for $L_0 = 0$ and is maximum for an empty enclosure.

References

1. Mezrhab A., Bouali H., Abid C. Modelling of combined radiation and convection heat transfer in an enclosure with a heat generating conducting body // International Journal of Computational Methods. 2005. Vol. 2, No. 3. P. 431-450.
2. Mezrhab A., Bouali H., Amaoui H., Bouzidi M. Computation of combined natural-convection and radiation heat-transfer in a cavity having a square body at its center // Applied Energy. 83 (2006) 1004–1023.
3. Nakamura H., Asko Y. Combined free convection and radiation heat transfer in rectangular cavities with a partition wall // Heat Transfer Japanese Research. 1986. P. 60-81.
4. Tadrari O, Abdelbaki A., Zrikem Z. Transfers thermiques couplés dans un système solaire à mur massif // Forum International des Energies Renouvelables, FIER'(2002), Tétouan-Maroc.
5. Buzzoni L., Dall'Olio R., Spiga M. Energy analysis of a passive solar system //Rev. Gén. Therm. (1998) 37, 411-416.
6. Gan G. A parametric study of Trombe walls for passive cooling of buildings // Energy and Buildings. 1998. 27 (1). 37-43.
7. Borgers T.R., Akbari H. Free convective turbulent flow with the Trombe wall channel // Solar Energy. 33 (1984). 251.
8. Ong K.S. A mathematical model of a solar chimney // Renewable Energy. 28 (2003). 1047–1060.
9. Awbi H.B., Gan G. Simulation of solar-induced ventilation // Renewable Energy Technology and the Environment. 4. (1992). 2016–30.

OPTIMIZATION OF THE NUMBER OF EFFECTS IN THE DESALINATION PLANTS FOR MULTIPLE EFFECTS

O. Sow, T. Maré**, J. Miriel**, M. Adj*, C. Tahya**

* Laboratoire d'Energétique Appliquée (LEA),
Ecole Supérieure Polytechnique
BP 633 Annexe Thiès, Sénégal
Tel: 825-34-26 E-mail: sowmane@yahoo.fr

**Laboratoire de Génie civil et de Génie Mécanique (LGCM),
INSA de Rennes, IUT Saint Malo, 35043 rennes, France
Tel: 02 99 21 95 05 / Fax: 02 99 21 95 41
E-mail: thierry.mare@univ-rennes1.fr

Received: 24 Sept 2007; accepted: 31 Oct 2007

By a thermodynamic approach, we determined the thermodynamic parameters characterizing the performances of the multiple effects system of desalination plant: ratios of brine and pure water recovery, salinity, energy, exergy, according to the provided necessary energy per unit of treated salt water mass. Thus, the model suggested in this present article allows, not only to arise all the characteristics common to the processes of desalination for multiple effects generally, but also to identify, for one kilogram of introduced salt water, the production in each effect, according to the provided energy, and the number of effects.

Keywords: ecology of water resources, optimization, energy, exergy

Ousmane Sow

Education: Université Cheikh Anta Diop (UCAD), Ecole Supérieure Polytechnique (ESP) Dakar (2003-2007).
Experience: ESP (Maître-Assistant), LEA (responsible of desalination) National Education (General inspector in mechanical engineering) (2004).
Main range of scientific interests: desalination of water, mechanics of the continuous mediums.
Publications: 2 papers in international scientific journals, 8 in international congress.

Thierry Maré

Education: IUT Saint Malo, University of Rennes1, INSA Rennes (1993-2007).
Experience: Maitre de conférences HDR, Head of Industrial Maintenance department, Head of International Relation, responsible of research committee IUT Saint Malo.
Main range of scientific interests: mixed convection, nanofluid, desalination, instability...
Publications: 12 papers in international scientific journals, 35 in international congress.

Introduction

An increase in population, a rural migration to cities, an increase in industrial demand, are independent factors of an increase in water requirements. Fresh water natural resources are no long driving sufficient, because more than 98 % of the earth resources have a too high content salt. The desalination of water thus becomes absolutely necessary and cannot be circumvented in order to dispose of sufficient quantities of consumable drinking water or for needs for irrigation or even for industries.

In Senegal in particular, this water deficit is now a critical national problem. Several projects were born in to yield fresh water by the localities far away from the big cities. It was proposed to exploit the brackish water (drilling, well, desalination…). Thus, the Laboratory of Applied Energy (LEA) of the Polytechnic University (ESP) of Dakar centred its research on the desalination of brackish water of the Saloum islands.

Let us note however that the majority of desalination techniques are to be met very high capital costs as well as his high running costs. These constraints push

developing countries into adopting with their economic reach. Consequently the major question which emerges is as follows:

How to manage the adopting of a powerful technique of desalination based on the use of easily accessible energy?

With respect to this problem, solar energy, an inexhaustible source, becomes a real candidate. In spite of the availability of this energy source, it is necessary to reduce the losses of energy in order to increase the output of the solar desalination plants. The increase in the output of these installations contributes to the reduction not only of their size, but also to decrease necessary size of solar collector to ensure the operation of desalination. Our study will be divided into two parts.

In the first part of this article, we will quantify with precision, the losses of energy by a second law analysis of multiple effect installations. Indeed, Spiegler and El Sayed [1], Yunus [2] have come to the obvious conclusion that, if the desalination process were to be fully reversible, the cost would be enormous since a plant of infinite size would be needed; an impossible endeavour. It follows that the only way process is to minimize the losses, thereby requiring a second law approach.

The exergetic analysis makes it possible to evaluate quantitatively and qualitatively the degree of degradation of energy, related to the thermodynamic irreversibilities, i.e. to correctly quantify the losses in the systems. Ali Mr. El Nashar and Atef Al Baghadi [3] presented a system of desalination for 18 effects laid in two parallel series of 9 effects. The exergetic losses in the installation were carefully highlighted. However, the gain output of the multiple effects process, the object of their article, was not approached. In the present work we were particularly interested in the losses generated in the system, when the number of effects and the quantity of provided energy vary. In all the study the results are in term of normalized 1 kg of treated salt water, i.e. all the characteristics are expressed per unit of introduced salt water mass.

The second part of this article presents a quantitative analysis of the production of water of installations for multiple effects, on the basis of the equations of steady state thermodynamics, applied to the various components of the total system. It is possible to consider not only the quantity of water being obtained and the water rejections, but also to have further information on the energy behavior of these processes, when one introduces into the system one kilogram of brackish water. As for the first part of the study, all the analysis was made according to the quantity of provided energy (basic variable of the study) and of the number of effects (principal parameter of the study).

Schematic description of the multi effect desalination

The system is presented Fig. 1.

In this description we consider the following notation: A_i for the effect A_i and $V_{4a_i\text{-}3a_i+1}$ for the valve located between items 4 and 3 of A_i effect.

Brackish water passing throw the P_1 pump, enters the various heaters (r_n, r_2,…r_1) in succession and arrives in the evaporator at a temperature close to that of saturation at the point 3_{a_1}. Because of energy provided by the $Ech_{11\text{-}12}$ exchanger, and of the vacuum which reigns in the tank (A_1), water passes in a state of a liquid-vapour mixture at the point 5_{a_1}. The vapour heat is incoming feed water at the point 6_{a_1} before reaching in the second evaporator by the point 7_{a_1}. This makes it possible to vaporize salt water of the second effect, i.e. the brine of the first outgoing effect of the valve between 4_{a_1} and 3_{a_2}. At the point 9_{a_1} pure water is extracted. The same process continues until the last effect where the vaporized fluid reaches the feed water in component r_n, before entering the condenser. After complete condensation of the vapour, the pure water is extracted by the pump $P_{ep}(n)$ and brackish water is extracted as at point 10 by the P_{sa} pump.

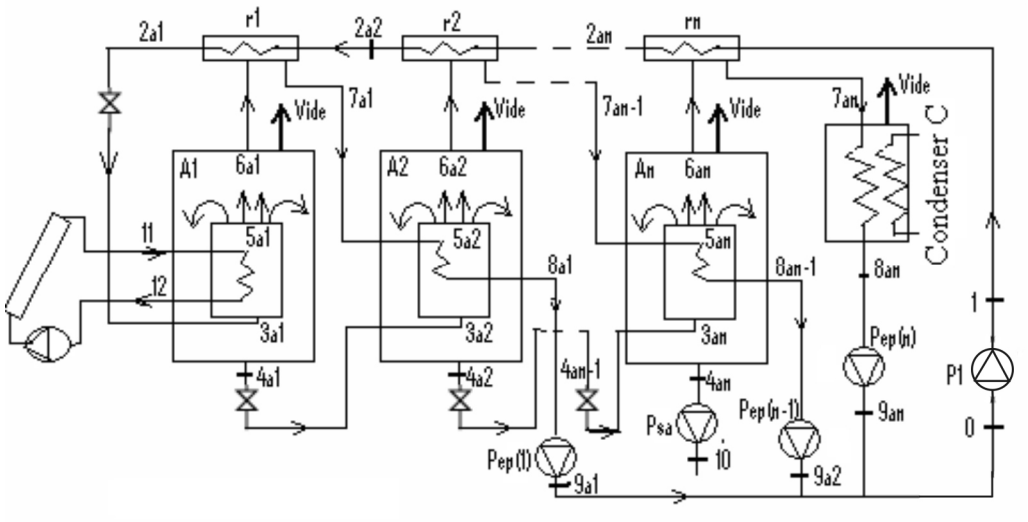

Fig. 1. *Presentation of a system of desalination to multiple effects*

Exergy analysis

Hypotheses

Leading causes of creation of entropy [4, 5] at the origin of the exergetic losses of importance in this work are:

a. The generation of entropy due to heat transfer between the various fluids of the system (evaporators, heaters, condenser, flows of water);

b. The generation of entropy in an isenthalpic relaxation due to the passage through the valves;

c. The generation of entropy due to viscous dissipation (neglected);

d. The generation of entropy due to thermal losses by conductivity (neglected);

e. Variations of kinetic and potential energy (neglected).

Mathematical model

Taking into account the assumptions quoted above (3.1), the exergy mass [6, 7] expresses itself as follows:

$$ex = h - T_0 s \tag{1}$$

The exergetic balance in steady state [7], in its general formulation is expressed as:

$$\Delta[q_m ex]_{ec} = W' + Ex'_q - Ex'_{\det} \tag{2}$$

With W' – mechanical power provided to the system, expressed in W, Ex'_q – exergetic flow provided to the system, expressed in W.

The enthalpy of the various points was calculated with the influence of the presence of salt [8, 9]. Equations (1) and (2) applied to all the components of the installation give the results of Table 1.

Table 1

Loss of exergy in the various components and flows of water

Expression of the exergetic losses due to the heat transfers		
Evaporator of effect 1 ($Ex_{\det a_1}$)	$Ex_{\det a_1} = \left(\frac{T_0}{T_{sat\,a_1}} - \frac{T_0}{\varepsilon_{11/12}\left(T_{11} - T_{sat\,a_1}\right)} \ln\left(\frac{T_{11}}{T_{12}}\right) \right) q_{11/12}$	(3)
Evaporator of an effect i ($Ex_{\det a_i}$ 2 ≤ i ≤ n)	$Ex_{\det a_i} = \left[\frac{T_0}{T_{sat\,a_i}} - \frac{T_0}{T_{sat\,a_{i-1}}} \right] \left(h_{6a_{i-1}} - h_{7a_{i-1}}\right) \prod_{i=2}^{n} x_{a_i} \left(1 - x_{a_{i-1}}\right)$ (avec pour $i = n$ alors $T_{2an+1} = T_1$)	(4)
Heater r_i ($Ex_{\det r_i}$)	$Ex_{\det r_i} = T_0 Cp \ln\left(\frac{T_{2a_i}}{T_{2a_{i+1}}}\right) - \left(\frac{T_0}{T_{sat\,a_i}}\right)\left(h_{7a_i} - h_{6a_i}\right) \prod_{i=1}^{n} x_{a_i}\left(1 - x_{a_{i-1}}\right)$	(5)
Condenser C ($Ex_{\det C}$)	$Ex_{\det C} = \left[-\frac{T_0}{T_{sat\,a_i}} + \frac{T_0}{\varepsilon_{ref}\left(T_{sat\,a_i} - T_{eref}\right)} \ln\left(\frac{T_{s\,ref}}{T_{eref}}\right) \right] q_{ref}$	(6)
The expression of the exergetic losses in the flows of water		
Feed water ($Ex_{\det 1}$)	$Ex_{\det 1} = \left[\left(h_1 - h_0\right) - T_0\left(s_1 - s_0\right) \right]$	(7)
Pure water ($Ex_{\det 9a_i}$)	$Ex_{\det 9a_i} = \prod_{i=1}^{n} x_{a_i}\left(1 - x_{a_{i-1}}\right) \prod_{i=1}^{n} \left(h_{9a_i} - h_0\right) - T_0\left(s_{9a_i} - s_0\right)$	(8)
Brackish water ($Ex_{\det 9sa}$)	$Ex_{\det sa} = \prod_{i=1}^{n} \left(1 - x_{a_i}\right) \left[\left(h_{10} - h_0\right) - T_0\left(s_{10} - s_0\right) \right]$	(9)
The expression of the exergetic losses in the valves		
Valve $V_{2a_1/3a_1}$ ($Ex_{\det(V2a_1/3a_1)}$)	$Ex_{\det(V_{2a_1/3a_1})} = \frac{T_0}{T_{sat\,a_1}} \left(\frac{p_1 - p_{sat\,a_1}}{\rho} \right)$	(10)
Valve $V_{4a_i/3a_i+1}$ ($Ex_{\det V_{4a_i}}$)	$Ex_{\det V_{4a_i}} = \left[T_0 \left(s_{3a_{i+1}} - s_{4a_i} \right) \right] \prod_{i=1}^{n-1} \left(1 - x_i\right)$	(11)

Energy loss results

Conditions of simulation

The equations presented in Table 1, were solved by matrix inversion with the Matlab software. As explained above, all the results are expressed per unit mass of salt.

In order to avoid the problems of building up salt on the components of the installation resulting from the highly salinities at high temperatures [10-12] processes of desalination is carried out at low pressure and low temperature. In any case the provision of energy at high temperature from solar prediction is expensive so this also drives us to use low temperatures and pressures. Thus the conditions of simulation are the following ones:

– Initial temperature of water (T_1) is 20 °C;

– Initial salinity of water (s_1) is of 1 %;

– Ambient temperature (T_0) 28 °C, s_0 entropy of the air with 28 °C, atmospheric pressure, h_0 is the corresponding enthalpy;

– Effectiveness of the heaters is 0.85;

– Temperatures of saturation of the various effects are: 75, 70, 65, 60, 55, 50, 45, 40, 35 °C.

The number of effects is an input to the program as is the heat input from the solar collector.

The variable of entry is the quantity of heat provided per unit of treated salt water mass ($q_{11/12}$).

Presentation of the results

Legend of the first part of the study:

– – – –	effect 1	———	effect 6
▪▪▪▪▪▪▪▪▪▪	effect 2	– – – –	effect 7
— . —	effect 3	·····	effect 8
·····	effect 4	———	effect 9
— . . —	effect 5		

The results of this study relate to various systems, energy of the simple effect (1 effect) to a system comprising 9 effects.

Fig. 2 presents the exergetic losses in the evaporators of the various effects according to the provided energy per unit of treated salt water mass ($q_{11/12}$).

With the first effect, the exergetic losses are due to the transfer of heat between the coolant of the heating circuit and salt water. For the other effects, these losses are due to the transfer of heat between the steams resulting from the effect (A_{i-1}) and salt water of the effect (A_i) also coming from the effect (A_{i-1}).

We note that these losses are proportional to the quantity of exchanged energy. What results not only in an increasing linearity of the curves representing these exergetic losses according to introduced energy, but also in the change of pace starting from the maximum values. It is explained by the progressive reduction of the quantity of salt water introduced into the various cells caused by the increase in the production of vapor.

The maximum exergy destroyed between the first and the last effect ranges between 35 and 5 kJ/kg of treated salt water.

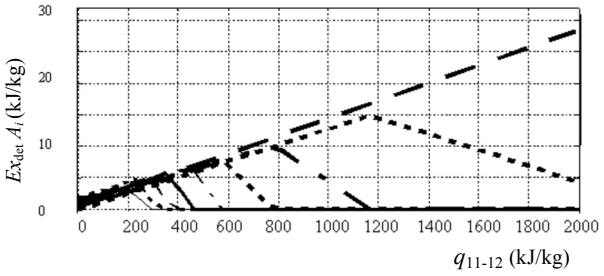

Fig. 2. *Exergy destroyed in the evaporators of the various effects*

Fig. 3 represents the exergy destroyed at the time of the passage through the valves of brine extraction, according to the provided energy per unit of treated salt water mass ($q_{11/12}$). The exergy destroyed in the valves of extraction has a maximum value at the beginning of the process because of the flows introduced into these components (quantity of brine) which start from a maximum value and decrease gradually with the increase in concerned energy. We also note that the speed of waning of these losses increases with the number of effects.

The maximum exergy destroyed between the first and the last effect ranges between 18.5 and 13 kJ/kg of treated salt water.

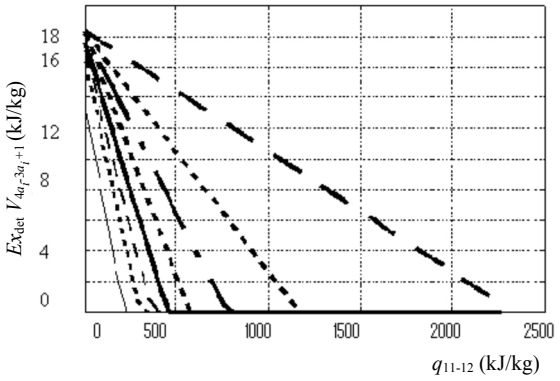

Fig. 3. *Exergy destroyed through the valves of brine extraction*

Fig. 4 makes it possible to evaluate the exergetic losses in the pure water flow by taking as reference the ambient conditions, according to the provided energy per unit of treated salt water mass ($q_{11/12}$).

These losses fall generally with the number of effects i.e. when the variation of temperature with the external medium decreases.

This figure also presents maximum values corresponding to vapor titles equal to 1 in the various effects. Consequently, the quantity of water (brine) introduced into the various effects, in connection with the quantity of produced vapor, decreases continuously when this one increases, until reaching a zero value.

The maximum values between the first and the last effect are between 60 and less than 4 kJ/kg of treated salt water.

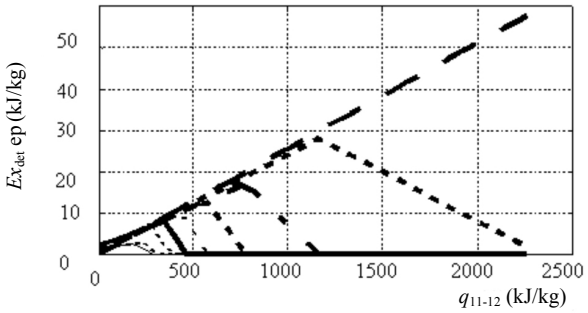

Fig. 4. *Exergetic losses during the flow of pure water*

Fig. 5 shows the exergetic losses in the brine rejections, according to the provided energy per unit of treated salt water mass ($q_{11/12}$). Like for the valves of brine extraction (Fig. 3), this Fig. 5 presents maximum values at the beginning of the operation which decrease in a linear way until reaching a zero value.

The maximum values between the first and the last effect range between 14 and 58 kJ/kg of treated salt water.

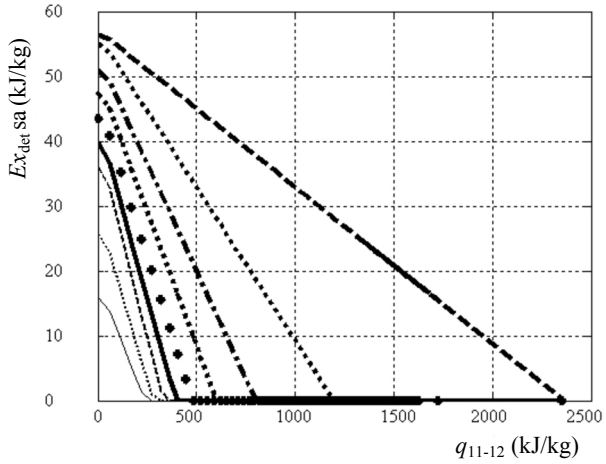

Fig. 5. *Exergetic losses of the rejections of the brine*

Fig. 6 presents the exergetic losses of the condenser according to the provided energy per unit of treated salt water mass ($q_{11/12}$).

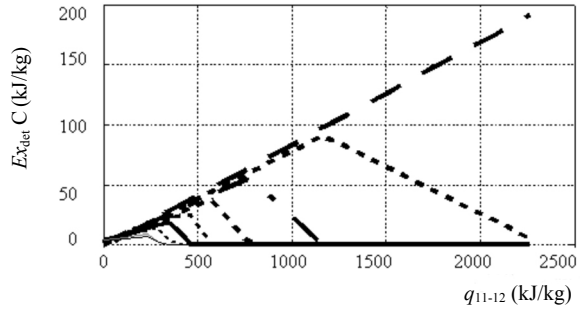

Fig. 6. *Exergetic losses in the condenser*

It gives an idea of these losses caused by heat exchange between the vapor resulting from the last effect and the coolant circuit of the condenser. These losses thus depend primarily on the quantity of the produced vapor. Thus, they increase with this one until reaching a maximum value corresponding to a title of value equal to 1, before starting to decrease. The shape of the curves of Fig. 3, 5, and 7 presents a similarity. In effect, these last all are in connection with the produced vapor. Between the first and the last effect, the maximum exergetic losses range between 200 and 12 kJ/kg of treated salt water.

Fig. 7 makes it possible to evaluate the exergy destroyed in the heaters (r_i, according to the provided energy per unit of treated salt water mass ($q_{11/12}$). The observations made on the preceding figures are checked on the level of the heaters. The exergetic losses in these components range between 35 (effect 1) and 17 kJ/kg of treated salt water (effect 9).

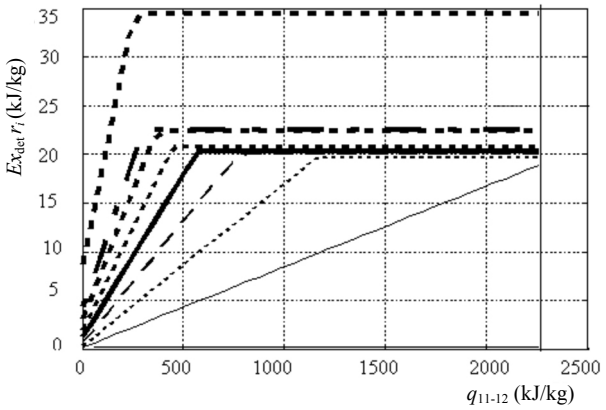

Fig. 7. *Exergy destroyed in the heater*

All in all, knowing that during a heat transfer between two fluids, the creation of entropy takes place when the heat transfer is carried out with a variation of temperature, then on the assumption of a condensation without under cooling and evaporation without overheating, one can admit that the creation of entropy is negligible. Under these conditions, and taking into account the assumptions of the study, the exergy destroyed in the cells where there is no sensible heat (of 2 to n), becomes also negligible. This would explain partly why the dominating losses of exergy are at the level of the condenser, in the heaters, the flows of water, and in effect 1. The localization of these losses makes it possible to realize, that a system for simple effect is not very possible in practice because would inevitably lead to a bad output exergetic (less than 4 % [13]).

Conclusion of the first study

This study made it possible to appreciate quantitatively the exergetic losses in a system for multiple effects. Thus, the results show that the highest losses are caused not only by the exchange between the coolants and salt water, but also by the condensation of the vapors produced in the last effect and the flows of water. The weakest losses are at the level of the valves of brine extractions. Generally these losses decrease when the number of effect increases. Consequently, this analysis recommends increasing the number of effect ad infinitum.

This conclusion raises another problem: which number of maximum effect does one have to implement to optimize the multiple effect desalination plant? We shall for that purpose, study the influence of the increase of the number of effect on the production of water.

Production analysis

Working hypotheses (same assumption as previously)

a) The presence of air in the production unit of fresh water is neglected.

b) The variations of kinetic and potential energy are neglected.

c) The thermal losses towards outside are negligible in the various tanks.

d) The extracted steam is free from salt.

Equations

– Conservation equation of the mass

$$\Delta[q_m]_{ec} = 0 \tag{12}$$

– Conservation equation of the energy

$$\Delta[hq_m]_{ec} = W'_E + Q' \tag{13}$$

The development of the equations (12) and (13) applied to all the components of the installation (evaporators, the condenser, heaters, and various extraction valves) leads to a series of coupled equations, given in Table 2.

Table 2

Results of the thermodynamic study

Enthalpy of the liquid mixture vapor of the first effect at the point $5_{a_1}(h_{5a_1})$	$h_{5a_1} - h_{3a_1} = q_{11/12}$	(14)
Enthalpy of the liquid mixture vapor in an effect i at the point $5_{a_i}(h_{5a_i})$	$h_{5a_i} = \frac{x_{a_{i-1}}}{1-x_{a_{i-1}}}\left(h_{7a_{i-1}} - h_{8a_{i-1}}\right) + h_{3a_i}$	(15)
Titrate vapor of an unspecified effect $A_i(x_{a_i})$	$x_{a_i} = \frac{h_{5a_i} - h_{4a_i}}{h_{6a_i} - h_{4a_i}}$	(16)
Report/ratio of pure water recovery of an effect $A_i(r_{ep\,a_i})$	$r_{ep\,a_i} = \frac{q_{mep\,a_i}}{q_{mes\,a_1}} = \frac{q_{mep\,a_i}}{q_{mes\,a_i}}\frac{q_{mes\,a_i}}{q_{mes\,a_1}} = \prod_{i=1}^{n} x_{a_i}\left(1-x_{a_{i-1}}\right)$	(17)
Report/ratio of brine recovery of an effect $A_i(r_{sa\,a_i})$	$r_{sa\,a_i} = \frac{q_{msa\,a_i}}{q_{mes\,a_1}} = \frac{q_{msa\,a_i}}{q_{mes\,a_i}}\frac{q_{mes\,a_i}}{q_{mes\,a_1}} = \prod_{i=1}^{n}\left(1-x_{a_i}\right)$	(18)
Total production of water in number of effect ($prod_{a_i}$)	$prod_{a_i} = \sum_{i=1}^{n}\prod_{i=1}^{n} x_{a_i}\left(1-x_{a_{i-1}}\right)$	(19)
Salinity of the brine extracted from an effect $A_i(s_{4a_i})$	$S_{4a_i} = \frac{S_{3a_i}}{(1-x_{a_i})}$	(20)
Enthalpy of the fluid at the entry of effect 1 i.e. at the exit of the heater r_1: h_{2a_1}	$h_{2a_1} = h_{3a_1}$	(21)
Enthalpy of salt water at the exit of the various effects (h_{4a_i})	$h_{4a_{i-1}} = h_{3a_i}$	(22)
Enthalpy on the outlet side of the heaters (h_{7a_i})	$h_{7a_i} = h_{6a_i} - \frac{h_{2a_i} - h_{2a_{i+1}}}{\prod_{i=1}^{n} x_{a_i}\left(1-x_{a_{i-1}}\right)}$	(23)
Energy of cooling per unit of introduced salt water mass ($q_{ref/es}$)	$q_{ref/es} = \frac{Q'_{ref}}{q_{mes\,a_1}} = \prod_{i=1}^{n} x_{a_i}\left(1-x_{a_{i-1}}\right)\left(h_{7a_n} - h_{8a_n}\right)$	(24)
Energy of cooling per unit of produced pure water mass ($q_{ref/ep}$)	$q_{ref/ep} = \frac{\prod_{i=1}^{n} x_{a_i}\left(1-x_{a_{i-1}}\right)\left(h_{7a_n} - h_{8a_n}\right)}{\sum_{i=1}^{n}\prod_{i=1}^{n} x_{a_i}\left(1-x_{a_{i-1}}\right)}$	(25)
Specific energy in the various effects ($q_{sp\,a_n}$)	$q_{sp\,a_n} = \frac{q_{11/12}}{\sum_{i=1}^{n}\prod_{i=1}^{n} x_{a_i}\left(1-x_{a_{i-1}}\right)}$	(26)

With these equations are added those giving the influence of the presence of salt on the characteristics of the mixture water-salt [8, 14, 15].

Results of the second study

Conditions of simulation

The conditions of simulation are the same ones as those presented in paragraph *Energy loss results*.

Thus, the parameter of simulation is always the number of effect, and the basic variable always remains the quantity of heat provided per unit of treated salt water mass ($q_{11/12}$).

Presentation of the results

Legend of the second part of the study:

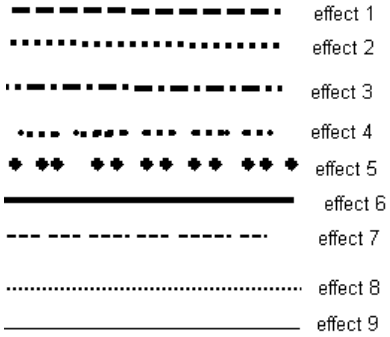

Fig. 8-11 respectively show the evolution of the ratios of recovery of pure water and brine rejection, the vapor title, the enthalpy of the liquid-steamer mixture and the production of pure water according to the variable $q_{11/12}$.

*Note:*An effect of superposition of the curves of Fig. 8 made up of two series of curves makes the reading difficult. This is why it is necessary to give following indications to guide the reader. The curves (*rep*) mark according to $q_{11/12}$ have the same pace as the curves of (*qref*) given to Fig. 13. Whereas the curves (rej) according to $q_{11/12}$ have the same pace as the curves of (ex_{det} $V_{4a_i-3a_i+1}$) given to has Fig. 3. These two series of curves (*rep* mark and *rej*) joined together in same Fig. 8 give points of intersection whose interpretations are rather interesting.

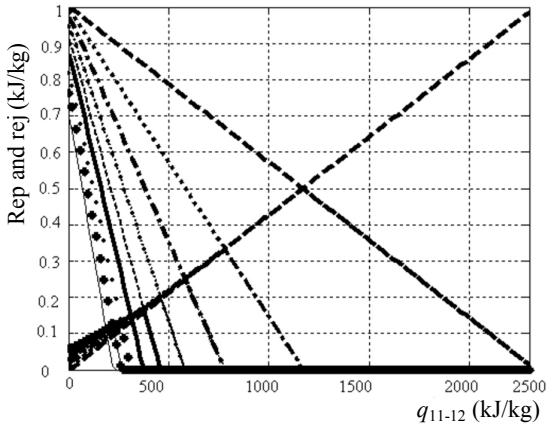

Fig. 8. *Report/ratio of recovery of pure water (rep) and brine rejection (rej) according to the energy provided per unit of salt water mass*

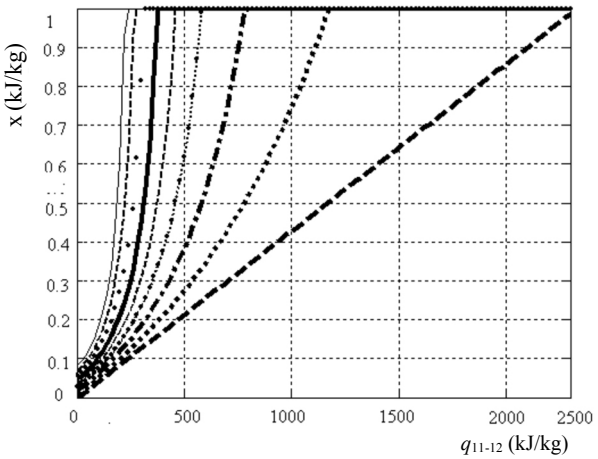

Fig. 9. *Titrate vapor according to the energy provided per unit of salt water mass*

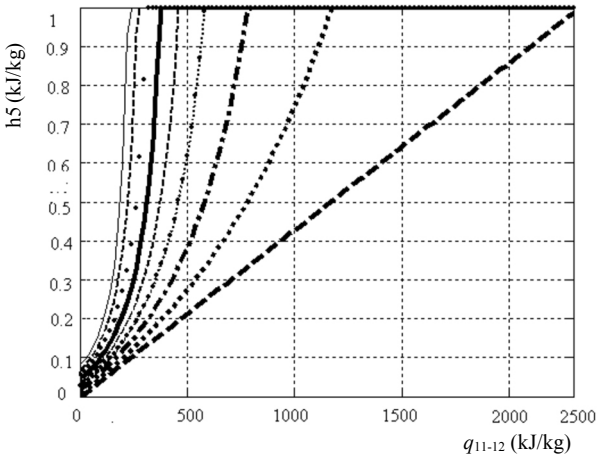

Fig. 10. *Enthalpy of the liquid-steamer mixture according to the energy provided per unit of salt water mass*

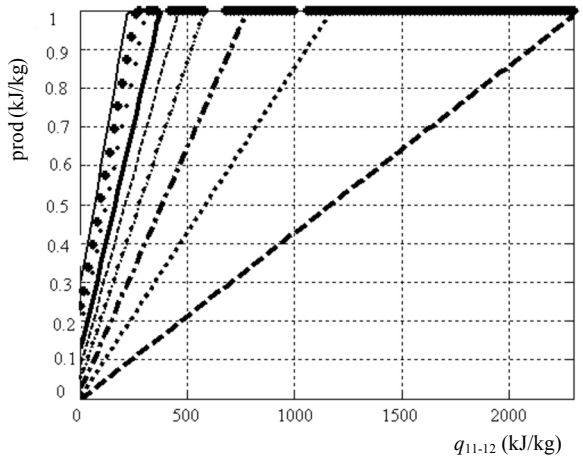

Fig. 11. *Production of one kg pure water per kg of salt water according to the energy provided per unit of salt water mass*

These four figures characterize perfectly the principle of the systems for multiple effects. Indeed, we note that, when the production reaches a maximum value in a given effect A_i (Fig. 8), that corresponds a minimal value

(zero value) to the level of the following effect (A_{i+1}). Beyond this maximum value, the report/ratio of pure water recovery in effect *i* (Fig. 8) is rigorously identical to that of the brine of the effect (A_{i-1}). Indeed, all the salt water introduced into effect (A_i), starting from the effect (A_{i-1}) vaporizes spontaneously, as soon as the vapor title reaches value 1 (Fig. 9). What implies a null production (Fig. 8) for all the effects located beyond cell A_i, i.e. the A_{i+1} cells, A_{i+2},….A_n. Fig. 10 and 11 give respectively the enthalpy of the liquid-steamer mixture and the production of pure water, according to provided energy but also according to the number of effects used. These four figures (8, 9, 10, 11) also inform about the quantity of energy necessary to reach the maximum production with the last effect, when (n) varies. What makes it possible to judiciously choose the number of effect constituting our system, according to the quantity of energy available. Table 3 below recapitulates energy $q_{max}(n)$ leading to a vapor title equal to the unit to the n_{th} effect (A_n), and the corresponding ratio (*rep*), according to the number of effect (n).

Table 3

Values of q_{max} (n) and *rep* according to the number of effects

(*n*)	1	2	3	4	5	6	7	8	9
$q_{max}(n)$	2308	1180	780	580	460	360	300	260	220
rep	1	0.5	0.33	0.25	0.2	0.165	0.13	0.1184	0.1
x	1	1	1	1	1	1	1	1	1

Remarks

R_1: The report of $q_{max}(n)$ on the ratio (*rep*) of pure water tends towards a constant. This constant represents the latent heat of phase shift of entering salt water.

This remark gives us a relation specific to the system for multiple effects:

$$\frac{q_{max}(n)}{n} = \text{const} \qquad (27)$$

R_2: It is clear that a vapor title equal to one cannot be reached in the cells of the systems for multiple effects, because that would lead to the crystallization of salt on the components. The values of (n) thus constitute a maximum threshold not being able to be reached. What makes it possible to delimit the zones of operation (Fig. 14).

A practical example validating this assertion is based on the study undertaken by El Nashar [3] which lays out two series of 9 effects to make 18 of them. In this precise case, where the rate of feed is worth 17.7 m^3/h in each series and the energy of provided heating of 176 kJ, the distillate flow rate is worth 3.1 m^3/h, and the provided energy per unit of salt water mass is of 35.5 kJ/kg, quite lower than 220 kJ/kg (Table 3). But while analyzing these experimental results of meadows, we realize that this value corresponds to a vapor title equal to 0.17 (i.e. 3.1/17.7). This is perfectly in phase with our results, because our calculations give 0.16 (i.e. 35.5/220); and we are well in the zone of operation (wet vapor) of Fig. 14.

In addition to these remarks, we generally note, a clear improvement of the production. Indeed, when the number of effect increases the aggregate output increases too. However, beyond 6_{th} and 7_{th} effects, this improvement of the system related to the increase in the quantity of recovered pure water, becomes increasingly weak, what is materialized in the present study, by the convergence of the curves towards n^{th} effect.

Fig. 12, 13 and 14 give further information on salinity, the energy of cooling, and specific energy.

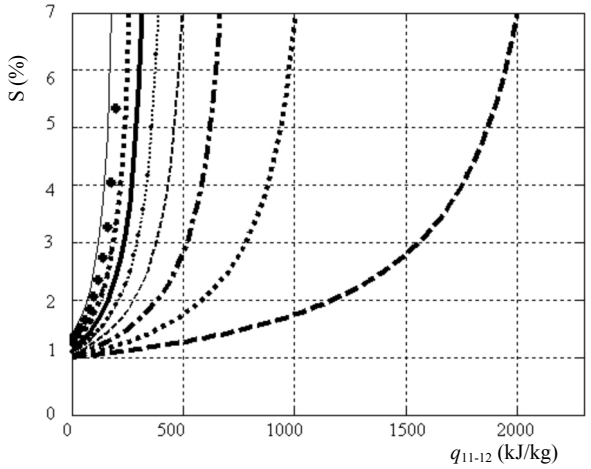

Fig. 12. *Salinity of the brine according to the energy provided per unit of salt water mass*

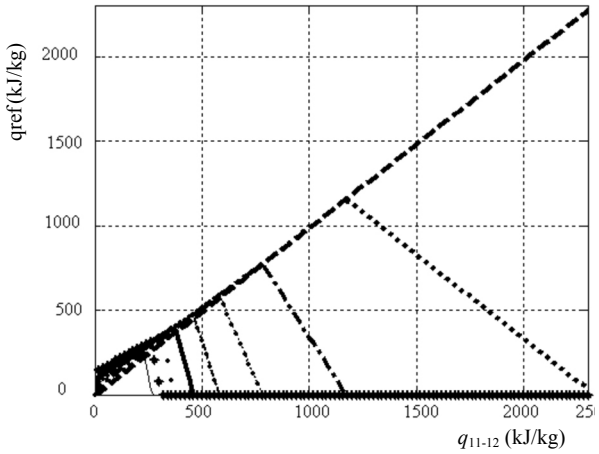

Fig. 13. *Energy of cooling per unit of salt water mass according to the energy provided per unit of salt water mass*

Fig. 12 gives salinity according to provided necessary energy, per unit of salt water mass ($q_{11/12}$). This figure

also makes it possible to delimit the maximum value of the size $q_{11/12}$ being likely to create the build up of salt on the components like the exchangers. Indeed, for the strong salt concentrations (beyond a salinity of 5.5 %) [15, 16] there is risk of salt build up.

Fig. 13 gives the energy of cooling, i.e. energy necessary to ensure the complete condensation of the vapors in the last effect, by the only condenser of the system for multiple effects. We naturally note that the maximum value of q_{ref} is equal q_{max}(n).

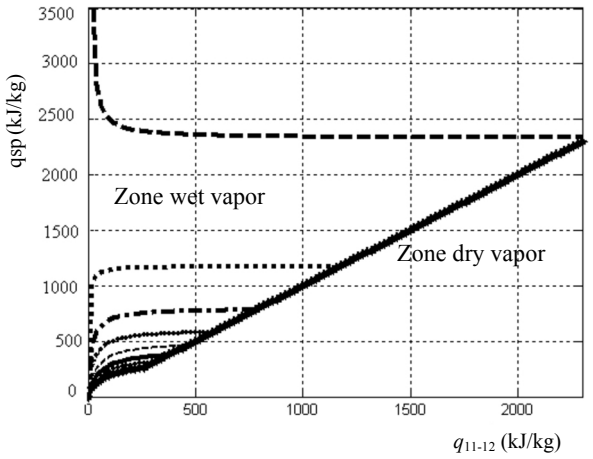

Fig. 14. *Energy provided to produce one kg of pure water according to the provided energy per unit of salt water mass*

Fig. 14 presents energy necessary to produce one kg of pure water (q_{sp}) according to the provided energy reported to the unit of salt water mass. We note a convergence of the various curves towards the value (*n*). All these values are on a linear line which is a "pivot" characteristic of the systems for multiple effects. This line is very useful not only to graphically determine (*n*) according to $q_{11/12}$, but also to delimit the zone of operation optimizing the contribution of energy (zone wet vapor). Indeed, beyond this zone, it is not useful any more to increase the number of effects or energy.

Conclusion of the second study

This second part of the study describes and generally gives the characteristics of the systems for multiple effects, while specifying their performances with respect to the number of effects used and provided energy. She thus gives an idea on the performances of desalination with multiples effects. Indeed, we can say at the conclusion of this study that for 1 kg of introduced salt water, the number of effect could be limited to 9. Indeed, the convergence of the curves towards the last effects shows that beyond 6_{th} and 7_{th} effects, the report/ratio of recovery becomes relatively weak and converges towards 0.1 kg_{ep}/kg_{es}: 0.16, 0.13, 0.12, 0.1 kg_{ep}/kg_{es} (see Table 1 and Fig. 8); this conclusion makes it possible to delimit the capital costs i.e. to limit the number of effects, the supply of energy, the entering salt water flow, and the quantity of pure water provided to the last effect.

General conclusion

The mathematical model presented here, constitutes a coherent analysis as a whole helping to come to a conclusion about the profitability of the installations for multiple effects.

Indeed, the first study, bearing on the exergetic analysis made it possible to show that the exergetic losses fall in a considerable way with the number of effects. Analysis of the production of water, object of the second study, shows that the production also increases with the number of effect, but this increase in production becomes increasingly weak when (*n*) increases. Thus, in our case of study the optimal situation would be to limit the number of effects to 9, and the quantity of energy required per unit of treated salt water mass less than 220 kJ/kg of treated salt water. Table 3 recapitulates the other cases of figure.

The study specifies energy thus leading to a vapor title equal to one according to the number of effects used, i.e. the operational limits of the systems for multiple effects according to the provided energy brought back to the unit of treated salt water mass, and of the number of effect.

Generally, this work gives interesting information on the process multiple effects, in particular on the energy cost of the production of water which could be definitely reduced by the optimization of the number of effects. The continuation of the study could give an alternative for developing countries.

Acknowledgements

Colonel Mbarek DIOP of Senegal, Antoninon ZICHICHI of Switzerland for the support brought to the Laboratory of Energy Applied (LEA) of ESP of DAKAR.

Symbols

c_p – specific heat at constant pressure, $kJ \cdot K^{-1} \cdot kg^{-1}$
Ex′ – exergy power, W
ex – specific exergy, kJ/kg
h – specific enthalpy, kJ/kg
m – mass, kg
p – pressure, Pa
prod – production of water, $kg \cdot kg^{-1}$
q – specific heat exchanged, kJ/kg
Q' – thermal power, W
q_m – mass flow rate, $kg \cdot s^{-1}$
rep – report/ratio of pure water recovery, $kg \cdot kg^{-1}$
rej – brine rejection, $kg \cdot kg^{-1}$
s – specific entropy, $kJ \cdot K^{-1} \cdot kg^{-1}$
S – salinity (%)
T – temperature, K
v – specific volume, $m^3 \cdot kg^{-1}$
x – titrate vapor, $kg \cdot kg^{-1}$
ε – first low efficiency, %

Component symbols

r – heater
V – Valve
Ech *i*/*j* – Exchanging located between items *i* and *j*
P – pump

Subscripts and superscripts

′– Relative to a flow
* – Relative to a saline solution
0 – Relating to the ambient conditions
det – Destroyed
es –Salted water
ep – Pure water
ec – Flow
a_i – Relating to effect A_i
(*i*-*j*) – component located between *i* and *j*
(*i*/*j*) – Component located between *i* and *j*
ref – Cooling
sa – Brine
sat – Relating to saturation
sp – Specific

References

1. Spiegler K.S. EL Sayed. The energetic of desalination processes // Desalination, 2001. No. 134. P. 109-128.
2. Yunus C. The minimum requirement for distillation processes // Exergy an international journal, 2002. Vol. 2. P. 15–23.
3. El Nashar A.M., Al Bagaghadi A.A. Exergy losses in a multiple-effect stack seawater desalination plant // Desalination, 1998. Vol. 116. P. 11–24. Elsevier.
4. Feidt J.M. Thermodynamique et optimisation énergétique des Systèmes, 1996, Edition Lavoisier, Technique et documentation.
5. Feidt M., Lallemand A., Benelmir R. Analyse exergétique // Technique de l'ingénieur, BE 8015. P. 1-15 (2001).
6. Corriou J.P. Thermodynamique chimique Définitions et relations fondamentales // Techniques de l'ingénieur, J 1 025 (2001).
7. Rollet Gilbert. Thermodynamique appliquée // L'exergie, techniques de l'ingénieur. B 1212 (2001).
8. Millero Chen, Bradshaw Schleicher. Technical papers in marine sciences international Oceanographic Tables, UNESCO, P. 97 (1987).
9. Grumbreg L., Miles M. Proceeding of 3rd International symposium of fresh water from sea, 1970.
10. Sow O., Siroux M., Desmet B. Gestion des rejets d'eau par régulation d'une installation de dessalement d'eau saumâtre de petite capacité, Congrès Français de Mécanique (CFM) Nice du 1-5 Sept. (2003).
11. Perry R.H., Chilton C.H. Chemical engineering, Hand Book, Mac Graw Hill, Book Company 5th edition. P. 3-121 (1973).
12. Sow O., Gning F., Mare T., Adj M. Caractérisation des procédés de dessalement à multiples effets, par approche thermodynamique. Modélisation et simulation. VIIIème Colloque Interuniversitaire Franco Québécois CIFQ 2007, Montréal, 28, 29, 30 Mai 2007.
13. Sow O., Siroux M., Desmet B. Energetic and exergetic optimization of a tripple effect desalination system by distillation with solar contribution // Desalination, 2005. No. 174.
14. Sow O. Analyse thermodynamique d'un système de dessalement par distillation avec apport solaire. Recherche des conditions optimales de fonctionnement en régime variable, Thèse de doctorat, Université de Valenciennes et du Hainaut-Cambrésis, Octobre (2003).
15. Evans R.B., Crelin G.L., Tribus M. Thermoeconomic considerations of seawater demineralization, Ouvrage Chap. 1 // Principles of desalination, part 1, 2nd edition, 1980.
16. Sow O., Desmet B., Mare T., Adj M. Modélisation et simulation en régime dynamique d'un système de dessalement à multiples effets couplés à un capteur solaire plan, VIIième Colloque interuniversitaire Franco-Québécois sur la thermique des systèmes, Saint Malo, du 23-25 Mai 2005.

SIMSPARK PLATFORM EVOLUTION FOR LOW-ENERGY BUILDING SIMULATION

P. Tittelein, E. Wurtz, G. Achard*

LOCIE, Université de Savoie, INES-RDI BP 332; F-73377 Le Bourget du Lac – CEDEX FRANCE
*E-mail: Etienne.Wurtz@univ-savoie.fr

Received: 21 Sept 2007; accepted: 31 Oct 2007

To counter the world's mounting energy demands, the energy efficiency of buildings is a major control lever. Therefore, low energy buildings and passive houses are increasingly in the news. But what does this mean?
Beginning with a simulation platform (SimSpark) based on the solver Spark, we aim to describe the thermo-aeraulic behaviour in buildings. From this platform, we can easily integrate all types of system.
Using the environment's modularity, it is possible to estimate the gain contributed by various types of envelope or by the addition of different systems. We can also determine the interactions that give the most effective associations. In this article, the results of simulations on the effect of counter-flow ventilation on the heating demand and the effect of adding overhangs above windows on the building's thermal behaviour will be presented. We will also present a method to simulate the earth-to-air exchanger.

Keywords: solar buildings, high efficiency building, SimSpark, simulation, earth-to-air exchanger

Pierre Tittelein

Organization(s): University of Savoie, France.
Education: ENS Cachan, Civil engineering (2001-2004), Master wood science and civil engineering Laval University – Canada (2004-2005), PhD Student, Savoie University, France (2005-2007).
Main range of scientific interests: building simulation, wood-cement composite.

Etienne Wurtz

Organizations: Leader of National Solar Energy Institute for CNRS and Savoie University in Chambery; IBPSA-France (building simulation association) president.
Experience: Research director of CNRS, Savoie University (from 2005); assistant professor in La Rochelle University (1996-2005), PhD: Zonal method modelling with different simulation tools (2005).
Projects in development: DYNASIMUL – New modelling concepts (coordinator); Maisonpassives - Passive houses studies (coordinator); ORASOL – State of the art from solar cooling (coordinator); ACTIFEN - New windows concept; GEOBAT – Geothermal studies.
Main range of scientific interests: modelling in oriented object tool, building energetic efficacy, solar cooling, heat and mass transfer, energy storage.
Publications: E. Wurtz, L. Mora, C. Inard, An equation-based simulation environment to investigate fast building simulation, Building and Environment (41): 1571-1583, 2006; E. Wurtz, F. Haghighat, L. Mora, K.C. Mendonca, C. Maalouf, H.Zhao, P. Bourdoukan, An integrated zonal model to predict transient indoor humidity distribution, ASHRAE Transactions (112)2: 175-186, 2006.

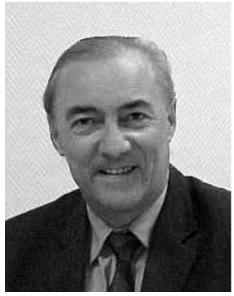

Gilbert Achard

Experience: Professor in the Savoie University (from 1992); assistant professor in Savoie University (1986-1992); assistant professor in INSA Lyon (1979-1986); PhD in INSA Lyon.
Projects in development: Solar energy valorization in buildings, energetic integration in buildings with use of multisources/multifunctions processes; artificial/natural lighting in tertiary buildings; environmental quality in buildings.
Main range of scientific interests: energy in buildings, buildings simulation, global comfort in buildings (hygrothermal, acoustical, visual...), natural lighting in premises, solar thermal energy, low temperature geothermal energy, high efficiency buildings, wood-made constructions acoustical and thermal behaviour, environmental quality of buildings.
Publications: C. Franzetti, G. Fraisse, G. Achard, Influence of the coupling between daylight and artificial lighting on thermal loads in office buildings, Energy and Buildings (36)2: 117-126, 2004;
G. Fraisse, K. Johannes, V. Trillat-Berdal, G. Achard, The use of a heavy internal wall with a ventilated air gap to store solar energy and improve summer comfort in timber frame houses, Energy and Buildings (38)4: 293-302, 2006.

Introduction

In a context of sustainable development, it is becoming necessary to limit energy consumption. As buildings today require a great deal of energy, the notion of the low- and ultra-low-consumption building is coming to the forefront.
In the first section, we will quickly discuss these notions. Then we will see approach used to simulate these buildings with the simulation platform SimSpark by taking two concrete applications to show the possibilities of this environment. We will finally present a new method to simulate the earth-to-air exchanger.

Energy efficiency in buildings

In the energy efficiency of buildings, two performance levels are distinguished. For a heating demand of 30–60 kW·h/(m²·yr), "low-energy" or "low-consumption" construction is used. For an "ultra-low-energy" building (or "ultra-low consumption" or "passive"), a heating demand criterion of 10–15 kW·h/(m²·yr) must be satisfied. In this second type of house, it is no longer necessary to set up a conventional heating system.
The graph below (Fig. 1) helps understand why these two categories are advantageous.

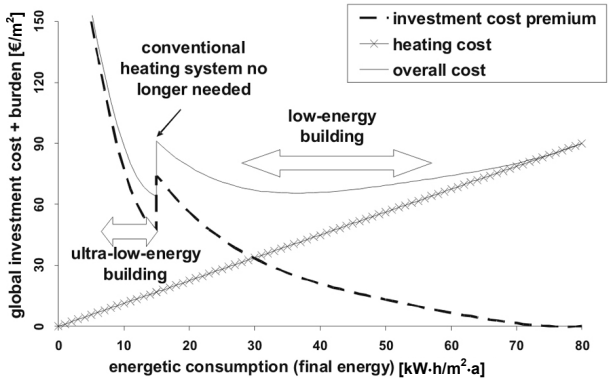

Fig. 1. *Global energy cost in a building [1]*

This graph shows that there are two economic optima: the first one for a consumption of approximately 40 kW·h/(m²·yr) and the second for a consumption of approximately 15 kW·h/(m²·yr). These two optima correspond to low- and ultra-low-energy buildings.
These two types of buildings are certified by two different companies in Europe: Minergie® (Switzerland) and Three Litters House (Germany), which certify low-energy consumption construction. Of the companies offering ultra-low-consumption buildings, the most widely recognized are Minergie-P® (Switzerland) and Passivhaus (Germany).
The maximal heating load required for a 150-m² ultra-low-consumption house is 1500 W, the power of a hairdryer.
According to a CSTB study [2], Germany has approximately 5000 passive houses and 12,000 low-consumption houses today. According to Minergie® [3], Switzerland has a total of 6000 low-consumption houses and 100 ultra-low-consumption houses. In France, there are only a few such homes and no operational ultra-low-energy building label exists at this time.
To describe high energy efficiency building thermo-aeraulic behaviour, simulation is necessary.

Numerical simulation with the platform SimSpark

To simulate building behaviour and use the experimental data, we chose to base our simulation platform, SimSpark [4], on the equation solver, Spark, developed by the Lawrence Berkeley National Laboratory. Spark is a general simulation environment in which a system of equations can be defined and solved by a robust algebro-differential solver according to Sowel et al. [5]. It is an object-oriented equation-based environment.

Description of Spark simulations

The basic object in Spark is the equation, which is shaped in what is called an "atomic class". One equation can communicate with another one with its variables, called ports.
To program in Spark, these equations simply need to be ordered with each other. This requires using another type of object, the "macro-class", in which we call the equations and make them communicate with their variables. "System of equations" objects can also communicate with the other objects through their variables, providing an object hierarchical organization, from the simplest, which represents an equation (for example, the convection equation in a wall) to the most complex system of equations (for example, the complete thermal simulation of a building) by way of intermediate objects (such as objects modelling a wall).
When all the equations are connected through several levels of objects, the system's input and output are identified in a last object called "program".
This procedure allows connecting models at various levels very easily. For example, using their variables, a solar panel model can be combined with a floor heating model that is connected to a model of thermo-aeraulic air transfers of a building combined with models of the walls, providing a model of a building equipped with a direct sun floor.
Like the other object-oriented environments, Spark possesses the property of data encapsulation. This means that the characteristics of an object are localized within it, making it is easy to change a model in a simulation.
In Spark, the equations are not defined in a directed way. When the basic problem is defined, a variable is not an input or an output. Therefore, Spark inverts a model very easily by changing the status of a variable using a keyword in the program file. A variable which resulting from the simulation then becomes an input.

Examples of simulations

The house on which this study is based was built on two full floors. Its net floor area is approximately 100 m. There is 13.5 m² glazing on the south facade (i.e. 28 % of the total surface of the wall), 6.5 m² on the west (18 %) and 3.5 m² on the east side (9 %). The front faces the south. The climatic conditions are those of Chambéry, France.

The wall is composed of mass concrete inside and external insulation to take advantage of thermal inertia (we consider a classical insulation of specific conductivity 0.04 W/(m·°C)).

A nodal method with one node per floor was used for calculation. The thermal transfers in the walls were estimated by discretization of the heat equation by finite difference.

Radiation was calculated using the fictitious domain method. To determine the sun's contributions through the windows, we made a geometrical calculation of the area of the sun task on each window. Then we considered that the flow was distributed throughout the surface of the wall reached by the sun's rays. The value obtained is considered as a direct primary flow in the fictitious domain method.

Both very simple studies were conducted to show that the simulation platform is operational and easily gives results of dynamic simulations for different configurations.

More complex configurations are being developed and will be explained in a later publication.

Comparison of two types of ventilation

This section compares the effect of single-flow ventilation to that of counter-flow ventilation.

Let us note first that the counter-flow heat exchanger is shunted in the summer because of the low temperature gradient between indoor and outside. Consequently, in the summer, both types of ventilation have the same behaviour, which is why the comparison element chosen here is the heating demand [kW·h/(m²·yr)].

For both models, each floor possesses an air inlet, in which the mass flow is fixed, and an air outlet. For air exchange, the volume flow rate is normally 0.5 volume per hour. In the summer, during the night, when the outside temperature is lower than the indoor temperature, overventilation is obtained with a volume flow rate of 3 volumes per hour.

For the single-flow ventilation, the heat flow entering the room by the air inlet is calculated by the equation:

$$\Phi_i = \dot{m} C_p T_{ext}\,, \tag{1}$$

where Φ_i – inlet heat flow [W], $\dot{m}$ – air mass flow [kg/s], C_p – air heat capacity [J/(kg·°C)], T_{ext} – external air temperature [°C].

The heat quantity going out via the air outlet is calculated by:

$$\Phi_0 = \dot{m} C_p T_{ind}\,, \tag{2}$$

where Φ_0 – outlet heat flow [W], T_{ind} – indoor temperature [°C].

Counter-flow ventilation is simulated very simply by evaluating the air-supplied indoor temperature calculated with the efficiency of the exchanger:

$$T_{si} = T_{ext} + \eta(T_{ind} - T_{ext}), \tag{3}$$

where T_{st} – air supplied inside temperature [°C], η – exchanger efficiency [-].

We then calculate the heat flow leaving the room using the same equation as for the single flow (2) and the flow entering using the equation:

$$\Phi_i = \dot{m} C_p T_{si}\,. \tag{4}$$

After several annual simulations with a time step of 30 minutes, we can deduct the following result (insulation thickness varies) (Fig. 2):

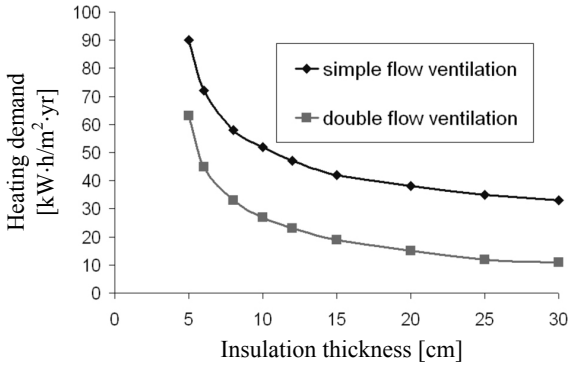

Fig. 2. *Heating demand for two types of ventilation*

On this curve, it should be noted that the difference in heating demand between the house equipped with single-flow ventilation and the one equipped with counter-flow ventilation is constant whatever the thickness of insulation. The value of this difference is approximately 25 kW·h/(m²·yr).

As a result, for a house with 5-cm-thick insulation, the energy savings gained from installing counter-flow ventilation is 30 %, while for a house with 30-cm-thick insulation (order of magnitude for German passive houses), the energy savings is roughly 70 %.

Thus, to obtain high energetic efficiency, counter-flow ventilation is completely warranted.

Passive treatment of summer comfort

In this section, we attempt to determine the effect of window overhangs on summer comfort and their impact on heating demand.

Summer comfort is estimated by the number of hours when the indoor air temperature exceeds 27 °C.

To model these overhangs, a geometrical calculation is made to determine at what height the window receives sunlight (Hfe) (Fig. 3).

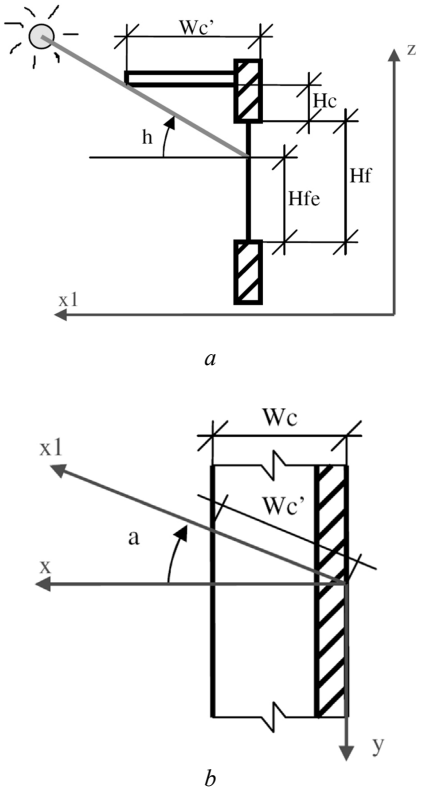

Fig. 3. *View in the solar ray plan of the overhang (a), top view of the overhang (b)*

Here a – directed angle between the normal for the window and the projection of the sunbeam on the ground; h – solar altitude.
Other symbols are explicit geometrical characteristics of the problem.
We can deduce the expression of Hfe:

$$Hfe = \min(Hf, Hf + Hc - W_c \tan h / \cos a) \qquad (5)$$

With this value, the window surface area by which the solar flow enters in the room can be calculated.
Overhangs are placed 60 cm above the south windows and their length is variable.
The results obtained are illustrated in Fig. 4.

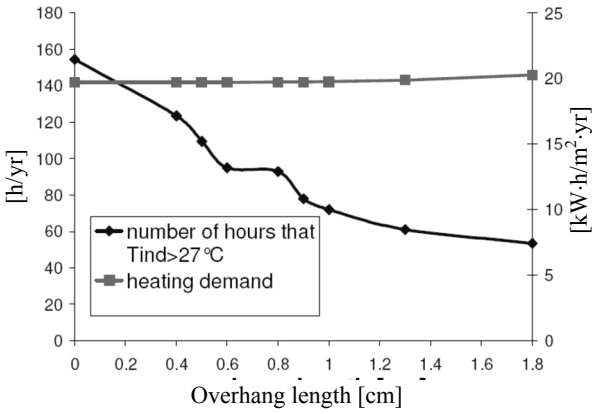

Fig. 4. *Effect of overhang length on heating demand and summer comfort*

According to the results, the number of hours that indoor temperature is over 27 degrees in the house can be divided by two with the south overhangs, without significantly increasing the heating demand.
This type of system is therefore very useful in a high efficiency building. Indeed, the problem of overhangs for classic houses is that between seasons, windows are shaded and energy consumption increases. Here, since heat is no longer needed between seasons, overhangs no longer have negative effect on the heating demand.

Earth-to-air exchanger simulation

The next stage of the simulation concerns systems used in high-efficiency buildings. Our first study concerns the earth-to-air exchanger.
The principle of the earth-to-air exchanger is very simple. Before being blown inside, the renewal air goes into a horizontal buried pipe. During the winter, air is preheated because the ground is warmer than the outside air and during the summer, air is cooled because the inverse phenomenon occurs.
The earth-to-air exchanger (Fig. 5) can be modelled in two different ways. In the first one, the pipe is submitted on its external face to a variable temperature calculated with its depth. The modification of the soil temperature is not considered. In the second one, the interaction between pipe and soil is considered [6]. The first simulation is not very realistic because it does not take into account ground depletion, which is why we chose the second category.
The 3D problem is divided into brackets of thickness: Δx.

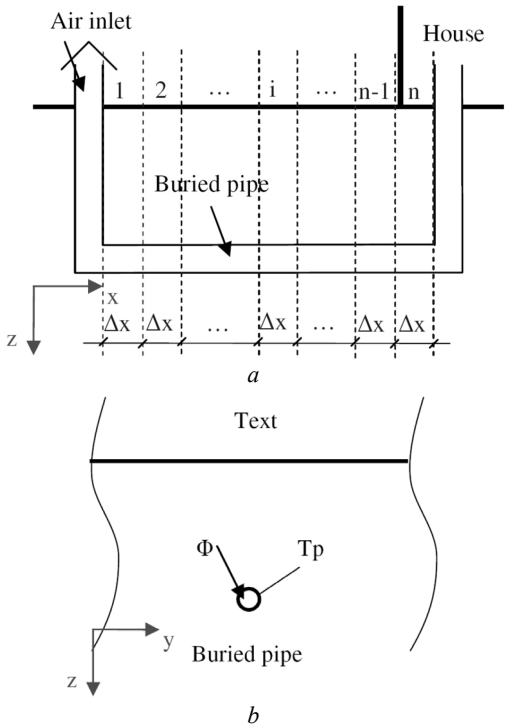

Fig. 5. *Earth-to-air exchanger: a – longitudinal view, b – cross-section view*

For each bracket, a simple power balance is made in the pipe:

$$\dot{m}C_pT_i = \dot{m}C_pT_{i-1} + \Phi\Delta x \qquad (6)$$

where $\dot{m}$ – air flow in the buried pipe, kg/s; C_p – air heat capacity, J/(kg °C); T_i – air temperature in the mesh, °C; Φ – heat flow brought to the pipe; Δx – bracket thickness, m.

To estimate the heat flow brought to the pipe (Φ), the response factor method is used on each bracket.

The problem is broken down assuming that soil is only submitted to two types of load: a temperature variation at the ground surface and a temperature variation of the external face of the buried pipe (linked to the temperature of air in the pipe).

On this 2D structure, the software Comsol will be used to determine the flow Φ (W/m) received by the stream for the following elementary load (Fig. 6):

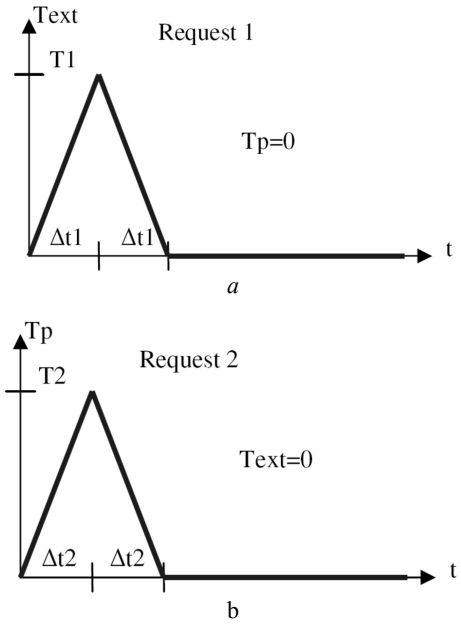

Fig. 6. *Elementary load: a – on the ground surface, b – in the pipe*

Δt_2 is lower than Δt_1 because the physical phenomenon is faster for the request 2.

Then response factors Y and Z are stored in tables to be input into SimSpark. For the first load, the response factor Y, which can be called transmittance, is evaluated by the expression:

$$Y = \Phi/T_1 \qquad (7)$$

For the second load, the response factor Z, which can be called admittance, is evaluated by the expression:

$$Z = \Phi/T_2 \qquad (8)$$

In order to determine the real heat flow received by the earth-to-air exchanger, both real loads must be broken down by superimposing elementary loads (Fig. 7).

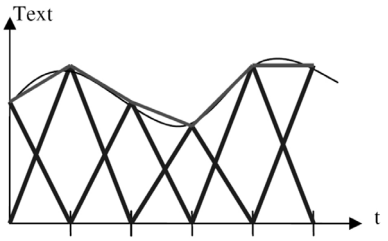

Fig. 7. *Breakdown of real load into elementary loads*

Then the superposition theorem can be applied and the heat flow received by the pipe can be deduced for each time step:

$$\Phi(t) = \sum_{i=i}^{\infty} Y_i T_{ext}\left(t - i\Delta T_1\right) + \sum_{j=i}^{\infty} Z_j T_{ext}\left(t - j\Delta T_2\right). \qquad (9)$$

With this expression, the temperature throughout the pipe can be estimated and the pipe air outlet temperature can be determined. The earth-to-air exchanger can be directly combined with the house's ventilation system (counter or single flow) to study the interactions. This simulation is in progress.

Conclusion

Finally, we have seen that it was possible to simulate the thermo-aeraulic behaviour of high-energy efficiency buildings with the simulation platform SimSpark.

Its modularity allows this platform to compare various types of systems easily, as well as various types of envelopes.

We showed that counter-flow ventilation is indispensable to obtain high energy efficiency; in that case, the heating demand is divided by 3 with regard to single-flow ventilation.

We also showed that adding overhangs above south windows greatly improves indoor comfort in summer without damaging the heating demand.

Finally a new method that will be integrated into SimSpark to treat the case of the earth-to-air exchanger has been discussed.

References

1. Passivhaus. Official site of Passivhaus. http:// www.passiv.de/

2. CSTB. Comparaison internationale bâtiment et énergie, intermediate report. Programme de Recherche et d'Expérimentation sur l'Énergie dans le Bâtiment. 2006.

3. Minergie ®. Official site of Minergie ®. http://www.minergie.ch/

4. Mora L. Prédiction des performances thermo-aérauliques des bâtiments par association de modèles de différents niveaux de finesse au sein d'un environnement orienté objet. Doctoral thesis. 2003.

5. Sowell E.F., Haves P. Efficient solution strategies for building energy system simulation // Energy and Buildings. 2001. No. 33(4). P. 309–317.

6. Hollmuller P. Utilisation des échangeurs air/sol pour le chauffage et le rafraîchissement des bâtiments. Doctoral thesis. 2002.

COUPLED HEAT TRANSFERS THROUGH BUILDING ROOFS FORMED BY HOLLOW CONCRETE BLOCKS

T. Ait-Taleb, A. Abdelbaki, Z. Zrikem

LMFE, Department of Physics
Cadi Ayyad University
Faculty of Sciences Semlalia, BP 2390, Marrakesh, Morocco
Tel.: +212-24-43-46-49 (post 489); Fax: +212-24-43-74-10
E-mail: zrikem@gmail.com, abdelbaki@ucam.ac.ma

Received: 23 Sept 2007; accepted: 31 Oct 2007

The aim of this work is to study numerically the coupled heat transfers by conduction, natural convection and radiation through building roofs constructed by hollow concrete blocks. Heat transfer is assumed to be two-dimensional and the fluid flow in the different air cells of the system under investigation is laminar. Equations governing heat transfer are discretized using the control volumes approach and are solved by the SIMPLE algorithm. Streamlines, isotherms and overall heat fluxes are presented for building roofs heated from below and formed by different types of hollow concrete blocks. Analysis of results obtained for different numbers of air cells in the horizontal direction shows that the study of the entire system can be reduced, with a very good approximation, to the study of a single hollow concrete block. This permits a very important reduction of the computational time.

Keywords: building roof, hollow concrete blocks, conduction, convection, radiation, numerical simulation

T. Ait-Taleb

Doctorat student at the Cadi Ayyad University, Faculty of Sciences Semlalia, Department of Physics, Fluid Mechanics and Energetics Laboratory, Marrakech, Morocco. He received the Licence (1997) and the DESA (2001) in physics from Cadi Ayyad University, Faculty of Sciences Semlalia, Marrakech, Morocco. It's research field is the study of coupled heat transfer by natural convection, conduction and radiation in building elements and the development of the heat transfer functions for these elements. About ten papers in international scientific journals and congresses was published.

A. Abdelbaki

Professor at the Cadi Ayyad University, Faculty of Sciences Semlalia, Department of Physics, Fluid Mechanics and Energetics Laboratory, Marrakech, Morocco. He received the DES (1993) and the Doctorat d'Etat (2000) in physics from the Cadi Ayyad University, Faculty of Sciences Semlalia, Marrakech, Morocco. The main range of scientific interests are the study of the coupled heat transfer by natural convection, conduction and radiation in different configurations; the heat transfer between soil and buildings, solar systems, the development of the heat transfer functions for the building elements. About seventy papers in international scientific journals and congresses was published.

Z. Zrikem

Professor at the Cadi Ayyad University, Faculty of Sciences Semlalia, Department of Physics, Fluid Mechanics and Energetic Laboratory, Marrakech, Morocco. He is Engineer (1981) in Mechanical Engineering from Ecole Mohammadia d'Ingénieurs, Rabat, Morocco and he received the Ph.D. (1988) in Mechanical Engineering from Ecole Polytechnique, Montreal, Canada. The main range of scientific interests are the study of the coupled heat transfer by natural convection, conduction and radiation in different configurations; the heat transfer between soil and buildings, solar systems, the development of the heat transfer functions for the building elements. About a hundred of papers in international scientific journals and congresses was published.

Introduction

Hollow concrete blocks are often used in the construction of building roofs. In general, each hollow block is formed by three cavities surrounded by solid concrete partitions. Thus, the heat transfer within such structures is done simultaneously by conduction in the solid partitions, natural convection inside the cavities and radiation between the internal faces of these cavities. Furthermore, the three heat transfer processes are intimately bound. Therefore, the fine study of the thermal behavior of the hollow blocks needs a simultaneous solving of the complex and sometimes non linear equations modeling the different thermal transfer mechanisms.

The coupling problem between the three modes of heat transfer was the subject of numerous investigations. The bibliographic studies presented in the works [1-6] show that the most of these investigations are generally limited to simple configurations constituted by rectangular cavities with one or several conducting walls and were especially has been interested to the study of the effects of conduction and/or radiation on natural convection in the cavities.

The coupled heat transfers in vertical alveolar building envelopes formed by hollow clay tiles have been studied by Abdelbaki and Zrikem [5]. Based on a detailed simulation model, the authors determined characteristic coefficients that permit fast and accurate estimation of heat exchanges through the alveolar walls without solving the complex coupled equations governing the different thermal mechanisms [6]. These characteristic coefficients are the overall heat exchange coefficients in the steady state regime and the transfer function coefficients in time varying regime.

Recently, the previous studies are extended to the case of hollow concrete blocks used in the construction of building roofs by Ait-Taleb et al. [7, 8]. In this case, the considered alveolar structures are horizontal but are subjected to a vertical gradient temperature. The two situations of heating have been considered: heating from below and from above.

In the practice, a building roof having, for example, 4 meters length contains about 8 units of hollow blocks. In construction, the hollow blocks are placed in such a way that each hollow blocks possesses 3 cavities (Nx = 3) in the horizontal direction separated by supporting girders. Therefore, the total number of alveolar in the considered building roof is about 24 cavities in the horizontal direction (Nx = 24). Consequently, the simulation of the global system requires an important computational time. Then, it is more interesting to reduce the size of the system under investigation. However, this reduction is only efficient if its influence on the global thermal behavior of the system is limited.

To examine this solution, this paper presents a numerical study of the vertical coupled heat transfers by conduction, convection and radiation through horizontal hollow structures that differ by the alveolar number (Nx) in the horizontal direction and by the aspect ratio of the internal cells.

Mathematical formulation

The studied alveolar system is sketched in Fig. 1 and is formed by a range of Nx rectangular cavities of width l and height h surrounded by vertical solid partitions of thickness ex_i ($1 \le i \le Nx + 1$) and horizontal partitions of thickness ey_j ($1 \le j \le 2$). The top and bottom sides of the hollow structure are considered isothermal and are maintained at constant temperatures T_0 and T_i respectively. The structure vertical sides are considered adiabatic or submitted to periodicity conditions.

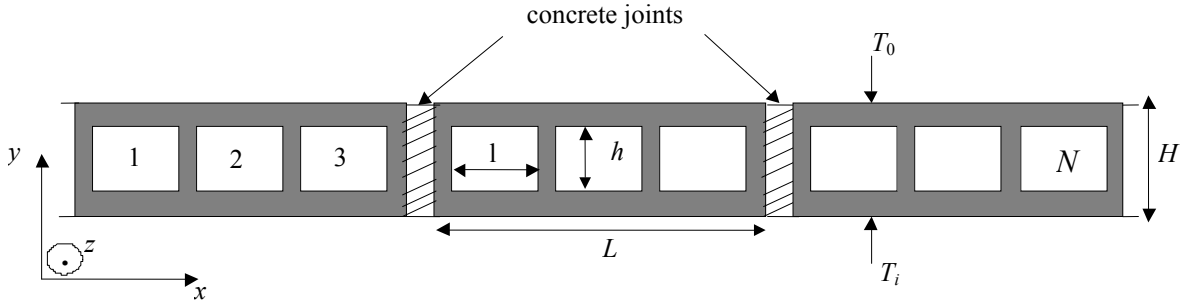

Fig. 1. *Schematic diagram of disposition of hollow blocks in building roofs*

In formulating governing equations, the fluid motion and the heat transfer are considered two-dimensional and the fluid flow is laminar. The solid and fluid properties are assumed to be constant except for the density in the buoyancy term where the Boussinesq approximation is utilized. Viscous heat dissipation in the fluid is neglected. The fluid is assumed to be non-participating to radiation and the inside surfaces of all cavities are considered diffuse-grey. The governing equations are written in dimensionless form as:

$$\frac{\partial U}{\partial X} + \frac{\partial V}{\partial Y} = 0 \quad (1)$$

$$\frac{\partial U}{\partial \tau} + U\frac{\partial U}{\partial X} + V\frac{\partial U}{\partial Y} = -\frac{\partial P}{\partial X} + Pr\left(\frac{\partial^2 U}{\partial X^2} + \frac{\partial^2 U}{\partial Y^2}\right) \quad (2)$$

$$\frac{\partial V}{\partial \tau} + U\frac{\partial V}{\partial X} + V\frac{\partial V}{\partial Y} = -\frac{\partial P}{\partial Y} + Pr\left(\frac{\partial^2 V}{\partial X^2} + \frac{\partial^2 V}{\partial Y^2}\right) + RaPr\theta_f \quad (3)$$

$$\frac{\partial \theta_f}{\partial \tau} + U\frac{\partial \theta_f}{\partial X} + V\frac{\partial \theta_f}{\partial Y} = \frac{\partial^2 \theta_f}{\partial X^2} + \frac{\partial^2 \theta_f}{\partial Y^2}, \quad (4)$$

where U and V are the dimensionless velocity components in X and Y directions respectively, P is the pressure, θ_f is the fluid temperature, Pr is the Prandtl number and Ra is the Rayleigh number given by: $Ra = \frac{g\beta H^3 \Delta T}{\nu^2} Pr$, $Pr = \frac{\nu}{\alpha_f}$, where ν and α_f are respectively the fluid kinematic viscosity and the thermal diffusivity.

The dimensionless equation of heat conduction in the solid walls is:

$$\frac{\alpha_f}{\alpha_s}\frac{\partial \theta_s}{\partial \tau} = \frac{\partial^2 \theta_s}{\partial X^2} + \frac{\partial^2 \theta_s}{\partial Y^2}, \quad (5)$$

where α_s is the solid thermal diffusivity and θ_s is the dimensionless solid temperature. The boundary conditions of the problem are:

* $U = V = 0$ on the inner sides of each cavity.
* $\theta_s(X,0) = 1$ and $\theta_s(X,1) = 0$ $(0 \leq X \leq L/H)$
* $\begin{cases} \theta_s(0,Y) = \theta_s(L/H,Y) \ (0 \leq Y \leq 1) \text{ for the periodicity condition} \\ \left(\frac{\partial \theta_s}{\partial X}\right)_{X=0;L/H} = 0 \ (0 \leq Y \leq 1) \text{ for the adiabaticity condition} \end{cases}$

The continuity of the temperature and the heat flux at the fluid-wall interfaces gives:

$$\theta_s(X,Y) = \theta_f(X,Y), \quad (6)$$

$$-\frac{\partial \theta_s}{\partial \eta} = -N_k \frac{\partial \theta_f}{\partial \eta} + N_r Q_r, \quad (7)$$

where η represents the dimensionless coordinate normal to the wall, N_k is the thermal conductivity ratio K_f/K_s, Q_r is the dimensionless radiative heat flux and N_r is the dimensionless radiation to conduction parameter defined by:

$$N_r = \frac{\sigma T_0^4 H}{k_s \Delta T}.$$

The dimensionless radiative heat flux Q_r is related to the radiative heat flux q_r by:

$$Q_r = \frac{q_r}{\sigma T_0^4}.$$

The net radiative heat flux $q_{r,k}(r_k)$ exchanged by the finite area dS_k, located at a position r_k on the surface k, is given by:

$$q_{r,k}(r_k) = J_k(r_k) - E_k(r_k), \quad (8)$$

where $J_k(r_k)$ is the radiosity and $E_k(r_k)$ is the incident radiative heat flux on the surface dS_k given respectively by:

$$J_k(r_k) = \varepsilon_k \sigma (T_k(r_k))^4 + (1-\varepsilon_k) E_k(r_k), \quad (9)$$

$$E_k(r_k) = \sum_{j=1}^{4} \int_{A_j} J_j(r_j) dF_{dS_k - dS_j(r_k, r_j)}, \quad (10)$$

where ε_k is the emissivity of the surface k and $dF_{dS_k - dS_j}$ is the view factor between the finite surfaces dS_k and dS_j located at r_k and r_j respectively. Taking into account equations (8) to (10), the dimensionless radiative heat flux can be expressed as:

$$Q_{r,k}(r'_k) = \varepsilon_k \left(\left| 1 - \frac{1}{G} \right| \theta_k(r'_k) + \frac{1}{G} \right)^4 - \varepsilon_k \sum_{j=1}^{4} \int_{S_j} J'_j(r'_j) dF_{dS_k - dS_j}, \quad (11)$$

where G is the temperature ratio T_0/T_i, $J'_j(r_j)$ is the dimensionless radiosity at the position r_j on surface j. By dividing the walls into finite isothermal surfaces, equation (11) leads to a set of linear equation where the unknowns are the dimensionless radiosities $J'_j(r_j)$.

The dimensionless average heat flux across the structure is given by:

$$Q_a = -\frac{H}{L} \int_0^{L/H} \left. \frac{\partial \theta_s}{\partial Y} \right|_{Y=0} dX = -\frac{H}{L} \int_0^{L/H} \left. \frac{\partial \theta_s}{\partial Y} \right|_{Y=1} dX. \quad (12)$$

The previous equations are discretized using the finites differences method based on the control volumes approach with a power law scheme and are solved by the SIMPLE algorithm. The resulting system of algebraic equations is solved by the Tri-Diagonal-Matrix-Algorithm. To accelerate the convergence of solutions, the governing equations are solved in their instationary form. The numerical code has been validated by comparing its results with those reported in reliable works in literature [4]. To realize a compromise between accuracy and computation time, a study on the effects of both grid spacing and time step on the simulation results has been conducted. It was found that a no uniform grid size of 185×20 is sufficient to model accurately the heat transfer and fluid flow inside the hollow block. The dimensionless time used is 10^{-4}. The convergence criterion is 10^{-4}.

Results and discussion

Results presented in this study (Table 1) are obtained for the hollow blocks mostly used in Morocco which are made in light concrete and characterized by a thermal conductivity K_s = 0.5 W/m·K and emissivity ε = 0.9. The geometrical parameters for the different hollow blocks considered are given in table 1 where l is the length and h is the height of the internal cavities, A_c is the aspect ratio of these cavities ($A_c = h/l$), e_x and e_y are respectively the thickness of the vertical and horizontal solid partitions. The Prandtl number is Pr = 0.71. The temperature difference ΔT = (T_0 − T_i) values vary between 1 °C and 30 °C in accordance with the practical conditions.

Table 1
Geometrical dimensions of the different studied hollow blocks

Aspect ratio	l (m)	h (m)	e_x (m)	e_y (m)	$A_c = h/l$
$A_c = A_{c1} \approx 1/4$	0.13	0.035	0.025	0.02	0.26
$A_c = A_{c2} \approx 1/2$	0.13	0.07	0.025	0.02	0.53
$A_c = A_{c3} \approx 1$	0.13	0.1	0.025	0.02	0.77

Streamlines and isotherms

Fig. 2 presents the streamlines contours and the isotherms obtained for $N_x = 12$, $\Delta T = 20$ °C, $G = 1.035$ and for the two considered types of hollow blocks characterized by $A_c \approx 1/2$ and $A_c \approx 1$. The other dimensionless parameters corresponding to these data are $Ra_H = 2.5 \cdot 10^6$ and $Nr = 5.850$ for $A_c \approx 1/2$, $Ra_H = 5.169 \cdot 10^6$ and $Nr = 4.596$ for $A_c \approx 1$. It should be mentioned that the effective Rayleigh numbers in the different internal cavities are $Ra_h = 5.13 \cdot 10^5$ for $A_c \approx 1/2$ and $Ra_h = 1.53 \cdot 10^6$ for $A_c \approx 1$ in such way the air flow remains laminar. Results of the Fig. 2 show that the flow structures and the temperature fields in the different cells of the same building roof are practically similar. Indeed, it is shown a nearly repetitivity of the flow structures and the temperature profiles in the different hollow blocks. It can be seen also that, the flow nature and temperature distribution are significantly affected by the aspect ratio of the alveolar. In fact, natural convection in the hollow block of aspect ratio $A_c \approx 1/2$ is characterized by the formation of two adjacent cells circulating in opposite directions and symmetrical with respect the central vertical axis of the cavity. However, for the same temperature difference, the flow structure in the hollow block of aspect ratio $A_c \approx 1$, is characterized by a single cell. The concentration of the isotherms near the superior horizontal surfaces of the alveolar indicates an important gradient of temperature in these regions. This is due essentially to the motion of the fluid going up following the alveolar vertical axis. Toward the central and low parts of the cavities, the heat transfer is less important but has a very marked two dimensional character.

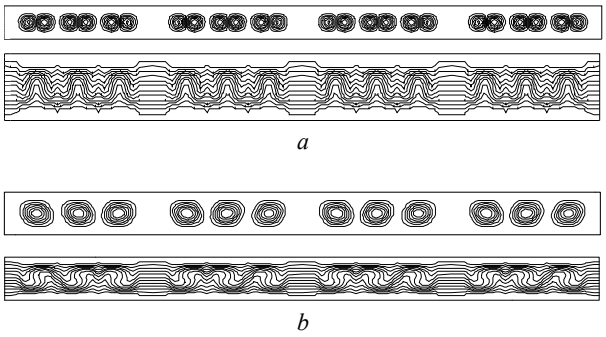

a

b

Fig. 2. *Streamlines (at the top) and isotherms (at the bottom) obtained for ΔT = 20 °C and for the aspect ratios: (a) $A_c \approx 1/2$; (b) $A_c \approx 1$*

As expected, in the solid partitions separating the hollow blocks (concrete joints). the stratification of the isotherms indicates the linear character of the conductive heat transfer through these partitions.

Heat transfer

In order to show the effect of the alveolar number Nx on the global heat transfer through the system, Fig. 3 presents the variation of the dimensional heat flux Q (W/m^2) crossing the structure as a function of the temperature difference ΔT for $A_c \approx 1/2$ and different values of Nx. The heat fluxes obtained for $Nx = 3$, 6, 9 and 12 by applying adiabatic boundary condition imposed on the vertical limits of the system (building floor) are compared to those calculated for $Nx = 3$ using the periodicity condition at the system vertical limits. Fig. 3 shows that the results obtained in the five considered situations are in very good agreement. Indeed, the observed difference on heat fluxes calculated for different values of ΔT and Nx are lower than 0,5 %. This result confirms the observations made in the previous paragraph when the analysis of the structures flow and the temperature fields has indicated a repetitively physical phenomenon in the different hollow blocks of the same building roofs.

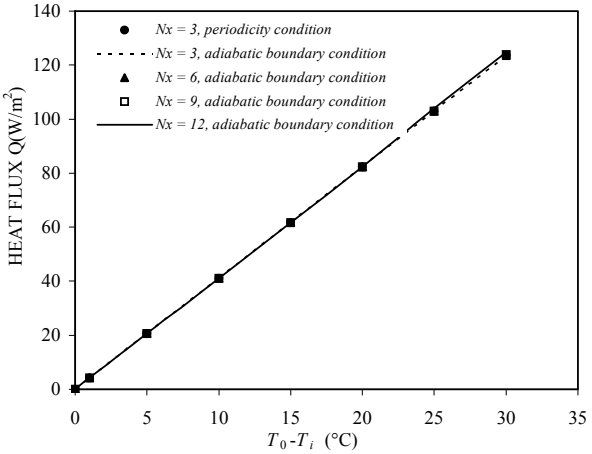

Fig. 3. *Effects of both alveolar number in the horizontal direction Nx and boundary conditions on the average heat transfer through the hollow block of aspect ratio $A_c \approx 1/2$*

The results established above are observed also for other alveolar aspect ratios. In fact, Fig. 4 presents the variations of the mean vertical heat flux Q (W/m^2) as a function of the temperature difference ΔT (°C) between the horizontal surfaces for $A_c \approx 1/4$, $A_c \approx 1/2$ and $A_c \approx 1$. This figure gives the results obtained for different values of Nx. It can be noted that, for each type of hollow block, the heat fluxes simulated in the different considered cases ($Nx = 3$, 6, 9 and 12) are in very good agreement. The maximal relative difference between the results obtained for the different values of Nx is lower than 0,7 %. Therefore the study of the entire system formed by Nx alveolar can be reduced with a very good approximation to that of hollow block with three alveolar

(*Nx* = 3). This approximation permits significant reduction in computational time especially in transient conditions where the latter becomes extremely high.

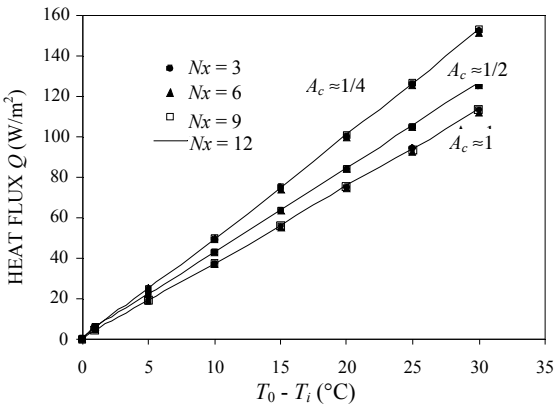

Fig. 4. *Variations of the global heat flux as function of the temperature differences ΔT for the three types of hollow blocks of aspect ratios $A_c \approx 1/4$; $A_c \approx 1/2$; $A_c \approx 1/4$ and different values of Nx*

Conclusion

The simulation results showed that the flow structures and the thermal behaviors in the different hollow blocks of a alveolar building roof are similar. For the different types of hollow block considered, the average heat flux crossing roofs that differ by the alveolar number *Nx* in the horizontal direction are practically the same. Therefore, the numerical simulation of the thermal behavior of the building roof can be reduced with a very good approximation to that of hollow block with three cells in the horizontal direction. This permits a considerable reduction of the computation time, especially in transient conditions where the latter becomes extremely important.

References

1. Kim D.M., Viskanta R. Study of the effects of wall conductance on natural convection in differentially oriented square cavities // J. Fluid Mech. 1984, Vol. 144. P.153-176.
2. Balaji C., Venkateshan S.P. Interaction of surface radiation with free convection in a square cavity // Int. J. Heat Fluid Flow. 1993, Vol. 14, P. 260-267.
3. Akiyama M., Chong O.P., Numerical analysis of natural convection with surface radiation in a square enclosure// Numer. Heat Transfer. 1997, Vol. 31, Part. A, P. 419-433.
4. Ramesh N., Venkateshan S.P., Effect of surface radiation on natural convection in a square enclosure // J. Thermophys. Heat Transfer. 1999, Vol. 13, P. 299-301.
5. Abdelbaki A., and Zrikem Z., Simulation numérique des transferts thermiques couplés à travers les parois alvéolaires des bâtiments // Int. J. Therm. Sci. 1999. Vol. 38, P. 719-730.
6. Abdelbaki A., Zrikem Z., Haghighat F., Identification of empirical transfer function coefficients for a hollow tile based on detailed models of coupled heat transfers // Building and Environment. 2001, Vol. 36, P. 139-148.
7. Ait-Taleb T., Abdelbaki A., and Zrikem Z., Etude numérique de l'interaction entre les transferts thermiques conductifs, convectifs et radiatifs dans une structure alvéolaire chauffée par le bas // Phys. and Chem. News, 2006, Vol. 30, P. 20-24.
8. Ait-Taleb T., Abdelbaki A., and Zrikem Z., Numerical simulation of coupled heat transfers by conduction, natural convection and radiation in hollow structures heated from below or above // Int. J. Therm. Sci. In press.

ELECTROCHEMICAL DESTRUCTION OF METHIDATHION BY ANODIC OXIDATION USING A BORON-DOPED DIAMOND ELECTRODE

F. Hachami*, R. Salghi**, M. Mihit*, L. Bazzi*, K. Serrano, A. Hormatallah****, M. Hilali****

*Faculté des Sciences d'Agadir, Laboratoire Environnement & Matériaux, Equipe de Chimie Physique Appliquées, BP 8106, 80000 Agadir, Morocco. Telephone 00 212 28 09 57 Fax 00 212 28 22 01 00
E-mail: lahcen_bazzi@yahoo.fr

**Ecole National des Sciences Appliquées d'Agadir, Laboratoire d'Ingénierie des Procédés de l'Energie & de l'Environnement, BP 1136, 80000 Agadir, Morocco. Telephone: 00 212 28 22 83 13 Fax: 00 212 28 23 20 07
E-mail: salghi@ensa-agadir.ac.ma

***Université Paul Sabatier, Faculté des Sciences, Laboratoire de Génie Chimique UMR 5503, 118 route de Narbonne, 31062 Toulouse cedex 04, France. Telephone: 00 33 5 61 55 86 77 Fax: 00 33 5 61 55 61 39
E-mail: serrano@chimie.ups-tlse.fr

****Institut Agronomique et Vétérinaire Hassan II, Complexe Horticole d'Agadir, Laboratoire des Pesticides, BP 18/S, Agadir. Telephone: (212)28-240155/241006 Fax: (212)48-242243 Maroc
E-mail: ahormatallah@yahoo.fr

****Author for correspondence, Pr. R. Salghi**
Ecole National des Sciences Appliquées d'Agadir, BP 1136, Agadir, Morocco.
Telephone: 00 212 28 22 83 13 Fax: 00 212 28 23 20 07 E-mail salghi@ensa-agadir.ac.ma

Received: 2 Aug 2007; accepted: 30 Aug 2007

The degradation of insecticide methidathion (organophosphorous pesticide) in aqueous medium has been studied by anodic oxidation using a boron-doped diamond (BDD) anode. The results obtained show that the application of electrolysis of pesticide allows to reduce the chemical oxygen demand (COD). For 2 % NaCl and 3 % NaCl solutions the achieved reduction was 85 % and 72 % respectively. In all cases, the pH of electrolysis was significantly reduced after 45 min. The COD of methidathion solution was observed to fall with pseudo first-order kinetics. An increasing of applied current leads to an increase of the rate of electrochemical oxidation process. The effect of temperature shows that for 25 °C and 65 °C the achieved reduction was 85 % and 66 % respectively. The activation energy indicates that the process of electrochemical degradation is a complex one.

Keywords: ecology of water resources, electrochemical oxidation, pesticide, methidathion, ecology

Fatima Hachami

Organization: Faculty of Science, Agadir, Morocco.
She is doctorant.
She is working on the electrochemical degradation of pesticide.

Rachid Salghi

Organization: Ecole Nationale des Sciences Appliquées of Agadir. He was awarded a PhD degree in Corrosion field in 1999. He is lecturer professor, his researcher is in the Laboratoire d'Ingénierie des procédés de l'Energie et de l'environnement (LIPEE). He is expert in the pesticide field.
Education: Ecole Nationale des Sciences Appliquées Agadir, Diplome d'habilitation (2005), Université Mohamed Premier, Faculté des Sciences d'Oujda, Ph.D. degree in Chemistry Sciences (1997-1999). Université Mohamed Premier, Faculté des Sciences d'Oujda, Diplôme d'Etude Supérieures in Chemistry Sciences (1994-1997).
Experience: Ecole Nationale des Sciences Appliquées d'Agadir, Lecturer professor (2005 – to date). Ecole Superieure de Technologie d'Agadir, Asistant professor (2001-2005). Ministère de l'Agriculture, Etablissement Autonome de Contrôle et de Coordination des Exportations; Chef of laboratory (2000–2001). Ministère de l'Agriculture, Etablissement Autonome de Contrôle et de Coordination des Exportations; Responsible of laboratory (1997–2000).
Main range of scientific interests: The research interest covers as well corrosion inhibition of aluminium, lead, tin and tinplate in industrial water by oxoanions, tetrazole, pyrazole and aminoacid and ester compounds as pesticide degradation in water, soil, fruits and vegetables.
Publications: More than 30 papers in corrosion and pesticide.

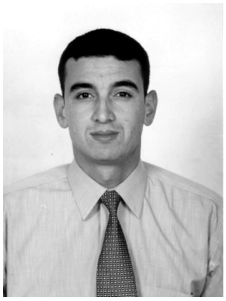

Mohammed Mihit

Organization: Faculty of Science, Agadir, Morocco.
He was awarded a PhD degree in Corrosion field in 2006.
Main range of scientific interests: corrosion and the inhibition of the corrosion of copper and its alloys by organics and inorganics compounds.
Publications: More than 10 papers in corrosion.

Lahcen Bazzi

Organization: Faculty of Science, Agadir, Morocco. He was awarded a PhD degree in Corrosion Science in 1995. He is currently a teacher and researcher in the Laboratory of Materials & Environment.
Education: University Ibn Zohr, Faculty of Science, PhD degree in corrosion (1995). Ecole Normale Supérieure Rabat, Doctorat (DES), 1987.
Experience: University Ibn Zohr, Faculty of Science, Agadir, Professor B (2003 − to date).
University Ibn Zohr, Faculty of Science, Agadir, Professor A (2000-2003).
University Ibn Zohr, Faculty of Science, Agadir, lecturer Professor (1995-1999).
University Ibn Zohr, Faculty of Science, Agadir, Assistant Professor (1988-1994).
Main range of scientific interests: The research interest covers corrosion inhibition of aluminium, tin and tinplate in industrial water by oxoanions, tetrazole, pyrazole and aminoacid and ester compounds. Additionally, he works on pesticide degradation in water, soil, fruits and vegetables.
Publications: More than 40 papers in corrosion and sensors fields.

Karine Groenen-Serrano

Karine Groenen-Serrano was born in 1969 in France.
Education: She was awarded a PhD degree in Electrochemistry 1998.
Organization: She is currently a teacher and researcher at Faculté des Sciences de l'Université Paul Sabatier de Toulouse in France.

Abderrahim Hormatallah

Hormatallah Abderrahim was born in 1957 in Khouribga, Morocco.
Education: He was awarded a PhD degree in Pesticides Science at 1996.
Organization: He is currently a teacher and researcher at Institute Agronomique et Vétérinaire Hassan II, Agadir, Morocco. He is currently the Head of Pesticide Management and Pesticide residues Analysis Laboratory.
Main range of scientific interests: All aspects of behavior of pesticides in soil, plant and water (residues; persistence…), pesticide management and monitoring programs, quality control of food, traceability in food production, implementation of good agricultural practice in field systems, packaging houses design and hygiene.
Publications: Approximately 24 scientific publications and review articles.

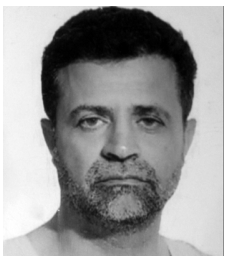

Mustapha Hilali

Prof. Mustapha Hilali was born in 1959 in Ksar El Kebir, Morocco.
Education: He was awarded a PhD degree in Theoretical Chemistry in 1992.
Organization: He is currently a professor in the Faculty of Science, University Ibn Zohr and researcher in the Laboratory of Materials & Environment.

Introduction

The disposal of pesticides can cause serious problems due to the chemical nature of the active ingredients in pesticide formulation and due to the large quantities of the unwanted products. These products undergo physical and chemical alterations either due to extended storage, beyond the recommended expiry date, or storage under improper conditions (high humidity and temperature). In many countries, large quantities of pesticides have accumulated since they have lost their desirable characteristics. Pesticides that have passed their self-life

can be included in this category. Although, these products are not suitable for use, they still contain toxic compounds. In addition, many surplus pesticides, still within their expiration limits, may become useless, when their future use is prohibited due to toxicological or environmental concerns [1].

Recently, there has been increased interest in the use of electrochemical method for wastewater treatment. Electrochemical methods have been successfully applied to the purification of wastewaters containing phenolic substances [2], cyanides [3], refractory organic pollutants [4], olive oil production units [5], wastewaters generated in textilemanufacture [6] and tanneries [7].

The recent use of a boron-doped diamond (BDD) thin film anode [8-12] in anodic oxidation has shown that its O_2 overvoltage is much higher than that of conventional anodes such as PbO_2, doped SnO_2, IrO_2 and Pt, then producing larger amounts of adsorbed OH• by reaction

$$Cl_2 + H_2O \Leftrightarrow HClO + H^+ + Cl^- \qquad (1)$$

giving a more rapid destruction of pollutants. Anodic oxidation with BDD then seems a suitable procedure to mineralize organics, as found for $HClO_4$ aqueous solutions containing carboxylic acids such as acetic, malic, formic and oxalic [8], 4-chlorophenol [9], phenol [10], and benzoic acid [11], as well as for malic acid at pH 2.7 and ethylendiaminitetraacetic acid at pH 9.2 [12].

The objective of this work is to investigate the electrochemical degradation of methidathion, in aqueous solution using a boron-doped diamond electrode (BDD).

Materials and methods

Boron-doped diamond films, Diachem®, were synthesized by the hot filament chemical vapor deposition technique (HF CVD) on conducting p-Si substrate (0.1Ω cm, Siltronix).The filament temperature ranged from 2440 to 2560 °C and the substrate one was kept at 830 °C. The reactive gas used was methane in an excess of dihydrogen (1 % CH_4 in H_2). The doping gas was trimethylboron with a concentration of 3 ppm. The gas mixture was supplied to the reaction chamber, providing a 0.24 μm·h^{-1} growth rate for the diamond layer. The diamond films were about 1μm thick. This HF CVD process produces columnar, randomly textured, polycrystalline films.

Electrochemical measurements using a computer controlled by Potentiostat/Galvanostat model PGP 201 associated to "Volta-Master1" software. A conventional three electrodes cell (100 cm^3) was used thermoregulated glass cell (Tacussel Standard CEC/TH). Saturated calomel electrode (SCE) and platinum electrode are used as reference and Auxiliary electrodes, respectively. Diamond was used as working electrode (1 cm^2 Methidathion [O,O-dimethylS-(5-methoxy-1,3,4-Thiadiazoliny-l-3-methyl) dithiophos-phate] (Fig. 1) is a widely used organophosphorous insecticide, was chosen as the target molecule for the present study because of chemical toxicity (the acute oral LD_{50}, for rats is approximately 54 mg/kg [13]).

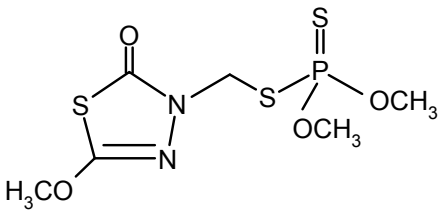

Fig. 1. *Structural formula of methidathion*

Galvanostatic electrolysis ware carried out with a volume of 75 cm^3 aqueous solution of methidathion 1.4 mM·L^{-1} during 120 minutes. The range of applied current density was 20 to 60 mA/cm^2 and samples were taken, at predetermined intervals during the experiment, and submitted for analysis. All tests have been performed at different temperature in magnetically stirred and aerated solutions. In all cases sodium chloride was added to the electrolytic cell, at different concentrations.

To characterize the toxicity removal, the global parameter, the chemical oxygen demand (COD) is measured according to the standard methods for examination of water and wastewater [14]. All measurements were repeated in triplicate and all results were observed to be repeatable within a 5 % margin of experimental error.

The commercial formulation Methidaxide (40 % methidation) was purchased from Bayer. The chemical sodium chloride used was of analytical-reagent grade and was obtained from Aldrich.

Results and discussions

Effect of chloride concentration

The Fig. 2 shows the effect of chloride ion concentration on the destruction of methidathion, carried out at 60 mA/cm^2.

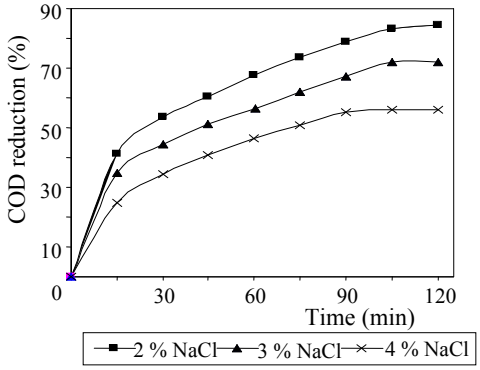

Fig. 2. *The chemical oxygen demand (COD) reduction (in %) for methidathion 1.4 mM/L solution for 120 min of electrolysis at 60 mA and 25 °C*

We observed that the application of electrolysis in this pesticide have the ability to reduce considerably the COD. For example, for 2 % mass NaCl and 3 % NaCl the achieved reduction was 85 % and 72 % respectively, while for 4 % NaCl was 56 %.

The mechanism of electrochemical mineralization can be direct, in this case there is oxidation of methidathion on the electrode or indirect via some mediators like chlorinated species or other radicals [15-16].
Since some oxidant compounds that are produced during oxidation of water (like O_2, O_3 or hydroxyl radical) or oxidation of chlorine ions following Eq (2) to (4):

$$Cl^- \Leftrightarrow Cl^{\bullet}_{ads} + e^- \quad (2)$$

$$Cl^- + Cl^{\bullet}_{ads} \Leftrightarrow Cl_2 + e^- \quad (3)$$

$$Cl_2 + H_2O \Leftrightarrow HClO + H^+ + Cl^- \quad (4)$$

As cited in reference [17], at pH higher than 4.5 the complete dismutation of Cl_2 into HClO and Cl^- is occurred.
An explanation of the mediating role of chloride ions has been proposed by Bonfatti et al [17].
The presence of a weak concentration of chloride ions allows to inhibit the water discharge into oxygen, and to favorise hydroxyl or chloride and oxycloride radicals, which are very powerful oxidants. It can been explain why until 2 % of NaCl concentration the COD removal increases with NaCl concentration.
Increasing the chloride concentration more than 3 % cause a "potentiostatic buffering" by the chlorine redox system and consequently a decrease of the anode potential. Another possibility is the presence of competitive reactions, in particular oxygen and chloride evolution due to recombination of radicals that becomes bigger with the increasing NaCl concentration. The balance of all these phenomena results that there is an optimum of NaCl concentration which is 2 % mass of NaCl for the degradation of methidathion.
Fig. 3 illustrates that the pH during the electrolysis is significantly reduced.

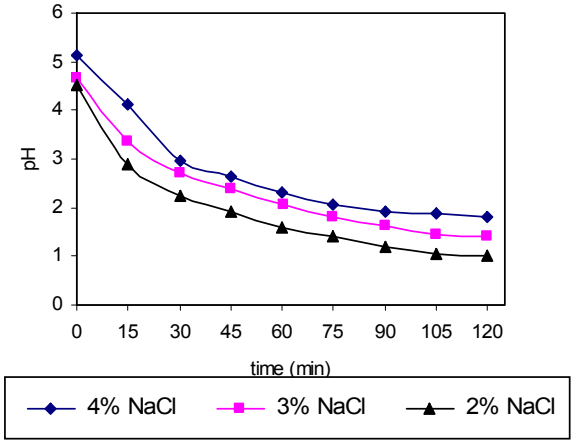

Fig. 3. *PH reduction for methidation 1.4 mM/L solution for 120 min of electrolysis at 60 mA and 25 °C*

Finally the pH in all cases became strong acidic. It is obvious that the continuous addition of high levels of organic matter in the electrolytic cell, resulted in the drop of pH. The electrolysis was more effective in terms of %COD reduction when the pH was in the acid range. This drop of the pH, during pesticides degradation, was also noted from Kotronarou et al [18]. It was also reported by Bonfatti et al [17] that while the mineralization goes to completion and the solution pH gets more and more acidic.

Effect of applied current

Applied current is an important factor affecting the electrolysis kinetics and process economics. The effect of applied current on the electrochemical process was demonstrated in several studies [19-20]. In Fig. 4 the % COD reduction for the methidathion is presented under different current inputs (chlorides = 2 %).

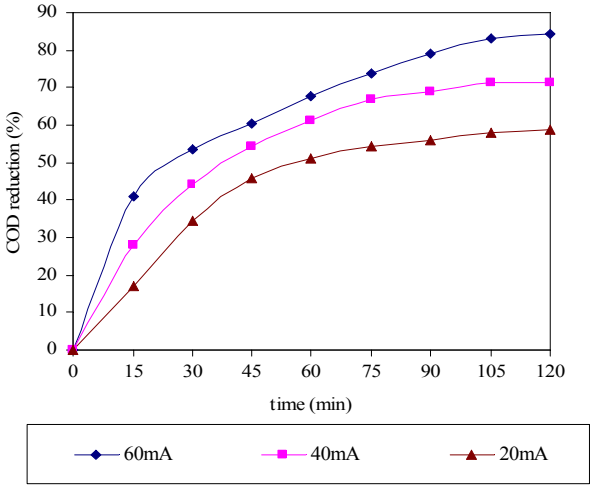

Fig. 4. *COD reduction (in %) for methidathion 1.4 mM/L solution under different current inputs (chlorides = 2 %) and 25 °C*

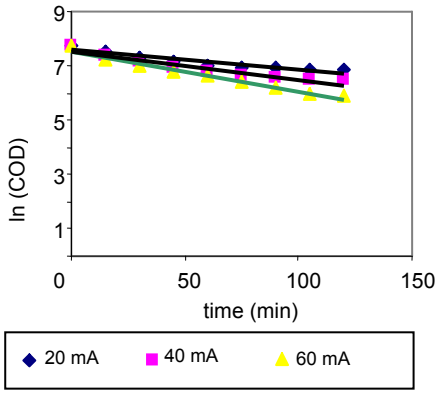

Fig. 5. *Pseudo first-order plot for oxidation of methidathion 1.4 mM/L solution in 2 % NaCl at 25 °C under different current inputs (COD at a given time, t, during electrolysis)*

These studies concluded that applied current increases the rate of electrochemical oxidation process.
The COD of methidathion was observed to fall with pseudo first-order kinetics, on all the surface studied. This is related to the dependence of the rate of oxidation on the rate of formation of the oxidising species at the electrode surface. The pseudo first-order constant of methidathion (k) varies from 0.0073 s^{-1} (20 mA) to 0.0146 s^{-1} (60 mA).

This is exemplified in Fig. 5 where the pseudo first-order plot is presented. From these results it was calculated that the best applied current is 60 mA.

Effect of temperature

In Fig. 6 the % COD reduction for methidathion at different temperatures under current input 60 mA is presented.

It is observed that for 25 °C and 65 °C the achieved reduction was 85 % and 66 % respectively.

The COD of methidathion was observed to fall with pseudo first-order kinetics (Fig. 7). The pseudo first-order constant of methidathion (k) varies from 0.0131 s^{-1} (25 °C) to 0.0077 s^{-1} (65 °C).

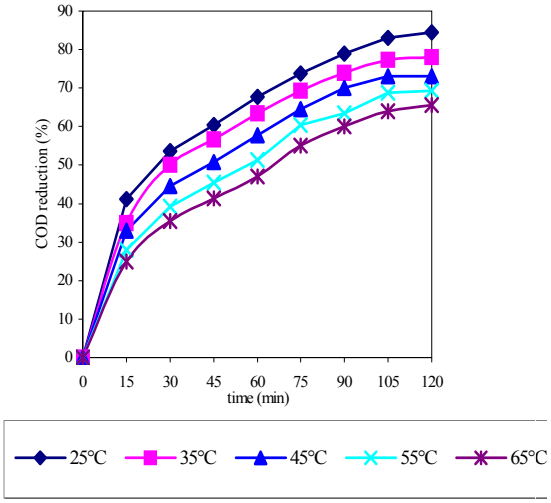

Fig. 6. *COD reduction (in %) for methidathion 1.4 mM/L solution in 2 % NaCl at 25 °C at different temperatures*

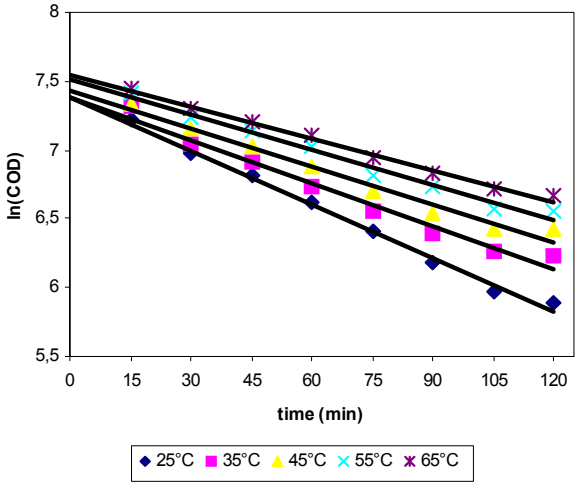

Fig. 7. *Pseudo first-order plot for oxidation of methidathion 1.4 mM/L solution in 2 % NaCl at 60 mA under different temperatures (COD at a given time, t, during electrolysis)*

The effect of temperature on the rates of constant was modelled using the Arrhenius plots, are shown in (Fig. 8). The apparent activation energies were determined by:

$$K = A \cdot \exp(-E_a/RT), \qquad (5)$$

where K is rate constant, A is constant, E_a is the activation energy, T is the temperature (K) and R is the gas law constant.

The obtained activation energy (−10.75 kJ) indicates that the process of electrochemical degradation is a complex one.

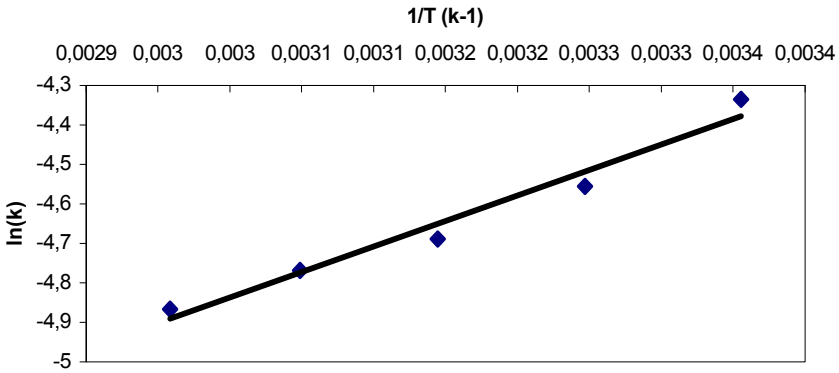

Fig. 8. *Arrhenius plote for oxidation of methidathion 1.4 mM/L solution in 2 % NaCl at 60 mA at various temperatures*

Conclusions

The conclusions of this study are as follows:

– The application of electrolysis in pesticide has the ability reduce the COD. For 2 % mass NaCl and 3 % mass NaCl the achieved reduction was 85 % and 72 % respectively. For 4 % NaCl was 56 %.

– In all cases the pH of electrolysis was significantly reduced after 45 min.

– The COD of methidathion was observed to fall with pseudo first-order kinetics, on all the surface studied.

– The applied current increases the rate of electrochemical oxidation process.

– The effect of temperature shows that for 25 °C and 65 °C the achieved reduction was 85 % and 66 % respectively.
– The activation energy indicates that the process of electrochemical degradation is a complex one.

References

1. FAO, (2000) Pesticide Disposal series, Baseline study on the problem of obsolete pesticide stocks, Rome.
2. Weiss E., Groenen-Serrano K., Savall A., Comninellis C. A kinetic study of the electrochemical oxidation of maleic acid on boron-doped diamond // J. Appl. Electrochem. 2007. Vol. 37, No. 1. P. 41-47.
3. Dhamo N. Electrochemical oxidation of cyanide in the hydrocyclone cell // Waste Manage. 1996. Vol. 16, No. 4. P. 257-261.
4. Saracco G., Solarino L., Aigotti R., Speccia V., Maja M. Electrochemical oxidation of organic pollutants at low electrolyte concentrations // Electrochim. Acta. 2000. Vol. 46, No. 2-3. P. 373-380.
5. Israilides G.J., Vlyssides A.G., Mourafeti V.N., Karvouni G. Olive oil wastewater treatment with the use of an electrolysis system // Bioresource Technol. 1997. Vol. 61, No. 2. P. 163-170.
6. Vlyssides A.G., Loizidou M., Karlis P.K., Zorpas A.A., Papaioannou D. Electrochemical oxidation of a textile dye wastewater using a Pt/Ti electrode // J. Hazard. Mater. 1990. Vol. 70, No. 1-2. P. 41-52.
7. Szpyrkowicz L., Naumczyk J., Zilio-Grandi Z. Electrochemical treatment of tannery wastewater using Ti/Pt and Ti/Pt/Ir electrodes // Water Res. 1995. Vol. 29, No. 2. P. 517-524.
8. Gandini D., Mahé E., Michaud P.A., Haenni W., Perret A., Comninellis C. Oxidation of carboxylic acids at boron-doped diamond electrodes for wastewater treatment // J. Appl. Electrochem. 2000. Vol. 30, No. 12. P. 1043-1051.
9. Rodrigo M.A., Michaud P.A., Duo I., Panizza M., Cerisola G., Comninellis C. Oxidation of 4-chlorophenol at boron-doped diamond electrodes for wastewater treatment // J. Electrochem. Soc. 2001. Vol. 148, No. 5.
10. Iniesta J., Michaud P.A., Panizza M., Cerisola G., Aldaz A., Comninellis C. Electrochemical oxidation of phenol at boron-doped diamond electrode // Electrochimica Acta. 2001. Vol. 46. P. 3573-3578.
11. Montilla F., Michaud P.A., Morallon E., Vasquez J.L., Comninellis C. Electrochemical oxidation of benzoic acid at boron-doped diamond electrodes // Electrochim. Acta. 2002. Vol. 47, No. 21. P. 3509-3513.
12. Kraft A., Stadelmann M., Blaschke M. Anodic oxidation with doped diamond electrodes: a new advanced oxidation process // J. Hazard. Mat. 2003. Vol. 103, No. 3. P. 247-261.
13. Hayes W.J., Jr. and Laws E.R., Jr. Pesticides derived from plants and other organisms. Handbook of Pesticide Toxicology. Academic Press, New York, NY. 1991.
14. Apha Awwa Wef. Standard Methods for the Examination of Water and wastewater, 13th ed. Apha, New York. 1971.
15. Tatapudi P., Fenton J.M. Electrolytic process for pollution treatment and pollution prevention. In Gerischer H. (Ed) // Advances in Electrochemical Engineering. VCH, Weinheim. 1994. P. 363-367.
16. Lin S., Shyu C., Sun M. Saline wastewater treatment by electrochemical method // Water Res. 1998. Vol. 32. P. 1059-1066.
17. Bonfatti F., D. Battisti A., Ferro S., Lodi G., Osti S. Anodic mineralization of organic substrates in chloride-containing aqueous media // Electrochim. Acta. 2000. Vol. 46, No. 2-3. P. 305-314.
18. Kotronarou A., Mills G., Hoffmann R.M. Decomposition of parathion in aqueous solution by ultrasonic irradiation // Environ. Sci.Technol. 1992. Vol. 26, No. 11. P. 1460-1462.
19. Mathis K. Treatment of industrial liquid wastes by electrofloatation // Water Pollut. Control. 1980. Vol. 19, No. 1. P. 136-143.
20. Lin S., Peng C. Treatment of textile wastewater by electrochemical method // Water Res. 1994. Vol. 28, No. 2. P. 277-282.

IMPROVEMENT OF IRRADIATION RESISTANCE OF SOLAR CELLS BY VARIATION OF THE DEVICE PARAMETERS: APPLICATION TO N+/P InGaP

M. Idali Oumhand[*], *Y. Mir*[**], *M. Khalis*[*], *M. Zazoui*[*]

[*]Laboratoire de Physique de la Matière Condensée, Université Hassan II Mohammedia
BP 146, Bd Hassan II, F.S.T. Mohammedia, Maroc
Telephone/fax: 023315353
E-mail: idali4@yahoo.fr

[**] Ecole Nationale des Sciences Appliquées de Safi, Université CADI AYYAD
BP 63 route Sidi Bouzid, Safi principale

Received: 8 Oct. 2007; accepted: 14 Nov. 2007

The degradation of solar cell materials in space has already been studied and is a consequence of the defects induced by electron and proton irradiation. The nature, characteristics and introduction rates of these defects are typical of a specific material. We propose here a method allowing to study the variation of the short circuit current J_{sc} and open circuit voltage V_{oc} versus the fluence of the irradiation using a new approach taking account of the dependence of two minority carriers lifetime τ_{0n} and τ_{0p} before irradiation. Then we show the effect of the device parameters, i.e. the variation of different values of parameters respectively the emitter thickness, base thickness, emitter doping, base doping and the front surface recombination velocity.

Keywords: photovoltaic effect in semiconductor structures; modelisation, degradation

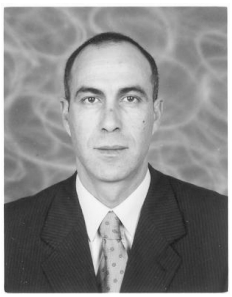

Mimoun Zazoui

Organization: Professor.
Education: Université Hassan II Mohammedia (1995-2007).
Main range of scientific interests: solar cells, semiconductor, condensed matter.
Publications: in Phys Rev, Appl. Phys. Letter, J. Appl. Phys, Semicond. Scien. Tech…

Mohammed Idali Oumhand

Organization(s): professor and thesis L.P.M.C. Laboratoire de Physique de la Matière Condensée.
Education: Université Hassan II. Mohammedia, Faculté des sciences et techniques F.S.T. Mohammedia. Maroc (2004-2007).

Introduction

Previously we have proposed a new method, justified theoretically and experimentally, allowing to deduce τ_{0n} versus τ_{0p}, the minority carriers lifetime respectively in the base and in the emitter of solar cell, before irradiation and τ_{jn} versus τ_{jp}, the minority carriers lifetime respectively in the base and in the emitter, after irradiation, and versus φ_j, the fluence irradiation. The validity of this method was illustrated in the case of the degradation of the *n*+/*p* InGaP cells [1]. In this paper, we recall briefly the calculation principle of new approach and we will show the effect of the device parameters, i.e. the emitter thickness and doping (X_n, N_d) and base thickness and doping (X_p, N_a) and the front surface recombination velocity, S_p, on the variation of characteristics and consequently on the resistance to electron irradiation of solar cells.

Principle of calculation of minority carrier lifetime

The electron or proton irradiation introduces recombination centres which tend to affect solar cell performance by reducing the minority carrier lifetimes τ_{jn} and τ_{jp} through equation [2],

$$\frac{1}{\tau_{jn}} = \frac{1}{\tau_{0n}} + k\sigma_n \nu_n \varphi_j , \quad \frac{1}{\tau_{jp}} = \frac{1}{\tau_{0p}} + k\sigma_p \nu_p \varphi_j ,$$

where the subscripts 0*n*, 0*p* and *jn*, *jp* indicate values before and after irradiation in the *n* and *p* region.
The lifetimes τ_{0np} associated with the recombination of minority carriers (electrons and holes in the emitter and (or) base before irradiation) depend on the nature and concentration of the native recombination centres, i.e. on the mode of growth of the material and on the process treatments which are applied to realize the cell.

In the previous work, we have shown that the minority carrier lifetime can be written as:

$$\tau_{jn} = \left[\left(a_j r_n \sqrt{\tau_{jp}} + b_j\right) \Big/ \left(J_{scj}\sqrt{\tau_{jp}} - a_j r_p\right)\right]^2.$$

The complete expressions for a_j, b_j, r_n and r_p of last equation were derived from [1].

Mecanism of degradation and parameters effects

Mecanism of degradation

It is possible to calculate, and hence predict, the degradation of n+/p InGaP solar cell, when the thickness and doping respectively of the emitter and base are given. The parameters of the studied cell are listed in Table 1 below.

Table 1

Calculated parameters of n+/p InGaP cells

Cell	$\tau_{0n}(s)$	$\tau_{0p}(s)$	$k\sigma_n(cm^{-1})$	$k\sigma_p(cm^{-1})$
InGaP (n+/p)	$3.44\cdot10^{-8}$	$7.2\cdot10^{-12}$	$1.2\cdot10^{-14}$	$8.6\cdot10^{-13}$

The knowledge of J_{sc0} and V_{oc0} under given illumination, before irradiation is also necessary in order to derive the minority carrier lifetimes τ_{0n}, τ_{0p} in the base and emitter. Once the initial values of the minority carrier lifetimes are determined, one inject them into calculation. The knowledge of J_{scj} and V_{ocj} under given illumination and amount of irradiation φ_j allow it to deduce the values of τ_{jn}, τ_{jp} and hence $k\sigma_n$, $k\sigma_p$.

Often some authors fits experimental data to the values normalized prior irradiation [3, 4]. In our case we calculate the absolute theoretical data as shown in Fig. 1, a and b where the absolute experimental [5] (with yellow star (*) symbol) and the theoretical data of V_{oc}, J_{sc} are represented.

From the parameters τ_{0n}, $k\sigma_n$ (in emitter region), and τ_{0p}, $k\sigma_p$ (in base region) (see Table 2) we derive the calculated values of V_{oc} and J_{sc}. We add that these values extracted from our analysis are different of the values determined by other authors [3, 4] because of the relationship between two carriers lifetime τ_{0n} and τ_{0p}.

Once the degradation of n+/p InGaP is calculated, we proceed to study the parameters effects on the degradation of V_{oc} and J_{sc} [6].

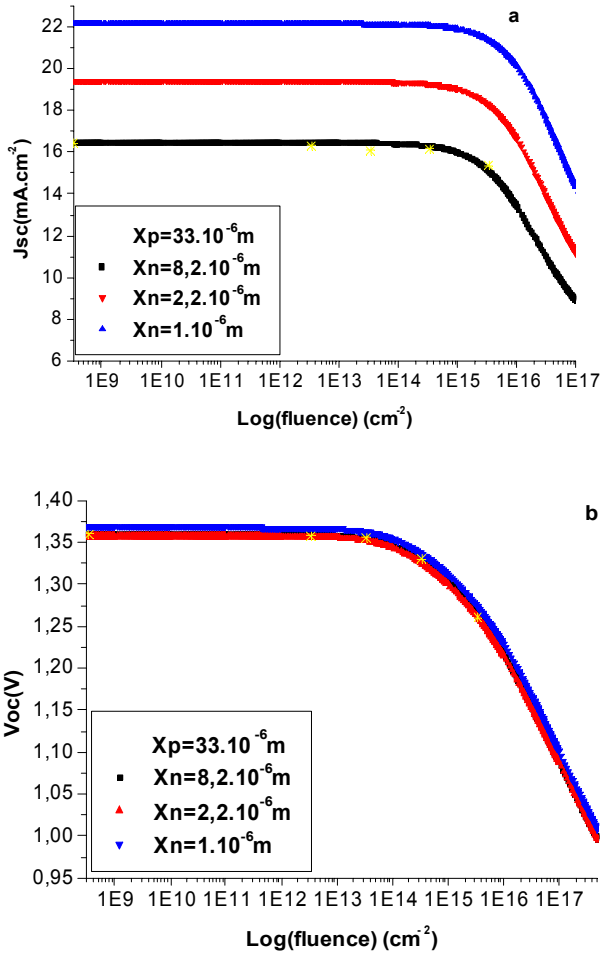

Fig. 1. *Variation (a) of the short circuit current, J_{sc}, and (b) of the open circuit voltage, V_{oc}, under 1 AM0 illumination, versus the fluence of 1 MeV electron irradiation, calculated for different values, X_n, of emitter thickness*

Table 2

Parameters of InGaP solar cells

InGaP-n^+/p	Emitter thickness X_n ($1\cdot10^{-6}$ m)	Base thickness X_p ($1\cdot10^{-5}$ m)	Emitter doping N_d ($1\cdot10^{18}$ cm^{-3})	Base doping N_a ($1\cdot10^{17}$ cm^{-3})	Recombination velocity S_p ($1\cdot10^5$ cm·s^{-1})
Solar cell parameters	8.2 2.2 1.0	3.3 2 1	4.5 1.5 0.85	4 2 1	5 1 0.5

In the present work, we interest to the effects of parameters as the emitter thickness and doping (X_n, N_d) and base thickness and doping (X_p, N_a) and the front surface recombination velocity, S_p. We show in Fig. 1-5 respectively the variation of the short circuit current, J_{sc}, and open circuit voltage, V_{oc}, under 1 AM0 illumination, (the AM0 spectrum is the relevant one for satellite and space-vehicle applications), versus the fluence of 1 MeV electron irradiation, calculated for different values of the emitter and base thickness and doping level and of the front surface recombination velocities.

The effect of the variation of the thickness

For the studied cell InGaP-*n*+/*p*, we vary only each of the emitter thickness, X_n, and the base thickness, X_p, the other parameters being fixed at the values of Table 2. The curves of J_{sc}, short-circuit current and the open circuit voltage, V_{oc}, obtained are represented in Fig. 1, 2.

We observe an important reduction in J_{sc} with the increase values of the emitter thickness, X_n. On the contrary J_{sc} increases but slightly with increasing values of the bases thickness, X_p.

Indeed, when the emitter thickness, X_n, will be big, enough carriers don't reach the base region, what causes a reduction of the spectral response and therefore an attenuation of the value of J_{sc}.

At high fluence of irradiation (Fig. 2, *a*), we note a fast decrease of the curves representing the cells of which the thickness X_p is large.

Not indeed of surprise for the V_{oc} parameter, it doesn't vary practically at the time of the variation of the X_n and X_p (in the Fig. 1, *b* and Fig. 2, *b*; the three representative curves are nearly confounded).

The effect of the variation of the level doping

The effect of the variation of the level doping of two regions, emitter and base, is illustrated in Fig. 3, 4.

The Fig. 3, *b* and Fig. 4, *b* show that the effect of the doping remains weak on the variation of the V_{oc} parameter.

The contribution of the two regions to the short circuit current, J_{sc}, is shown in Fig. 3, *a* and Fig. 4, *a*. This contribution takes place in opposite sense, i.e., the J_{sc} increases rapidly when the base is well doped by the quantity N_a whereas the emitter is doped weakly by the quantity N_d.

Moreover, at high fluence of irradiation, to see Fig. 3, *b* and Fig. 4, *a*, J_{sc} resists to the irradiations when the cell (*n*+/*p*) is doped weakly by the acceptors N_a, on the other hand V_{oc} resists well to the irradiations when the junction (*n*+/*p*) is doped weakly by the donors N_d.

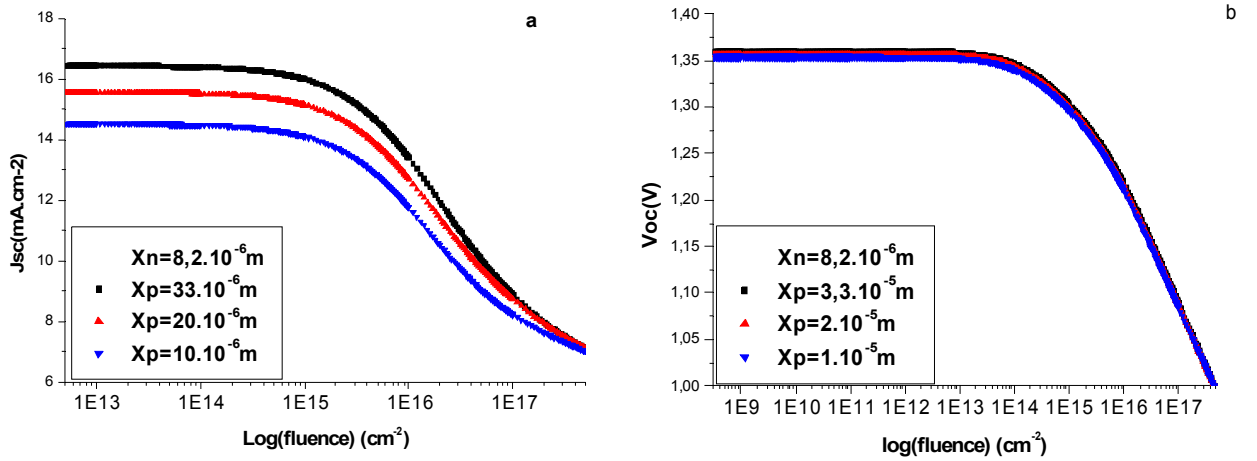

Fig. 2. *Variation (a) of the short circuit current, J_{sc}, and (b) of the open circuit voltage, V_{oc}, under 1 AM0 illumination, versus the fluence of 1MeV electron irradiation, calculated for different values, X_p, of base thickness*

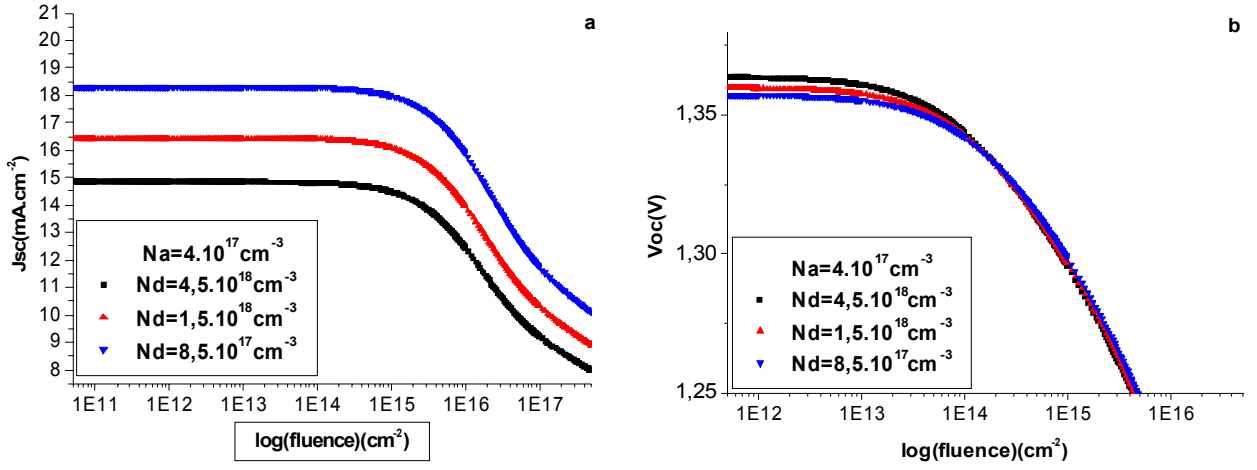

Fig. 3. *Variation (a) of the short circuit current, J_{sc}, and (b) of the open circuit voltage, V_{oc}, under 1 AM0 illumination, versus the fluence of 1 MeV electron irradiation, calculated for different values N_d of the emitter doping level*

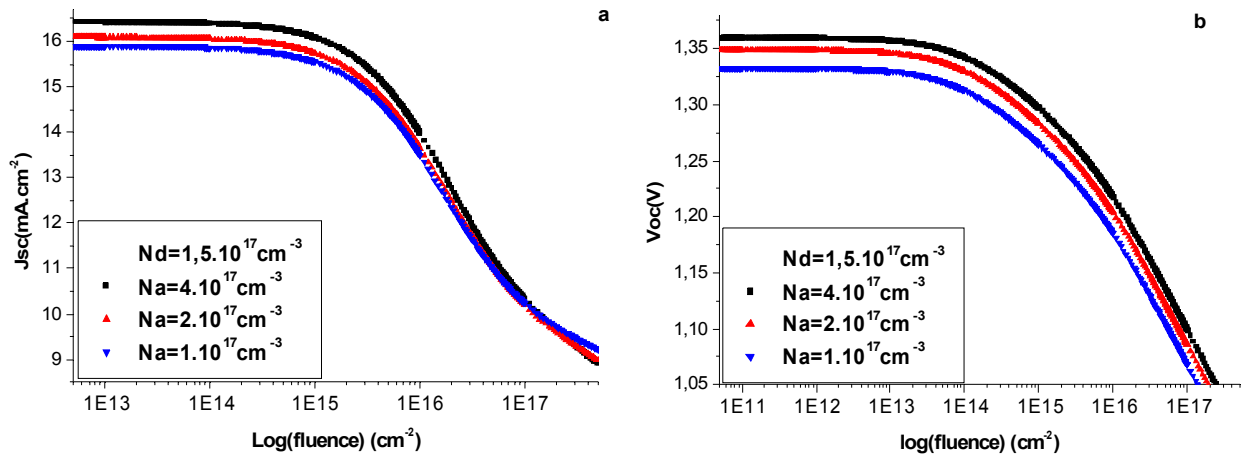

Fig. 4. *Variation (a) of the short circuit current, J_{sc}, and (b) of the open circuit voltage, V_{oc}, under 1 AM0 illumination, versus the fluence of 1 MeV electron irradiation, calculated for different values, N_a, of the base doping level*

The effect of the variation of the front surface recombination velocities

The Fig. 5 shows a not very significant effect of the front surface recombination velocities, S_p, on the characteristics J_{sc} and V_{oc} especially at low fluence of irradiation but at high fluence of irradiation, we can note a very significant effect of the S_p on the irradiation resistance of the J_{sc} and V_{oc} parameters, i.e., more the S_p decreases and more the J_{sc} and V_{oc} increase.

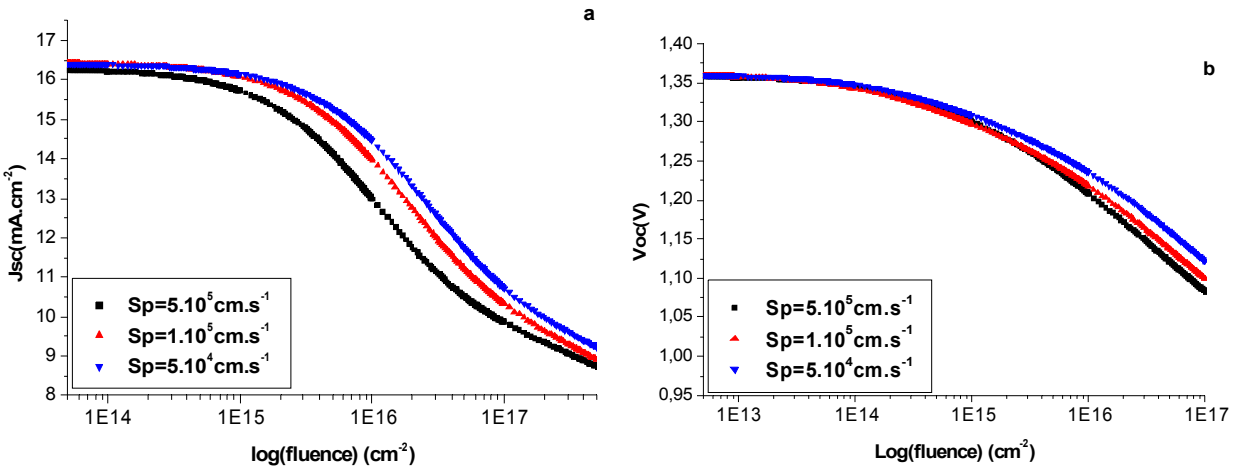

Fig. 5. *Variation (a) of the short circuit current, J_{sc}, and (b) of the open circuit voltage, V_{oc}, under 1 AM0 illumination, versus the fluence of 1MeV electron irradiation, calculated for different values, S_p, of front surface recombination velocities*

Conclusion

In this study, we have shown that the short circuit current, J_{sc}, is sensitive to variations of he emitter thickness, base thickness, emitter doping, base doping and the front surface recombination velocities.

At high irradiation of the *n+/p* InGaP solar cell and when the level of doping of the donors, N_d, is large then that of the acceptors, N_a, is low, we note a resistance of the two characteristics J_{sc} and V_{oc} to the electron irradiations. Finally, the front surface recombination velocities, S_p, has a profound effect on the short circuit current, J_{sc}, especially at high fluence irradiation.

References

1. Idali Oumhand M., Zazoui M. M. // J. Condensed Matter.
2. Sze S.M. // Physics of Semiconductors Devices. Murray Hill New-Jersey. 1991.
3. Makham S. et al. // Semicond. Sci. Technol. 20 (2005). P. 699-704.
4. Bourgoin J.C., Angelis N. // Solar Energy Material & Solar Cell. 66 (2001). P. 467-477.
5. Yamaguchi M., Takamoto T., Araki K., Ekins-Daukes N. // Solar Energy. 79 (2005). P. 78-85.
6. Hadrami M. // Solar Energy Material & Solar Cell. 90 (2006). P. 1486-1497.

PREPARATION AND CHARACTERIZATION OF $CuInS_2$ THIN FILMS FOR LOW COST SOLAR CELLS

A. Ihlal, K. Bouabid*, D. Soubane*, A. Elfanaout*, E. Elhamri*, M. Nya*, G. Nouet***

*Laboratoire Matériaux et Energies Renouvelables (LMER), Faculté des Sciences, BP 8106, Hay Dakhla, Agadir, Maroc.
E-mail: ihlal_ahmed@yahoo.fr
**Structure des Interfaces et Fonctionnalité des couches minces (SIFCOM), Ensicaen, Bd du Maréchal Juin, 14050 Caen, France
E-mail: gerard.nouet@ensicaen.fr

Received: 26 Oct 2007, accepted: 6 Nov 2007

Thin films of copper indium disulphide were grown on indium tin oxid (ITO) coated glass substrates using a two stage process: electrodeposition of Cu-In alloys and subsequent sulfurisation. The influence of sulfurisation temperature was investigated with X-ray diffraction, scanning electron microscopy and optical measurements. Single phase chalcopyrite $CuInS_2$ films were obtained after treatment of Cu-In alloys in 5 % H_2S/Ar at 500 °C for 10 min. Indeed, only peaks from $CuInS_2$ are present in the XRD pattern after KCN etching. SEM analyses have shown that the film consisted of homogeneous grains with sizes of about few hundreds of nm in good agreement with TEM investigations. The films were copper-rich as evidenced by EDS analysis. The band gap value deduced from the optical measurements is about 1.44 eV. This value is in good agreement with that measured on sulphurised Cu-In layers obtained by high vacuum process.

Keywords: solar energy, structural materials

Ahmed Ihlal

Organization(s): Université Ibn Zohr, Faculté des sciences, Professeur, directeur laboratoire matériaux et énergies renouvelables (LMER), lauréat prix Ibn Zohr de la recherche scientifique (2007).
Education: 1988 − présent; Professeur de physique, faculté des sciences, Université ibn Zohr, Agadir. 1985: DEA énergétique, Université Paris VII; 1988 Doctorat de l'université, Université de Caen, France; 1995: Doctorat d'Etat, Université Ibn Zohr, Agadir, Maroc.
Experience: Engineer (1986-1994). Chief scientist (1994-1998). Scientific research projects.
Main range of scientific interests: energies renouvelables, photovoltaique, matériaux, couches minces, physique de l'état solide.
Publications: Une trentaine de publications dans des revues de renomée internationale et plusieurs dizaines de communications dans les conférences internationals.

Gérard Nouet

Organization(s): Université de Caen, Ecole Nationale Supérieure d'Ingénieurs de Caen (France) Laboratoire Structure des Interfaces et Fonctionnalité des Couches Minces, Directeur de Recherche CNRS
Education: 1972: Doctorat d'Etat Université de Caen.
Experience: Engineer (1986-1994). Chief scientist (1994-1998). Scientific research projects.
Main range of scientific interests: structure atomique des défauts structuraux: microscopie électronique en transmission, calcul énergétique. Couches minces des semiconducteurs nitrures, des matériaux photovoltaiques.
Publications: Plus de deux cents publications dans les revues internationales, et de nombreuses communications dans les conférences internationals.

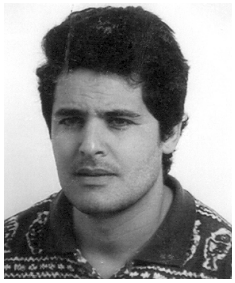

Khalid Bouabid

Organization(s): Université Ibn Zohr, Faculté des sciences, Professeur assistant.
Education: 1994 − présent; Professeur de physique, faculté des sciences, Université ibn Zohr, Agadir; 2004 Doctorat d'Etat, Université Ibn Zohr, Agadir, Maroc.
Main range of scientific interests: energies renouvelables, photovoltaique, matériaux, couches minces, physique de l'état solide.
Publications: Une vingtaine de publications dans des revues de renomée internationale et plusieurs dizaines de communications.


M'barek Nya

Organization(s): Université Ibn Zohr, Faculté des sciences, Professeur assistant.
Education: 1987 − présent; Professeur de physique, faculté des sciences, Université ibn Zohr, Agadir; 1986 Doctorat de l'université, Université de Marseille, France.
Main range of scientific interests: energies renouvelables, photovoltaique, matériaux, couches minces, physique de l'état solide.
Publications: Une dizaine de publications dans des revues de renomée internationale et plusieurs dizaines de communications.

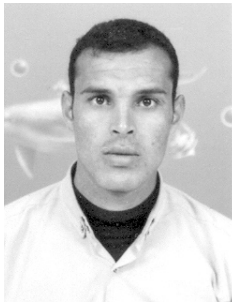
Elhoucine Elhamri

Organization: Etudiant en DESA.
Education: Ibn Zohr University, Faculty of science.
Main range of scientific interests: chimie, matériaux en couches minces.

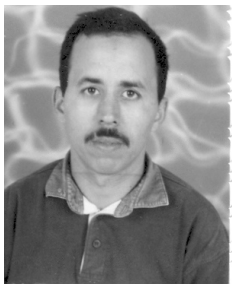
Abdessalam Elfanaout

Organization: Doctorant.
Education: Ibn Zohr University, Faculty of science.
Main range of scientific interests: physique de l'état solide.

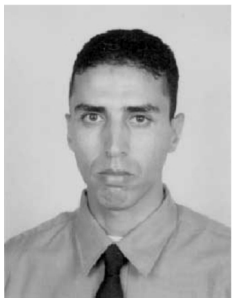
Driss Soubane

Organization: Doctorant.
Education: Ibn Zohr University, Faculty of science.
Main range of scientific interests: enérigie solaire, couches minces, simulations.
Publications: trois publications et plusieurs dizaines de commuinications.

Introduction

Because of the growing emissions of greenhouse gases like CO_2, due to the burning of fossil fuels, the average planet surface temperature is expected to rise drastically in the 21^{th} century [1]. Such temperature increase (phenomenon known as global warming) will have a negative impact on our environment. Searching alternative sources of energy is then a vital issue for our planet. Solar energy is not only renewable and abundant but also environmentally friendly. Power obtained from solar energy finds more and more utilization worldwide. Among these alternatives, photovoltaic (PV), (direct conversion of sun energy into electricity) holds the best promise for the reduction of CO_2 emissions. Unfortunately, the price per kW for photovoltaic-electricity remains higher than its traditional energy counterpart because of the high cost of silicon single crystal based solar cells processing. Reducing the price of PV-electricity is then a major challenge for scientists

and industrials. One approach to bring down the costs is the developpment of thin film solar cells. In this way, ternary chalcopyrite semiconductors, $CuInSe_2$ (CISe) and their alloys with gallium CIGSe are becoming among the leading candidates for high efficiency and low-cost terrestrial photovoltaic devices. Indeed, polycrystalline CISe and CIGSe based solar cells have achieved efficiencies of about 19 % on a laboratory scale [2-4] and around 14 % for modules [5]. However, selenium is harmful and should be avoided in mass production. Chalcogene elements such as sulphur is environmentally friendly and could be used instead of Se. $CuInS_2$ (CIS), is Se free compound and exhibits a direct band gap value of 1.5 eV suitable for efficient sun light conversion. Unfortunately, the best reported conversion efficiency for CIS based solar cells is 12.7 % [6, 7] less than those obtained with CISe based solar cells. In the present paper we report on some results concerned with $CuInS_2$ (CIS) thin films prepared by a simple, cost-effective non-vacuum process (electrodeposition).

Experimental methods

Electrochemical process was used to prepare CuIn thin films onto commercially available indium tin oxide (ITO) coated glass substrates. The substrates were thoroughly degreased with isopropanol, and cleaned ultrasonically in distilled water and finally dried under nitrogen. The deposition was carried out at room temperature using three electrodes potensiostat system with a saturated calomel electrode (SCE) as the reference electrode and platinum as the counter electrode. The concentration of precursors were chosen to be $CuSO_4$ $3\cdot10^{-3}$ M, $In_2(SO_4)_3$ $3\cdot10^{-3}$ M. The pH of the solution was adjusted to 2 using concentrated sulfuric acid. Citric acid (0.1 M) was used as a complexing agent and K_2SO_4 (0.1 M) was used as supporting electrolyte. The polarization curves were investigated at a sweep rate of 10 mV/s. All the films were grown at a potential of -0.6 V (vs. SCE). The obtained films were then sulfurised under a continuous flow of 5 % H_2S/Ar atmosphere at 300, 400 and 500 °C for 10 minutes. The optical properties were carried out with a spectrophotometer Cary 500 (Varian) and Shimadzu UV-3101 UV-Visible-IR spectrophotometer operating in the wavelength range 320 to 3200 nm.
The structural properties of all the obtained films were analyzed by X-Ray diffraction (XRD) using Philips PW 1840 diffractometer with CuK_α source (λ = 15418 Å). The morphology of the samples surface was investigated with the help of JEOL 5500 electronic microscope for scanning electronic microscopy (SEM) and transmission electron microscopy (TEM).

Results and discussion

Fig. 1 shows the SEM micrographs of the CuIn layer sulfurized at 500 °C under 5 % H_2S/Ar atmosphere during 10 min.

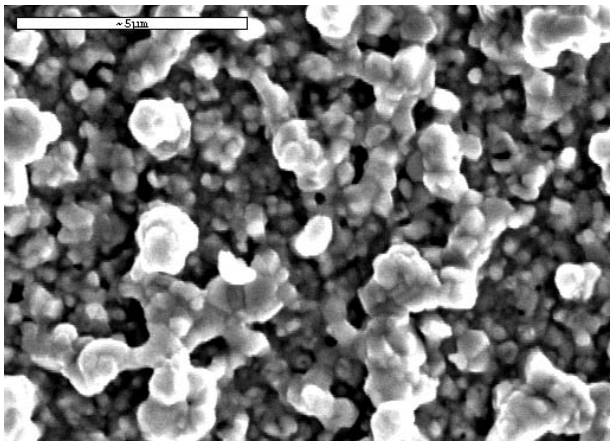

Fig. 1. *SEM micrograph of CuIn layer sulfurised at 500 °C under 5 % H_2S/Ar during 10 min*

This figure suggests a good morphological aspect of the CIS film. It shows a good and uniform coverage of the surface of the substrate. The film consists of grains with a size of about 1 µm. No pinholes are observed. However, one can notice the blurred structure of the film probably due to the presence of secondary phases like Cu_xS. These results are comparable to those reported on $CuInS_2$ thin films prepared by rf-sputtering in our previous work [8].
The XRD pattern corresponding to this sample is shown in Fig. 2:

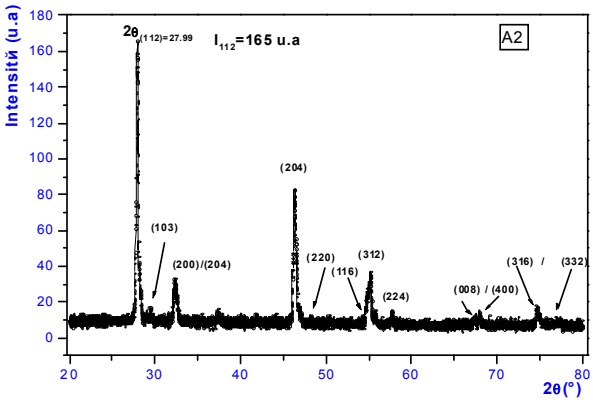

Fig. 2. *XRD pattern of CuIn layer sulfurised at 500 °C under 5 % H_2S/Ar during 10 min*

The sharpness of the peak at 2θ = 27.6° suggests a good cristallinity of the film. This observation is in good agreement with that reported by other authors [9].
EDS analyses performed on this sample have shown that our film is copper-rich. Atomic percentage of the elements are the next: Cu: 35.65 %, In: 17.24 %, S: 47.11 %. Fig. 3 shows the SEM micrograph of the sample of Fig. 1 after KCN etching.
This attack has removed the superficial layer and has lead the appearance of weak coverage of the substrate. The atomic percentage of the elements deduced from EDS analysis is the next: Cu: 28.05, In: 22.57, S: 49.38. The film is still copper rich, however, the atomic ratio Cu/In is 1.24 instead of 2 before KCN etching.

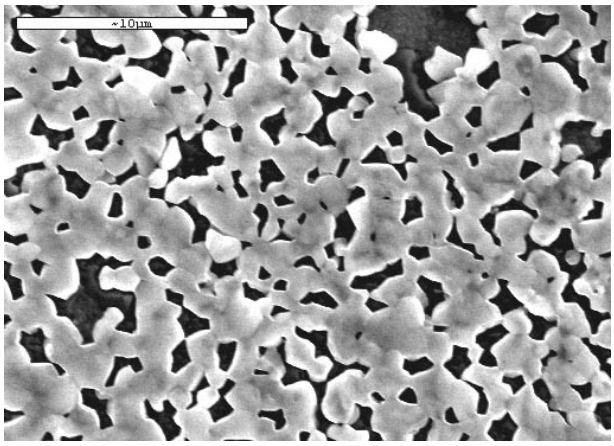

Fig. 3. *SEM micrograph of the sample of Fig. 1 after KCN etching during 3 min*

TEM image of the film of Fig. 3 is shown in Fig. 4. The film consists on grains of about few hundreds of nm, in good agreements with SEM observations.

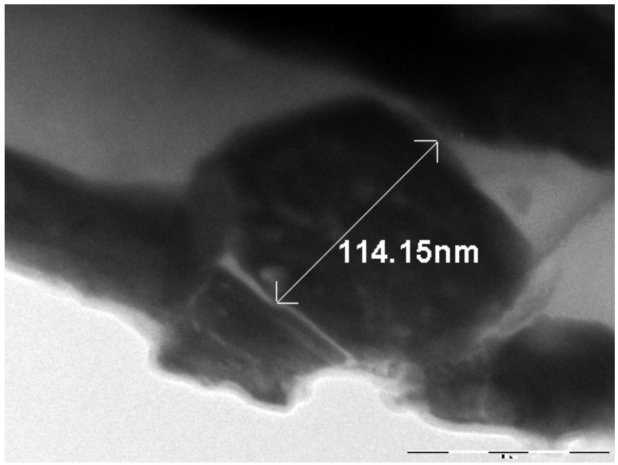

Fig. 4. *TEM image of the sample of Fig. 3*

Optical measurements have shown that our film is highly absorbing. Absorption values as high as 10^5 cm^{-1} were measured on our sample. The band gap value deduced from optical measurements is about 1.44 eV. This value is in good agreement with that measured on sulfurised Cu-In layers obtained by high vacuum process [8] and close to 1.5 eV suited for the photovoltaic conversion of solar energy.

Conclusion

Non-vacuum process was used to prepare good quality $CuInS_2$ thin films. The technique consists in the preparation of CuIn layers by electrodeposition and a subsequent sulfurisation in 5 % H_2S/Ar atmosphere. The obtained films were polycrystalline and copper rich. The grain size is about few hundreds nm. KCN etching procedure has lead to the formation of the well known chalcopyrite $CuInS_2$ single phase. The films are highly absorbing with an absorption coefficient close to 10^5 cm^{-1} and exhibit a band gap value close to 1.5 eV suitable for solar energy conversion.

Acknowledgements

This work was partially supported by the CNRST/CNRS cooperation program (Chimie 05/07).

References

1. http://yosemite.epa.gov/oar/globalwarming.nsf/content/index,html.
2. Ramanathan K., Contreras M.A., Perkins C.L., Asher S., Hasoon F.S., Keane J., Young D., Romero M., Metzger W., Noufi R., Ward J., Duda A. // Prog. Photovoltaics: Res. Appl. 2003. No. 11. P. 225.
3. Contreras M.A., Ramanathan K., Abushama J., Hasoon F., Young D.L., Egaas B., Noufi R. // Prog. Photovoltaics: Res. Appl. 2005. No. 13. P. 209.
4. Contreras M.A., Egaas B., Ramanathan K., Hiltner G., Swartzlander A., Hasoon F., Noufi R. // Prog. Photovoltaics. 1999. No. 7. P. 311.
5. Powalla M., Dimmler B., Chaeffler R., Woorwenden G., Stein U., Mohring H.D., Kessler F., Hariskos D. // Proc. 19th European Photovoltaic Solar Energy Conference (EPSEC) and Exhibition, Paris, June. 2004. P. 1663.
6. Klenk R., Dobson P., Falz M., Janke N., Luck I., Pérez-Rodriguez A., Scheer R., Terzini E. // Proc. 16th EPVSEC, 2000.
7. Siemer K., Klaer J., Luck I., Burns J., Klenk R., Braunig D. // Solar Energy Materials and Solar Cells. 2001. No. 67. P. 159.
8. Ihlal A., Bouabid K., Soubane D., Nya M., Ait-Taleb-Ali O., Amira Y., Outzourhit A., Nouet G. // Thin Solid Films. 2007. No. 515. P. 5852.
9. Sartale S.D., Ennaoui A., Lux-Steiner M. // Proc. of 19th EPSEC, Paris. 2004. P. 1988.

FACTORS AFFECTING THE VALORIZATION OF PHOTOVOLTAIC WATER PUMPING PROJECTS FOR IRRIGATION IN THE ADAMAWA PROVINCE (CAMEROON)

M. Kamta*, O. Bergossi**

*University of Ngaoundere, ENSAI, Department of Electrical engineering, Energetic and Automation
BP 455, Ngaoundere, Cameroon
Mobile phone: (237) 77 52 79 65, E-mail: martin_kamta@yahoo.fr

**CREIDD, Troyes University of Technology,
12 rue Marie Curie, BP 2060, 10010 Troyes cedex, France,
E-mail: olivier.bergossi@utt.fr

Received: 3 Oct 2007; accepted: 25 Oct 2007

The CESAM method has been adapted to design a photovoltaic water pumping system in the state-of-the-art, according to the farmers' needs in Marza area. An experimental agricultural structure has been implemented to overcome factors affecting the valorization of new technologies for irrigation in dry season such as the lack of modern technological knowledge by farmers, the lack of affordable means by farmers, the lack of interface between the researchers and the users of research results. Convincing results revealed that the farmers could afford to invest in the photovoltaic water pumping projects for irrigation, the incomes being better than the ones in raining season.

Keywords: solar water-lifting systems, economic aspects, CESAM method, RETScreen International software

Martin Kamta

Organization: National School of Agro-Industrial Sciences (ENSAI), University of Ngaoundere, Cameroon.
Education: Doctorate in physics of semiconductor devices, 1998. Cycle Doctorate in physics of semiconductor devices, 1989. Post-graduate, 1984. Master's degree in physics, 1983. Graduate in physics and chemistry, 1982. Faculty of sciences, University of Yaounde, Cameroon.
Experience: Senior lecturer in electronics (ENSAI). Research activities: Cirad of Montpellier, February and March, 2007. Lab. of ESR spectroscopy, Louis Pasteur's University of Strasbourg, France (1987-1989) and (1992-1995). Lab. of solid state chemistry, University of Nancy 1, France, 1986.
Main range of scientific interests: physics of semiconductor devices, photovoltaic systems.
Publications: 3 articles in electron spin resonance (ESR) of defects in III-V materials, 2 articles in superconducting materials, 2 communications about renewable energy.

Olivier Bergossi

Organization: Center for Research and Interdisciplinary Studies on Sustainable Development (CREIDD), University of technology of Troyes (UTT, France).
Education: Doctorate in Engineering Sciences, 1995, University of Franche-Comté (France), Master degree in Industrial Ecology, 2003, UTT.
Experience: Assistant-professor (UTT, 1996-2005), Research on near-field optics (1996-2001, UTT) and sustainable development (since 2003, UTT), Technology of Information and Communication in Education (TICE) for engineering (since 2001, UTT) – French cooperation in Cameroon, project "Comètes" (2005-2007).
Main range of scientific interest: physics (optoelectronics and nanotechnologies), TICE, sustainable development (industrial ecology, ecological footprint).
Publications: 11 articles about Near-field optics, 2 articles about TICE and 2 articles about Sustainable development.

Introduction

In the Adamawa province (Cameroon), the bulk of rural inhabitants reside in dispersed homesteads. They are poor, with irregular income from the agricultural activities. Indeed, it is estimated that 68 % of inhabitants of sub-Saharan Africa reside in rural areas [1]. In such a dispersed rural settlements, there is no conventional electric grid. Therefore, an ideal market for decentralized energy technologies that better match the dispersed rural settlements in the Adamawa province is welcomed.
The Adamawa province is known as the water tower of Cameroon, with an average groundwater level at 20 m in most plain areas [2]. These plain areas are farmable and are mainly cultivated in raining season. Unfortunately the unavoidable use a lot of herbal medicine in raining

season leads to the reduction of farmers' income, even if there are high yield crops. On the other hand, in dry season the farmers' income may be higher than in raining season, due to the use of a bit of herbal medicine. However, farms have to be irrigated. As a matter of fact, most streams dry off from February to April. In this case, farmers have to select an irrigation system that best fits their incomes. For example, if farmers have access to sufficient surface water for irrigation, then it is usually the cheapest option [3]. Otherwise, in the areas were the groundwater level is less than 5 m, the use of diesel pump units could be more cheaper than other water pumping system [4]. Therefore, what is the matter for farmable areas where groundwater level is up to 20 m?

In this paper, a discussion on the specific factors affecting the valorization of photovoltaic water pumping projects in Adamawa province is presented. The CESAM method carried out at CIRAD of Montpellier (France) [5] is adapted to design a photovoltaic water pumping system which satisfies the adamawa farmers' needs in dry season, especially in the Marza area in Ngaoundere.

The CESAM method for system design

The potential utilization of photovoltaic water pumping systems for irrigation in the Adamawa province depends on factors such as the high difference in air temperature, the lack of modern technological knowledge by farmers, the lack of affordable means by farmers, the lack of interface between the researchers and the potential users of research results, etc. While the issues relating to the first factor may vary considerably from one site to another, the issues concerning the other factors really affect the development of the country. Indeed, a lot of hydraulic projects consisting of boreholes equipped with manual pump units have been carried out in the Adamawa province [2]. Unfortunately, a manual pumping system is not suitable for irrigation. In addition, the users are not qualified to maintain the system.

The CESAM method has been adapted in this paper to find out the adequate solutions to the afore-mentioned problems. This method is an approach of participatory and pluridisciplinary design, aimed to perform small scale farming equipments for sub-Saharan countries. The mean objective is to design equipments in the state-of-the-art, according to the users' needs. Therefore, the design team may be built up by researchers, manufacturers and users. They have to work together from the beginning to the end of the project. This method has been disseminated in several countries in West Africa [6-7], and has registered widespread success, mainly due to the user's satisfaction. To the best of our knowledge, this method is almost unknown in Central Africa.

Generally, the CESAM method is organized in 8 stages. Here, some of these stages have been adapted in a particular case of photovoltaic water pumping project for irrigation in the Adamawa province, especially in the Marza area. The adapted stages can be expressed in terms of the following questions. First of all, is the project profitable? Who are the partners? Who are the final users? Are the financial resources available? Is the equipment to be used local? What is the planning of the project? What is the usual agricultural technique? Etc. The answers to these fundamental questions give rise to innovative ideas which connect the technology to the market.

Within the framework of this project, inquiries have been made, where the following farmers' questions have been registered: Is the investment cost affordable? What is the rate of return on investment? How can the system be maintained and managed? Etc.

The afore-mentioned questions have enabled us to analyse and design a photovoltaic water pumping system taking into account the whole factors affecting the operation system during the dry season and its valorization. To that effect, the RETScreen International software [8] have been used and the sizing of photovoltaic pumping system have been made by the manufacturer [9]. Finally, the photovoltaic water pumping system for irrigation in the Marza area has been implemented by a team of researchers, manufacturers and farmers.

Experimental agricultural structure

There are numerous possibilities of making connexion between the technology and the market. For example, an experimental agricultural structure would be adequate for meetings of researchers and farmers. In this way, the valorization of research results may take place, particularly in the field of irrigation in dry season. This experimental agricultural structure is built up at the Mgr. Yves Plumey's foundation in Ngaoundere at the latitude of 7.3 °N and longitude of 13.3 °E, where large farmable areas and groundwater are available.

System implementation

The implementation of actual photovoltaic water pumping project for irrigation has taken into account the affordable means by farmers, their usual agricultural practice, the profit rate on investment and the system management. The configuration system drawn in Fig. 1 is not quite new. The previous photovoltaic water pumping systems for irrigation which have been the subject of numerous papers [10-11], mainly aimed to reduce the initial investment cost. For our project, all relevant system elements have been dimensioned by the manufacturer with the best up to date selling price. So, one SQFlex solar pump with internal inverter and CU 200 SQFlex controller, and three Helios Technology's solar photovoltaic modules have been purchased. The system has been designed so as to yield the surface water for irrigation in the dry season as it is shown by Fig. 1.

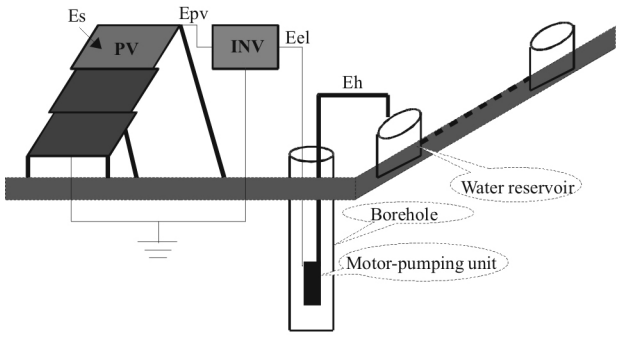

Fig. 1. *Schematic diagram of configuration system*

System analysis

The actual project has been analysed using RETScreen International software, the nominal operating cell temperature being 45 °C with efficiency of 13.3 %. The groundwater availability has been assumed to be sufficient for irrigation according to the agriculture expert's report [2]. The results are shown in Table 1 below, for the month of February.

Table 1
Performance of the system in the month of February

Mean daily production of water Q_D (m^3/day)	6
Total head lift including the head friction loss H_T (m)	24.5
Maximum flow rate Q_{max} (m^3/h)	1.1
Mean daily hydraulic energy E_H (kW·h/day)	0.4
Mean daily solar radiation on PV panel E_S (kW·h/m^2/day)	6.41
Tilt angle of the PV panel θ (deg)	9
Nominal electric power of the PV panel P_{el} (kWp)	0.18
Surface of the PV panel S_{PV} (m^2)	1.3
Total efficiency of the photovoltaic pumping system η (%)	4.6
Daily minimum temperature of photovoltaic solar cells $Tcell_{min}$ (°C)	28
Daily maximum temperature of photovoltaic solar cells $Tcell_{max}$ (°C)	65

Economic analysis

Few of the farmers in the Marza area use diesel pump units for irrigation in dry season. An inquiry has been opened on them, aimed to know if this irrigation technique is profitable; but no answer was registered. However, we assume that an assessment of the affordable means by farmers to invest in a photovoltaic water pumping project can be made by a comparison with a diesel pump unit taken as a reference within the RETScreen International software. The results are presented in Table 2 below.

Table 2
Economic analysis of the project (1 € = 655,957 XAF)

Investment cost.	
Feasibility studies (XAF)	50,000
Engineering (XAF)	350,000
Photovoltaic equipment (XAF)	852,000
Pump unit and closely related infrastructure (XAF)	2,279,745
Miscellaneous (XAF)	349,270
Total investment cost (XAF)	3,881,015
Financial parameters	
Paid-up capital (XAF)	1,552,406
Loan (XAF)	2,328,609
Loan duration (year)	4
Interest-loan (%)	15
Payment of loan (XAF/year)	815,631
Annual savings (XAF/year)	772,810
Total interest-loan (XAF)	933,915
Total payment of loan (XAF)	3,262,524
Rate of return on investment (year)	6.23

Discussion

The temperature dependence on the efficiency of photovoltaic solar cells has been the subject of numerous papers based on numerical simulations [12-16]. The high daily temperature (65 °C) of photovoltaic solar cells (Table 1) really affect the daily production of renewable energy and that remains a great preoccupation in the field of experimental research. In fact, RETScreen International software does not allow us to find out the effect of temperature higher than the nominal operating value on photovoltaic solar cells. Anyway, the manufacturer has found the same nominal electric power of photovoltaic array as the one in Table 1 for a daily water production of 6 m^3 at the head lift of 24.5 m. So, the proposed simplest configuration system for irrigation may operate well in the optimal conditions. However, a malfunction of the system could occur at the cell temperature higher than the nominal operating value.

The actual project has been awarded by the French cooperation in Cameroon (Comètes project) [17] in the frame of a call for proposal dealing with finalized research in the laboratories of the Cameroon Technology Institutes and Engineering School. The detailed expenses in the Table 2 are aimed to prove the affordable means by farmers to invest in the photovoltaic water pumping projects. It is obvious that a few group of farmers can afford 40 % of the total investment cost, the balance of 60 % corresponding to a loan with 15 % interest. The rate of return on investment is less than 7 years.

Conclusion

In the Marza area (Adamawa province), a few farmers having access to sufficient surface water for irrigation in dry season may considerably increase their income from agricultural activities. Unfortunately, large farmable areas are not worked in dry season because of the lack of sufficient surface water and also, the lack of modern technological knowledge by farmers in the field of irrigation.

To overcome these problems, the CESAM method is adapted to design a photovoltaic water pumping system for irrigation in the state-of-the-art, according to the farmers' needs. A system analysis using the RETScreen International software has yielded convincing results so that the farmers could afford to invest in the photovoltaic water pumping projects for irrigation. Another factor affecting the valorization of this technology is the lack of interface between the researchers and the potential users of research results. As a solution, an experimental agricultural structure is built up at the Mgr. Yves Plumey's foundation in Ngaoundere, where large farmable areas and groundwater are available.

In perspective, the effect of high daily temperature (65 °C) of photovoltaic solar cells which really affects the daily production of renewable energy will be a great preoccupation in the field of experimental research.

Acknowledgements

The authors would like to acknowledge the support of French cooperation in Cameroon through the Comètes project.

References

1. World Bank, 2000a. African Development Indicators 2000. World Bank, Washington, 2000.

2. Contract №07-1/C/06/MINADER/PARFAR. Programme d'amélioration du revenu familial rural dans les provinces septentrionales (P.A.R.FA.R). B.P. 1805 Garoua, Cameroun. E-mail: parfarmcm@yahoo.fr, 2006.

3. World Bank. Power supply to agriculture, Vol. 1. Report no. 22171-IN. World Bank, Washington DC, 2001.

4. Atul Kumar, Tara C. Kandpal. Renewable energy technologies for irrigation water pumping in India: A preliminary attempt toward potential estimation // Energy. 2007. Vol. 32. P. 861-870.

5. Marouze C. Proposition d'une méthode pour piloter la trajectoire technologique des équipements dans les pays du sud. Application au secteur agricole et agroalimentaire. Paris: "ENSAM", 1999.

6. Anon. Approches participatives, décentralisation et participation. Priorité aux producteurs. Spore CTA, No. 99. 2002.

7. Anon. Etude des potentiels techniques et économiques de la transformation primaire des tubercules vivriers dans la région de l'Afrique de l'Ouest. Etude exploratoire au Bénin. Rapport CFD, 1998.

8. RETScreen International. Centre d'aide à la décision sur les énergies propres. Canada. www.retscreen.net, 2004.

9. Champ G. Energies Nouvelles Entreprises. Grundfos. Mas d'Eole-St Come, 2007.

10. Glasnovic Z., Margeta J. A model for optimal sizing of photovoltaic irrigation water pumping systems. Solar Energy. 2007. Available online at www.sciencedirect.com.

11. Vilela O.C., Bione J., Fraidenraich N. Simulation of grape culture irrigation with photovoltaic V-trough pumping systems // Renewable energy. 2004. Vol. 29. P. 1697-1705.

12. Meneses R.D., Horley P.P., Gonzalez H.J., Vorobiev Y.V., Gorley P.N. Photovoltaic solar cells performance at elevated temperatures // Solar Energy. 2005. Vol. 78. P. 243-250.

13. Pacca S., Sivaraman D., Keoleian G.A. Energy Policy. 2006. Article in press.

14. Mattei M., Notton G., Cristofari C., Muselli M., Poggi P. Calculation of the polycrystalline PV module temperature using a simple method of energy balance // Renewable Energy. 2006. Vol. 31, No. 4. P. 553-567.

15. Chenni R., Makhlouf M., Kerbache T., Bouzid A. A detailed modeling method for photovoltaic cells // Energy. 2005. Available online at www.sciencedirect.com.

16. Hove T. A method for predicting long-term average performance of photovoltaic systems // Renewable Energy. 2000. Vol. 21. P. 207-229.

17. Comètes: Cooperation and Modernization of the Cameroon Technological Universities and Institutes, www.projetcometes.org.

COUPLED UTILIZATION OF SOLAR ENERGY AND LOCAL MATERIALS IN BUILDING

H. Kazeoui, A. Tahakourt*, A. Ait-Mokhtar**, R. Belarbi***

*Laboratory of Technology of Materials and Engineering Process (LTMGP), University A. Mira
Targa Ouzemour, Bejaia, 06000, Algeria
Tel: 00 213 34 21 45 01; Fax: 00 213 34 21 60 98; E-mail: hkazeoui@yahoo.fr

**Laboratory of Study of Transfer Phenomena Applied to Buildings (LEPTAB), University of La Rochelle
Av. Michel Crépeau 17042 La Rochelle cedex, France
Tel: +33 (0) 5 46 45 72 39; Fax: + 33 (0) 5 46 45 82 4; E-mail: karim.ait-mokhtar@univ-lr.fr

Received: 16 Oct 2007, accepted: 2 Nov 2007

The aim of this study is to present possibilities of associating the solar energy with local materials in buildings under the Mediterranean climate since the solar energy is a renewable, economical and not pollutant energy, the local materials offer comfort to users, protect the environment and have a low price. The performances of the Direct Solar Floor (DSF) are presented. This method of proceeding is one of the most used solutions in the solar heating field. The application of this method in the south Mediterranean side could bring about interesting results with respect to the importance and availability of the solar bearing. The effects are not only relevant to the energy saving or the thermal comfort that the DSF procures, but include also the environmental aspects of quality. One example of study carried on an experimental cell equipped with the DSF in the west of Algeria is presented. A behavior model of DSF was realized and integrated in the computing simulation system TRNSYS. The results obtained are very promising because the heating and the warm sanitary water needs are satisfied at more than 60 % with an area ratio captor/ground = 0.1. These results are then compared to the other results obtained from equipment realized in France in order to estimate the solar bearing influence on this type of system.
On the other hand the incorporation of local materials, especially those based on the stabilized clay in cold conditions, in the building is an important element of thermal comfort. Simulations were carried out on a building of a given design by changing the building materials. These simulations show clearly the supply of comfort in terms of thermal stability, surrounding conditions and building energetic needs. Thus, the coupling system DSF/ local materials will certainly allow to improve the building energy performances, hence the reduction of the user's energy bill.

Keywords: solar buildings, heating, direct solar floor, heating needs, local materials, thermal comfort

Abdelkader Tahakourt

Diplome: Doctorat Thesis at The National Institute of Applied Science, (INSA) Rennes, France, July, 1992.
Education: Professor of Bejaia University since 1993.
Main range of scientific interests: reinforced concrete, heat transfer, thermal modelling in building.
Experience: Head of "Construction Materials team" at the LTMGP laboratory.
Research fields: heat transfer in building and local materials.
Publications: in Revue Générale de Thermique (now: International Journal of Thermal Science).

Abdelkarim Ait-Mokhtar

Diplome: Doctorat Thesis at The National Institute of Applied Science, (INSA) Rennes, France, January, 1993.
Education: Professor of La Rochelle University since 1994.
Main range of scientific interests: construction materials, behaviour laws of materials, diffusion through porous media.
Experience: Head of "Construction Materials team" at the LEPTAB laboratory.
Research fields: mass and aggressive agents transfer in porous materials, with application to the durability of materials and constructions. Development of new construction materials.
Publications: Publications in many international scientific journals.

Introduction

The European energetic bill in the building sector represents 40.7 % of the total energetic expenses. Besides, the heating of the residential premises represents the biggest part of the energy consumed for the house keepings of the European state members (57 %) followed by the production of domestic hot water needs (25 %) [1]. Also, the improvement by one point per year (1 %) of the energetic intensity in the final consumption will lead into more than 55 Mtep of economy over the whole energy consumption in the building sector. This leads to avoid 100 million tons of CO_2 emission per year; a quantity representing 20 % of EU commitment kept in Kyoto.

In order to reduce the energetic consumption in buildings and to improve the quality environmental aspect and the thermal comfort, several studies have been carried out [2-6]. To contribute to this research work, the energetic performance of a direct solar floor (DSF) system and local materials in building in the south-Mediterranean climate has been analysed. The reasons of our interest in the heating techniques by DSF are the large advantages such as availability of the solar energy in Algeria [7]; a uniform temperature so there is no cold or hot area [8], simple and not encumbering system contrarily to the classical solar heating systems, free energy.

Furthermore, the use of local materials known for their thermal and hygrometrical properties (absorption and adsorption of steam present in the ambient medium) allows to the indoor ambient conditions to be regulated (temperature, moisture), thus providing comfort for the occupiers [9].

The present work constitutes the first step of the study centred on the evaluation of a DSF performance using local materials. The aim of this phase is to show the impact of these two processes on the building comfort, the air quality and the energy consumption.

On one hand, an evaluation of DSF performance was realized (through a comparative study over two sites with different climates); on the other hand, an evaluation of the influence of using local materials was carried out (through a study on two buildings; one commonly used in current constructions with standard materials such as concrete and the other with bioclimatic architectural design in which the envelope is made of local materials.

Direct solar floor

The technique of heating using heating floors with hot water is particularly well adapted to low temperatures generators (high output boiler, condensation boiler, heating pump, solar collectors). In France, more than 20 % of the new houses use this technique for domestic hot water needs. However, this proportion remains small compared to other European countries (40 % in Germany and 50 % in Switzerland) [1].

The physical phenomena governing the thermal behaviour of the solar direct heating floor are difficult to approach, because of the inertia emitter and the coupling between the direct solar floor input and radiance input of transparent surfaces. In order to conduct this study, a bidimensional model of the DSF was developed [10, 11] and integrated in the TRNSYS environment [12]. The model is obtained after dividing the floor into a multitude of unites and nodes. The writing of equations of thermal assessment for the different nodes leads to a complex system of non linear equations. The problem solving is done by using thermal response factors method. The meshes system adopted is the one of a bidimensional model with finite differences (Fig. 1). This method considers linear thermal exchanges (conduction, convection and radiation) and assumes invariant character of the couple excitations/responses where the same reasons produce the same effects.

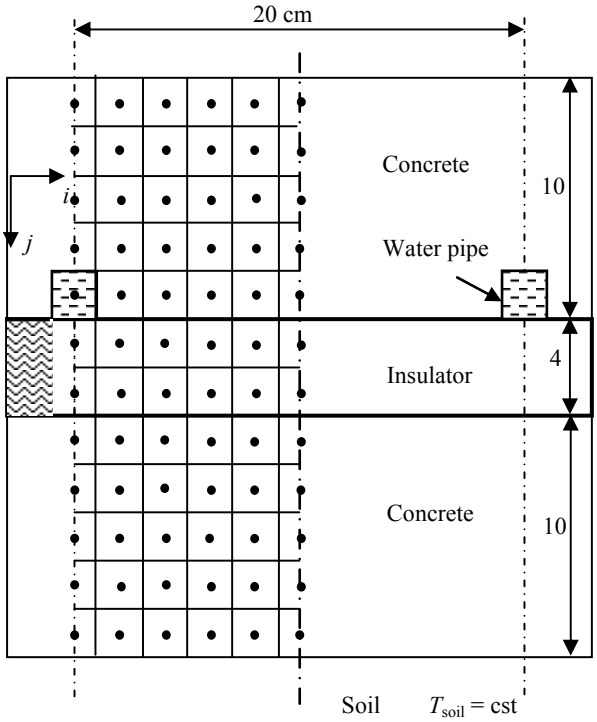

Fig. 1. *Meshing scheme of the model*

The response factors method principle consists in following the evolution of the system response to a triangular or rectangular excitation (Fig. 2). The unitary triangular excitation response is sampled following a time step taken usually equal to an hour.

So, we obtain a series of discrete values. Since the system is linear, the superposition of effects is adopted. Thus, each sollicitation can be decomposed into a series of discrete triangular elements and the system response will be the sum of responses corresponding to each triangular solicitation. For the direct solar floor, the excitations to consider are of four types: air temperature, floor surface temperature, injected power in pipes and absorbed solar flow on surface. The response factors are numerically calculated using the differences method with

alternated directions (ADI) [13]. In this method, Δt is divided to two time steps. In first time step, $T^{t+\Delta t/2}$ is calculated, implicitly according to x and explicitly according to y. In the second one, $T^{t+\Delta t}$ is calculated implicitly according to y and explicitly according to x. Such a method is unconditionally convergent.

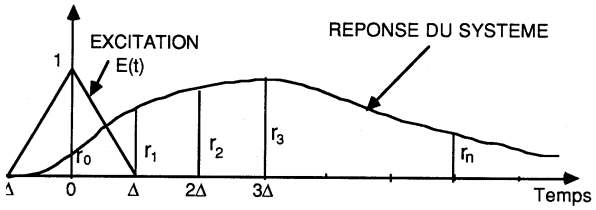

a

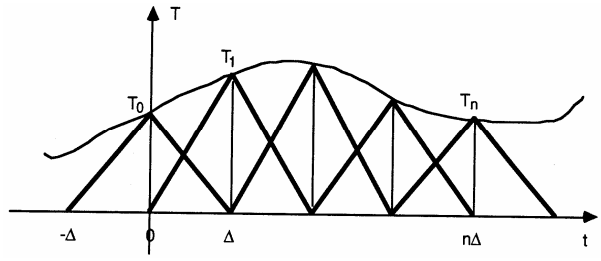

b

Fig. 2. *The principle of the method of the response factors: a – sampling of the response to a triangular unitary solicitation; b – decomposition of the solicitation into triangular elements*

Theoretical analysis

An orthogonal mishe of Δx and Δy dimensions is used (Δx and Δy variable). Thermal energy balance equations are written for the different floor nodes.

The basic equation of heat transfer in bidimensional model is written:

$$\frac{\partial^2 T}{\partial x^2}+\frac{\partial^2 T}{\partial y^2}=\frac{1}{a}\frac{\partial T}{\partial t};$$

$$\frac{\partial^2 T}{\partial x^2}=\frac{1}{\Delta x}\left[\frac{T^t_{(i+1,j)}-T^t_{(i,j)}}{\Delta x}+\frac{T^t_{(i-1,j)}-T^t_{(i,j)}}{\Delta x}\right];$$

$$\frac{\partial^2 T}{\partial x^2}=\frac{1}{\Delta x^2}\left[T^t_{(i+1,j)}-2T^t_{(i,j)}+T^t_{(i-1,j)}\right];$$

$$\frac{\partial^2 T}{\partial y^2}=\frac{1}{\Delta y^2}\left[T^t_{(i,j+1)}-2T^t_{(i,j)}+T^t_{(i,j-1)}\right];$$

$$\frac{\partial T}{\partial t}=\frac{T^{t+\Delta t}_{(i,j)}-T^t_{(i,j)}}{\Delta t},$$

where a – material diffusivity: $a = \lambda/\rho c$, where λ – thermal conductivity, c – specific heat, ρ – density, Δt – time step.

**** Interior nodes (concrete, insulator, soil)***

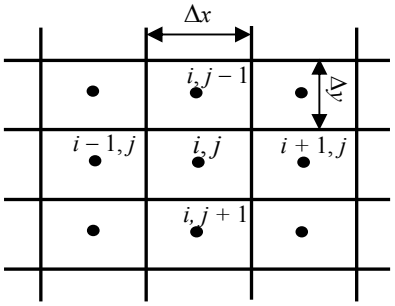

For (i, j) node, the following equation is obtained:

$$\frac{T_{(i,j)}\left(t+\frac{n\Delta t}{2}\right)-T_{(i,j)}\left(t+\frac{(n-1)\Delta t}{2}\right)}{\Delta t/2}=$$
$$=\frac{a}{\Delta x^2}\left[T_{(i+1,j)}-2T_{(i,j)}+T_{(i-1,j)}\right]+$$
$$+\frac{a}{\Delta y^2}\left[T_{(i,j+1)}-2T_{(i,j)}+T_{(i,j-1)}\right]; \qquad (1)$$

n values are 1 then 2.

$\underline{n = 1}$:

$$-\frac{a}{\Delta x^2}T_{(i+1,j)}\left(t+\frac{\Delta t}{2}\right)+\left(\frac{2a}{\Delta x^2}+\frac{2}{\Delta t}\right)T_{(i,j)}\left(t+\frac{\Delta t}{2}\right)-$$
$$-\frac{a}{\Delta x^2}T_{(i-1,j)}\left(t+\frac{\Delta t}{2}\right)=\frac{a}{\Delta y^2}T_{(i,j+1)}(t)+$$
$$+\left(\frac{-2a}{\Delta y^2}+\frac{2}{\Delta t}\right)T_{(i,j)}(t)+\frac{a}{\Delta y^2}T_{(i,j-1)}(t),$$

$\underline{n = 2}$:

$$-\frac{a}{\Delta y^2}T_{(i,j+1)}(t+\Delta t)+\left(\frac{2a}{\Delta y^2}+\frac{2}{\Delta t}\right)T_{(i,j)}(t+\Delta t)-$$
$$-\frac{a}{\Delta y^2}T_{(i,j-1)}(t+\Delta t)=\frac{a}{\Delta x^2}T_{(i+1,j)}\left(t+\frac{\Delta t}{2}\right)+$$
$$+\left(\frac{-2a}{\Delta x^2}+\frac{2}{\Delta t}\right)T_{(i,j)}\left(t+\frac{\Delta t}{2}\right)-\frac{a}{\Delta x^2}T_{(i-1,j)}\left(t+\frac{\Delta t}{2}\right).$$

**** Nodes on symmetry axes:***

Nodes on axis of symmetry of pipes

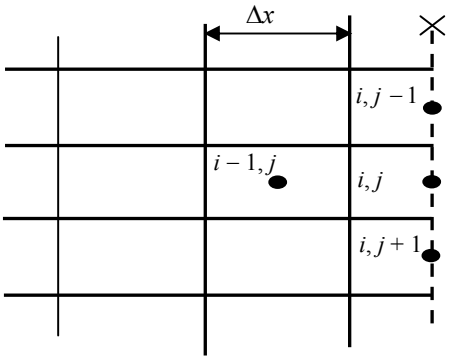

$$\frac{T\left(i,j\left(t+\frac{n\Delta t}{2}\right)-T\left(i,j\left(t+\frac{(n-1)\Delta t}{2}\right)\right.\right.}{\Delta t/2}=$$

$$=\frac{a}{\Delta x^2}\left(T_{(i-1,j)}-T_{(i,j)}\right)+\frac{a}{\Delta y^2}\left(T_{(i,j-1)}-2T_{(i,j)}+T_{(i,j+1)}\right)$$

Nodes along pipes

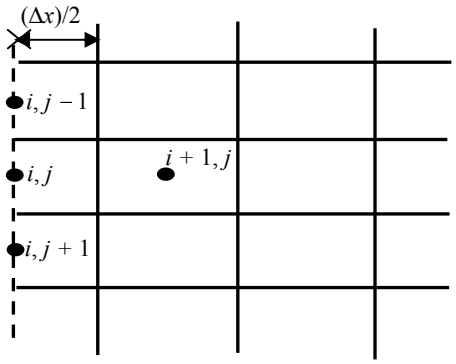

$$\frac{T_{(i,j)}\left(t+\frac{n\Delta t}{2}\right)-T_{(i,j)}\left(t+\frac{(n-1)\Delta t}{2}\right)}{\Delta t/2}=$$

$$=\frac{a}{\Delta x^2}\left(T_{(i+1,j)}-T_{(i,j)}\right)+\frac{a}{\Delta y^2}\left(T_{(i,j-1)}-2T_{(i,j)}+T_{(i,j+1)}\right)$$

**** Surfaces floor nodes***

These nodes are characterized by a limit condition of Dirichlet (imposed surface temperature) or of Fourier (imposed ambient temperature and conductance). When the floor rests on soil, the temperature of soil is considered constant.

Upper surface

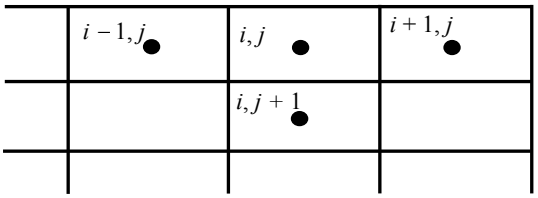

$$\frac{T_{(i,j)}\left(t+\frac{n\Delta t}{2}\right)-T_{(i,j)}\left(t+\frac{(n-1)\Delta t}{2}\right)}{\Delta t/2}=$$

$$=\frac{a}{\Delta x^2}\left[T_{(i+1,j)}-2T_{(i,j)}+T_{(i-1,j)}\right]+$$

$$+\frac{1}{\Delta y}\left[\frac{a}{\Delta y}T_{(i,j+1)}-\left(\frac{a}{\Delta y}+\frac{2a}{\Delta y+2\frac{\lambda}{h}}\right)T_{(i,j)}+\frac{2a}{\Delta y+2\frac{\lambda}{h}}T\right], \quad (2)$$

where T – imposed temperature (surface temperature or ambient temperature).

When a surface temperature is imposed, the equation (2) remains valid on condition to take a large value of h ($\lambda/h \to 0$).

Surface below

$$\frac{T_{(i,j)}\left(t+\frac{n\Delta t}{2}\right)-T_{(i,j)}\left(t+\frac{(n-1)\Delta t}{2}\right)}{\Delta t/2}=$$

$$=\frac{a}{\Delta x^2}\left[T_{(i+1,j)}-2T_{(i,j)}+T_{(i-1,j)}\right]+$$

$$+\frac{1}{\Delta y}\left[\frac{a}{\Delta y}T-\left(\frac{a}{\Delta y}+\frac{2a}{\Delta y+2\frac{\lambda}{h}}\right)T_{(i,j)}+\frac{2a}{\Delta y+2\frac{\lambda}{h}}T_{(i,j-1)}\right]$$

**** Nodes in concrete-insulator interface***

It concerns the nodes situated in concrete (or insulator) which change heat with the nodes situated in insulator (or in concrete). The case of nodes in concrete is developed below.

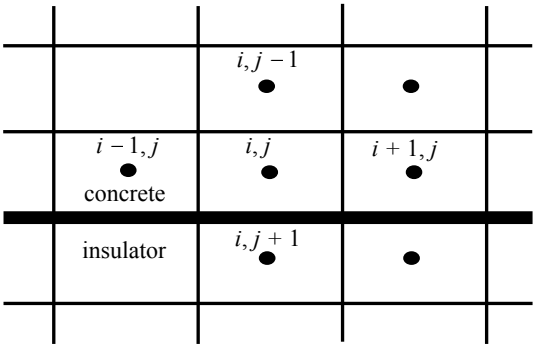

Thermal resistance concrete-insulator:

$$R_1=\frac{\Delta y/2}{\lambda_1}+\frac{\Delta y/2}{\lambda_2}=\frac{\Delta y}{2}\left[\frac{1}{\lambda_1}+\frac{1}{\lambda_2}\right]=\frac{\Delta y}{2}\frac{\lambda_1+\lambda_2}{\lambda_1\lambda_2},$$

where λ_1 – thermal conductivity of concrete, λ_2 – thermal conductivity of insulator.

The conductance K_1

$$K_1=\frac{1}{R_1}=\frac{2\lambda_1\lambda_2}{\Delta y(\lambda_1+\lambda_2)}$$

The energy balance for these nodes:

$$\frac{T_{(i,j)}\left(t+\frac{n\Delta t}{2}\right)-T_{(i,j)}\left(t+\frac{(n-1)\Delta t}{2}\right)}{\Delta t/2}\rho_1 c_1\Delta x\Delta y=$$

$$=\frac{\lambda_1}{\Delta y}\Delta x\left[T_{(i,j-1)}-T_{(i,j)}\right]+\frac{2\lambda_1\lambda_2}{\Delta y(\lambda_1+\lambda_2)}\Delta x\left[T_{(i,j+1)}-T_{(i,j)}\right]+$$

$$+\frac{\lambda_1}{\Delta x}\Delta y\left[T_{(i-1,j)}-2T_{(i,j)}+T_{(i+1,j)}\right],$$

$$\frac{T_{(i,j)}\left(t+\frac{n\Delta t}{2}\right)-T_{(i,j)}\left(t+\frac{(n-1)\Delta t}{2}\right)}{\Delta t/2}=$$

$$=\frac{a_1}{\Delta y^2}T_{(i,j-1)}-\left[\frac{2a_1\lambda_2}{\Delta y^2(\lambda_1+\lambda_2)}+\frac{a_1}{\Delta y^2}+\frac{2a_1}{\Delta x^2}\right]T_{(i,j)}+$$

$$+\frac{a_1}{\Delta x^2}\left[T_{(i-1,j)}+T_{(i+1,j)}\right]+\frac{2a_1\lambda_2}{\Delta y^2(\lambda_1+\lambda_2)}T_{(i,j+1)}.$$

**** Nodes in contact with water pipe***

The water temperature T_F is considered constant $T_F=\frac{T_E+T_S}{2}$, where T_E, T_S are respectively inlet and outlet water temperature in pipe.

These nodes change heat with water through the pipe. The expression of the conductance K_1 between water and the node (i, j) in concrete (or in insulator K_2) is given as a function of convection coefficient in water h and concrete (or in insulator) thermal resistance R.

$$K_1=\frac{1}{R_1},\quad R_1=\frac{1}{h}+\frac{e_t}{\lambda_t}+\frac{\Delta x}{\lambda_1},\ h=\frac{Nu\cdot\lambda_3}{D},$$

where e_t – pipe thickness, λ_t – pipe conductivity, Nu is Nusselt number which is calculated as a function of Reynolds Re and Prandt Pr numbers, pipe length and internal diameter.

The thermal balance for (i, j) node in concrete is:

$$\frac{T_{(i,j)}\left(t+\frac{n\Delta t}{2}\right)-T_{(i,j)}\left(t+\frac{(n-1)\Delta t}{2}\right)}{\Delta t/2}\rho_1 c_1\Delta x\Delta y=$$

$$K_1\Delta y\left[T_F-T_{(i,j)}\right]+\frac{2\lambda_1\lambda_2}{\Delta y(\lambda_1+\lambda_2)}\Delta x\left[T_{(i,j+1)}-T_{(i,j)}\right]+$$

$$+\frac{\lambda_1}{\Delta x}\Delta y\left[T_{(i+1,j)}-T_{(i,j)}\right]+\frac{\lambda_1}{\Delta y}\Delta x\left[T_{(i,j-1)}-T_{(i,j)}\right].$$

Local materials

The thermal behaviour of traditional houses using clay-based local materials "adobe" was analysed [9]. So, the thermal and mechanical characterization of these materials was realized, in addition a simplified model of the material behaviour was used. The traditional material characteristics used in the simulation were measured in the laboratory on the adobe samples with the following composition; 100 g of clay, 10 g of ACP-CEMI 52.5 (stabilizing agent) and 2 g of straw with a ratio water/clay = 50 %.

The performances of this type of house were compared to those obtained with a "modern" house using brick walls.

Results and discussion

Direct solar floor

For a better approach of the feasibility of the DSF, we have compared its performance using two climatic sites; Oran (Algeria) and Carpentras (France) sites [14, 15]. The simulated building represents an experimental cell composed with two rooms of the same dimensions but only one is equipped with DSF, the second one is considered as a reference room. Concerning the floor, we used two heating slabs of reinforced concrete (10 cm) separated with a layer of polystyrene (4 cm) where the network of pipes is put directly on the insulating material [10].

The simulations results show that in Oran, the rate of the solar coverage is about 64 % (heating HEA and domestic hot water DHW) with a collecting ratio about 0.1. In this case, the additional energy to supply is only about 36 % of the needs (Fig. 3). This coverage goes up to 89 % with a collecting ratio equal to 0.2 against 45 % for the French climate; that is to say about 50 % fewer (Fig. 4).

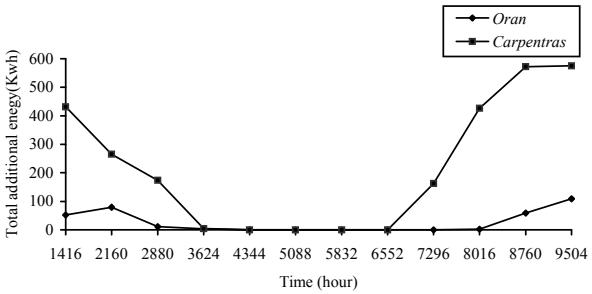

Fig. 3. *The evolution of the necessary additional energy quantity in the two regions; Oran and Carpentras*

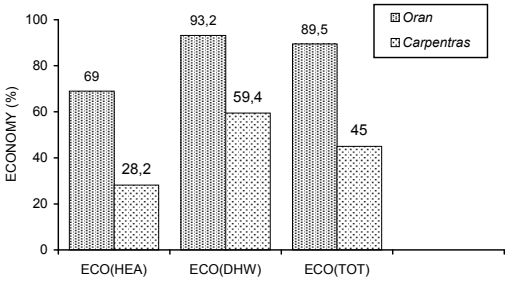

Fig. 4. *The evolution of the solar coverage in the two regions (collecting ratio = 0,2)*

Concerning free temperature evolution (without auxiliary system), we notice that the internal temperature close the comfort temperature (Fig. 5). So, we can forward that DSF heating technique applies in the southern Mediterranean climate.

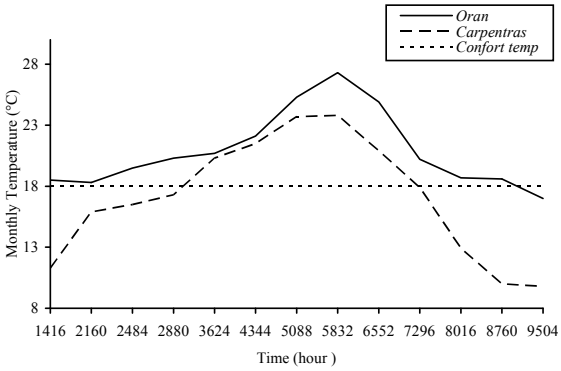

Fig. 5. *Free evolution of internal temperature with DSF only*

Another installation which has been realized in "Chartres de Bretagne" (west of France) [12], shows that for oceanic climate, where the diffused radiance is predominant, the energetic bill is covered at 40 %. The follow up of the installation performances was realized for two consecutive periods of heating on a house built on earth platform and having one floor under roof. The south façade consists of 15 m^2 glasshouse. The DSF system was installed in both floors (platform and floor). The solar collectors are of 12.15 m^2 (collecting ratio equal to 0.1) and are built-in the south roof. The Fig. 6 summarizes the installation energy balance. In summer, the installation supplies 100 % of domestic hot water, so, the annual thermal production is about 416 Wh per 1 m^2 of collectors.

The results show the influence of solar potential on the energetic needs cover of buildings, hence the interest in the use of DSF as an alternative heating solution.

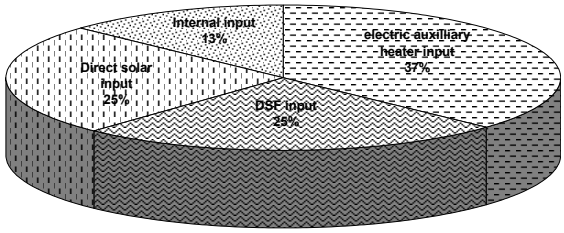

Fig. 6. *Repartition of different sources of energy contributions*

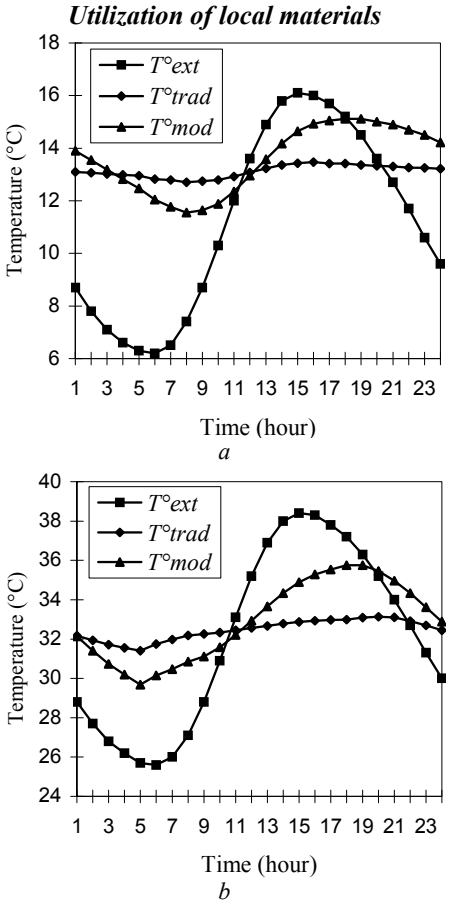

Fig. 7. *Temperature evolution in the two buildings: a – typical January day; b – typical August day*

Simulations were carried out on two buildings with the same habitable area, one with a traditional architecture using local materials like adobe, the other one with a modern architecture (classic flat) [9]. The results are presented for two typical days: wintry and summery. It is necessary to point that no heating system was used.

Analysing the free external and internal temperatures evolution (Fig. 7), we have observed that the traditional house presents better insulating and thermal comfort in summer. However, it is necessary to heat in winter in order to reach the comfort temperature.

he humidity evolution (Fig. 8) is more stable in summer. Its level, lower than the one in modern house, shows the possibilities of utilization of passive cooling systems.

We conclude that, by using local materials, the internal temperatures and relative humidity are almost constant and are close to the building comfort conditions.

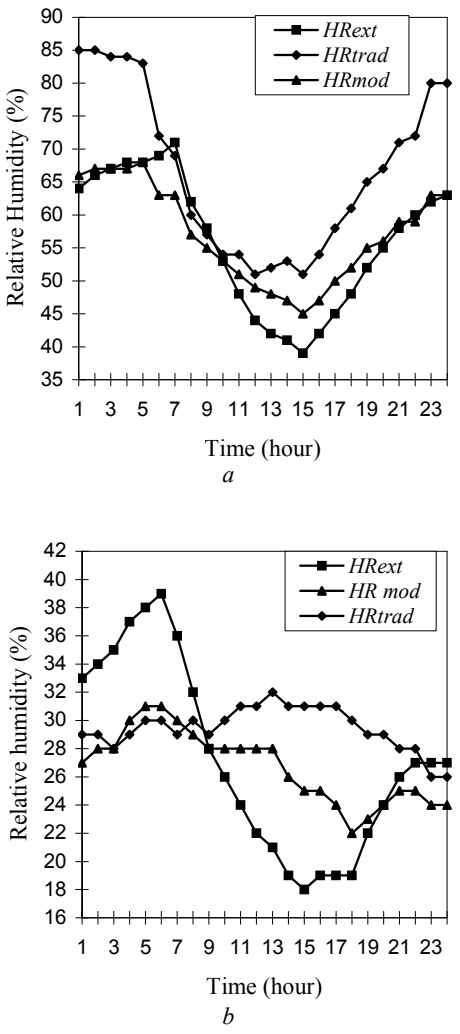

Fig. 8. *The evolution of relative humidity in the buildings: a – typical January day, b – typical August day*

Coupled utilization of direct solar floor and local materials

The interesting results on the solar cover rate of DSF system with a ratio of 0.1 on one hand, and the thermal comfort without conditioning during summer and a small contribution of heating during winter using local materials on the other hand, lead us to the idea of coupling both systems to assure the thermal comfort with lesser cost and above all to protect the environment. We test this system by using the DSF in a building with local materials (traditional building) on one hand and with brick walls (modern building) on the other hand. The data used are those of Bechar city.

Internal temperatures and thermal comfort

The temperatures obtained in the traditional building change very little. The difference between the maximal temperatures and the minimal one is about 2 °C during the coldest week compared to 4 °C in the second building (Fig. 9, *a*). During the very coldest day where the average external temperature recorded is 4.75 °C, we noted 16.16 °C in the modern building and only 11.96 °C in the other one (Fig. 9, *b*).

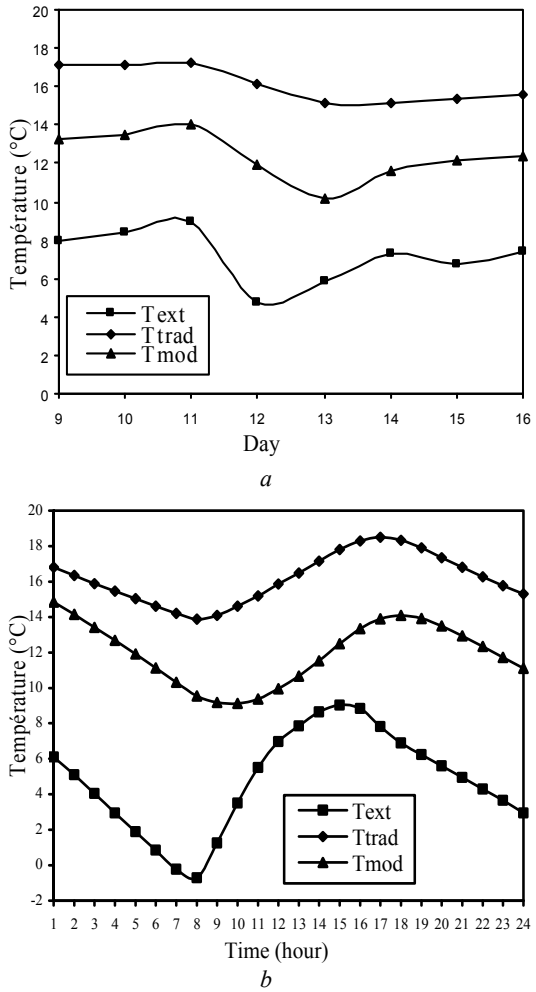

Fig. 9. *Temperature evolution in the two buildings with DSF: a – 9 to 16 January week, b – 12 January day*

We also compared internal temperatures before and after using DSF in both buildings (Fig. 10). We saw that the DSF brings a distinct improvement of comfort conditions in the traditional house (Fig. 10, *a*) where the increase in temperature reached 6 °C against only 3 °C in the second one (Fig. 10, *b*). This is due to the inertia effect of the adobe which has an important storage potential. This permits it to accumulate heat and to release it to the internal ambiance when the external temperature decreases. With bricks materials, the internal temperature evolution follows, without redemption, the external temperature fluctuations.

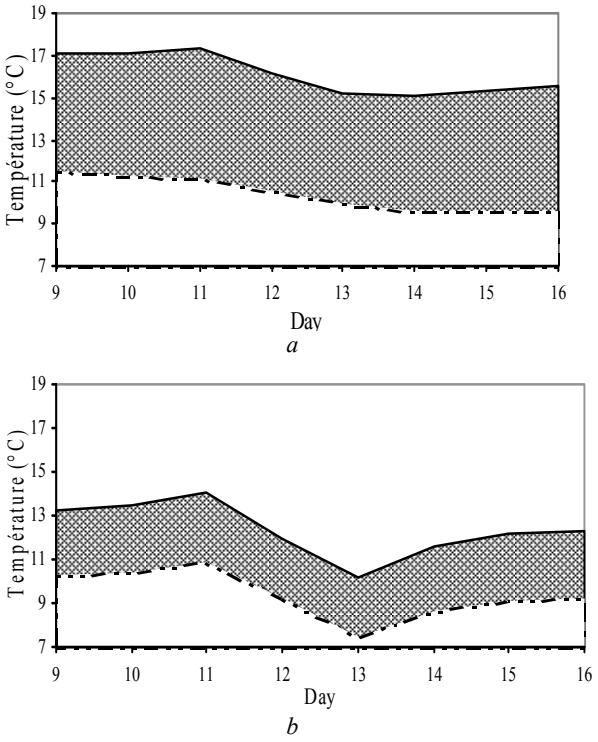

Fig. 10. *Temperature evolution in the two buildings before and after DSF incorporation: a – traditional building, b – modern building*

Performance and energetic saving

We also analysed the influence of coupled utilization of DSF and local materials on energy saving. We noted solar cover rates (COS) varying from 60 to 100 % (Fig. 11). During April month, the difference noted is about 47 % between the tow buildings. In the same way, cooling needs during summer were evaluated. Concerning the hottest month, the needs are three times as big in modern building (Fig. 12). We come back to the storage capacity of adobe which stores coolness during night and releases it during day. This particularity shows that the construction with adobe walls is particularly adapted to climates which have great difference between diurnal and nocturnal temperatures.

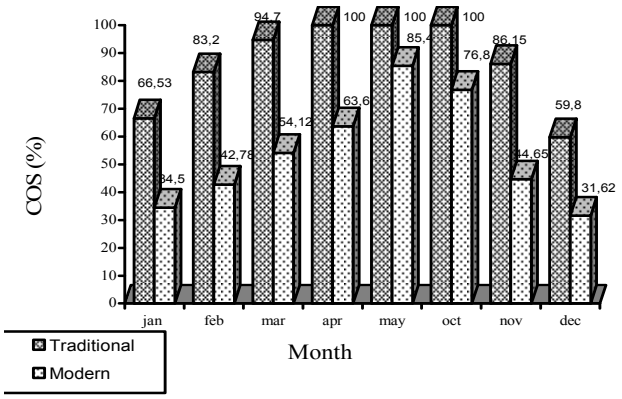

Fig. 11. *Evolution of heating saving brought by using DSF in the two buildings*

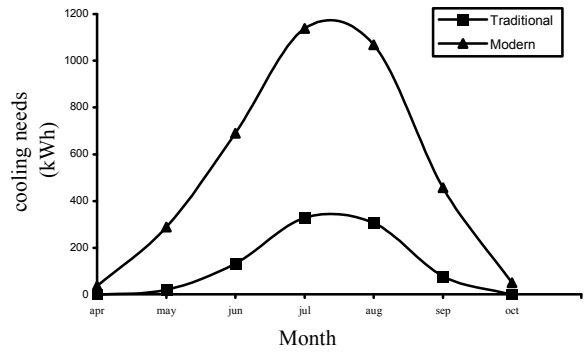

Fig. 12. *Evolution of cooling needs in the two buildings*

Conclusion

The results obtained for systems, direct solar floor and the utilization of local materials, put in evidence a lot of information. Indeed, in desert regions, construction using local materials offers better insulation and comfort during summer than the modern materials.

Also, the passive systems of cooling seem to adapt easily this type of construction.

The results obtained on the three installations of the same type showed the important role played by the solar bearing in the case of the direct solar floor heating. Excellent performance was obtained in Algeria with solar cover rates reaching 90 %. The simultaneous use of the two techniques underlined the interest of this solution in order to reduce energy use in buildings and ameliorate comfort conditions in hot climates. Also, it is imperative to pay attention to the choice of materials according to climatic data in the conception phase of buildings.

References

1. CEE report, Directive proposition European parliament and council about the energetic performance of buildings, Brussels 11/05/2001.

2. Sockolay S.U. Climate analysis based on the psychometric chart // International Journal of Ambient Energy. Vol. 7, No. 4. October 1986. Australia.

3. Givoni B. Man, climate and architecture. Second edition // Applied Sciences Publication, London, 1976.

4. Santamouris M. (Coordinator). Natural Cooling Techniques. Design Methodology and Application to Southern Europe. Pascool Final Report, European Commission, Directorate General XII For Science Research and Development, edited in 1995.

5. Belarbi R., Allard F. Atlas of natural cooling techniques application of evaporative cooling system. Second European Conference on Energy Performance and Indoor Climate in Buildings (EPIC'98), Lyon, November 1998.

6. Belarbi R. Développement d'outils méthodologiques d'évaluation et d'intégration des systèmes évaporatifs pour le rafraîchissement passif des bâtiments. Thèse de Doctorat Université de La Rochelle (France), July 1998.

7. Lalonde B. Du neuf sous le soleil // Solar systems revue. 64-65 (1991).

8. Jean A., Papillon P. Direct solar floor development. Journeys "Thermal Solar". Paris, October 1994.

9. Benhabib R., Ait-Mokhtar A., Allard F. Bioclimatic analysis of traditional houses in the north-Sahara regions.

10. Kazeoui H. Direct solar floor influence on the conditioning of buildings in Maghreb context. Magister Thesis, USTO (Algeria) 1997.

11. Tahakourt A. The study of the thermal behaviour of direct solar floors in the transient regime using the response factors method: experimental validation. Doctorate Thesis, INSA Rennes, France, 1992.

12. TRNSYS, Transient simulation system. Software of thermal simulation of buildings. University of Madison (Wisconsin, USA).

13. Larbi Youcef M.H. Contribution à l'étude d'un PSD sur terre-plein. Thèse de Doctorat, INSA Toulouse, 1987.

14. Kazeoui H., Mokhtari A., Achard G., Boukezzi Y. Climatic conditioning of buildings in the Maghrebin context: Direct solar floor for heating / Hydraulic floor for cooling. 8th international days of thermic (JITH), Marseille, July, 1997.

15. Papillon P. Contribution to the amelioration of direct solar floor technique. The analyses of thin slabs solution and optimized management of auxiliary heating. Doctorat thesis. University of Savoie, 1992.

EXPERIMENTAL STUDY ON STRUCTURAL AND OPTICAL PROPERTIES OF ZnO THIN FILMS PREPARED BY SPRAY PYROLYSIS TECHNIQUE

Z. Kebbab, M. Medles, F. Miloua, R. Miloua, F. Chiker, N. Benramdane

Laboratoire d'Elaboration et de Caractérisation des Matériaux (LECM)
Université Djillali Liabès, BP 89, Sidi Bel Abbès, 22000, Algérie
E-mail: kebbab_zoubir@yahoo.fr

Received: 24 Sept 2007; accepted: 5 Nov 2007

In this work, thin films of the ZnO material were deposited on glass substrates using spray pyrolysis technique. The obtained films are good in quality, adhere well to the substrate and do not present any apparent visual defect. The structural study by X-ray diffraction (XRD) presents a spectrum with very fine peaks, proof of a good crystallization. The study of this spectrum shows a privileged orientation (002) and indicates the presence of structure wurtzite, the cell parameters found are respectively about 3.245 and 5.189 Å. These results are in very good agreement with ASTM card No. 36-1451. The grain size measured at the most important peak (002) is about 263 Å. Moreover, an optical study using (UV-VIS-NIR Jasco V-570) spectrometer was undertaken on these films. A new approach for evaluation thickness is proposed. All the optical constants were given. The direct gap is evaluated at 3.27 eV, value in good agreement with the literature.

Keywords: structural materials, photoelectric cells, spray technique; thin films

Zoubir Kebbab

Organization(s): Djillali Liabes University.
Education: Djillali Liabes University: Magister (1995), Doctorat d'Etat (2004).
Experience: Engineer in ENIE (Entreprise National des Industries de l'Electronique), Sidi Bel Abbès, Algeria (1975-1985). Teaching at Djillali Liabes University (1985 – today). Member of the Laboratoire d'Elaboration et de Caractérisation des Matériaux (LECM), Djillali Liabes University, Sidi Bel Abbès, Algeria (1990 – today).
Main range of scientific interests: thin solid films, structural, optical and electrical properties of semiconductors, ab initio calculations.
Publications: 1 publication in materials chemistry and physics; 1 publication in materials science and engineering; 1 publication in microelectronic engineering; 1 publication in solar energy and solar cells; 1 publication in thin solid films.

Introduction

The zinc oxide (ZnO) is among the most transparent oxides in the visible range. In its aspect, it looks as glass. In addition to its character semiconductor, it seems to be a good protective agent against corrosion. Judiciously doped, the ZnO can give a good conducting and transparent product, like a conducting glass. So its use is irreproachable as windows in the solar cells.

However, the problem of suitable doping remains posed; many attempts, like doping with aluminum, fluorine or lithium gave promising results [1, 2]. This compound which belongs to the II-VI group, offers varied applications; In addition to its employment like gas-detector, it can be also used like pressure sensor; it has also the quality to be piezoelectric.

ZnO compound is a semiconductor with a large gap; all the optical studies give a direct gap whose value is in the interval: 3.22-3.32 eV [3]. ZnO presents also two possible phases of crystallization; rocksalt structure and wurtzite one, the latter is the most frequent in nature [4-6].

Experiments

ZnO thin films were prepared using the spray pyrolysis technique. Used solution is 0.1 M of molarity; it is prepared with zinc nitrate $Zn(NO_3)_2$-$6H_2O$ and bidistilled water as solvent. The obtained solution is pulverised on glass substrates with compressed air (2 bars) as carrying gas. The solution flow is adjusted at 5 ml/min. The substrate temperature is regulated at 350 °C; it is controlled by a chrome-nickel thermocouple. The distance from the spray nozzle to the heater is kept approximately at 30 cm. Under these deposit conditions, good films are obtained. They are uniform, very adherent to the substrates and do not present apparent visual defects.

The structural characterisation of these films is undertaken, at the ambient temperature, using Rigaku Miniflex diffractometer. This equipment utilize the Bragg-Brentano assembly in the θ-2θ configuration. The X-ray source is a monochromatic beam with $\lambda_{K\alpha 1}$ = = 1.5406 Å as wavelength and 1 kW as power. All the

optical measurements were carried out using a Jasco model V-570 (UV-VIS-NIR) spectrophotometer. The apparatus has a double beam and covers the interval: (200-2500 nm).

Results and discussions

Structural properties

Fig. 1 represents the experimental spectrum diffraction obtained for the as deposit film. It presents very fine peaks, proof of a good crystallization. Moreover, according to the existence of a dominant peak, the material presents necessarily a privileged orientation.

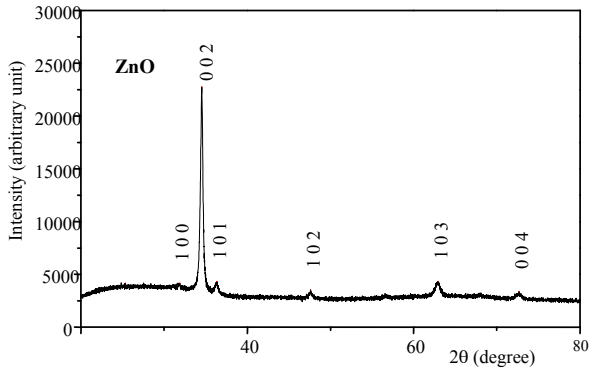

Fig. 1. *X-ray diffraction spectra of ZnO*

By using Bragg relation ($2d\sin(\theta) = \lambda$) on the one hand, and the ASTM diffraction card No. 36-1451 on the other hand, one can easily proceed to the indexing of the spectrum and the identification of the material. After indexing, the follow well solved peaks appear: (100), (002), (101), (102), (103) and (004). As seen on the Fig. 1, this material has the privileged orientation (002). This spectrum is obviously the signature of the ZnO material crystallising in the wurtzite structure where the distance $d_{(hkl)}$ is governed by the following law:

$$d_{hkl} = \frac{a}{\sqrt{\frac{4}{3}\left(h^2 + k^2 + hk + \frac{l^2 a^2}{c^2}\right)}}. \qquad (1)$$

This relation applied to the two most intense peaks, peaks (002) and (101), one can be able to determine the cell parameters (a and c). These parameters are estimated to be about: $a = 3.245$ Å; $c = 5.189$ Å.

One can note the good agreement by comparing our results with those given in the literature [6]. Certain results for comparison are given in Table 1.

Table 1

Cell parameters of ZnO

	Our results	Other results [6]	ASTM card of ZnO No. 36-1451
a (Å)	3.245	3.257	3.24982
c (Å)	5.189	5.219	5.20661

The estimated average grain size was evaluated using the well known Scherrer formula [7] given by the following relation:

$$G = \frac{K\lambda}{D\cos\theta}. \qquad (2)$$

In this relation, the different parameter means:

G: average grain size (Å), K: form factor, its value is in the interval: 0.7-1.7, λ: X-ray wavelength used in the handling (Å), D: half peak width of the considered peak (radian), θ: Bragg diffraction angle of the considered peak (radian).

The half peak width D is obtained by fitting the most intense peak to the Lorentz law given by the following equation:

$$y = y_0 + \frac{2A}{\pi}\frac{D}{4(x - x_c)^2 + D^2}. \qquad (3)$$

In this last relation, the different parameters represent:

y_0: initial ordinate or "offset"; A: surface under the peak; x_C: central x-coordinate; D: half peak width.

The fitting operation applied to the peak (002) gives a D value of about 0.352 rd (see Fig. 1). By taking form factor $K = 1$, it follows a grain size G of about: $G = 263$ Å.

Optical properties

Determination of the transmittance and the reflectance of the film

A thin film is not dissociable of its support, any optical measurement leads ineluctably to a complex result. The obtained result is always made up of the useful optical signal due to the film and the undesirable one coming from the substrate. Thus, we propose a measurement method to outline this difficulty and to isolate the useful signal of the film. For this purpose, we used the simplified diagram of a multiple reflection represented in the Fig. 2.

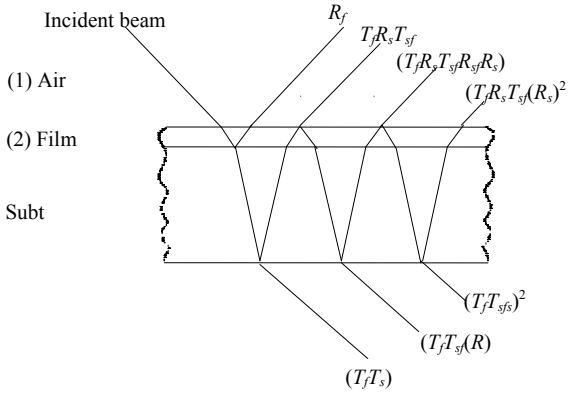

Fig. 2. *Simplified diagram of the multiple reflections phenomenon in a thin film according to [7]*

According to the last figure, it is easy to establish respectively the relationship relating to the transmittance T and reflectance R; that is as follow [7]:

$$T = \frac{T_F T_S}{1 - R_{SF} R_S}, \quad (4)$$

$$R = R_F + \frac{T_F R_S T_{SF}}{1 - R_{SF} R_S}. \quad (5)$$

In the previous relations, each parameter means: T_F: transmittance of the film; T_S: transmittance of the substrate; R_F: reflectance of the film; R_S: reflectance of the substrate; T_{SF}: transmittance of the system substrate-film; R_{SF}: reflectance of the system substrate-film.
It is clear that during a normal measurement; only the parameters T and R are accessible. The other parameters intervening in the relations (4) and (5) remain always unknown. So one proposes the measurement process schematized in the Fig. 3.

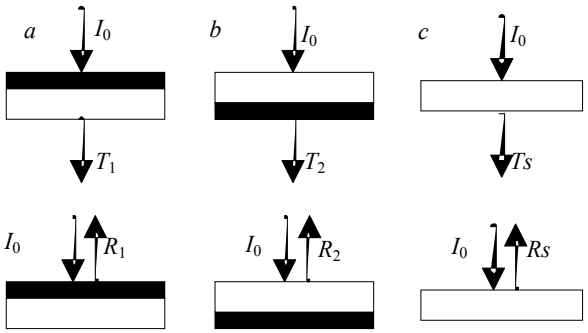

Fig. 3. *Schematic diagram of adopted measurements*

In this figure, one can note three steps of measurement:
− The sample being taken in the usual direction, one measures the transmittance T_1 and the reflectance R_1 of the film-substrate system; Fig. 3, *a*.
− The sample being taken in the opposite direction of the previous case, one measures the transmittance T_2 and the reflectance R_2 of the substrate-film system; Fig. 3, *b*.
− Finally, the substrate being taken alone, one measures the transmittance T_S and the reflectance R_S of the substrate; Fig. 3, *c*.
From all the previous stages, if the substrate is weakly absorbent, it is easy to see that the terms T_{SF} and R_{SF} are identified respectively with T_2 and R_2 ($T_{SF} \approx T_2$ and $R_{SF} \approx \approx R_2$) so that the relations (4) and (5) become:

$$T_1 = \frac{T_F T_S}{1 - R_2 R_S}, \quad (6)$$

$$R_1 = R_F + \frac{T_F R_S T_2}{1 - R_2 R_S}. \quad (7)$$

One can deduce in that case the required expression for T_F and R_F respectively the transmittance and the reflectance of the film lonely:

$$T_F = \frac{T_1}{T_S}\left(1 - R_2 R_S\right), \quad (8)$$

$$R_F = R_1 - \frac{T_F R_S T_2}{1 - R_2 R_S} = R_1 - \frac{T_1 R_S T_2}{T_S}. \quad (9)$$

Determination of the film thickness:
Let us suppose that $X = e^{-ad}$ in the transmittance formula of a layer with parallel faces which has a thickness d and an absorption coefficient α, it is always possible to write it in the form:

$$T_F = \frac{AX}{1 + BX^2 + CX\cos\varphi}. \quad (10)$$

A, B and C are constants and the parameter φ represents the dephasing given by the relation:

$$\varphi = \frac{4\pi nd}{\lambda}, \quad (11)$$

where n is the refraction index and λ *the* wavelength of the radiation used.
In the absence of any interference, the average transmittance T_m is obtained obviously when the term cos(φ) is null, in which case one will have:

$$T_m = \frac{AX}{1 + BX^2}. \quad (12)$$

Taking into account the equations (10) and (11), it is easy to establish the following relation:

$$T_F = \frac{T_m}{1 + K_C T_m + \cos\left(\frac{4\pi nd}{\lambda}\right)}. \quad (13)$$

In the previous equations, K_C is a constant.
If the refraction index n is approximately constant, that is always true in the transmitted part of the energy; it is possible to obtain the parameters n and d by fitting the experimental curve T_F to the equation (13) if the average T_m is available.

Optical characterisations
The optical measurements of transmittance and reflectance were undertaken according to the procedure described before. All the range wavelengths offered by the spectrophotometer was explored (200-2500 nm). The obtained results are represented on the Fig. 4 and 5. The interference phenomenon is quite visible, mainly in the reflectivity spectrum.

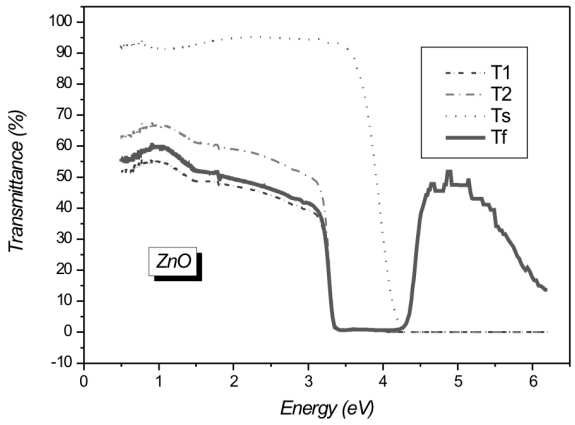

Fig. 4. *Transmittance spectra versus energy according to previous procedure*

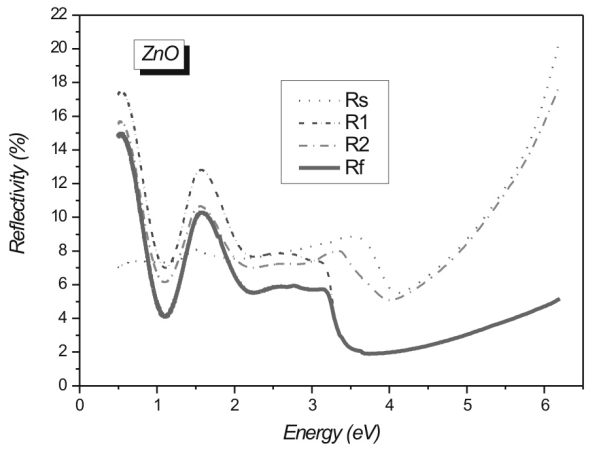

Fig. 5. *Reflectivity spectra versus energy according to previous procedure*

Because of the presence of interference, it is imperative to determine T_m and R_m; respectively average transmittance and reflectance of the film. Fig. 6 and 7, where the useful energy rang was limited between 0.5 and 4 eV, give a solution to this problem.

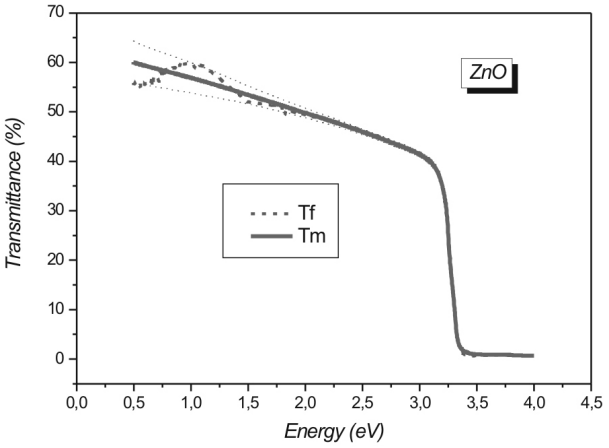

Fig. 6. *Average transmittance spectra T_m versus energy*

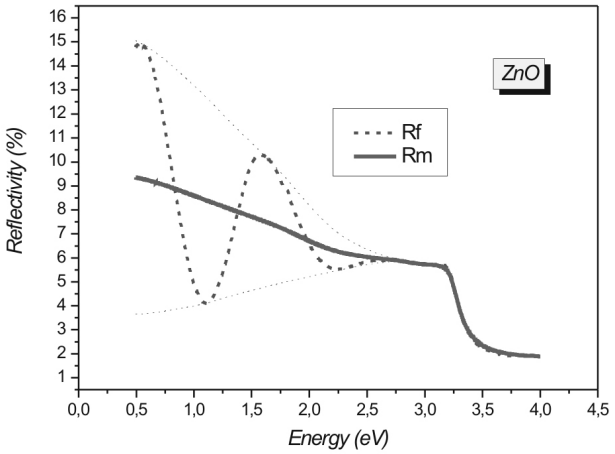

Fig. 7. *Average reflectance spectra R_m versus energy*

Once T_m and R_m determined, the thickness d is obtained by fitting the experimental result to the equation (13). As shown clearly in Fig. 8, the obtained thickness is evaluated to d = 486 nm.

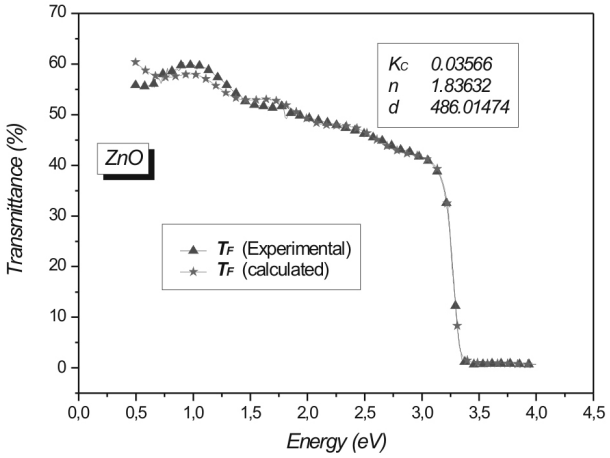

Fig. 8. *Determination of film thickness by fitting experimental transmittance T_F to equation (13)*

Transmittance T_F and reflectance R_F being now available, the film thickness d being determined, the absorption coefficient α is obtained using the well known relation:

$$\alpha = \frac{1}{d}\ln\left(1-\frac{R_F}{T_F}\right). \qquad (14)$$

Fig. 9 shows the absorption coefficient versus energy. It increases abruptly in the interval of the energy rang (3-3.5 eV), i.e. in the vicinity of a zone noted (zone A). The study of the curve $(\alpha h\nu)^2 = f(h\nu)$, in the vicinity of this zone, enables us to highlight the fundamental transition *Eg* (direct gap), characteristic of the ZnO material. Fig. 10 shows it clearly, the obtained value for *Eg* is about 3.27 eV.

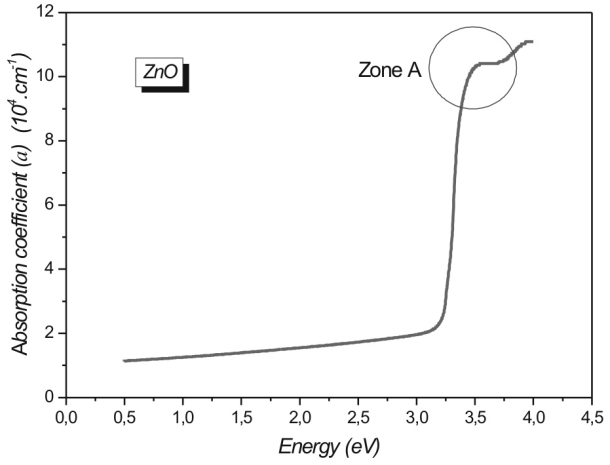

Fig. 9. *Absorption coefficient α versus energy (hν)*

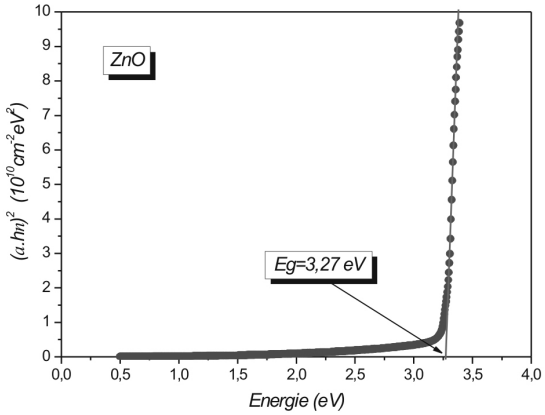

Fig. 10. *Curve $(\alpha h\nu)^2$ versus energy (hv) in the vicinity of zone A*

Table 2 which contains empirical values is given for comparison. The direct gap found is in a great agreement with the literature [3].

Table 2

Direct gap *Eg* of ZnO

Direct gap *Eg* (eV)	
Our results	**Other results [3]**
3.27	3.22-3.32*

(*) Values found for ZnO doped with boron.

From the following equations (15) and (16) we can reach easily the extinction coefficient k and the refraction index n.

$$\alpha = 4\pi\frac{k}{\lambda} \Rightarrow k = \frac{\alpha\lambda}{4\pi}, \qquad (15)$$

$$n = \frac{1+R}{1-R} + \sqrt{\frac{4R}{(1-R)^2} - k^2}\ . \qquad (16)$$

The coefficients n and k are also linked to the real and imaginary part of the dielectric function. The real part ε_1 as well as the imaginary part ε_2 are easily obtained using the following equations:

$$\varepsilon_1 = n^2 - k^2, \qquad (17)$$

$$\varepsilon_2 = 2nk. \qquad (18)$$

Fig. 11 shows the variations of n and k, Fig. 12 shows those of ε_1 and ε_2.

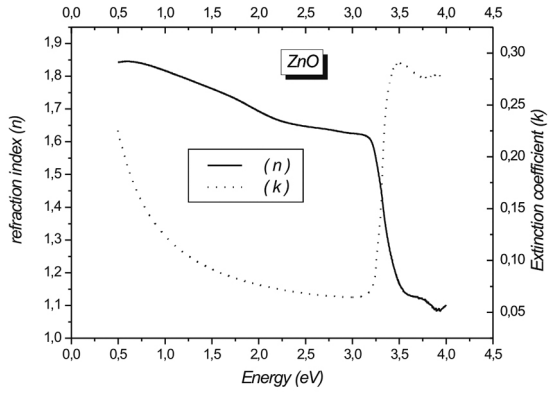

Fig. 11. *Curves n and k versus energy (hv)*

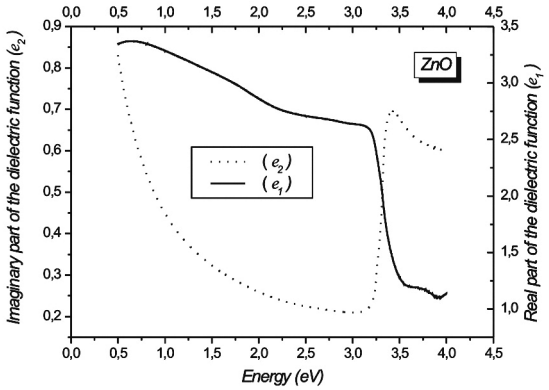

Fig. 12. *Curves ε_1 and ε_2 versus energy (hv)*

Conclusion

This work shows in a clear way the possibility of manufacturing thin films of ZnO by the spray technique. This simple and economic technique proves to be easy to implement. It allows the realisation of compound like oxides or sulphides. The ZnO object of this study is found to be polycrystalline, crystallises in a wurtzite structure and shows a privileged orientation (002). The cell parameters are evaluated respectively at (a = 3.245 and c = 5.189 Å). The optical study shows that the material is very transparent in the visible region and that it is a semiconductor with large gap. This study reveals the existence of a direct fundamental transition; the optical gap determined is about 3.27 eV. Moreover all the optical constants were given.

References

1. Mondragon-Suarez H., Maldonado A., Olvera M. de la L. et al. ZnO:Al thin films obtained by chemical spray: effect of the Al concentration // Applied Surface Science. 2002. 7794. P. 1-8.
2. Shinobu F., Chikako S., Toshio K. Crystallization behavior and origin of c-axis orientation in sol-gel-derived ZnO:Li thin films on glass substrates // Applied Surface Science. 2001. 180. P. 341-350.
3. Lokhande B.J., Patil P.S., Uplane M.D. Studies on structural, optical and electrical properties of boron doped zinc oxide films prepared by spray pyrolysis technique // Physica B. 2001. 302-303. P. 59-63.
4. Sze S.M. Modern semiconductor device physics. John Willey & Sons, Inc. 1998.
5. Van Heerden J.L, Swanepoel R. XRD analysis of ZnO thin films prepared by spray pyrolysis // Thin Solid Films. 1997. 299. P. 72-77.
6. Riad A.S., Mahmoud S.A., A. Ibrahim A. Structural and DC electrical investigations of ZnO thin films prepared by spray pyrolysis technique // Physica B. 2001. 296. P. 319-325.
7. Blaine Johns, Roger H. French, Franklin D. Kalk, William A. McGahan, John A. Woollam. Optical Interference Coatings, SPIE Vol. 2253, Edited by F. Abelès, 1098. 1994.

A DETAILED ANALYSIS OF THE PRODUCTIVITY OF PHOTOVOLTAIC SYSTEMS FOR HOUSEHOLD USE IN AN AMAZONIAN ENVIRONMENT

L. Linguet

University of the French Antilles and French Guiana's
Research Group on Renewable Energies (GRER)
Campus Saint-Denis, Avenue d'Estrées
97337 Cayenne Cedex, France
Phone: (33) 0594296209/(33) 0594296279; e-mail: llinguet@guyane.univ-ag.fr
http://calamar.univ-ag.fr/uag/physique/grer/grer.html

Received: 23 Sept 2007; accepted: 29 Oct 2007

This study was conducted in French Guiana, a region characterized by specific human and environmental conditions, by members of the University of the French Antilles and French Guiana's Research Group on Renewable Energies (GRER) in collaboration with the regional office of ADEME (Agency for the Environment and Energy Management) and the companies that installed the photovoltaic systems.
Its aim was a better understanding of the attitudes, expectations, and relationship of the users towards the photovoltaic installations. The data collected made it possible to make suggestions for adapting the photovoltaic systems to their environment by taking into account social, cultural, and geoclimatic specificities. Analysis of on-site productivity provides valuable information on energy profiles and types of use. Field surveys made it possible to associate users' perception of the energy production equipment and their degree of satisfaction with operating efficiency and on-site maintenance. This aspect is essential for analyzing the actual rate of use of the energy that is theoretically available.
Parallel to these surveys, the results of the study carried out on the performance of the photovoltaic systems made it possible to learn the quantitative aspects of the energy produced and consumed as well as the qualitative aspects of the parameters that condition the performance of the photovoltaic systems.
After keyboarding, the subjective, qualitative as well as the quantitative variables were processed using a statistical analysis program in order to determine the correlations between them and to prepare the final conclusions. These surveys and measurements were carried out simultaneously over the 2004-2005 period.

Keywords: silicone solar thermal electric plants, economical aspects, solar energy

Laurent Linguet

Organization(s): University of the French Antilles and French Guiana, researcher, PhD degree.
Education: University Paul Sabatier (1982-1990), Université d'Orsay Paris XI (1990-1993).
Experience: Thomson-CSF Company, Engineer (1990-1993), Université des Antilles et de la Guyane, Maître de Conférences (1994-2007).
Main range of scientific interests: renewable energy, converters, sustainable development.
Publications: Papers in EPE, EPF, PCIM, 1 patent.

Introduction

It is widely accepted today that technological progress cannot be pursued as an end in itself, without taking into account its impact on users. Scientific efforts are expected to have a true impact on the comfort of individuals, improvement of the economy, and how societies function.
The study presented in this article deals with the issue of photovoltaics (PV) in French Guiana, considered as a technique imported into a region characterized by specific human and environmental conditions.

Granted, the issue of "classic photovoltaics" has been studied extensively. The notion of "classic photovoltaics" refers to:
– the implementation of the technical system under optimal operating conditions (that is, in a temperate climate or in the laboratory);
– adaptation of the technical system for a Western, urban, or semi-urban public.
However, there are several fundamental reasons why it can be said that photovoltaic systems are not suitably adapted to living and operating conditions encountered in French Guiana.

Environmental conditions are not always favorable:
– A long rainy season during which solar radiation is low (6 months/year).
– High humidity, which promotes the growth of moss on the panels.
– High humidity, which promotes battery discharge.
Specific social and geographical conditions characterized by:
– The presence of non-homogenous populations stemming from various cultures.
– The presence of isolated villages and municipalities which are difficult to reach (no road access, access only possible by river or helicopter).
It must be noted that in a real-life situation, the notion of reliability no longer covers only those parameters recognized in the laboratory. Other parameters linked to user perception and operating conditions have to be taken into account. The concept of reliability covers not only certainty of correct performance but also overall productivity and includes the human factor. This distinction is particularly important for photovoltaic installations located in isolated areas. It is therefore necessary to conduct a study on the habits and expectations of the populations, taking sociocultural parameters into account.

Study parameters

PV performance

One aspect of this work studies the operating characteristics of the photovoltaic systems currently installed in French Guiana. The aim is to define the average productivity of these photovoltaic systems compared to production rates announced by the manufacturer.
A series of measurements was taken on photovoltaic systems installed at pre-selected sites. These measurements provide quantitative and statistical data on the operating conditions of the modules, as well as data concerning the characteristics linked to the quantities of energy produced and the quantities of energy consumed.
We identified:
– the quantity of energy produced by each photovoltaic system;
– the quantity of energy consumed by each home;
– failures of photovoltaic modules;
– complete discharges of batteries;
– maximum solar radiation levels.
Correlations were established between:
– solar radiation and the quantity of energy produced;
– the quantity of energy produced and the quantity of energy consumed;
– solar radiation and the quantity of energy consumed.
Analysis of these measurements provides:
– an evaluation of average operating conditions for the modules;
– consumption rates of produced energy;
– the ratio between measured kW·h and kW·p announced by the manufacturer.

Socio-anthropological surveys

The second aspect of this work introduces questions about the use of photovoltaic equipment by populations whose culture differs from Western culture. The cultural differences of the societies in which this equipment was set up make it impossible to transpose identical energy use inspired by the Western model. In addition, access conditions, demands, and practices diverge according to cultural affiliation and place of residence.
Although introducing photovoltaic systems enables the vast majority of these populations to benefit from access to electrical energy, a thorough understanding of its effects is necessary in order to increase its chances of being efficient.
In order to understand the complex situation created by introducing new technologies into non-westernized or minimally westernized societies, the following elements should be studied: the perception of energy among these populations, the overall perception of the system or technology introduced, the degree of acceptation of its constraints, and the impact on the economic, social, and cultural aspects of their way of life.
Socio-anthropological surveys were conducted at several sites equipped with individual photovoltaic units spread throughout French Guiana. These surveys made it possible to associate users' perception of the energy production equipment with their degree of satisfaction with operating efficiency and on-site maintenance. This aspect is decisive and will be compared with the actual rate of use of the energy that is theoretically available.
These socio-anthropological surveys were carried out by meeting with several categories of users. Besides their cultural affiliation and their place of residence, other parameters were also taken into account, such as: age, socio-professional category, marital status, income, household composition, practices linked to use of household appliances, and acculturation phenomena caused by introducing a technical progress previously unknown to certain populations.
We will also attempt to answer the following questions:
Which aspects of the technology were best accepted? Which factors may incite users to cooperate or on the contrary reject the system? What would be the impact of a more or less significant implication of the users in the running of the system? What types of maintenance activities would be most adapted? What type of training should be planned for?

Selection of sampling sites

Definition of the sampling and measurement sites was carried out in coordination with the locally-based companies that installed the photovoltaic systems. Sites were chosen according to two criteria:
1. Carry out measurements in several different areas spread over the entire territory of French Guiana.
2. Favor sites that are geographically isolated and/or hard to reach.
The areas selected and shown on the Fig. 1 are:
– Municipality of Roura;

– Municipality of Saül;
– Maroon villages of Maroni Valley-Apatou;
– Municipality of Saint Laurent and Mana;
– The Amerindian village of Favard.

Fig. 1. *The areas selected for study*

Socio-anthropological surveys results

Municipality of Roura

Study surveyors visited twenty-three homes equipped with photovoltaic systems scattered over various areas in the municipality of Roura.

The homes are located far from the main village of the municipality in areas not reached by EDF's electrical grid. Nevertheless, these homes are easily reachable by dirt roads suitable for vehicles which branch off from a national or departmental road. They are therefore only relatively isolated.

The persons surveyed were heads of households, RMI (guaranteed minimum income) recipients, and resided in the Roura area (mainly French Guianese Creoles and Metropolitan French). The majority of them had regular incomes of between 500€ and 999€. These were mainly families composed of three children under 15 and three adults (15 and over).

Most of the people interviewed had benefited from the installation for 3-4 years.

Inside the houses, the main electrical appliances were televisions (91 %), refrigerators (65 %), and stereo systems (47 %). We also observed that many had video recorders, microwave ovens, computers, and satellite television service.

Daily use of the television is significant. It is the main entertainment and "standby" mode seems to be the first choice of the people questioned when they are not watching. Indeed, the television was mentioned first among appliances that are always on.

A broad majority of users are satisfied with solar energy which they find "useful", "indispensable for all" and ecological, but a broad majority regretted the fact that the system functions poorly in rainy weather.

60 % are not prepared to break their contract with the company that installed the photovoltaic system as they are satisfied with the service, but certain users would prefer a type of installation that would provide more constant production and have fewer constraints. Being dependent on weather conditions and having to maintain the installations and manage energy consumption appear to detract from the image of the photovoltaic system.

Municipality of Saül

The village of Saül is located in the middle of French Guiana, in the heart of the forest, cut off from any road or river access. The village can only be reached by air, a trip that takes approximately one hour from Cayenne, the capital.

The village is equipped with autonomous solar generators in order to satisfy the energy needs of the inhabitants. Twenty-three users of photovoltaic systems were questioned (Fig. 2, 3).

The majority of the persons questioned were men (68.42 %), heads of households, and RMI recipients. They were mainly French Guianese Creoles (57.89 %) and Metropolitan French (31.58 %).

36.84 % of them had regular incomes of between 250€ and 499€. The people questioned were mainly couples without children.

Most of the people interviewed had benefited from the installation for 2 years.

Inside the houses, the main appliances were electric refrigerators (100 %), freezers (94.74 %), stereo systems (63.16 %), and televisions (21 %).

A broad majority of the users are satisfied that they can keep their food refrigerated. But a broad majority of them regretted the high cost and the maintenance and repairs required by the system.

Client perception of the company that installed the PV systems can be summed up as follows:

– 46.67 % of the clients are satisfied and acknowledge "having no problem" with the company.

– 33.9 % of the clients, who could be termed "indifferent", are not concerned by the image transmitted by the company.

– 13.34 % of the clients are dissatisfied and accuse the company of not repairing system failures.

Half of those questioned consider that they do not have a satisfactory relationship with the installation company and deplore the fact that they are not completely satisfied with the photovoltaic system. A high proportion of the users questioned also complained about the cost, which they considered high.

Many clients used a generator before the introduction of solar energy. They acknowledge the improvement in family living conditions since the change to solar energy and the fact that the system is more economical and quieter than using a generator. But they admitted that, if they no longer had electricity, they would use gas and would go back to living "like they did before". Electricity is considered indispensable (38.84 %) but the percentage of people without an opinion is identical.

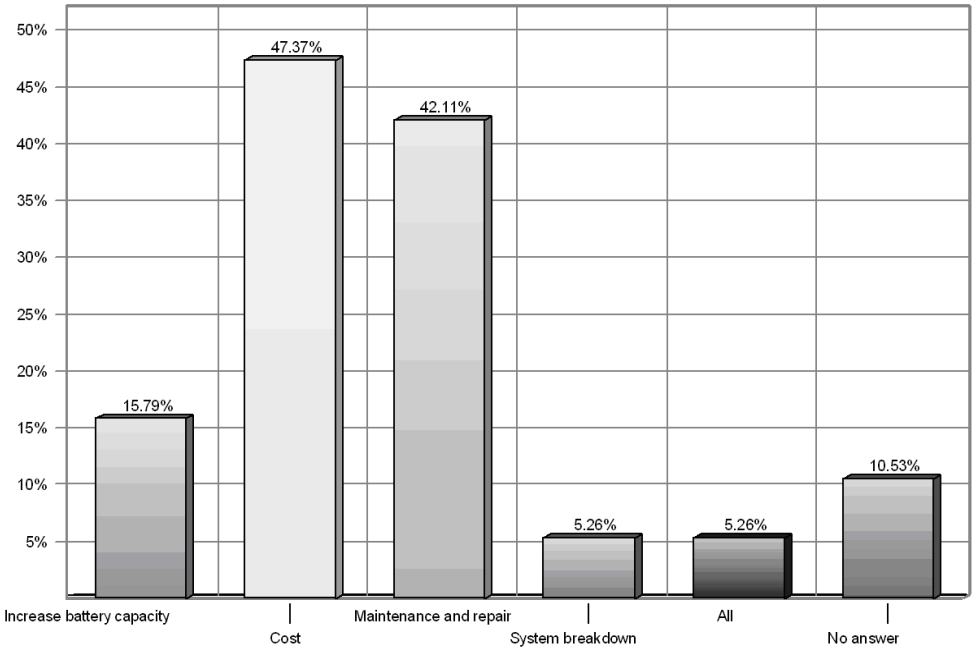

Fig. 2. *(Saül) Answers to the question: What are the drawbacks of the photovoltaic system?*

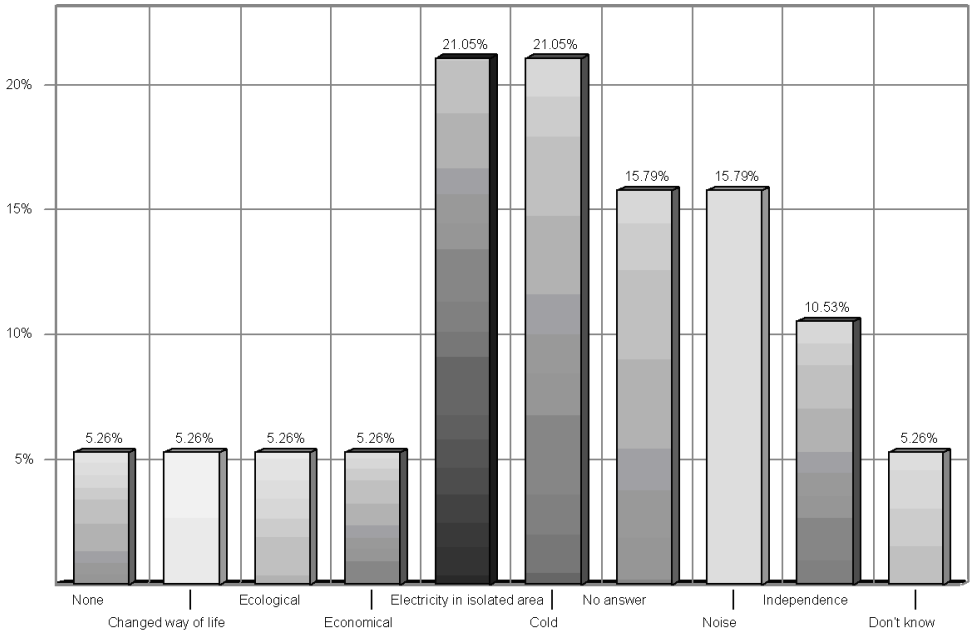

Fig. 3. *(Saül) Answers to the question: What are the advantages of the photovoltaic system?*

Municipality of Mana and Saint-Laurent

The homes visited for the survey were located away from the main villages (Mana and Saint Laurent), off the EDF electricity grid, but easily reachable by car by following dirt tracks branching off of the main roads for a few minutes. The EDF electricity grid runs alongside the main roads.

Men and women were equally represented (50 % each) among the persons questioned. The most highly represented cultural group (80 %) were the Metropolitan French.

Half of the people surveyed were teachers and the average monthly income of the clients who answered the question was between 1000€ and 1499€ (62.5 %). 100 %

of these incomes were monthly. 25 % of the clients had had access to solar energy for 4 years and 25 % for 7 years.

62.5 % of the persons questioned are satisfied with solar energy, which they describe as ecological and natural. The following drawbacks were mentioned:

– The low capacity of the batteries (37.5 %), insufficient energy during rainy weather.

Concerning the changes in their life since the system was installed:

– 25 % think that "it's good": life is easier, safer, more comfortable; they highlighted the possibility of having appliances and the economic aspect. However, the same proportion

– (25 %) gave no answer.

The appliances owned were stereo systems (100 %), refrigerators (100 %), televisions (62.5 %), and computers (62.5 %).

75 % consider electricity "indispensable" and 62.5 % are not prepared to break their contract. 62.5 % consider their relationship with the installation company to be "satisfactory" and 50 % claim to have no problem.

Having electricity has:

– led to new evening activities (25 %);

– enabled the use of new tools (12.5 %);

– created new activities within the family (12.5 %).

The majority of clients at this site were of european origin and had fairly high incomes (the highest of all the clients in the study). They were all located close to roads and were isolated mainly in terms of access to the electricity grid.

Maroon villages of Maroni Valley - Apatou

The photovoltaic installations and homes visited are located on the banks of the border river, the Maroni. They can only be reached by river; the trip from Saint Laurent takes two hours. The homes visited were located in several villages scattered along the river, which constitutes the sole transportation route between them: Spawine, Patience, Petit Patience, Anaoulaondo, and New-Campo. The EDF electricity grid stops at Saint Laurent and is not extended along the Maroni river up to a point near these living places.

Twenty-five clients who use the photovoltaic systems were questioned (Fig. 4, 5).

All of the users and persons questioned belonged to the Maroon cultural group. Women were broadly represented (72 %).

The main sources of income were the RMI (44 %) and child benefits (44 %).

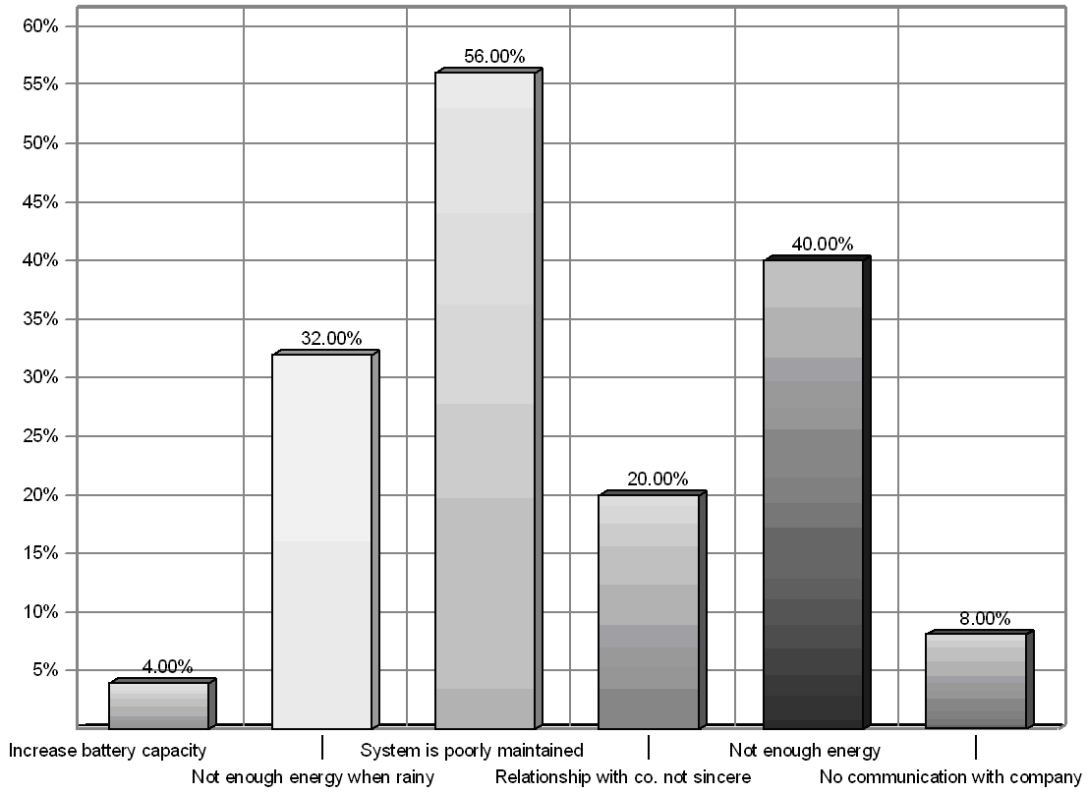

Fig. 4. *(Apatou) What are the drawbacks? (What should be changed?)*

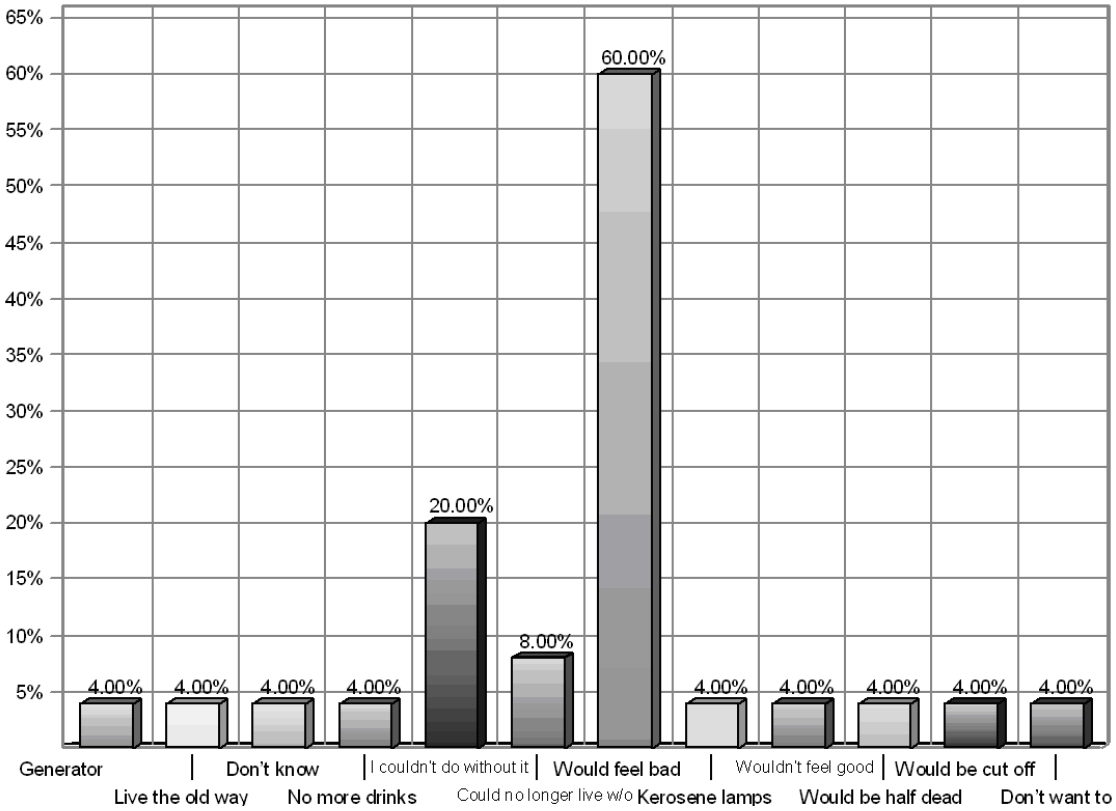

Fig. 5. *(Apatou) Explain what it would be like if you no longer had electricity?*

The persons questioned stated that they had incomes under 249€ per month (44 %); it should be pointed out that 56 % did not answer that question.

36 % of the clients had had access to solar energy for 7 years.

Certain advantages were acknowledged, namely:

– the quietness of the system compared to generators (48 %);

– the possibility of using electricity day and night (24 %);

– the possibility of benefiting from electricity in an isolated area (24 %).

The drawbacks highlighted were:

– poor maintenance of the system (56 %);

– low capacity of the batteries (40 %);

– power failures during rainy weather (32 %);

– lack of sincerity between them and the installation company (20 %).

88 % of the users admitted to not having understood the agreements signed with the installation company and 84 % described their relationship with the latter as "not at all satisfactory". The main reasons stated were the lack of maintenance and follow-up (29.17 %), the company's lax attitude (16.67 %), and the lack of visits to check installations (16.67 %).

A majority of the clients (64 %) are not satisfied with solar energy. The main reasons mentioned were maintenance of the system (32 %); others thought that this represented a defect (20 %).

Before the system was installed, 28 % of users used kerosene lamps and 24 % a generator. Since the system was installed, they acknowledge the following changes:

– the advantage of having light at night (25 %);

– the possibility of refrigerating food (16.67 %);

– the possibility of having more leisure activities (16.67 %).

60 % admitted that they would feel "bad" if they didn't have electricity. Thus, 88 % would not be prepared to break their contract. However, among those who would, 66 % admitted that they would be motivated by the fact that the system breaks down and has defects.

The appliances owned are as follows, by order of importance:

– televisions (69.57 %), freezers (65.22 %), stereo systems (56.52 %).

Amerindian village of Favard

The Amerindian village of Favard is located in the municipality of Roura, on the right bank of the Oyack river, fifteen minutes by canoe from the village of Roura. It can be reached by taking a road (which is in very bad condition due to the rains) that goes through the forest; the trip from Roura takes less than an hour. The EDF electricity grid does not pass near the road.

All twelve clients who use the photovoltaic systems in the village were questioned (Fig. 6, 7).

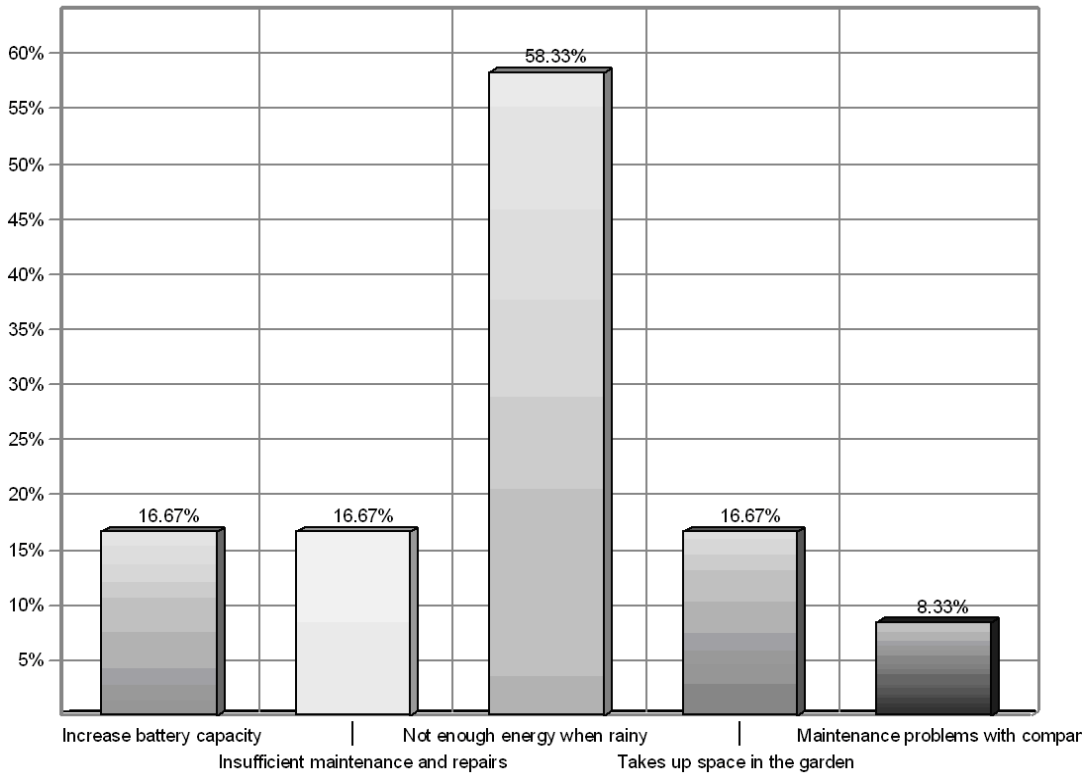

Fig. 6. *(Favard) What are the drawbacks?*

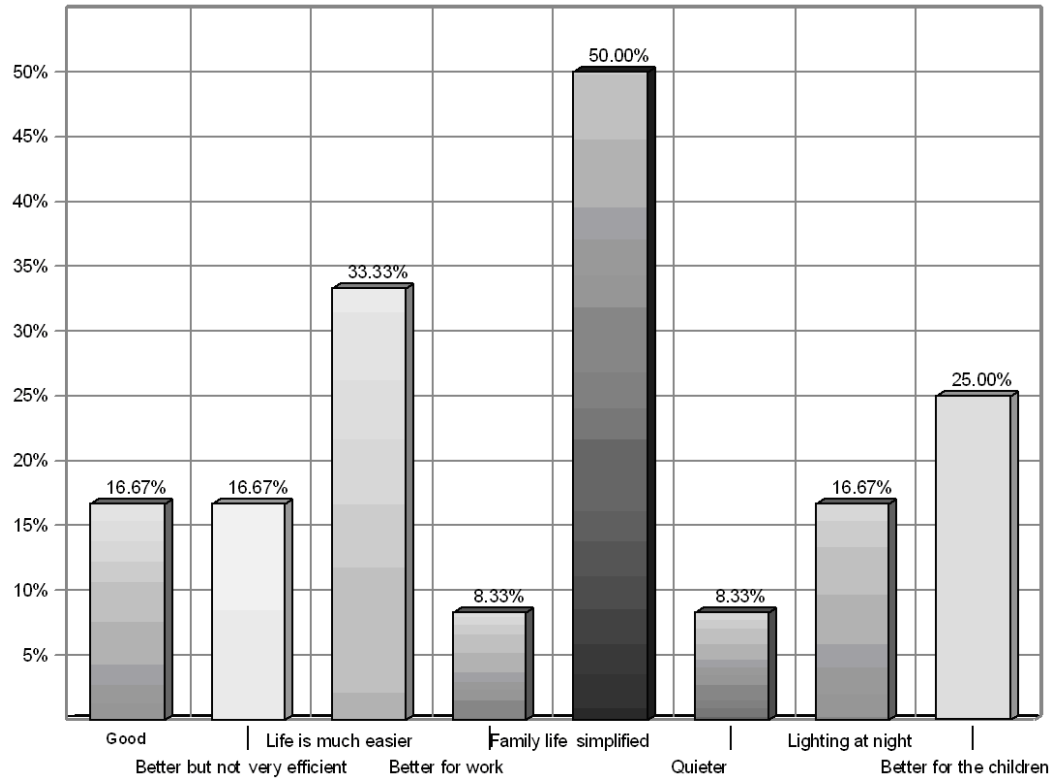

Fig.7. *(Favard) What has changed in your life since the system was installed?*

All the users and inhabitants of this village belong to the Amerindian cultural group. 41.67 % of the people surveyed were between 25 and 29 years of age and 75 % were men.
60 % of the clients questioned are employed, 50 % are RMI recipients, and 16.67 % are farmers. Their average monthly income (45.45 %) is between 250€ and 499€.
50 % have had access to solar energy for 6 years.
Electricity was described as indispensable by 91.67 % of the clients. If they no longer had electricity, 41.67 % would go back to the old ways and 25 % would look for another way to satisfy their energy needs.
A considerable proportion of the clients (66.67 %) claim to be satisfied with the presence of the photovoltaic system. The advantages stated were having electricity in an isolated zone (58.33 %) and the ecological aspect (16.67 %).
Nevertheless, the clients appeared to be dissatisfied with the performance of the system. The main drawbacks noted by the clients were:
– there is "not enough energy in rainy weather" (58,33 %);
– maintenance and repair are insufficient (16.67 %);
– battery capacity is low (16.67 %);
– the installation takes up room in the garden (16.67 %).
33.33 % described the nature of their relationship with the company as "not at all satisfactory" and 25 % considered it to be "satisfactory". However, 16.67 % did not answer and 33.33 % don't know. How should this "heavy" silence be interpreted?
Concerning the reasons for this opinion, of the total number of persons questioned:
– 16.67 % accused the company of carrying out "insufficient maintenance";
– 8.33 % think that there are "a lot of mistakes";
– 8.33 % wonder how the company regards them.
50 % of the clients stated that they did not understand the agreements signed with the installation company.
We should emphasize the fact that 66.67 % are not prepared to break their contract with the installation company for several reasons: they have no problem for the moment (62.50 %) and think that they would have "more problems afterwards" (25 %) if they didn't have access to electrical energy.
However, 25 % of the clients would agree to do without it, and 33.33 % would do it "if there were a new solution" that would replace the solar energy.
The appliances owned were:
– refrigerators (83.33 %), gas cooking stoves (58.33 %), stereo systems (25 %).
The main change mentioned by the clients was the simplification of family life (50 %). They specified that "life is much easier" (33.33 %) and better for the children (25 %).
91 % stated that there were people at home all day long. These were mainly members of the family. These people do the housekeeping and, during the day, energy is also used to watch television and listen to the radio.
Most of the clients in this residential area are not satisfied with the services of the installation company. System failures (due to the weather, breakdowns), combined with incorrect use of electrical appliances by the clients, exacerbate this dissatisfaction.

PV performance results

Analysis of performance data for the first two years following commissioning of PV systems

The numerous performance data recorded by the PV systems' calculators were integrated into a calculation program (Excel) which made it possible to extract the average values per site. Useful variables for our study are presented in the Table 1.
We observed that the energy potential captured by the solar panels and recorded by the installations' data logging systems (SUNPAC or ENERPEC) varies considerably from one site to another. There is a 20 % gap between the highest energy potential and the lowest. The gap between the highest energy level and the lowest increases to 40 % when we evaluate the energy actually captured.

Table 1

Average daily and annual values drawn from the data recorded on the PV systems

Identified values	Potential energy of solar panels or average theoretical producible solar energy per day (kW·h)	Average actual solar energy supplied per day (kW·h)	Daily consumption profile (kW·h)	Average consumption rate of average actual solar energy supplied (%)	Average consumption rate of average producible energy (%)	Estimated proportion of defects in the battery bank (%)	Average maximum current during the 1st year (A)
Apatou	3.3	3.18	2.7	85	82	45	28.6
Favard	2.83	2.1	1.29	62	45.5	57	19.6
St. Laurent and Mana	3.3	3.24	2.25	69	68	5	38.7
Roura	3	2.8	2.3	83	77	5	
Saul	2.64	1.9	1.3	70	50	0	

The measurements of the average energy consumption of users at each site during the first two years of PV system operation reveal significant differences that cannot be explained by the variation in potential solar energy alone. There is a 50 % gap between extreme consumption levels. The lowest consumption levels were found in Saül and Favard.
Table 2 highlights the rapid deterioration of proper PV system performance, particularly at the sites inhabited by Amerindian (Favard) and Maroon (Apatou) populations. These high defect rates are mainly due to insufficient battery maintenance and repair, both by clients and by the installation company.
The defect rates recorded at the more accessible sites of Mana and St. Laurent were lower, as clients of Metropolitan French origin played a greater role in battery inspection and maintenance, which made it possible to keep the installation in good working order.

Cross analysis of current data

Table 2

Average daily and annual values drawn from the data recorded on the PV systems

Identified values	**Potential energy of solar panels or average theoretical producible solar energy per day (kW·h)**	**Average actual solar energy supplied per day (kW·h)**	**Daily consumption profile (kW·h)**	**Average consumption rate of average actual solar energy supplied (%)**	**Average consumption rate of average producible energy (%)**	**Estimated proportion of defects in the battery bank (%)**
Apatou	3.3	3.18	1	30	31.4	80
Favard	2.83	2.1	0.6	21	29	80
St.-Laurent and Mana	3.3	3.24	2.25	69	68	5
Roura	3	2.8	2.3	83	77	5
Saul	2.64	1.9	1.3	70	50	0

Discussion

This study shows that the issue of energy in truly isolated areas is considered vital by the populations who live in these areas and who do not have other similar-strength energy sources available to them (Apatou, Favard). We observed that the users belonging to the Amerindian and Maroon communities who have access to electrical energy and currently have the lowest consumption rates are also the most numerous in percentage terms to consider it indispensable (Fig. 8).

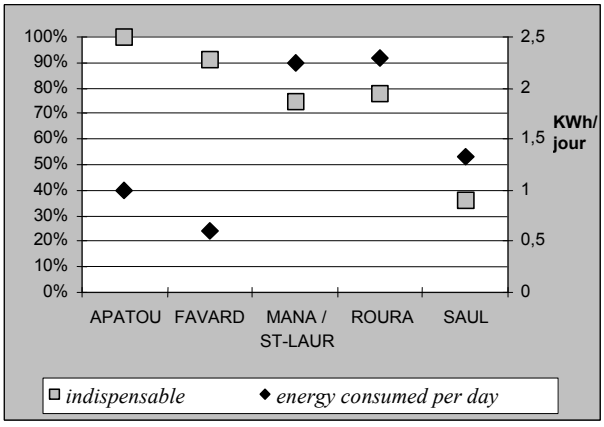

Fig. 8. *A correlation between user perception of PV electrical energy and energy consumed per day*

The downward trend over the past few years of consumption levels of solar energy actually supplied to the system at the Apatou and Favard sites has not had a negative impact on user perception concerning electrical energy. On the other hand, the Saül site shows low adherence to the need for solar-derived electrical energy even though the clients' battery bank is in good condition, but its solar potential is lower than all the other sites. Strangely, when we examined the possible correlation between the users' interest in solar-derived electricity and the solar potential of the site, we discovered that these data were proportional: the lower the solar potential, the weaker the users' interest in solar energy. This was particularly true for Saül.
The study point out that introducing new technologies into populations with different socio-cultural backgrounds produces specific responses. The following examples will illustrate our statements (Fig. 9):
– At the Saül site, we observed that the insufficiency of potential energy available seemed to be at the root of a marked deterioration of solar installation performance. The discrepancy between announced and actual performance and the desire of the installers to maintain this type of production system in spite of poor performance appears to have produced an attitude of rejection of the technology among the population of Saül, composed mainly of Creoles.

– At the Favard site, where the population is exclusively Amerindian, a low solar energy potential and a high rate of battery defects during the first years of operation did not bring about rejection of the technology, but did create an unsatisfactory relationship with the installer. We observed that all forms of obligation (agreements, payment) were rejected.
– At the Apatou site, where the population is exclusively of Maroon origin, a high energy potential available during the first years of operation certainly attracted and convinced users of the need to have electrical energy. However, insufficient maintenance, the presence of operating defects, and deterioration of system performance brought about an even stronger rejection of the technology as well as an unsatisfactory relationship with the installer. There appears to be a strong misunderstanding concerning the agreements signed and the terms of payment.
– We observed that the users at the Mana/St. Laurent site, who were mainly of European origin, were those who best willingly accept the technology and its constraints, but do not view the need to have electrical energy as essential, contrary to the other sites. They have a good relationship with the installation company.

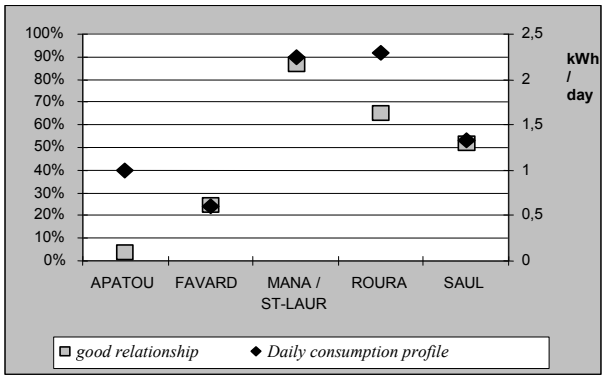

Fig. 9. *Correlation between relationship quality with PV installers and daily consumption profile*

Several complementary analyses can been carried out using the data collected and presented in this report.
Daily television use is significant. Television is the main source of entertainment and "standby" mode is the first choice of the persons questioned when they are not watching television. Moreover, we observed a certain confusion between standby mode and operation of the appliances. Certain clients thought that, during standby, the appliance was turned off, while others thought that refrigerators and freezers did not run continuously but that they remained in standby mode. It seems necessary to provide information on these different concepts.
In this discussion, we concentrated on answering the questions raised at the beginning of the report.
What factors can lead to rejection of the system?
Several factors were revealed. First of all, dissatisfaction due to insufficient available electrical energy. This insufficiency appears to have different origins:
– Low solar energy potential that the installation does not manage to exploit in order to satisfy user needs, or a high defect rate concerning battery voltage (maybe due to intensive use?).
– The attitude of the installation company appears to be considered as a factor in the rejection of the technology. Users complained of the lack of a relationship, insufficient contact, and the absence of on-site presence, which were felt to indicate an attitude of contempt on the part of the company. This attitude led to deterioration of the installations.
– Generally speaking, users acknowledged that they hadn't understood the agreements and what their implication in the system was supposed to be. The users' relationship to the system should not be confused with their relationship to the installer. For example, the users in Saül who received training on the use of the system all said that they hadn't understood the agreements signed with the installer, and their relationship with the latter is quite unsatisfactory.
– The obligation to pay are factors which lead to conflict and deterioration of the relationship between users and the installation company.
We would like to point out that particular attention should be paid to the potential solar energy available at a site and the dimensioning of the installations. The study appears to indicate that a slightly insufficient energy potential can lead to much lower productivity than that which could have been expected. Unless there is another explanation which could elucidate this phenomenon, it would appear that photovoltaic systems degrade low-level quantities of solar energy excessively (generating a yield which is proportionately lower).
What factors can incite users to cooperate?
We observed a strong attachment to the service provided by the photovoltaic system (except in Saül), the only positive point the study highlighted. This is a sign that allows us to conclude that trust in the technology and the company that installed it can be re-established. In order for this to happen, each population's modes of relating would have to be taken into account very carefully and true personal contact re-established. The most important concern should not be profit or economic equilibrium but the initial objective intended for the photovoltaic installations: supplying energy in isolated areas.
By what means can users be incited to become more involved in operating the system?
The possibility for users to get in touch with the installer appears to be a priority expectation. The users have many questions about the system and routine maintenance. They need to be listened to and reassured, especially when the availability of electrical energy is considered vital.
What type of maintenance program would be the most adapted? What type of training should be planned for? The questions asked by the users during the interviews indicate that priority should be given to battery maintenance. The first training program to carry out

should be on battery maintenance (adding water, acid, cleaning corroded terminals, measuring voltage, pH, etc.) It is this element of the photovoltaic system which appears to be the main cause of failures.
The maintenance program to adopt should be a joint approach involving one or several users at the different sites and the installation company's technicians.

Conclusion

The study on photovoltaic system productivity in an Amazonian environment carried out on the socio-anthropological and technical levels has yielded a large amount of information and a wealth of results.
A total of 91 homes equipped with photovoltaic systems were visited at different sites having different meteorological conditions. All these homes were off the EDF electricity grid. The relative distance from transportation routes was different and specific to each site: certain sites can only be reached by air, others only by river, and still others can be reached by road.
We deliberately chose clients belonging to different cultural groups. Therefore, the study includes clients of Amerindian, Maroon, Creole, and European origin.
The first conclusion that can be drawn from the study is that introducing new technologies into populations with different socio-cultural backgrounds produces specific responses that should be taken into account very early on; care should be taken not to neglect them in order to avoid rejection of the technology and its players.
Generally speaking, client perception of the photovoltaic system is mixed. They consider several aspects of the technology to be ecological (it is silent, natural, and linked to sunshine) and they willingly use the electrical energy generated, which most consider indispensable.
However, the major drawbacks highlighted by the clients are the low capacity of the batteries, the poor performance of the system during rainy weather, and the lack of system maintenance.
Still, the majority of them would not be prepared to break their contract with the installation company.
The main concerns involve the disfunctioning of the photovoltaic system. On this point, the clients in Apatou and Favard consider that they do not get any attention from the installation company and they would like more visits and more contact.
System failures (meteorology, breakdowns), coupled with incorrect use of electrical appliances by the clients, exacerbate the dissatisfaction experienced.
This study shows that the issue of energy in truly isolated areas (not reachable or very difficult to reach by road) is considered vital by the populations who live in these areas and who do not have other similar-strength energy sources available to them (Apatou, Favard).
It appears that heavy economic constraints combined with differing cultural approaches may hampered the proper productivity of the photovoltaic installations present at these sites.

References

1. Tsoutsos T., Frantzeskaki N., Gekas V. Environmental impacts from the solar energy technologies, Elsevier 2003, Energy Policy.
2. Gaunt C.T. Meeting electrification's social objectives in South Africa, and implications for developing countries, Elsevier 2004, Energy Policy.
3. Chakrabarti S., Subhendu C. Rural electrification programme with solar energy in remote region – a case study in an island, Elsevier, Energy Policy 30 (2002) 33–42.

EFFECT OF SOLUTAL BUOYANCY FORCES ON THERMAL CONVECTION IN CONFINED NON-NEWTONIAN POWER-LAW FLUIDS

T. Makayssi*, M. Naïmi*[a], M. Lamsaadi*, M. Hasnaoui**, A. Raji*, A. Bahlaoui*

[*]Sultan Moulay Slimane university, Faculty of Sciences and Technologies, Physics Department, UFR of Sciences and Engineering of Materials, Team of Flows and Transfers Modelling (EMET), BP 523, Béni-Mellal, Morocco

[**]Cadi Ayyad University, Faculty of Sciences Semlalia, Physics Department, UFR TMF, Laboratory of Fluid Mechanics and Energetics (LMFE), BP 2390, Marrakech, Morocco

[a]Corresponding author. Tel.: (212) 23 48 51 12/22/82; Fax: (212) 23 48 52 01.
E-mail: naimi@fstbm.ac.ma, naimima@yahoo.fr

Received: 24 Sept 2007; accepted: 5 Nov 2007

This paper reports the results of an analytical and numerical study on natural convection heat transfer with and without solutal buoyancy forces in a non-Newtonian power-law fluid contained in a horizontal rectangular shallow enclosure submitted to uniform heat and mass fluxes along its short vertical sides, while the horizontal ones are insulated and impermeable. An approximate theoretical solution is developed, on the basis of the parallel flow assumption, and validated numerically by solving the full governing equations. A comparison between results obtained in presence and in absence of solutal buoyancy forces is done. The effect of the non-Newtonian behavior on fluid flow and heat transfer characteristics is examined.

Keywords: thermodynamic analysis in renewable energy, thermal natural convection, double diffusive convection, rectangular enclosures, non-Newtonian fluids

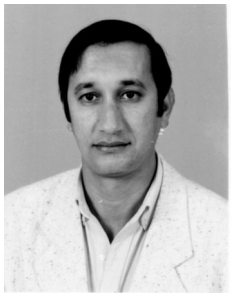

Mohamed Naïmi

Education: A national doctorate (INPL, Nancy, France, 1989) and a doctorate of state (University Cadi Ayyad, Marrakech, Morocco, 2001). The title of the former is: "Etudes des lois d'écoulement et de transfert de chaleur pour des fluides non-Newtoniens en espace annulaire tournant: approche réaliste de l'échangeur de chaleur à surface raclée" while the latter entitled: "Contribution à l'étude de l'effet Marangoni thermique dans les fluides non-Newtoniens en conditions de gravité et de microgravité".
Experience: A teacher researcher, with the degree of higher teaching Professor, at the Faculty of Sciences and Technologies of Sultan Moulay Slimane University (Béni-Mellal, Morocco).
Main range of scientific interests: natural, double diffusive and capillary convections in non-Newtonian fluids.
Publications: 8 main papers since 2005.

Nomenclature

A – aspect ratio of the cavity, Eq. (11)
C_T – dimensionless temperature gradient in the x-direction
C_S – dimensionless concentration gradient in the x-direction
D – mass diffusivity (m^2/s)
g – gravitational acceleration (m/s^2)
H' – height of the enclosure (m)
j' – constant mass flux per unit area ($kg/m^2 \cdot s$)
K – consistency index for a power-law fluid at the reference temperature ($Pa \cdot s^n$)
Le – Lewis number, Eq. (11)
L' – length of the rectangular enclosure (m)
N – buoyancy ratio, Eq. (11)
n – flow behavior index for a power-law fluid at the reference temperature
Nu – local Nusselt number, Eqs. (12), (13) and (33)
$\overline{Nu}$ – average Nusselt number, Eqs. (14) and (33)
Pr – generalised Prandtl number, Eq. (11)
q' – constant heat flux per unit area (W/m^2)
Ra_T – generalized thermal Rayleigh number, Eq. (11)
S – dimensionless concentration $\left[= \left(S' - S'_c\right) / \Delta S^*\right]$
S'_c – reference concentration at the geometric center of the enclosure (kg/m^3)
Sh – local Sherwood number, Eqs. (12), (13) and (33)
$\overline{Sh}$ – mean Sherwood number, Eqs. (14) and (33)
T – dimensionless temperature $\left[= \left(T' - T'_c\right) / \Delta T^*\right]$
T'_c – reference temperature at the geometric center of the enclosure (K)
ΔT^* – characteristic temperature $\left[= q'H'/\lambda\right]$ (K)
ΔS^* – characteristic concentration $\left[= j'H'/D\right]$ (kg/m^3)
(u, v) – dimensionless axial and transverse velocities $\left[= (u', v') / (\alpha / H')\right]$
(x, y) – dimensionless axial and transverse co-ordinates $\left[= (x', y') / H'\right]$

Greek symbols

α – thermal diffusivity of fluid at the reference temperature (m^2/s)

β_T – thermal expansion coefficient of fluid at the reference temperature (1/K)

β_S – solutal expansion coefficient of fluid at the reference concentration (m^3/kg)

λ – thermal conductivity of fluid at the reference temperature (W/m·C)

μ – dynamic viscosity for a Newtonian fluid at the reference temperature (Pa·s)

μ_a – dimensionless apparent viscosity of fluid, Eq. (7)

ρ – density of fluid at the reference temperature (kg/m^3)

Ω – dimensionless vorticity $\left[=\Omega/\left(\alpha/H'^2\right)\right]$

ψ – dimensionless stream function $\left[=\psi/\alpha\right]$

Superscript

′ – dimensional variable

Subscripts

c – value relative to the centre of the enclosure $(x, y) = (A/2, 1/2)$

* – characteristic variable

Introduction

Thermal or simple natural convection is a flow due to density variations with temperature in gravitational field. Double-diffusive natural convection, i.e. flows generated by buoyancy due to simultaneous temperature and concentration gradients, can be found in wide range of situations. In nature, such flows are encountered in the oceans, lakes, solar ponds, shallow coastal waters and the atmosphere. In industry, examples include chemical processes, crystal growth, energy storage, material and food processing, etc... For a review of the fundamental works in this area see, for instance, [1].

The literature on double-diffusive natural convection shows that the majority of investigations were focused on the enclosures of rectangular form [2].

In the past, many studies concerning Newtonian fluid flows in enclosures, driven simultaneously by thermal and solutal buoyancy effects, were carried out. These can be classified under three types, according to the thermal and solutal boundary conditions adopted. In the first type, the cavity is subjected to a vertical solutal gradient and a horizontal thermal one [3]. In the second type, both the temperature and concentration gradients are imposed transversally [4]. In the third type, which is the present case, both the thermal and solutal gradients are imposed laterally [5].

To our knowledge, for non-Newtonian fluids, except the work performed by Benhadji et al. [6] in the case of a porous horizontal rectangular layer, where double-diffusive convection is generated inside a power-law fluid by application of horizontal or vertical uniform heat and mass fluxes, there is no investigations dealing with fluid-filled enclosures.Otherwise, the majority of investigations concerning non-Newtonian fluids dealt with thermal driven buoyancy convection [7, 8].

Non-Newtonian flows are of importance and very present in many industrial applications such as paper making, oil drilling, slurry transporting, food processing, polymer engineering and many others. Some of these applications are discussed in Jaluria [9].

In order to contribute to fill the gap left by the lack of studies on the field, at least partly, the present investigation focuses on the effect of solutal buoyancy forces on natural convection heat transfer inside a two-dimensional horizontal rectangular enclosure, filled with a non-Newtonian fluid. The cavity is submitted to uniform heat and mass fluxes from its short vertical sides, while its long horizontal boundaries are insulated and impermeable.

Mathematical formulation

The studied configuration, sketched in Fig. 1, is a rectangular enclosure of height H' and length L' with the long horizontal rigid walls insulated and impermeable and the short vertical ones submitted to constant heat and mass densities of fluxes, q' and j', respectively.

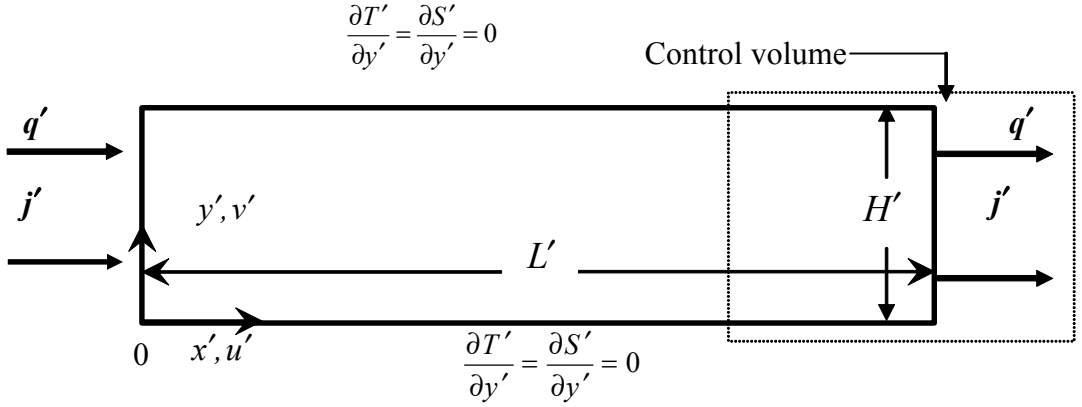

Fig. 1. *Sketch of the cavity and co-ordinates system*

The non-Newtonian fluids considered here are those for which the rheological behavior can be described by the power-law model, proposed by Ostwald-De Waele [10], whose expression, in term of laminar apparent viscosity, is

$$\mu'_a = k\left(2\left(\left(\frac{\partial u'}{\partial x'}\right)^2+\left(\frac{\partial v'}{\partial y'}\right)^2\right)+\left(\frac{\partial u'}{\partial y'}+\frac{\partial v'}{\partial x'}\right)^2\right)^{\frac{n-1}{2}}, \quad (1)$$

where n is the power-law index and k is an empirical coefficient known as the consistency factor, which is an indicator of the degree of fluids viscosity. Note that for $n = 1$ the power-law model reduces to the Newton's law by setting $k = \mu$. Thus, the deviation of n from unity characterizes the degree of non-Newtonian behavior of the fluid. Specifically, when n is in the range $0 < n < 1$ the fluid is said to be pseudo-plastic (or shear-thinning) and the viscosity is found to decrease by increasing the shear rate. On the other hand when $n > 1$ the fluid is said to be dilatant (or shear-thickening) and the viscosity increases by increasing the shear rate. Dilatant fluids are generally much less frequent than pseudo-plastic ones. Though the Ostwald-de Wale model does not converge to a Newtonian behavior in the limit of zero and maximum shear rates, it presents however the advantage to be simple and mathematically tractable. In addition, the rheological behavior of many substances can be adequately represented by this model for relatively large range of shear rates (or shear stresses) making it useful, at least for engineering purpose, and justifying its use in most theoretical investigations of fluids having pseudo-plastic or dilatant behaviors. On the other hand, the main assumptions made here are those commonly used, i.e., the flow is laminar and two-dimensional, the viscous dissipation is negligible, the interactions between heat and mass exchanges, known under the name of Soret and Duffour effects, are negligible, the fluid is incompressible and its physical properties are considered temperature independent except the density in the buoyancy term which obeys the Boussinesq approximation. Then, the dimensionless governing equations, written in terms of vorticity, Ω, temperature, T, concentration, S, and stream function, ψ, are:

$$\frac{\partial \Omega}{\partial t}+\frac{\partial(u\Omega)}{\partial x}+\frac{\partial(v\Omega)}{\partial y}=$$

$$=Pr\left[\mu_a\nabla^2\Omega+2\left[\frac{\partial\mu_a}{\partial x}\frac{\partial\Omega}{\partial x}+\frac{\partial\mu_a}{\partial y}\frac{\partial\Omega}{\partial y}\right]\right]+S_\Omega \quad (2)$$

$$\frac{\partial T}{\partial t}+\frac{\partial(uT)}{\partial x}+\frac{\partial(vT)}{\partial y}=\nabla^2 T \quad (3)$$

$$\frac{\partial S}{\partial t}+\frac{\partial(uS)}{\partial x}+\frac{\partial(vS)}{\partial y}=\frac{1}{Le}\nabla^2 S \quad (4)$$

and

$$\nabla^2\psi=-\Omega, \quad (5)$$

where

$$u=\frac{\partial\psi}{\partial y};\ v=-\frac{\partial\psi}{\partial x} \quad (6)$$

$$\mu_a=\left[2\left[\left(\frac{\partial u}{\partial x}\right)^2+\left(\frac{\partial v}{\partial y}\right)^2\right]+\left[\frac{\partial u}{\partial y}+\frac{\partial v}{\partial x}\right]^2\right]^{\frac{n-1}{2}} \quad (7)$$

and

$$S_\Omega=Pr\left[\left[\frac{\partial^2\mu_a}{\partial x^2}-\frac{\partial^2\mu_a}{\partial y^2}\right]\left[\frac{\partial u}{\partial y}+\frac{\partial v}{\partial x}\right]-2\frac{\partial^2\mu_a}{\partial x\partial y}\left[\frac{\partial u}{\partial x}-\frac{\partial v}{\partial y}\right]\right]+$$

$$+PrRa_T\left(\frac{\partial T}{\partial x}+N\frac{\partial S}{\partial x}\right). \quad (8)$$

Such a formulation presents the advantage to reduce the number of equations, by eliminating the pressure, which is without interest in this study, and to be more appropriate for two-dimensional flows.

The dimensionless boundary conditions, for the physical system considered here, are

$$u=v=\psi=0,\ \ \frac{\partial T}{\partial x}=\frac{\partial S}{\partial x}=1 \ \text{ for } x=0 \text{ and } A \quad (9)$$

$$u=v=\psi=0,\ \ \frac{\partial T}{\partial y}=\frac{\partial S}{\partial y}=0 \ \text{ for } y=0 \text{ and } 1 \quad (10)$$

On the other hand, for the vorticity, which is unknown at the boundaries, the relation of woods [11] is used, for its accuracy and stability.

The dimensionless variables are obtained by using the characteristic scales H', H'^2/α, α/H', α/H'^2, $q'H'/\lambda$, $j'H'/D$ and α corresponding to length, time, velocity, vorticity, characteristic temperature, characteristic concentration, and stream function, respectively.

In addition to the power-law index, n, the present problem is governed by five other dimensionless parameters, namely, the aspect ratio of the enclosure, A, the Lewis number, Le, the buoyancy ratio, N, the generalized Prandtl, Pr, and thermal Rayleigh, Ra_T, numbers, whose expressions are

$$A=\frac{L'}{H'},$$

$$Le=\frac{\alpha}{D},$$

$$N=\frac{\beta_S\Delta S^*}{\beta_T\Delta T^*},$$

$$Pr = \frac{(k/\rho)\,H'^{2-2n}}{\alpha^{2-n}}$$

and

$$Ra_T = \frac{g\beta H'^{2n+2} q'}{(k/\rho)\alpha^n \lambda}. \qquad (11)$$

Notice that it is possible to recover the Newtonian expressions of Pr and Ra_T by setting n = 1 and replacing k by the Newtonian viscosity μ.

Numerics

The two-dimensional governing equations are solved by using the well known second order central finite difference method with a regular mesh size. The integration of Eq. (2), (3) and (4), is performed with the alternating-direction implicit method (ADI). This method, frequently used for Newtonian fluids, was successfully extended to non-Newtonian power-law fluids in the past by Ozoe and Churchill [7] and recently by Lamsaadi et al. [8]. To satisfy the mass conservation, Eq. (5) is solved by a point successive over-relaxation method (PSOR) with an optimum relaxation factor calculated by the Franckel formula [11]. The mesh size is chosen on the basis of a compromise between running time and accuracy of the results. The procedure is based on grid refinement until the numerical results agree with the parallel flow ones, presented below, within reasonable accuracy. Hence, a uniform grid of 321×81 is found sufficient to model accurately the flow, temperature and concentration fields within a cavity of A = 24 (value used for the numerical computations). To satisfy the continuity equation, the convergence criterion $\sum_{i,j} \left|\psi_{i,j}^{k+1} - \psi_{i,j}^{k}\right| < 10^{-4} \sum_{i,j} \left|\psi_{i,j}^{k+1}\right|$ is adopted, where $\psi_{i,j}^{k}$ is the value of the stream function at the kth iteration level. The time step size, δt, is varied in the range $10^{-7} \le \delta t \le 10^{-4}$, depending on the values of the governing parameters. More precisely, the small values of δt are used for high values of n and Ra_T.

With the Ostwald power-law model, the dimensionless viscosity, given by Eq. (7), tends towards infinity, for, $0 < n < 1$ at the level of the cavity corners, where the velocity gradients tend towards zero, which renders impossible direct numerical computations. This difficulty is, however, overcome by using average values for the corner viscosity making, thus, the computations possible and stable.

The local heat and mass transfers through the fluid layer filling the cavity can be expressed in terms of the local Nusselt and Sherwood numbers, respectively, defined as

$$Nu(y) = \frac{q'}{(\lambda \Delta T'/L')} = \frac{A}{\Delta T} = \frac{1}{(\Delta T/A)}$$

and

$$Sh(y) = \frac{j'}{(D\,\Delta S'/L')} = \frac{A}{\Delta S} = \frac{1}{(\Delta S/A)}, \qquad (12)$$

where $\Delta T = T(0,y) - T(A,y)$ and $\Delta S = S(0,y) - S(A,y)$ are the side to side dimensionless local temperature and concentration differences, respectively. This definition is, however, notoriously inaccurate owing to the uncertainty of the temperature and concentration values evaluated at the two vertical walls (edge effects). Instead, the Nusselt and Sherwood numbers are calculated on the basis of a temperature and concentration differences between two vertical sections, far from the end sides. Thus, by analogy with Eq. (12), and considering two infinitesimally close sections, the local Nusselt and Sherwood numbers can be defined by

$$Nu(y) = \lim_{\delta x \to 0} \delta x/\delta T = \lim_{\delta x \to 0} \frac{1}{\delta T/\delta x} = -\frac{1}{(\partial x/\partial T)_{x=A/2}}$$

and

$$Sh(y) = \lim_{\delta x \to 0} \delta x/\delta S = \lim_{\delta x \to 0} \frac{1}{\delta S/\delta x} = -\frac{1}{(\partial x/\partial S)_{x=A/2}}, \qquad (13)$$

where δx is the distance between two symmetrical sections with respect to the central one. The corresponding average Nusselt and Sherwood numbers are, respectively, calculated at different locations, as follows

$$\overline{Nu} = \int_0^1 Nu(y)\,dy$$

and

$$\overline{Sh} = \int_0^1 Sh(y)\,dy. \qquad (14)$$

As an additional check of the results accuracy, energy and matter balances are systematically verified for the system at each numerical code running. Thus, the overall heat and mass transfers, through each vertical plane, are evaluated and compared with the quantities of heat and mass furnished to the system at x = 0. For the results reported here, the energy and matter balances are satisfied within 2 % as a maximum difference.

Typical numerical results, in terms of streamlines (a), isotherms (b) and isoconcentrations, are presented in Fig. 2, obtained, for A = 24, Le = 10, $Ra_T = 10^5$ and various values of n and N. As appears, from these figures, the flow is parallel to the horizontal boundaries of the enclosure and the temperature and the concentration are linearly stratified in the x-direction of the core region. The approximate analytical solution, developed in the next section, relies on these observations.

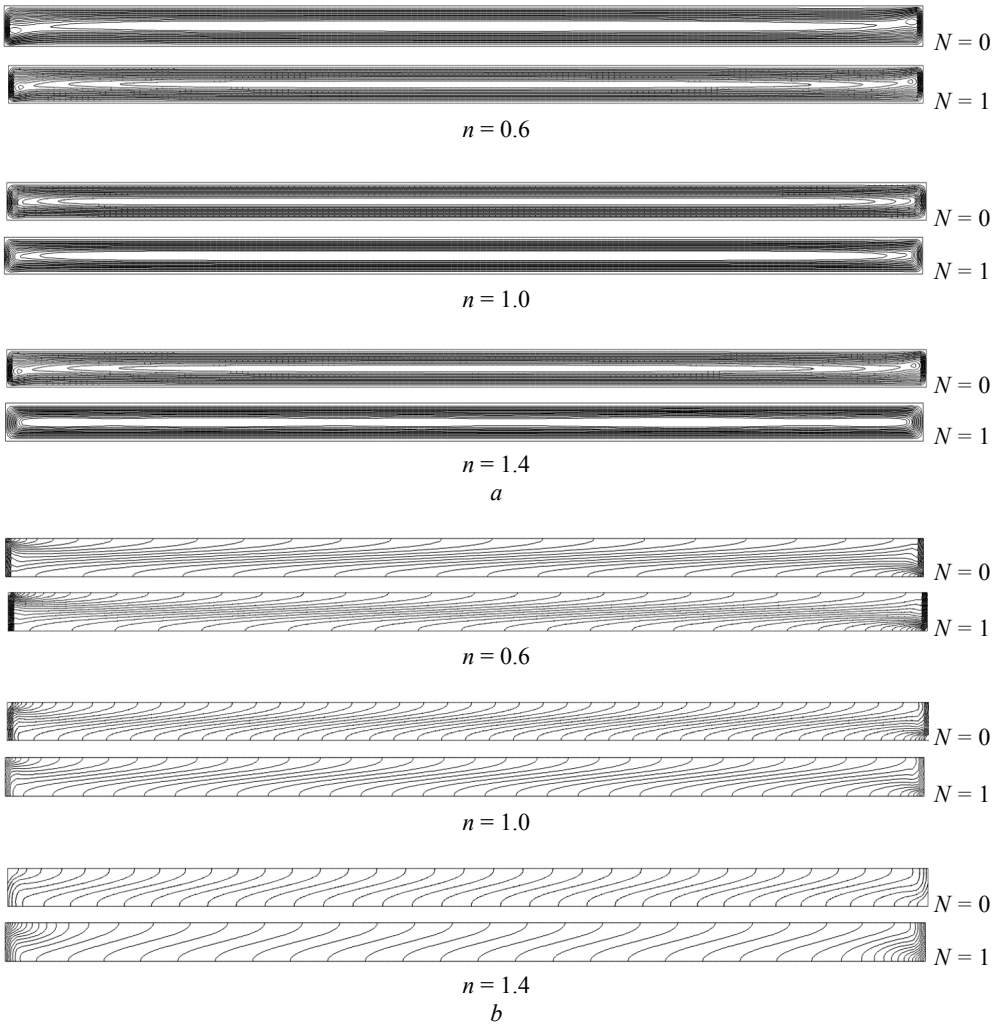

Fig. 2. *Combined effect of N and n on: a) – streamlines; b) – isotherms*

Approximate parallel flow analytical solution

The results presented in Fig. 2, allow the following appropriate simplifications:

$$\psi(x,y)=\psi(y),\ T(x,y)=C_T(x-A/2)+\theta_T(y)$$

and

$$S(x,y)=C_S(x-A/2)+\theta_S(y), \qquad (15)$$

where C_T and C_S are unknown constant temperature and concentration gradients in the x-direction. On the basis of this, the non-dimensional governing equations become

$$\frac{d^2}{dy^2}\left[\left|\frac{du}{dy}\right|^{n-1}\frac{du}{dy}\right]=(C_T+NC_S)Ra_T=ERa_T, \qquad (16)$$

$$C_T u=\frac{d^2\theta_T}{dy^2} \text{ and } LeC_S u=\frac{d^2\theta_S}{dy^2} \qquad (17)$$

with

$$u=\frac{d\theta_T}{dy}=\frac{d\theta_S}{dy}=0 \text{ for } y=0 \text{ and } 1, \qquad (18)$$

$$\int_0^1 u(y)\,dy=0 \qquad (19)$$

as boundary and return flow conditions, respectively.

Recently, the above concept has been successfully used by Lamsaadi et al. [8] to predict the thermal convection flow behavior in the case of a non-Newtonian power-law fluid.

The integration of Eq. (16) and (17), coupled with the conditions (18) and (19), leads to analytical expressions of velocity, temperature and concentration. However, such an operation is difficult to carry out owing to the particular nature of the governing equations and requires, therefore, a special numerical treatment. In fact, the non-linearity of the fluid behavior and the change of du/dy sign, due to the return flow, impose that the velocity

expressions are different depending on whether $0 \le y \le y_0$, $y_0 \le y \le y_1$ or $y_1 \le y \le 1$, where y_0 and $y_1 = 1 - y_0$ (because of the centro-symmetry of the core flow) are the vertical coordinate values for which $du/dy = 0$. They are derived from Eq. (19), which is numerically solved by using a combination of the Regula-Falsi iteration method [12] and the Gauss-Legendre integration method [13]. To reduce the velocity, temperature and concentration expressions, the function $f(y) = \left(y^2 - y + y_0 y_1\right)/2$ is introduced. Thus, for

$0 \le y \le y_0$

$$u(y) = E^{1/n}\ Ra_T^{1/n}\left[\int_0^y [f(y)]^{1/n}\,dy\right], \tag{20}$$

$$\theta_T(y) = C_T E^{1/n} Ra_T^{1/n}\left[\int_0^y\left[\int_0^y\left[\int_0^y [f(y)]^{1/n}\,dy\right]dy\right]dy\right] + \theta_T(0)\,. \tag{21}$$

$y_0 \le y \le y_1$

$$u(y) = E^{1/n}\ Ra_T^{1/n}\left[\int_0^y [f(y)]^{1/n}\,dy + \int_y^y [-f(y)]^{1/n}\,dy\right], \tag{22}$$

$$\theta_T(y) = C_T E^{1/n}\ Ra_T^{1/n}\left[\frac{(y-y_0)^2}{2}\int_0^{y_0}[f(y)]^{1/n}\,dy + \int_{y_0}^y\left[\int_{y_0}^y\left[\int_y^{y_0}[-f(y)]^{1/n}\,dy\right]dy\right]dy\right] +$$
$$+ (y-y_0)\int_0^{y_0}\left[\int_0^y [f(y)]^{1/n}\,dy\right]dy + \int_0^y\left[\int_0^y\left[\int_0^y [f(y)]^{1/n}\,dy\right]dy\right]dy\right] + \theta_T(0)\,. \tag{23}$$

$y_1 \le y \le 1$

$$u(y) = E^{1/n}\ Ra_T^{1/n}\left[\int_0^{y_0} [f(y)]^{1/n}\,dy + \int_{y_1}^{y_0} [-f(y)]^{1/n}\,dy + \int_{y_1}^y [f(y)]^{1/n}\,dy\right], \tag{24}$$

$$\theta_T(y) = C_T E^{1/n}\ Ra_T^{1/n}\left[\frac{1}{2}(y-y_1)(y+y_1-2)\left[\int_0^{y_0}[f(y)]^{1/n}\,dy + \int_{y_1}^{y_0}[-f(y)]^{1/n}\,dy\right] +\right.$$
$$+ \int_{y_1}^y\left[\int_1^y\left[\int_{y_1}^y [f(y)]^{1/n}\,dy\right]dy\right]dy + \int_{y_0}^{y_1}\left[\int_{y_0}^y\left[\int_y^{y_0}[-f(y)]^{1/n}\,dy\right]dy\right]dy +$$
$$\left. + \frac{1}{2}(y_1-y_0)^2\int_0^{y_0}[f(y)]^{1/n}\,dy + (y_1-y_0)\int_0^{y_0}\left[\int_0^y [f(y)]^{1/n}\,dy\right]dy + \int_0^{y_0}\left[\int_0^y\left[\int_0^y [f(y)]^{1/n}\,dy\right]dy\right]dy\right] + \theta_T(0)\,. \tag{25}$$

The expression of $\theta_s(y)$, given by

$$\theta_S(y) = Le\frac{C_S}{C_T}\theta_T(y) \tag{26}$$

is obtained by eliminating u from Eq. (17) and (18), and integrating twice the resulting equation taking into account of Eq. (19) and the centro-symmetry of thermal and solutal fields in the core region. The exploitation of such a property and the use of Eq. (26) give, respectively:

$$\theta_T(0) = -C_T E^{1/n}\ Ra_T^{1/n}\left[\frac{(1/2-y_0)^2}{2}\int_0^{y_0}[f(y)]^{1/n}\,dy + \int_{y_0}^{1/2}\left[\int_{y_0}^{y}\left[\int_{y}^{y_0}[-f(y)]^{1/n}\,dy\right]dy\right]dy + \right.$$

$$\left. + (1/2-y_0)\int_0^{y_0}\left[\int_0^{y}[f(y)]^{1/n}\,dy\right]dy + \int_0^{y_0}\left[\int_0^{y}\left[\int_0^{y}[f(y)]^{1/n}\,dy\right]dy\right]dy\right] \quad (27)$$

and

$$\theta_S(0) = Le\frac{C_S}{C_T}\theta_T(0)\,. \quad (28)$$

The expression of $\psi(y)$ can be deduced from that of $u(y)$ by integration of Eq. (6) taking into account of Eq. (10). Therefore, the stream function at the center of the enclosure, which is a measure of the flow intensity, can be expressed by

$$\psi_c = \psi(A/2,1/2) = E^{1/n}Ra_T^{1/n}\left[(1/2-y_0)\int_0^{y_0}[f(y)]^{1/n}\,dy + \int_0^{y_0}\left[\int_0^{y}[f(y)]^{1/n}\,dy\right]dy + \int_{y_0}^{1/2}\left[\int_{y}^{y_0}[-f(y)]^{1/n}\,dy\right]dy\right]. \quad (29)$$

On the other hand, C_T and C_S are evaluated from thermal and solutal boundary conditions imposed on the end walls. Because of the turning flow at the end regions of the fluid layer, the boundary conditions in the *x*-direction, Eq. (9), could not be satisfied by the parallel flow approximation. Instead, the expressions of C_T and C_S are determined by matching the core solution, Eq. (15), to the integral solution for the end regions, which consists on the integration of Eq. (3) and (4), together with the boundary conditions (9) and (10), by considering the arbitrary control volume of Fig. 1. This yields:

$$C_T + 1 = \int_0^1 u(y)\theta_T(y)\,dy$$

and

$$C_S + 1 = Le\int_0^1 u(y)\theta_S(y)\,dy \quad (30)$$

to which the substitution of the expressions of $u(y)$, $\theta_T(y)$ and $\theta_S(y)$ gives:

$$C_T = \frac{1}{A_n E^{1/n} Ra_T^{1/n} - 1} \text{ and } C_S = \frac{1}{A_n Le^2 E^{1/n} Ra_T^{1/n} - 1} \quad (31)$$

On the other hand, knowing that $E = C_T + NC_S$, the following transcendental equation is obtained

$$Le^2 A_n^2 Ra_T^{4/n} E^{1+4/n} - A_n(1+Le^2)Ra_T^{2/n}E^{1+2/n} -$$

$$-(Le^2+N)A_n Ra_T^{2/n}E^{2/n} + E + (N+1) = 0\,, \quad (32)$$

where the coefficient A_n, which depends only on *n*, is calculated with the Gauss-Legendre integration method and its values are presented with those of y_0 in Table 1.

Table 1

Dependence of y_0 and A_n on *n*

n	y_0	A_n
0.6	0.199	$-0.485\cdot10^{-7}$
1.0	0.211	$-0.276\cdot10^{-5}$
1.4	0.219	$-0.160\cdot10^{-4}$

It should be point out, from Table 1, that y_0 is an increasing function of *n*, which means that the velocity maximum is displaced away from the lower wall by increasing *n*. Moreover, Eq. (19)-(27) indicate that *n* is the only parameter that affects the shape of *u*, ψ, θ_T and θ_S profiles.

To determine the value of *E*, Eq. (32) is solved by the Regula-Falsi iteration method and the values of C_T and C_S are deduced from Eq. (31), for each given value of *Le*, *N*, *n* and Ra_T.

Finally, taking into account of Eq. (13) and (14), the Nusselt and Sherwood numbers are constant and can be expressed as

$$Nu = -1/C_T = \overline{Nu}$$

and

$$Sh = -1/C_S = \overline{Sh}\,. \quad (33)$$

Results and discussion

The fact of imposing uniform heat and mass fluxes, as boundary conditions, leads to flow characteristics independent on the aspect ratio, *A*, when this parameter is large enough. The approximate solution, developed in the preceding section, on the basis of the parallel flow assumption, is thus valid asymptotically in the limit of a shallow cavity $A >> 1$. In this respect, after some

numerical tests (results not presented here), 24 is found as being the smallest value of A leading to results reasonably close to those of the large aspect ratio approximation. In fact, the asymptotic analytical limits are largely reached in such a situation. This value reduces to $A = 8$ in pure thermal convection ($N = 0$) as obtained by Lamsaadi et al. [8], which shows the retarding role of the double diffusion with respect to the asymptotic state. On the other hand, for the non-Newtonian fluids considered here, the Prandtl number, Pr, is large enough such that the convection becomes insensitive to any change of the large values of this parameter [4, 8]. On the basis of this, the simulations are conducted with $Pr - \propto$, i.e. by neglecting the convective terms on the left hand side of Eq. (2), which presents the advantage of making the computations faster than with finite large values of Pr [10]. Therefore, the natural double-diffusive convection flow developed inside the enclosure is governed by the thermal Rayleigh number, Ra_T , the buoyancy ratio, N, the Lewis number, Le, and the power-law index n, which is varied, in this study, from 0.6 to 1.4 to include shear-thinning $(0 < n < 1)$, Newtonian $(n = 1)$ and shear-thickening $(n > 1)$ fluids.

Validation of the approximate parallel flow analytical solution

The inspection of the streamlines (*a*) and isotherms (b), depicted in Fig. 2, allows affirming the existence of an analytical solution, for the present problem, owing to the parallelism and the stratification aspects that flow and temperature fields exhibit, respectively, in the central part of the enclosure, i.e. somewhat far from the side edges. Moreover, Fig. 3, comparing the corresponding horizontal velocity (top) and temperature (bottom) profiles, calculated analytically (continuous lines) and numerically (black dots) at mid-length of the cavity, along the vertical direction, testify to the almost perfect agreement between the two types of solutions.

Another confirmation of this is given by Table 2 where the relative difference between analytical and numerical results does not exceed 0.61 % for $|\psi_c|$ and 0.38 % for $\overline{Nu}$.

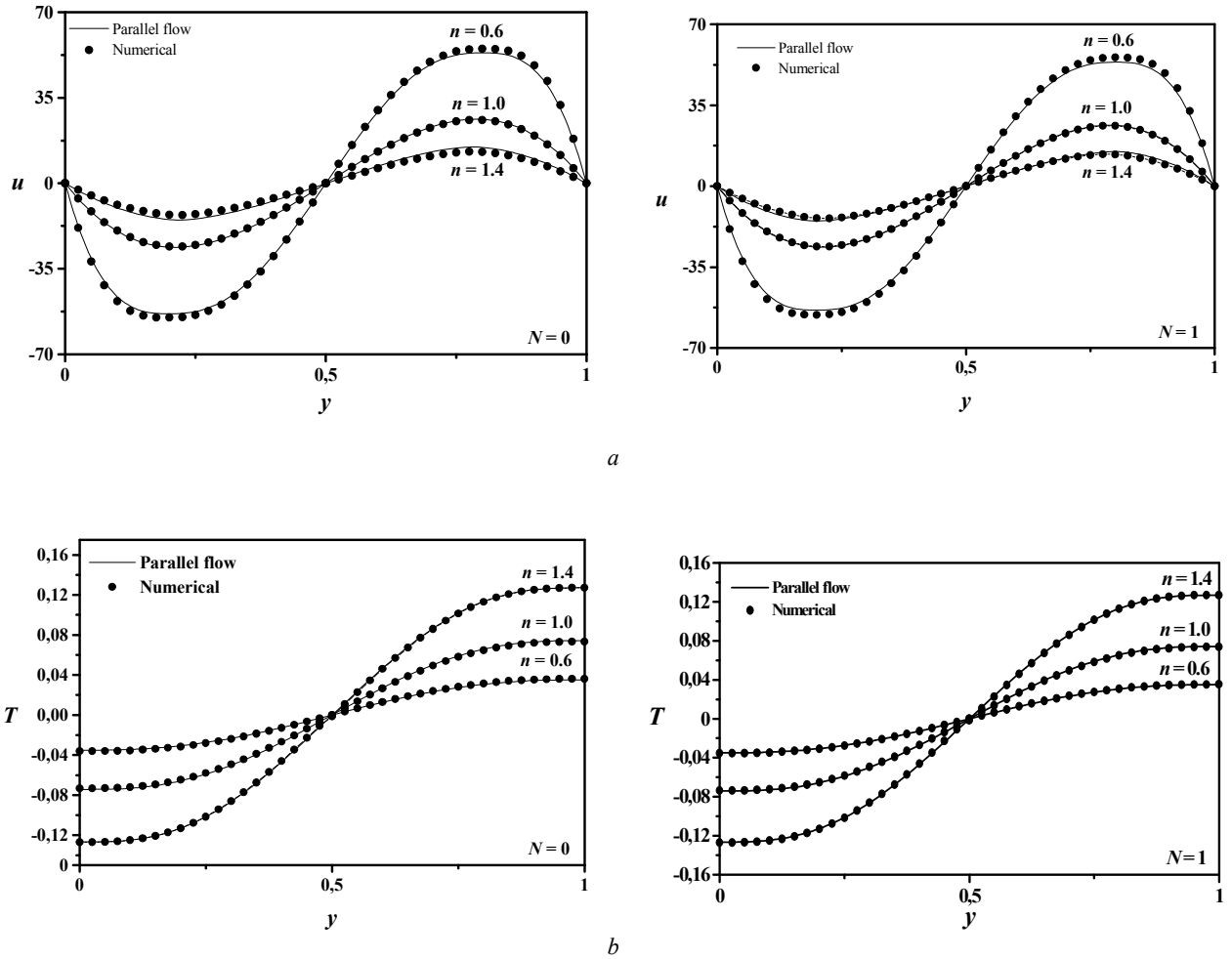

***Fig. 3**. Velocity (a) and temperature (b) profiles for $Ra_T = 10^5$, Le = 10 and different values of n and N*

Table 2

Comparison between the analytical and numerical results for $N = 0$, $Ra_T = 10^5$ and $Le = 10$

$N = 0$		$\lvert\psi_c\rvert$		$\overline{Nu}$	
		Parallel flow	**Numerical**	**Parallel flow**	**Numerical**
n	0.6	19.016	18.991	139,835	139.8
	1.0	8.035	8.01	30.115	30.08
	1.4	4.045	4.02	9.145	9.11
$N = 1$		$\lvert\psi_c\rvert$		$\overline{Nu}$	
		Parallel flow	**Numerical**	**Parallel flow**	**Numerical**
n	0.6	19.1	19.12	140.3	140.33
	1.0	8,51	8.53	30.549	30.58
	1.4	4.57	4.59	9.652	9.68

Hence, it appears clear, from what precedes, that the results of the two approaches adopted in this study agree, at least for the governing parameters selected values, which validates the parallel flow assumption used in section 4 and justifies the choice of $A = 24$ as a large aspect ratio approximation value.

Thermal convection with and without solutal buoyancy forces

At first, it is advisable to recall that the case of natural simple convection (thermal) corresponds to $N = 0$, i.e. the case where solutal buoyancy forces are absent, whereas in presence of these forces, which corresponds to $N \neq 0$, it is about the natural double diffusive convection.

It seems obvious from Fig. 2, where are depicted the streamlines (*a*) and isotherms (*b*), that the flow structure and the thermal field do not undergo qualitative change when N passes from 0 to 1 (case where thermal and solutal buoyancy forces act in the same direction with the same intensity), since the isolines indicate a unicellular regime with a parallel aspect and thermal stratification in the core region of the cavity and this independently on N. The flow and heat transfer intensities, whose numerical values are given in Table 3, show also this fact.

Table 3

Effect of n and N on the flow intensity and heat transfer rate for $Ra_T = 10^5$ and $Le = 10$

		$\lvert\psi_c\rvert$		$\overline{Nu}$	
		$N = 0$	$N = 1$	$N = 0$	$N = 1$
n	0.6	18.991	19.1	139.8	140.3
	1.0	8.01	8.51	30.08	30.549
	1.4	4.02	4.57	9.11	9.652

For a fine examination of the effect of solutal buoyancy forces on thermal convection, the horizontal velocity (*a*) and temperature (*b*)profiles are displayed in Fig. 4.

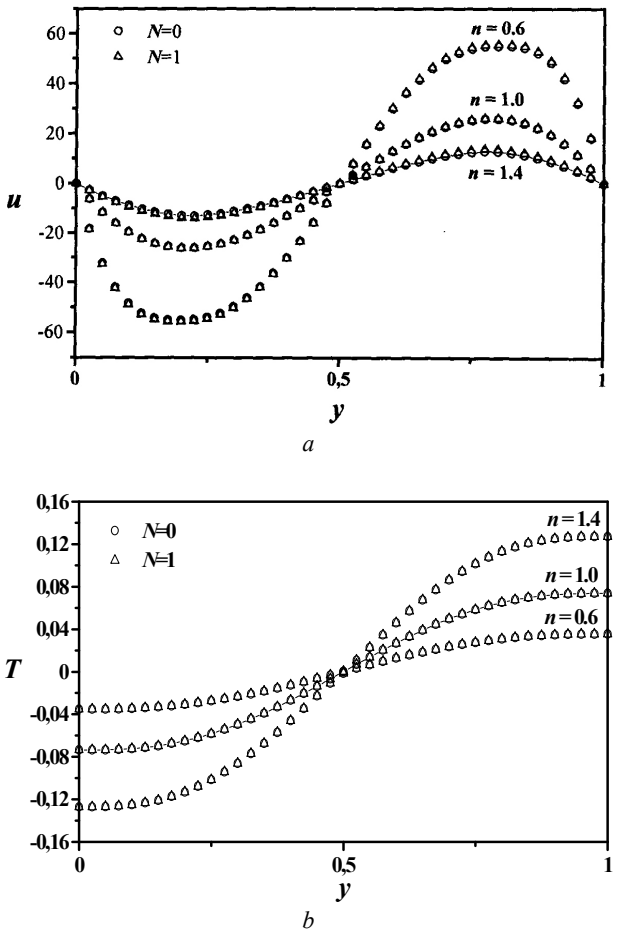

***Fig. 4**. Velocity (a) and temperature (b) profiles for $Ra_T = 10^5$, $Le = 10$ and different values of n and N*

As can be seen, for all the considered values of n, the profiles remain almost identical while passing N from 0 to 1, which means that this parameter does not affect the dynamical and thermal fields. This is related essentially to the fact that the contribution of the solutal effects in the convection is negligible (Le = 10). Such a situation can be described as a regime of prevailing thermal effects.

Influence of the power-law non-Newtonian behaviour on thermal convection

Useful information, concerning the influence of the non-Newtonian rheological behavior on the flow and thermal fields, can be obtained from the examination of Fig. 2. Thus, although the streamlines do not show a qualitative modification in the flow global structure, which keeps a unicellular and parallel aspect in the central part of the cavity independently on the value of n, the flow intensity, ψ_c, undergoes significant quantitative variations with n. In fact $|\psi_c|$ is seen to decrease with n passes, as shown in Table 3, which means, thus, a slowing down of the fluid circulation in such a situation. This trend is confirmed by the velocity profiles (a) of Fig. 3. On the other hand, the corresponding isotherms appear much more affected by the rheological behavior , since they become less and less inclined, with regard to the vertical direction, while increasing n, which testifies, thus, to the reduction of the flow intensity with this parameter. Moreover, Figs. 3 (b) show an increase, in absolute values, of the temperature with n, which indicates that the flow loses its intensity in such circumstances. This type of evolution, with n, is found also on the level of the mean heat transfer rate, $\overline{Nu}$, whose values decrease while increasing n, illustrated by Table 3.

Such results can be explained while referring to Eq. (7), where an increase of n causes an increase of the apparent viscosity, whose slowing-down role on the fluid motion is well known. It results, from what precedes, that, compared to Newtonian case (n = 1), the shear-thinning behavior ($0 < n < 1$) enhances the convection whereas the shear-thickening one ($n > 1$) reduces it.

Conclusion

The present paper is devoted to numerical and analytical experiments on natural simple and double-diffusive convections in a two-dimensional horizontal shallow enclosure ($A >> 1$), filled with non-Newtonian power-law fluids, in the case where both short vertical sides are submitted to uniform heat and mass fluxes while the horizontal boundaries are insulated and impermeable. The main conclusions of the present investigation are summarized as follows:

- The approximate analytical solution, developed on the basis of the parallel flow hypothesis in the core region of the cavity, is found to agree perfectly with the numerical solution, obtained by solving numerically the full governing equations.
- The buoyancy ratio, N, seems not influencing the convection heat transfer while passing from 0 to 1 being given the value of the Lewis number, Le = 10.
- The fluid flow and heat transfer characteristics seem to be rather sensitive to the flow behavior index, n. Thus, compared to Newtonian case (n = 1), the shear-thinning behavior ($0 < n < 1$) enhances the fluid circulation and the convection heat and mass transfers while the shear-thickening one ($n > 1$) produces an opposite effect.

In the future an extent for this study will be carried out with moderate and high values of N in order to examine widely the effect of this parameter on convection heat transfer.

References

1. Viskanta R., Bergman T.L., Incopera F.P. Double-diffusive natural convection. In Natural Convection, Fundamentals and Applications. Hemisphere, Washington DC; 1985.
2. Nield D.A., Bejan A. Convection in Porous Media, Springer Verlag; 1992.
3. Kalla L., Vasseur V., Benacer R., Beji H., Duval R. Double-diffusive convection within a horizontal porous layer salted from the bottom and heated horizontally // Int Comm Heat Mass Transfer. 2001. 28. P. 1-10.
4. Mamou M., Vasseur P., Hasnaoui M. On numerical stability analysis of double-diffusive convection in confined enclosures // J Fluid Mech. 2001. 433. P. 209-250.
5. Ouriemi M., Vasseur P., Bahloul A., Robillard L. Natural convection in a horizontal layer of a binary mixture // Int J Thermal Sciences. 2006. 45. P. 752–759.
6. Benhadji K., Vasseur P. Double-diffusive convection in a shallow porous cavity filled with a non-Newtonian fluid // Int Comm Heat Mass Transfer. 2001. 28. P. 763-772.
7. Ozoe H., Churchill S.W. Hydrodynamic stability and natural convection in Ostwald-De Waele and Ellis fluids: the development of a numerical solution // AIChE J. 1972. 18. P. 1196-1207.
8. Lamsaadi M., Naimi M., Hasnaoui M. Natural convection heat transfer in shallow horizontal rectangular enclosures uniformly heated from the side and filled with non-Newtonian power law fluids // Energy Conversion and Management. 2006. 47. P. 2535-2551.
9. Jaluria Y. Thermal processing of materials: From basic research to engineering // Journal of Heat Transfer. 2003. 125. P. 957-979.
10. Bird R.B., Armstrong R.C., Hassager O. Dynamics of polymeric liquids // Fluid Mechanics. Willey, New York, 1987. Vol. 1.
11. Roache P.J. Computational fluid dynamics. New Mexico, Albuquerque: Hermosa Publishers, 1982.
12. Gourdin A., Boumahrat M. Applied numerical methods. Technique and Documentation-Lavoisier, Paris, 1989.
13. Sibony M., Mardon J-CI. Numerical Analysis II, Approximation and differential equations. Paris: Hermann, 1982.

AB INITIO STUDY OF PHASE SEPARATION AND ORDERING IN II-IV-BASED TERNARY ALLOYS

R. Miloua*, F. Miloua*, A. Arbaoui**, Z. Kebbab*, N. Achargui, N. Benramdane****

*Laboratoire d'Elaboration et de Caractérisation des Matériaux,
Faculté des Sciences de l'Ingénieur, BP 89, Université Djillali LIABES
Sidi-Bel-Abbès, Algeria.
Tel: 00 213 50 71 61 56; E-mail: mr_lecm@yahoo.fr

**Laboratoire de Physique des Matériaux, Faculté des Sciences,
Université Mohammed V-Agdal, Rabat, Morocco.

***Faculté des Sciences et Techniques Guéliz, Département de Physique,
Université Cadi Ayyad, Marrakech, Morocco.

Received: 31 July 2007; accepted: 26 Aug 2007

First-principles calculations of the ground-state properties and the stability of $Cd_{1-x}Zn_xTe$ solid solutions are presented using the full-potential linearized augmented plane wave (FP-LAPW) method in combination with the local density approximation (LDA). It is found that the structural parameters, i.e. lattice constants and bulk moduli follow a linear function of the composition *x.* The stability of the alloys is viewed as an energetic balance between pure structural constraints and quantum chemical effect. Our calculations yield to the prediction of an ordering tendency for low Zn content, occurrence of an intermediate disordered phase at 50-50 % of composition and phase separation for the Zn-rich range. These results agree well with the recent experimental work by Arbaoui et al. Sol. Ene. Mater. Sol.-Cells. 2006. 90. P. 1364.

Keywords: materials for solar-hydrogen energy, photovoltaic effect in semiconductor structures

Fodil Miloua

Organization(s): Scientist researcher at Laboratoire d'Elaboration et de Caractérisation des Matériaux.
Education: D.E.A in electronics at Université des Sciences et Techniques of Lille, France (1986).
Doctorate in Physics and materials science at Claude Bernard University- Lyon I, France (1992).
Main range of scientific interests: Materials science, surfaces and interfaces.
Some publications (number of publications: 11)**:** F. Miloua et al. Structural and electrical characterzation of Ag-InP(100) interfaces stabilized by antimony // Materials Chemistry and Physics 1993. 33. P. 85.; M. Bouslama, B. Khelifa, F. Miloua et al. Interaction of phosphorus with Indium // Appl. Surf. Sciences. 1992.; F. Miloua et al. Structural and electrical characterizations of Ag-InP(100) interfaces stabilized by antimony // 3ème Rencontre de Physique: ''Sciences des Surfaces des Matériaux''. Oran. 1991.

Introduction

The mixed crystals of II-VI compounds semiconductors have attracted mush attention in recent years because of the relevance of their optical properties. These materials permit many applications as infrared detectors, solar cells and other optoelectronic devices [1]. The CdZnTe (CZT) alloy is one of the most promising II-IV-based alloys that have been the subject of many interesting experimental studies. CZT was successfully grown both in bulk and in thin film forms by different techniques such as two-stage process [2], molecular beam epitaxy [3], chemical vapour deposition [4, 5] and electrodeposition technique [6].

Very recently, Arbaoui et al. [7] reported on the growth of CZT by the RF magnetron sputtering technique. They showed that the formation of the polycrystalline ternary alloy is favoured for a small concentration of Zn. In contrast, for samples with higher Zn content, the XRD spectra showed no formation of CdZnTe. The measured lattice constants are found to vary linearly with Zn composition as expected from the Vegard's law.

The main goal of the present work is to investigate theoretically the possibility to form the CZT ternary alloys with varying Zn composition. Since ordering phenomena can influence directly both electronic and optical properties of a material, it motivates us to investigate the stability of $Cd_{1-x}Zn_xTe$ ordered structures by using the Full-Potential Linearized Augmented Plane Wave (FP-LAPW) method [8]. This method is one of the most accurate schemes to calculate structural, electronic and thermodynamic properties of materials. We considered that the ternary alloys are cubic pseudo-binary semiconductors with one of the two fcc sublattices occupied by Te atoms and the other by Cd

and Zn. Furthermore, we introduce the disordering effect and predict that the alloys prefer ordering for low Zn content and clustering elsewhere.

The paper is organized as follows. In section 2, we briefly describe the calculation procedure. Results and discussions are presented in section 3 and the paper is summarized in section 4.

Method of calculation

Our calculations have been made using FP-LAPW approach within the framework of the Density Functional Theory (DFT) [9, 10] as implemented in WIEN2K [11] code. The exchange-correlation contribution to the total energy is described within the Local Density approximation (LDA) [12].

Kohn-Sham wave functions were expanded in terms of spherical harmonic functions inside the non-overlapping muffin-tin spheres surrounding the atomic sites (MT spheres) and in Fourier series in the interstitial regions. Inside the MT spheres of radius R_{MT}, the l-expansion of the wave function were carried out up to $l_{\max} = 10$ while the charge density was Fourier expanded up to $G_{max} = 14$ $(\text{Ryd})^{1/2}$. In order to achieve energy eigenvalues convergence, the wave functions in the interstitial region were expanded in plane waves with a cut-off parameter of $K_{\max} = 8/R_{MT}$ for both binary and ternary alloys. R_{MT} values were assumed to be 2,2 a.u. for Zn, 2,6 a.u. for Cd and 2,4 a.u. for Te atoms, respectively for all structures. A mesh of 30 special k-points for both binary and ternary compounds was taken in the irreducible wedge of the Brillouin zone. Both the MT radius and the number of k-points were varied to ensure total energy convergence. The core states that are completely confined inside the corresponding MT spheres were treated fully relativistic, while for the valance states we used the scalar relativistic approach that includes the mass velocity and Darwin s-shift, but omits spin-orbit coupling.

Results and discussions

Structural parameters

First, we calculated the structural properties of the binary compounds CdTe and ZnTe in the zinc blend structure. Then, the ordered ternary alloys $Cd_{1-x}Zn_xTe$ were simulated at the compositions x = 0,25, 0,5 and 0,75. For each composition, we carried out a structural optimization by minimizing the total energy with respect to the cell volume and also the atomic positions. A simple cubic structure (luzonite) of eight atoms is used to model compositions of x = 0,25 and x = 0,75. For x = 0,5 the smallest ordered structure is a four-atom tetragonal cell, which corresponds to the (001) superlattice.

The calculated lattice constants and bulk moduli were obtained by fitting the total energy versus unit cell volume to the Murnaghan's equation of state [13]. In Fig. 1 and Fig. 2 we depicted, respectively the lattice constants and the bulk moduli as a function of the composition x. From Fig. 1, one can see that the calculated lattice parameters are close to those obtained by considering an ideal mixing between CdTe and ZnTe, the differences between theme are less than 0.4 %. The calculated lattice constants follow a decreasing linear function of composition x as expected by the Vegard's law, this concords well with the results reported in Refs. [7, 14-16]. A fitting of both the experimental data reported in Ref. [7] and the calculated ones leads to the following linear equations:

$$a_{\exp}(x) = 6.479 - 0.432x, \quad (1)$$

$$a_{th}(x) = 6.421 - 0.411x. \quad (2)$$

Considering the general trend that the LDA usually underestimates the lattice parameters, our LDA results are in reasonable agreement with experiment and the other theoretical values. In Fig. 2, the composition dependence of the bulk moduli is compared with the results predicted by the linear concentration dependence (LCD). The bulk moduli exhibit a small deviation from the LCD and are in reasonable agreement with those obtained by Wei et al. [17].

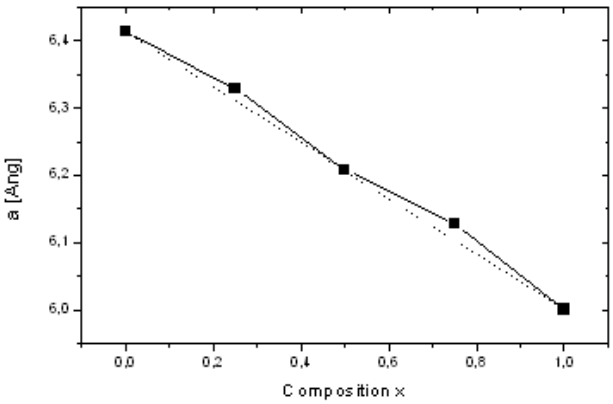

Fig. 1. *The calculated lattice constants (solid squares) and lattice constants of ideal mixing solid solutions (doted line) for the five ordered structures* $(Cd)_{1-n}(Zn)_nTe$ *(n = 0, 1, 2, 3, 4)*

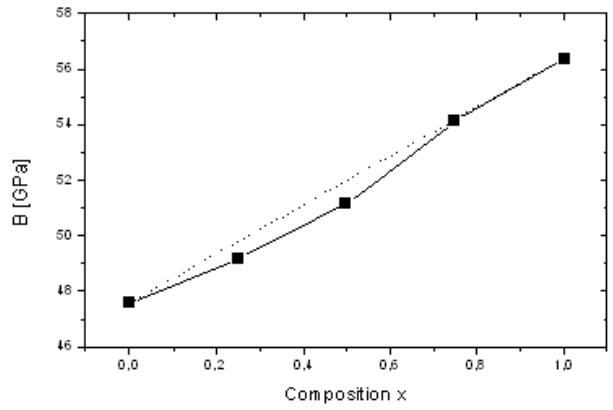

Fig. 2. *Calculated bulk moduli (solid squares) and those of ideal mixing (dotted line) as a function of composition*

Stability of the ordered phase

In order to study the stability of CdZnTe in the ordered form. we calculated the formation energies of the five (n = 0, 1, 2, 3, 4) structures using the following relation

$$E_{form}(n) = E_{(Cd)_{1-n}(Zn)_n Te} - \frac{n}{4}E_{ZnTe} - \left(1-\frac{n}{4}\right)E_{CdTe}, \quad (3)$$

where $E_{(Cd)_{1-n}(Zn)_n Te}$ is the total energy of the *n*th ordered alloy, E_{ZnTe} and E_{CdTe} are total energies of ZnTe and CdTe binaries, respectively. The results are viewed in Fig. 3 (solid squares) together with those for disordered alloys (solid line).

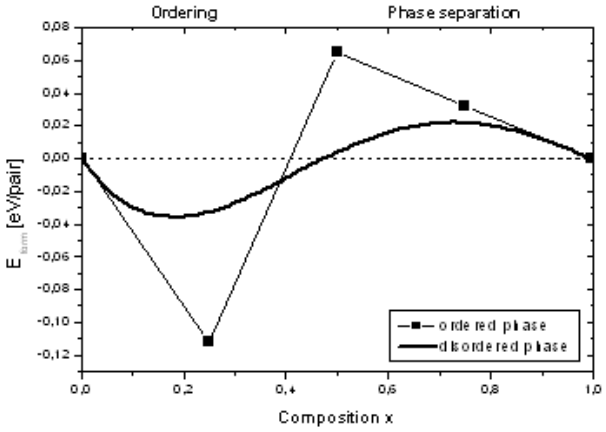

Fig. 3. *The calculated formation energies for ordered structures and disordered alloys*

The formation energy can give a measure of the stability of a material. For low Zn compositions we notice that it is negative below $x = 0.41$ and positive elsewhere. This trend indicates an ordering tendency that occurs for low Zn content and a phase separation for Zn-rich range. Thus, our results are consistent with the experimental ones from Ref. [7].

In order to clarify the physical origin of this behaviour, we decompose E_{form} into three physically recognizable contributions [18-20] as follows:

$$E_{form} = E_{VD} + E_{CE} + E_{ER}, \quad (4)$$

where E_{VD} is the hydrostatic "volume deformation" contribution due to the dilatation of ZnTe and compression of CdTe from their equilibrium lattice constants (6.00 Å and 6.414 Å, respectively) to the common (Vegard-like) lattice constant of the alloy;

E_{CE} is the "charge exchange" energy that releases when ZnTe and CdTe, taken at common lattice constant, combine to give $Cd_{1-x}Zn_xTe$ ordered alloy. The internal relaxation effects are not included in this energy;

E_{ER} is the "structural relaxation" term due to the full relaxation of cell-internal degrees of freedom.

From the equation (2), one can derive two different energetic terms E_{struct} and E_{elec} that have different physical meanings:

$$E_{form} = E_{chem} + E_{struct}, \quad (5)$$

where E_{chem} means a chemical contribution associated to an electronic mismatch between cations and E_{struct} means a structural contribution (positional relaxation + volume deformation) induced by both lattice and atom-size mismatches.

Fig. 4 shows the splitting of the formation energies of the ternary alloys into the three physical contributions; we can deduce the following important remarks:

– The large lattice mismatch (≈ 6 %) between the binary constituents leads to a large and positive E_{VD} that tends to decrease the stability of CdZnTe alloys over the whole range of composition. Because of the atom-size mismatch, including one Zn atom in a CdTe host leads to a less strained structure then including one Cd atom in a ZnTe host. This behaviour can be deduced form the fact that E_{VD} ($x = 0.25$) < E_{VD} ($x = 0.75$).

– In contrast to E_{VD}, internal relaxations tend to increase the stability of the alloys by taking a negative E_{SR} values. However, the sum E_{VD} + E_{SR} remains positive and increases with increasing the concentration.

– The electronic contribution E_{CE} to the formation energies appears to be a relevant term.

For $x = 0.25$, the energy E_{CE} is negative and overwhelms the E_{VD} + E_{SR} term. This let us to conclude that the expected stability of CdZnTe alloys for low Zn content have a chemical nature.

– At 50-50 % content, both structural and chemical parts are positive, leading to a phase separation. We notice that the chemical part contributes significantly to the formation energy. For the highest Zn composition (i.e. $x = 0{,}75$), the alloy instability takes a structural nature and the structural energy contribution overwhelms the chemical one.

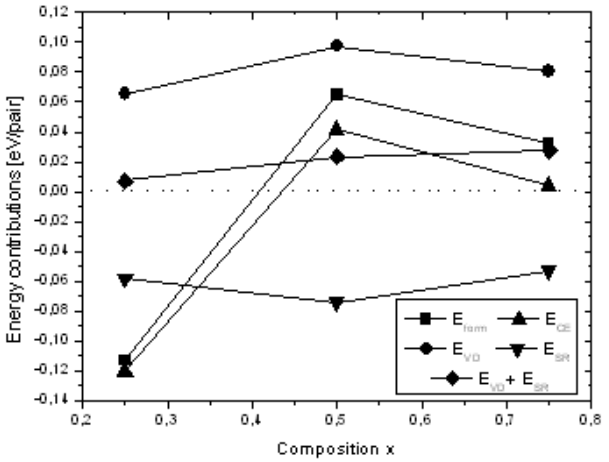

Fig. 4. *Energy contributions to the formation energies of ordered alloys*

Stability of the disordered phase

In this section, the energetics of the disordered alloys are calculated using a cluster expansion. Following the idea of Connolly and Williams [21], the energy of formation of the disordered solid solutions can be written as

$$E_{form}^{dis}(x) = \sum_{n=0}^{4} P_n(x) E_{form}^{n}(x); \quad (6)$$

$$P_n(x) = \binom{4}{n} x^n (1-x)^{4-n}, \quad (7)$$

where $E_{form}^{dis}(x)$ is the energy of formation of each of the five ordered structures. $P_n(x)$ is a statistical weight representing the probability that the nth short-range ordered structure occurs in the alloy. From Fig. 3 (solid line), it is observed that a maximum of alloy stability is attained at $x = 0.22$ and that a negative curvature appears. Calculating inflexion points of the curve corresponding to $\partial^2 G(x)/\partial x^2 = 0$ where $G(x)$ is the Gibbs free energy of mixing, leads to the concentrations $(c_1, c_2) = (0.409, 0.997)$ that delimit a spinodal decomposition domain.

Comparing both ordered and disordered phases for the whole range of x leads to the evidence that ordered phase remains more stable then the disordered one for compositions less than $x = 0.38$. From the later concentration to $x = 0.41$, the coexistence of the two phases is predicted. Then, the disordered phase becomes more stable than the ordered phase until $x = 0.48$, in this range the ordered phase is unstable. Finally, both phases become unstable for higher Zn content and a miscibility gap is expected.

Then, our explanations on the stability trends of the alloys may be suggested as follows. First, the ordering at low composition of Zn needs the intermixing of Cd and Zn elements and rearrangements of atoms. This is induced by the long time and the high temperature of the annealing of the samples [7]. Also, as explained before, the charge exchange between Cd, Zn and Te atoms acts like a driving force that tends to stabilize the alloy. All these factors cause the interdiffusion of Cd and Zn, which results in a grain nucleation and growth leading to a polycrystalline material. By increasing Zn content, the electronic contribution to the formation energy increases rapidly and tends to separate the alloy into regions with short-range periods consisting of the mixed clusters (Cd_3ZnTe_4, $Cd_2Zn_2Te_4$ and $CdZn_3Te_4$). After that, the system exhibits an excess of the "pure" (Cd_4Te_4 and Zn_4Te_4) clusters and a deficiency in the mixed ones.

Conclusion

In summary, we performed accurate FP-LAPW calculations to investigate the structure and the stability of $Cd_{1-x}Zn_xTe$ solid solutions in the ordered and disordered forms. It was shown that the lattice constants are a decreasing linear function of composition, in agreement with available experimental works. The calculated formation energy of the ordered structures is resulting from a competition between three different physical contributions, i.e. the volume deformation, the internal relaxation and the charge exchange. The ordering tendency for low Zn content is explained to have a chemical nature.

The experimental threshold reported in Ref. [7] at which a phase separation occurs ($x < 0.4$) is well predicted by our calculations.

References

1. Gunshor R.L., Nurmiko A.V. II-VI blue/green light emitters: devices physics and epitaxial growth // Semiconductors and Semimetals. 1997. Vol. 44. Academic press, New York.
2. Basol B.M., Kapur V.K., Ferris M.L. Low cost technique for preparing CdZnTe films and solar cells // J. Appl. Phys. 1989. 66. P. 1816.
3. Ringel S.A., Sudharsanam R., Rohatgi A. et al. A study of polycrystalline Cd(Zn, Mn)Te/CdS films and interfaces // J. Electron. Mater. 1990. 19. P. 259.
4. Chu T.L., Chu S.S., Ferekids C. et al. Films and junctions of cadmium zinc telluride // J. Appl. Phys. 1992. 71. P. 5635.
5. Cohen K., Stolyarova S., Amir N. et al. MOCVD growth of ordered $Cd_{1-x}Zn_xTe$ epilayers // J. Cristal Growth. 1999. 198. P. 1174.
6. Bansal A., Rajaram P. Electrochemical growth of CdZnTe thin films // Mater. Lett. 2005. 59. P. 3666.
7. Arbaoui A., Outzourhit A., Achargui N. et al. Effect of the zinc composition on the formation of ternary alloy $Cd_{1-x}Zn_xTe$ thin films // Sol. Ene. Mater. Sol.-Cells. 2006. 90. P. 1364.
8. Andersen O.K. Linear methods in band theory // Phys. Rev. B 1975. 42. P. 3060.
9. Hohenberg P., Kohn W. Inhomogeneous electron gas // Phys. Rev. 1964. 136. P. B864.
10. Kohn W. Sham L.S. One-particle properties of an inhomogeneous interacting electron gas // Phys. Rev. 1965. 140. P. A1133.
11. Blaha P., Schwarz K., Madsen G.K.H. Electronic structure calculations of solids using the WIEN2k package for material sciences // Comput. Phys. Commun. 2002. 147. P. 71.
12. Ceperley D.M., Alder B.J. Ground state of the electron gas by a stochastic method // Phys. Rev. Lett. 1980. 45. P. 566.
13. Murnaghan F.D. The compressibility of media under extreme pressures // Proc. Natl. Acad. Sci. USA. 1944. 30. P. 244.
14. Ammar A.H. Studies on some structural and optical properties of $Zn_xCd_{1-x}Te$ thin films // App. Surf. Sci. 2002. 201. P. 9.
15. Soliman H.S., Allam F.M., El-Shazily A.A. Structural and optical properties of $Cd_{1-x}Zn_xTe$ thin films // J. Mater. Sci. Mater. Elect. 1996. 7. P. 233.
16. Schenk M., Hähnert I., Duong L.T.H. et al. Validity of the lattice-parameter Vegard-rule in $Cd_{1-x}Zn_xTe$ solid solutions // Crys. Res. Tech. 1996. 31. P. 665.
17. Wei S.H., Ferreira L.G., Zunger A. First-principles calculation of temperature-composition phase diagrams of semiconductor alloys // Phys. Rev. B 1990. 41. P. 8240.
18. Satani M., Hart G.L.W., Zunger A. Ordering tendencies in octahedral MgO-ZnO alloys // Phys. Rev. B 2003. 68. P. 155210.
19. Bernard J.E., Zunger A. Electronic structure of ZnS, ZnSe, ZnTe, and their pseudobinary alloys // Phys. Rev. B 1987. 36. P. 3199.
20. Zunger A., Wei S.-H., Ferreira L.G. et al. Special quasirandom structures // Phys. Rev. Lett. 1990. 65. P. 353.
21. Connolly J.W.D., Williams A.R. Density-functional theory applied to phase transformations in transition-metal alloys // Phys. Rev. B 1983. 27. P. 5169.

FIRST-PRINCIPLES INVESTIGATION THE PHASE SEPARATION IN $Ca_{1-x}Mg_xO$ ALLOYS

R. Miloua, F. Miloua, Z. Kebbab, N. Benramdane

Laboratoire d'Elaboration et de Caractérisation des Matériaux,
Faculté des Sciences de l'Ingénieur, BP 89, Université Djillali LIABES
Sidi-Bel-Abbès, Algeria.
Tel: 00 213 50 71 61 56; E-mail: mr_lecm@yahoo.fr

Using the full-potential linearized augmented plane wave (FP-LAPW) method in combination with the local density approximation to the exchange-correlation potential, we investigated the ground-state properties and the stability of $Ca_{1-x}Mg_xO$ mixed oxides. It is found that the structural parameters, i.e. lattice constants and bulk moduli deviate slightly from the linear function of the composition *x*. We determined the equation of state of the alloys and showed an increasing compressibility function of composition. We expressed the formation energy as an energetic balance between pure structural constraints and quantum chemical effects. Thus, a phase separation over the whole range of concentration is expected. The origin of the miscibility gap has a chemical nature. Also, we performed a thermodynamic study of the stability of the alloys.

Keywords: development and study of material properties to form catalytic layers in fuel cells, new structural materials for renewable energy structures

F. Miloua

Organization(s): Scientist researcher at Laboratoire d'Elaboration et de Caractérisation des Matériaux.
Education: D.E.A in electronics at Université des Sciences et Techniques of Lille, France (1986). Doctorate in Physics and materials science at Claude Bernard University- Lyon I, France (1992).
Main range of scientific interests: Materials science, surfaces and interfaces.
Some publications (number of publications: 11)**:** F. Miloua et al. Structural and electrical characterzation of Ag-InP(100) interfaces stabilized by antimony // Materials Chemistry and Physics 1993. 33. P. 85.; M. Bouslama, B. Khelifa, F. Miloua et al. Interaction of phosphorus with Indium // Appl. Surf. Sciences. 1992.; F. Miloua et al. Structural and electrical characterizations of Ag-InP(100) interfaces stabilized by antimony // 3ème Rencontre de Physique: ''Sciences des Surfaces des Matériaux''. Oran. 1991.

Introduction

The alkaline earth oxides CaO and MgO, as well as their mixtures have been in focus both theoretically and experimentally. Because of their interesting physical and chemical properties, they found a wide range of applications ranging from catalysis to microelectronics. They have been used as catalysts for the steam gasification of naphthalene [1], in oxidative coupling reaction of methane [2] and for soot combustion [3]. Recently, $Ca_{1-x}Mg_xO$ solid solutions have been demonstrated as an alternative dielectrics to SiO_2 due to favourable properties such as high dielectric constant, wide bandgap, and notable lattice compatibility with SiC [4]. CaMgO films grown by rf plasma-assisted molecular beam epitaxy and capped with Sc_2O_3 are promising candidates as surface passivation layers and gate dielectrics on GaN-based high electron mobility transistors (HEMTs) and metal-oxide semiconductor HEMTs (MOS-HEMTs) [5, 6].

Due to the large difference in ionic radius between Mg and Ca, solid-solution CaO-MgO is difficult to synthesize using bulk techniques, i.e. a severe immiscibility is observed [7]. However, the use of MBE as a film growth technique often allows for the formation of metastable phases. In fact, $Ca_{1-x}Mg_xO$ ternaries were grown as solid solution films covering the entire compositional range when grown at a remarkably low temperature of 300 °C [8]. Also, using pulsed laser deposition, Nishii et al. have grown metastable solid solution films on ZnO layers [9].

In the present paper we report on the structural and thermodynamic stability of $Ca_{1-x}Mg_xO$ alloys. We employed the Full-Potential Linearised Augmented Plane Wave (FP-LAPW) method [10] to study the ground-state properties and the formation energy of the alloys. The disordering effect on the formation energy is introduced using a cluster expansion approach. The predicted trends are explained on the basis of a structural-chemical energetic balance. Further, the thermodynamic phase diagram is established and the critical temperature is estimated.

The rest of the paper is organized as follows. In section 2, we briefly describe the calculation procedure. Results and discussions are presented in section 3 and the paper is concluded in section 4.

Method of calculation

Our calculations have been made using FP-LAPW approach within the framework of the Density Functional Theory (DFT) [11, 12] as implemented in WIEN2k [13] code. The exchange-correlation contribution to the total energy is described within the Local Density approximation (LDA) [14]. Kohn-Sham wave functions were expanded in terms of spherical harmonic functions inside the non-overlapping muffin-tin spheres surrounding the atomic sites (MT spheres) and in Fourier series in the interstitial regions. Inside the MT spheres of radius R_{MT}, the l-expansion of the wave function were carried out up to $l_{max} = 10$ while the charge density was Fourier expanded up to $G_{max} = 14$ (Ryd)$^{1/2}$. In order to achieve energy eigenvalues convergence, the wave functions in the interstitial region were expanded in plane waves with a cut-off parameter of $K_{max} = 8/R_{MT}$ for both binary and ternary compounds. R_{MT} values were assumed to be 2.0 a.u. for Mg, 2.2 a.u. for Ca and 1.6 a.u. for O atoms, respectively for all structures. A mesh of 30 special k-points for both binary and ternary compounds was taken in the irreducible wedge of the Brillouin zone. Both the MT radius and the number of k-points were varied to ensure total energy convergence. The core states that are completely confined inside the corresponding MT spheres were treated fully relativistic, while for the valance states we used the scalar relativistic approach that includes the mass velocity and Darwin s-shift, but omits spin-orbit coupling.

Results and discussions

Structural parameters

First, we calculated the structural properties of the binary compounds CaO and MgO in the rock-salt structure. Then, the ordered ternary alloys $Ca_{1-x}Mg_xO$ ($0 \le x \le 1$) were simulated at compositions $x = 0.25$, 0.5 and 0.75 by substituting cations. For each composition, we carried out a structural optimization by minimizing the total energy with respect to the cell volume and also the atomic positions. The calculated lattice constants and bulk moduli (see Table 1) were obtained by fitting the total energy versus unit cell volume to the Murnaghan's equation of state [15].

Table 1

Calculated lattice constants and bulk moduli, compared to experimental and other theoretical results

$Ca_{1-x}Mg_xO$	Lattice constants, a (Å)			Bulk moduli (GPa)		
x	This work	Exp	Other calc	This work	Exp	Other calc
0	4.71	4.81 [16]	4.72 [17]	127	110 [16]	128 [17]
0.25	4.61			135.84		
0.5	4.49			144.41		
0.75	4.35			157.12		
1	4.17	4.213 [18]	4.165 [17]	173.15	160 [18]	171 [17]

In Fig. 1 and Fig. 2 we depicted, respectively the lattice constants and the bulk moduli as a function of the composition x. From Fig. 1, one can see that the calculated lattice parameters deviate slightly from those obtained from the Vegard's law. The differences between themes are less than 5.5 %. The calculated lattice constants follow a decreasing quadratic function of composition x

$$a(x) = 4.70961 - 0.32582x - 0.21422x^2. \quad (1)$$

In Fig. 2, the composition dependence of the bulk moduli is compared with the results predicted by the linear concentration dependence (LCD). The bulk moduli exhibit a strong deviation from the LCD. Considering the general trend that LDA usually underestimates the lattice constant and overestimates the bulk modulus, our results are in good agreement with the experimental and other calculated values (see Table 1).

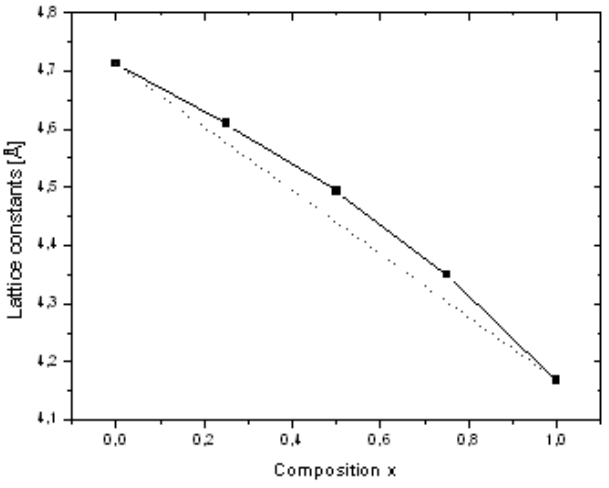

Fig. 1. *The calculated lattice constants (solid squares) and lattice constants of ideal mixing solid solutions (doted line) for the five ordered structures $Ca_{1-n}Mg_nO$ (n = 0, 1, 2, 3, 4)*

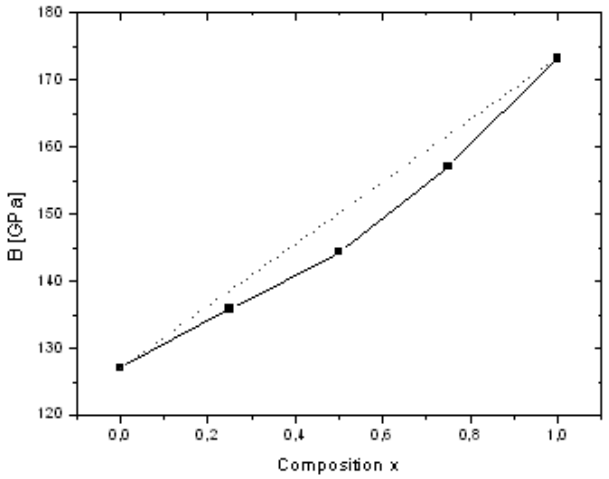

Fig. 2. *Calculated bulk moduli (solid squares) and those of ideal mixing (dotted line) as a function of composition*

Equation of state

The calculated equation of state for the $Ca_{1-x}Mg_xO$ alloys is plotted in Fig. 3. The relationship of the strain volume V/V_0 (where V is the unit cell volume under pressure, V_0 is the volume without pressure) under the same pressure P among the different compositions can be written as

$$(V/V_0)_{CaO} < (V/V_0)_{Ca_3MgO_4} < (V/V_0)_{CaMgO_2} < < (V/V_0)_{CaMg_3O_4} < (V/V_0)_{MgO}. \quad (2)$$

The relationship shows that CaO can be compressed more easily than MgO, this trend is observed in the bulk modulus ($B_{CaO} < B_{MgO}$). The compressibility decreases when the composition x increase.

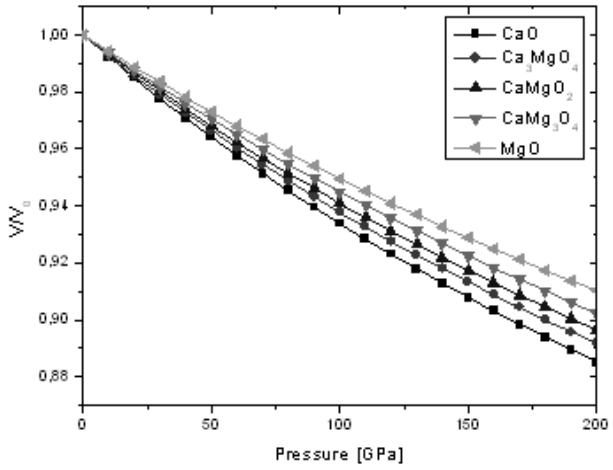

Fig. 3. *Equations of state of the $Ca_{1-x}Mg_xO$ alloys*

Phase separation of the CaMgO alloys

The ordered phases

In order to study the stability of CaMgO in the ordered form, we calculated the formation energies of the five (n = 0, 1, 2, 3, 4) structures using the following relation

$$E_{form}(n) = E_{Ca_{1-n}Mg_nO} - \frac{n}{4}E_{MgO} - \left(1 - \frac{n}{4}\right)E_{CaO}, \quad (3)$$

where $E_{Ca_{1-n}Mg_nO}$ is the total energy of the nth ordered alloy, E_{MgO} and E_{CaO} are total energies of MgO and CaO binaries, respectively. The results are viewed in Fig. 4 (solid squares) together with those for disordered alloys (solid line).

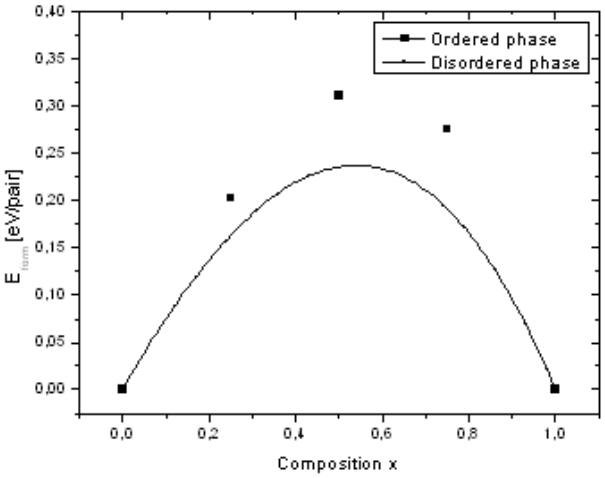

Fig. 4. *The calculated formation energies for ordered structures and disordered alloys*

The formation energy can give a measure of the stability of a material. We notice that it is positive for the whole range of composition, this indicates that it is energetically unfavourable for CaO and MgO to mix and form alloys. In order to clarify the physical origin of this behaviour, we decompose E_{form} into three physically recognizable contributions [19-21] as follows:

$$E_{form} = E_{VD} + E_{CE} + E_{SR}, \quad (4)$$

where E_{VD} is the hydrostatic "volume deformation" contribution due to the dilatation of MgO and compression of CaO from their equilibrium lattice constants (4.17 Å and 4.71 Å, respectively) to the common (Vegard-like) lattice constant of the alloy;

E_{CE} is the "charge exchange" energy that releases when MgO and CaO, taken at common lattice constant, combine to give $Ca_{1-x}Mg_xO$ ordered alloy. The internal relaxation effects are not included in this energy.

E_{SR} is the "structural relaxation" term due to the full relaxation of cell-internal degrees of freedom.

Fig. 5 shows the splitting of the formation energies of the ternary alloys into the three physical contributions; we can deduce the following important remarks:

– The large lattice mismatch (≈ 12%) between the binary constituents leads to a large and positive E_{VD} that tends to decrease the stability of CaMgO alloys over the whole range of composition.

– In contrast to E_{VD}, internal relaxation tends to increase the stability of the alloys by taking a negative E_{SR} value. However, E_{SR} is very small, compared to E_{VD} and the sum $E_{VD} + E_{SR}$ remains positive.

– The E_{CE} contribution remains positive and is higher than $E_{VD} + E_{SR}$, so can say that the phase separation has a chemical nature.

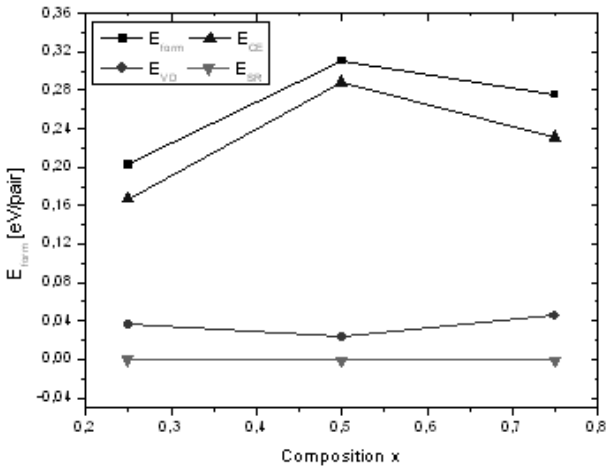

Fig. 5. *Energy contributions to the formation energies of ordered alloys*

The disordered phase

In this section, the energetic properties of the disordered alloys are calculated using a cluster expansion method. Following the idea of Connolly and Williams [22], the energy of formation of the disordered solid solutions can be written as

$$E_{form}^{dis}(x) = \sum_{n=0}^{4} P_n(x) E_{form}^{n}(x) \qquad (5)$$

$$P_n(x) = \binom{4}{n} x^n (1-x)^{4-n} \qquad (6)$$

where $E_{form}^{n}(x)$ is the energy of formation of each of the five ordered structures. $P_n(x)$ is a statistical weight representing the probability that the nth short-range ordered structure occurs in the alloy. In Fig. 4 (solid line), the formation energy of the disordered alloys is depicted. It is lower than that of the ordered structures.

Thermodynamic properties

The thermodynamic properties of $Ca_{1-x}Mg_xO$ are calculated by estimating the solubility limit. Following the approach of Neugebauer and Van de Walle [23], we use the calculated formation energy to construct a lower limit $\Delta H^{\min}(x)$ for each composition

$$\Delta H^{\min}(x) = 4x(1-x)\Delta H^0, \qquad (7)$$

where $\Delta H^0 = 0.1351863$ eV ($\Delta H^{\min}(x) = 0.1013897$ eV with $x = 0.25$). Then, the miscibility gap is analytically estimated and its behaviour as a function of temperature is given by the binodal line, as shown in Fig. 6 (solid line) [24, 25]

$$k_B T / \Delta H^0 = (8x-4)/[\ln x - \ln(1-x)]. \qquad (8)$$

The region below the spinodal line is unstable (as indicated by doted line)

$$k_B T / \Delta H^0 = 8x(1-x). \qquad (9)$$

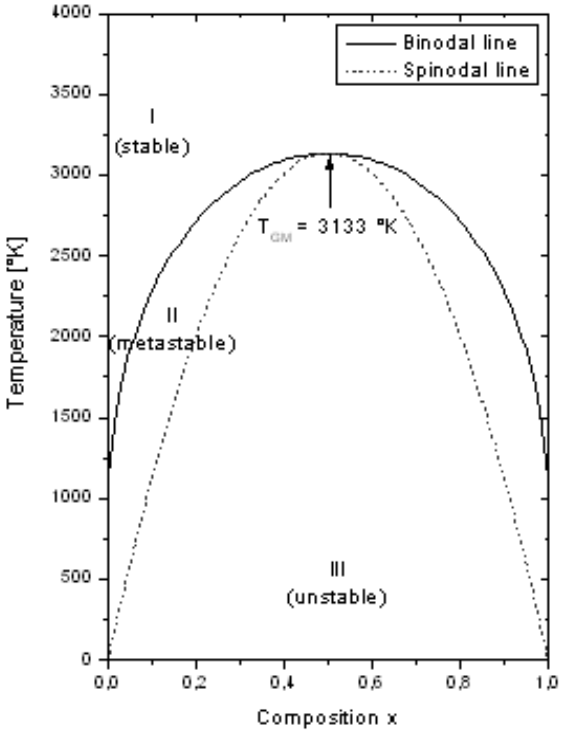

Fig. 6. *T-x phase diagram of $Ca_{1-x}Mg_xO$ alloys, solid line: binodal curve, doted line: spinodal curve*

The critical temperature of the miscibility gap is thus $T_{GM} = 2\Delta H^0/k_B = 3133$ K.

The spinodal curve in the phase diagram marks the equilibrium solubility limit, i.e., the miscibility gap. For temperatures and compositions above this curve a homogeneous alloy is predicted. The wide range between spinodal and binodal curves indicates that the alloy may exist as metastable phase.

Conclusion

In summary, we performed accurate FP-LAPW calculations to investigate the structure and the stability of $Ca_{1-x}Mg_xO$ solid solutions in the ordered and disordered forms. It is shown that the lattice constants and bulk moduli exhibit a strong deviation from the linear law. The compressibility of the alloys decreases when the composition x increase. The calculated formation energies for both ordered and disordered phases are positive and yield to a miscibility gap. Then, the origin of phase separation was determined to be of a chemical nature. Further, the thermodynamic phase diagram is calculated and a critical temperature of T_{GM} = = 3133 K is found.

References

1. Alarcón N., García X., Centeno M. et al. Catalytic cooperation at the interface of physical mixtures of CaO and MgO catalysts during steam gasification of naphthalene // Surface and Interface Analysis. 2001. 31. P. 1031.
2. Omata K., Aoki A., Fujimoto K. Oxidative coupling of methane over CaO-MgO mixed oxide // Catalysis Letters. 1990. 4. P. 241.
3. Jiménez R., García X., Gordon A. CaO-MgO catalysts for soot combustion: KNO_3 as source for doping with potassium // J. Chil. Chem. Soc. 2005. 50. P. 651.
4. Stodilka D.O., Gerger A.P., Hlad M. et al. Alternative magnesium calcium oxide gate dielectric for silicon carbide MOS application // Mater. Res. Soc. Symp. Proc. 2006. 911. P. 3.
5. Gila B.P., Thaler G.T., Onstine A.H. et al. Novel dielectrics for gate oxides and surface passivation on GaN // Solid-State Electronics. 2006. 50. P. 1016.
6. Hlad M., Voss L., Gila B.P. et al. Dry etching of MgCaO gate dielectric and passivation layers on GaN // Applied Surface Science. 2006. 252. P. 8010.
7. Doman R.C., Barr J.B., McNally R.N. et al. Phase equilibria in the system CaO-MgO // J. Am. Ceram. Soc. 1963. 46. P. 314.
8. Hellman E.S., Hartford E.H. Epitaxial solid-solution films of immiscible MgO and CaO // Appl. Phys. Lett. 1994. 64. P. 1341.
9. Nishii J., Ohtomo A., Ikeda M. et al. High-throughput synthesis and characterization of $Mg_{1-x}Ca_xO$ films as a lattice and valence-matched gate dielectric for ZnO based field effect transistors // Applied Surface Science. 2006. 252. P. 2507.
10. Andersen O.K. Linear methods in band theory // Phys. Rev. B 1975. 42. P. 3060.
11. Hohenberg P., Kohn W. Inhomogeneous Electron Gas // Phys. Rev. 1964. 136. P. B864.
12. Kohn W., Sham L.S. One-particle properties of an inhomogeneous interacting electron gas // Phys. Rev. 1965. 140. P. A1133.
13. Blaha P., Schwarz K., Madsen G.K.H. Electronic structure calculations of solids using the WIEN2k package for material sciences // Comput. Phys. Commun. 2002. 147. P. 71.
14. Ceperley D.M., Alder B.J. Ground state of the electron gas by a stochastic method // Phys. Rev. Lett. 1980. 45. P. 566.
15. Murnaghan F.D. The compressibility of media under extreme pressures // Proc. Natl. Acad. Sci. USA. 1944. 30. P. 244.
16. Richet P., Mao H.K., Bell P.M. Static compression and equation of state of CaO to 1.35 Mbar // J. Geophys. Res. 1988. 93. P. 15279.
17. Baltache H., Khenata R., Sahnoun M. et al. Full potential calculation of structural, electronic and elastic properties of alkaline earth oxides MgO, CaO and SrO // Physica B. 2004. 344. P. 334.
18. Fei Y. Effects of temperature and composition on the bulk modulus of (Mg,Fe)O // Am. Mineral. 1999. 84. P. 272.
19. Wei S.H., Ferreira L.G., Zunger A. First-principles calculation of temperature-composition phase diagrams of semiconductor alloys // Phys. Rev. B 1990. 41. P. 8240.
20. Satani M., Hart G.L.W., Zunger A. Ordering tendencies in octahedral MgO-ZnO alloys // Phys. Rev. B 2003. 68. P. 155210.
21. Bernard J.E., Zunger A. Electronic structure of ZnS, ZnSe, ZnTe, and their pseudobinary alloys // Phys. Rev. B 1987. 36. P. 3199.
22. Zunger A., Wei S.-H., Ferreira L.G. et al. Special quasirandom structures // Phys. Rev. Lett. 1990. 65. P. 353.
23. Connolly J.W.D., Williams A.R. Density-functional theory applied to phase transformations in transition-metal alloys // Phys. Rev. B 1983. 27. P. 5169.
24. Lambrecht W.R.L., Segall B. Electronic structure of (diamond C)/(sphalerite BN) (110) interfaces and superlattices // Phys. Rev. B 1989. 40. P. 9909.
25. Lambrecht W.R.L., Segall B. Anomalous band-gap behaviour and phase stability of c-BN–diamond alloys // Phys. Rev. B 1993. 47. P. 9289.

MODELLING AND ELEMENTS OF VALIDATION OF SOLAR DRYING: APPLICATION TO ACTIVATED SLUDGE DRYING OF WASTE WATER

D. Morau, J.P. Praene, L. Adelard, J.-C. Gatina

Université de la Réunion Faculté des Sciences de l'Homme et de l'Environnement, Laboratoire de Physique du Bâtiment et des Systèmes
117 rue du Général Ailleret 97430 Le Tampon, REUNION (FRANCE)
00 262 57 95 50 / 00 262 57 95 41; E-mail: dominique.morau@univ-reunion.fr

Received: 19 Sept 2007; accepted: 10 Oct 2007

This paper presents a simulation code for the solar drying of sludge. This code is using a model of the drying kinetics of wastewater sludge, and takes into account water transport in the product during drying.
An application of the FAST method for the parametric sensitivity test of this code has been used in order to highlight influencial parameters on the solar collector model. Finally, it is shown that outputs of the model, could be approached by a regression polynomial called "metamodel" created from sensitivity analysis. Sensitivity analysis becomes an alternative in order to model a system, working under various weather conditions.

Keywords: solar energy, simulation, sensitivity analysis, mass flux, spectral analysis

Dominique Morau

Organization: Reunion Island University, Environmental and Human Sciences Faculty, Building Physics and Systems Laboratory.
Education: I received the Bachelor of Science degree in Physics in 1997. I then moved to France at Institute National Polytechnique de Lorraine where I received a Masters degree of Mechanical engineering in 2003. The PhD degree in 2006 was made at University of Reunion Island.
Experience: Engineer Consultant in Acoustics and Renewable Energy in Buildings (2007). I actually participate to two French research projects: VEOLIA (2007, on solar Drying of sludge), INCIVOL (2007, on incineration of waste) and DYNASIMUL (2007, on building simulation).
Main range of scientific interests: My main range of scientific interests relate to the study of solids and liquids wastes treatment.
Publications: Modelling of drying activated sludge: effects of the sludge turn over on drying kinetics, International Conference on Advances in Mechanical Engineering and Mechanics, ICAMEM 06, December, 2006, Tunisia.
Theoretical and Experimental study of activated sludge drying of waste water, International Conference on Engineering for Waste Treatment, May, 2005, Albi, France.
Drying granular porous media: mixing effects of activated sludge on the kinetics of drying, International Communication of Heat and Mass Transfer, 2007 (under review).

Introduction

Since 1 July 2002 in Europe, the law No. 92-646 of 13th July 2002 has prohibited the disposal of sludge that contains less than 30 % dry matter in storage centers. Studies of methods of drying the sludge using a renewable energy are an attempt to solve this problem.
The present theoretical study focuses on modelling the solar drying. A practical application of solar drying is the activated sludge of waste water drying. The paper also focuses on modelling the drying kinetics of the sludge. The model takes into account water transport between the sludge and drying air during drying that would occur within a laboratory solar dryer operating at low temperatures.
Then we conducted a parametric sensitivity analysis, using the FAST (Fourier Amplitude Sensitivity Technique) method, on the elaborated model. The analysis is concerned with the sensitivity of the model in relation to functional parameters (e.g., meteorological parameters, flow rate, and temperature) and structural parameters (e.g., geometrical parameters, orientation of the collector, and thermo-physical features).
The new sensitivity testing technique outlined in this study identifies the most influential parameters.
This approach will demonstrate the influence of functional parameters such as the temperature, flow rate, and relative humidity of the drying air, parameters that can be perfectly controlled during the drying. This analysis will show that the influence of product size is less significant than the effects of these three parameters.
In order to improve the model it is important to control these parameters or accurately measuring them. In this way, the gain of heat conveying air temperature at the output of the solar collector model could be represented by a polynomial of regression called "metamodel". This model is a combination of the most important parameters.
In the first part of this article, the dynamic model will be presented, and then the sensitivity analysis will be applied to improve the modelling.

Theoretical analysis

Modelling of the solar drying system

Modelling of the drying system

The solar drying is composed of a drying room coupled with two solar collectors. This kind of dryer belongs to the family of the active driers [1]. The solar collectors are placed upstream drying room and set aside to heat or to preheat air before make one's entrance into the drying room.

Functional and architectural description of the dryer

The dryer is a cupboard-shaped room, with the lower part containing drying air that is aspirated from ambient air by a centrifugal fan and heated by an electric balance system of heating. This hot air is blown upward and into contact with the product sample. The samples are spread in thin layers in the shape of small disks placed on one or more trays arranged vertically. Humid air is removed from the dryer via evacuation openings.

Fig. 1 is a schematic diagram of the dryer and shows how the product samples are situated within the drying room.

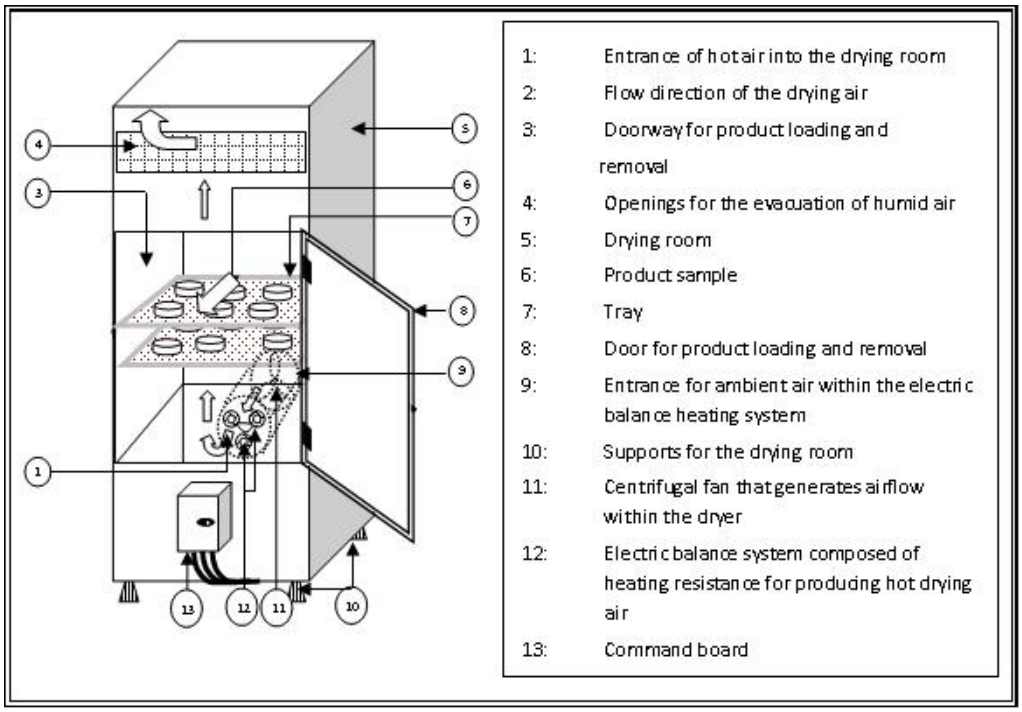

Fig. 1. *Schematic drawing of the studied drying system*

Simplifying hypotheses for dryer modelling

As simplifying hypothesis for modelling the drying room [1], the following transfers were neglected:

– heat exchange with the ceiling and the floor of the room;

– thermal exchange related to the condensation of humid air on the internal surfaces of the drying room;

– heat exchange with trays, heat exchange related to the thermal inertia of the drying air;

– heat and mass exchanges between samples.

In addition, it was assumed that samples are shaped like small disks, the solar flux density received by the four surfaces of the drying room is uniform, and that the sludge temperature on each tray is uniform. (diameter, thickness).

Equations of thermal balance

The drying room was subdivided such that each sub-area slice contains a tray. Thus, Fig. 2 describes the thermal exchange phenomena [2] taking place with the *i*-th representative slice of the drying room. On the basis of analogy between electric and thermal factors, an electric circuit equivalent to all the thermal exchanges occurring with this sub-area slice is shown on Fig. 3.

By applying Ohm's law to every node of the circuit, we derive a non-linear system of five partial derivative equations of the following shape:

$$C_k \frac{dT_k}{dt} = \sigma_k + \sum_{j=1}^{n} \left[\left(R_{kj} + H_{kj} + C_{kj} \right) \left(T_j - T_k \right) \right]. \quad (1)$$

The differential equation system is solved for each segment in the time domain using 4th order Runge-Kutta method.

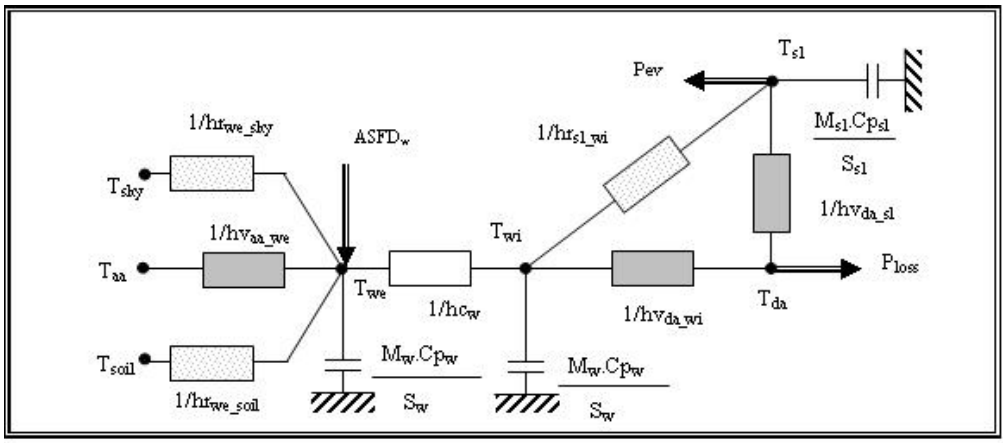

Fig. 2. *Schematic description of thermal exchange phenomena taking place at the i- th fictitious representative slice of the drying room*

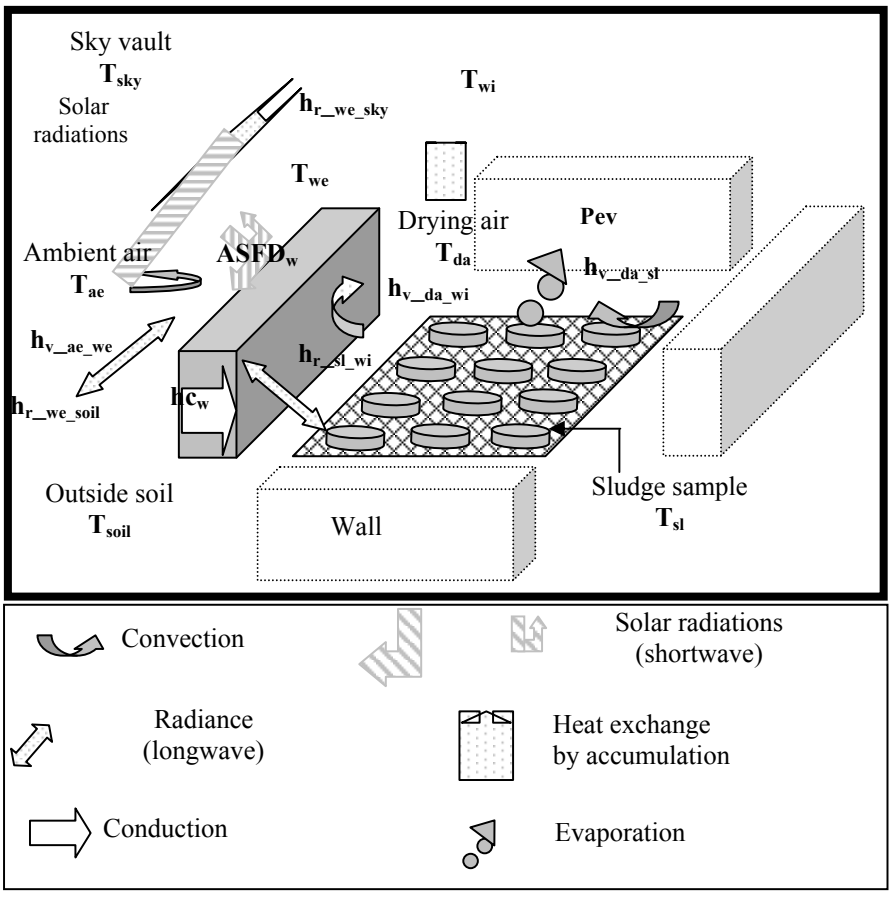

Fig. 3. *Equivalent electric circuit related to the i-th fictitious representative slice of the drying room*

Solar collector modelling

Functional and architectural description of the dryer

In the present study, the developed model corresponds to a plane collector (Fig. 4). This kind of model is often used in active drying [3].

On the basis of analogy between electric and thermal factors, an electric circuit equivalent to all the thermal exchanges occurring with this sub-area slice is shown on Fig. 5.

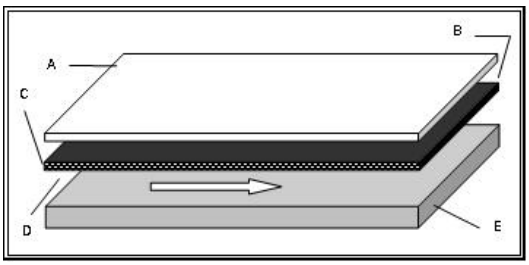

Fig. 4. *Schematic drawing of the studied solar collector*

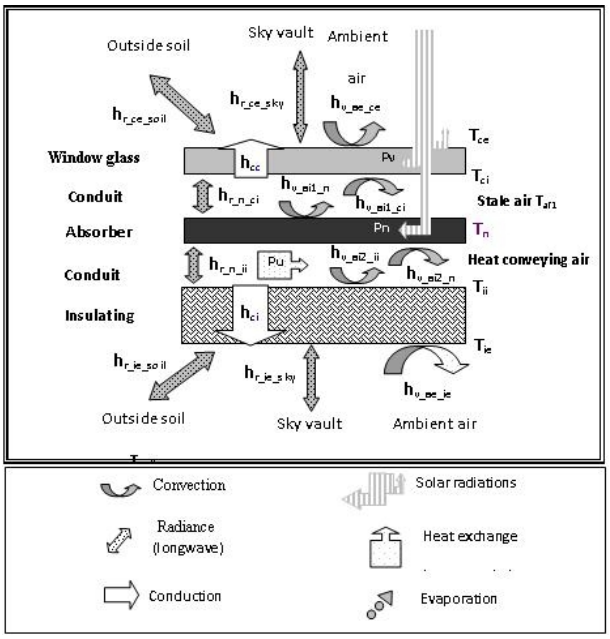

Fig. 5. *Schematic description of thermal exchange phenomena taking place at the i-th fictitious representative slice of the solar collector*

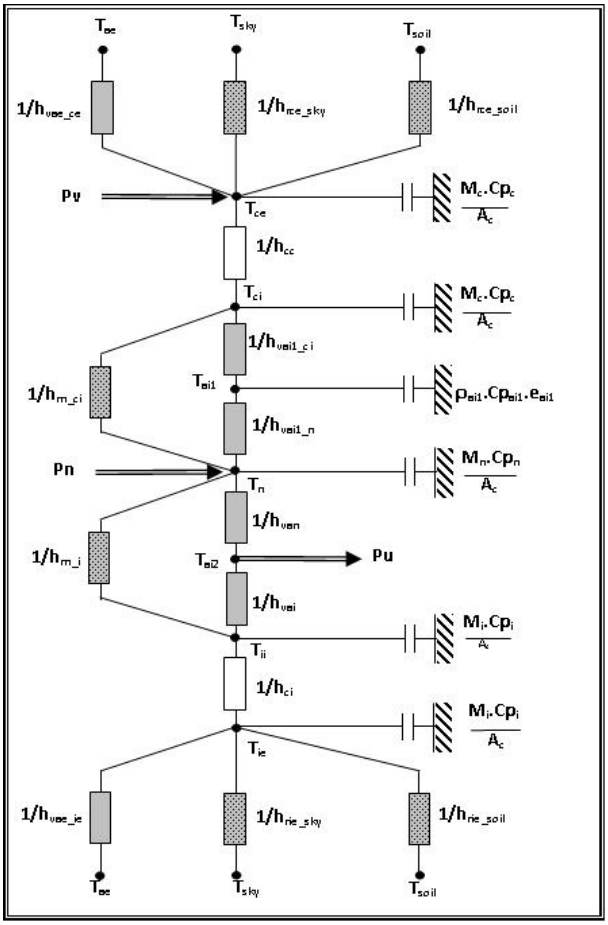

Fig.6. *Equivalent electric circuit related to the i-th fictitious representative slice of the solar collector*

By applying Ohm's law to every node of the circuit, we derive a non-linear system of six partial derivative equations. The equations are same shape as equation (1). Equivalent electric circuit related to the *i*-th fictitious representative slice of the solar collector is represented in Fig. 6.

Model of the kinetics of drying sewage sludge

The model of sewage sludge drying kinetics, which was used for the system modeling, was proposed by Léonard et al. [4]. This model takes in account the existence of two critical values of product moisture content: W_{crit1} and W_{crit2} [$kg_{water} \cdot kg^{-1}_{dry\ matter}$], which subdivide the sludge volumetric shrinkage curve into three distinct zones. Thus, the cross-sectional mass flux F_m has three expressions:

– Constant drying-rate period: $W > W_{crit1}$

$$F_m = F_{\text{const}} = \frac{A_0}{S} k_c \rho_a \left(Y_{sat}\left(T_w\right) - Y_\infty\right). \qquad (2)$$

– First decreasing drying-rate period: $W_{crit1} > W > W_{crit2}$

$$F_m = F_{\text{const}} = \left(\frac{V(W)}{V_0}\right)^{2/3}. \qquad (3)$$

– Second decreasing drying-rate period: $W < W_{crit2}$

$$F_m = F_{\text{const}} = \left(\frac{V(W_{crit2})}{V_0}\right)^{2/3} \left(\frac{W}{W_{crit2}}\right)^{\alpha}, \qquad (4)$$

where α is a tuning parameter that is dependent on the drying conditions.

Experimental set up and simulation

An experimental solar dryer has been set up in a treatment plant at Reunion Island (21°S, 55°E) (Fig.7), under a tropical humid climate. The meteorological conditions used are showed below (Fig. 8).

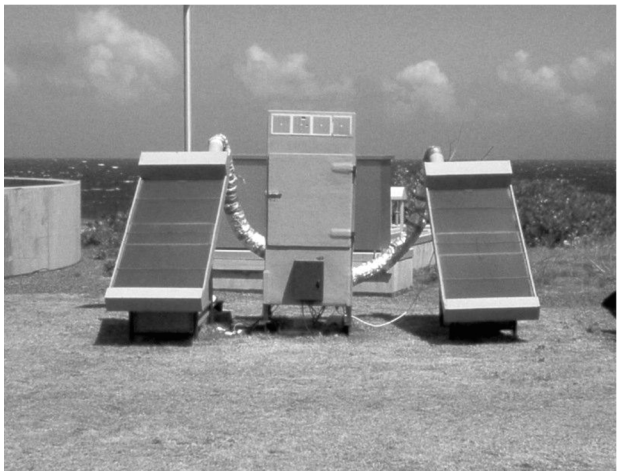

Fig. 7. *Solar dryer in the treatment plant*

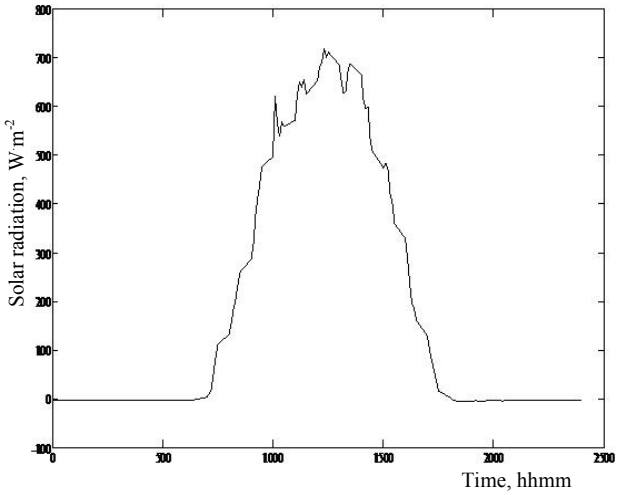

Fig. 8. *Global solar irradiance during the day*

The first objective is to follow the behaviour of the solar collector according to the heat conveying air flow but also to highlight the efficiency according to the solar radiation from weather conditions database.

According to the Fig. 9, the increase in useful output, collected on the outlet side of the solar collector, does not give a positive effect on the gain of air temperature when the flow increases. Indeed more the flow is raised, less the heat conveying air will not have time to recover the heat by convection.

The useful output (Fig. 10) increases with the solar radiation. However the diffuse radiation has more influence than the direct radiation on the useful output. More the solar radiation increases more the efficiency of the solar collector decreases (Fig. 11). Nevertheless the minimal efficiency is superior at 45 %.

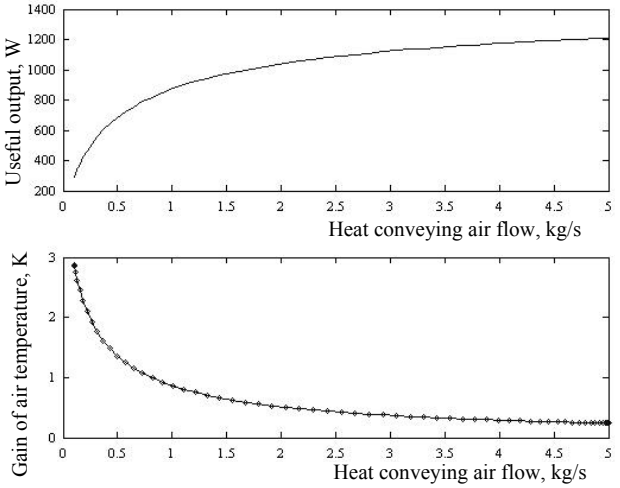

Fig. 9. *Influence heat conveying air flow on the useful output and on the gain of air temperature*

The useful output (Fig. 10) increases with the solar radiation. However the diffuse radiation has more influence than the direct radiation on the useful output. More the solar radiation increases more the efficiency of the solar collector decreases (Fig. 11). Nevertheless the minimal efficiency is superior at 45 %.

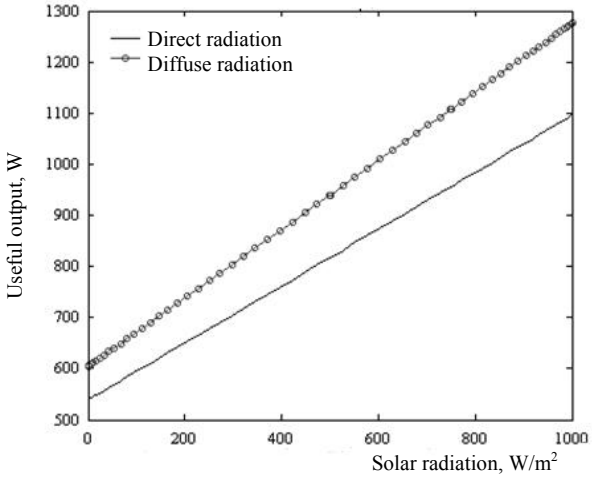

Fig. 10. *Influence solar radiation on the useful output*

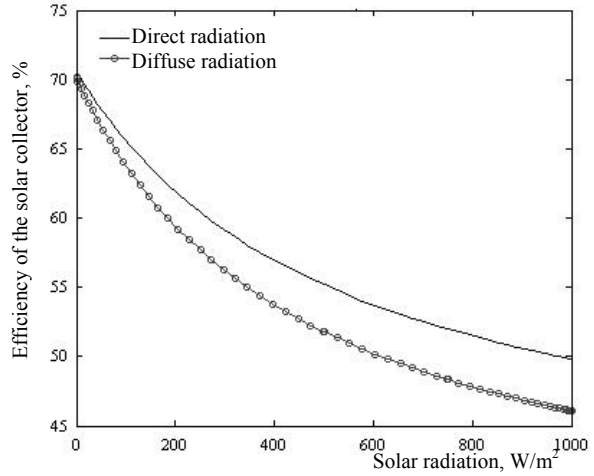

Fig. 11. *Influence solar radiation on the efficiency of the solar collector*

The wind, as the solar radiation, has an influence on the useful output and on the efficiency of the solar collector (Fig. 12). But effects are less important. The losses are tiny. On the other hand the surface of the solar collector has a considerable influence on the parameters (Fig. 13).

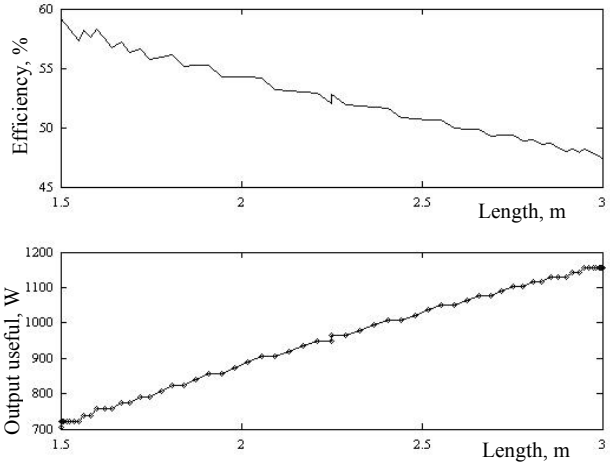

Fig. 12. *Influence of the wind speed on the efficiency of the solar collector and the output useful*

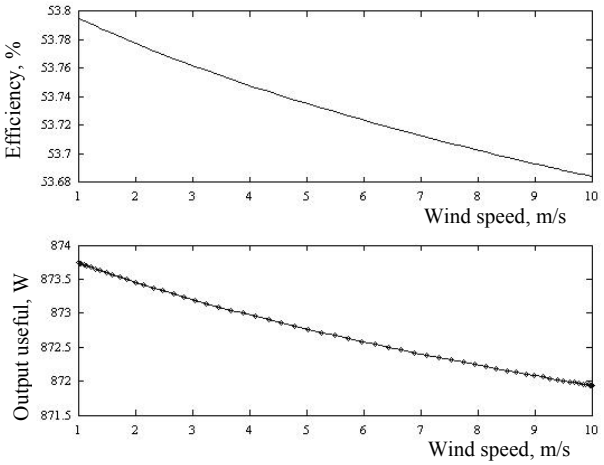

Fig. 13. *Influence of the length of solar collector on the efficiency and the output useful*

Multiplying by two the length of the solar collector decreases by 10 % the efficiency of the solar collector.

Results of experiments

The kinetics of drying (Fig. 14) has been studied while drying 24 kg of sludge (6 kg·4). The samples have been numbered in ascending order as a function of their position in the trays.

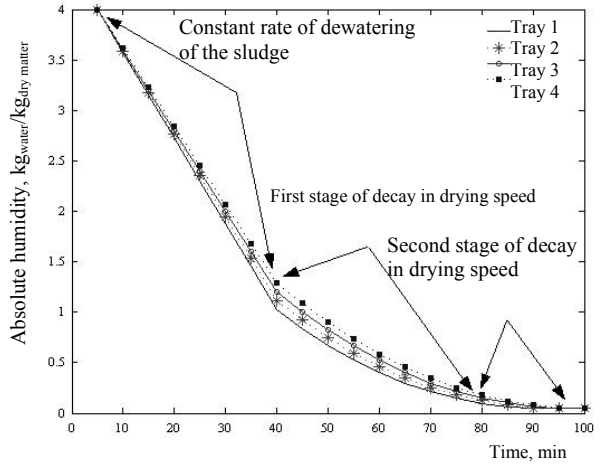

Fig. 14. *Kinetics of drying*

Experimental characteristics

Experimental characteristics are showed in Table 1.

We can note from Fig. 14 that:

– Sludge samples dry faster at lower levels within the drying room. The greater the increase in draining air within the drying room, the higher the rate of moisture increase. The drying power of the air gradually decreases as it moves along the trays.

– During the first 40 % of the drying time, the drying rate of the sludge is constant; it is independent free of evaporated water. After this stage, we can observe the first stage of decay in the rate of drying, where steam–water exchanges reduce slowed. The difference in the moisture content of samples on Trays 1 and 4 becomes significant. After 80 % of the drying time, the drying rate decreases for a second time. During this stage, the sludge approaches a hygroscopic balance. The flux mass transfer decreases over the period of drying time. At this stage, water molecules within the samples are not free as in the first stage, but are linked with others molecules via intracellular connections. This water is termed "Water linked". To break these molecules much more energy and time are required.

Table 1

Characteristics of the sludge and drying conditions

Shape	**Cylindrical**
Thickness, cm	1
Diameter, cm	6
Dry matter, g/l	1.62
Volatile matter, g/l	1.38
Relative humidity of the incoming air, %	60
Relative humidity of the outgoing air, %	20
Drying temperature, °C	60

– At the end of the drying time, the four curves concur perfectly after having deviated for the major part of the drying time. The reason for this trend is as follows: once Tray 1 samples had dried, the steam pressure of water in the air is saturated when it arrives at the level of Tray 2, and the drying power of the air is reduced. Consequently, sludge on Tray 2 will exhibit the same behaviour as sludge on Tray 1 and will dry until reaching the moisture of balance. The same applies to Trays 3 and 4.

This study of the kinetics of drying led us to follow the evolution of the flow of mass according to the absolute humidity (Fig. 15).

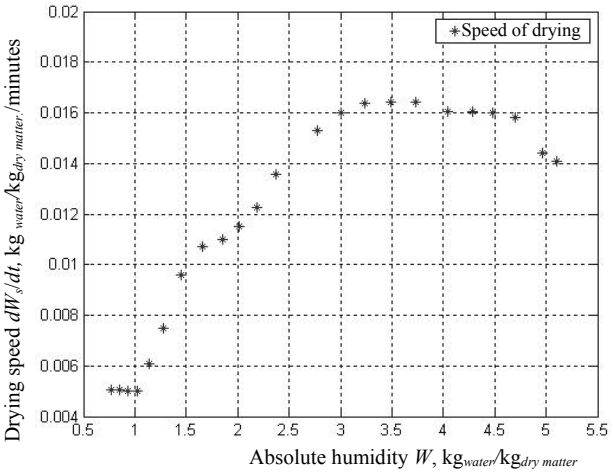

Fig. 15. *Kinetics of drying according to absolute humidity*

This study of the kinetics of drying led us to follow the evolution of the flow of mass according to the absolute humidity (Fig. 15).
The two critical values of the absolute humidity are:

$$\begin{cases} W_{crit1} = 3 \cdot \mathrm{kg}_{water} / kg_{dry\,matter} \\ W_{crit2} = 1.1 \cdot \mathrm{kg}_{water} / kg_{dry\,matter} \end{cases}$$

The existence of these two critical values of absolute humidity arises from the fact that sludge is a hygroscopic product. In general, these values depend on the speed of drying and dimensions of the product, as well as mechanisms of moisture migration. These characteristics increase with the increasing of the drying speed and the thickness of the product. It should also be noted that the initial absolute humidity content of the product has an influence on the value of W_{crit}. These considerations explain the fact that the absolute humidity W_{crit1} and W_{crit2} can differ from one test to another.

Sensitivity analysis

The principal objective of sensitivity analysis (SA) is to ascertain how a given output depends on its input factors, Saltelli [5].
The study concerns a one output (y) model (e.g gain of air temperature) with p input parameters $y = f(x_1, x_2, \ldots, x_p)$. The approach of the proposed parametric sensitivity lays on FAST method (acronym of Fourier Amplitude Sensitivity Test) which has been developed for the first time by Cuckier and al. [6]. It consists in a first step of making several simulations modifying each parameter x_h, so that each of them includes a periodical function G_h characterised by a frequency w_h (distinct for each parameter). The frequency is the "signature" of the parameter. The Fourier coefficients corresponding to each frequency (and their harmonics) leads to the estimation of their influence.
So the sampling of the parameter x_h can be expressed by the following formula:

$$x_{h,k} = G_h(\sin(w_h s_k)). \quad (5)$$

The transformation function G_h is generally chosen to assure a good representation of the wide range of parameters (a good "cover"). That means that the variable x_h has to be sampled following a precise given density probability (corresponding to the uncertainty on its value). Mara et al. [7] proposed to sample the parameters with the following manner:

$$x_{h,k} = x_{h,0} + \delta_h \sin(w_h s_k) \quad \text{with } s_k = 2\pi k / N_s, \quad (6)$$

where k represents the simulation number ($k = 1, N_s$), $x_{h,0}$ is the basis value of the parameter h and δ_h is chosen such as $x_{h,k} \in [x_{h,0} - \delta_h, x_{h,0} + \delta_h]$, N_s is the number of simulations. Mara [7] has shown that it is possible to represent the model output by polynomial regression based on the most important parameters of the model, as described in the following equation:

$$y_k = \beta_0 + \underbrace{\sum_{h=1}^{p} \beta_h \sin(w_h s_k)}_{\text{Term 1}} + \underbrace{\sum_{h=1}^{p}\sum_{h'=1}^{p} \frac{\beta_{hh'}}{2}\left[-\cos((w_h + w_{h'})s_k) + \cos((w_h - w_{h'})s_k)\right]}_{\text{Term 2}}. \quad (7)$$

The term 1 corresponds to the linear effects of the parameters (the Fourier coefficients δ_h = standard linear regression coefficient).

$$\beta_h = \frac{2}{N}\sum_{k=o}^{N} y \sin(w_h s_k). \quad (8)$$

The term 2 corresponds to the non linear effects including the interactions between two parameters x_h and $x_{h'}$ and also the quadratic effects of x_h.

$$\beta_{hh'} = -\frac{4}{N}\sum_{k=0}^{N} y \cos((w_h + w_{h'})s_k) = \frac{4}{N}\sum_{k=0}^{N} y \cos((w_h - w_{h'})s_k). \quad (9)$$

The interactions between the parameters produce additional frequencies with the same magnitude. So a one order interaction causes the apparition of two frequencies which are $|w_h - w_{h'}|$ and $|w_h + w_{h'}|$.
More precisely, to determine the surface response of the studied model, Mara [8] proposed a method. The following steps of this approach are described beneath:
− Sampling of the parameters of the model in their respective range of variation. A distinct frequency is attributed to each parameter and the simulations are made.
− The Fourier transform calculation of the output of the model y : the spectrum drawing:
We identify the frequencies which appear at each step of our exploration in order to determine the "metamodel" components.
– βi coefficients values estimation using the relations (8-9) or by using an optimisation algorithm.
− Analysis of the residue or correlation coefficient R^2 calculation to appreciate the validity of the identified response surface.
− Comparison of the linear regression coefficients to determine the effects of the parameters on the output of the model.
Such an approach is an element of validation of our model. Fig. 16 shows the results of the FAST method used to determinate the most important parameters. In this step, the parameters studied are the structural and functional parameters of the model, as described in Table 2.
It is important to notice that the SA method of used is a local method. In this way, the range of variation used, approximately 10 % of the optimal value is the domain of validity.

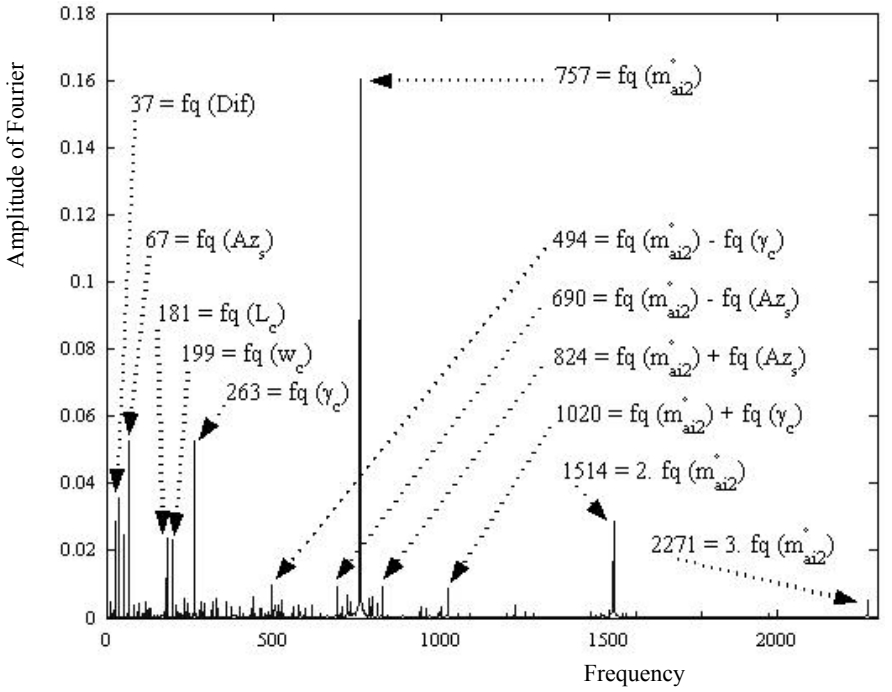

a

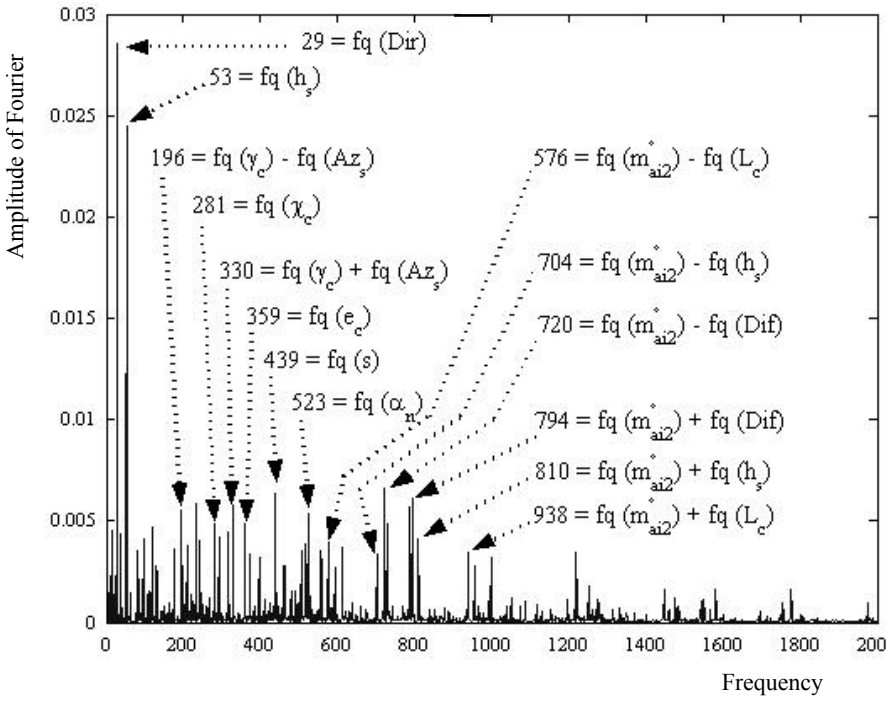

b

Fig. 16. *The results of the FAST method: a – identification according to their frequency of the influential parameters; b – zoom*

This spectral analysis (Fig. 16) has showed that the influential parameters on the heat conveying air were: the flow, the structural parameters of solar collector (length and width), but also the meteorological conditions, azimuth and height of the sun, absorption coefficients of the absorber which represent the reality of influence of solar energy in a solar collector model.

This analysis allows us to determine a polynomial of regression corresponding to an output of the solar collector model that is the gain of heat conveying air temperature.

The "metamodel" is presented by equation (10). The polynomial regression is obtained by optimizing the coefficient using a Levenberg Marquart algorithm

$$\Delta T_{air} = 0.866 - 0.03\langle T_{ae}\rangle + 0.053\langle Dir\rangle + 0.066\langle Dif\rangle + \\ + 0.011\langle \alpha_n\rangle + 0.007\langle \alpha_{nd}\rangle + 0.109\langle AZ_s\rangle + 0.047\langle L_c\rangle - \\ - 0.291\langle m_{ai2}\rangle - 0.010\langle \chi_c\rangle - 0.110\langle \gamma_c\rangle . \quad (10)$$

Table 2

Frequency associated to the input parameters of the solar collector model

Factors	Range of variation	$x_{h,0}$	Frequency
Dif	[200; 400]	300	37
Dir	[600; 800]	700	29
AZ_s	[-180; 180]	15	67
L_c	[1.5; 3]	2	181
w_c	[0.9; 1.1]	1	199
α_n	[0.8; 0.99]	0.91	523
m_{ai2}	[0.8; 1]	0.9	757
χ_c	[24; 26]	25	281
e_c	[0.003; 0.005]	0.004	359
k_c	[1; 1.2]	1.08	373
γ_c	[-180; 180]	90	263
ε_c	[0.8; 0.95]	0.88	397
α_{nd}	[0.7; 0.95]	0.9	557
K_{is}	[0.042; 0.044]	0.043	641
ε_{is}	[0.8; 0.95]	0.89	673
s	[20; 22]	21	439

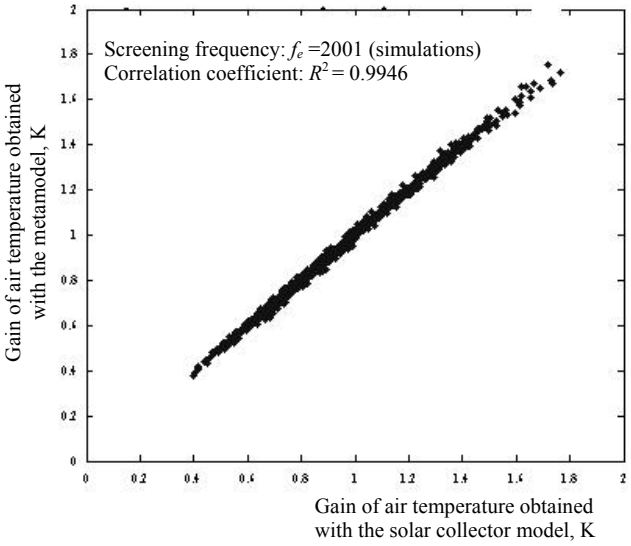

Fig. 17. *Comparison between results simulated with metamodel and the solar collector model*

The comparison of results (Fig. 17) obtained between the metamodel and the solar collector model gives a correlation coefficient equivalent to 0.9946. The metamodel proposed gives satisfaction. As a result the metamodel becomes an alternative for the modelling. The most influential variables can be identified by comparing the regression coefficients of the linear terms of the metamodel. The results of such a comparison are presented in Fig. 18, in which a positive effect of a parameter indicates that an increase in its value entails an increase in the value of the observed output parameter. A negative effect indicates that an increase in the parameter value results in a decrease in the value of the chosen output parameter (Fig. 18).

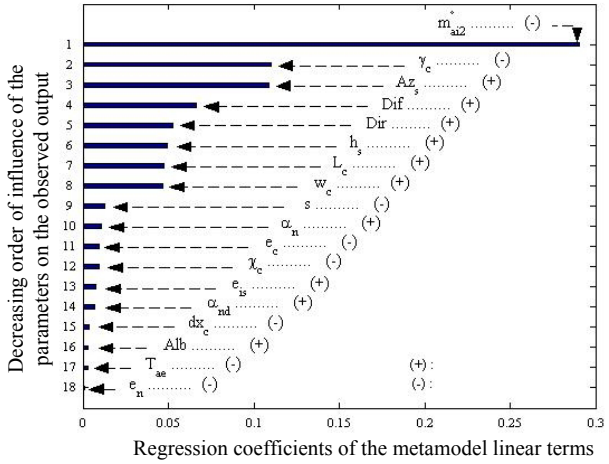

Fig. 18. *Comparison of the regression coefficients of the 18 most influential parameters of the solar collector model*

Conclusion

The objective of this wok was to model the solar drying active system using equations of thermal balance. But also, used sensitivity analysis in order to determine influential parameters on the output model and prove this method could be an alternative to traditional modelling method. The main advantages of this approach compared to conventional are simplicity and speed.

The accuracy of the metamodel obtained is fine considering that the comparison with the model give a good correlation coefficient. The metamodel brings a fine approximation of the solar collector behavior. In this case of this we focus on meteorological conditions, functional and architectural parameters of the solar collector.

This work highlighted the drying speed of sludge and characterized the kinetics of drying via the determination of hygrometric parameters. Further research in this field will consist in a study of the incineration of sludge with or without the addition of household waste.

Acknowledgement

This work was supported financially by Regional Council of Reunion Island.

Nomenclature

Key to abbreviations

A_0: sample initial exchange area, m^2
Alb: albedo
ASFD: absorbed solar flux density, $W \cdot m^{-2}$
AZ_s: azimuth of the sun, °
C_k: heat capacity, $J \cdot K^{-1}$
C_{kj}: coefficient of conductive heat exchange between the *k* and *j* nodes, $W \cdot K^{-1}$
C_p: mass heat capacity, $J \cdot K^{-1} \cdot kg^{-1}$
Dif: diffuse solar irradiance in the plane of the collector,$W \cdot m^{-2}$
Dir: direct solar irradiance in the plane of the collector, $W \cdot m^{-2}$
e: thickness, m
F_{const}: cross-sectional mass flux during the constant drying-rate period , $kg \cdot m^{-2} \cdot s^{-1}$
H_{kj}: coefficient of convective heat exchange between the *k* and *j* nodes, $W \cdot K^{-1}$
hc: conduction heat coefficient, $W \cdot K^{-1} \cdot m^{-2}$
hr: radiance heat coefficient, $W \cdot K^{-1} \cdot m^{-2}$
h_s: angular height of the sun, °
hv: convection heat coefficient, $W \cdot K^{-1} \cdot m^{-2}$
k_c: external mass transfer coefficient, $m \cdot s^{-1}$
L_c: solar collector length, m
M: mass, kg
m_{ai2}: heat conveying air flow, $kg \cdot s^{-1}$
Pev: product humidity evaporation heat density, $W \cdot m^{-2}$
Ploss: heat loss density, $W \cdot m^{-2}$
R_{kj}: coefficient of long wave radiation heat exchange between the *k* and *j* nodes, $W \cdot K^{-1}$
S: surface, m^2
s: inclination of the solar collector, °
T: temperature, K
T_w: wet bulb temperature, K
V: sample instantaneous volume, m^3
V_0: sample initial volume, m^3
W: sample humidity content, $kg_{water} \cdot kg^{-1}_{dry\ matter}$
W_c: solar collector width, m
$Y_{sat}(T_w)$: air saturation humidity at wet bulb temperature, $kg_{water} \cdot kg^{-1}_{dry\ air}$
Y_∞: bulb external gas phase humidity, $kg_{water} \cdot kg^{-1}_{dry\ air}$

Key to subscripts

ae: ambient air
*ai*1: stale air
*ai*2: heat conveying air
c: window glass
ce: external face of window glass
ci: internal face of window glass
da: drying air
ie: external face of insulating
ii: internal face of insulating
is: insulating
n: absorber
sl: sludge sample
sky: sky vault
soil: outside soil
w: drying room wall
we: external face of the drying room wall
wi: internal face of the drying room wall

Greek symbol

α_n: absorption coefficient direct irradiance of absorber
α_{nd}: absorption coefficient diffuse irradiance of absorber
β: coefficients of polynomial regression
ε: emissivity
χ_c: extinction coefficient, m^{-1}
γ_c: orientation of the solar, °
ρ_a: density of humid air, $kg \cdot m^{-3}$
σ_k: heat source, W

References

1. Daguenet M. Les séchoirs solaires: théorie et pratique, UNESCO, 1985, P. 489-494.
2. Sacadura J.F. Initiation aux transferts thermiques, 2000. 6ième édition.
3. Daguenet M. Les séchoirs solaires: théorie et pratique, UNESCO, 1985, P. 320-343.
4. Léonard A., Salmon T., Janssens O., Crine M. Kinetics modelling of convective heat drying of wastewater treatment sludge, Acte de Congrés ECCE2 1999.
5. Saltelli A., Tarantola S., Chan K.P.S. A quantitative Model-independent method for global sensitivity analysis of model output // Technometrics. 1999. Vol. 41. No. 1.
6. Cukier R.I. et al. Study of the sensitivity of coupled reaction systems to uncertainties in rate coefficients. Part I Theory // Journal of Chemical Physics. 1973. Vol. 59. P. 3873-3878.
7. Mara T.A. Contribution à la validation d'un logiciel de simulation de thermo-aéraulique du bâtiment: Proposition de nouveaux outils d'aide à la validation. PhD Thesis, Université de la Réunion, 2000.
8. Mara T.A., Boyer H., Garde F. Parametric sensitivity analysis in thermal building using a new method based on spectral analysis // Transactions of ASME – International Journal of Solar Energy Engineering. 2002. No. 124. P. 237–242.
9. Duffie J.A., Beckman W.A. Solar engineering of thermal processes, 1991. 2nd edition.

MODELLING OF A BIOCLIMATIC ROOF USING NATURAL VENTILATION

I. Ouédraogo, A. Ouédraogo*, K. Palm*, B. Zeghmati***

*Laboratoire de Chimie Organique et Appliquée UFR\SEA Université de Ouagadougou BP 7021 Burkina Faso.
Fax: (+226) 50 30 72 42, e-mail**:** issaka.ouedraogo@univ-ouaga.bf
**Laboratoire de Mathématiques et Physiques de Systèmes Université de Perpignan
66860 Perpignan France

Received: 11 Oct 2007, accepted: 7 Nov 2007

The traditional techniques of air-conditioning present considerable disadvantages of the point of view of the energy consumption and especially of the environmental pollution. So the promotion of new technologies of air-conditioning to low fuel consumption of energy and the improvement of the energy effectiveness of the habitats prove to be essential. The air-conditioning passivates which minimizes the thermal energy of the sun by various techniques and which exploits the architectural characteristics of the buildings is very promising. Thus, the bioclimatic term refers to some guiding principles where the design and construction of the buildings take account of the environment to create an interior environment in conformity with thermal comfort.

Keywords: solar buildings, natural ventilation, bioclimatic roof, thermal comfort

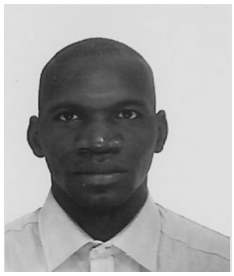

Issaka Ouedraogo

Master degree at ISFRA of Bamako (Mali), 1999.
Teacher of physique to the college Zinda of Ouagadougou, 1999-2002.
Master degree at University of Perpignan (France), 2002.
Assistant monitor in charge of undergraduate Physics lab at University of Ouagadougou, 2004.
Scientific interests: modelling and heat transfer.

Alioune Ouedraogo

Laboratoire de Chimie Organique Appliquee UFR/SEA University of Ouagadougou.
Pr, Head of Physics Department of IMP, 1981-1984.
Coordinator of Physics-Chemistry section, 2004, UFR/SEA.
Decoration: Chevalier of Academic Palm, 2002.
Fullbright grant (USA) 1986-1987 at UC-Davis, and UGa-Athens CIUF grant for 3 months training (Belgium), 1999-2002, at ULB.
Scientific interests: solid state physics, ferroelectrics, essential oils and aromatic plants.
Publications: 4 in Mechanics (BUP); 6 in Solid State (Journal de Physique, Ferroelectrics and European Physical Journal); 2 in Journal of SOACHIM; 2 on Essential Oils (Journal of Applied Sciences and Annals of UO).
2 scientific projects.

Nomenclature

T = Temperature (K)
t = Time (s)
L = Length (m)
l = Width (m)
H = Height of the channel (m)
S = Surface (m^2)
k = Thermal conductivity ($W \cdot m^{-1}K^{-1}$)
Ep = Thickness (m)
M = Mass (kg)
Cp = Specific heat constant ($J \cdot kg^{-1}K^{-1}$)
hr = Radiation transfer coefficient ($W \cdot m^{-2}K^{-1}$)
hc = Free convection transfer coefficient ($W \cdot m^{-2}K^{-1}$)
F = Geometrical factor form
γ = Roof thermal absorptivity ($W \cdot m^2$)
ε = Emissivity
α = Angle inclination (°)
η = Flux density collected by Absorber ($W \cdot m^2$)
Pu = Flux puissance ($W \cdot m^2$)
ϕ = Solar flux ($W \cdot m^2$)

Indices

be = External roof
bi = Interior roof
a = Air of the channel
p = Absorber
is = Insulator
amb = Ambient
v*c* = Vault of heaven
amp = The air enters the insulator and the ceiling
pl = Ceiling

Introduction

In the world and particularly the emerging countries like Burkina Faso, energy is a factor very determining to ensure a minimum of the economic and social activity. The problem of energy is essential to reduce the great consumption related to the HVAC (Heating Ventilating and Air Conditioning) by the techniques of passive air-conditioning. So it is allowed that the combination of various techniques passive air-conditionings decreases the energy loads considerably and to improve comfort of the buildings [1]. Our model of bioclimatic roof designed to trap the solar radiation involves local materials [2]. Plexiglas and clay tiles, a channel where circulate the air of the enclosure, and a sheet painted in black being the absorber. Finally an insulator is constituted of *Ceiba Pentandra* fibres. In this work the model is compared to a plane sensor of air of rectangular and tilted section. Distribution of the temperatures of various materials of the roof, and the air flow depends on the coefficients of heat transfer by natural convection and radiation [3]. However these coefficients are characterized by the number of Nusselt for a given geometrical configuration. We retain the number of Nusselt proposed by Holland et al [4]. The air flow is estimated by the equation of Bansal, Mathur and Bhandari [5]. Finally we numerically simulate the performances of the model of a bioclimatic roof in a hot and dry tropical climate, in order to optimize the dimensional parameters of buildings.

Description of the model

The roof model is similar to that studied by Khedari et al [6] in a hot and wet climate (Thailand). The process consists in making the air inside the building circulate by natural convection in the roof by creating temperature gradients between the components of the roof made up of local materials (Fig. 1).
On one hand it is possible to act on dimensions of bricks and their sites and on the other hand on the optical properties of these bricks. The study of this roof can be performed primarily according to two steps:
1. The first takes account of the space-time evolution of the temperature of all the speed and roofing units, to which the air circulates in this roof. This method requires the resolution of the equations of transfers by natural convection coupled with the equation of transfer of heat by conduction in various materials (Table 1).

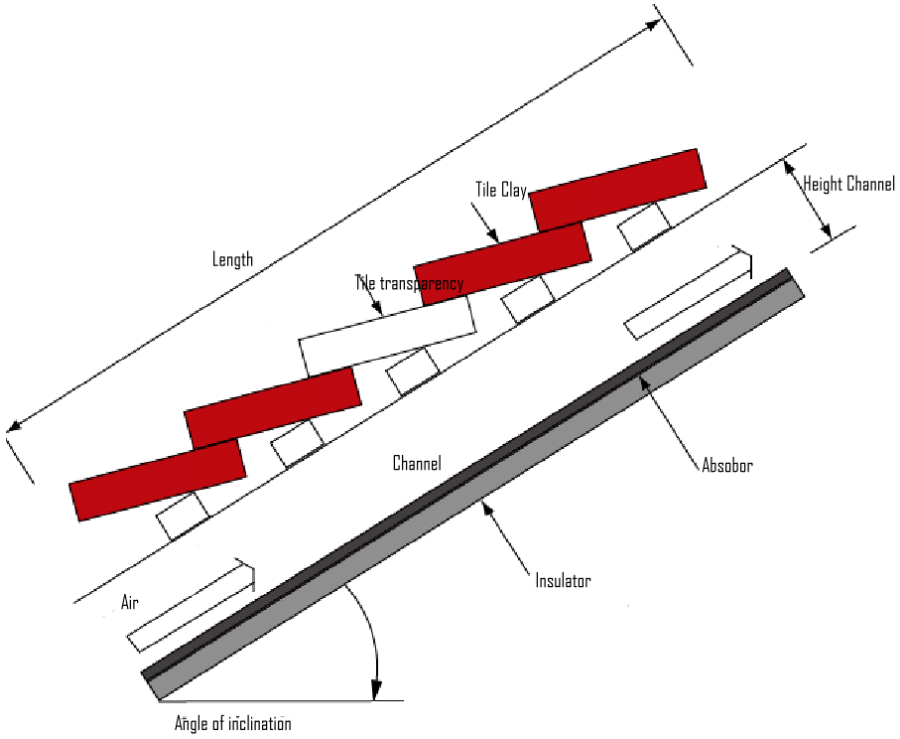

Fig. 1. *Bioclimatic roof model*

Table 1

Thermal properties of materials

Materials	Density, ρ (kg/m^3)	Specific heat, C_p (J/kg/K)	Absorptivity, γ	Thermal conductivity, K (W·m^{-1}K^{-1})	Emissivity, ε
Clay tiles	1800	780	0.485	0.685	0.834
Plexiglas tiles	1200	800	0.128	0.752	0.010
Absorber	2700	920	0.945	180	0.880
Insulator	530	950	0.237	0.016	0.15

2. The second consists in allotting to the various roofing units arbitrary average temperatures. It allows gives an account of their temporal evolution, and evaluates the air flow which circulates in the roof. This method rests on the use of the analogies between the thermal and electric transfers.

For modelling, the following simplifying assumptions were made:

1) The constituent materials of the roof are homogeneous.

2) The physical properties of materials and the air are supposed to be constant.

3) The transfers are one-dimensional.

4) The thermal inertia of the air is negligible.

Mathematical formulation

The method consists in cutting out the roof in fictitious sections in the direction of the air flow. To write the heat balances in each section we use analogies which exist between the thermal transfers and the transfers of electricity. The application of the Ohm's law to each section leads to the following heat balances:

The external

$$\frac{M_{be}CP_{be}}{S}\frac{\partial T_{be}}{\partial t} = \varepsilon\gamma_{be}\eta_{be} + \frac{k_{be}}{EP_{be}}\left(T_{bi} - T_{be}\right) + hr_{be}\left(T_{vc} - T_{be}\right) + hc_1\left(T_{amb} - T_{be}\right) + hr_{amb}\left(T_{amb} - T_{be}\right). \quad (1)$$

The internal

$$\frac{M_{bi}CP_{bi}}{S}\frac{\partial T_{bi}}{\partial t} = \frac{k_{bi}}{EP_{bi}}\left(T_{be} - T_{bi}\right) + hc_2\left(T_a - T_{bi}\right) + hr_{p\to bi}\left(T_p - T_{bi}\right). \quad (2)$$

Air channel

$$\frac{M_aCP_a}{S}\frac{\partial T_a}{\partial t} = +hc_2\left(T_p - T_a\right) + hc_3\left(T_{bi} - T_a\right) + Pu\,. \quad (3)$$

Absorber

$$\frac{M_pCP_p}{S}\frac{\partial T_p}{\partial t} = \varepsilon\gamma_p\eta_p + \frac{k_p}{EP_v}\left(T_p - T_{is}\right) + hc_2\left(T_a - T_p\right) + hr_{p\to vc}\left(T_{vc} - T_p\right) + \sum_{i=1}^{3} hr_{i\to t_p}F_{i,t_p}\left(T_i - T_p\right) + \Phi\,. \quad (4)$$

Insulator

$$\frac{M_{is}CP_{is}}{S}\frac{\partial T_{is}}{\partial t} = \frac{k_{is}}{EP_{is}}\left(T_p - T_{is}\right) + hc_4\left(T_{amp} - T_{is}\right) + \sum_{i=1}^{2} hr_{i\to pl}F_{i,pl}\left(T_i - T_{is}\right). \quad (5)$$

Resolution algorithm

The discretization using an implicit method with the finished differences of the equations (1 to 5) led to a system of algebraic equation which is solved, in each section of the roof, by using the method "Diabolo Sablier". An iterative calculation is necessary because the heat transfer coefficients by convection and radiation are a function of the roof temperatures.

Results and discussion

The space-time knowledge of the distributions of the temperatures of the whole of materials of the roof of the building and the air flow to ventilate by natural convection proves to be necessary to determine optimal dimensions. Thus we study the influence of the physical properties of materials of the roof (B = tiles out of clay and P = plexiglass tiles). Of sound inclination (α) compared to the horizontal one for values ranging between 30° with 75° and of sound geographical orientation on the distributions of the temperatures of the air in the roof and the enclosure of the building. We consider the influence height (H) of the channel where the air flow circulates. We present them below numerical results with the following parameters: α = 50°, H = 0.15 m, L = 2 m, l = 0.3 m. For our calculations we used the weather data of the town of OUAGADOUGOU (in the center of Burkina Faso) [7] standard day of June, May, July.

While comparing the profile of the temperatures of air and of different materials (Fig. 2) it is noticed that the temperature of the air is (T_a) is higher than that of other materials of the roof, except the one of the absorber (T_p). This seems to be in contradiction with the concept of passive air-conditioning. It can be explained by the presence of the plexiglas tiles which cause an increase in the solar flow collected by the elements of the lower part of the roof which is accompanied by an increase in the intensity of the radiative exchanges inside the roof.

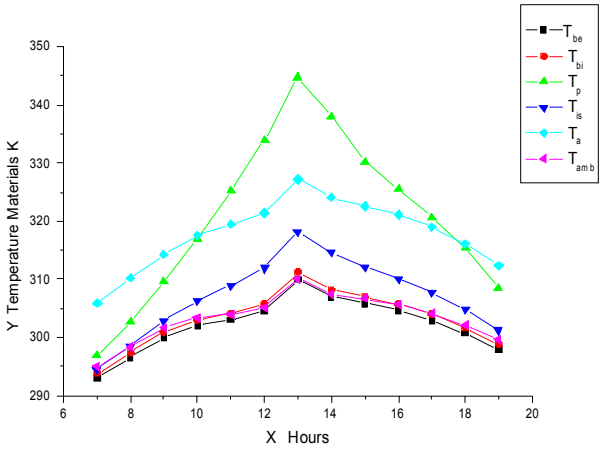

Fig. 2. *Space-time evolution of the temperatures of materials of the roof*

To follow the evolution of the air flow to the course time, and to seek an optimal flow in conformity with the Adaptive Standard Comfort (ACS), we planned several types of roof. It is about the higher part of roof contacts some with the ambient conditions. As illustrated by Fig. 3, when this part is completely covered with the clay tiles (BBBBB), one notes very week air flow, therefore a thermal discomfort inside the building. While an entirely covered roof of plexiglass tiles (PPPPP), the air flow is very appreciable but for the reason of expensive cost of the materials, we did not consider this case in practice.

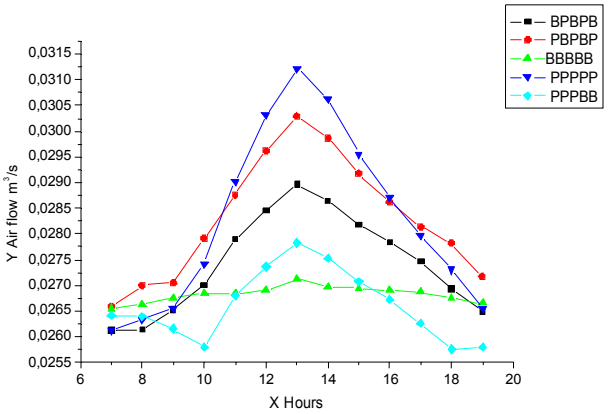

Fig. 3*. Space-time evolution of the flow circulating in the roof*

While varying the height of the channel H = 0,12 m (Fig. 4) and 0,15 m, we notice in (Fig. 5) when one intercalates the tiles out of clay and plexiglas that the air flow decrease and increases. However the temperature of the air (T_a) is not very sensitive to this variation.

The angle of inclination influences considerably the temperature and the air flow which circulates. When the angle of inclination is higher than 45°, the intensity of the flow collected by the roof decreases. For an angle of inclination α = 50°, we observe that the average temperature of the air inside is lower than that of ambient. Let us add that other parameters influence the environment of the enclosure of the building, such as the thickness of the walls and the height of the windows. In order to validate our numerical results, we compare these results with the works of Jompob Waewsak [8] on a similar roof in Thailand and those of Richard J. de Dear and Gail S. Brager [9] on the thermal index of satisfaction of Adaptive Comfort Standards (ACS).

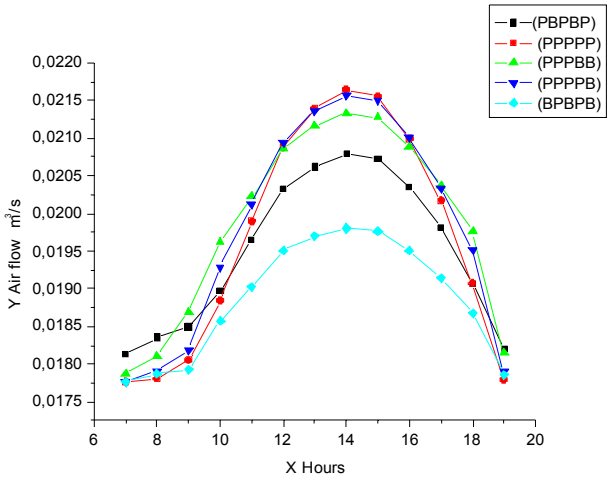

Fig. 4. *Space-time evolution of the flow circulating in the roof an influence height of the channel*

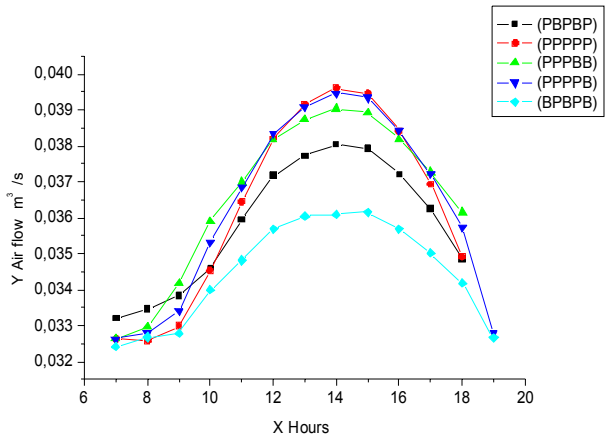

Fig. 5. *Space-time evolution of the flow circulating in the roof an influence height of the channel*

Conclusion

Our study explores the effects of natural ventilation in a hot and dry tropical climate inside a building to save energy in a city like Ouagadougou in Burkina Faso. It comes out from our calculations to reach an optimal flow in the enclosure of a building, synonymous with satisfactory thermal feeling: the building must be directed in North-South and the roof should be inclined with an angle of 50° with a maximum of the influence of channel for an height of 0.15 m. In spite of that the thermal feeling depends also on the relative humidity of the city, the clothing and finally of the psychological factor of the occupants of the building.

Aknowlegements

The authors wish to thank the CUD (Belgium) for the grant (CIUF/UO/06) to Mr. Ouedraogo Issaka.

References

1. Depecker P. et al. Design of building shape and energy consumption // Building and environment. 2006. No. 36 (5). P. 627-635.
2. Awbi H. B. Design consideration for naturally ventilated buildings, Renewable Energy. 1994. No. 5. P II. P. 1081-1090.
3. Rodigues A.M., Canha da Piedade A., Lahellec A., Grandpeix J. Y. Modelling natural convection in heated verticale channel for room ventilation // Building and Environment. 2000. No. 35. P. 455-469.
4. Duffie J. A., Beckman W.A. Solar Engineering of thermal Processes. 2nd edition. New York: John & Sons Inc., 1991. P. 919.
5. Bansal N.K., Mathur R., Bhandari M. S. Solar chimney for Enhanced Stack Ventilation // Buildings and Environment. 1992. No. 28. P. 373-377.
6. Khedari J. et al. New configuration of a roof solar collector maximizing natural convection // Buildings and environment. 2001. No. 36. P. 383-391.
7. Lui B.Y.H., Jordan R.C. The interrelationship and characteristic distribution of direct diffuse and total radiation // Solar Energy. 1961. No. 4. P. 1-19.
8. Waewsak J. These de doctorat. Designing of an original Thai-Bioclimatic Roof. 2001. University of Perpignan.
9. Richard J. de Dear, Gail Brager S. Thermal comfort in naturally ventilated buildings: revision to ASHRAE standard 55 energy and building. 2002. No. 36. P. 549-561.
10. Fange P.O. Thermal comfort-Analysis and Application in Environmental Engineering, Danish Technical Press Copenhagen. 1970.
11. Agrawal P.C. A review of passive system for natural heating and cooling of buildings // Solar and wind Technology. 1989. No. 6. P. 557-567.

SIMULATION OF A SOLAR ABSORPTION COOLING SYSTEM

J.P. Praene, D. Morau, F. Lucas, F. Garde, H. Boyer*

Laboratoire de Physique du Bâtiment et des Systemes
117 rue du Général Ailleret, Tampon, 97430, REUNION
262 692 23 34 11 / + 262 57 95 41; *E-mail: praene@univ-reunion.fr

Received: 18 Sept 2007; accepted: 15 Oct 2007

This paper describes the dynamic modeling of a solar absorption cooling plant that will be built for both research and demonstration purposes by the end of 2007. The synchronizing of cooling loads with solar radiation intensity is an important advantage when utilizing solar energy in air conditioning in buildings. The first part of this work deals with the dynamic modeling of an evacuated tube collector. A field of these collectors feed a single-effect absorption chiller of 35 kW nominal cooling capacity. The simulation model has been done in a modular way under TRNSYS16. In a second part, simulation and optimization of the system has been investigated in order to determine the effect of several parameters (collector area, tank volume...) on chiller performance.

Keywords: solar collectors, solar refrigerators, solar energy

J.P. Praene

Education: At the University of Reunion Island, I received the Bachelor of Science degree in Physics in 1999. I then moved to France at Institut National Polytechnique de Lorraine where I received a Masters degree of Mechanical engineering in 2001. The PhD degree in 2007 was made at University of Reunion Island.
Experience: Engineer Consultant in Acoustics and Renewable Energy in Buildings (2007). I worked as assistant engineer in LL&A's Consulting (2002). I actually participate to two French research projects: RAFSOL, ORASOL (2006-2008, on solar cooling) and DYNASIMU (2007, on building simulation).
Main range of scientific interests: Study of building comfort in hot climates and the use of renewable energy as alternative to face buildings loads.
Publications: Dynamic modeling and elements of validation of solar evacuated tube collectors. The Ninth IBPSA Conference and Exhibition, 2005; Simulation and optimization of a solar absorption cooling system using evacuated tube collectors. CLIMA 2007, 2007; Steady state model of an evacuated tube collector − Sensitivity analysis approach. Journal of Solar Energy Engineering, 2007 (under review).

Introduction

The possible use of solar energy as an alternative heat input for a cooling system has led to several studies of available cooling technologies that use solar energy and was initiated by the technological developments in the solar field [1]. The demand for cooling energy closely matches the availability of solar energy, both in seasonal and the daily variations. A state-of-art of solar absorption cooling systems (SACs) have been proposed [2-4]. An overview of recent development and many projects is also given and control strategy of such plants is approached. Much more investigation has to be done in computer models field in order to improve development of accurate forecast tools to predict SACs performance.

Reunion Island is a French overseas department located in the southern hemisphere characterized by a tropical humid climate. In few years, conventional energy will not be enough to meet the continuously increasing demand of energy. Building remains at the present time the most consuming sector in electricity. Under our latitudes, the demand for electricity greatly increases because of the extensive use of heating ventilation air conditioning (HVAC) systems, which increase the peak electric load during summer period (November to April). Of share our insularity an orientation towards renewable energies is actually is an attractive concept to obtain an energy independence. This orientation was initiated during 90's, Fig. 1.

One of the many categories of solar cooling systems is the solar absorption cooling. As no CFC are used, absorption systems are friendlier to the environment. At present the market of sorption refrigeration systems is dominated by LiBr–H_2O systems [5]. Absorption air-conditioning systems are similar to vapor compression air-conditioning systems, but differ in the pressurization stages. In general an absorbent in the low pressure side absorbs an evaporating refrigerant (H_2O). The most usual combinations of chemical fluids used include lithium bromide-water (LiBr–H_2O), where water vapor is the refrigerant, and ammonia–water (NH_3–H_2O) system where ammonia is the refrigerant [6]. The electric quantity of power consumed by the pump is almost negligible. One needs nevertheless a contribution of heat, Fig. 2.

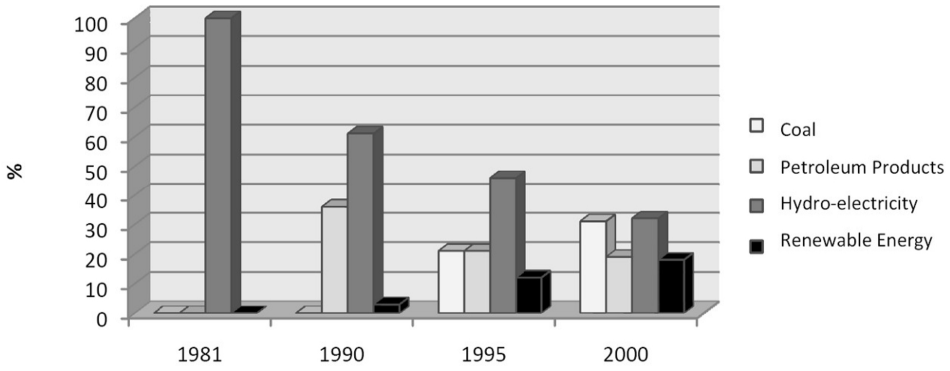

Fig. 1. *Evolution of the energy production repartition in Reunion Island since 80's*

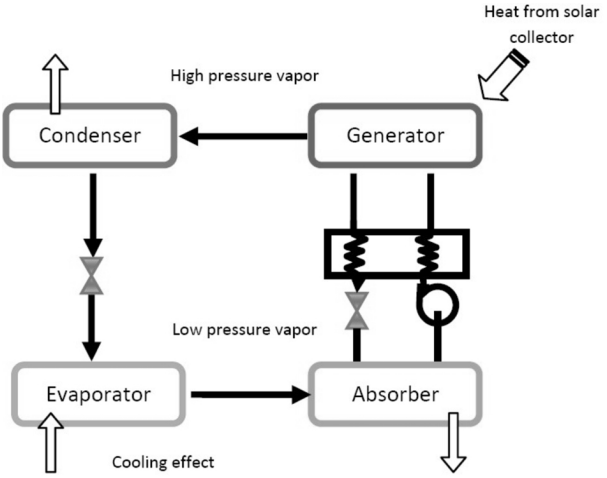

Fig. 2. *The basic principle of the absorption air-conditioning system*

Single effect absorption chillers require for their operation a hot water temperature on the level of the generator of 80 °C − 150 °C. Moreover, the temperature of cooling water must lie between 7 °C and 43 °C [2]. The higher limit is founded in order to limit the differences in pressure between the generator and the absorber and the condenser and the evaporator. The lower limit makes it possible to avoid the crystallization of lithium bromide which is carried out at low temperature [6].

The main focus of this study is concentrated on the development of dynamic simulation of SACs that can be used for installation design. The purpose of this article is to study the effect of several parameters on the SACs performance. The analysis and optimization is carried out with the TRNSYS 16 software.

Dynamic evacuated-tube collector (ETC) modeling

Solar collector represent the heart of SACs performance and investments (~ 57%). Thus, an accurate forecast of the solar collector field performance is particularly judicious. This part of the paper deals with the development of ETC dynamic modeling.

There are three types of solar collectors which can be used within the framework of solar cooling: flat-plate, parabolic and vacuum collectors, see Fig. 3. In the present work, an ETC with selective absorber plate surface is considered.

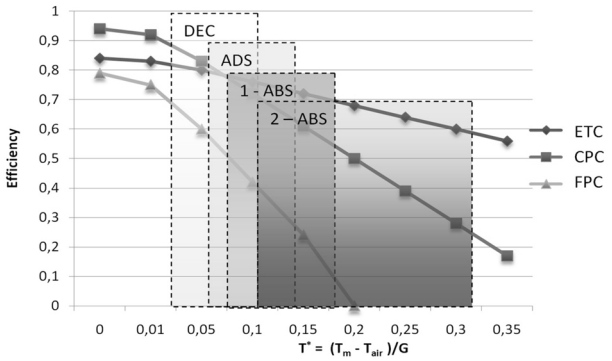

Fig. 3. *Comparison of ETC / Compound parabolic/ Flat-plate performance for different solar cooling systems (Desiccant /Adsorption/ Absorption)*

Such collectors are highly efficient due to the fact that the space between the glass and the absorber is evacuated. The main advantage of ETC is the possibility to obtain a good efficiency at high temperature. The studied model consists of vacuum tubes mounted three by three in series. The heat transfer fluid flows in a copper U-tube which is welded to a narrow flat absorber. Thus, the inlet and the outlet are situated at the same end of the ETC, see Fig. 4.

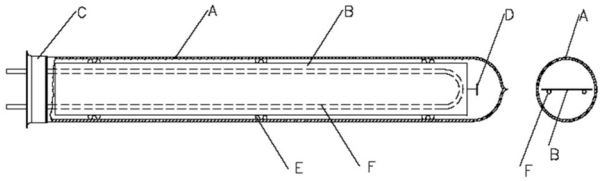

A – Evacuated glass tube
B – Absorber
C – Metal header
D – Getter
E – Support spring
F – Copper U-tube

Fig. 4. *Evacuated tube collector model*

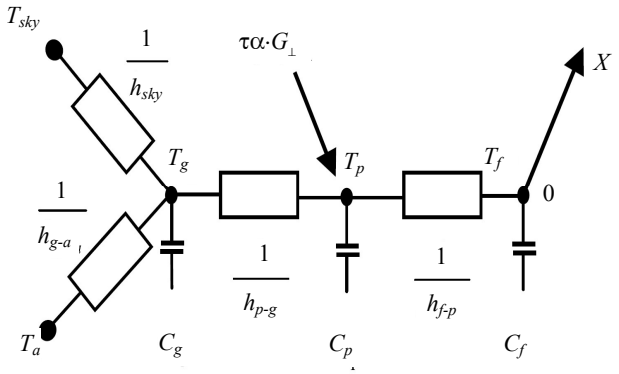

Fig. 5. *Thermal networks for the 3-node dynamic model*

The literature contains numerous works on the modeling of solar collectors. These models developed have different levels of complexity. Usually, solar collectors are described by stationary models, considering the collector working under steady-state conditions. These approaches are generally based on the work of Klein [7]. A number of simplifying assumptions have to be made for the modeling. Most of these have been previously described by Duffie [8]:

– material properties are not dependent on temperature;

– temperature gradients along the absorber length can be neglected;

– temperature gradients inside the glass cover is assumed to be negligible;

– dust and pollution over the collector can be neglected;

– perfect insulation at the edges of the collector is assumed.

The model (Fig. 5) consists on three nodes corresponding to the fluid, the absorber plate and the transparent glass cover. It is considered that the temperature of the fluid is a function of x. The fluid is moving in a single channel with the velocity *u*, along *x*-axis.

Applying heat balances at different parts of the collector, the temperature in the nodal points can be described by a set of three differential equations:

$$C_g \frac{\partial T_g}{\partial t} = \varepsilon_g \sigma\left(T_{sky}^4 - T_g^4\right) + h_{g-a}\left(T_a - T_g\right) + \varepsilon_g \sigma\left(T_p^4 - T_g^4\right) \quad (1)$$

$$C_p \frac{\partial T_p}{\partial t} = \tau\alpha G_\perp + \varepsilon_g \sigma\left(T_g^4 - T_p^4\right) + h_{f-p}\left(T_f - T_p\right) \quad (2)$$

$$C_f\left(\frac{\partial T_f}{\partial t} + u\frac{\partial T_f}{\partial x}\right) = h_{f-p}\left(T_p - T_f\right). \quad (3)$$

The details of the model developed and elements of validation associated have been previously described by Praene [9]. A comparison between model forecast and measurements is presented in Fig. 6. The simulation is carried out at the minute time step. A new type has been created under TRNSYS, in order to coupling with the rest of the solar cooling system. We have chosen to numerically solve this system using finite difference approach. In this case, the collector is defined as single fluid channel, which is divided into N segments.

The differential equation system is solved for each of segments using a Total Variation Diminishing scheme based on Lax Wen Droff Method. The final outlet temperature obtain for segment (*xi*-1) is the initial or inlet fluid temperature for segment *xi*. The final outlet temperature is obtained by connecting the *N* segments of the collector.

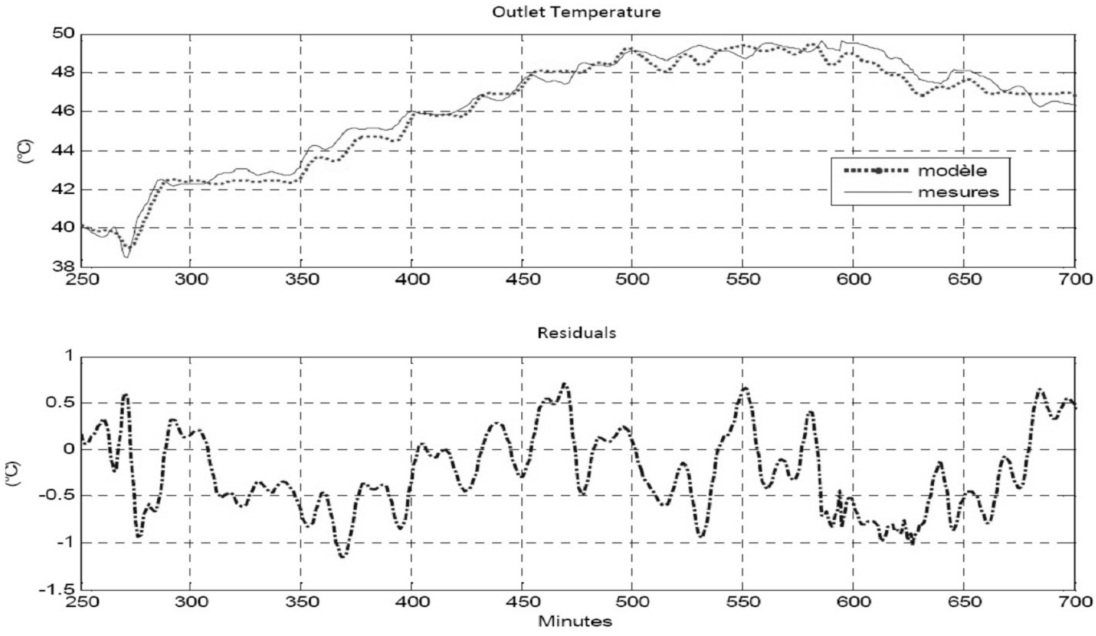

Fig. 6. *Comparison between measurements and model prediction at minute time step*

Thermal building simulation

A detailed building thermal simulation software is employed for the modeling of the different studied zone. This software called CODYRUN, developed in our laboratory, is both regrouping a design and research aspects. The description of this software has already been covered in various publications [10-13]. The CODYRUN program was translated under TRNSYS 16 environment in order to replace the TYPE 56 subroutine. The main advantages are a good accuracy for short time step (less than the hour) and several tests have been carried out to validate the code for tropical humid climates. One of the most important developments is the dynamic link between cold production for absorption and the building loads. Thanks to CODYRUN, as we simulate at short time step (1/8 hour), thus it is possible to observe the impact of variation of cooling rate on air temperature inside the building.

The different studied zones are classroom of the Civil Engineering Department of University of Reunion Island. The first step of simulation is about evaluate air temperature inside classroom under natural ventilation during one year. An accurate climatic database is needed for the study. The meteorological database from our experimental setup was used. The department becomes located close to sea level (50 meters high).

As shown at Fig. 7, the period from May to October corresponding to our southern winter offering natural comfort condition. A temperature lower than 25 °C is fixed as thermal comfort condition inside classroom relative humidity is also an important factor for comfort. In reality, no direct control of humidity rate is possible on absorption chiller. However, many researches were carried out by the researchers in order to create simplified tools of indication of comfort [14-15]. We were thus based on the computation results of these comfort index within the framework of our simulations over the whole year, in order to determine the interesting building load period to study. The starting point for the definition of the levels of comfort is based on the value recommended of PMV* (Predicted Mean Vote). That involves values of $-0.5 < PMV^* < +0.5$. Regarding our work, only the positive part is considered. Fig. 8 presents the PMV* evolution and confirms the same period of natural comfort shown previously.

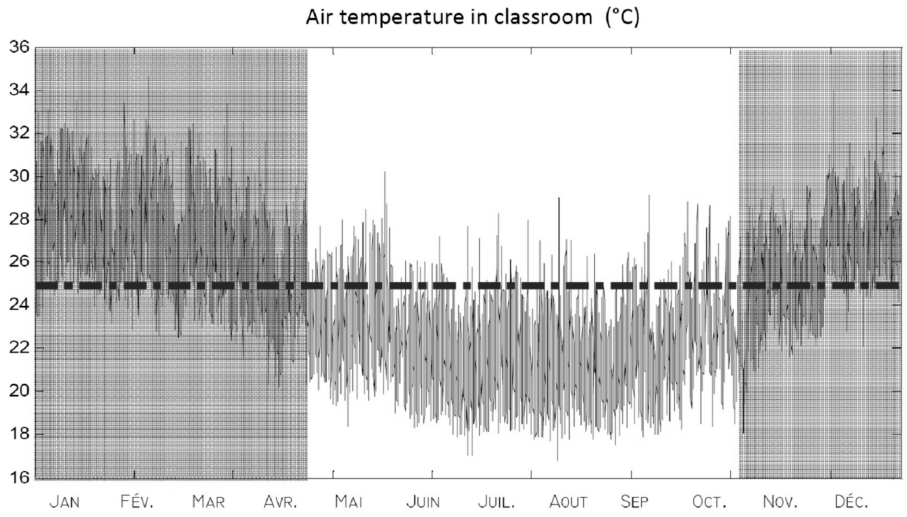

Fig. 7. *Yearly evolution of air temperature in classroom*

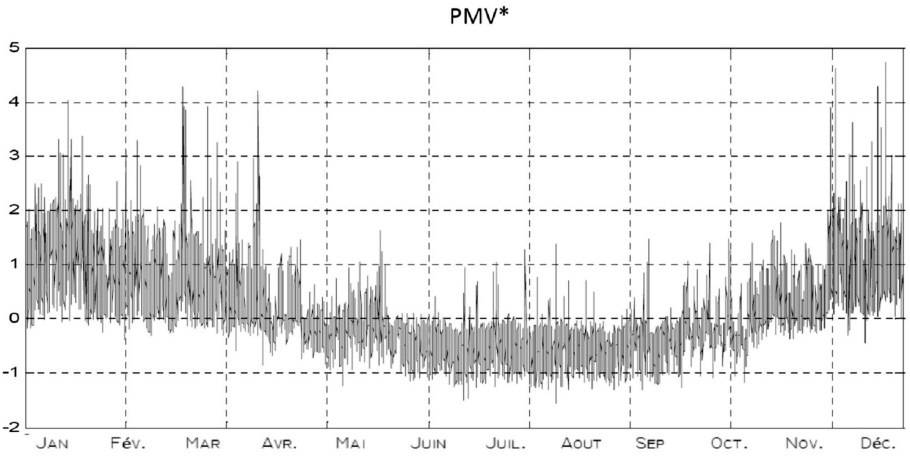

Fig. 8. *Yearly evolution of PMV* in clasroom under natural ventilation condition*

The period from November to April is clearly identify as cooling period. In a second time, CODYRUN ensured in the evaluation of building loads during summer. January was chosen as month of reference. Simulations were carried out for the classroom using the following assumptions:

– Inside air temperature of 25 °C.

– Relative humidity of 55 %.

As presented on Fig. 9 the maximum classroom load is 9.5 kW. This peak occurs after midday that is due to the inertia of the building and consequently restitution of this heat. Thus, for all the classrooms of the Civil Engineering Department a 35 kW absorption chiller is necessary. Simula has been extended to the summer period in order to determine a daily cooling rate for the classroom. The maximum value is 1.2 kW·h/m²·day during January, see Fig. 10.

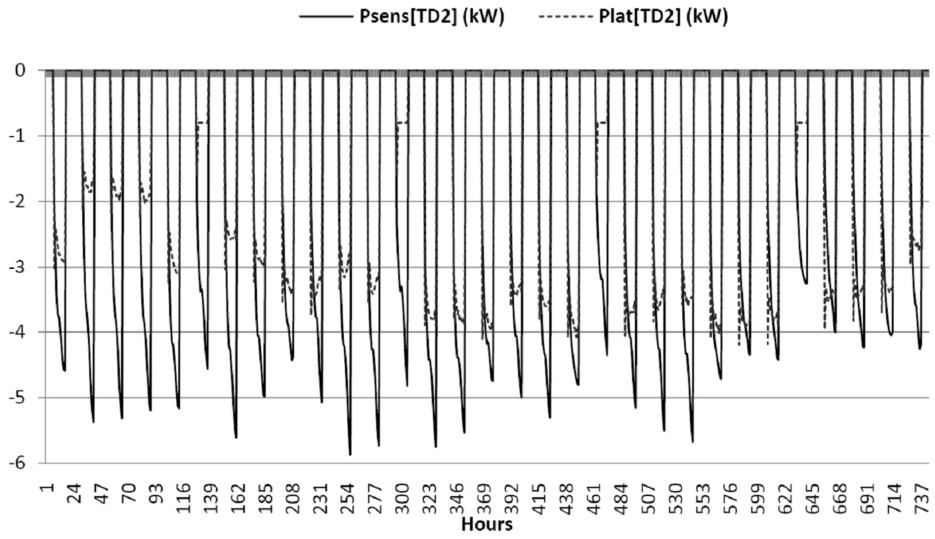

Fig. 9. *Sensible and latent power called by a classroom during January*

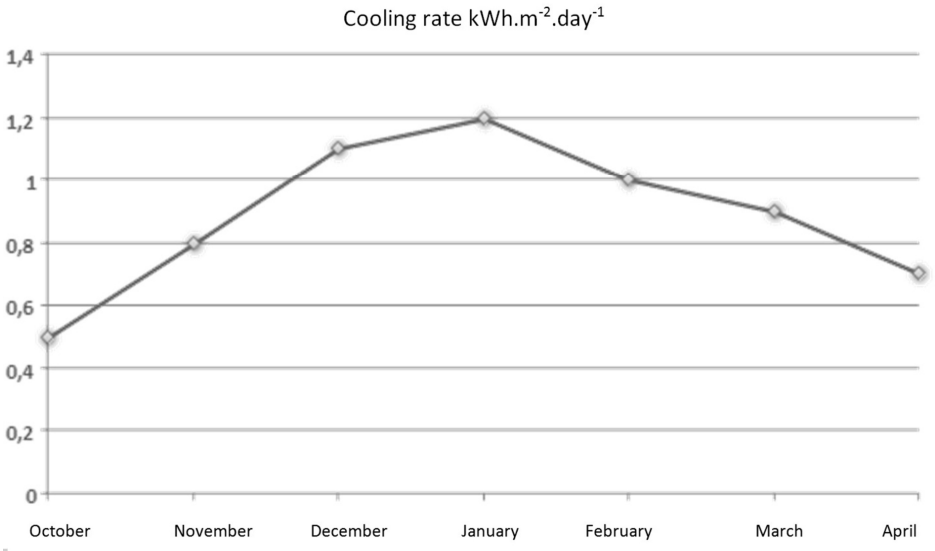

Fig. 10. *Daily average cooling demand for a classroom*

Absorption cooling system simulation

This section presents the principal results obtain under TRNSYS for simulation of the global solar absorption cooling system. This program consists of the use of several "subroutines" which represents the components of the system described by ordinary or algebraic equations. The LiBr–water absorption air conditioner employed is a single-effect unit, based on Arkla model WF-36. Auxiliary heater is not used. Two new types were added to the existing models under TRNSYS. It is about the model of simulation of the building and the model of vacuum collector. The useful surface area of collector used during simulation is 60 m². The storage of

hot water uses Type 38. That corresponds to a vertical roll of 800 L made up of copper insulated thematically with polyurethane. A sequence of January is considered in order to carry out our simulation, as shown on Fig. 11 and 12.

The average temperature in classroom is near 27 °C during the day. The difference between inside and outside air temperature is about 4 °C.

Absorption chiller works without additional contribution of an auxiliary heat unit. As we can see on Fig. 12, the 60 m² of ETC is enough to meet the minimum inlet temperature of 80 °C for the generator. If the inlet temperature is too low, the water flows through a by pass to the solar loop to be heat again.

A number of simulation are carried out in order to evaluate the effect of various parameters on the performance of the system. All runs consider the meteorological data of University during January. One of the most important points from an economic point of view of a solar cooling plant is the solar loop. The field of solar collectors accounts for approximately 60 % of the total investment (in particular if it is vacuum collector). So it is important to dimension in a first place the needs for the building then the total surface of the field of solar collectors. Three points go in general to the decision of the field of solar collectors:

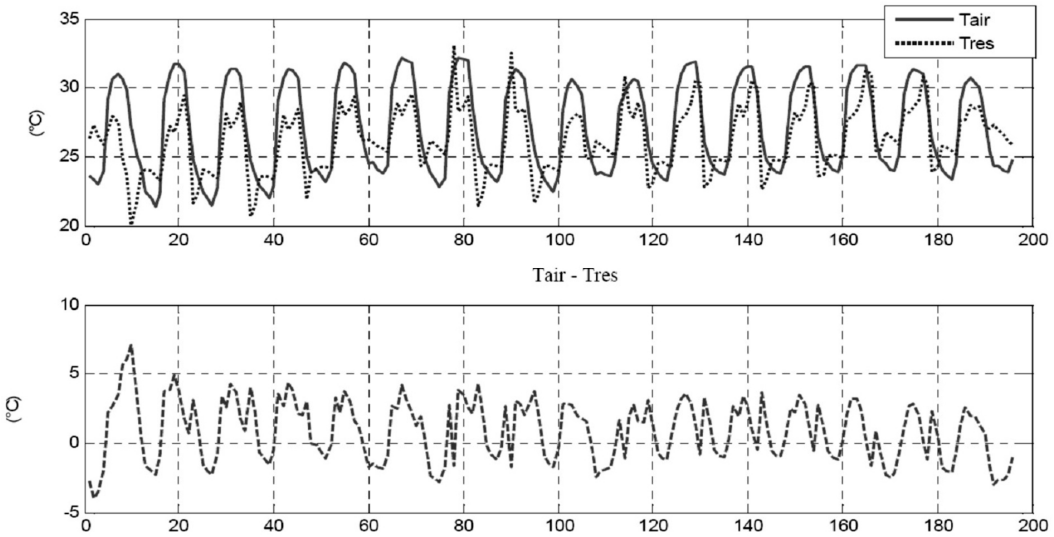

Fig. 11. *Comparison between inside air temperature (Tres) and outside air temperature (Tair)*

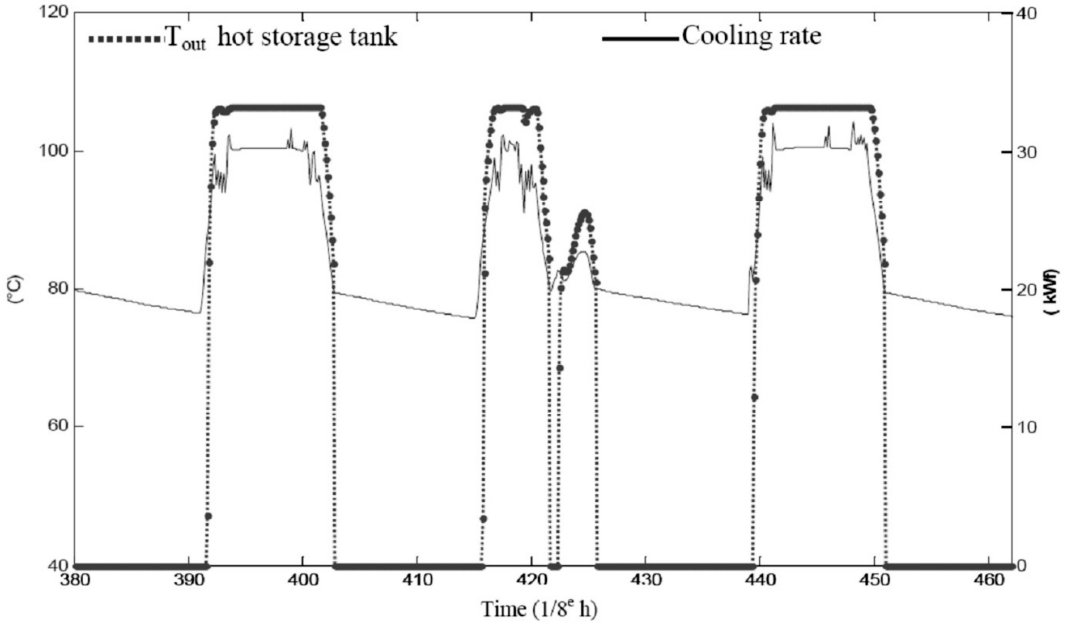

Fig. 12. *Evolution of absorption chiller cooling rate and outlet temperature of hot water storage tank*

− Economic constraint: Budget dedicated to the project.

− Space constraint: surface available for the solar field.

− Weather constraint: average numbers of good days during the hot period.

Also, it is important to quantify the influence of the elements of the solar loop, of as much we are in the case of an operation of solar cooling, without auxiliary contribution.

Many tests have been investigated to evaluate the sensitivity of the machine performance for different volume of storage tank, see Fig. 13. For a volume superior than 2.5 m^3, the outlet temperature is lower than 80 °C, thus the cold production will stop. Storage volume plays a dominating part because it has a buffering effect to the abrupt weather variations and makes possible to continue the hot water supply of absorption chiller. The total solar collector area is the most important point (performance and economy). Several area of solar collectors have been tested (Fig. 14.)

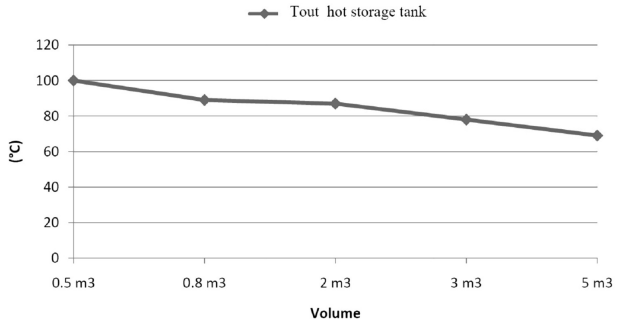

Fig. 13. *Effect of tank size on hot water temperature for generator*

The effect of solar collector is evaluated against the energy rate from absorption chiller. The cooling rate from 60 m² to 40 m² is near. This production reaches to low value for a solar area less than 20 m². Thus, to have continuous condition for cold production a collector area of 60 m² is required.

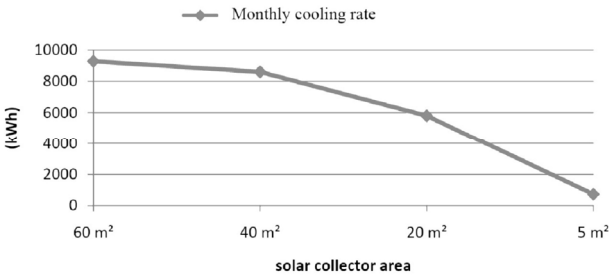

Fig. 14. *Energy production from absorption chiller for different solar collectors areas*

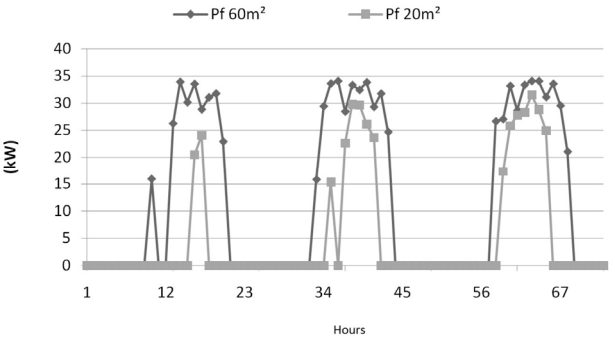

Fig. 15. *Cooling rate for 60 and 20 m² of ETC surface area*

As shown on Fig. 15, 20 m² of ETC create an intermittent working. The cold production is not available during the all day, furthermore the cooling rate is lower than the second case. Same conditions has been considered to evaluate the effect of solar collectors are on air temperature inside the classroom.

Inside air temperature (Tres) is higher than outside temperature (Tair ext), see Fig. 16. A solar collectors surface area of 20 m² is clearly not enough to meet comfort conditions in the building. This results shows the dynamic link between cooling rate and inside air temperature.

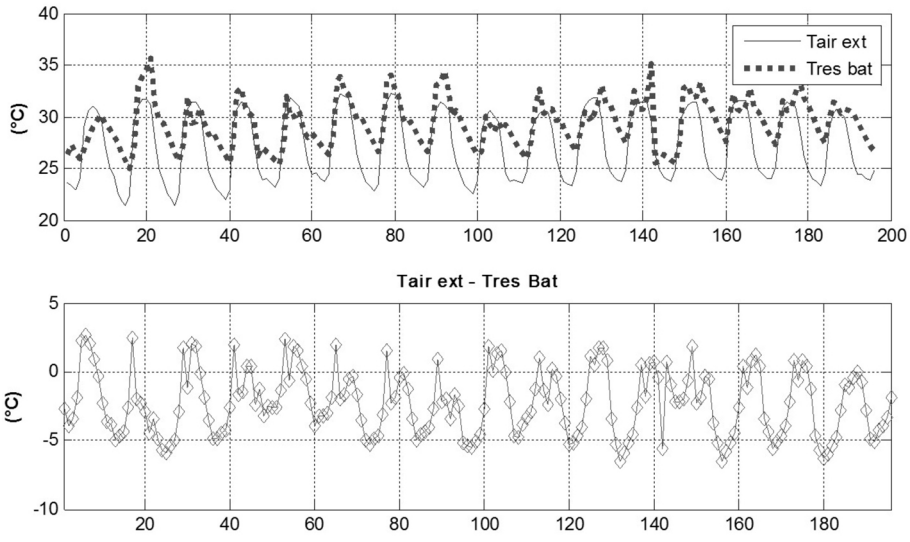

Fig. 16. *Impact of 20 m² collector on inside air temperature (Tres)*

Conclusion

The aim of this work is to present the development of a dynamic model of a solar cooling plant. The system is modeled with the TRNSYS program. For the requirements in cooling for classrooms, an optimum of the components consists of the use of 60 m² of vacuum solar collectors associated a storage tank of 0.8 m^3. We also fixed the nominal capacity of the absorption chiller with 33 kW. The final objective of this work was to set up a simulation tool representing a solar cooling plant. This environment will be used as basic support with the simulation of various configurations. The developed program can be used both for design and research studies. These simulations have been used to dimensioning an installation at University. The cooling plant will be setup on November 2007, in order to be in function in summer. This experiment will bring important element of validation on the different components of the solar cooling plant simulation.

Nomenclature

C_f – fluid heat capacity (J/m²·K)
C_g – heat capacity of glass cover (J/m²·K)
C_p – heat capacity of absorber (J/m²·K)
$G\perp$ – global solar irradiance in the plane of the collector (W/m²)
$h_{f\text{-}p}$ – heat transfer coefficient fluid – absorber (W/m²·K)
$h_{g\text{-}a}$ – heat transfer coefficient glass – ambient (W/m²·K)
h_{sky} – heat transfer coefficient glass – sky (W/m²·k)
T_a – ambient temperature (°C)
T_{sky} – sky temperature (°C)
u – fluid velocity (m/s)
v – wind velocity (m/s)

Greek symbols

α – absorptivity coefficient
ε – emissivity
σ – Stefan-Boltzmann constant ($5.67\cdot10^{-8}$ W·m^{-2}·K^{-4})

Subscripts

f – fluid
g – glass
p – absorber plate

References

1. Tabor H.Z. Use of solar energy for cooling purposes // Solar Energy. 1962. Vol. 6. P. 136-141.
2. Henning H.-M. Solar assisted air conditioning of buildings – an overview // Applied Thermal Engineering. 2007. Vol. 27, No. 10. P. 1734–1749.
3. Florides G.A., Tassou S.A., Kalogirou S.A., Wrobel L.C. Review of solar and low energy cooling technologies for buildings // Renewable Sustainable Energy Rev. 2002. Vol. 6. P. 557–572.
4. Fan Y., Luo L., Souyri B. Review of solar sorption refrigeration technologies: Development and applications // Renewable and Sustainable Energy Reviews. 2007. Vol. 11, No. 8. P. 1758-1775.
5. Lamp P., Ziegler F. Review paper, European research on solar assisted AC, Elsevier Science Ltd. and IIR. 1998.
6. Dorgan C.B., Leight S.P., Dorgan C.E. ASHRAE. Handbook of fundamentals. Application guide for absorption cooling/refrigeration using recovered heat. American Society of Heating, Refrigerating and Air Conditioning Engineers. 1995.
7. Klein S.A, Duffie J.A., Beckman W.A. Transient considerations of a flat-plate solar collectors // ASME. J. Eng. Power. 1974. Vol. 96A. P. 109-113.
8. Duffie J.A., Beckman W.A. Solar engineering of thermal processes, 2nd edition, 1991.
9. Praëne J.P., Garde F., Lucas F. Dynamic modelling and elements of validation of a solar evacuated tube collector. Building Simulation. 2005. P 953–960.
10. Boyer H. Conception thermo-aeraulique de Batiments multizones proposition d'un outil à choix multiples de modèles. PhD Thesis, INSA de Lyon, France. 1993.
11. Boyer H., Garde F., Brau J.C., Gatina J.C. A multi model approach of thermal building simulation for and research approach // Energy and Building. 1998. Vol. 28. P. 71-78.
12. Boyer H., Chabriat J.P., Grondin Perez B., Tourrand C., Brau J. Thermal building simulation and computer generation of nodal models // Building and Environment. 1996. Vol. 31, No. 3. P. 207–214.
13. Boyer H., Lauret A.P., Adelard L., Mara T.A. Building ventilation: a pressure airflow model computer generation and elements of validation // Energy and Buildings. 1999. Vol. 29. P. 283–292.
14. Gagge A.P., Fobelets A., Berglund L.G. A standard predictive index of human response to the thermal environment // ASHRAE Trans. 1986. Vol. 92 (2B). P. 709-731.
15. Humphreys M.A., Fergus Nicol J. The validity of ISO-PMV for predicting comfort votes in every day thermal environments // Energy and Buildings. 2002. Vol. 34, No. 6. P. 2553-2565.

THE PEGASE PROJECT

A. Ferrière

PROMES
UPR CNRS nr 8521
7, rue du Four Solaire 66120 Font Romeu Odeillo FRANCE
Phone: +33 468 30 77 49; E-mail: Alain.Ferriere@promes.cnrs.fr
http://www.promes.cnrs.fr

The project PEGASE (Production of Electricity with Gas Turbine and Solar Energy) aims at setting up and testing a solar power demonstrator of 1.4 MW based on a thermodynamic gas cycle (at high temperature). As such, this project aims at carrying out R & D work needed to prepare and to develop the future of solar power plants with very high conversion efficiency (30 %) through the implementation of an innovative solar receiver technology feeding a gas turbine with a bottom combined cycle.

Keywords: solar power plants, thermodynamic analysis of basic energy generation processes in alternative energy

Alain Ferrière

Organization: Senior scientist at Centre National de la Recherche Scientifique (CNRS), Processes, Materials and Solar Energy Laboratory (PROMES), Sustainable Energy Carriers group.
Experience: Engineer in electrical engineering, PhD in thermal engineering science.
Main range of scientific interests: heat and mass transfers, solar flux measurements and instrumentation, surface modifications of materials at high temperature, solar energy conversion with solar thermal concentrating technologies.
Publications: 27 publications, 35 communications, 6 invited lectures.

Introduction

Concentrated solar facilities are used to achieve power of several dozen MWe. The solar power plants under construction now, in Spain for example, implement technological solutions but little innovative (reduction of industrial risk). Therefore, a major effort of R & D is required to propose alternatives that increase yields and lower production costs per kW·h.

Description

The proposed thermodynamic cycle is a Brayton cycle. The project requires the restoration of 100 heliostats (5400 m^2). Under a normal direct sunlight of 950 W/m^2, the power supplied to the thermal cycle by the solar receiver is 3620 kW_{th}, which represents a contribution of solar electricity of 61 % for a nominal production of 1.4 MWe (turbine GPB15 Kawasaki).

The objectives of this pilot experiment (Fig. 1) are science and technology. They are:

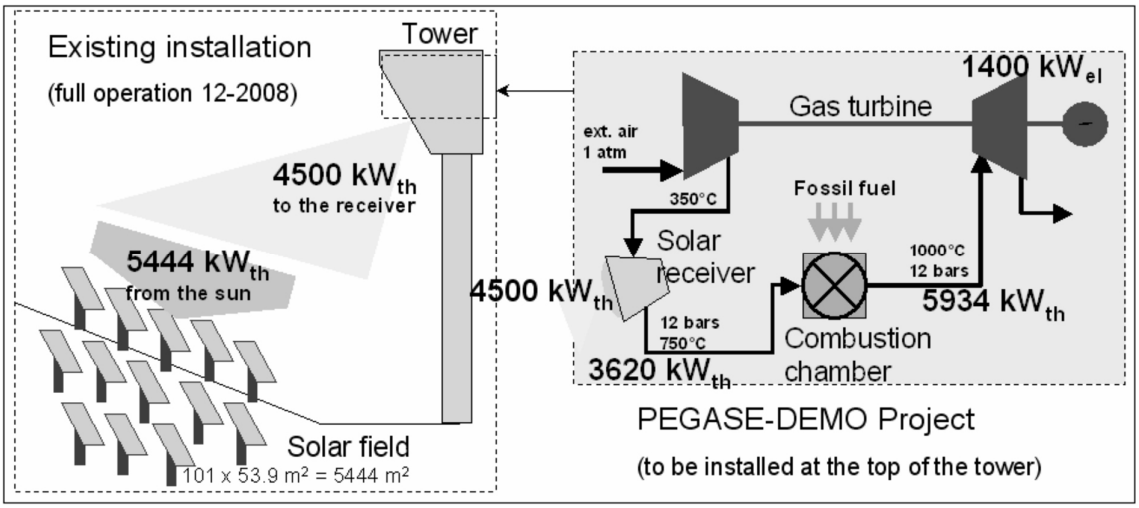

Fig. 1. *Scheme showing the principle of the thermodynamic cycle PEGASE installed at the top of the Themis tower*

• To validate a methodology for scaling up (from 0.23 to 1.4 MWe, namely a factor 6 in comparison with SOLGATE, single similar project (European) of R & D performed in Almeria-Spain between 2001 and 2003). From this point of view, the PEGASE experimentation has clearly a European dimension.
• To achieve the transformation of solar energy into electricity with high solar fractions: 60-80 % in instantaneous value and 50-60 % in average annual value.
• To develop solar receivers (research and technology) that can reach outlet air temperatures of 1000 °C and above. The involved research concern, in particular, the mechanics of turbulent flows (parietal transfers under strong gradients), and high-temperature materials.
• To establish a database allowing the conception and the reliable performance forecast of this technical solution for various conditions of sunlight and various powers.
• To establish collaborations (research organizations and industries) to ensure a future development of the sector.

Necessary scale

The unit power of the commercial power plants planned with hybrid technology solar-fossil gas turbine is typically 10 to 25 MWe with combined cycles. Today, only one experience at 230 kWe (scale 1/50) was carried out within the framework of a European research project (FP6 project Solgate, Almeria, 2001-2003), with a volumetric solar receiver. The PEGASE project aims at achieving an intermediate step at a power of 1.4 MWe, corresponding to the scale 1/10. This is a necessary step, particularly for a reliable receiver solar technology industrial design (outer wall receiver). The coupling with a combustion turbine will also be validated on a large scale. Based on the results observed on this demonstrator PEGASE, extrapolation to a commercial power plant with better economic performance will be possible without major technological barrier.

Technological barriers over passed by the technology demonstrator

1. Development of a pressurized gas solar receiver at very high temperature. Works on two levels are necessary:
− Basic research on materials and on heat transfers between flow and wall at very high temperature.
− Development of receiver prototypes on the basis of based on the most advanced technologies of compact exchangers and evaluation of their performance on PROMES solar installations in Odeillo (solar furnaces). It should be noted that the modeling of turbulent flows in the vicinity of walls with high temperature gradients is a new field of knowledge.
2. Combustion of fossil fuels or biogas at high pressure and high temperature. The hybrid nature of the concept imposes to adjust the combustion chamber of the gas turbine to varying conditions of the receiver output power. Special attention will be paid to the regulation of the regime of the turbine.
3. Integration of components and system analysis. A solar power plant is a complex set of subsystems whose operation is characterized by variable regimes and frequent transient during startup and shutdown. The performance analysis of the PEGASE cycle and the prediction of production of the chain as a function of the climate require the development of adapted software tools. Similarly the command and control system must meet the requirements of sometimes contradictory optimal production and guaranteed security of components.

The timing of the project

The project will last 5 years: 2009-2013.
The renovation of the field of heliostats Themis for PEGASE, started in 2007 (Fig.2), will be completed by the end of 2008. This initial phase is already funded (1050 k€), in the frame of a public-private partnership including CNRS, ADEME, the Languedoc-Roussillon Region, the Department of Pyrenees-Orientales, the groups Total and EDF.

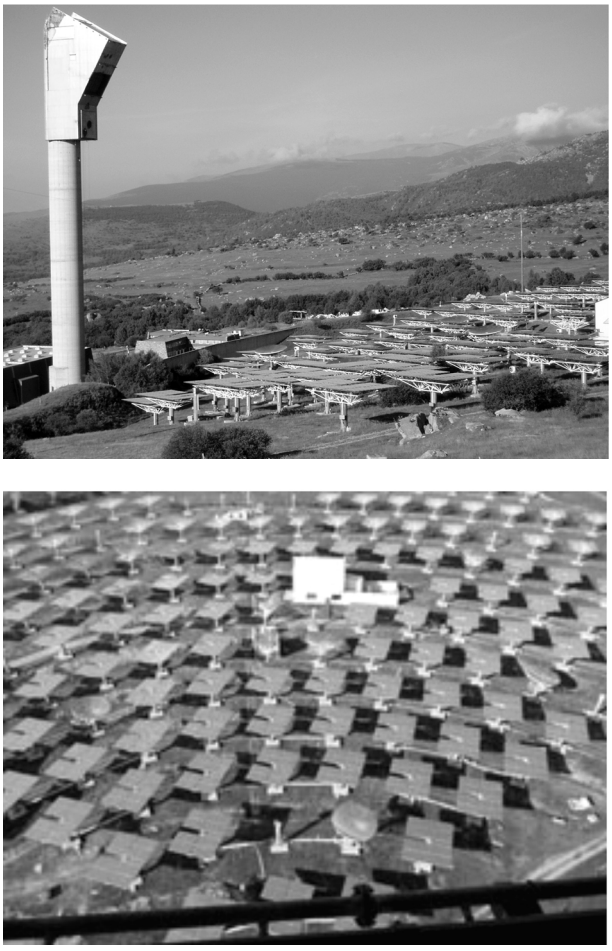

Fig. 2. *Pictures of the tower and of heliostats*

The demonstrator will be installed during the period 2009-2010. The installation covers the purchase of equipment and engineering work needed for installation.
The experiment is scheduled for 4 years (2010-2013). The program will focus on:

– The heliostat field: optical efficiency, concentration, availability.

– The solar receiver: air and walls temperatures, thermal efficiency, material behaviour.

– Turbine: performance, management mode of solar and fuel input power, and transients.

The complete cycle: overall performance of solar energy/electricity conversion (instantaneous and average efficiency), solar fraction, transient behavior, performance evaluation of more powerful commercial power plants (10 MWe).

NUMERICAL STUDY OF THE EFFECT OF THE INSULATION OF THE WALLS ON NATURAL CONVECTION IN A DIFFERENTIALLY HEATED CAVITY

A. Raji, M. Hasnaoui**, S. Goujon-Durand***, P. Vasseur*****

*Faculty of Sciences and Technologies, Department of Physics, University Sultan Moulay Sliman, Team of Flows and Transfers Modeling (EMET), Laboratory of Physics and Mechanics of Materials, BP 523, Béni-Mellal, Morocco
Tel.: 00212 23 48 51 12; fax: 00212 23 48 52 01, E-mail: abderaji@fstbm.ac.ma; abderaji@yahoo.fr

**Faculty of Sciences Semlalia, Department of Physics, University Cadi Ayyad, UFR TMF, BP 2390 Marrakesh, Morocco
Tel.: 00212 44 43 46 49; fax: 00212 44 43 74 10, E-mail: hasnaoui@ucam.ac.ma

***Université Paris XII, France

****Ecole Polytechnique de Montréal, Canada

Received: 27 Sept 2007; accepted: 31 Oct 2007

In this work, we study numerically the natural convection in a square cavity using the Navier-Stokes equations with the Boussinesq approximation. A finite difference method based on the control volume notion is used to resolve, in nondimensional forms, the natural convection equations. The results are obtained for various combinations of the parameters of base, such as the Rayleigh number ($10^3 \le Ra \le 5 \cdot 10^6$), the relative thermal conductivity ($0.1 \le K \le \le 100$), the relative width of the walls ($0 \le e \le 0.2$) and the relative spacing ($0.05 \le e_{spa} \le 0.3$). The numerical simulations of natural convection in a cavity having walls of finite width have shown the possibility to reduce significantly the heat transfer by using appropriate isolation techniques.

Keywords: natural convection, numerical study, effect of the insulation

Abdelghani Raji

Organization: Teacher at the Faculty of Sciences and Technics in Beni Mellal (Morocco).
Education: Doctorates in heat transfer (1994 and 2000) after attending Cadi Ayyad University. The title of the first doctorate was: "Etude numérique des écoulements et des transferts de chaleur par convection dans des cavités en interaction et dans un canal de longueur finie". The title of the second thesis was: "Etude numérique du phénomène de la convection mixte dans des cavités ventilées avec et sans effet de rayonnement".
Experience: Head of the physics department from 2000 to 2003.
Main range of scientific interests: heat transfer by conduction, convection, radiation, porous media…
Publications: from 2004:
− Coupling between mixed convection and radiation in an inclined channel locally heated. *Journal of Mechanical Engineering, 2004.*
− Interaction between natural convection and radiation in a square cavity heated from below. *Numerical Heat Transfer, Part – A: Applications, 2004*.
− Multiple steady state solutions resulting from coupling between mixed convection and radiation in an inclined. *Heat and Mass Transfer, August 2005.*
− Combined effect of radiation and natural convection in a rectangular enclosure discreetly heated from one side. *International Journal of Numerical Methods for Heat & Fluid Flow, 2006.*
− Multiplicité de solutions en convection naturelle couplée au rayonnement dans une cavité horizontale. *Physical & Chemical News, 2006.*
− Mixed convection in a horizontal channel with emissive walls and partially heated from below. *Numerical Heat Transfer, Part – A: Applications, 2007.*
− Multiple steady state solutions for natural convection in a tilted rectangular slot containing non-Newtonian power-law fluids and subject to a transverse thermal gradient. *Numerical Heat Transfer, Part – A: Applications, 2007.*
− Parallel flow convection in a shallow horizontal cavity filled with non-newtonian power-law fluids and subject to horizontal and vertical uniform heat fluxes. In Press in *Numerical Heat Transfer, Part – A: Applications, 2007.*
− Coupled natural convection and radiation in a horizontal rectangular enclosure discretely heated from below. *Accepted in Numerical Heat Transfer, Part – A: Applications, 2007*.

Nomenclature

A – aspect ration of the cavity, $H′/L′$
e – relative width of the wall, $l′/L′$
e_{ins} – relative width of the insulating layer, $l′_{ins}/L′$
e_{spa} – spacing between the walls, $l′_{spa}/L′$
g – acceleration due to gravity, m/s^2
h – mean convection heat transfer
K – relative conductivity, λ/λ_f
$l′$ – dimensional width of the wall, m
$l′_{ins}$ – dimensional width of the insulating layer, m
$l′_{spa}$ – dimensional spacing between the walls, m
P – dimensionless pressure, $(P′ + \rho_0 g y′)/\rho_0(\alpha/L′)^2$
Pr – Prandtl number, ν/α
Ra – Rayleigh number, $g\beta\Delta T′L′^3/(\nu\alpha)$
r_w – relative conductivity of the wall, λ_w/λ_f
r_{ins} – relative conductivity of the insulator, λ_{ins}/λ_f
$\Delta T'$ – temperature difference, $(T′_H - T′_C)$
(u, v) – dimensionless horizontal and vertical velocities, $(u′, v′)/(a/L′)$
(x, y) – dimensionless Cartesian coordinates, $(x′, y′/L')$

Greek letters

α – thermal diffusivity (m^2·s^{-1})
β – thermal expansion coefficient of the fluid (K^{-1})
Γ – diffusion coefficient
λ – thermal conductivity (W·m^{-1}·K^{-1})
ν – kinematic viscosity of fluid (m^2·s^{-1})
ψ – dimensional stream function (m^2·s^{-1})
Ψ – dimensionless stream function, ψ/α
θ – dimensionless temperature, $\theta = (T′ - T′_C)/(T′_H - T′_C)$
ρ_0 – fluid density at the temperature T_0 (kg·m^{-3})

Subscripts and Superscripts

board – boarding
C – cooled
cond – conduction
f – fluid
H – heated
ins – insulator
max – maximum
r – relative
s – solid
spa – spacing
w – wall
′ – dimensional variables

Introduction

During the last decades, natural convection in closed cavities has received great efforts of research. This special attention was dictated by the importance of this phenomenon in the design of the physical models related to the field of solar engineering, the cooling of the printed circuit boards and the design of buildings. Hence in several practical applications, the use of materials with high thermal conductivity will lead to an undesirable increase of the temperature of the fluid inside the cavity. The maintenance of a desirable temperature can be achieved if an adequate insulation of the walls of the cavity is taken into account. Heat exchange between the walls of the cavity and the fluid can be controlled by recourse to thermally insulating materials. A problem of base well documented in the literature specialized in heat transfer is that of a rectangular enclosure without partition. An exhaustive review on this subject is presented in references [1-4]. Compared to the studies relating to rectangular cavities, those concerning partially or completely partitioned cavities are relatively less documented. It is obvious that the addition of one or more partitions has a considerable effect on the heat transfer and the fluid flow structure inside the cavity. Thereafter, the subject needs to be further explored and other works are necessary to improve our knowledge in this field by taking account of the influence of partitions; especially if it is known that their dimensions, their conductivities, their number and the way in which they are placed are among the parameters which control the importance of this influence in various technological aspects [5-10].

The main goal of this study consists in numerically simulating the two-dimensional natural convection in a differentially heated cavity whose vertical walls have a finite conductivity and a thickness. The effect of the insertion of an insulating material on the internal surfaces of the walls will be also investigated in parallel with the technique of the thermal boarding (use of a double wall separated by an insulator). The effects of these various techniques of insulation on the heat transfer and the fluid flow will be studied for various values of the Rayleigh number, *Ra*, the relative thermal conductivities r_w and r_{ins} and for various combinations of the geometrical parameters.

Problem formulation

The configurations under study with the system of coordinates are sketched in Fig. 1. They consist of a differentially heated cavity whose vertical walls have a finite thickness without insulation (Fig. 1, *a*), with an internal insulation (Fig. 1, *b*) and with an insulation using the thermal boarding technique (Fig. 1, *c*). For these three types of configurations, the horizontal walls are adiabatic. The fluid flow is assumed to be laminar

and two-dimensional and the Boussinesq approximation is adopted for the variations of the density in the buoyancy term.

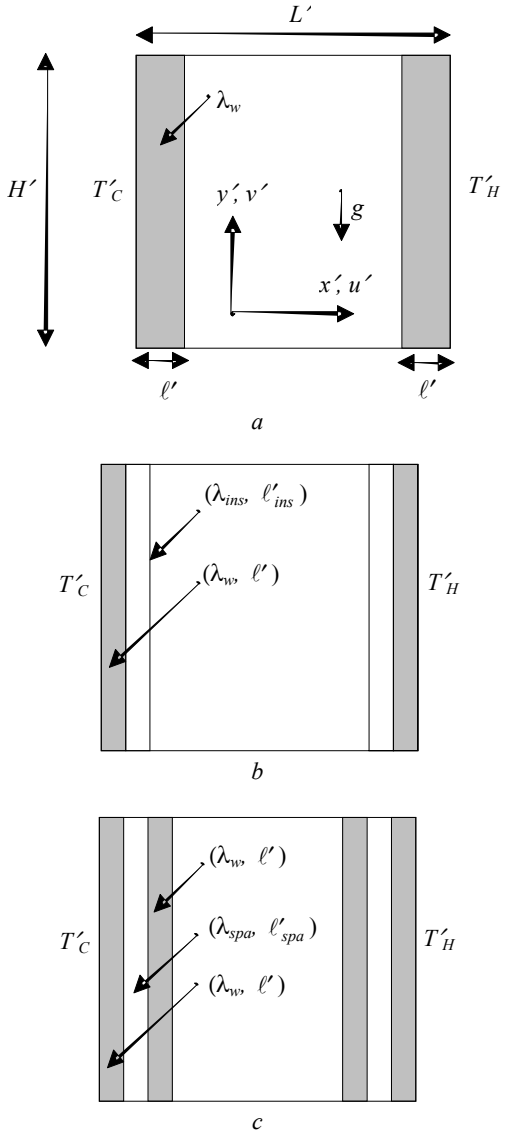

Fig. 1. *Studied configurations*

The equations governing the dynamic and thermal fields are those of Navier-Stokes coupled with the equation of energy transport. In stationary and non-dimensional form, they are written as:

$$u\frac{\partial u}{\partial x}+v\frac{\partial u}{\partial y}=-\frac{\partial P}{\partial x}+\Gamma\left(\frac{\partial^2 u}{\partial x^2}+\frac{\partial^2 u}{\partial y^2}\right), \quad (1)$$

$$u\frac{\partial v}{\partial x}+v\frac{\partial v}{\partial y}=-\frac{\partial P}{\partial y}+\Gamma\left(\frac{\partial^2 v}{\partial x^2}+\frac{\partial^2 v}{\partial y^2}\right)+RaPr\theta, \quad (2)$$

$$u\frac{\partial \theta}{\partial x}+v\frac{\partial \theta}{\partial y}=K\left(\frac{\partial^2 \theta}{\partial x^2}+\frac{\partial^2 \theta}{\partial y^2}\right). \quad (3)$$

The parameters Γ and K are respectively the diffusion coefficient and the relative thermal conductivity. A value of unity is allotted to Γ in the fluid area while an "infinite" value (1015) is affected for it in the solid area. The relative thermal conductivity K is equal to unity in the fluid medium and its value is k_r for the solid walls. The parameters Γ and K are easily implanted in the numerical code and their use satisfies automatically the boundary conditions at the solid-fluid interfaces.

The thermal and dynamic boundary conditions associated to this problem are:

$$\begin{aligned} &\theta = 0 && \text{for } x = 0;\\ &\theta = 1 && \text{for } x = 1;\\ &\frac{\partial \theta}{\partial y} = 0 && \text{for } y = 0 \text{ and } y = 1;\\ &u = v = \Psi = 0 && \text{on the solid walls.} \end{aligned} \quad (4)$$

The average heat quantity transferred through the active walls of the cavity is defined by mean of the following expression:

$$Q=\int_0^1 \frac{\partial \theta}{\partial x}dy \quad (5)$$

$$Nu=\frac{Q}{Q_{cond}}, \quad (6)$$

where Q_{cond} is the heat flux by conduction evaluated by equation (5) for $Ra = 0$.

Numerics

The discretization of the governing equations, written in primitive variables, is carried out by using a finite difference method and the numerical integration is based on the control-volume approach with the SIMPLER algorithm and the hybrid scheme for interpolation [11]. The technique of the finite volume method is based on the principle of conservation of the various physical quantities (mass, momentum and energy). In order to prevent that physical incompatibilities of the pressure do not generate a convergence of the total solution towards a nonphysical solution, a uniform shifted grid was used for the velocity. The numerical code was validated by comparing the results obtained in the case of a differentially heated cavity with those of the Bench-Mark solution of De Vahl Davis [3]. As it can be seen in Table 1, the agreement observed is excellent and the maximum relative deviation remains less than 1.67 and 1.34 % respectively in terms of Ψ_{max} and Q. The numerical code was also validated by comparing our results with those of the references [12-14] in the case of a cavity containing an obstacle placed at its centre. The comparative results, presented in Table 2, show an excellent agreement with a maximum deviation less than 1 %. Also for all the computations, it was carefully verified that the heat provided by the heated wall to the fluid is equal to that leaving the cavity through the cold wall with 0.2 % as a maximum difference. It is interesting to announce also that in the pure conduction

mode, the heat flux through a cavity containing various solid layers, having each one a thermal conductivity, coincides perfectly with that calculated analytically by using the concept of thermal resistance. The agreement is excellent and the maximum deviation remains lower than 0.5 %. The sensitivity of the results with respect to grid size is summarized in Table 3 in terms of Ψ_{max} and *Nu*. It can be retained that a uniform grid of 80×80 can describe correctly the heat transfer and fluid flow. In fact, a refinement of the mesh to 120×120 involves relatively weak maximum deviations but induces consequently higher computing times. The parameter of relaxation varies between 0.4 for low values of *Ra* and 0.1 for high values of this parameter. Finally, the convergence criterion, based on the correction of the pressure, is checked when the corrected terms are sufficiently weak and the existing difference between the fields of pressure before and after each correction is nonsignificant.

Table 1
Validation of the numerical code in terms of the maximum stream function and the average heat quantity

	Present study		**Bench Mark [3]**	
Ra	Ψ_{max}	*Q*	Ψ_{max}	*Q*
10^3	1.176	1.102	1.174	1.117
10^4	5.078	2.221	5.071	2.238
10^5	9.642	4.496	9.612	4.509
10^6	17.031	8.880	16.750	8.817

Table 2
Comparative results of the average heat quantity for a square enclosure containing a conducting square solid body at the centre

Ra	k_r	**Present study**	**House et al. [12]**	**Merrikh and Lage [13]**	**Lee and Ha [14]**
10^5	0.2	4.623	4.624	4.605	4.631
10^5	5	4.317	4.324	4.280	4.324

Table 3
Variations of the maximum stream function, Ψ_{max}, and the average heat quantity, *Q*, according to the grid size for $Ra = 10^6$

Mesh	Ψ_{max}	***Q***	**CPU(s)**
40×40	17.55	9.14	191
80×80	17.03	8.86	1031
120×120	16.92	8.82	6346

Results and discussion

1st configuration: walls without insulation

Typical results of the streamlines and the isotherms illustrating the effect of the relative conductivity of the walls are presented in Fig. 2 for $Ra = 10^6$, $e = 0.05$ and r_w ranging between 0.1 and 50. For walls with a low thermal conductivity ($r_w = 0.1$), Fig. 2, *a* shows that the fluid circulation is relatively weak. The corresponding isotherms indicate that the horizontal heat gradients in the solid walls are important indicating a great resistance to the heat flux between the extreme faces of each wall.

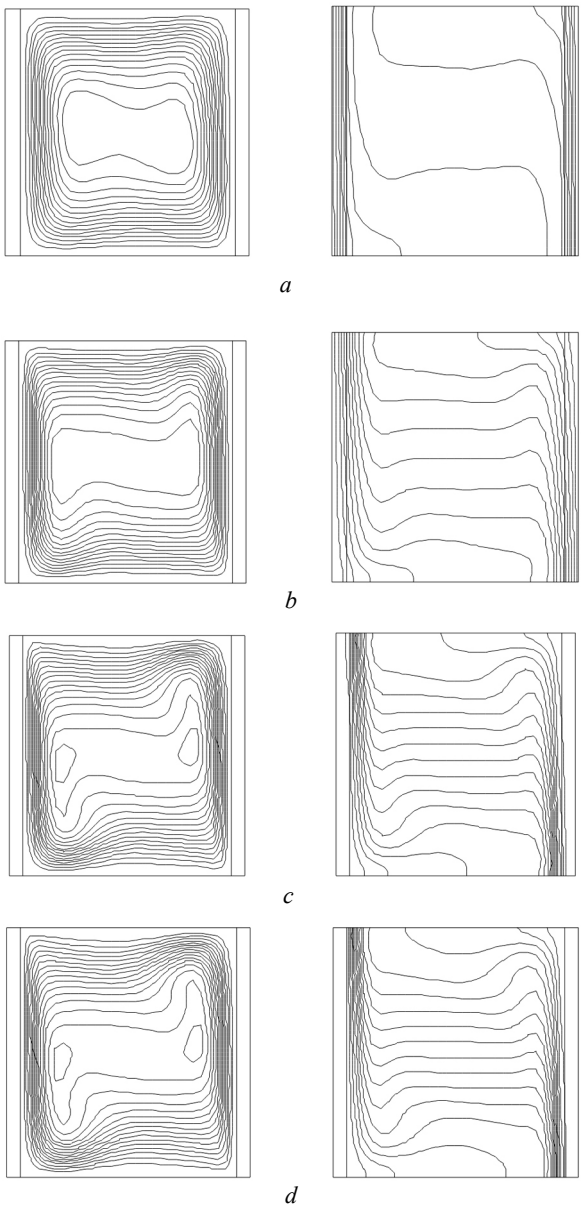

Fig. 2. *Streamlines and isotherms for $Ra = 10^6$, $e = 0.05$ and different values of r_w:*
a) $r_w = 0.1$ ($\Psi_{max} = 6.62$, $Nu = 1.46$),
b) $r_w = 1$ ($\Psi_{max} = 11.42$, $Nu = 3.92$),
c) $r_w = 10$ ($\Psi_{max} = 16.01$, $Nu = 7.13$)
d) $r_w = 50$ ($\Psi_{max} = 16.85$, $Nu = 7.76$)

This will lead to a limited interaction with the fluid inside the cavity. For r_w = 1, Fig. 2, *b* shows an improvement of the fluid circulation characterized by higher values of Ψ_{max} and a spacing of the isotherms at the level of the walls as a consequence of the reduction in their thermal resistance. By increasing r_w to 10, Fig. 2, *c* shows that the fluid circulation continues to be intensified. The corresponding isotherms show an uniformisation of the temperatures of the two walls and a better interaction of the latters with the fluid. For high values of relative conductivity (r_w = 50), Fig. 2, *d* shows that the flow and temperature fields are qualitatively similar and quantitatively comparable to those described in the preceding figure corresponding to r_w = 10.

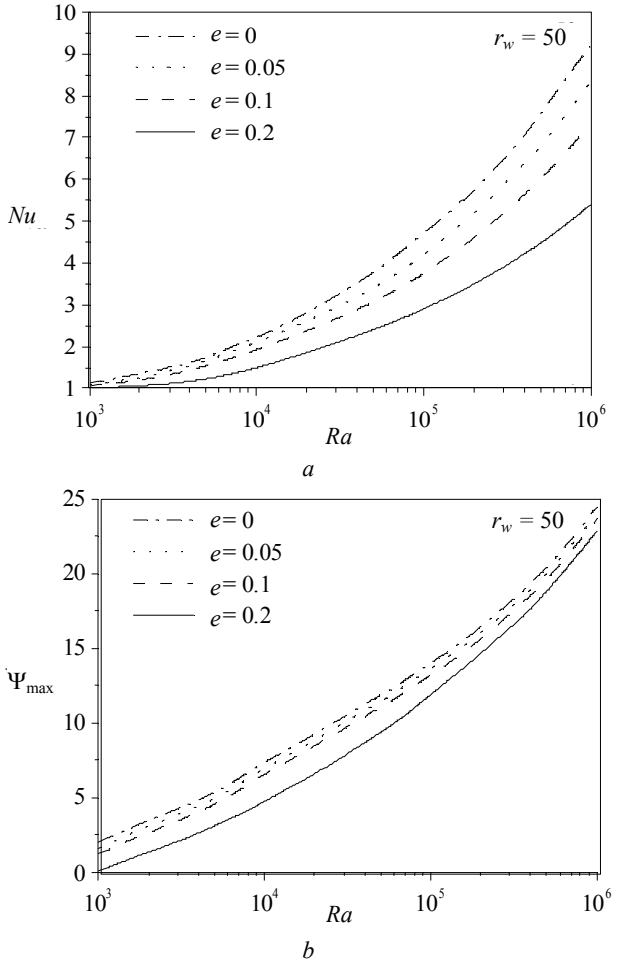

Fig. 3. *Variations of Nu and Ψ_{max} with Ra for e = 0.05, r_w = 50 and different values of the relative width of the walls*

The thickness of the walls was varied in the range $0 \le e \le 0.2$ in order to analyze its effect on the fluid flow and heat transfer. The results obtained are presented in Fig. 3 in terms of variations of *Nu* and Ψ_{max} with *Ra* for r_w = 50 and various values of *e*. The results of base obtained for *e* = 0 (absence of conduction in the walls) are also presented for a comparison purpose. For values of *Ra* ≤ 1500, the heat transfer is done mainly by conduction and is slightly affected by the thickness of the walls. For higher values of *Ra*, the effect of the thickness becomes visible and the Nusselt number decreases when this last parameter increases. For *Ra* = 106 and *e* = 0.2, the reduction of *Nu* reaches approximately 48 % when compared to the reference case (*e* = 0). This tendency is a consequence of the increase in the conductive thermal resistance of the walls with the thickness.

The effect of the Rayleigh number on the Nusselt number and the maximum stream function is presented in Fig. 4 for *e* = 0.05 and various values of relative conductivity r_w of the walls. For the lower considered value of r_w (r_w = 0.1), the Nusselt numbers remain generally close to unity, showing thus the resistant effect of the walls to the heat transfer and this even for high values of the Rayleigh number. For a given value of *Ra*, we can note an increase in the heat quantity restored to the fluid by the active surfaces. This increase of *Nu* with r_w cease as soon as this last parameter becomes higher than 50 as it can be seen in Fig. 5 where the Nusselt number and the maximum stream function tend asymptotically to limiting values. For *Ra* = 10^6, it is interesting to note that the use of walls with a conductivity such r_w = 10 would lead to a reduction of 9.8 % of *Nu* when compared to walls of relative conductivity r_w = 50. This reduction reaches 16.6 % when the conductivity of the walls is r_w = 5.

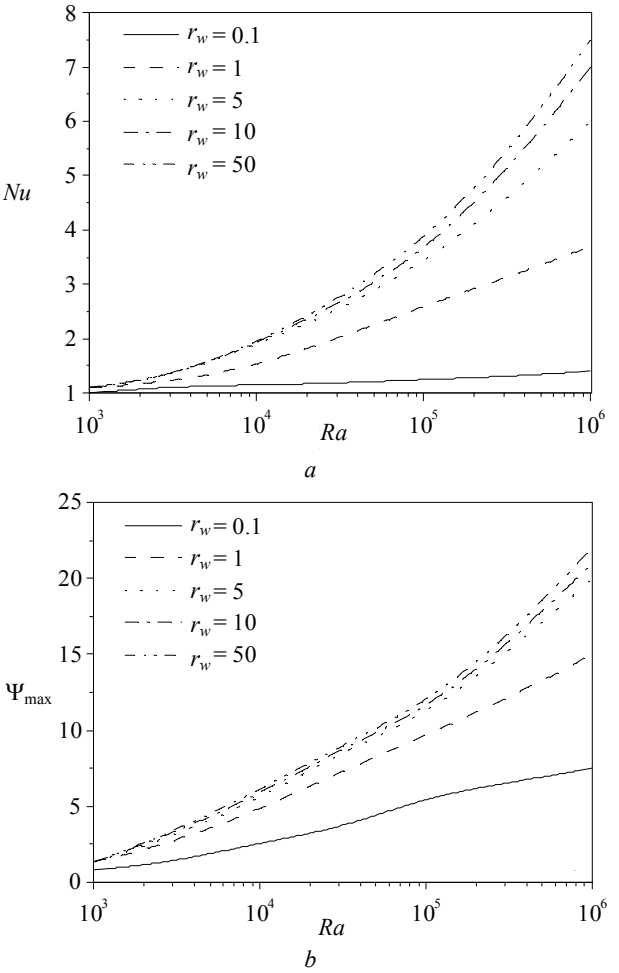

Fig. 4. *Variations of Nu and Ψ_{max} with Ra for e = 0.05 and different values of the relative conductivity r_w of the walls*

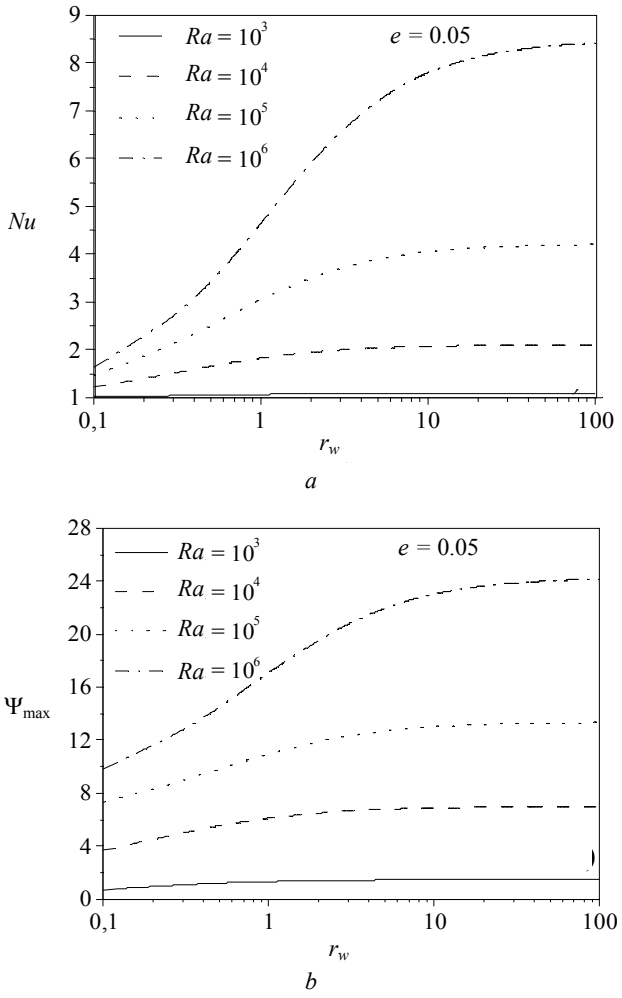

Fig. 5. *Effect of the relative thermal conductivity r_w of the walls on Nu and Ψ_{max} for e = 0.05 and different values of the Rayleigh number*

2nd configuration: walls with insulation

In this section, we will examine the effect of the increase of the thermal resistance of the walls by adding an insulating layer on the interior surfaces. The conductivity of this layer will be varied in order to obtain a rate of heat transfer comparable or lower than that obtained by using materials of relative conductivities of r_w = 5 or 10. The thicknesses of the insulating layer and that of the wall are fixed respectively at e_{ins} = 0.0125 and e = 0.0375, in such a way that the total thickness remains equal to that of the already studied configuration ($e_{ins} + e = 0.05$).

The effect of the addition of an insulating layer on internal surfaces of the walls will be examined for a relative conductivity of the walls fixed at r_w = 50 and a thickness e = 0.0375. Hence, variations of *Nu* and Ψ_{max} with *Ra* are shown in Fig. 6 for e_{ins} = 0.0125 and various values of the relative conductivity of the insulator. It can be seen that for the low values of *Ra*, the Nusselt number is practically independent of the relative conductivity of the insulator. It is a foreseeable result since these values of *Ra* correspond to a mode for which conduction contributes largely to the heat transfer. The increase of *Ra* supports the fluid circulation within the cavity and generates consequently an increase of *Nu*. Also, for a given value of *Ra*, the Nusselt number decreases when relative conductivity of the insulator decreases. A comparison with the results of the already studied configuration shows an appreciable reduction of the rate of heat transfer. The percentages of this reduction compared to walls of different relative conductivities are presented in Table 4 for $Ra = 10^6$ and for various values of the relative conductivity of the insulator.

Table 4

Percentage of reduction of *Nu* due to the addition of an insulation for $Ra = 10^6$ and various values of the conductivity of the insulator

$\frac{Nu - Nu_{ins}}{Nu} \times 100$	r_{ins}				
	0.1	**0.2**	**0.5**	**1.0**	**5.0**
$r_w = 50$	68.3	56.6	38.4	26.2	11.2
$r_w = 10$	64.8	52.0	31.6	18.1	1.6
$r_w = 5$	62.0	48.1	26.1	11.4	---

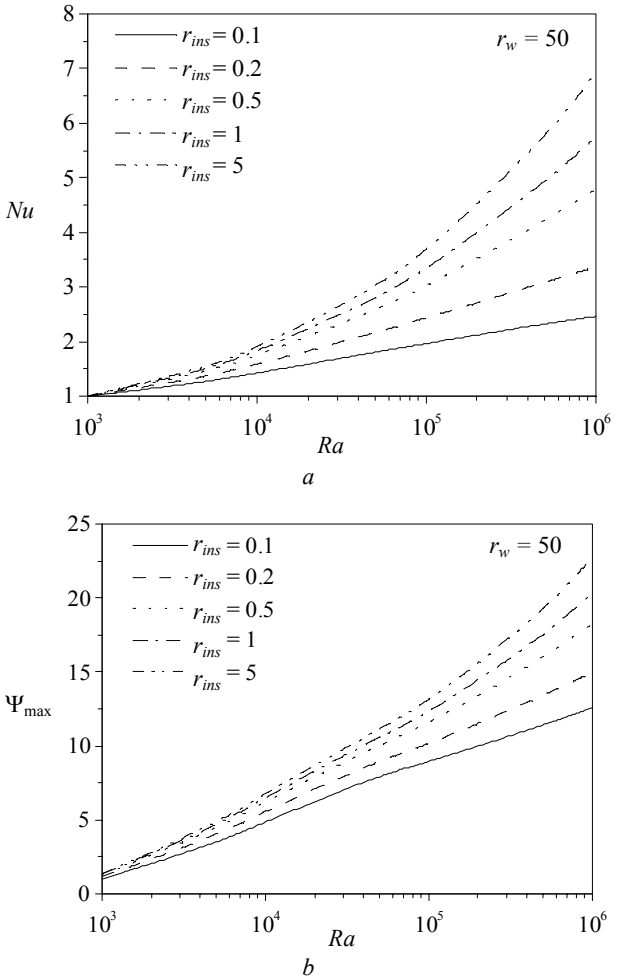

Fig. 6. *Effect of Ra on Nu and Ψ_{max} for rw = 50 and various values of the relative thermal conductivity r_{ins} of the insulating layer*

3rd configuration: case of thermal boarding

Another technique of insulation consists in using two walls separated by a fluid or solid layer playing the role of an insulator. The thickness of the space between the two walls is taken equal to that of the insulator (e_{spa} = = 0.0125). The results obtained by using this technique of insulation are found identical to those of the second configuration. For the same values of r_{ins}, the maximum deviation compared to this situation remains lower than 0.45 %. Hence, the air was considered as insulator and its thickness was varied to study its impact on the heat transfer.

The effect of the spacing between the walls is examined in this section by producing streamlines and isotherms for $Ra = 5 \cdot 10^6$, $r_w = 50$ and different values of e_{spa}. The walls have each one a thickness equal to $e = 0.025$ so that the total thickness is equal to that of the wall of Fig. 1, *a*. For an air layer of thickness $e_{spa} = 0.05$, Fig. 7, *a* shows a structure close to that obtained for a differentially heated cavity. The corresponding isotherms show a clear stratification in the central part of the cavity. An increase of e_{spa} to 0.1 supports the formation of convective cells of low intensities in the insulating layers (Fig. 7, *b*). The examination of the isotherms between the walls shows that conduction is the heat transfer dominating mode in these areas. From Fig. 7, *c*, it can be seen that an increase of e_{spa} to 0.15 is accompanied by an improvement of the fluid circulation in the insulating fluid layers and of a reduction of the general circulation of the fluid within the cavity which will lead to a reduction of the Nusselt number. The numerical tests carried out showed that $e_{spa} = 0.15$ is the optimum value which tolerates a weaker thermal interaction between the active walls of the enclosure for the considered value of *Ra*. A spacing beyond this critical value supports the role of natural convection in the insulating layers and generates a better interaction between the active walls of the cavity and the fluid. This results in a noticeable improvement of the general circulation of the fluid and an increase of *Nu*. The Fig. 7, *d* corresponding to $e_{spa} = 0.2$, shows a distortion of the isotherms between the walls resulting from the intensification of the flow in the insulating layers and a stratification of the temperature better than that observed in the case of Fig. 7, *c*.

The effect *Ra* on the Nusselt number and the maximum stream function is presented in Fig. 8 for $r_w = 50$ and various values of e_{spa}. It can be seen that, for a fixed value of *Ra*, the Nusselt number decreases with the increase of the thickness of separation. Compared to the case of a wall without insulation, the technique of the boarding appears effective to reduce the rate of heat transfer through the cavity. This technique leads to performances better than those of materials having conductivities of r_w = 5 and 10. Quantitatively, the percentage of this reduction is presented in Table 5.

Table 5

Percentage of reduction of *Nu* in comparison with a cavity without insulation for $r_w = 50$, $Ra = 10^6$ and different values of the spacing

$\frac{Nu - Nu_{board}}{Nu} \times 100$	e_{spa}			
	0.05	**0.1**	**0.2**	**0.3**
$r_w = 50$	39.88	62.03	74.22	70.36

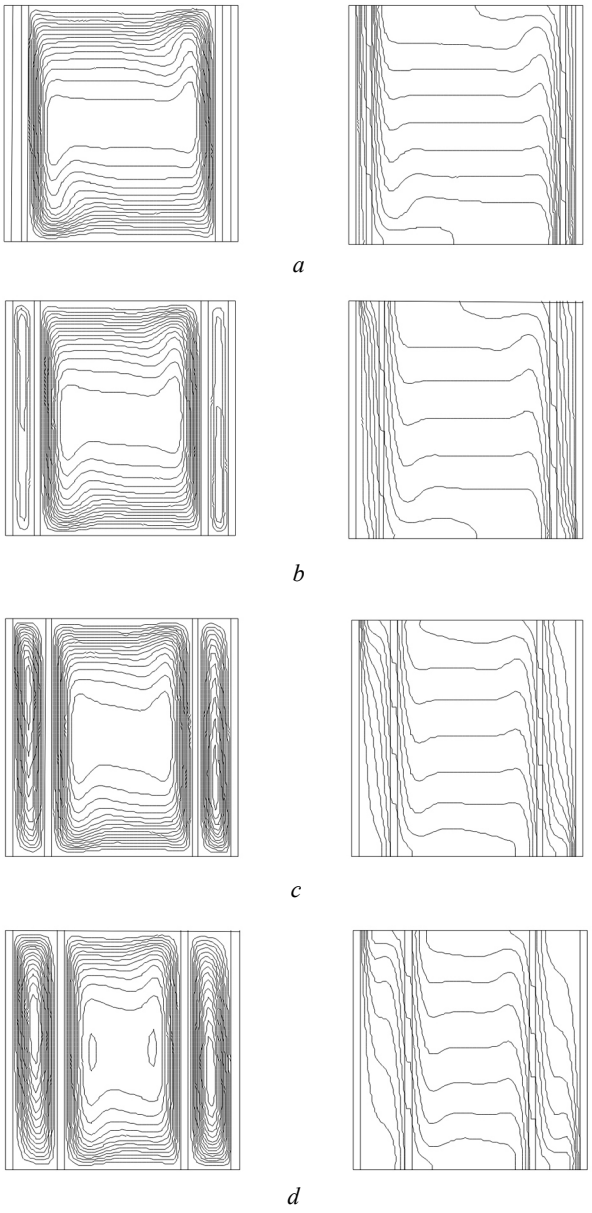

Fig. 7. Streamlines and isotherms for $Ra = 5 \cdot 10^6$, $r_w = 50$, $e = 0.025$ and different values of the spacing between the walls: a) $e_{spa} = 0.05$ ($\Psi_{max} = 18.78$, $Nu = 6.82$), b) $e_{spa} = 0.1$ ($\Psi_{max} = 14.96$, $Nu = 4.17$), c) $e_{spa} = 0.15$ ($\Psi_{max} = 12.82$, $Nu = 3.90$) d) $e_{spa} = 0.2$ ($\Psi_{max} = 15.28$, $Nu = 4.13$)

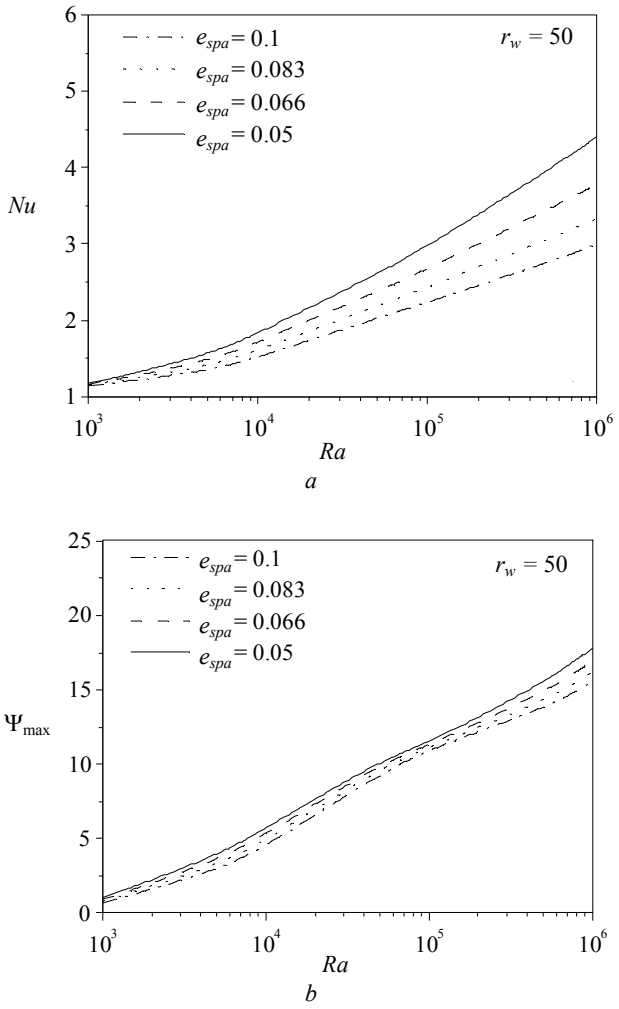

Fig. 8. Effect of the Rayleigh number on Nu and Ψ_{max} for r_w = = 50 and various values of the relative spacing between the walls

From Table 5, it can be seen that the percentage of reduction of the heat transfer increases with e_{spa} as long as this parameter is lower or equal to 0.2. Beyond this value a decrease is observed for e_{spa} = 0.3. This testifies of the existence of a critical value of the spacing between the walls which would engender the maximum reduction of the heat transfer. In Fig. 9, the variations of the Nusselt number, with e_{spa}, are presented for r_w = 50, e = 0.025 and different values of *Ra*. The examination of this curve confirms well that a spacing of about 0.2 induces a minimum heat transfer for $Ra = 10^6$. Beyond this critical value, any increase of e_{spa} would lead to an increase in the intensity of the flows in the space between the walls and consequently to an increase in the resulting heat transfer. For $Ra = 5 \cdot 10^6$, it can be seen that the value of the critical spacing inducing a minimum heat transfer is of about 0.15. This critical value, lower than that corresponding to $Ra = 10^6$, is due to the early development of the effect of the natural convection in the fluid layers intended to play an insulating role. It appears thus obvious that the technique of the thermal boarding is effective to ensure a good insulation. But, it is important to underline that the performances of this technique are achieved to the detriment of the space allowed to the fluid inside the cavity.

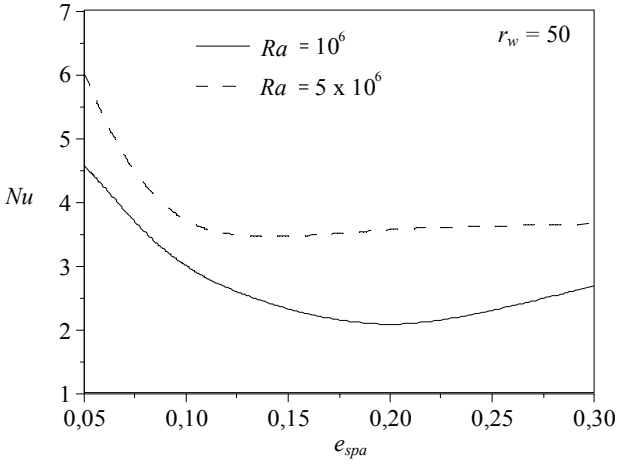

Fig. 9. *Variations of the Nusselt number with the spacing between the walls for various Ra*

Conclusion

In this work, a numerical study was carried of on the natural convection in a square cavity with conducting vertical walls by using two techniques of heat insulation. The obtained results show that the thermal performances of walls with high relative conductivities can be improved considerably by using an insulating layer. The technique of the thermal boarding was found interesting to reduce in an appreciable way the heat transfer in comparison to the cases of the walls with or without insulation. In this technique, the existence of a range of the spacing between the walls which generates weak interactions with fluid medium was observed.

References

1. Bejan A. Convective heat transfer. John Wiley & Sons, 1984.
2. Yang K.T. Natural convection in enclosures. In Hand Book of Single Phase Convective Heat Transfer. New York, 1987.
3. De Vahl Davis G. Natural convection of air in a square cavity: a bench-mark numerical solution // Int. J. for Numerical Methods in Fluids. 1983. Vol. 3. P. 249-264.
4. Rasoul I., Prinos P. Natural convection in an inclined enclosure // Int. J. for Numerical Methods for Heat & Fluid Flow. 1997. Vol. 7, No. 5. P. 438-478.
5. Acharya S. and Jetli R. Heat transfer due to buoyancy in a partially divided square box // Int. J. Heat Mass Transfer. 1990. Vol. 33, No. 5. P. 931-942.
6. Kelkar K.M., Patankar S.V. Numerical prediction of natural convection in square partitioned enclosures // Num. Heat Transfer. 1990. Part A. Vol. 17. P. 269-285.

7. Ntibarufata E., Hasnaoui M., Bilgen E., Vasseur P. Natural convection in partitioned enclosures with localized heating // Int. J. for Numerical Methods for Heat & Fluid Flow. 1993. Vol. 3. P. 133-143.
8. Vasseur P., Hasnaoui M., Bilgen E. Analytical and Numerical study of natural convection heat transfer in inclined composite enclosures // Applied Scientific Research. 1994. Vol. 52. P. 187-207.
9. Mamou M., Hasnaoui M., Bilgen E., Vasseur P. Natural convection heat transfer in inclined enclosures with multiple conducting solid partitions // Num. Heat Transfer. Part A. 1994. Vol. 25. P. 295-315.
10. Raji A., Hasnaoui M., Zrikem Z. Natural convection in interacting cavities heated from below // Int. J. for Numerical Methods for Heat & Fluid Flow. 1997. Vol. 7, No. 6. P. 580-597.
11. Patankar S.V. Numerical heat transfer and fluid flow. New York: Hemisphere, 1980.
12. House J.M., Beckermann C., Smith T.F. Effect of a centered conducting body on natural convection heat transfer in an enclosure // Numer. Heat Transfer. Part A. 1990. Vol. 18. P. 213–225.
13. Merrikh A.A., Lage J.L. Natural convection in an enclosure with disconnected and conducting solid blocks // Int. J. Heat Mass Transfer. 20005. Vol. 48, No. 7. P. 1361–1372.
14. Lee J.R., Ha M.Y. Numerical simulation of natural convection in a horizontal enclosure with a heat-generating conducting body // Int. J. Heat Mass Transfer. 2006. Vol. 49. P. 2684–2702.

NUMERICAL STUDY OF MIXED CONVECTION COUPLED WITH RADIATION IN A VENTED PARTITIONED ENCLOSURE

A. Bahlaoui*, A. Raji*, M. Hasnaoui**, R. El Ayachi*, M. Naïmi*, T. Makayssi*, M. Lamsaadi*

*Faculty of Sciences and Technologies, Department of Physics, University Sultan Moulay Sliman, Team of Flows and Transfers Modeling (EMET), Laboratory of Physics and Mechanics of Materials, BP 523, Béni-Mellal, Morocco
Tel.: 00212 23 48 51 12; Fax: 00212 23 48 52 01, E-mail: abderaji@fstbm.ac.ma; abderaji@yahoo.fr

**Faculty of Sciences Semlalia, Department of Physics, University Cadi Ayyad, UFR TMF, BP 2390 Marrakesh, Morocco
Tel.: 00212 44 43 46 49; Fax: 00212 44 43 74 10, E-mail: hasnaoui@ucam.ac.ma

Received: 27 Sept 2007; accepted: 29 Oct 2007

The present work reports numerical results of mixed convection and surface radiation within a horizontal ventilated cavity, with an aspect ratio $A = L'/H' = 2$, heated from below and provided with an adiabatic partition, of a fine thickness, on the heated surface. Air, a radiatively transparent medium, is considered to be the cooling fluid. The effect of the governing parameters, which are the Reynolds number, $200 \le Re \le 5000$, the partition position from the inlet, $0.25 \le L_b \le 1.75$, and the emissivity of the walls, $0 \le \varepsilon \le 0.85$, on the fluid flow and heat transfer characteristics is studied in detail. The relative height of the partition, $H_b = H'_b/H'$, and the relative height of the openings, $B = h'/H'$, are kept constant at 1/2 and 1/4 respectively.

Keywords: mixed convection, surface radiation, ventilated cavity, adiabatic partition

Abdelghani Raji

Organization: A teacher at the Faculty of Sciences and Technics in Beni Mellal (Morocco).
Education: Doctorates in heat transfer (1994 and 2000) after attending Cadi Ayyad University. The title of the first doctorate: "Etude numérique des écoulements et des transferts de chaleur par convection dans des cavités en interaction et dans un canal de longueur finie". The title of the second thesis: "Etude numérique du phénomène de la convection mixte dans des cavités ventilées avec et sans effet de rayonnement".
Experience: Head of the physics department from 2000 to 2003.
Main range of scientific interests: Heat transfer by conduction, convection, radiation, porous media…
Publications: from 2004: – Coupling between mixed convection and radiation in an inclined channel locally heated. *Journal of Mechanical Engineering, 2004.* – Interaction between natural convection and radiation in a square cavity heated from below. *Numerical Heat Transfer, Part – A: Applications, 2004.* – Multiple steady state solutions resulting from coupling between mixed convection and radiation in an inclined. *Heat and Mass Transfer, August 2005.* – Combined effect of radiation and natural convection in a rectangular enclosure discreetly heated from one side. *International Journal of Numerical Methods for Heat & Fluid Flow, 2006.* – Multiplicité de solutions en convection naturelle couplée au rayonnement dans une cavité horizontale, *Physical & Chemical News, 2006.* – Mixed convection in a horizontal channel with emissive walls and partially heated from below. *Numerical Heat Transfer, Part – A: Applications, 2007.* – Multiple steady state solutions for natural convection in a tilted rectangular slot containing non-Newtonian power-law fluids and subject to a transverse thermal gradient. *Numerical Heat Transfer, Part – A: Applications, 2007.* – Parallel flow convection in a shallow horizontal cavity filled with non-Newtonian power-law fuids and subject to horizontal and vertical uniform heat fluxes². *In press in Numerical Heat Transfer, Part – A: Applications, 2007.* – Coupled natural convection and radiation in a horizontal rectangular enclosure discretely heated from below. *Accepted in Numerical Heat Transfer, Part – A: Applications, 2007.*

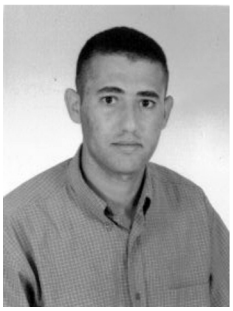

Ahmed Bahlaoui

Education: A diploma of higher studies in Fluid Mechanics and Energetics (2000) of the Faculty of Sciences Semlalia, Marrakech, Morocco and a National Doctorate in Fluid Mechanics and Heat Transfer of the Faculty of Sciences and Technologies (F.S.T.), Béni-Mellal, Morocco (2006).
Organization: A teacher in the F.S.T., Béni-Mellal, Morocco, during the period 2004-2007. Member of the Team of Flows and Transfers Modeling (EMET) in the F.S.T., Béni-Mellal, Morocco.
The principal **publications** which I carried out are those cited above.

Nomenclature

A – aspect ratio of the cavity $(= L'/H')$
B – relative height of the openings $(= h'/H')$
cv – convection
F_{ij} – view factor from S_i surface to S_j one
g – acceleration due to gravity, m/s^2
h' – height of the openings, m
H' – height of the cavity, m
H_b – relative height of the partition $(= H'_b / H')$
I_i – dimensionless irradiation $(= I'_i/\sigma T'^4_C)$
J_i – dimensionless radiosity $(= J'_i/\sigma T'^4_C)$
L' – length of the cavity, m
L_b – dimensionless x-direction distance of the partition from the inlet $(= L'_b / H')$
Nr – convection-radiation interaction parameter $(= \sigma T'^4_C / q')$
Nu – average Nusselt number
Pr – Prandtl number $(= \nu/\alpha)$
q' – imposed wall heat flux, W/m^2
Q_r – dimensionless radiative heat flux $(= Q'_r/\sigma T'^4_C)$
Ra – Rayleigh number $(= g\,\beta\, q' H'^4/\alpha\nu\lambda)$
rd – radiation
Re – Reynolds number $(= u'_0 H'/\nu)$
t – dimensionless time $(= t' u'_0 / H')$
T – dimensionless fluid temperature $(= \lambda(T' - T'_C)/q' H')$
T' – dimensional fluid temperature, K
$\overline{T}$ – dimensionless mean temperature
T_{max} – dimensionless maximum temperature
T'_C – common temperature of the left vertical cold wall and imposed flow, K
T_0 – dimensionless reference temperature $(= \lambda T'_C / q' H')$
u'_0 – velocity of the imposed flow, m/s
(u, v) – dimensionless horizontal and vertical velocities $(= (u', v')/u'_0)$
(x, y) – dimensionless coordinates $(= (x', y')/H')$

Greek symbols

α – thermal diffusivity of fluid, m^2/s
β – thermal expansion coefficient of fluid, 1/K
Δt – dimensionless time step
ε – walls emissivity
λ – thermal conductivity of fluid, W/(K·m)
ν – kinematic viscosity of fluid, m^2/s
Ω – dimensionless vorticity $(= \Omega' H'/u_0)$
Ψ – dimensionless stream function $(= \Psi'/u'_0 H')$
σ – Stéfan-Boltzman constant (= 5.67·10^{-8} W/m^2·K^4)

Subscripts and Superscripts

$_C$ – cold temperature
$_H$ – heated wall
$_{max}$ – maximum value
$_{min}$ – minimum value
$'$ – dimensional variable

Introduction

Mixed convection heat transfer in ventilated systems continues to be a fertile area of research, due to the interest of the phenomenon in many technological processes, such as the design of solar collectors, thermal design of buildings, air conditioning and recently the cooling of electronic circuit boards. In the literature, numerous analytical, numerical and experimental studies dealing with mixed convection in ventilated geometries have been reported without radiation effect. The effect of the latter can be neglected in the case of configurations with non emissive or weakly emissive boundaries which is not the case in general since the contribution of radiation to the overall heat transfer could be significant. In the absence of radiation, mixed convection in a square enclosure provided with a partially dividing partition was studied numerically by Hsu et al. [1], How and Hsu [2] and Hsu and Wang [3]. Results of the simulations indicate that the heat transfer and flow structure are strongly dependent on the height, the conductivity ratio and the location of the conducting baffles. Laminar mixed convection in a two-dimensional enclosure with assisting and opposing flows was studied numerically by Raji and Hasnaoui in the case of a cavity uniformly heated from one or two side walls [4-6]. The obtained results show that the *Re-Ra* plane can be divided in regions corresponding to the dominance of the forced convection or to the mixed convection regime where the heat transfer is maximum. Recently, mixed convection from a flush-mounted uniform heat sources in a rectangular enclosure with openings was numerically investigated by Bhoite et al [7]. and Saha et al. [8]. In the case of ventilated cavities, the numerical study, conducted by Raji and Hasnaoui [9] on combined mixed convection and radiation, showed that the contribution of radiation could be important even though the cooling fluid is transparent to radiation. The neglected effect of thermal radiation is mainly justified by the fact that the heat transfer is especially ensured by mixed or forced convection. However, moderate temperature differences give rise to significant radiation effects and the fact of neglecting their contribution becomes non realistic.

The main objective of the present study consists of examining the effect of the Reynolds number, *Re,* the horizontal position of partition, L_b, and the emissivity of the walls, ε, on flow and thermal fields. Variations, versus the main controlling parameters, of maximum and mean temperatures are also explored.

Problem formulation

The configuration under study, together with the system of coordinates is depicted in Fig. 1. It consists of a ventilated rectangular cavity. The bottom wall is uniformly heated with a constant heat flux and provided with a vertical adiabatic baffle. The upper horizontal and right vertical walls are considered insulated, while the

left side of the cavity is cooled with a constant temperature. The system is submitted to an imposed flow of ambient air through an opening located on the lower part of left vertical wall. The forced flow leaves the cavity through an outflow opening placed on the higher part of the right vertical wall. The inner surfaces, in contact with the fluid, are assumed to be gray, diffuse emitters and reflectors of radiation with identical emissivities. The fluid properties are evaluated at a mean temperature and the airflow is assumed to be, two-dimensional, laminar, incompressible and obeying the Boussinesq approximation. Under these assumptions, the dimensionless governing equations, written in terms of vorticity and stream function formulation, are as follows:

$$\frac{\partial \Omega}{\partial t} + u\frac{\partial \Omega}{\partial x} + v\frac{\partial \Omega}{\partial y} = \frac{1}{Re}\left[\frac{\partial^2 \Omega}{\partial x^2} + \frac{\partial^2 \Omega}{\partial y^2}\right] + \frac{Ra}{Re^2\ Pr}\ \frac{\partial T}{\partial x}, \quad (1)$$

$$\frac{\partial T}{\partial t} + u\frac{\partial T}{\partial x} + v\frac{\partial T}{\partial y} = \frac{1}{Re\ Pr}\left[\frac{\partial^2 T}{\partial x^2} + \frac{\partial^2 T}{\partial y^2}\right], \quad (2)$$

$$\frac{\partial^2 \Psi}{\partial x^2} + \frac{\partial^2 \Psi}{\partial y^2} = -\Omega\,. \quad (3)$$

The stream function and the vorticity are related to the velocity components by the following expressions:

$$u = \frac{\partial \Psi}{\partial y}\ ,\ \mathrm{v} = -\frac{\partial \Psi}{\partial x}\ \text{and}\ \Omega = \frac{\partial v}{\partial x} - \frac{\partial u}{\partial y}\,. \quad (4)$$

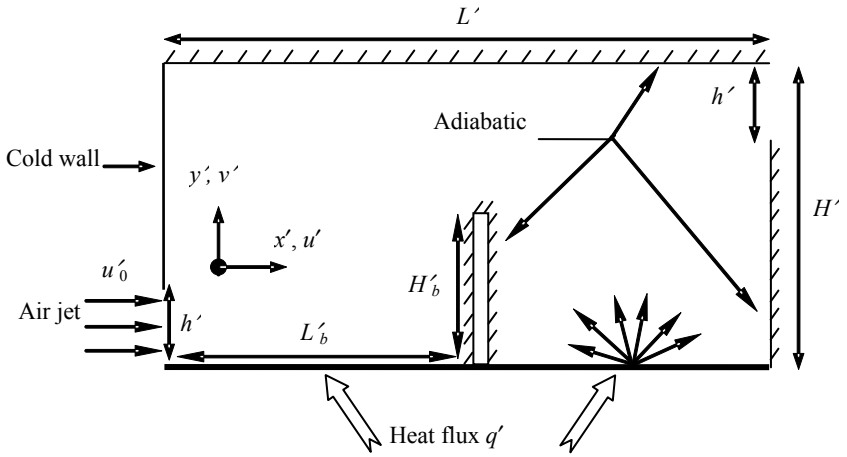

Fig. 1. *Schematic of the studied configuration*

Boundary conditions

The boundary conditions, associated to the problem are as follows: $u = v = 0$ on the rigid walls; $T = v = \Omega = 0$, $u = 1$ and $\Psi = y$ at the inlet of the cavity; $T = 0$ on the left vertical cold wall; $-\frac{\partial T}{\partial \mathrm{y}} + N_r Q_r = 1$ on the lower horizontal heated wall; $-\frac{\partial T}{\partial n} + N_r Q_r = 0$ on the adiabatic walls; "n" being the normal direction to the considered adiabatic wall.

For this problem, the boundary conditions are unknown at the outflow opening. Values of u, v, T, Ψ and Ω are obtained at each time step by mean of an extrapolation technique [9-11].

Radiation equations

The calculation of the radiative heat exchange between the cavity and its surrounding (through the inlet and the exit) is based on the radiosity method. In addition, the radiative heat transfer between the system surfaces is expressed by the following set of equations in non-dimensional form:

$$J_i = \varepsilon_i\left(\frac{T_i}{T_0} + 1\right)^4 + (1-\varepsilon_i)\sum_{j=1}^{N} F_{ij}\ J_j \quad (5)$$

The dimensionless net radiative heat flux leaving an element of surface S_i is evaluated by:

$$Q_r = J_i - I_i = \varepsilon_i\left[(\frac{T_i}{T_0} + 1)^4 - \sum_{j=1}^{N} F_{ij}\mathrm{J_j}\right] \quad (6)$$

Heat transfer

The average Nusselt numbers, characterizing the contributions of mixed convection and thermal radiation through the heated wall, are respectively defined as:

$$Nu_H(cv) = -\frac{1}{A}\int_0^A -\frac{1}{T}\left(\frac{\partial T}{\partial y}\right)\Big|_{y=0} dx\,;$$

$$Nu_H(rd) = \frac{1}{A}\int_0^A \frac{1}{T}\left(N_r Q_r\right)\Big|_{y=0} dx\,. \quad (7)$$

The total Nusselt number, Nu, is evaluated as being the sum of the corresponding convective and radiative Nusselt numbers, i.e. $Nu = Nu(cv) + Nu(rd)$.

Method of solution

The non linear partial differential governing equations, Eq. (1)-(3), were discretized using a finite difference technique. The first and second derivatives of the diffusive terms were approached by central differences while a second order upwind scheme was used for the convective terms to avoid possible instabilities frequently encountered in mixed convection problems. The integration of equations (1) and (2) was ensured by the Alternating Direction Implicit method (ADI). At each time step, the Poisson equation, Eq. (3), was treated by using the Point Successive Over-Relaxation method (PSOR) with an optimum over-relaxation coefficient equal to 1.88 for the grid (81×41) adopted in the present study. The set of Eq. (5), representing the radiative heat transfer between the different elementary surfaces of the cavity, was solved by using the Gauss-Seidel method. The numerical code was validated against the results of Akiyama and Chong [12] obtained in the case of a square cavity differentially heated. Comparisons, made in terms of convective Nusselt numbers, evaluated at the heated wall, showed a fairly good agreement with relative maximum deviations limited to 1.07 %/(1.36 %) for ε = 0 / (1) for *Ra* varying in the range $10^3 \le Ra \le 10^6$ (Table 1).

Table 1

Effect of *Ra* and ε on the mean convective Nusselt number, Nu_{cv}, evaluated on the heating wall of a square cavity for T'_H = 298.5 K and T'_C = 288.5 K

	ε = 0				**ε = 1**			
Ra	10^3	10^4	10^5	10^6	10^3	10^4	10^5	10^6
Present work	1.118	2.257	4.627	9.475	1.250	2.242	4.192	8.100
Akiyama and Chong [12]	1.125	2.250	4.625	9.375	1.250	2.250	4.250	8.125

Results and discussion

In the present study, the value of Rayleigh number, *Ra,* is fixed at $5 \cdot 10^6$.

The effect of radiation on the flow structure and temperature distribution inside the cavity is illustrated in Fig. 2 for *Re* = 250 and various values of ε.

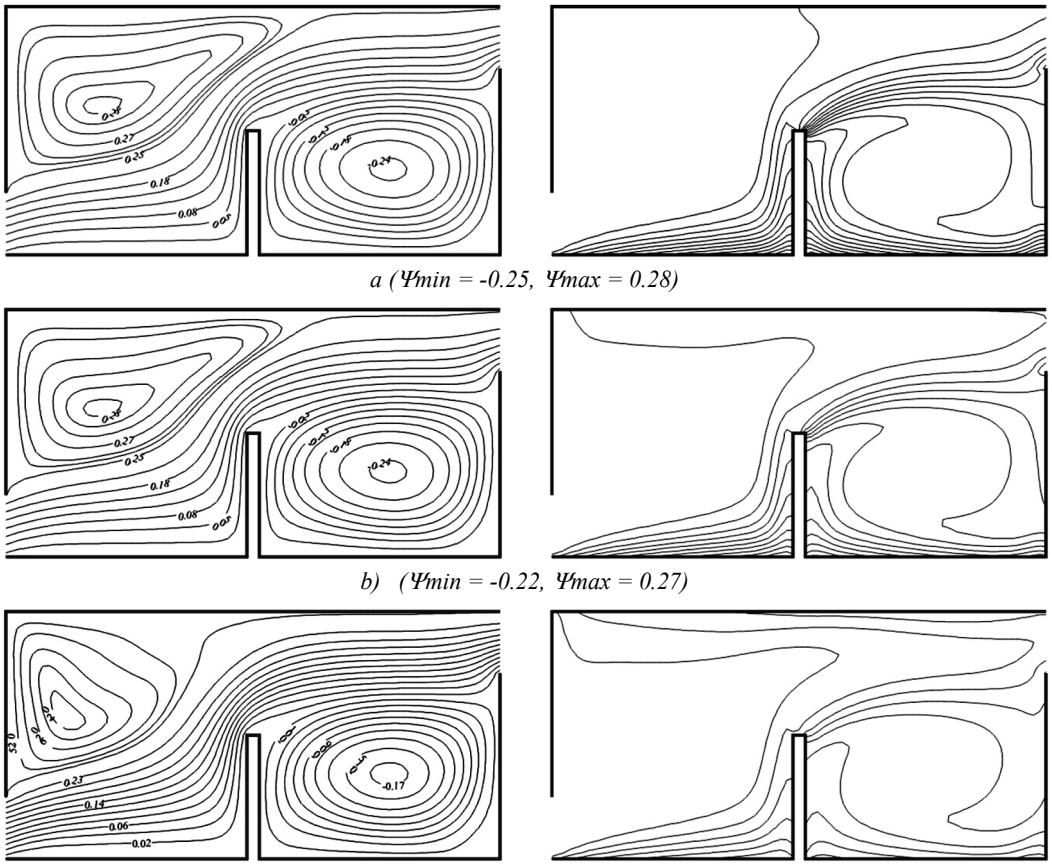

a (Ψmin = -0.25, Ψmax = 0.28)

b) (Ψmin = -0.22, Ψmax = 0.27)

c) (Ψ_{min} = -0.17, Ψ_{max} = 0.27)

Fig. 2. *Streamlines and isotherms obtained for Re = 250, L_b = 1 and different values of ε: a) ε = 0, b) ε = 0.15 and c) ε = 0.85*

The analysis of the streamlines in Fig. 2, *a*, obtained for ε = 0, reveals the existence of open lines surmounted by a trigonometric cell whose formation is rather due to the shearing effect and a clockwise natural convection cell (its direction of rotation is imposed by the forced flow) under the open lines, located on the right of the baffle. The corresponding isotherms are tightened at the level of the heating wall indicating a good convective heat exchange between this wall and the open lines/(closed cell) on the left/(right) side of the baffle. An important heat exchange can also be seen between the lower cell and the open lines while this interaction is quasi absent between the forced flow and the upper cell. Consequently, the cold zone occupies a non negligible part of the available space on the left part of the fin (in the entrance region of the cavity), visibly reduced by increasing the emissivity. The reduction of the cold zone space, following the increase of ε, indicates that the wall's radiation plays an important role in the homogenization of the fluid temperature inside the cavity. In addition, the increase of the emissivity reduces the importance of the upper cell (size and intensity) in favor of the open lines (Fig. 2, *b, c*) and leads to an increasing spacing of the isotherms in regions where the thermal interaction is important in the absence of radiation. Moreover, when the inner surfaces are radiatively participating, a heating of the adiabatic upper wall is observed and presents increasingly significant thermal gradients as the emissivity increases.

Variations, versus *Re*, of the average Nusselt numbers, resulting from contributions of convection and radiation and the total Nusselt number, evaluated along the heated wall, are presented in Fig. 3, *a-c* for various values of ε. As expected, Fig. 3, *a* shows a monotonous increase of $Nu_H(cv)$ with *Re* either with or without radiation effect. The rate of this increase becomes more important from *Re* ~ 1000 (an increase in the slope of the curves is observed from this threshold). This tendency is justified by the flow intensification with the inertia effect, promoted by the increase of *Re*. For a fixed value of this parameter, the increase of the emissivity of the walls leads to a noticeable decrease of the convection effect. The negative role of radiation on the natural convection is well known and it is confirmed here in the case of mixed convection. The effect of the emissivity of the walls on the radiative heat transfer component is presented in Fig. 3, *b* in terms of $Nu_H(rd)$ variations with *Re* for ε = 0.15, 0.5 and 0.85. Globally, it can be deduced that, for a given value of *Re*, the effect of radiation is important for ε = 0.5 and 0.85 and it is characterized by an important increase of $Nu_H(rd)$ with ε. Also, the effect of *Re* on $Nu_H(rd)$ is limited in the case of ε = 0.15 but becomes increasingly positive by increasing ε. The variations of the total Nusselt number with *Re*, presented in Fig. 3, *c*, show increasing tendencies of Nu_H with *Re* and ε which means that the positive impact of radiation on the radiative Nusselt number is more important than its negative effect on the convective Nusselt number.

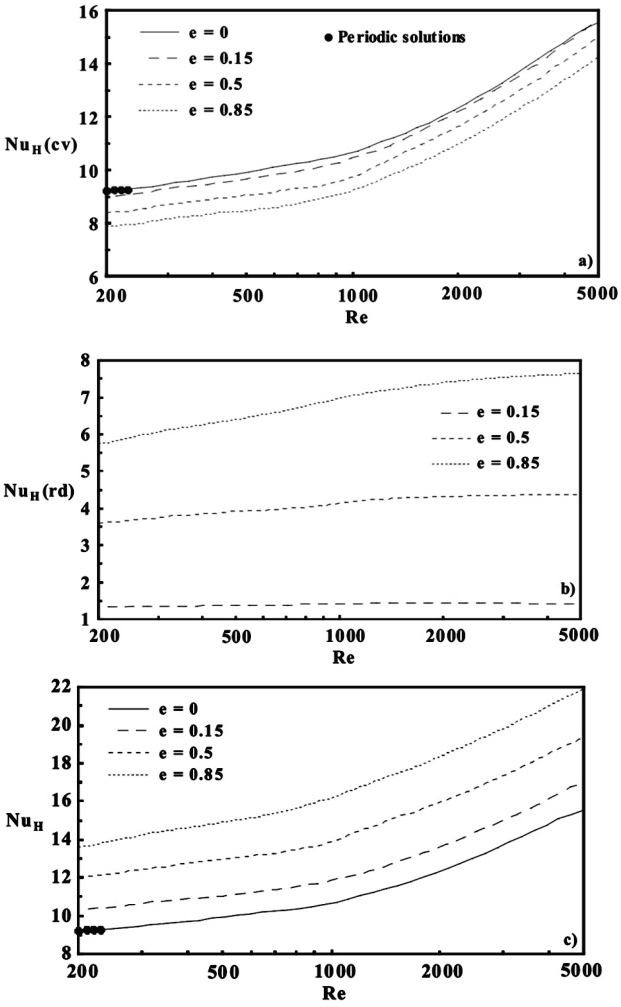

Fig. 3. *Variations, with Re, of the average Nusselt numbers on the heated wall for L_b = 1 and various values of ε : a) $Nu_H(cv)$, b) $Nu_H(rd)$ and c) Nu_H*

For practical applications, it is of great importance to know the impact of the governing parameters on mean and maximum temperatures of the fluid inside the cavity. Thus, the variations of these quantities with *Re* are presented in Figs. 4, *a*, *b* for different values of ε. For all considered values of ε, Fig. 4, *a* shows that the evolution of $\overline{T}$ is characterized by a continuous decrease by increasing *Re*. In addition, for a given *Re*, the increase of ε is accompanied by a decrease of the average temperature since the part of energy provided by the hot wall and leaving directly the cavity through the openings, without being transported by the fluid, increases with ε. The evolution of the maximum temperature, presented in Fig. 4, *b* and generally located on the heated wall, is marked also by a monotonous decrease with *Re* and ε which means that the overheating phenomenon can be avoided by increasing the emissivity of the walls and the velocity of the external imposed flow. Quantitatively, for *Re* = 200, the increase of the walls emissivity from zero to 0.85 generates a decrease in mean and maximum dimensional temperatures by

about 7.25 °C and 60.83 °C, respectively but this decrease drops to about 1.37 °C (case of ε = 0) and 35.28 °C (case of ε = 0.85) for *Re* = 5000.

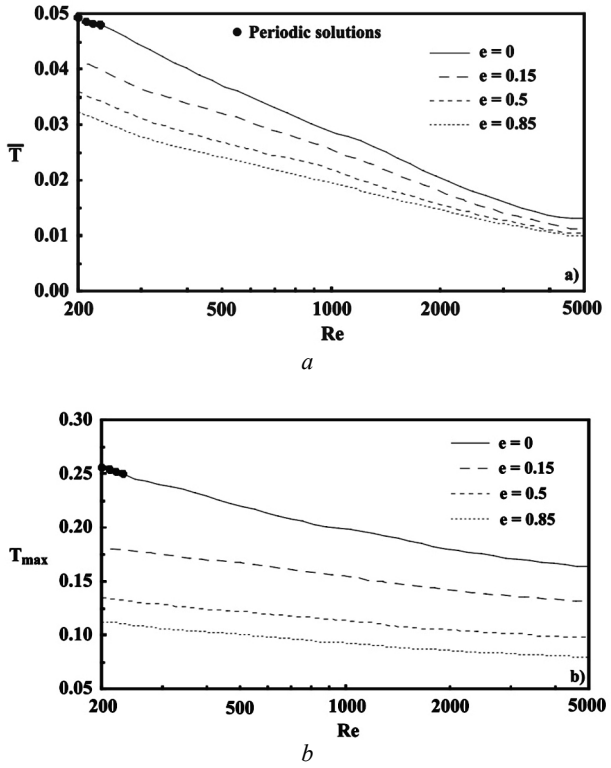

a

b

Fig. 4. *Variations, with Re, of the temperature for L_b = 1 and various values of ε: a) mean temperature $\overline{T}$, b) maximum temperature T_{max}.*

Variations of the Nusselt numbers, with the position L_b of the baffle, are presented in Fig. 5 for *Re* = 300 and different values of ε. Fig. 5, *a* shows that the convective component of heat transfer increases by moving away the partition from the cold wall but the rate of this increase becomes limited beyond L_b = 1.5; critical value from which the reduction of the space between the partition and the adiabatic vertical wall leads to a limited interaction between the closed cell and the open lines. Fig. 5, *b* shows that the increase of L_b is characterized by a limited decrease of $Nu_H(rd)$ what means that the latter is almost independent of L_b. However, the figure shows clearly an increasing positive effect of radiation when ε is increased leading to an enhancement of the total heat transfer (Fig. 5, *c*) and the latter is favored also by the increase of L_b. Improvements in terms of the total heat transfer of about 28.2 % and 18.1 % are obtained respectively for ε = 0 and 0.85, when the parameter L_b is varied from 0.25 to 1.75. It should be mentioned that the solution is unsteady for L_b = 1.5. The corresponding results, presented by full circles in Figs. 5, *a-c*, were obtained as averaged values during flow cycles.

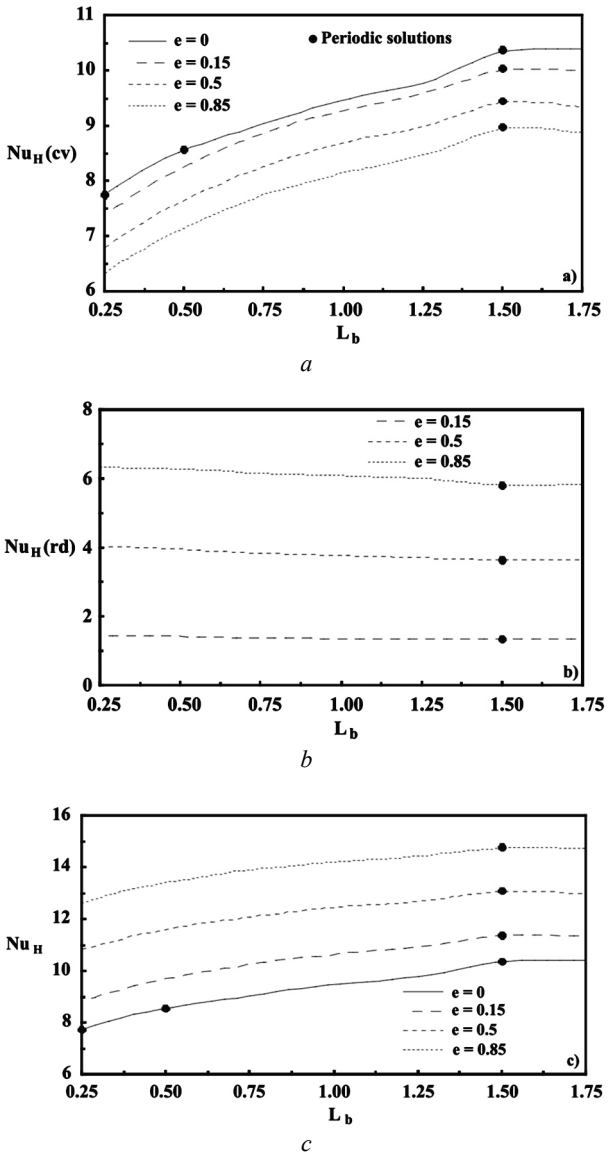

a

b

c

Fig. 5. *Variations, with L_b, of the average Nusselt numbers on the heated wall for Re = 300 and various values of ε : a) $Nu_H(cv)$, b) $Nu_H(rd)$ and c) Nu_H*

Variations, with L_b, of mean and maximum temperatures are presented in Figs. 6 for *Re* = 300 and different values of ε. It is seen from Fig. 6, *a* that $\overline{T}$ decreases by increasing ε and L_b. In fact, the increase of the overall heat transfer with both ε and L_b (Fig. 5, *c*) and the mixed convection heat transfer component with L_b (Fig. 5, *a*), contributes to a better cooling within the cavity. It should be noted that for L_b > 1.5, the effect of the emissivity ε on $\overline{T}$ becomes limited. The variations of the maximum temperature, T_{max}, reported in Fig. 6, *b*, show a decrease of this parameter by increasing ε or L_b with a drastic decrease from L_b = 1.25, due to the competition between natural and forced convections, towards a minimum reached at L_b = 1.5, position for which the maximum of the overall heat transfer is reached.

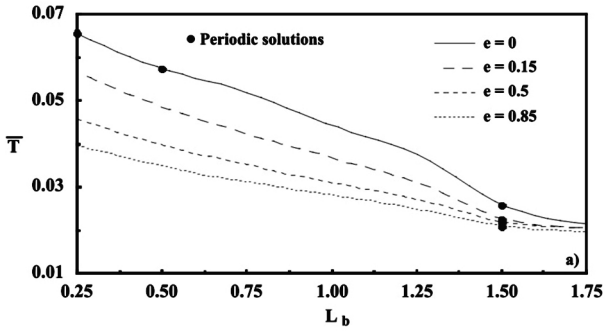

a

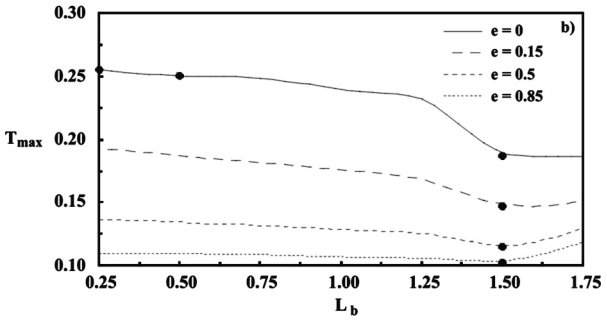

b

Fig. 6. *Variations, with L_b, of the temperature for Re = 300 and various values of ε: a) mean temperature $\overline{T}$, b) maximum temperature T_{max}*

Concluding remarks

The problem of combined mixed convection and radiation inside a partitioned ventilated cavity has been studied numerically. Results of the study show that the radiation effect leads to a better homogenization of the temperature inside the cavity by reducing the cold zone space in the entrance region. It is found that the radiation effect reduces the convective Nusselt number component and the latter is favored by the Reynolds number, *Re*, and the displacement of the partition away from the inlet, L_b. All the parameters *Re*, L_b and ε are found to have a positive effect on the total heat transfer. The better cooling of the cavity, expressed by the decrease of mean and maximum temperatures of the fluid, is obtained by the increase of the parameters *Re*, L_b and ε. Also, the contribution of radiation to the overall heat transfer is generally not negligible even for the weaker value (ε = = 0.15) considered for ε.

References

1. Hsu T.H., Hsu P.T., How S.P. Mixed convection in a partially divided rectangular enclosure // Num. Heat Transfer. Part A. 1997. Vol. 31. P. 655–683.
2. How S.P., Hsu T.H. Transient mixed convection in a partially divided enclosure // Comput. Math. Appl. 1998. Vol. 36. P. 95–115.
3. Hsu T.H., Wang S.G. Mixed convection in a rectangular enclosure with discrete heat sources // Num. Heat Transfer. Part A. 2000. Vol. 38. P. 627–652.
4. Raji A., Hasnaoui M. Mixed convection heat transfer in a rectangular cavity ventilated and heated from the side // Num. Heat Transfer. Part A. 1998. Vol. 33. P. 533–548.
5. Raji A., Hasnaoui M. Corrélations en convection mixte dans des cavités ventilées // Revue Générale de Thermique. 1998. Vol. 37. P. 874–884.
6. Raji A., Hasnaoui M. Mixed convection heat transfer in ventilated cavities with opposing and assisting flows // Engineering Computations. Int. J. for Computer-Aided Engineering and Software. 2000. Vol. 17. P. 556–572.
7. Bhoite M.T., Narasimham G.S. V.L., Krishna Murthy M.V. Mixed convection in a shallow enclosure with a series of heat generating components // Int. J. Thermal Sciences. 2005. Vol. 44. P. 121–135.
8. Saha S., Saha G., Ali M., Quamrul Islam M. Combined free and forced convection inside a two-dimensional multiple ventilated rectangular enclosure // ARPN Journal of Engineering and Applied Sciences. 2006. Vol. 1, No. 3. P. 23–35.
9. Raji A., Hasnaoui M. Combined mixed convection and radiation in ventilated cavities // Engineering Computations. Int. J. for Computer-Aided Engineering and Software. 2001. Vol. 18. P. 922-949.
10. Bahlaoui A., Raji A., Hasnaoui M. Coupling between mixed convection and radiation in an inclined channel locally heated // Journal of Mechanical Engineering. 2004. Vol. 55. P. 45-57.
11. Bahlaoui A., Raji A., Hasnaoui M. Multiple steady state solutions resulting from coupling between mixed convection and radiation in an inclined channel // Heat and Mass Transfer. 2005. Vol. 41. P. 899-908.
12. Akiyama M., Chong Q.P. Numerical analysis of natural convection with surface radiation in a square enclosure // Num. Heat Transfer. Part A. 1997. Vol. 31. P. 419–433.

THE DEVELOPMENT OF A NEW MAXIMUM POWER POINT TRACKER FOR A PV PANEL

M. Salhi, R. El-Bachtiri*, E. Matagne***

*REPEER Group, LESSI laboratory, Faculty of sciences dhar el-Mehrez, USMBA University
Higher school of technology, km5, R^{te} Imouzzer, BP 2427, Fez, Morocco.
Telephone: +212 35 600584/Fax: +212 35 600588
E-mail: Salhi_estf@yahoo.fr; bachtri@yahoo.fr

**LEI laboratory, Université Catholique de Louvain
Louvain-la-Neuve, Belgium
E-mail: Ernest.matagne@uclouvain.be

Received: 21 Sept 2007; accepted: 29 Oct 2007

The PV systems are rapidly expanding and have increasing roles in electric power technologies, providing more secure power sources and pollution free electric supplies. Since the PV electricity is expensive compared to the electricity from the utility grid, users want to use all the available output PV power. Therefore, the PV systems should be designed to operate at their maximum output power for any temperature and solar radiation level. In this paper, we consider a photovoltaic panel supplying a battery. For maximizing the output power of this panel, we have using a boost dc/dc converter controlled by a PI regulator. For synthesizing this regulator, we have replaced the converter with an equivalent continuous model when we have considered the mean values, over the chopping period, of the electric quantities. Then, we have developed the transfer function of the system by using the small signal modeling around an optimal operating point. A PI synthesis has been achieved by using Bode method. In the study, we have taken into account the converter losses. Coefficients K_p and K_I obtained of PI regulator lead to good simulations. The theoretical results confirm excellent tracking effectiveness response. The regulator operates correctly on a large range.

Keywords: solar powerplants, photovoltaic panel, maximum power point tracking, boost dc/dc converter, losses

M. Salhi

Organization: Assist master in Sidi Mohamed Ben Abdellah University (USMBA), Higher School of Technology (EST), in Fèz, Morocco.
Education: – Diploma of thorough higher study (DESA) in automatic and systems analysis (2002-2004) from faculty of sciences dhar el-Mehrez at Sidi Mohamed Ben Abdellah University (USMBA).
– Researcher student in solar energy photovoltaic since January 2005.
Experience: Member of "Team research in electrical engineering, power electronics and renewable energies" (REEPER at the higher school of technology in Fez) belonging to the "Laboratory of electronics, signal-systems and data processing" (LESSI at the Faculty of Science in Fez).
Main range of scientific interests: renewable energy, optimal use of the photovoltaic power.
Publications: participation at congress on renewable energy; automatic control and systems engineering.

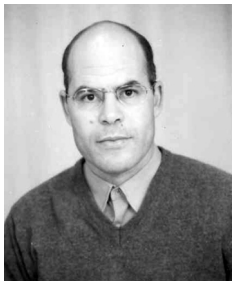

Rachid El-Bachtiri

Organization: Researcher teacher in Sidi Mohammed Ben Abdellah University (USMBA), Higher School of Technology (EST), in Fès, Morocco. Assisting Master (21/10/88). Ability Professor (22/01/97). Higher teaching Professor (22/01/01).
Education: Engineer (July 1988); Mohamed V University (Rabat), Mohammadia School of Engineers (EMI, 1983-1988), Electrical engineering, Electrotechnics and Industrial Electronics. Doctor of Sciences Applied (January 1997), Catholic University of Louvain (UCL, 1992-1997) at Louvain-La-Neuve (Belgium), Faculty of Science Applied (FSA), Department of electricity, Laboratory of electrotechnics and instrumentation (LEI).
Experience: Lectures and directed work: Power electronics and electrotechnics.
– Person in charge for a "Team of research in electrical engineering, power electronics and renewable energies" (REEPER at the higher school of technology in Fez) belonging to the: "Laboratory of electronics, signal-systems and data processing" (LESSI at the Faculty of Science in Fez).
Main range of scientific interests: electrical engineering and industrial electronics; resonance static conversion, effects of the harmonics, and their attenuation. Renewable energies; optimal use of the photovoltaic electrical power.
Publications: Papers in the power electronics and renewable energy field.

Ernest Matagne

Organization: Associate Professor in Université catholique de Louvain (UCL), Belgium, Assistant (1974), Senior staff member (1979), Associate professor (1999).
Education: Engineer (1971) in UCL, Doctor in Applied Sciences (1991).
Experience: Lectures and directed work in physics, electrical machines, power electronics, instrumentation and sensors, mechatronics, photovoltaic energy.
Main range of scientific interest: physics, analytical field computation, optimal design of electromechanical and electrical converters.
Publications: Physics, circuit theory, electrical machines, photovoltaic energy.

Introduction

Photovoltaic energy is a promising alternative energy source for the future, due to the world's limited conventional energy sources. Its disadvantages are that the initial cost is very high and the energy conversion efficiency is relatively low. Therefore, it is desirable to extract the highest possible power at any moment from the solar array source. The amount of power obtained from a photovoltaic array depends on its operating voltage. From its typical *V-I* and *V-P* characteristics (Fig. 1, *a* and *b* respectively), a unique operating point ($v = V_{mpp}$), known as the maximum power point (MPP), delivers the maximum available power $P_{\max}$. When operated at the MPP, the array is best utilized. The MPP of a photovoltaic array varies with irradiation, temperature and other effects. Up to now, a large variety of MPP seeking algorithms exists: look-up table [1, 2], perturbation and observation (P&O) [3], incremental conductance [4, 5] etc. Another maximum power point tracking (MPPT) is proposed in [6, 7], where a dc/dc converter is controlled so that $\partial I_{out}/\partial V$ and $\partial P/\partial V$ equal zero, where I_{out} and P are the dc/dc converter output current and input power respectively. However, these methods cannot take into account the losses in the dc/dc converter, particularly, the switch losses in the MOSFET transistor.

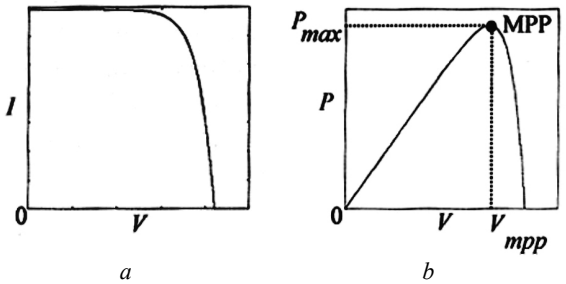

a *b*

Fig. 1. *Typical PV module: a – current-voltage and b – power-voltage characteristic*

In this paper, we pick up the work exposed in [7], and we consider that the dc/dc converter is not ideal. This converter is used between the PV and the battery to track the maximum power point of the PV module (Fig. 2, *a*).

The battery is considered as a constant voltage E in series with a constant resistance R_b [8, 9]. The MPP (V_{mpp}, P_{max}) is reached when $\partial P/\partial V = 0$, $P = VI$ being the PV power. Then, the control circuit must keep $(\partial P/\partial V)$ equals zero. That is possible with action on duty cycle α ($0 \le \alpha \le 1$) according to the solar irradiation λ and the temperature T. Duty cycle is a signal produced by a PI regulator. For synthesizing this regulator, we have developed a transfer function for the system using the small signal model. The coefficients K_p and K_i of the PI regulator are obtained by frequency synthesis.

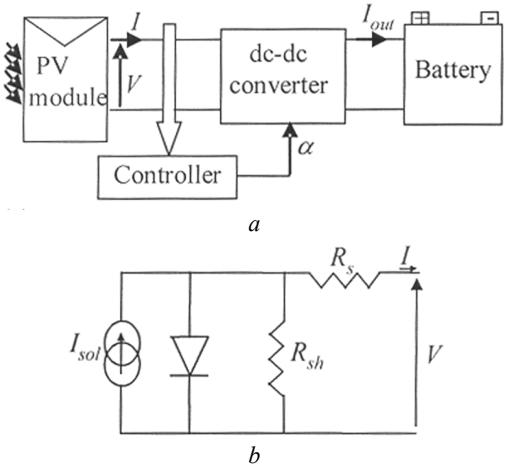

a

b

Fig. 2. *System bloc diagram (a) and – equivalent circuit(b) of a PV module*

Theoretical analysis

The power electronic converter is a boost converter inserted between the PV generator and the battery. It is characterised by its duty cycle α ($0 \le \alpha \le 1$) that gives the ratio input between the input and the output voltage when the conduction is continuous (Fig. 3).

The transistor is ON during αT and OFF during the rest of the period i.e. $(1 - \alpha)T$. The diode state, in continuous conduction, is complementary of the transistor one. The inductance is charged by the input through the transistor, and it discharges at the output through the diode.

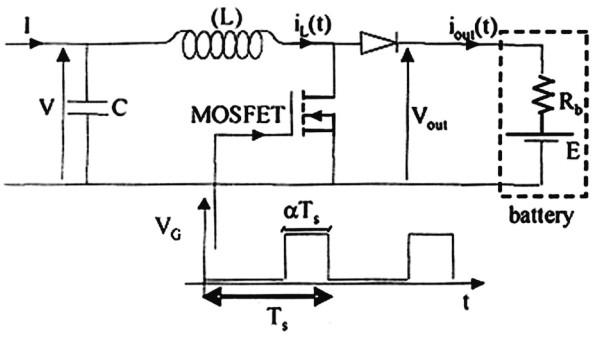

a

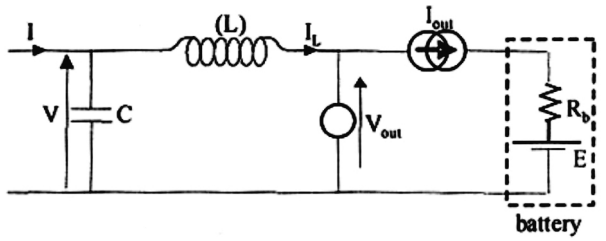

b

Fig. 3. *Boost converter (a); converter "mean" (b) equivalent circuit*

If the chopping frequency is sufficiently higher than the system characteristic frequencies, we can replace the converter with an equivalent continuous model. We will consider, for that, the mean values, over the chopping period, of the electric quantities (Fig. 3, *b*). The transistor can be replaced by a voltage source whose value equals its mean voltage. At the same, the diode can replaced by a current source.

Optimal operating point of PV module

The equivalent circuit of the PV module considered in this paper is shown in Fig. 2, *b*. The relationship between *V* and *I* is given by [10, 11]:

$$I - I_{sol} - I_{os}\left\{\exp\left[\frac{q}{\gamma kT}\left(V + R_s I\right)\right] - 1\right\} - \frac{V + R_s I}{R_{sh}}, \quad (1)$$

where:

$$I_{os} = I_{or}\left[\frac{T}{T_r}\right]^3 \exp\left[\frac{qE_{GO}}{\beta k}\left(\frac{1}{T_r} - \frac{1}{T}\right)\right] \quad (2)$$

$$I_{sol} = \left[I_{SC} + K_I\left(T - 298.18\right)\right]\frac{\lambda}{1000} \quad (3)$$

and *I* and *V* – cell output current and voltage, I_{or} – cell reverse saturation current, *T* – cell temperature in degree Kelvin, *k* – Boltzmann's constant (1.381e^{-23} J/K), *q* – electronic charge (1,602e^{-19} C), K_I – short-circuit current temperature coefficient at I_{sc} (= 0,0004 A/K), I_{sc} – short-circuit current at 25 °C and 1000 W/m^2, λ – solar irradiation in W/m^2, I_{sol} – light-generated current, E_{GO} – band gap for silicon (= 1.12 eV), γ (= β) – ideality factor (= 1,740), T_r – reference temperature (= 298,18 K), I_{or} – cell saturation current at T_r, R_{sh} – shunt resistance, R_s – series resistance.

The output power of PV panel is $P = VI$, at optimal point, we have:

$$\frac{\partial P}{\partial V} = I + V\frac{\partial I}{\partial V} = 0 \rightarrow \frac{\partial I}{\partial V} = \frac{-I}{V}. \quad (4)$$

Hence:

$$I = \left(V - R_s I\right)\left\{I_{os} A \exp\left[A\left(V + R_s I\right)\right] + \frac{1}{R_{sh}}\right\}, \quad (5)$$

where: $A = q/(\gamma kTN_{cell})$ and N_{cell} is the number of series cells in the module.

The PV module considered in this paper is the SM55. It has 36 series connected mono-crystalline cells. The manufacturer ratings of this PV photovoltaic under standard conditions (irradiation λ = 1000 W/m^2, A.M. 1.5, solar spectrum and cell temperature *T* = 25 °C) is shown in Table 1. The values of the rest parameters are as follow: R_s = 0,1124 Ω, R_{sh} = 6500 Ω and I_{or} = 4,842 μA.

Table 1

PV module specifications under standard test conditions (STC)

Cell temperature, °C	25
Open-cicuit voltage, V	21,7
Short-circuit current, A	3.45
Maximum power current, A	3.15
Maximum power voltage, V	17.4
Maximum power, W	55

Choice of *L* and *C*

The inductor value, *L*, required such the converter operates in the continuous conduction mode (Fig. 4, *a*) is calculated such that the peak inductor current at maximum input power does not exceed the power switch current rating [12]. Hence, *L* is calculated as:

$$L \geq \frac{V_{om}(1-\alpha_m)\alpha_m}{f_s\left|\Delta I_{Lm}\right|}, \quad (6)$$

where f_s (= $1/T_s$) – switching frequency, α_m – duty cycle at maximum converter input power, ΔI_{Lm} – peak-to-peak ripple of the inductor current, V_{om} – maximum of dc component of the output voltage, I_{om} – dc component of the output current at maximum output power.

Taking into account that the ripple of the PV output current must be less than 2 % of its mean value [12], the input capacitor value is calculated to be:

$$C \geq \frac{I_{om}\alpha_m^2}{0.02(1-\alpha_m)V_{mn}f_s}, \quad (7)$$

where V_{inm} – PV input voltage at the maximum power point.

When the boost converter is used in PV applications, the input power, voltage and current change continuously with atmospheric conditions. Thus, the converter conduction mode could change since it depends on them. Also, the duty cycle α is changed continuously in order to track the maximum power point of the PV array. The choice of the converter switching frequency and the inductor value is a compromise between the converter efficiency, the cost, the power capability and the weight. For example, higher is the switching frequency, lower is the inductor core size, but the power switch losses increase. Also, by using a large L value, the peak-to-peak current ripple ΔI_L is smaller; requiring lower current rating power switches. But the converter size is increased substantially because a larger inductor core is required.

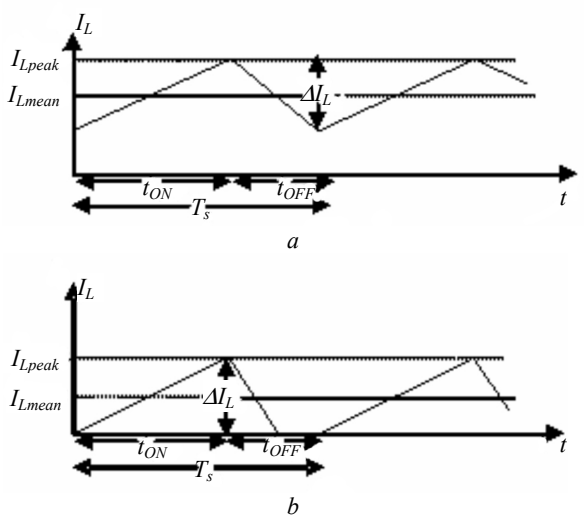

Fig. 4. *Boost converter waveforms: (a) continuous conduction mode and (b) discontinuous conduction mode*

Losses in the MOSFET transistor

In this study, we have taken into account the losses in the MOSFET transistor for determining the power transmitted to the battery at the optimal operating point. At ON state (Fig. 5), the transistor is equivalent to the R_{DSon} resistance. This resistance is considered as a constant. The average switching power dissipation in dc/dc converter is given as follow [13]:

$$P_{on-off} = \frac{1}{2} V_{DS} I_{DSon} \frac{t_{cON} + t_{cOFF}}{T_s} = \\ = \frac{1}{2} V_{DS} I_{DSon} f_s \left(t_{cON} + t_{cOFF} \right), \quad (8)$$

where:

$$V_{DS} = E + V_s + R_b I_{out}, \quad V_{DSon} \approx I_L, \quad t_{cON} = t_{ri} + t_{fv} \\ t_{cOFF} = t_{rV} + t_{ft} \quad (9)$$

and P_{on-off} – switching losses, V_{DS} – drain-to-source voltage, I_{DSon} – drain-to-source current, t_{ri} – rise time of transistor current, t_{fv} – fall time of the voltage, t_{rv} – rise time of the voltage, t_{ft} – fall time of current at the state OFF.

The switching power losses in the diode are neglected. And

$$P_d \approx R_{DSon} I_{DSon}^2 \alpha + V_s I_{out} + r_L I_L^2, \quad (10)$$

where P_d – average power dissipation in dc/dc converter, R_{DSon} – static drain-to-source on-resistance, α_{mpp} – duty cycle at MPP, V_s – threshold voltage of diode, I_D – average current of diode, r_L – resistance of inductor, I_L – average current of inductor.

So, the output power of dc/dc converter at optimal operating point (P_{out}) is:

$$P_{out} = P_{mpp} - (P_{on-off} + P_d), \quad (11)$$

where P_{mpp} – maximum power point.

The efficiency (η) of dc/dc converter is defined as:

$$\eta = \frac{P_{out}}{P}. \quad (12)$$

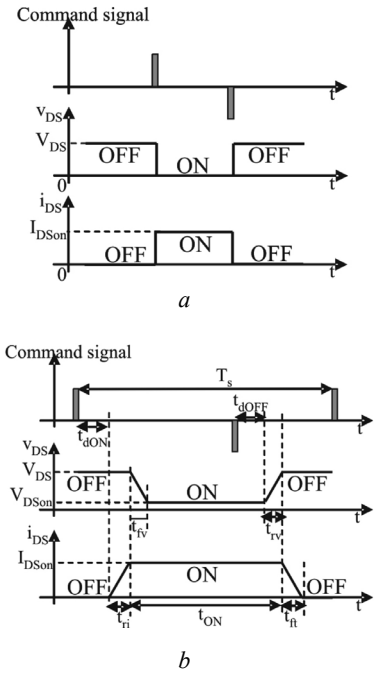

Fig. 5. *Switching time: a – ideal waveforms and b – real waveforms*

Frequencial synthesis of PI regulator

We deduce from the continuous model equations (Fig. 3, *b*) the following equations:

$$C \frac{dV}{dt} = I - I_L \quad (13)$$

$$V = L\frac{dI_L}{dt} + r_L I_L + V_{out} \quad (14)$$

$$I_{out} = (1 - \alpha) I_L, \quad (15)$$

where:

$$V_{out} = R_{DSon}\alpha I_L + R_b(1 - \alpha) I_L + (E + V_s)(1 - \alpha) \quad (16)$$

and r_L – inductor resistance, R_b – battery resistance, V_s – threshold voltage of the diode.

For expanding in series equations (11-14) around an optimal operating point, we write: $q = q_{mpp} + \Delta q$, for each quantity q in the set $\{V, \alpha, I_L, I, I_{out}\}$ defining the operating point. So, the equations system become:

$$C\frac{d\Delta V}{dt} = \Delta I - \Delta I_L \quad (17)$$

$$L\frac{d\Delta I_L}{dt} = \Delta V - \left(r_L + \alpha_{mpp} R_{DSon}\right)\Delta I_L - \\ - R_b \Delta I_{out} + \left(E + V_s - R_{DSon} I_{lmpp}\right)\Delta\alpha \quad (18)$$

$$\Delta I_{out} = \left(1 - \alpha_{mpp}\right)\Delta I_L - I_{Lmpp}\Delta\alpha \quad (19)$$

At steady state, we have:

$$I_{mpp} = I_{Lmpp} \quad (20)$$

$$V_{mpp} = \left(r_L + \alpha_{mpp} R_{DSon}\right) I_{Lmpp} + \\ + R_b \Delta I_{outmpp} + \left(E + V_s\right)\left(1 - \alpha_{mpp}\right) \quad (21)$$

$$I_{outmpp} = \left(1 - \alpha_{mpp}\right) - I_{Lmpp} \quad (22)$$

For a small variation around an optimal operating point, the system can be shown by a functional diagram like that used in [14] for synthesizing the regulator. Thus, the system can be presented as (Fig. 6):

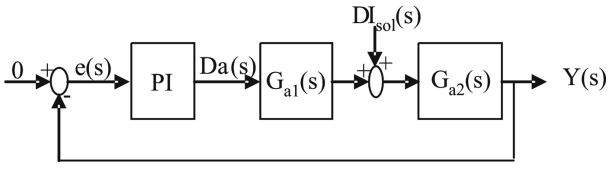

Fig. 6. *Functional diagram of the system*

According to [14], the transfer function $G_{a1}(s)$ and $G_{a2}(s)$ must have the following form:

$$G_{a1}(s) = K_{a1}\frac{R_{a1}(s)}{s^{\alpha_1}} \text{ and } G_{a2}(s) = K_{a2}\frac{R_{a2}(s)}{s^{\alpha_2}}, \quad (23)$$

where $R_{a1}(s)$ and $R_{a2}(s)$ – rational fractions with $R_{a1}(0) = R_{a2}(0) = 1$, K_{a1} and K_{a2} – static gains of $G_{a1}(s)$ and $G_{a2}(s)$, α_1 and α_2 – integration numbers of $G_{a1}(s)$ and $G_{a2}(s)$ respectively.

In this paper, we have obtained:

$$K_{a1} = \frac{\left(K_1 G - K_2\right)\left(1 + R_s G_m\right)\left\{E + V_s + \left(R_b - R_{DSon}\right) I_{Lmpp}\right\}}{K_1 + K_2 K_3} \quad (24)$$

$$K_{a2} = \frac{K_1 + K_2 K_3}{\left(1 + R_s G_m\right)\left(1 + GK_3\right)} \quad (25)$$

$$R_{a1}(s) = \frac{1}{\frac{K_1 LC}{K_1 + K_2 K_3}s^2 + \frac{K_1 K_3 C + K_2 L}{K_1 + K_2 K_3}s + 1} \quad (26)$$

$$R_{a2}(s) = \frac{\frac{K_1 LC}{K_1 + K_2 K_3}s^2 + \frac{K_1 K_3 C + K_2 L}{K_1 + K_2 K_3}s + 1}{\frac{LC}{1 + GK_3}s^2 + \frac{GL + GK_3}{1 + GK_3}s + 1}, \quad (27)$$

where:

$$K_1 = 1 + \frac{AR_s\left(R_s I_{mpp} - V_{mpp}\right)}{R_{dm}\left(1 + R_s G_m\right)},$$

$$K_2 = \frac{A\left(R_s I_{mpp} - V_{mpp}\right)}{R_{dm}\left(1 + R_s G_m\right)} - G$$

$$K_3 = r_L + \alpha_{mpp} R_{DSon} + R_b\left(1 - \alpha_{mpp}\right),\ G = \frac{G_m}{1 + R_s G_m},$$

$$G_m = \frac{1}{R_{dm}}, \text{ and } R_{dm} = \frac{1}{I_{os} A \exp\{A(V_{mpp} + R_s I_{mpp})\}}.$$

K_{a1} and K_{a2} are constants for a given temperature T and solar irradiation λ.

The transfer function of the open loop used to synthesizing a PI regulator is:

$$G_0(s) = G_{a1}(s) G_{a2}(s) = \\ = \frac{\left(K_1 G - K_2\right)\left\{E + V_s + \left(R_b - R_{DSon}\right) I_{Lmpp}\right\}}{1 + GK_3} \times \\ \times \frac{1}{\frac{LC}{1 + GK_3}s^2 + \frac{GL + CK_3}{1 + GK_3}s + 1} \quad (28)$$

Simulation procedure

The bloc used for simulations is given by Fig. 7, *a*. In PV module block, equations (1-3) are used; and in block (converter + battery) equations (11-14) are used. The switching losses are cutting off the output converter power according to equations (8-11).

The proposed controller circuit that forces the system to operate at its optimal operating point under variable temperature and insolation conditions, is shown in Fig. 7, *b*. On one hand, we multiply the PV output current I by the PV output voltage V. Then, we obtain the PV output power P who is derived in order to obtain the (dP/dt) signal. On the other hand, we drive the signal voltage and invert it. Thus, the signal $1/(dV/dt)$ is obtained.

The product of 1/(*dV*/*dt*) by (*dP*/*dt*) signals gives the (*dP*/*dV*) signal, who is compared to zero. The resulting difference signal (error signal) is the input signal of the PI regulator. This PI regulator is used to regulate the duty cycle signal of the *dc*/*dc* converter until that the condition: *dP*/*dV* = 0 is satisfied.

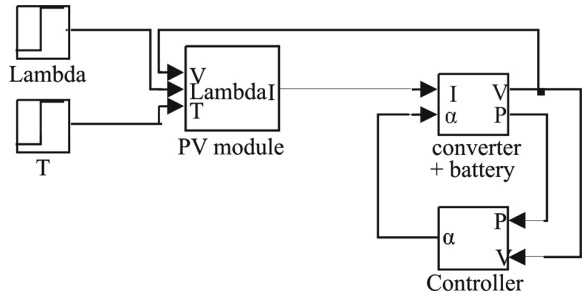

a

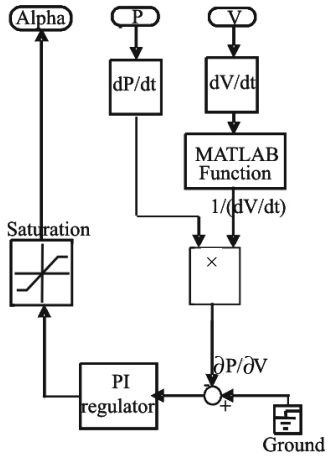

b

Fig. 7. *a – bloc diagram for system and b – MPPT tracker circuit*

Results and discussion

Theoretical results

The battery voltage, the threshold voltage of the diode, the resistance of battery and the series resistance of the inductor, used in this paper, are respectively $E = 24$ V, $V_s = 0.7$ V, $R_b = 0.65$ Ω and $r_L = 0.05$ Ω. The MOSFET transistor utilized here, is an IRFP250. Their characteristics used in this paper are: $R_{DSon} = 0.085$ Ω, $t_{fv} = 86$ ns, $t_{rv} = 62$ ns, $t_{ri} = 16$ ns and $t_{ft} = 70$ ns. Fifty kilohertz switching frequency is used.

The PI controller gain and the integral time constant obtained by frequency synthesis using Bode method are respectively $K_p = 0.01$ and T_i ($= 1/K_i$) = 1.8 ms. Using equation (6), the boost inductance choice is $L = 1$ mH. With equation (7), the choice of input capacitance is $C = 4.7$ μF.

For different values of irradiation λ and temperature T, the computation of the theoretical optimum quantities V_{mpp}, P_{mpp}, P_{out} and η are assembled in Table 2.

Table 2

Theoretical quantities V_{mpp}, P_{mpp}, P_{out} and η for different values of λ and T

Values of λ (W/m^2) and T (K)	**Optimum voltage V (V)**	**Optimum power P (W)**	**Optimum power P_{out} (W)**	**Efficiency η (%)**
λ = 100 and T = 298.18	14.25	4.393	4.224	96.16
λ = 1000 and T = 298.18	17.39	54.80	52.07	95.01
λ = 1000 and T = 320.18	15.65	48.61	46.07	94.76
λ = 100 and T = 320.18	12.31	3.715	3.570	96.11

Simulation results

The simulation study was made to illustrate the response of the proposed method to rapid temperature and solar irradiance change. For this purpose, the irradiance λ and the temperature T, which are initially 100 W/m^2, and 298.18 K, are switched, at 0.02 s and 0.05 s, to 1000 W/m^2 and 320.18 K respectively (Fig. 8, *a* and *b*). and vice versa (Fig. 9 *a* and *b*), i.e., the solar irradiance changes from 1000 W/m^2 to 100 W/m^2 at 0.02 s and the temperature changes from 320.18 K to 298.18 K at 0.05 s.

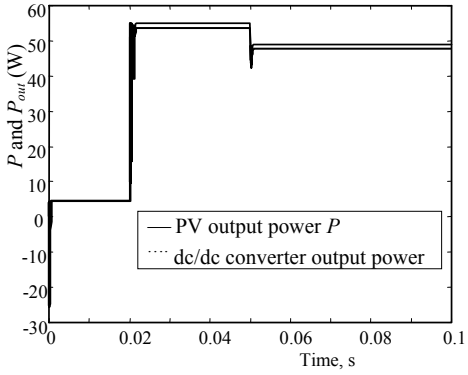

a

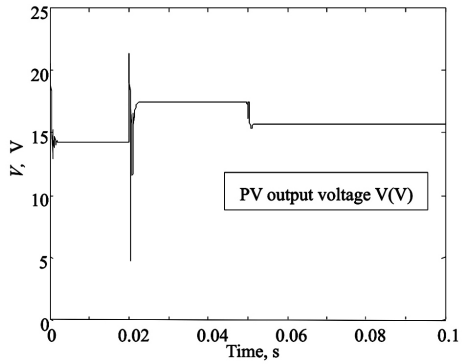

b

Fig. 8. *Variation of: a – PV output power and dc/dc converter output power, and b – PV output voltage for a step change on irradiation and temperature from 100 W/m^2 to 1000 W/m^2 and 29818 K to 320.18 K respectively*

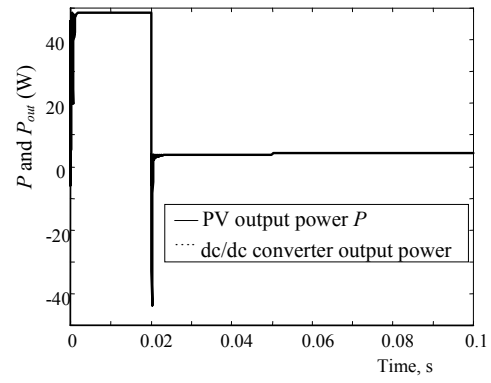

a

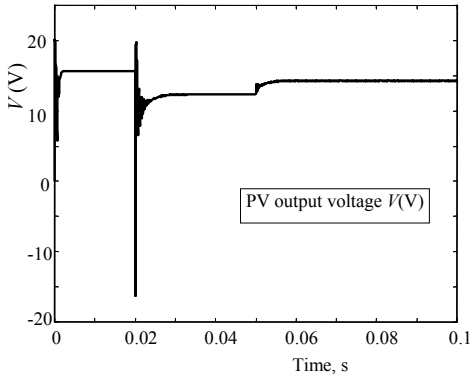

b

Fig. 9. *Variation of: a – PV output power and dc/dc converter output power; b – PV output voltage for a step change on irradiation and temperature from 1000 W/m² to 100 W/m² and 320.18 K to 298.18 K respectively*

In Fig. 8, *a* and 9, *a* the variation of instantaneous PV power *(P)* and dc/dc converter output power for a step change of temperature and solar irradiance are shown. And the Fig. 8, *b* and 9, *b* give the variation of PV output voltage for a step change of temperature and solar irradiance.

The optimum values of PV output voltage, instantaneous PV power and dc/dc converter output power obtained by simulations are assembled in Table 3.

Table 3

Simulated quantities V_{mpp}, P_{mpp}, P_{out} and η for different values of λ and T

Values of λ (W/m²) and T (K)	**Optimum voltage V (V)**	**Optimum power P (W)**	**Optimum power P_{out} (W)**	**Efficiency η (%)**
λ = 100 and T = 298.18	14.25	4.396	4.205	96.66
λ = 1000 and T = 298.18	17.41	54.83	51.99	94.82
λ = 1000 and T = 320.18	15.66	48.64	45.95	94.47
λ = 100 and T = 320.18	12.31	3.717	3.549	95.48

To watch Tables 2 and 3, then Fig. 8 and 9, it is clear, on one hand, that the average voltage (V), instantaneous PV power (P) and dc/dc converter output power (P_{out}) are very close to their optimal values V_{mpp}, P_{mpp} and P_{outmpp}. And on the other hand, the values obtained by simulation coincide with their obtained by programming.

The losses in the dc/dc converter varies from 0.168 W to 3.04 W for λ =100 W/m², T = 320.18 K, and λ = 1000 W/m², T = 298.18 K respectively. They can be minimized for adequate choices of the component of dc/dc converter.

The simulations of the MPPT show that the system is stable. The oscillations about the computed optimal operating point are due to the switching action of the dc/dc converter. The transients between operating points are natural for a dynamic system which is controlled by a PI type controller.

Conclusion

In this paper, a method that forces a photovoltaic panel to operate at its maximum power point under variable temperature and irradiation conditions is developed. This method is tested by simulations in Matlab software. It has been concluded that the method was able to track the irradiance and the temperature level change rapidly. The PI regulator used in this work for controlling the boost dc/dc converter in order to get the system operating at the PV maximum power is synthesized by frequencial synthesis using Bode method. So, we have developed a transfer function of global model using a small signal method by taking into account the losses in the dc/dc converter. Simulations show that the regulation is robust against disturbances.

References

1. Hohm D., Ropp M. Comparative study of maximum power point tracking algorithms // Progr. photovoltaics: Res. Appl. 2003. No. 11. P. 47-62.

2. Salas V., Manzanas M.J., Lazaro A. The control strategies for photovoltaic regulators applied to stand-alone systems // 28th annual conference of the IEEE Industrial Electronics Society, Sevilla. 2002. Vol. 4. P. 3274-3279.

3. Kislovski A., Redl R. Maximum power-tracking using positive feedback // Proceedings of IEEE Power Electronics Specialist Conference. 1994. P. 1065-1068.

4. Wolf S., Enslin J. Economical, PV maximumpower point tracking regulator with simplistic controller // Proceedings of IEEE Power Electronics Specialist Conference. 1993. P. 581-587.

5. Hiyama T., Kitabayashi K. Neural network based estimation of maximum power generation // IEEE Trans. Energy Convers. 1997. Vol. 12. P. 241-247.

6. Salhi M., El-Bachtiri R. A PI regulator synthesis for tracking the optimal operating point of photovoltaic system supplying a battery // World renewable energy

congress IX (WREC-IX), RT 15 (CD proceeding). Florence. Italy. 19-25 August. P. 515 (abstract), 2006.
7. Salhi M., El-Bachtiri R., Matagne E. Boost dc/dc converter control for tracking the maximum power of PV system supplying a battery // Conference on Systems and Control (CSC). Marrakech, Morocco, May 16-18, 2007.
8. Min Chen, Gabriel A. Rincon-Mora. Accurate Electrical Battery Model capable of Predicting Runtime and I-V Performance // IEEE Transactions on Energy Conversion. June 2006. Vol. 21. No. 2. P. 504-511.
9. Eakburanawat J., Boonyaroonate I. Development of a thermoelectric battery-charger with Microcontroller-based maximum power point tracking technique // Applied Energy. 2006. Vol. 83. P. 687-704.
10. Vachtsevanos G., Kalaitzakis K. A hybrid photovoltaic simulator for utility interactive studies // IEEE Trans. Energy Conv. June 1987. Vol. EC-2. P. 227-231.
11. Jaboori M.G., Saied M.M., Hanafy A.A. A contribution to the simulation and design optimization of photovoltaic systems // IEEE Trans. Energy Conv. Sept 1991. Vol. 6. P. 401-406.
12. Mohan N. et al. Power Electronics-Converters, Applications and Design. New York: Wiley, 1989.
13. Salhi M., El-Bachtiri R. Evaluation des pertes dans un convertisseur dc/dc utilisé pour la poursuite du point à puissance maximale dans un panneau photovoltaique alimentant une batterie // Colloque international sur les energies renouvelables (CER'2007). Oujda, Maroc. 4-5 Mai. 2007.
14. Maret L. Regulation automatique. Lausanne: Presses polytechniques romandes, 1987.

THEORETICAL AND EXPERIMENTAL STUDY OF CdS

K. Ouari, N. Benramdane*, Z. Kebbab*, A. Bouzidi*
H. Tabet-Drraz, R. Desfeux***

[*]Laboratoire d'Elaboration et de caractérisation des matériaux, département d'électronique,
Université Djillali Liabes, BP89, Sidi Bel Abbès, Algérie, E-mail: ouari_k@yahoo.fr

[**]Laboratoire de Physico-Chimie des Interfaces et Applications, Université d'Artois,
Faculté Jean Perrin, Rue Jean Souvraz, SP18, 62307 Lens, France

Received: 1 Oct, accepted: 6 Nov 2007

In the present paper, we investigate theoretically and experimentally the structural and optical properties of wurtzite (WZ) CdS semiconductor. The reflectance and transmittance spectra in the [1.5-3.5] eV range of a thin CdS film prepared by spray pyrolysis has been carried out. The first principles full potential linearized augmented plane wave (FPLAPW) method has been utilized to complete the study.

Keywords: structural materials, photovoltaic effect in semiconductor structures, FPLAPW method, spray pyrolysis technique, wurtzite CdS.

Kheira Ouari

Organization(s): Université de Sidi Bel Abbès.
Education: Université de Sidi Bel Abbès, Faculté des sciences et sciences de l'ingénieur, Engineer (1992-1996), Magister (2001-2004).
Experience: Teaching in university, member in research laboratory.
Main range of scientific interests: microelectronic**,** semiconductor, photo voltaic.
Publications: Theoretical and experimental study of wurtzite CdO (Communication). N. Benramdhane, K. Ouari, Z. Kebbab, A. Bouzidi, H. Boudaoud, R. Desfeux. Drip XI (Beeging chine).

Introduction

Cd-based II-IV semiconductor compounds are of considerable interest due to their applications in solar cells, optical detectors, field effect transistors and optoelectronic devices [1, 2]. Among these materials, CdS thin films are regarded as one of the most promising materials for heterojunction thin film solar cells. Wide bandgap CdS (E_g = 2.4 eV) has been used as a window material together with several semiconductors such as CdTe, Cu_2S, InP and $CuInSe_2$ with 14-16 efficiency [3, 4]. Depending on the growth temperature, it can stabilise in both zinc-blende (below 150 °C) or WZ phases (above 170 °C) [5, 6].
In this work, structural and optical properties of WZ CdS films grown using spray pyrolysis technique have been studied both experimentally and theoretically. This paper describes a combinatoric exploratory approach to bulk and thin film of CdS, combining theory and experimentation.

Experimental details

CdS thin films were prepared on glass substrates by spray pyrolysis technique. The experimental set-up is similar to that described in Ref. [7]. The glass substrates were cleaned with freshly prepared chromic acid, detergent solution and distilled water. The spray solution consisting of 0.05 M $CdCl_2$ and 0.05 M CH_4N_2S were dissolved in bi-distilled water. Compressed air of pressure 6 N/cm^2 was used as a carrier gas with a solution flow of 5 cm^3/min. The substrate temperature was fixed at 350 °C and controlled through a thermocouple (Chrome-Nickel). Structural characterisation was carried out at room temperature in the θ-2θ scan mode using a Rigaku Miniflex diffractometer (Cukα, radiation, λ = 1.5406 Å). Transmittance and reflectance were measured in the wavelength range of [1.5-3.5] eV using a UV-Visible – NIR JASCO type-570 double beam spectrophotometer.

Computational details

Theoretical calculations were performed using the FPLAPW method [8] based on the density-functional theory (DFT) [9, 10]. The exchange-correlation energy of the electrons is described in the local-density approximation (LDA) using the Perdew-Zunger scheme [11] as implemented in the WIEN 97 code [12]. Basis functions were expanded in combinations of spherical harmonic functions inside non-overlapping spheres surrounding the atomic sites (muffin-tin spheres) and in Fourier series in the interstitial region. In the muffin-tin spheres (MTS), the *L*-expansion of the non-spherical

potential and charge density was carried out up to $L_{MAX} = 12$. Consequently, 2554 plane waves have been utilized, and the energy cut off was set such as $R_{MT} \cdot K_{MAX} = 8$ (K_{MAX} being the maximum modulus for the reciprocal lattice vector and R_{MT} is the radius of the MTS). Furthermore, we adopted the value of 1.8 a.u for S and 2 a.u for Cd.

The electronic configuration of CdS is: Cd: [Kr] $4d^{10}5s^2$ and S: [Ne] $3s^23p^4$. In WZ, the Cd atoms are located at (0,0,0), (1/3,2/3,1/2) and the S atoms are located at (0,0,*u*), (1/3,2/3,1/2+*u*). The internal parameter *u* was fixed to the ideal value of a WZ crystal.

Results

Fig. 1 shows the X-ray diffraction pattern of our CdS film which indicates that the deposited film is polycrystalline with a hexagonal WZ structure of spatial group 186 ($P6_3/mc$). The peaks were indexed by comparing our measured inter-reticular distances $d_{(hkl)}$ and their intensities *I* to the 41-104 JCPDS X-ray powder data file. The lattice constants *a* and *c* were determined by using the following quadratic relation:

$$d_{hkl} = \frac{a}{\sqrt{\frac{4}{3}(h^2 + k^2 + hk) + \frac{l^2 a^2}{c^2}}}, \quad (1)$$

and were found to be 4.117 Å and 6.696 Å respectively. These values are in good agreement with previous results [13].

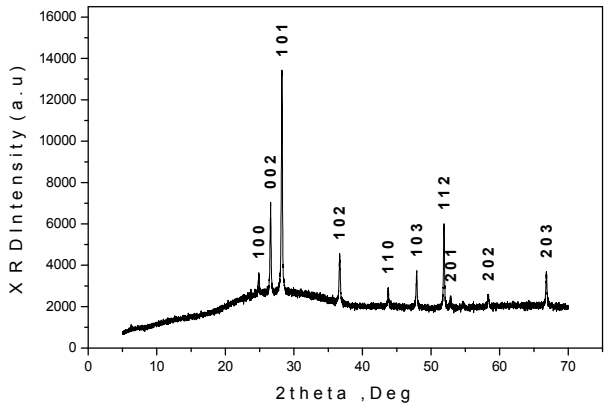

***Fig. 1**. XRD spectra of wurtzite CdS*

For reasons of comparison, we have also calculated theoretically the structural properties of our compound. The total energies were calculated in two steps. First, we varied the *c*/*a* ratio at a fixed volume and a stable *c*/*a* ratio was obtained by a parabolic fit. The equilibrium *c*/*a* value was found to be 1.626. In the second step, we fixed the equilibrium *c*/*a* and we varied the volume which was then fitted to Murnaghan's equation of state [14] as given by:

$$E(v) = \frac{B_0 v}{B_0'}\left[\frac{(v_0/v)^{B_0'}}{B_0' - 1} + 1\right] + cst \quad (2)$$

B and *B*′ being the bulk modulus and its pressure derivative at the equilibrium volume V_0.

Fig. 2 shows the total energy as a function of the volume for wurtzite CdS. The calculated lattice parameters are *a* = 4.108 Å and *c* = 6.679 Å which are found to be less than the experimental values because of LDA. The LDA calculations show a number of systematic shortcomings.

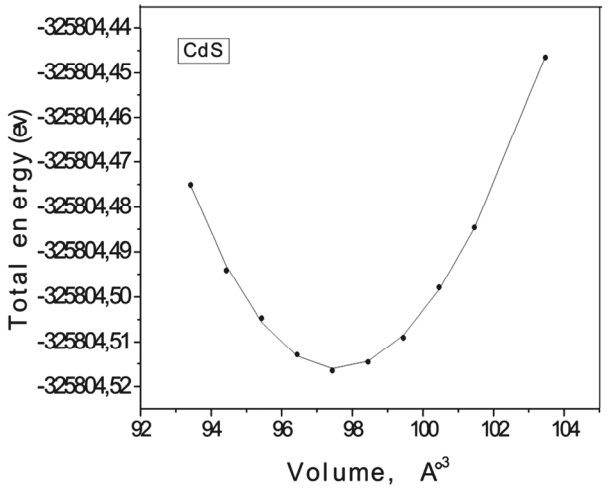

***Fig. 2.** Calculated total energy as a function of volume of CdS*

In the Fig. 3, we show the band structure of CdS obtained by the FPLAPW method. The calculated band gap is found to be only 1 eV. However, the experimental gap of CdS is 2.5 eV [15]. It is well known that the LDA based FLAPW underestimates gaps by 50 % or more, especially for II–VI compound semiconductors [16].

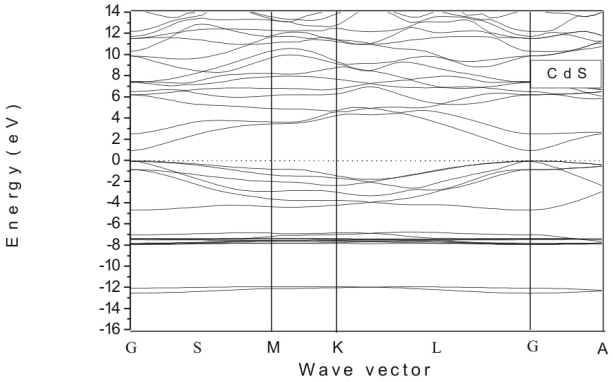

***Fig. 3.** Band structure for CdS in wurtzite structure*

In order to understand the general feature of the bonding in this compound, the total and partial densities of states (DOS and PDOS) integrated over the atoms and the interstitial region outside the MTS are shown in Fig .4.

The total DOS presents three regions: the lower band at around -8 to -7 eV is derived from the cadmium 4*d* states. The bands between -5 eV and the valence band maximum are mostly derived from the S *p*-states hybridised with Cd *s*-states. The states of the conduction band are mainly S *p*-states hybridised with Cd *s*-states with only small admixture of Cd 4*d*-states.

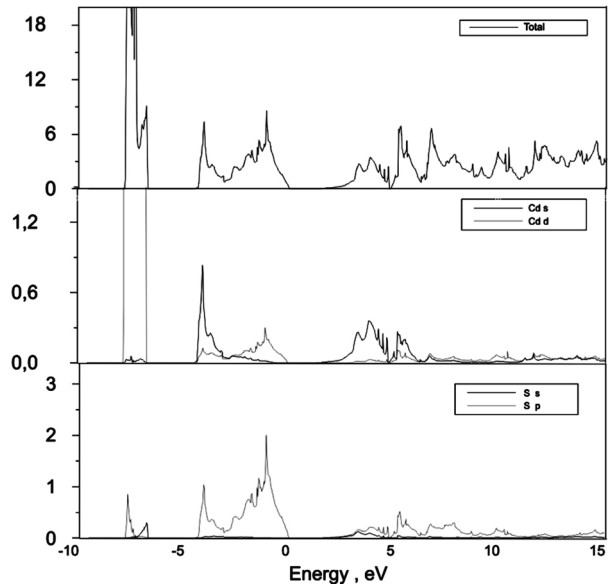

Fig. 4. *Total and partial density of states (DOS and PDOS) for CdS*

The total valence charge density is displayed along the Cd-S bonds and in the (110) plane containing Cd and S atoms (Fig. 5). The charge transfer gives rise to the ionic character of CdS similar to that found in other II-VI compound semiconductors. The driving force behind the displacement of the bonding charge is the greater ability of S to attract electrons towards it due to the difference in the electronegativity between Cd and S.

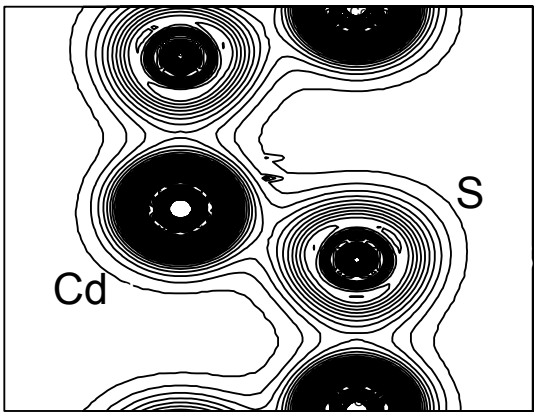

Fig. 5. *Contour plot of the total valence charge density in the (110) plane of CdS*

In order to investigate the optical properties of CdS, we used a mesh of 200 irreducible K points in the Brillouin zone and we shifted the conduction bands. The imaginary part of the dielectric constant $\varepsilon_2(E)$ was calculated by considering summation over all conduction and valence bands and over the first Brillouin zone. The real part $\varepsilon_1(E)$ was then obtained from $\varepsilon_2(E)$ by the use of the Kramers-Kronig relations. The other parameters follow straightforwardly.

Experimentally, optical transmittance and reflectance for CdS film were measured in the range [1.5-3.5] eV using a JASCO V-570 spectrophotometer. Fig. 6 shows the transmittance and reflectance spectra.

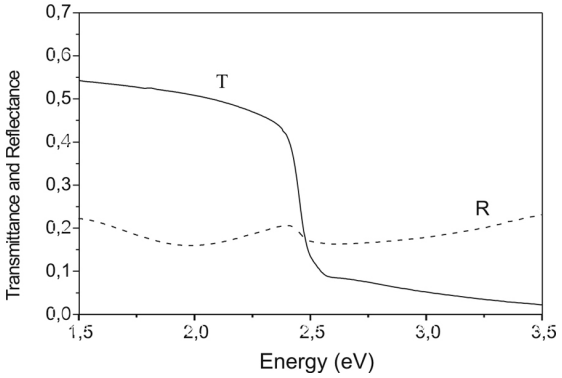

Fig. 6. *Transmittance and reflectance of CdS film*

T is in order of 5 % for higher energies values, and it increases to 50 % for low energy. *R* roughly levels off in the range [1.5, 2.5] eV energy and it increases from 2.5 to 3.5 eV. Similar behaviour in the transmission and reflectance spectra of CdS films prepared by other techniques have been reported in the literature [17-19]. The absorption coefficient α was calculated from the relation [20]:

$$T = \frac{(1-R)^2 e^{-\alpha d}}{R^2 e^{-2\alpha d}}, \qquad (3)$$

R and *T* being the spectral reflectance and transmittance and *d* the film thickness. The value of the energy band gap was calculated using the formula:

$$(\alpha h\nu)^2 = A(h\nu - E_g), \qquad (4)$$

where *A* is a constant which is related to the effective masses associated with the bands and E_g is the bandgap energy. Plot of $(\alpha h\upsilon)^2$ versus the photon energy $h\upsilon$ for film is shown in Fig. 7.

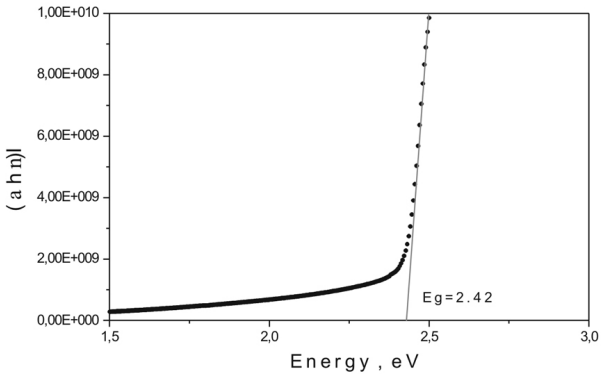

Fig. 7. *$(\alpha h\nu)^2$ vs. $(h\nu)$ plot for CdS film*

The linearity of the plot indicates that the material is of direct band gap nature. Extrapolation of linear portion of the graph to the energy axis at $\alpha = 0$ gives the value of the band gap energy, which is found to be 2.42 eV, in good agreement with Pal et al [21].

Fig. 8, 9 and 10 show the theoretical and experimental curves respectively in [1.5-3.5] eV range.

Fig. 8 shows the theoretical and experimental absorption coefficient. Good agreement is found between theory and measurement. However, due to the polycrystalline structure of the thin film, extra absorption of light occurs at the grain boundaries. This leads to non-zero value of α for photon energies smaller than the fundamental absorption edge.

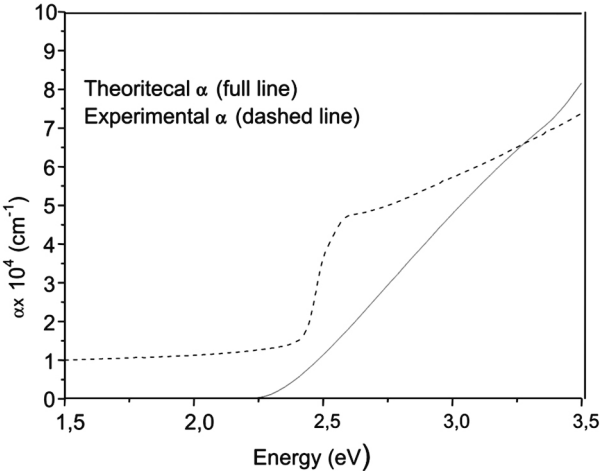

Fig. 8. *Theoretical and experimental α(E)*

In Fig. 9 the theoretical and experimental refractive index are presented. It is observed that for the experimental index there is one well-defined maximum. This observation is accounted to the particular structure of the film and it thickness [22, 23]. The peak value of the experimental of the refractive index is 2.45. The values of theoretical *n* increase with increasing photon energy. The smaller *n* experimental values in the range [2, 3.5] eV may be due to the polycrystalline structure of the film investigated.

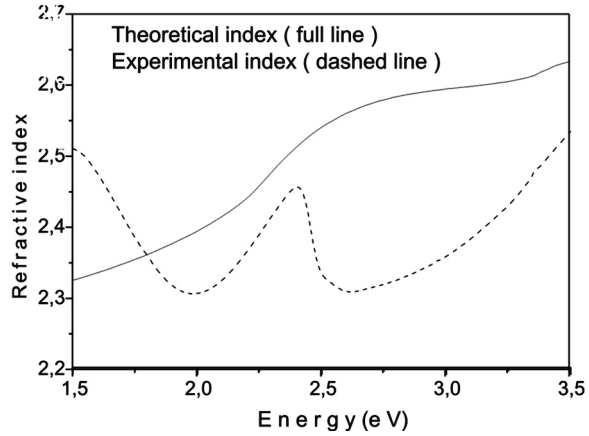

Fig. 9. *Theoretical and experimental n(E)*

Finally, Fig. 10 shows the theoretical and experimental reflectance. A good correspondence of the measured reflectance spectrum and the theoretical model in the range [2.5, 3.5] eV, only minor difference can be observed. Due to the transparency of the film, experimental *R* roughly levels off below 2.5 eV.

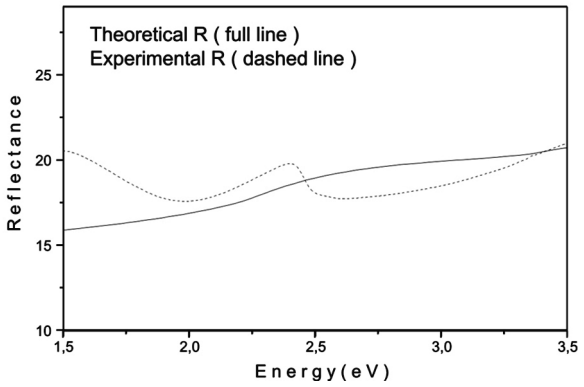

Fig. 10. *Theoretical and experimental R(E)*

Conclusion

In summary, we have presented a study of structural and optical properties of bulk and thin film of WZ CdS. The main conclusion can be summarized as follows:

– WZ CdS is a semiconductor with a direct optical band gap of about 2.42 eV witch is located at the Γ point of the BZ.

– The density of states on both sides of the gap has predominantly *s-p* character with only small admixture of *s*-states.

– The calculated electron charge distribution indicates an ionic character.

– The film exhibit high transmittance (more than 50 %) and low reflectance in the visible-near infrared region (2.48, 1.127) eV region, making the film suitable for optoelectronic devices, for instance as window layers in solar cells.

– The absorption coefficient α and refractive index *n* values ad reflectance *R* using the optical measurement are found to agree well with the results obtained using theoretical calculations.

References

1. Das S., Datta S.K., Saka H. Structure of vacuum, evaporated $Cd_xZn_{1-x}S$ thin films // Phys. Stat. Sol. 1993. Vol. a, No. 136. P. 251.

2. Touskova J., Kindl D., Tousek J. Preparation and characterization of CdS/CdTe thin film solar cells // Thin Solid Films // Phys. Stat. Sol. 1997.Vol. 293, No.142. P. 272-276.

3. Su B., Choy K.L. Growth behavior and microstructure of CdS thin films deposited by an electrostatic spray assisted vapor deposition (ESAVD) process // Thin Solid Films. 2001. Vol. 338. P. 9-14.

4. Wu X., Keane J.C., DeHart R.G., Albin D.S., Duda A., Gessert T.A., Asher S., Levi D.H., Sheldon P. Proceeding of the 17th European Photovoltaic Solar Energy Conference, Munich, Germany, 2001. P. 995.
5. Landolt-Bornstein: Numerical Data and Functional Relationships in science and technology, edited by O. Madelung, M. Schultz, and H. Weiss (Springer–Verlag, Berlin, 1982). Vol. 17b.
6. Vankar V.D., Das S.R., Prem Nath, Chopra K.L. Structure of vacuum, evaporated $Cd_xZn_{1-x}S$ thin films // Phys. Stat. Sol. 1978. Vol. 45. P. 665-669.
7. Chalapathy R.B.V. PhD Thesis, Sri Venkateswara University, Tirupati, India, 2001.
8. Jansen H.J.F., Freeman A.J. Total-energy full-potential linearized augmented-plane-wave method for bulk solids: Electronic and structural properties of tungsten // Phys. Rev. 1984. Vol. B, No. 30. P. 561.
9. Hohenberg P., Kohn W. One-particle properties of an inhomogeneous interacting electron gas // Phys. Rev. 1964. Vol. B, No. 136. P. 864.
10. Sham L.J., Kohn W. One-particle properties of an inhomogeneous interacting electron gas // 1965. Vol. B, No. 145. P. 561.
11. Perdew J.P., Wang Y. Accurate and simple analytic representation of the electron-gas correlation energy // Phys. Rev. 1992. Vol. B, No. 45. P. 13244.
12. Blaha P., Schwarz K., Luitz J. WIEN97, Vienna University of Technology, Vienna, 1997.
13. Razik N., Mater J. Use of a standard reference material for precise lattice parameter determination of materials of hexagonal crystal structure // Sci. Lett. 1987. Vol. 6, No. 12. P. 1443.
14. Murnaghan F.D. The compressibility of media under extreme pressures // 1944. Vol. 30. P. 244-247.
15. Polmann Johannes, Vogel Dirk., Krüger Peter. Self-interaction and relaxation-corrected pseudopotentials for II-VI semiconductors // Phys. Rev. 1996. Vol. B, No. 54. P. 5495.
16. Cardona M., Christensen N.E., Lew Yan Voon L.C., Willatzen M. Terms linear in k in the band structure of wurtzite-type semiconductors // Phys. Rev. 1996. Vol. B, No. 53. P. 10703.
17. Moon Byung-Sik, Lee Jae-Hyeong, Jung Hakkee. Comparative studies of the properties of CdS films deposited on different substrates by R.F. sputtering // Thin Solid Films. 2006. Vol. 511-512. P. 299-303.
18. Senthil K., Mangalaraj D., Narayandass Sa., Adachi Sadao. Mat. Sci. Eng. B 78, 53 (2000).
19. Achour A., Al-kadry N., Mahmoud S.A. Defect distribution in electron-irradiated CdS materials // Thin Solid Films. 1995. Vol. 238. P. 110-114.
20. El Manduh Z.S., Selim M.S. Physical properties of vanadium pentoxide sol gel films // Thin Solid Films. 2000. Vol. 371. P. 259-263.
21. Pal U., Silva-Gonzalez R., Martinez-Montes G., Gracia-Jemenez M., Vidal M., Torres S. Optical characterization of vacuum evaporated cadmium sulfide films // Thin Solid Films. 1997. Vol. 345. P. 345-350.
22. Yamaguchi K., Nakayama N., Matsumoto H., Iegami S. 8.5 % efficient screen-printed CdS/CdTe solar cell produced on a 5×10 cm^2 glass substrate // Appl. Phys. 1977. Vol. 16. P. 1203.
23. Tepehan F., Ozer N. Sol. En. Mater. // Sol Cells 30, 353 (1993).

SPECTROSCOPIC FT-IR STUDY OF TiO_2 FILMS PREPARED BY SOL-GEL METHOD

A. Merouani, H. Amardjia-Adnani

Department of physics, Laboratory of Dosage, Analyse and Characterization in high Resolution,
Ferhat Abbas University , Sétif, 19000, ALGERIA

E-mail: adnani2dz@yahoo.fr; E-mail: amerouani2001@yahoo.fr Tel/ Fax: 00213 36 92 51 33

Received: 26 Jul 2007; accepted: 30 Aug 2007

TiO_2 thin films used like a photoanode in dye sentisitized solar cells (DSSC), were prepared on conductor glass (FTO) by sol-gel method. They were studied by FT-IR spectroscopy in order to determinate a film composition and structural properties. The results showed that the thin layers of TiO_2 achieved with speed of 16 cm/min and annealed at 400 C° present important morphological and structural properties.

Keywords: structural materials; solar energy; TiO_2, sol-gel, dip-coating, DSSC.

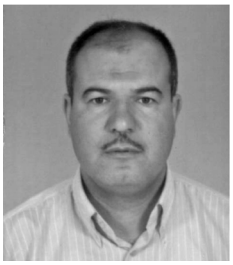

Merouani Amar

Organization: Doctorant.
Education: Electrochemical Engineer, 1989, Ferhat abbas, University(UFA), Master, 2004, UFA.
Experience: Member of team's research, since 2001.
Main range of scientific interests: renewable energy.
Publications: 2.

Introduction

These last years the protection of the environment became major preoccupation. Numerous ways of research moved therefore toward the investigating in the renewable energies, of which the solar energy, nevertheless on a terrestrial scale applications of the solar generators remain limited because of the method of the photobattery production that is laborious and difficult, therefore too dear. Scientists wanted to find an alternative to constituted traditional solar cells of semiconductor as silicon, who permits the conversion of light in electricity. These materials although steady must be to elevated temperature constituted of an atom network very pure, what returns their costly manufacture and therefore their difficult on a big scale use. It appears however laborious to increase the output or to reduce costs of production. The solar cell of Graetzel or dye cell appear then in 1990, to palliate to this problem. The professor Michael Graetzel of Swiss Federal Institute of Technology, put to the point for the first time a solar cell that uses the principle close to the photosynthesis. It replaces the mechanism used by plants to transform rays of the sun in electric energy.

Our work has for objectives, the survey and the characterisation of materials nanocrystallines semiconductors that is used in the Graetzel cell as the TiO_2 [1]. TiO_2 film can be prepared by methods such as ion beam assisted deposition (IBAD) or chemical vapor deposition etc… However, it's difficult and expensive to deposit a uniform layer of TiO_2 on the substrate with complex shapes or geometry by these methods. Sol-gel technology is a low temperature method of preparing film from chemical routes. The advantages of using a sol gel dip coating technique are that it is independent of the substrate shape, and can achieve a good control of surfaces properties such as composition, thickness and topography [2]. Our gait consists in synthesizing the oxide of titanium by sol gel way, then to make some thin layer deposits on supports in conductor glass (FTO) with different speeds of immersion, and in very controlled humid atmosphere, with technical deep-coating. In order to study morphologic and microstructuralesproperties of our samples, we have proceed to the application of FT-IR analysis method.

Experimental details

Film preparation

Titanium isopropoxyde ($Ti(OC_3H_7)_4$ from Aldrich 97 %, was used as TiO_2 precursor [3]. First, 1.6 ml of $Ti(OC_3H_7)_4$ was dissolved in 4.65 ml of isopropanol. The solution was let under agitation to plug closed during 10 min with heating to 60 °C. Then one adds 5.15 ml of acetic acid, while letting agitate during 15 min under heating to 60 °C. One finally adds 12 ml of methanol and one lets agitate during 2 h. The second phase of synthesis consists in preparing the thin layers of TiO_2 by

dip-coating process. The deposit of the thin layers of TiO_2 is achieved on blads of conductor glass (Fluor Tin Oxide, FTO) in device dip-coating. This device (achieved in our laboratory) is constituted of a surrounding wall squared in glass permitting nevertheless the passage of a flux of the Ar gas through two cracks on the lateral faces. The Humidity inside it limps is controlled by thermohygrometre (C62916, Bioblock Scientific, French), because the conditions of deposit influence on the quality of layers. It limps is surmounted of a motor permitting the control of the speed of immersion and withdrawal of the sample in the solution. The dip-coating sol-gel process consist in the immersion to a weak speed of an oblong plate of glass conductor (FTO) substrate [4]. Inside the solution of TiO_2 and to make take it with the same speed. For our work we achieved some thin layers with speeds of immersion of: 4, 8, 12, and 16 cm/min. The obtain samples were dried at 100 °C for 10 min, after they are annealed at 400 °C for 1 h.

Surface characterization

The film thickness and refractive index were measured by spectroscopic ellipsometre SOPRA GESP5, and the IR spectra of the samples on silicon wafers were recorded on the Nicolet 6700 FT-IR spectrometer.

Results and discussion

Formation of TiO_2 film

According to the literature [5] a rate of humidity of 20 % and temperature of 25 °C represent the best conditions for the adhering, transparent and homogeneous deposit obtaining. For the same conditions of deposit and of anneal, we varied the speed of immersion in order to study the effect of this last on thickness of layers, on their refractive index, on their structures and morphology. The thickness of the TiO_2 film is very important for the transportation of electrons as well as adsorption of the dye and it's another crucial factor contributing to cell efficiency. Although a thinner film has high transmittance, and the thicker ones have high dark current, it's workable and necessary to achieve optimum film thickness for energy conversion efficiency [6]. The thickness of the compacts films obtained from a sol gel in different speeds was measured by Ellipsometre according to the Table 1.

Table 1

Indicate the variation of refractive index and thickness of layers of TiO_2 according to the speed of immersion

The speed (cm/min)	4	8	12	16
Refractive index	1.8	2.15	2.40	2.55
Thickness (nm)	113.63	115.35	121.27	123.55

One also notices that when the speed increases the refractive index increases also. This proportionality between (speed, thickness, refractive index) is bound to the weight. That is to say that more the speed is big and more the set down matter quantity on our samples is big. Therefore, more thickness of layers is important more the refractive index is important and more matter is dense. This densification of layers is obtain after annealed it [7]. Nanostructures layers of TiO_2 obtain by sol-gel process are spongy, indeed they are constituted of grains of gleams and of holes or empty.

This densification is therefore the report between the total volume of the layer, that it's thickness multiplied by the surface of the layer and the volume of the nanocrystal of TiO_2. Thus, if we have to choose the best deposit for the photovoltaic use take the case where we have a large domain in the visible where the transmittance is maximal. In our case we will take the case where the speed is 16 cm/min. This case allows the large spectra of light to cross the layer of TiO_2 to arrive to the dye and so to excite him.

IR Study 3-2

The IR spectra of TiO_2 films deposited by dip-coating at 16 cm/min, dried at 100 °C and annealed at 300, 400 and 500 °C under oxygen atmosphere are presented in Figs.1, 2, 3 and 4.

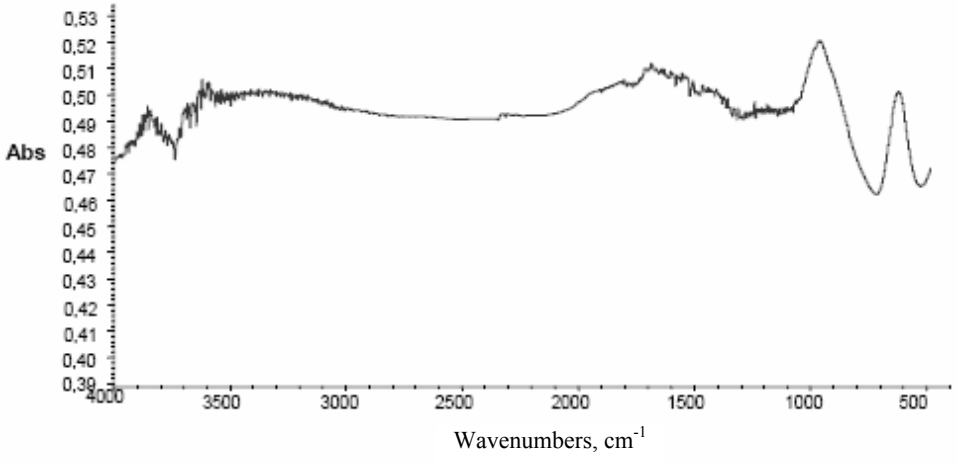

Fig. 1. *FT-IR spectra of TiO_2 prepared by dip-coating as deposited at 16 cm/min, and dried at 100 °C*

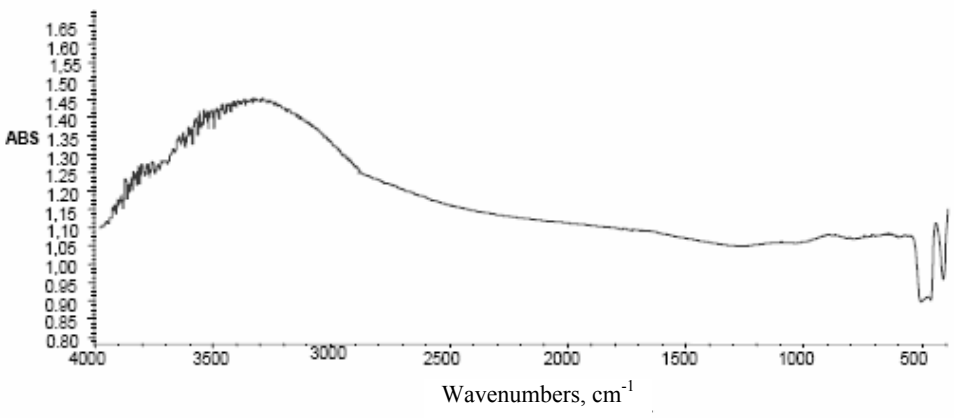

Fig. 2. *FT-IR spectra of TiO_2 prepared by dip-coating as deposited at 16 cm/min, dried at 100 °C and annealed at 300 °C*

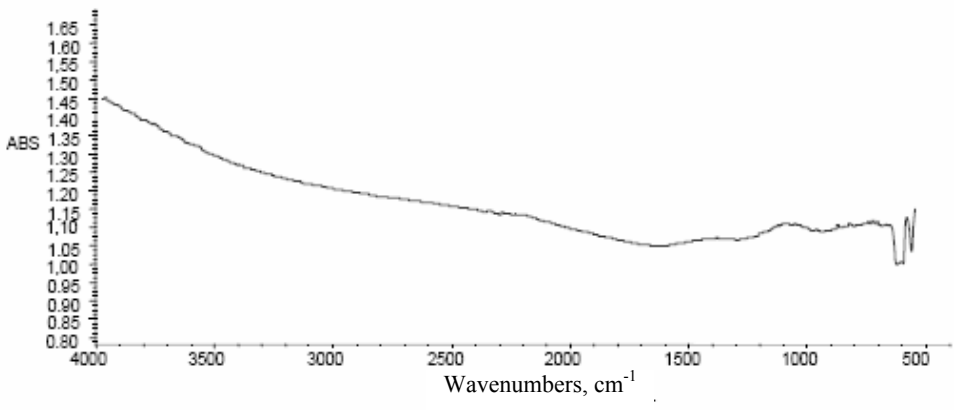

Fig. 3. *FT-IR spectra of TiO_2 prepared by dip-coating as deposited at 16 cm/min, dried at 100 °C and annealed at 400 °C*

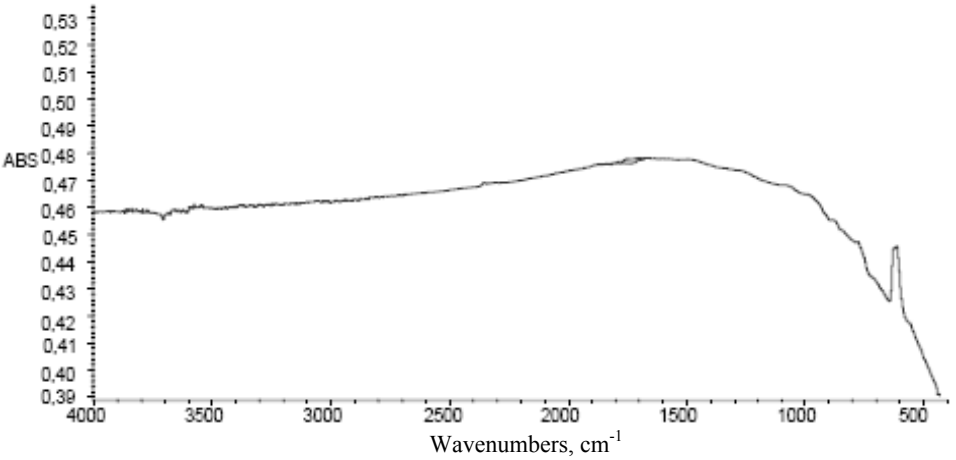

Fig. 4. *FT-IR spectra of TiO_2 prepared by dip-coating as deposited at 16 cm/min, dried at 100 °C and annealed at 500 °C*

For the sample prepared at 16 cm/min and dried at 100 °C (Fig. 1), the absorption bands at 500 cm^{-1} are assigned for aliphatic bonds of type C-C and the absorption bands between 560 and 700 cm^{-1} are assigned for O-N=O deformation which are very intense in IR spectra. The absorption bands at 1097 cm^{-1} are assigned for C-O-Ti. The acetyl and hydroxyl bonds were determinate at 1300 and 3600 cm^{-1} successively. For the sample prepared at 16 cm/min, dried at 100 °C and annealed at 300 °C (Fig. 2), we let's notice the presence of hydroxyl bonds and the disappearence or the shrinkage of organic origin. But the important fact is the apparition of pick at 430 cm^{-1} assigned for Ti-O-Ti bonds.

Let's note that J.Sabataityté et al had determined the strip of absorption of the Ti-O-Ti bonds at 440 cm^{-1} [8]. We find also the O-N=O bonds. Further annealing at

temperature of 400 °C, (Fig. 3) we note the disappearance of hydroxyl bonds, what confirms himself distinctly in Fig. 4, for the sample prepared at 500 °C and where one only finds the Ti-O-Ti bonds.

Conclusion

Through results of survey spectroscopic in FT-IR, we notice that our samples undergo amore and more important purification, every time hat one increases the temperature until 500 °C. We can conclude that the nonporous film of TiO_2 in thickness is 123.55 and have been prepared by sol-gel method with speed of immersion of 16 cm/min with and annealed at 500 °C has a perfect crystalline structure. The formation of the Ti-O-Ti bonds in films is observed after annealing at 300 °C. However the film became crystalline after annealing at 500 °C. But we show the sample prepared at 400 °C present a good absorbance (1.45) than a sample prepared at 500 °C (0.45).

Acknowledgements

The authors wish to acknowledge the financial support from the both department of Physics and Genius Process of Ferhat Abbas University. Our consideration for team of Unit of Development of Silicon Technique , UDTS, Algiers.

References

1. J. Kruger, R. Plass, L.Cevey, M.Piccirelli, M.Graetzel and U.Bach, Appl Phys Lett. (121). 2001.P. 2085-2087.
2. J. Xiaoliu, D.Zhiyang, F. Shi, Y. Jicai , Thin Solid Films 429 (2003) P. 225-230.
3. M. Takahashi, K. Tsukigi, T. Uchino, T. Yoko, Thin Solid Films 388 (2001) P. 231-236.
4. J.P. Chatelon, C.Terrier, E.Bernstein, R. Berjoan, and J.A. Roger., Thin Solid Films, 247 (1994) P. 162-168.
5. W.P.Tai , J. H. Oh Sensors and Actuators B85 (2002) P 154-157.
6. S.Dai, J. Weng, Y. Sui, C.Shi, Y.Huang, S.Chen, X.Pan, X.Fang, L.Hu, F.Kang, K.Wang, Solar Energy Materials and Solar Cells 84 (2004) P. 125-133.
7. G.P. Smestad, S. Spiekermann, J. Kowalik, C.D. Grant, A.M. Schwartzebrg, J.Zhang, L.M. Tolbert, E.Moons, Solar Energy Materials and Solar Cells. 2003. P. 85-105.
8. J. Sabataityté, I.Oja, F.Lenzmann, O.Volobujeva, M.Krunks, C.R. Chimie 9 (2006).

ALGERIA WIND ENERGY RESOURCES

R. Maouedj, S. Bousalem, B. Benyoucef*

Unité de Recherche des Matériaux et Energies Renouvelables (URMER)
BP 119, 13000 Tlemcen, Algérie
*E-mail: ra_maouedj@yahoo.fr

Received: 24 Sept 2007; accepted: 5 Nov 2007

The wind energy is a solar resource of origin, created by the differences in temperature between the sea, the earth and the air like by the variations in temperature between the equator and the poles of planet. Approximately 0.25 % of the total solar radiations are converted into wind power. The wind power knew a very strong growth during the last decade thanks to the advantages which it has for the environment, with the related technological breakthroughs and with the governmental programmes of encouragement in the world.
This article gives a report on the recent developments concerning the conversion systems of the wind power as well as welfare benefits and environmental which are associated there. It presents also a modelling and simulation of a conversion system wind on the sites of Alger, Oran, Tlemcen, Chlef, Djelfa, Tiaret, Tindouf and In Salah (Algeria) by using the weather and radio parameters metric and the determination of the parameters of Weibull *K* and *C* and the power recovered (mean velocities of the wind) according to altitude and of roughness of the site.

Keywords: wind energy, wind conversion system, wind speeds, power

Rachid Maouedj

Organization(s): Tlemcen university, Unit of Research on Materials and Renewable Energies. Tlemcen, URMER, PhD student.
Education: High level degree on physics Tlemcen University, Faculty of sciences (1999-2002), master degree on physics (2003-2005).
Experience: Attached of research to the Unit of Research in Renewable Energies in Saharan Medium URER-MS, Adrar (2006-2008), Scientific research projects: hybrid systems (photovoltaic, wind), application on optic telecommunication in Algeria.
Main range of scientific interests: renewable energies.
Publications: 1 paper in international scientific journal and 2 papers (in press).

Souad Bousalem

Organization(s): Tlemcen University, Unit of Research on Materials and Renewable Energies. Tlemcen (URMER), PhD Student.
Education: High level degree on physics Tlemcen University, Faculty of sciences (1997-2001), master degree on physics (2003-2005).
Experience: Tlemcen University, associate researcher (2006-2007), Scientific research projects: study, modeling and simulation of hybrid systems wind/PV.
Main range of scientific interests: renewable energies: wind and solar.
Publications: 1 paper in international scientific journal (in press).

Pr. Boumediene Benyoucef

Organization(s): Professor at Tlemcen University, Director of the Unit of Research on Materials and Renewable Energies, University of Tlemcen, Faculty of Science, Department of Physics, BP 119, 13000, Tlemcen. Algeria.

Introduction

The estimate of the wind power resources presents a major difficulty. Contrary to the fossil fuel reserves, the quantity of energy available varies with the season and the hour of the day. The wind power of advantage is influenced by topography that solar energy. Moreover, the total quantity of convertible wind power on the territory of a nation depends to a significant degree of the characteristics, the hoped output, the dimensioning and the horizontal distribution of the wind-engines (Tables 1, 2, Fig. 1).

Table 1

Geographical data of the selected sites [1, 2]

Sites	Longitude	Latitude	Altitude (m)	Topographic situation
Alger	03°15′ E	36°43′N	24	Coastal zone
Oran	00°37′ W	35°38′N	90	
Tlemcen	01°17′ W	34°57′N	592	North of the Tellien mountains
Chlef	01°20′ E	36°12′N	143	
Djelfa	03°15′ E	34°40′N	1144	Highlands
Tiaret	01°28′ E	35°21′N	977	
Tindouf	08°06′ W	27°40′N	401	Sahara
In Salah	02°28′ E	27°12′N	268	

Table 2

Weibull, hybrid Weibull parameters [1, 2, 3]

Sites	Roughness (m)	Frequency at V = 0 m/s (%)	Weibull parameters		V (m/s)
			K	C (m/s)	
Alger	0.01	34.0	2.03	5.0	2.9
Oran	0.01	06.0	1.26	4.1	3.6
Tlemcen	0.01	52.0	2.12	4.7	2.0
Chlef	0.01	36.0	1.82	4.5	2.5
Djelfa	0.08	36.5	1.71	4.4	2.5
Tiaret	0.02	20.0	1.74	6.3	4.3
Tindouf	0.00	16.0	1.90	5.4	4.0
In Salah	0.02	23.0	1.68	5.8	4.0

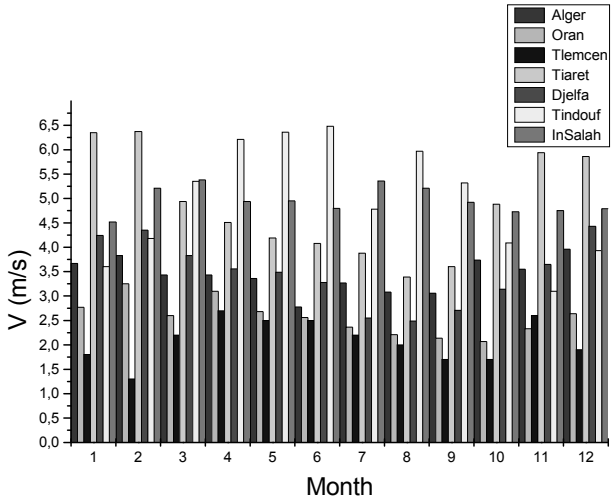

Fig. 1. *Monthly average wind speed*

Power available in the wind spectra [3, 4, 5]

The kinetic energy of a stream of air with mass m and moving with a velocity V is given by

$$E = \frac{1}{2}mv^2 \tag{1}$$

Consider a wind rotor of cross sectional area A exposed to this wind stream. The kinetic energy of the air stream available for the turbine can be expressed as:

$$E = \frac{1}{2}\rho_a v V^2 , \tag{2}$$

where ρ_a the density of air and V is the volume of air parcel available to the rotor.

The air parcel interacting with the rotor per unit time has a cross-sectional area equal to that of the rotor (A_T) and thickness equal to the wind velocity (V). Hence energy per unit time, that is power, can be expressed as

$$P = \frac{1}{2}\rho_a A_T V^3 . \tag{3}$$

From Eq. (3), we can see that the factors influencing the power available in the wind stream are the air density, area of the wind rotor and the wind velocity.

Effect of the wind velocity is more prominent owing to its cubic relation ship with the power.

Variation of the density of the air with the temperature, the pressure and of altitude

Factors like temperature, atmospheric pressure, elevation and air constituents affect the density of air. Dry air can be considered as an ideal gas. According to the ideal gas law [4, 6],

$$pV_G = nRT , \tag{4}$$

where p is the pressure, V_G is the volume of the gas, n is the number of kilomoles of the gas, R is the universal gas constant and T is the temperature. Density of air, which is the ratio of the mass of 1 kilomole of air to its volume, is given by:

$$\rho_a = \frac{m}{V_G} . \tag{5}$$

From Eqs. (4) and (5), density is given by:

$$\rho_a = \frac{mP}{RT} . \tag{6}$$

If we know the elevation Z and temperature T at a site, then the air density can be calculated by:

$$\rho_a = \frac{353.049}{T} e^{\left(-0.034\frac{Z}{T}\right)} . \tag{7}$$

The density of air decreases with the increase in site elevation and temperature as illustrated in Fig. 2-3.The air density may be taken as 1.225 for most of the practical cases. Due to this relatively low density, wind is rather a diffused source of energy. Hence large sized systems are often required for substantial power production.

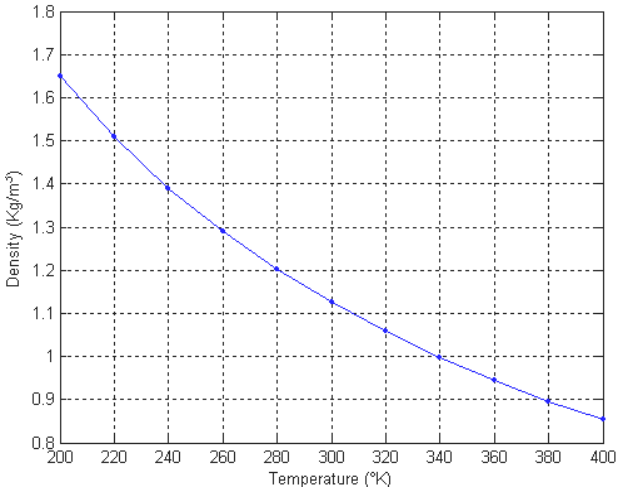

Fig. 2. *Effect of elevation on air density*

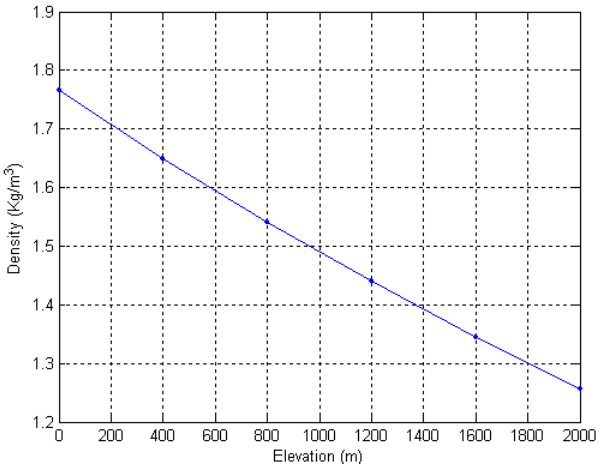

Fig. 3. *Effect of temperature on air density*

Effect of height

The wind shear at ground surface causes the wind speed increase with height in accordance with the expression [6, 7]

$$V_2 = V_1\left(\frac{h_2}{h_1}\right)^{\alpha}, \qquad (8)$$

where V_1: wind speed measured at the reference height h_1; V_2: wind speed estimated at height h_2; α: ground surface friction coefficient.

The friction coefficient is low for smooth terrain and high for rough ones (Fig. 4).

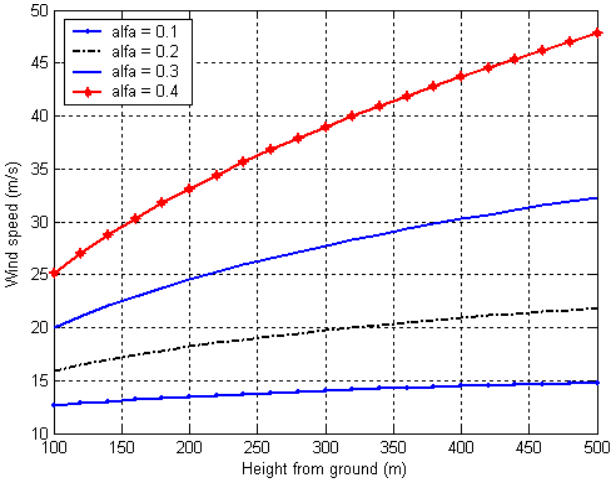

Fig. 4. *Wind speeds variation with height over different terrain. Smooth terrain has lower friction, developing a thin layer above*

The values of α for typical terrain classes are given in Table 3.

Table 3

Friction coefficient of various terrains

Terrain type	Friction coefficient α
Lake, ocean and smooth hard ground	0.10
Foot high grass on level ground	0.15
Tall crops, hedges, and shrubs	0.20
Wooded country with many trees	0.25
Small town with some trees and shrubs	0.30
City area with tall buildings	0.40

Transmission and generator efficiencies

The basic system is then as shown in Fig. 5. We star with the power in the wind, P_w. After this power passes through the turbine, we have a mechanical power P_m at the turbine angular velocity ω_m, which is then supplied to the transmission. The transmission output power P_t is given by the product of the turbine output power P_m and the transmission efficiency η_m [8],

$$P_t = \eta_m P_m. \qquad (9)$$

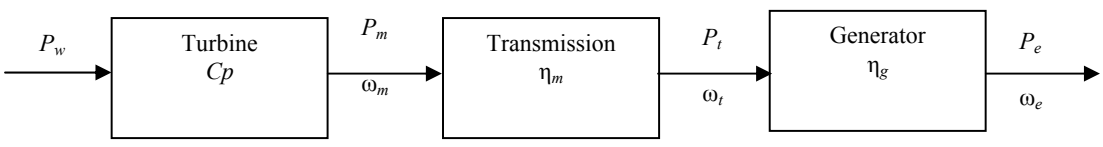

Fig. 5. *Wind electric system*

Similarly, the generator output power P_e is given by the product of the transmission output power and the generator efficiency η_g:

$$P_e = \eta_g P_t. \quad (10)$$

The generator output power P_e can be expressed as:

$$P_e = C_p \eta_m \eta_g P_\omega. \quad (11)$$

At rated wind speed, the rated electrical power output can be expressed as

$$P_{eR} = C_{PR} \eta_{mR} \eta_{gR} \frac{\rho}{2} A V_R^2, \quad (12)$$

where C_{PR} is the coefficient of performance at the rated wind speed V_R, η_{mR} is the transmission efficiency at rated power, η_{gR} is the generator efficiency at rated power, ρ is the air density, and A is the turbine area.

The quantity $C_{PR}\eta_{mR}\eta_{gR}$ is the rated overall efficiency of the turbine. We shall give this quantity a symbol of its own, η_0:

$$\rho_0 = C_{PR}\eta_{mR}\eta_{gR}. \quad (13)$$

Power curve of the wind turbine [9, 10]

The important characteristic speeds of the turbine are its cut-in velocity (V_I), rated velocity (V_R) and the cut-out velocity (V_0). The cut-in velocity of a turbine is the minimum wind velocity at which the system begins to produce power. It should not be confused with the start-up speed at which the rotor starts its rotation. The cut-in velocity varies from turbine to turbine, depending on its design features. However, in general, most of the commercial wind turbines cut-in at velocities between 3 to 5 m/s (Fig. 6).

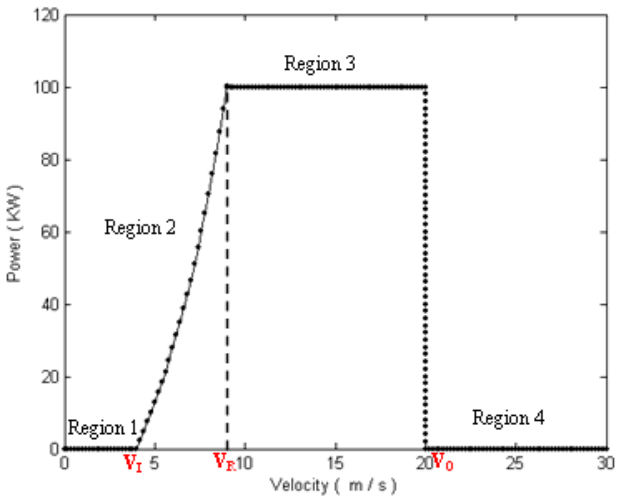

Fig. 6. *Ideal power curve of a pitch controlled wind turbine*

Due to technical and economical reasons, the wind turbine is designed to produce constant power – termed as the rated power (P_R) – beyond its rated velocity.

Table 4

Performance regions of a wind turbine

Velocity range	Power
Region 1: 0 to V_I	No power as the system is idle
Region 2: V_I to V_R	Power increases with V
Region 3: V_R to V_0	Constant power P_R
Region 4: Greater than V_0	No power as the system is shut down

Hence, the turbine has four distinct performance regions as indicated in Table 4. The power produced by the system is effectively derived from performance regions corresponding to V_I to V_R and V_R to V_0. Let us name these as region 2 and 3. The velocity-power relationship in the region 2 can be expressed in the general form

$$P_V = aV^n + b, \quad (14)$$

where a and b are constants and n is the velocity-power proportionality. Now consider the performance of the system at V_I and V_R. At V_I, the power developed by the turbine is zero. Thus

$$aV_I^n + b = 0. \quad (15)$$

At V_R power generated is P_R. That is:

$$aV_R^n + b = P_R. \quad (16)$$

Solving Eqs. (15) and (16) for a and b and substituting in Eq. (14) yields

$$P_V = P_R\left(\frac{V^n - V_I^n}{V_R^n - V_I^n}\right) \quad (17)$$

Finally we get:

$$\begin{cases} Pv = 0 & v < v_I \\ Pv = P_R\left(\dfrac{V^n - V_I^n}{V_R^n - V_I^n}\right) & v_I \le v \le v_R \\ Pv = P_R & v_R \le v \le v_0 \\ Pv = 0 & v > v_0 \end{cases} \quad (18)$$

Energy production and capacity factor

The average power output from a wind turbine is the power produced at each wind speed times the fraction of time that wind speed is experienced, integrated over all possible wind speeds [8].

In integral from, this is:

$$P_{e,ave} = \int_0^\infty Pvf(v)dv. \quad (19)$$

After calculate in finds

$$P_{e,ave} = P_R \left(\frac{\exp\left[-\left(\frac{v_I}{C}\right)^K\right] - \exp\left[-\left(\frac{v_R}{C}\right)^K\right]}{\left(\frac{v_I}{C}\right)^K - \left(\frac{v_R}{C}\right)^K} - \exp\left[-\left(\frac{v_0}{C}\right)^K\right] \right). \quad (20)$$

$P_{e,ave}$ can be expressed as:

$$P_{e,ave} = P_R(CF) = \eta_0 \frac{\rho}{2} A v_R^3 (CF), \quad (21)$$

where *CF* is the capacity factor.

The choice of rated wind speed will not depend on the rated overall efficiency, the air density, or the turbine area, so these quantities can be normalized out. Also, since the capacity factor is expressed entirely in normalized wind speed, it is convenient to do likewise in normalizing Eq. (21) by dividing the expression by C^3 to get term $(V_R/C)^3$. We therefore define a normalized average power P_N as:

$$P_N = \frac{P_{e,ave}}{\eta_0 \left(\frac{\rho}{2}\right) A C^3} = (CF)\left(\frac{v_R}{C}\right)^3. \quad (22)$$

The yearly energy production of such a turbine is:

$$W = P_{e,ave}(time) = (CF) P_R (8760), \quad (23)$$

where 8760 is the number of hours in a year of 365 days and P_R is expressed in kilowatts.

Mathematical models

The average wind velocity is given by [2, 4, 6]:

$$\overline{V} = \int_0^\infty f(V) dV, \quad (24)$$

where the standard GAMMA function Γ is defined by the following relation:

$$\Gamma(x) = \int_0^\infty \exp(-t) t^{x-1} dt \quad (25)$$

with $x > 0$.

The average cubic speed of the wind is given by the following relation:

$$\left\langle V^3 \right\rangle = \int_0^\infty V^3 P(V) dV. \quad (26)$$

The variance:

$$\sigma^2 = \int_0^\infty (V - < V >) f(V) dV. \quad (27)$$

Weibull distribution

In Weibull distribution, the variations in wind velocity are characterized by the two functions; (1) The probability density function and (2) The cumulative distribution function.

The probability density function $f(v)$ indicates the fraction of time (or probability) for which the wind is at a given velocity *V*. It is given by [2, 4, 6]:

$$f_W(V) = \left(\frac{k}{C}\right) \cdot \left(\frac{V}{C}\right)^{k-1} \exp\left[-\left(\frac{V}{C}\right)\right]^k. \quad (28)$$

Here, *K* is the Weibull shape factor and *C* is scale factor. The cumulative distribution function of the velocity *V* gives us the fraction of time (or probability) that the wind velocity is equal or lower than *V*. Thus the cumulative distribution *F(V)* is the integral of the probability density function. Thus,

$$F(V) = \int_0^\alpha f(V) dV = 1 - e^{-\left(\frac{V}{C}\right)^K}. \quad (29)$$

Average wind velocity of a regime, following the Weibull distribution is given by

$$\overline{V} = C \cdot \Gamma\left(1 + \frac{1}{k}\right). \quad (30)$$

The average cubic speed of the wind is given by the following relation:

$$\left\langle V^3 \right\rangle = C^3 \cdot \Gamma\left(1 + \frac{3}{k}\right). \quad (31)$$

The variance:

$$\sigma^2 = C^2 \left[\Gamma\left(1 + \frac{2}{K}\right) - \Gamma^2\left(1 + \frac{1}{K}\right) \right]. \quad (32)$$

Rayleigh distribution

Rayleigh distribution is a simplified case of the Weibull distribution which is derived by assuming the shape factor as 2. Owing to its simplicity, this distribution is widely used for wind energy modelling. Under the Rayleigh based approach, the cumulative distribution and probability density functions of wind velocity are given by [3, 4]:

$$f_R(V) = \frac{\pi}{2} \frac{V}{C^2} \exp\left[-\frac{\pi}{4}\left(\frac{V}{C}\right)^2\right]. \quad (33)$$

Similarly, the cumulative distribution is given by:

$$F(V) = 1 - e^{-\frac{\pi}{4}\left(\frac{V}{C}\right)^2}. \quad (34)$$

The average wind velocity is given by the distribution of Rayleigh by:

$$\overline{V} = 0{,}8862 C. \quad (35)$$

The average cubic speed of the wind is given by the following relation:

$$\langle V^3 \rangle = 1{,}3293 C^3 . \quad (36)$$

The variance:

$$\sigma^2 = 0{,}2146 C^2 . \quad (37)$$

***Hybrid of Weibull distribution** [11]*

$$\begin{cases} f(V) = (1-ff_0)\left(\frac{k}{C}\right)\left(\frac{V}{C}\right)^{k-1} \exp\left[-\left(\frac{V}{C}\right)\right]^k & V > 0 \\ f(V) = ff_0 & V = 0 \end{cases} \quad (38)$$

The mean velocity of the wind is given by the hybrid distribution of Weibull by:

$$\overline{V} = (1-ff_0) C \cdot \Gamma\left(1+\frac{1}{k}\right). \quad (39)$$

The average cubic speed of the wind is given by the following relation:

$$\left\langle V^3 \right\rangle = (1-ff_0) C^3 \cdot \Gamma\left(1+\frac{3}{k}\right). \quad (40)$$

The variance:

$$\sigma^2 = (1-ff_0) C^2 \left[\Gamma\left(1+\frac{2}{K}\right) - \Gamma^2\left(1+\frac{1}{K}\right)\right]. \quad (41)$$

Results and discussion

Weibull, Rayleigh, Hybrid of Weibull probability density function, Weibull, Rayleigh, Hybrid of Weibull cumulative distribution function for different shape factors (different sites) are presented in Fig. 7-12.
Calculation of the wind potential by the methods of Weibull, Rayleigh and Hybrid of Weibull distribution is presented in Table 5

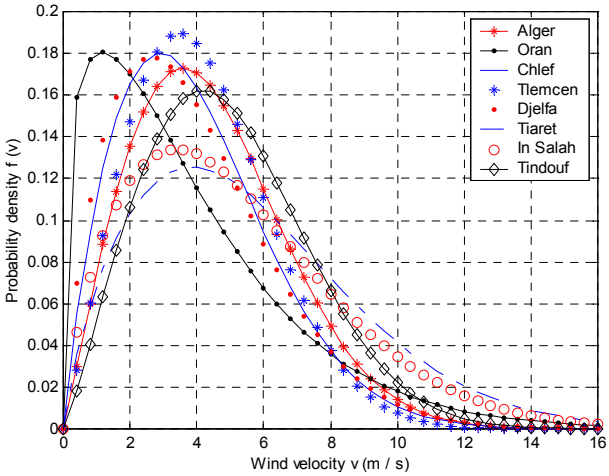

***Fig. 7.** Weibull probability density function for different shape factors (different sites)*

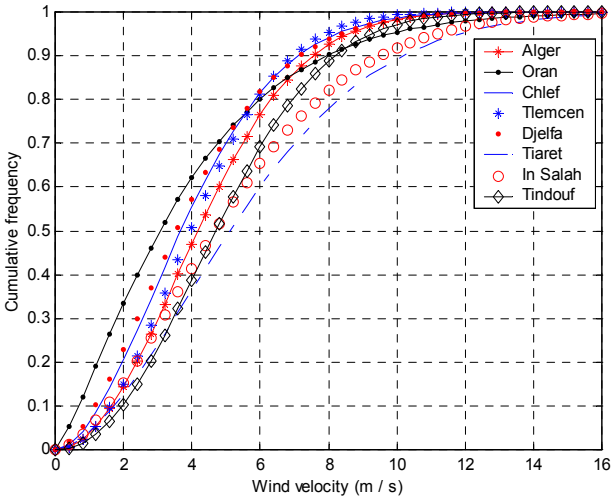

***Fig. 8.** Weibull cumulative distribution function for different shape factors (different sites)*

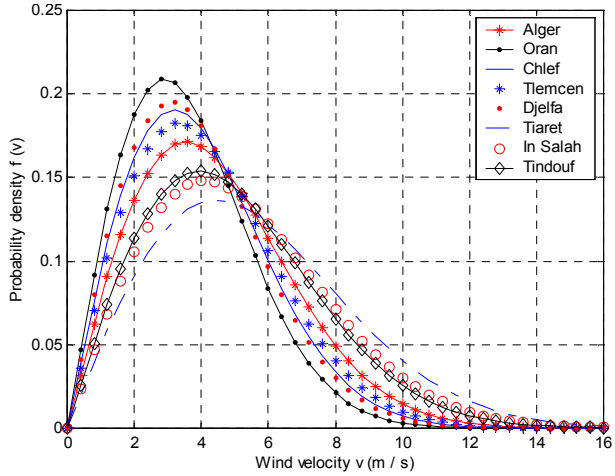

***Fig. 9.** Rayleigh probability density function for different shape factors (different sites)*

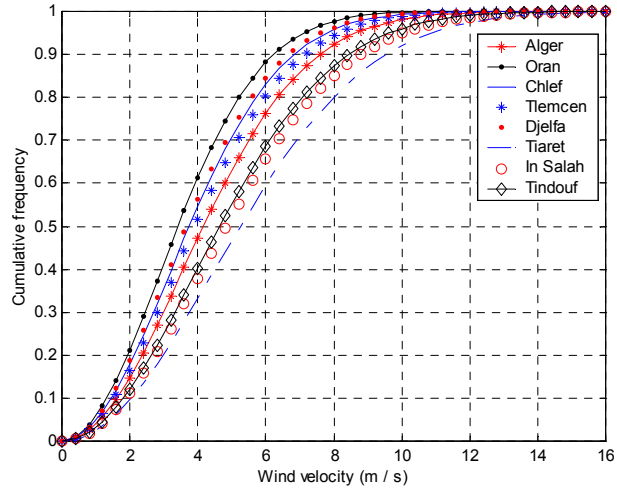

***Fig. 10.** Rayleigh cumulative distribution function for different shape factors (different sites)*

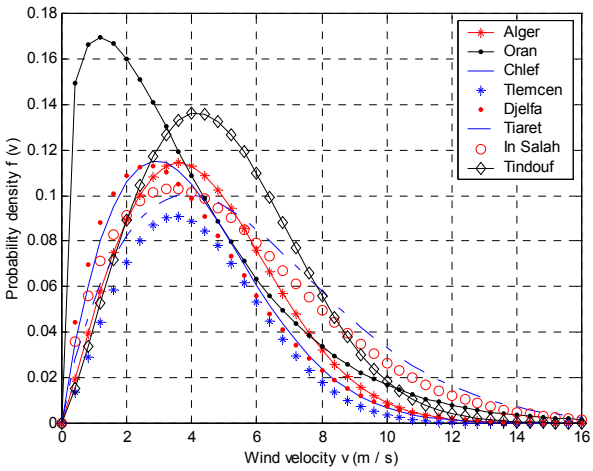

Fig. 11. *Hybrid of Weibull probability density function for different shape factors (different sites)*

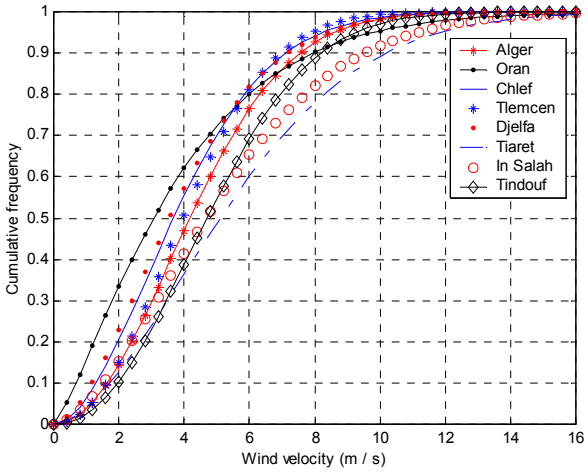

Fig. 12. *Hybrid of Weibull cumulative distribution function for different shape factors (different sites)*

Table 5

Calculation of the wind potential by the three methods [12, 13]

	Weibull distribution	**Rayleigh distribution**	**Hybrid of Weibull distribution**
		Alger	
$\overline{V}$ (m/s) V^3 (m^3/s^3) P (W/m^2)	4.43 163.62 100.22	4.43 166.17 101.78	2.92 107.99 66.14
		Oran	
$\overline{V}$ (m/s) V^3 (m^3/s^3) P (W/m^2)	3.81 201.34 123.32	3.63 91.62 56.12	3.58 189.26 115.92
		Chlef	
$\overline{V}$ (m/s) V^3 (m^3/s^3) P (W/m^2)	3.99 135.17 82.79	3.99 121.14 74.20	2.56 86.51 52.98
		Tlemcen	
$\overline{V}$ (m/s) V^3 (m^3/s^3) P (W/m^2)	4.16 130.25 79.78	4.16 138.02 84.54	1.99 62.52 38.29
		Djelfa	
$\overline{V}$ (m/s) V^3 (m^3/s^3) P (W/m^2)	3.92 137.50 84.22	3.90 113.24 69.36	2.49 87.31 53.48
		Tiaret	
$\overline{V}$ (m/s) V^3 (m^3/s^3) P (W/m^2)	5.61 393.80 241.20	5.58 332.40 203.59	4.49 315.04 192.96
		In Salah	
$\overline{V}$ (m/s) V^3 (m^3/s^3) P (W/m^2)	5.18 323.21 197.97	5.14 259.37 158.86	3.99 248.87 152.44
		Tindouf	
$\overline{V}$ (m/s) V^3 (m^3/s^3) P (W/m^2)	4.79 221.61 135.73	4.79 209.32 128.21	4.02 186.15 114.02

In the Fig. 13 we can see various wind regimes in Algeria [2].

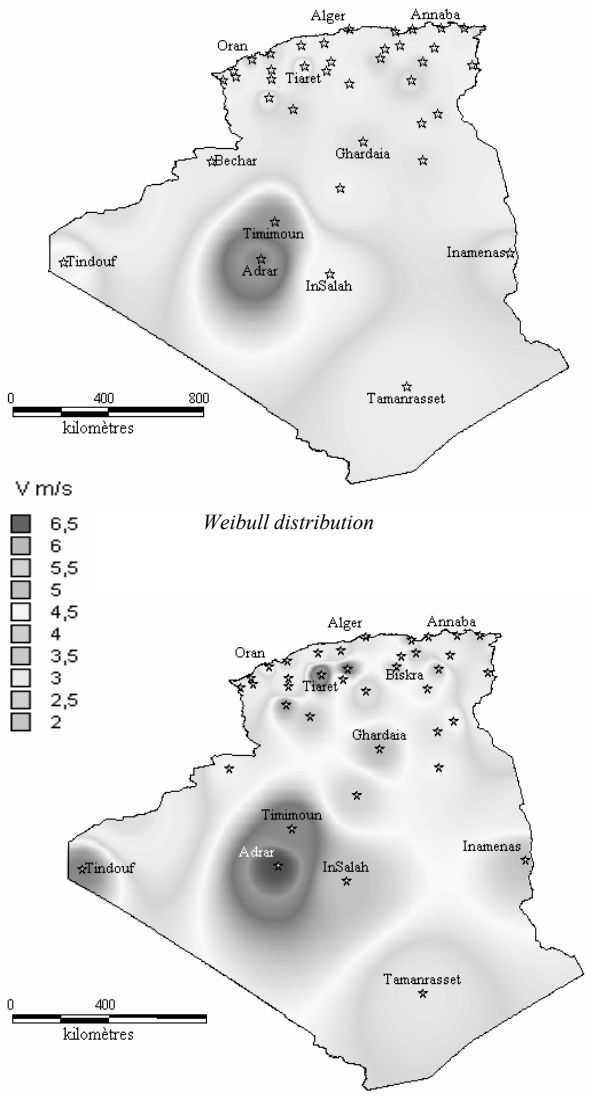

Weibull distribution

Hybrid of Weibull distribution

Fig. 13. *Various wind regimes in Algeria*

Conclusion

The most important remark is that Algeria has an appreciable wind energy potential, particularly in the south of the country and in some microclimates of the north. In the northern part, with a mean speed of the order of 5.6 m/s, Tiaret is the region that offers the most possibilities.

The three caused methods were compared for Algerian sites. These sites were selected because of the variety which represent the curves of distribution (difference of the shape factor *K* and of form and scale factor *C*) and in more difference average monthly speeds for the sites.

For a more precise evaluation of the performances of the wind-engines, it is preferable to use the law of distribution of Weibull. This method is based on the use the mean velocity of the wind and the two parameters of Weibull (*K* and *C*), even the method of Rayleigh gives good results for the sites characterized by a factor of form $K \approx 2$ like the site of Alger and Tlemcen, on the other hand on the site of Oran and In Salah in remark a great difference between the model of Rayleigh and the others models calculation.

The exploitation of the wind power is possible for several of the Algerian sites even for the installations of great power.

References

1. Capderou M. Atlas solaire de l'Algérie, Tome 2, Aspect énergétique.
2. N. Kasbadji Merzouk. Evaluation du gisement énergétique éolien contribution a la détermination du profil vertical de la vitesse du vent en Algérie. Thèse de doctorat, Université de Tlemcen. Algérie. Mai 2006.
3. Maouedj R., Bousalem S., Benyoucef B. Etude des performances d'un système éolien pour le site d'Adrar. Le 7eme congrès national de la physique et ses applications (CNPA' 2006) a Béchar du 18 au 20 Décembre 2006.
4. Sathyajith M. Wind energy fundamentals, resource analysis and economics. Faculty of Engineering, KCAET. Tavanur, Malapuram, Kerala. India.
5. Burton T., Sharpe D., Jenkins N., Bossanyi E. Wind energy handbook. England, 2001.
6. Justis C.G. (Traduit et adapté par J.L. Plazy). Vent et performances des éoliennes. Paris, 1980.
7. Extrait du rapport de synthèse ECRIN L'electronique de puissance vecteur d'optimisation pour les energie renouvelables. Paru mai en 2002. Paris.
8. Johnson G.L. Wind energy systems. November 21, 2001.
9. Bianchi F.D., De Battista H., Mantz R.J. Wind turbine control systems principles, modelling and gain scheduling design. Germany.
10. Hau E. Wind turbines fundamentals, technologies, applications, economics, 2nd edition, Germany.
11. N. Kasbadji Merzouk. Wind energy potential of Algeria // Renewable Energy. 21 (2000). P. 553-562.
12. Maouedj R., Deliou A., Benyoucef B. Estimation du potentiel énergétique éolien sur les sites de Tlemcen et d'Adrar. Le congrès international sur les énergies renouvelables et le développement durable ICRESD_07. Tlemcen, du 21 au 24 Mai 2007.
13. Maouedj R., Bousalem S., Khelifi C., Draou D., Benyoucef B. Modélisation et simulation d'un système de pompage éolien. Inernational conference on modeling and simulation MS'07, July 02-04, 2007. Algiers.

EXPLORATION AND NUMERICAL SIMULATION OF WIND TURBINE WAKE

F. Massouh, I.K. Dobrev***

Ecole Nationale Supérieure d'Arts et Métiers (ENSAM)
bvd. L'Hôpital, 151, Paris, 75013, France
+33 1 44246256/+33144246266;
*E-mail: fawaz.massouh@paris.ensam.fr
**E-mail: ivan.dobrev@paris.ensam.fr

Received: 24 Sept 2007; accepted: 31 Oct 2007

In this article, the flow behind a horizontal axis wind turbine (HAWT) is investigated and the obtained data is compared to the results of numerical simulation. The aim is to test reliability of random averaged Navier-Stokes (RANS) solver to model the wake behind a wind turbine. The experimental investigations are carried out by means of the 2D PIV measurements. The flow field is obtained in rotating frame of reference in which the rotor appears fixed by means of the phase-locked technique. Explorations are carried out in different azimuth planes. Because of large dimensions of the flow field, each azimuth plane is divided into several windows. For each window, the instantaneous velocity field is measured and stored successively to enable obtaining the averaged velocity field. Then, the flow in each azimuthal plane is reconstructed by stitching the averaged velocity field of these windows. Finally, the 3D velocity field is reconstituted by treating the results of images resulting from the different explored azimuth planes. These results are compared with RANS calculations. In general the numerical results show agreement with experiment, but some inconsistency concerning obtained power is revealed.

Keywords: wind energy

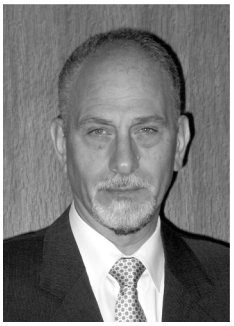

Fawaz Massouh

Organization(s): Ecole Nationale Supérieure d'Arts et Métiers, Researcher, Assoc. Prof.
Education: PhD − Paris-VI University (1984).
Experience: ENSAM (1979 to now).
Main range of scientific interests: fluid mechanics, wind energy.
Publications: 7 papers in international scientific journals.

Ivan Dobrev

Organization(s): Ecole Nationale Supérieure d'Arts et Métiers.
Education: Tech. Univ.-Sofia, Faculty of Energetic Machines (1978-1983).
Experience: Tech. Univ.-Sofia, assistant (1983-2003). ENSAM, researcher (2004 to now).
Main range of scientific interests: wind turbine, aerodynamics.
Publications: 2 papers in international scientific journals.

Introduction

The investigation of the wake development downstream wind turbines is required for the design of wind farms. In this case the wake is influenced by the presence of atmospheric boundary layer, atmosphere instabilities and "ground-wake" interaction. The flow is very complex and it is very difficult to obtain the velocity field downstream the rotor even with most sophisticated Navier-Stokes solvers. In such case there is need of experimental results that can validate calculations and adjust some parameters. There exist experiments in-situ, which permit to understand the wake structure [1]. However, in the case of large-scale experiments and due

to the sensors applied for velocity measurements, it is difficult to acquire with sufficient spatial and temporal resolution the development of the wake. As results, the usefulness of the obtained velocity field to serve as reference for CFD modeling is limited. Fortunately, there exist investigations of wake flows, which are realized in wind tunnel. These measurements are carried out in controlled flow conditions and more precise methods for the velocity measurement are applied.

Numerous studies were performed in wind tunnels in order to reveal the development of wake behind a wind turbine and to obtain precise results. These studies [2-6] were carried out using a Pitot tube or hot wire anemometry (HWA). The main disadvantage of these experiments is due to one-point measurement capabilities of applied sensors. Thus it is not possible to obtain instantaneous velocity simultaneously in the entire field of investigation. Also, due to limited directional sensibility, it is not possible to obtain the velocities in core of the blade tip vortices. However, the particle image velocimetry (PIV) is a non-intrusive method that permits to measure the instantaneous velocity vectors in plane. But researchers used PIV technique for the exploration of wind turbine wakes are few and their results are rather qualitative. Here we might mention the papers [7-12]. Recently, stereo PIV measurements are carried in out the case of HAWT with diameter of 4.5m and first results are published in [13].

The aim of this study is to present the quantitative information about the wake downstream of model wind turbine. This information is acquired by means of the PIV technique and cannot be obtained by techniques of HWA or pneumatic sensors. For example, the possibility of obtaining numerical data on velocity field around the tip vortices is of great interest. Moreover, the quality of data obtained in case of yaw and non-yaw flow conditions permits to use these results as reference in case of CFD computing of flow around the model wind turbine. Finally in this study, the numerical simulation is carried out in the case of non-yaw conditions. The comparison of obtained results with experiment permits to reveal some particularities of the used random averaged Navier-Stokes (RANS) solver.

Experimental results

The Fluid Mechanics Laboratory at ENSAM, Paris has a closed circuit wind tunnel with a semi-open test section. A settling chamber is equipped with a convergent nozzle which has contraction ratio of 12. This contraction ratio ensures a uniform flow and the turbulence intensity does not exceed 0.5 % for a velocity of 35 m/s. The test section has working dimensions 1.35 m by 1.65 m and 2 m of length. The investigation is carried out in wind tunnel using a modified commercial wind turbine Rutland 503.

This horizontal axis wind turbine has a three blade rotor with diameter of 500 mm and hub diameter of 135 mm. The blades are tapered and untwisted. They have a pitch angle of 10° and a chord of 45 mm at tip and 65 mm at the root. The rotational speed is 1000 rpm with a free-stream velocity of 9.3 m/s. Hence, the TSR is equal to 3, which is lower than the case of market wind turbines. The wind turbine is mounted on a support tube of 37 mm of diameter ensuring a sufficient height in order to allow the lasers fixed above the transparent roof to illuminate the explored plane with a sufficient intensity, Fig. 1.

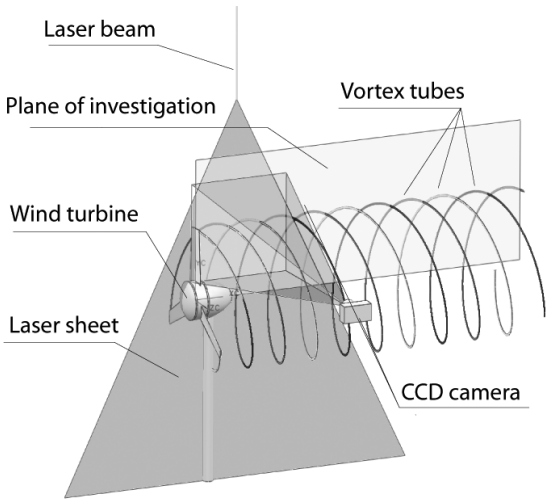

Fig. 1. *Experimental test bench*

The PIV technique is applied to obtain the velocity field in the wake downstream the turbine rotor. Here, a double cavity Quantel "Blue Sky" Nd:YAG pulsed laser (532 nm), which produce approximately 120 mJ per pulse, is installed above the transparent roof of the wind tunnel test section. A cylindrical lens is used to create a thin vertical sheet of laser light, which passes through the center of the rotor. As the test section is semi-open and without sidewalls, it is possible to place the camera outside the tunnel, Fig. 1. Olive oil droplets are introduced for seeding on the inlet of the wind tunnel diffuser.

In order to carry out the phase-locked measurements, the test bench is equipped with an optical sensor. This sensor synchronize the lasers pulses and a reference angular position of the blade. The sensor tracks a reflecting target fixed on the rotor hub and emits a signal, each time when the target passes. Then the emitted signal is sent via a delay circuit. The change of delay time permits to change the angular distance between the reference position of blade and the plane of exploration.

As the plane of exploration passes trough the rotor axis and the PIV used in this study is planar, then it is only possible to obtain radial and axial velocities. However the tangential velocity of the flow downstream the rotor is not zero and time interval between two laser pulses is set to 150 μs, it is probable that the tracked particles will be blown out of the illuminated volume. Therefore, it is needed to adjust the laser sheet thickness to nearly 3-4 mm.

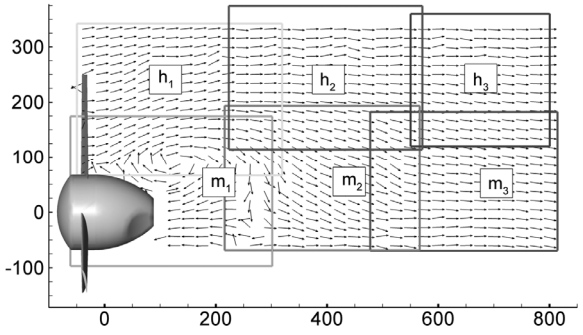

Fig. 2. *Flow map reconstruction*

Exploration of flow downstream the rotor is carried out in four azimuth planes with angles 0°, 30°, 60° and 90º. Here, the plane of 0° corresponds to the vertical position of the reference blade, Fig. 2. Because of the laser output power limitation and the camera resolution of 1600x1200 pixels, it is not possible to obtain with sufficient precision a velocity field larger than 300 mm. As a consequence to widen the explored area, the investigated velocity field is divided into six windows (3 horizontal by 2 vertical) with a certain overlapping. The scale of windows and their relative positions are defined using calibration markers placed in known positions inside the interrogation area. For this purpose, the images of these markers are taken after each series of tests.

For each explored window the imagery is repeated 95 times synchronously with rotor rotation. Hence temporal sequence is acquired during approximately 12 seconds in order to improve the precision of averaged velocity calculation.

Totally, four series of 6 by 95 pairs of images were acquired for different planes with azimuth angles of 0°, 30°, 60° and 90º; with zero corresponding to the vertical position of the reference blade.

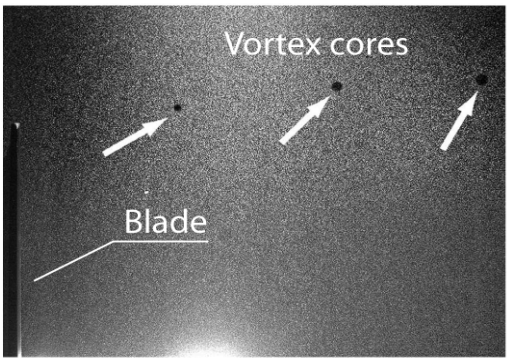

Fig. 3. *Raw image taken immediately behind the rotor in the h1 window*

The raw images have a resolution of 1600×1200 pixels and 12 bits of grayscale resolution. Thanks to the synchronization between the laser pulse and the rotor position detected by the optical sensor, we can distinguish a blade frozen in vertical position, on the left. It can be seen also the cores of vortex tubes emitted from the tips of other blades, Fig. 3. Due to velocities induced by these vortices the seeding particles are turned around the vortex core center and the centrifugal forces carry out these particles outside of the vortex center. As results the vortex tube core appears on the images like a black spot because the quantity of the seeding particles decreases inside.

Statistical processing of the raw images is carried out by means of Matpiv ver.1.6.1 developed by Sveen [14]. The "multi-pass" algorithm with 3 pass is applied, the final size of interrogation window is 16x16 pixels and the overlapping is 75 %. The obtained results are filtered by means of signal-to-noise (SNR), median and mean filter, then all vectors marked as "spurious" are discarded and new values are obtained by interpolation from nearest points. The criterion for discarding is the quality of velocity and vorticity fields. If the level of cut-off SNR is too high the flow is smoothed and some vorticity structures disappear, but if the SNR is too low then vorticity field is very noisy. Then instantaneous velocity fields resulting from each time series of 95 captured images are used to obtain the average fields in each of the investigated windows. Finally, the processing of the calibrating images makes it possible to obtain the scale constants, true velocity and the position of each window relative to the rotor. In this manner the fields of instantaneous and averaged velocity are calculated for each window.

Some uncertainty on the velocity measurement in the vicinity of the blade comes from the specific difficulties of the PIV technique to explore flow field close to the walls due to reflection. It must be noted also, that the high levels of the tangential velocities can take place just a few millimeters from the blades. This does not permits that the same seeding particles remain in the laser sheet between consecutive lase pulses. As result, the cross-correlation algorithm used in PIV image analysis fails to obtain the instantaneous velocity field.

The Fig. 4 shows the field, which results from averaged velocity fields for windows h1. Here, it can be observed the intersection between the plane of exploration defined by the laser sheet and the helical vortex tubes emanating from blade tips. Also it can be seen the effect of flow deceleration created by the wind turbine rotor whose consequence is shown by the increase of the downstream flow tube diameter. It must be noted that the flow tube is not cylindrical as assumed in the linear theory of propellers. We clearly see the deformation of flow tube surface due to the presence of tip vortices. It should be noted that there is a large vortex structure, which results from a detachment behind the hub. In the vicinity of the blade, the flow field is not well resolved, because of the presence of walls.

The analysis of near rotor wake shows that the hub is a major source of disturbances and unsteady aerodynamic effects. This is due to the bluff shape of the rotor hub, which contains the electric generator. The flow detachment from the hub is intensified due to the highly loaded root blade sections. For this reason high axial

velocities are induced; the flow on the hub surface is decelerated and then separated in vicinity of the blade attachment to the hub. The results of this phenomenon are visible in Fig. 4 where we note a return flow up to approximately 40 % of the diameter of the rotor.

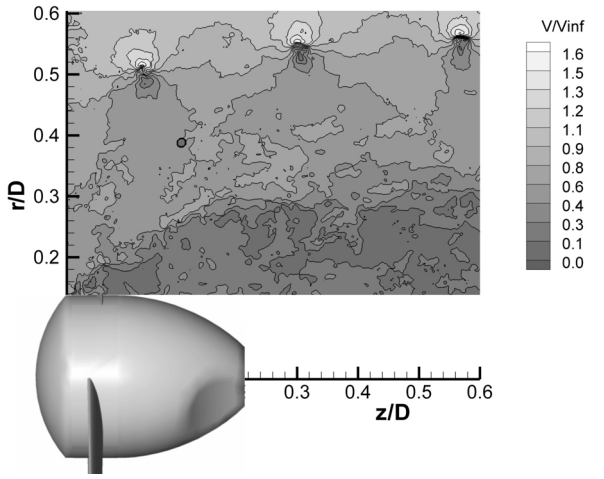

Fig. 4. *Contours and vectors of average velocity in h1*

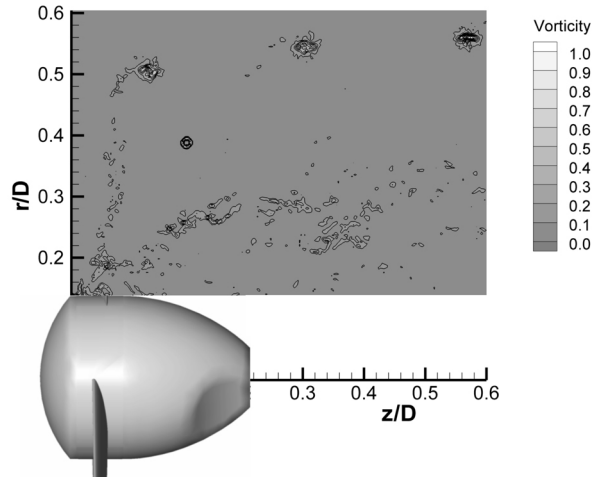

Fig. 5. *Vorticity of instantaneous velocity in h1 window*

The investigation of the time series of instantaneous vorticity fields, Fig. 5, shows that there is a fluctuation in the position of the cores of the tip vortices. These fluctuations, known as vortex wandering, produce an artificial reduction of vortex intensity when the average values are calculated from the instantaneous fields. The fluctuation of vortex center behind the rotor is shown on Fig. 6. It can be observed that the amplitude of the fluctuations increases downstream the rotor. In reality, in spite of vortex position instability, the vortex intensity and vortex core velocity does not decrease not as rapidly, see Fig. 7 and Fig. 8, as the averaged velocity field predict. Consequently, the average velocity field is not completely representative for comparison with steady numerical simulations.

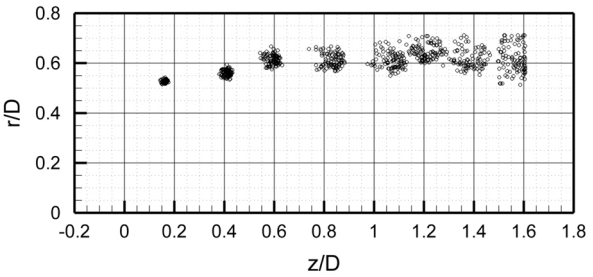

Fig. 6. *Vortex wandering behind the rotor*

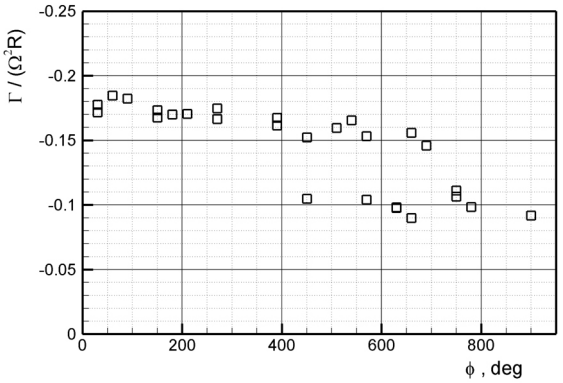

Fig. 7. *Vortex intensity behind the rotor*

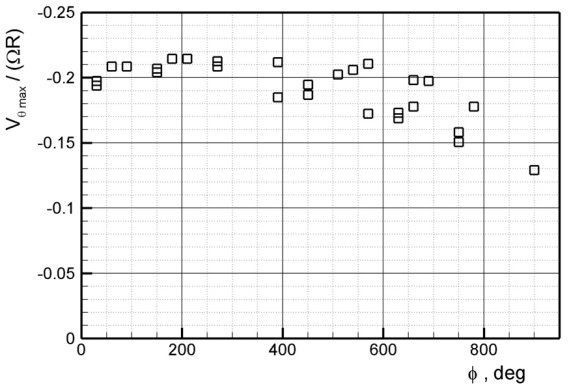

Fig. 8. *Vortex core maximum velocity*

Numerical simulation

To investigate flow downstream the rotor a computational analysis is carried out using commercial CFD code Fluent 6.3. In this simulation the rotational periodicity is not used and the flow past the rotor is modeled completely and not only one period. The periodicity is not used because this improve the unsteady simulation. In order to model the flow blockage the rotor is modeled as it rotates in the wind tunnel. Therefore, the tunnel walls are modeled to confine the flow about the rotor and this creates more realistic induced velocities.
Because CFD Fluent does not support chimera grid, the blade rotation around the rotor axis is modeled using a sliding mesh technique. Hence, the flow field is divided in two distinct cell zones; one that represents the wind

tunnel and other that represents the turbine rotor. In Fluent, these adjacent cell zones are associated to form three grid interfaces.

During the calculation, the cell zones rotate relative to one another along the grid interface in discrete steps. The cylinder, which represents the rotor and includes the blades, has the diameter 1.5D and the length 0.4D. In order to create a more regular grid around the suction and pressure surfaces of the blades, the rotor domain is divided along the blades by means of three parallelepipeds. Then the internal volume is divided once again in four sectors. Finally, the hexagonal volumes that include the pressure and suction surfaces blade surfaces are meshed using the hexagonal cells structured grid, Fig. 9.

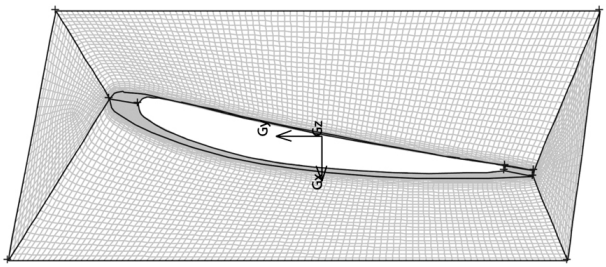

Fig. 9. *Grid blocks around the blade*

The blade suction and pressure surfaces are divided in the chordwise direction into 90 intervals, which are slightly refined near the leading and trailing edges where the velocity gradient is strongest. In spanwise direction the blade is divided into 90 intervals equally spaced. In order to improve the mesh in the boundary layer, 10 mesh layers in vicinity of blade walls are used. Here, the initial cells size in normal direction is 0.15 percent of chord lenghts and the growth factor of 1.25 is used. Totally 6 million hexahedral cells are used in rotor grid zone. To model the wind tunnel a multi-block grid of 10 hexahedral million cells is used. In order to decrease the cell number on tunnel walls we specify a wall shear stress of 0 Pa, so there is no need of boundary layer modeling. To compute this model divided in 8 partitions we employ a cluster of 4 PC with Pentium IV processors of 3.4 GHz and 4 GB of RAM each.

The Reynolds number of the blade tip sections is near 70,000. For this reason the turbulence model used is k-ω Shear Stress Transport (SST) which is considered to be more robust than others low-Reynolds number k-ω or standard k-ε models. This model employs a standard k-ω model in the inner region of the boundary layer, and a high-Reynolds number k-ε model in the rest. For the "pressure-velocity" coupling we use the SIMPLE algorithm and a second-order upwind differencing discretization scheme for the momentum equations. The time step is equivalent to a blade rotation of 1° about the rotor axis; each time step has 10 iterations and the results repeatability is obtained after 3 rotor turns.

In general the obtained results by Fluent correspond to experimental values. Unfortunately, it is seen that vortex core radii are lower and the distance between vortex cores is greater compared to experimental results, Fig. 10. This is due to the fact that the obtained power is lower. Also it must be noted that the flow separation downstream the rotor hub is strongest. This is a consequence of the RANS models failure to predict the flow separation. For regret, the other turbulence models, for example RSM or V2F also do not allow to obtain more realistic results for flow downstream of the rotor. Probably, to obtain better results it is necessary to use LES or DES model.

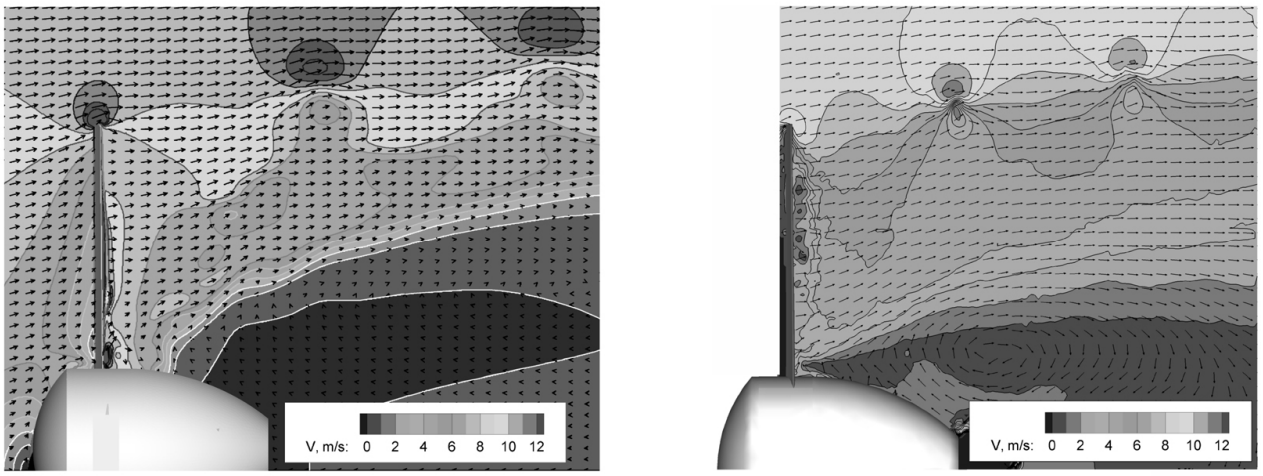

a *b*

Fig. 10. *Velocity field downstream rotor obtained by simulation (a) and by experiment (b)*

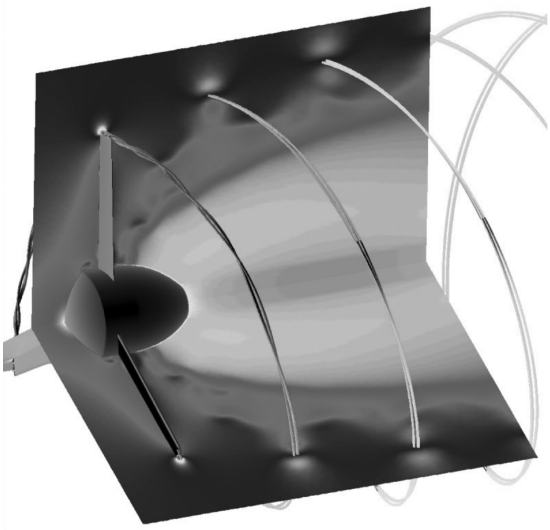

Fig. 11. *Velocity field and vortex tube issued from the blade tip*

Conclusion

In the present study, the PIV technique is successfully applied for investigation of the wake behind a horizontal axis wind turbine. The phase-locked measurements are applied and the images retrieval is synchronized with azimuth position of the blade. This permits to carry out flow measurements in the reference frame of the rotor and makes possible to reconstruct the 3D velocity field of the wake. To widen the measured field, the azimuthal plane of exploration is divided into 6 windows with some overlap. Then, by means of the position markers, these windows are stitched and the velocity field in the complete plane is obtained. Thus, the helical pitch and the radial position of the tip vortices, compared to the rotor, can be localized.

The results show that the radius of the tip vortices issued from the blade tips is not constant as it is assumed in linear propeller theory. In reality, the diameter of the flow tube increases as the simple theory of Froude-Rankine predicts it. Measurements revealed also the presence of important vortex structures downstream the hub and near the root of the blade. Some instability of the helical tip vortices, so called vortex wandering is also to be noted. Because of these fluctuations, the instantaneous velocity field is very rich with information. The numerical data concerning the instantaneous field constitutes a useful database for the validation of models of wind turbine rotors and the prediction of near wake development.

The RANS calculation is carried out in order to show a potential of numerical simulation of the flow behind the wind turbine. From the computation results presented above, it can be seen that the obtained CFD results show good agreement with experiments. However, there are some discrepancy due to incapability of CFD to resolve well the detached flows and also the need to introduce a transition model.

References

1. Vermeer L.J., Sorensen J.N., Crespo A. Wind turbine wake aerodynamics // Progress in Aerospace Sciences. 2003. Vol. 39. P. 467–510.
2. Massouh F. Dobrev I., Dejean F., Laborie A. Etude du sillage d'une éolienne à axe horizontal. 16ème Congrès Français de Mécanique CFM 2003, Nice, 2003.
3. Vermeer L.J. A review of wind turbine wake research at TU Delt, 2001 AIAA paper 2001-0030.
4. Ebert P.R., Wood D.H. The near wake of a model horizontal axis wind turbine–I. Experimental arrangments and initial results // Renewable Energy. 1997. Vol. 12, No. 3. P. 225-243.
5. Ebert P.R., Wood D.H. The near wake of a model horizontal axis wind turbine – Part 3: properties of tip and hub vortices // Renewable Energy. 2001. Vol. 22. P. 471-472.
6. Massouh F., Dobrev I. Investigation of wind turbine near wake. Int. Conf. on Jets, Wakes and Separated Flows, ICJWSF-2005, Toba-shi, Mie, Japan, Oct. 5-8, 2005.
7. Mast E.H.M., Vermeer L.J., van Bussel G.J.W. Estimation on the circulation distribution on a rotor blade from detailed near wake velocities // Wind Energy. 2004. Vol. 7. P. 189-209.
8. Grant I., Parkin P., Wang X. Optical vortex tracking studies of a horizontal axis wind turbine in yaw using laser-sheet flow vizualisation // Experiments in Fluid. 1997. Vol. 23. P. 513-519.
9. Grant I., Parkin P. A DPIV study of the trailing vortex elements from the blades of a horizontal axis wind turbine in yaw // Experiments in Fluids. 2000. Vol. 28. P. 368-376.
10. Grant I., Mo M., Pan X., Parkin P., Powell J., Reinecke H., Shuang K., Coton F., Lee F. and D. An experimental and numerical study of the vortex filaments in the wake of an operational horizontal-axis wind turbine // Journal of Wind Engineering and Industrial Aerodynamics. 2000. Vol. 85. P. 177-189.
11. Whale J., Helmis C., Papadopolous K.H., Anderson C.G., Skyner D.J. A study of the near wake structure of a wind turbine comparing measurements from laboratory and full-scale experiments // Solar Energy. 1996. Vol. 56, No. 6. P. 621-633.
12. Maeda T., Kinpara Y., Kakinaga T. Wind tunnel and field experiments on wake behind horizontal axis wind turbine // Trans. of Jap. Soc. Mec. Eng. 2005. Vol. 71, No. 701. P. 162-170.
13. The MEXICO project: Snel, Shepers J.G. and Montgomerie H. The database and first results on data processing and interpretation // Journal of Physics: Conference Series. 2007. Vol. 75.
14. Sveen J.K., Cowen E.A. Quantitative imaging techniques and their application to wavy flows, in PIV and Water Waves, editors J. Grue, P.L.F. Liu and G. Pedersen // World Scientific. 2004.

STUDY OF THE SURFACE HETEROGENEITY OF HYDROTHERMAL KAOLINITE

N. Hezil, K. Guerfi, S. Hazourli, A. Hammadi, S. Zeroual

Laboratory of Water Treatment and valorization of the Industrial Waste, Department of Chemistry
Faculty of Science, Badji Mokhtar University, BP 12, Annaba, Algeria.
E-mail: nawel_hez@yahoo.fr

Received: 23 Sept 2007; accepted: 25 Oct 2007

The hydrophilic and hydrophobic components of the surface of the hydrothermal kaolinite has been characterized using adsorption of passively and negatively charged surfactants in aqueous solution.
The hydrophilic and hydrophobic surface areas are inferred from the amount of probe molecule adsorbed and the structure of the adsorbed layer. The hydrophilic structure area of kaolinite is estimated from the adsorption of cationic surfactant: benzyl-demethyl-dodecyl-ammonium bromide (BDDAB). The adsorption of anionic surfactant; sodium dodecyl sulfate (SDS) onto kaolinite surface particles has been performed to assess their hydrophobic surface area.

Keywords: structural materials, kaolinite, surface heterogeneity, adsorption, surfactant

Nawel Hezil

Organization(s): Badji Mokhtar University (Algeria), faculty of science, Laboratory of Water Treatment and valorization of the Industrial Waste, Chemistry Department.
Education: Badji Mokhtar University, Faculty of science, Chemistry Department (1999-2007).
Experience: Badji Mokhtar University, responsible of practical works (2005-2007).
Main range of scientific interests: water treatment, materials, valorization of the industrial waste.

Introduction

Kaolinite is one of the most wide-spread minerals of the earth crust [1]. It occurs naturally in the form of clay-sized particles. The presence of kaolinite clays in the earth soils may strongly affect mass-transfer processes in natural environments. On the other hand, kaolinite clays are widely used in various industrial applications, such as production of ceramics, paper, pigments, and aluminium. Knowledge of the structural and surface properties of kaolinite is essential in optimizing the above mentioned applications [2]. Therefore, the characterization of the surface properties of kaolinite and other divided solids is a fundamental feature of real solid surfaces [3].
However, it is well known that most exhibit a superficial heterogeneity that is caused by surface topology and the chemical composition. This surface heterogeneity is a crucial parameter involved in interaction between the mineral surface and the different molecules [4].
Most methods designed to study the surface properties such as gas adsorption, immersion calorimetry, and determination of contact angles. However there is no a standard method to determine the hydrophilic/ hydrophobic balance [5]. An alternative method of assessment of the hydrophilic/ hydrophobic balance for heterogeneous surfaces consists of studying the adsorption of anionic and cationic surfactants onto hydrothermal kaolinite materials.

Experimental

Materials solid:

The kaolinite-type clay used in this study was obtained from Guelma region of Algeria.
The chemical composition of kaolinite was found to be as follows: 43.82 % SiO_2, 0.20 % Fe_2O_3, 36.90 % Al_2O_3, 0.025 % MnO, 0.23 % CaO, 0.03 % MgO, 18.51 % H_2O [6].
The sample was characterized by BET, SEM, and thermogravimetric.
Specific surfaces areas (SSA) were determined from adsorption of nitrogen at 77 K by applying the BET equation [7]. The SSA of kaolinite measured is 48.75 m^2/g.

Thermogravimetric analysis was performed using a TGA 2050 thermogravimetic analyser (TA Instruments). Fig. 1 shows a thermogravimetric curve with an endothermic peak clearly accentuated at the temperatures 500-520 °C corresponding to the disordered kaolinite.

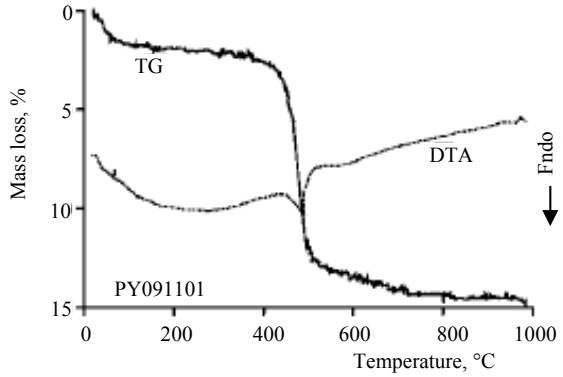

Fig. 1. *DTA and TG curves of the kaolinite*

The kaolinite sample was studied by scanning electron microscopy (Fig. 2), which indicated that the sample was uniform in content, containing a lot of tubular material, as well as large undesirable particle agglomerates.

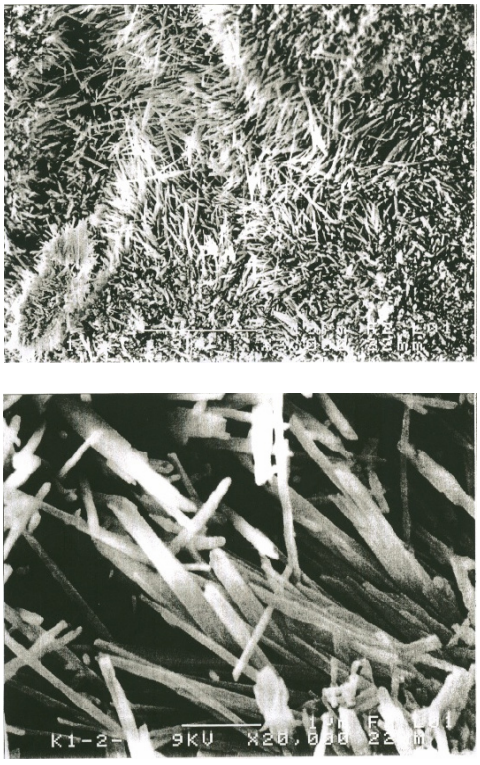

Fig. 2. *The kaolinite sample studied by scanning electron microscopy*

Surfactants

The cationic surfactant was benzyl-demethyl-dodecyl-ammonium bromide (BDDAB), C_6H_5-CH_2-$N^+(CH_3)_2C_{12}H_{25}Br^-$(NW = 384 g/mol), supplied by Fluka (purity > 99 %). The anionic surfactant was sodium dodecyl sulphate (SDS) $C_{12}H_{25}SO_4^-Na^+$ (NW = 288 g/mol), supplied by Biochima (purity > 99 %). The CMC of the two surfactants in pure water as determinated by surface tension measurement, were respectively; $5.36 \cdot 10^{-3}$ and $8.5 \cdot 10^{-3}$ mol/kg [8].

The cross section areas per molecule at the air/ water interface at 25 °C for BDDAB and SDS are 71 and 47 $Å^2$ respectively [8].

Method: surfactant adsorption isotherms

Isotherms are obtained from the measurement of surfactant concentrations in the initial solution (Co) and in the supernatant at the adsorption equilibrium after long-time contact between the solid and the surfactant solution. In a typical experiment, 0.5 g of kaolinite was mixed with 20 g of surfactant solution. These suspensions were sealed in clean glas ,s tubes from the solid and then agitated for 24 hours at 25 °C. The supernatant was separated from the solid by filtration and the surfactant concentration was measured. The amount of adsorbed surfactant Γ was calculated according to the equation:

$$\Gamma = \left(\frac{C_0 - C_{eq}}{1000M} \right) V , \qquad (1)$$

where: C_0 − the initial concentration of surfactant; C_{eq} − the equilibrium concentration of surfactant; V − the solution volume; M − the mass of the solid.

Results and discussion

Adsorption of cationic surfactant from water

Sorption of cationic surfactants, such as alkylammoniumon clays were attributed to both cation exchange and hydrophobic bonding [9].

The adsorption isotherm of BDDAB onto kaolinite at 25 °C is shown in Fig. 3.The adsorption isotherm the initial section of the isotherm, corresponding to very low equilibrium concentrations suggests very strong adsorption; at this step of adsorption, the individual surfactant molecules are bound to the surface of kaolinite by an electrostatic interaction between the positively charged head group of $BDDA^+$ ion and the negatively charged group of kaolinite surface [10].

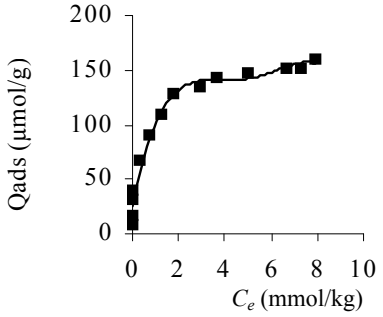

Fig. 3. *Adsorption isotherm of BDDAB at 25 °C and free pH onto kaolinite*

The maximum quantity of surfactant adsorbed is about 3.31 μmol/m^2; at this section the adsorption of BDDAB is attributed to hydrophobic interactions due to the surfactant ions bound to the surface by the polar head group. The alkyl chains are oriented toward the solution. The geometric cross-sectional area of BDDAB head at liquid-air interface is 71 Å^2, if the adsorption of BDDAB is performed by the polar head of the surfactant on one charged site; from the amount of adsorbed surfactant (3.34 μmol/m^2) and the cross sectional-area of the polar head, it is possible to calculate approximately the hydrophilic part of the kaolinite surface according to the equation:

$$N_a \cdot 3.34\ \mu mol/m^2 \cdot 71\ Å^2 = 1.42\ m^2/g, \qquad (2)$$

where: N_a is the Avogadro's number.
The value represents 3 % of the total surface area.

Adsorption of anionic surfactant from water

The adsorption of isotherm of SDS onto kaolinite is shown in Fig. 4. The adsorption isotherm shows two plateaus, the quantity adsorbed at the first plateau is about 1.23 μmol/m^2. The Γ(max) at the second isotherm plateau is about 4.8 μmol/m^2.The negatively charged surfactant cannot be adsorbed on the negatively charged kaolinite sites. This adsorption is due to direct interactions between the aliphatic parts of SDS molecules and the hydrophobic parts of kaolinite surface.
The hydrophobic contribution of the kaolinite surface can be estimated according to the following relationship:

$$S_{hydrophobic} = n_{aggregate} \cdot \sigma_{aggregate}. \qquad (3)$$

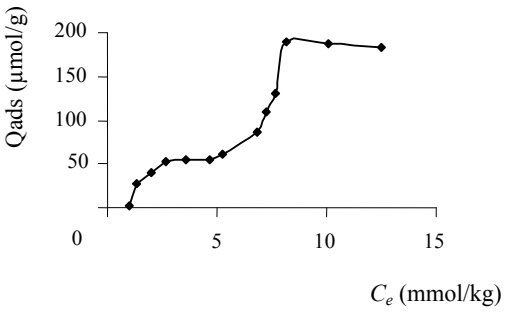

Fig. 4. *Adsorption isotherm of SDS at 25 °C and free pH onto kaolinite*

For a spherical micelle of SDS in aqueous solution, the aggregation number has been stated to be 60 monomers [8, 11]. The adsorbed aggregates were assumed semicircular, thus giving a value of $\sigma_{aggregate}$ = 10 nm.
The area of the hydrophobic parts of kaolinite was found to be 37 m^2/g. The sum of the hydrophilic (1.42 m^2/g) and the hydrophobic surface (37 m^2/g) gives 38.42 m^2 /g, a value which is only 21 % smaller than BET surface area.

Conclusion

In common with other clay minerals, hydrothermal kaolinite show polar and non-polar surface inhomogeneity related to their layer structure.
Adsorption of cationic and anionic surfactants on kaolinite was applied to determine the hydrophilic / hydrophobic balance. Adsorption of cationic surfactant occurs through electrostatic interaction between the positively charged head group of BDDAB ion and the negatively charged group of kaolinite surface.
It is shown that the adsorption of SDS essentially occurs through dispersive interactions between the nonpolar hydrocarbon chain of the probe molecule and the hydrophobic mineral surface. The sum of hydrophilic and hydrophobic surface area of kaolinite obtained with cationic and anionic surfactants is consistent with the value of the BET surface area.

References

1. Moore D.M., Reynolds R.C. X-ray diffraction and the identification and analysis of clay minerals. England: Oxford University Press, 1989.
2. Bereznitski Y., Jaroniec N., Maurice. Adsorption characterization of two clay minerals society standard kaolinites // J Colloid Interface Sci. 1998. 205. P. 528-530.
3. Drach M., Lajtar L., Narkicvicz-Michalck J., Rudzinski W., Zajac J. Adsorption of cationic surfactants on hydrophilic silica // J. Colloid Surfaces A: Physicochem. Eng. Aspects. 1998. 145. P. 243-261.
4. Charnay C., Lagerge S., Partyka S. Assessment of the surface heterogeneity of talc materials // J. Colloid Interface Science. 2001. 233. P. 250-258.
5. Cases J.M., Villiéras F., Michot L.J. Adsorption, exchange and retention phenomena at the solid-aqueous solution interface // Earth and Planetary Sciences. 2000. 331. P. 763-773.
6. Boulmoukh A., Berrdjem Y., Guerfi K., Gheid A.H. Kaolin from Djebel Dbbagh mine, Guelma, Algeria // Research J. Applied Science. 2007. 2 (4). P. 430-445.
7. Adamson A.W. Physical chemistry of surfaces. New York: Wiley, 1976.
8. Zajac J., Partyka S. Adsorption of new and modified inorganic sorbents. Netherlands. Elsevier Sciences, 1996.
9. Zhang R, Somasundaran P. Advances in adsorption of surfactants and their mixtures at solid/solution interfaces // J. Colloid Interface Science. 2006. 123-126. P. 213–229.
10. Rosen M. Surfactants and interfacial phenomena. New York: Wiley, 1989.
11. Cases J.M., Mielezarski J., Mielezarska E., Michot L.J., Villieras F., Thomas F. Ionic surfactants adsorption on heterogeneous surfaces // C R Geosciences. 2003. 334. P. 675-688.
12. Luciani L., Denoyel R., Rouquerol J. Poly (ethoxy) anionic surfactants: micellization and adsorption at the

solid: liquid interface // J Colloid Surfaces A: Physicochem. Eng. Aspects. 2001. 178. P. 297-312.
13. Torn L.H., Keizer A., Koopal L.K., Lyklema J. Mixed adsorption of poly (vinyl pyrrolidone) and sodium dodecyl benzene sulfonate on kaolinite // J Colloid Interface Sci. 2003. 260. P. 1-8.
14. Cases J.M., Villiéras F., Michot L.J., Bersillo J.L. Long chain ionic surfactants: the understanding of adsorption mechanisms from the resolution of adsorption isotherms // J Colloid Surfaces A: Physicochem. Eng. Aspects. 2002. 205. P. 85-99.

SOME TETRAZOLIC COMPOUNDS AS CORROSION INHIBITORS FOR COPPER IN NITRIC ACID MEDIUM

M. Mihit, L. Bazzi*, R. Salghi**, B. Hammouti***, S. El Issami*, E. Ait Addi*****

*Faculté des Sciences d'Agadir, Laboratoire Environnement & Matériaux, Equipe de Chimie Physique Appliquées, BP 8106, 80000 Agadir, Morocco. Telephone 00 212 28 09 57 Fax 00 212 28 22 01 00,
E-mail: lahcen_bazzi@yahoo.fr

**Ecole National des Sciences Appliquées d'Agadir, Laboratoire d'Ingénierie des Procédés de l'Energie & de l'Environnement, BP 1136, 80000 Agadir, Morocco. Telephone 00 212 28 22 83 13 Fax 00 212 28 23 20 07,
E-mail: salghi@ensa-agadir.ac.ma

***Faculté des Sciences d'Oujda, Laboratoire de Chimie Appliquée & Environnement,B. P 717, Oujda, Morocco.
Telephone 00 212 68 63 22 73 Fax 00 212 36 500 603, E-mail: hammoutib@gmail.com

****Ecole Supérieure de Technologie d'Agadir, Département Bio-industrie, BP 33/S, 80000 Agadir, Morocco.
Telephone 00 212 28 23 25 83 Fax 00 212 28 22 78 24, E-mail: habib@esta.ac.ma

***Author for correspondence, Pr. R. Salghi,* Ecole National des Sciences Appliquées d'Agadir, BP 1136, Agadir, Morocco.
Phone 00 212 28 22 83 13 Fax 00 212 28 23 20 07, E-mail salghi@ensa-agadir.ac.ma

Received: 31 July 2007; accepted: 25 Aug 2007

The corrosion inhibition of copper in 0.1 M HNO_3 was studied by gravimetric, potentiodynamic polarization and electrochemical impedance spectroscopy (EIS) measurements by the use of tetrazolic compounds such as 1,2,3,4-tetrazole (TTZ), 1-phenyl-1,2,3,4-tetrazole (PT), 5-amino-1,2,3,4-tetrazole (AT) and 1-phenyl-5-mercapto-1,2,3,4-tetrazole (PMT). The addition of these compounds acts differently on the kinetic of corrosion process of copper in nitric medium. The comparative study indicates that PMT is the best inhibitor. Its inhibition efficiency increases while its concentration increases in solution to attain 97 % at 10^{-3} M. Electrochemical measurements show that both polarization and transfer resistances increase with PMT concentration. The adsorption of PMT on the copper surface followed the Frumkin isotherm model. The results obtained from the various methods are in good agreement.

Keywords: thermodynamic analysis in alternative energy, corrosion, inhibition, copper, nitric acid, tetrazole

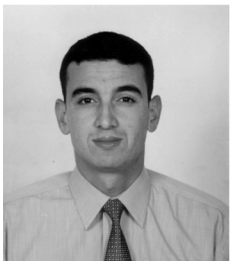

Mohammed Mihit

Organization: Faculty of Science Agadir Morocco. He was awarded a PhD degree in Corrosion field in 2006.
Main range of scientific interests: Corrosion and the inhibition of the corrosion of copper and its alloys by organics and inorganics compounds.
Pubications: More than 10 papers in corrosion.

Lahcen Bazzi

Organization: Faculty of Science Agadir Morocco. He was awarded a PhD degree in Corrosion Science in 1995. He is currently a teacher and researcher in the Laboratory of Materials & Environment.
Education: University Ibn Zohr, Faculty of Science, PhD degree in corrosion (1995). Ecole Normale Supérieure Rabat, Doctorat (DES), 1987.
Experience: University Ibn Zohr, Faculty of Science Agadir, Professor B (2003 − to date).
University Ibn Zohr, Faculty of Science Agadir, Professor A (2000-2003).
University Ibn Zohr, Faculty of Science Agadir, lecturer Professor (1995-1999).
University Ibn Zohr, Faculty of Science Agadir, Assistant Professor (1988-1994).
Main range of scientific interests: The research interest covers corrosion inhibition of aluminium, tin and tinplate in industrial water by oxoanions, tetrazole, pyrazole and aminoacid and ester compounds. Additionally, he works on pesticide degradation in water, soil, fruits and vegetables.
Pubications: He has published more than 40 papers in corrosion and sensors fields.

Rachid Salghi

Organization: Ecole Nationale des Sciences Appliquées of Agadir. He was awarded a PhD degree in Corrosion field in 1999. He is lecturer professor, his researcher is in the Laboratoire d'Ingénierie des procédés de l'Energie et de l'environnement (LIPEE). He is expert in the pesticide field.
Education: Ecole Nationale des Sciences Appliquées Agadir, Diplome d'habilitation (2005), Université Mohamed Premier, Faculté des Sciences d'Oujda, PhD degree in Chemistry Sciences (1997-1999). Université Mohamed Premier, Faculté des Sciences d'Oujda, Diplôme d'Etude Supérieures in Chemistry Sciences (1994-1997).
Experience: Ecole Nationale des Sciences Appliquées d'Agadir, Lecturer professor (2005 – to date). Ecole Superieure de Technologie d'Agadir, Asistant professor (2001-2005). Ministère de l'Agriculture, Etablissement Autonome de Contrôle et de Coordination des Exportations; Chef of laboratory (2000–2001). Ministère de l'Agriculture, Etablissement Autonome de Contrôle et de Coordination des Exportations; Responsible of laboratory (1997–2000).
Main range of scientific interests: The research interest covers as well corrosion inhibition of aluminium, lead, tin and tinplate in industrial water by oxoanions, tetrazole, pyrazole and aminoacid and ester compounds as pesticide degradation in water, soil, fruits and vegetables.
Pubications: More than 30 papers in corrosion and pesticide.

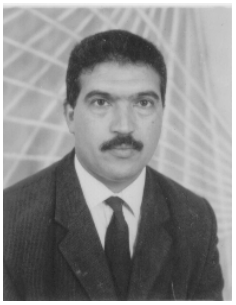

Belkhir Hammouti

Organization: University of Mohammed 1st Faculty of Science Oujda. He was awarded a PhD degree in Corrosion Science in 1994. He is currently a professor and the Director of the Laboratory of Applied Chemistry and Environment.
Education: University of Mohammed 1st Faculty of Science Oujda, Faculty of Science, Ph.D. degree in corrosion (1994). Ecole Normale Supérieure Rabat, Doctorat (DES), 1987.
Experience: University of Mohammed 1st Faculty of Science Oujda Professor B (2003 − to date).
University of Mohammed 1st Faculty of Science Oujda, Professor A (1999-2003).
University of Mohammed 1st, Faculty of Science Oujda, lecturer Professor (1994-1998). University of Mohammed 1st Faculty of Science Oujda, Assistant Professor (1988-1994).
Main range of scientific interests: Prof. Hammouti's research interest covers acidity sensors and corrosion inhibition of iron, steel, lead, aluminium and copper in mineral acids by tetrazole, pyrazole, polymer, thiophene, pyridine, peptide, aminoacid and ester compounds. Additionally his research interest is moreover directed towards the field of the pesticides and selective electrodes.
Pubications: More than 100 papers in corrosion and sensors fields.

Souad El Issami

Organization: Faculty of Science Agadir Morocco. She was awarded a PhD degree in Corrosion Science in 2005. She is currently a teacher and researcher in the Laboratory of Materials & Environment.
Education: University Ibn Zohr, Faculty of Science, PhD degree in corrosion (2005). University Ibn Zohr, Faculty of Science, Doctorat (DES), 1994.
Experience: University Ibn Zohr, Faculty of Science Agadir, lecturer Professor (2005 − to date). University Ibn Zohr, Faculty of Science Agadir, Assistant Professor B (2003-2005). University Ibn Zohr, Faculty of Science Agadir, Assistant Professor A (1995-2003).
Main range of scientific interests: The research interest covers as well corrosion inhibition of aluminium, lead, tin and tinplate in industrial water by oxoanions, tetrazole, pyrazole and aminoacid and ester compounds as pesticide degradation in water, soil, fruits and vegetables.
Pubications: More than 12 papers in corrosion.

El Habib Ait Addi

Organization: Ecole Supérieure de Technologie of Agadir. He was awarded a PhD degree in Corrosion Science in 2005. He is currently an assistant professor.
Education: University Ibn Zohr, Faculty of Science, PhD degree in corrosion (2005).
Experience: Ecole Superieure de Technologie d'Agadir, Asistant professor (2006 − to date). Ministère de l'Agriculture, Etablissement Autonome de Contrôle et de Coordination des Exportations; Chef of laboratory (2001–2006). Ministère de l'Agriculture, Etablissement Autonome de Contrôle et de Coordination des Exportations (1995–2001).
Main range of scientific interests: The research interest covers corrosion inhibition of tin and tinplate in industrial water by oxoanions, tetrazole, pyrazole and aminoacid and ester compounds, pesticide persistence and the dissipation of their residues in water, soil, fruits and vegetables and chemical quality of the industrial wastewater.
Pubications: More than 16 papers in corrosion and pesticide.

Introduction

Numerous investigations have been performed on the corrosion inhibition of copper and its alloys by the use of different organic compounds [1-9]. Among the practical interest of these later are the chemical bond that linked the inhibitors and the metal. Therefore, the organic inhibitors provide often an excellent protection against corrosion phenomenon. This protection was explained by the presence of heteroatoms (S, N, P, Se) in the molecular structure of the inhibitors [8-12].

The addition of an inhibitor at certain concentration minimises the direct interaction between the metal and corrosive agents. In some cases, the coordination of the inhibitor molecules to the surface is weak, and their presence in the corrosive solutions required maintaining the desired concentration of these agents to attain a minimal protection of the metal [10-13]. As some inhibitor molecules also serve as reducing agents for the copper oxidation products, they must be continuously added to avoid other possible type of corrosion [14].

In the last few decades, numerous investigations were performed by using the traditional electrochemical methods [15-17], but recently, many research groups try to understand processes taking place at electrode surfaces by using in situ different accelerated corrosion techniques coupled by surface sensitive techniques like quartz crystal microbalance (QCM) and scanning probe microscopy (SPM) [18-22]. These in situ techniques have fostered a better understanding of dissolution/deposition of metals and adsorption of different ions by measuring mass differences in order of nanogram per surface area or visualizing the surface morphological changes in nanometer or even atomic scale. Related to this issue, several investigations [23-27] reported that the inhibition effectiveness might be due to the formation of thin layers of copper-inhibitor complexes. It's found also that 5-mercapto-1-phenyl-tetrazole (PMT) was an efficient inhibitor against the dissolution of various metals in different acid mediums [5, 6, 28]. This molecule adsorbs probably through the sulphur atom or through coordination with nitrogen from the tetrazole ring [29]. Ye et al. [30] demonstrate also that copper surface is normally coated with cuprous oxide layer (Cu_2O), and PMT forms protective barriers of inert, insoluble and long-lasting polymeric Cu(I) complex coating on the Cu_2O substrate.

The aim of this paper is to study the corrosion behaviour of copper in 0.1 M HNO_3 in the presence and in the absence of the tetrazolic compounds at 25 °C by the use of gravimetric measurements combined with linear potential scan voltammetry (I-E) and electrochemical impedance spectroscopy (EIS) methods.

Experimental methods

Materials

The material used was prepared from copper (99.99 %). The specimens used in the gravimetric tests have a rectangular form (2×3 cm). For the electrochemical studies, the electrode was provided in rod form and was embedded in epoxy resin in a Teflon holder with electrical contact being achieved by means of a copper wire threaded into the base of the metal sample. The surface of the specimen was 0.35 cm^2. Prior to each test, the exposed surfaces were abraded successively with different emery paper up 1200 grade, washed thoroughly with acetone and rinsed with double distilled water. The experiments were carried out in aerated 0.1M HNO_3 solution which was prepared using analytical grade reagent (65 %) and double distilled water. All experiments have been performed at temperature 25 ± 1 °C. Tetrazolic compounds tested (at 10^{-3}M) were 1,2,3,4-tetrazole (TTZ), 1-phenyl-1,2,3,4-tetrazole (PT), 1-phenyl-5-mercapto-1,2,3,4-tetrazole (PMT), and 5-amino-1,2,3,4-tetrazole (AT). They are Aldrich commercial products (> 99 % purity). Their molecular structures are shown in Fig. 1.

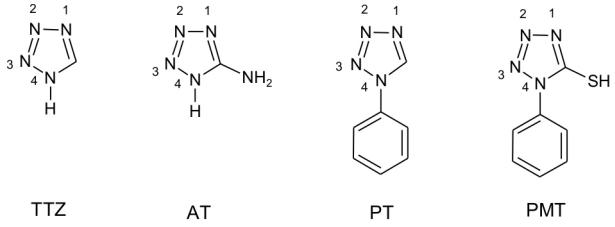

Fig. 1. *Molecular structures of organic compounds tested*

Gravimetric and electrochemical measurements

Gravimetric measurements were carried out in a double walled glass cell equipped with a thermostat-cooling condenser. All experiments were carried out under total immersion in 75 ml of test solutions at temperature 25 °C. Mass loss was recorded by an analytical balance with 0.1 mg accuracy at 72 hours of immersion.

Steady-state polarization experiments were conducted with a potentiostat PGP 201. The polarization curves were obtained by means of the linear potential sweep of 60 mV min^{-1} after the working electrode was left under free corrosion (for about 30 min) to reach a stable potential. The electrochemical measurements were performed in a conventional three-electrode electrochemical cell (Tacussel Standard CEC/TH). Saturated calomel electrode (SCE) and platinum electrode are used as reference and auxiliary electrodes, respectively.

Electrochemical impedance spectroscopy (EIS) was carried out with a voltalab PGZ 100 electrochemical system at E_{corr} after immersion in solution. After determination of the steady-state current at a given potential, sine wave voltage (10 mV) peak to peak, at frequencies between 100 kHz and 10 mHz was superimposed on the rest potential. Computer programs (Voltamaster4) automatically controls the measurements performed at rest potentials after 30 min of exposure. The impedance diagrams were given in the Nyquist representation.

Results and discussion

Comparative study

The effect of the addition of tetrazolic compounds on the corrosion of copper in aerated nitric acid solution was studied by gravimetric measurements after 72 hours of immersion period and at 25 °C. The concentration of these inhibitors of 10^{-3} M was chosen to compare the inhibition efficiency of the four compounds toward the

generalised corrosion. The value of the inhibition efficiency (E_G/%) was determined using the equation (1).

$$E_G = \frac{W_{corr} - W'_{corr}}{W_{corr}} \times 100, \qquad (1)$$

where W_{corr} and W'_{corr} (mg·h^{-1}·cm^{-2}) are the corrosion rate in absence and presence of the inhibitor, respectively.

The corrosion data for different inhibitors tested are reported in Table 1.

Table 1

Corrosion rate of copper in 0.1 M HNO_3 with and without tetrazole at 10^{-3} M, and the corresponding inhibition efficiency

Solution	W_{corr} / μg cm^{-2}·h^{-1}	E_G / %
Blank	3.65	-
TTZ	2.50	31
AT	1.51	58
PT	0.20	94
PMT	0.09	97

According to this data, it is clear that the addition of tetrazolic compounds reduces the corrosion rate of copper in nitric acid solution. The inhibition efficiency was found to depend on the nature of substituents.

Potentiokinetic polarization curves were plotted for copper in 0.1M HNO_3 solution in the presence of TTZ, PMT, AT or PT at 10^{-3} M (Fig. 2).

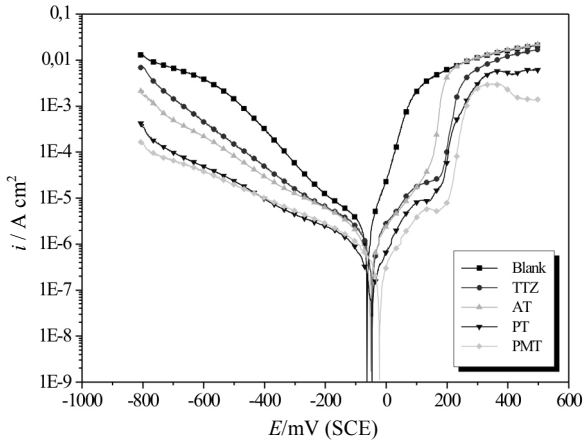

Fig. 2. *Polarization curves of copper in 0.1 M HNO_3 with and without tetrazole at 10^{-3} M*

A linear region with apparent Tafel was observed. The cathodic reaction was activation-controlled and the addition of the compounds tested decreased the current densities in large anodic and cathodic domains of potential. This result indicated that the compounds studied acted as mixed-type inhibitors. Generally, the addition of mixed inhibitors in solution does not change corrosion potential significantly because they inhibit both the anodic and cathodic reactions. Small changes in potentials can be a result of the competition of the anodic and the cathodic inhibiting reactions, and of the metal surface condition.

Table 2 gives the values of the associated electrochemical parameters.

Table 2

Electrochemical parameters of copper in 0.1 M HNO_3 with and without tetrazole at 10^{-3} M, and the corresponding inhibition efficiencies

Solution	E_{corr} / mV (SCE)	I_{corr} / μA cm^{-2}	R_p / Ω cm^2	βc / mV dec^{-1}	E_I / %	E_{Rp} / %
Blank	−63	4.3	4050	−85	–	–
TTZ	−49	3.0	5525	−73	30	27
AT	−54	1.7	11065	−74	60	63
PT	−51	0.3	92500	−75	94	96
PMT	−27	0.2	133320	−75	95	97

The inhibition efficiency (E_I / %) was determined using the equation (2) :

$$E_I = \frac{I_{corr} - I'_{corr}}{I_{corr}} \times 100 \ , \qquad (2)$$

I_{corr} and I'_{corr} are the uninhibited and inhibited corrosion current densities, respectively, determined by extrapolation of the cathodic Tafel lines to corrosion potential (E_{corr}).

From Table 2, it was clearly seen that cathodic slope was found equal indicating that the reduction of hydrogen did not modified in the presence of the inhibitors tested. Thus, the presence of tetrazolic compounds at 10^{-3} M leads to decrease in the values of I_{corr}, which was particularly significant in the case of PMT.

The inhibition properties of tetrazolic compounds were evaluated also by polarization resistance method. Fig. 3 presents plots of the current densities as a function of over-voltage near the corrosion potential E_{corr}.

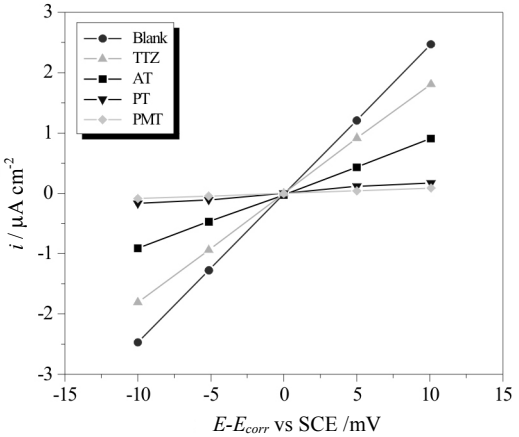

Fig. 3. *Linear polarization curves of copper in 0.1 M HNO_3 with and without tetrazole at 10^{-3} M*

Table 2 gathered the corresponding values of polarization resistance R_p and the inhibition efficiency (E_{Rt}/ %) which is calculated using the equation (3).

$$E_{Rp} = \frac{Rp'-Rp}{Rp'} \times 100 \ , \qquad (3)$$

R_p and R'_p are the polarization resistance values without and with inhibitor, respectively.

From polarization resistance measurements, the weakest value of R_p is found for copper in 0.1 M HNO_3 without inhibitor. However, the addition of the tetrazole in solution leads to an increase in the polarization resistance values. In fact, the value of R_p is 5525 Ω cm^2 in the case of TTZ and increases for AT (11065 Ω cm^2), PT (92500 Ω cm^2) and PMT (R_p = 133320 Ω cm^2). This in turn leads to a decrease in corrosion current density I_{corr} values because this later is inversely proportional to R_p.

Furthermore, corrosion behaviour of copper, in acidic solution with and without addition of tetrazole at 10^{-3} M, is investigated by electrochemical impedance spectroscopy (EIS) measurement at corrosion potential (E_{corr}) and after 30 min of immersion (at 25 °C). The corresponding Nyquist diagrams are shown in Fig. 4.

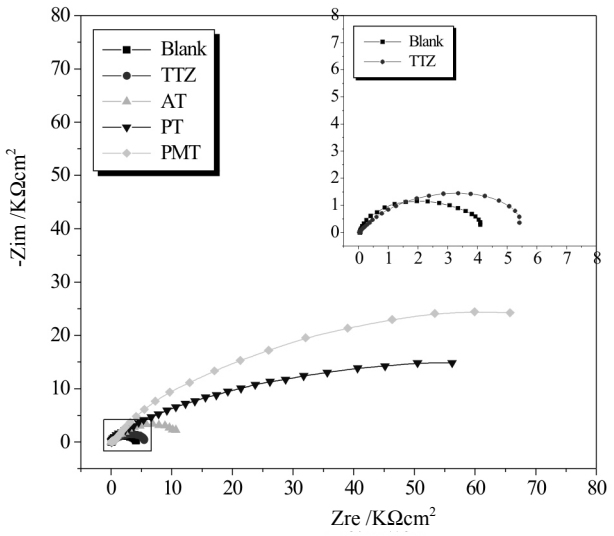

Fig. 4. *Nyquist plots obtained for copper in 0.1 M HNO_3 without and with tetrazole at 10^{-3} M (at E_{corr})*

The charge-transfer resistance (R_t) values are calculated from the difference in impedance at low and high frequencies, as suggested by Tsuru et al. [31]. The double layer capacitance (C_{dl}) was obtained, at the frequency fm at which the imaginary component of the impedance is maximum ($-Z_{im.}$), using the equation (4):

$$C_{dl} = \frac{1}{2\pi f_m R_t} . \qquad (4)$$

The impedance parameters derived from this investigation are mentioned in Table 3.

Table 3

Impedance parameters for copper in 0.1 M HNO_3 with and without addition of tetrazolic inhibitors at 10^{-3} M, and the corresponding inhibition efficiency

Solution	R_s / Ω cm^2	R_t / Ω cm^2	f_m / Hz	C_{dl} / μF cm^{-2}	E_{R_t} / %
Blank	14	4096	0.63	61.6	-
TTZ	16	6020	0.63	41.9	32
AT	18	13250	0.4	30.0	69
PT	21	90770	0.2	8.7	95
PMT	22	135170	0.2	5.9	97

The inhibition efficiency (E_{R_t} / %) got from the charge-transfer resistance is calculated using the following equation:

$$E_{Rt} = \frac{R'_t - R_t}{R'_t} \times 100 \qquad (5)$$

R_t and R'_t are the charge-transfer resistance values without and with inhibitors, respectively.

As we notice, Fig. 4, the impedance diagram, corresponds to the blank, shows perfect semi-circle indicating a charge transfer process mainly controlling the corrosion of copper. The addition of tetrazolic compounds enhances the value of the transfer resistance in acidic solution. EIS study confirms that the tested compounds are efficient inhibitors.

From the impedance data reported in Table 3, the values of R_t increase according to the sequence TTZ < AT < < PT < PMT. This behaviour reveals the adsorption of inhibitors on the copper surface, and an increasing in the values of corrosion inhibition efficiency. The value of double-layer capacitance decreases in the presence of tetrazole. This decrease confirms the adsorption of these compounds on the metal surface leading to a film formation on the copper surface. The inhibition efficiency obtained from EIS measurement are close to those deduced from polarization and gravimetric methods.

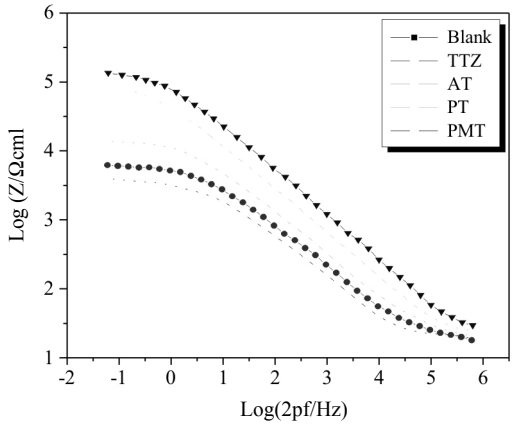

Fig. 5. *Bode plots of copper in 0.1 M HNO_3 containing different tetrazolic compounds at 10^{-3} M (at E_{corr})*

As the impedance diagrams obtained in the case of PT and PMT inhibitors, the semi-circles are more nonperfect. In this subject, several studies showed that the semi-circle is imperfect while the inhibition effect of the inhibitors is important [32-36].
Fig. 5 shows the Bode plots on the electrodes made of these samples.
The EIS results for the liquid and steam-treated samples can be explained by the simple equivalent Randles circuit [37], Fig. 6, which consist of a solution resistance R_s in series with a component composed of parallel film capacitance C_{dl} and transfer resistance R_t [38].

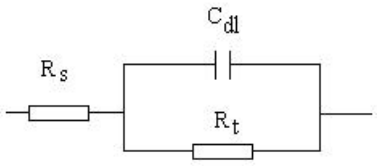

Fig. 6. *A simple Randles-type equivalent circuit for EIS measurements*

The values of the inhibition efficiency obtained from different methods are in good agreement. Therefore, the inhibiting effect was found to increases according to the following sequence: TTZ < AT < PT < PMT.
This order is mainly due to the nature of the substituents and its position. It's well known that different substituents on the organic molecule polarize the functional group in a different manner [39] and the inhibition efficiency of organic inhibitor containing heteroatoms should follows the sequence O < N < S < P [40]. The presence of NH_2 in AT, phenyl in PT, SH and phenyl in PMT may increase the polarity and the adsorbability of inhibitors on the metal surface. Therefore, the inhibition efficiency of TTZ is about 30 % and increases to 63 % in the cases of AT, then it attain 97 % with PMT. These jumps may be explained by the calculation of the net atomic charges [41]. The net charge of sulphur atom being −0.061 e, is adsorbed on the surface of metal. The presence of both phenyl and SH groups in PMT leads to synergistic intramolecular effect (Table 4) [30, 42-43].

Table 4

Net atomic charges of tetrazolic compounds calculated by PETRA program [41]

Inhibitor	***N*(1)**	***N*(2)**	***N*(3)**	***N*(4)**	***S***	E_{LUMO} **/ eV**	E_{HOMO} **/ eV**	**Δ*E* / eV**
TTZ	-0.2439	-0.1391	-0.1743	0.1502	-	-0.085	-11.413	11.32
AT	-0.1658	-0.1101	-0.1176	0.1950	-	0.018	-10.084	10.10
PT	-0.2212	-0.1165	-0.1559	0.1852	-	-0.765	-9.893	9.128
PMT	-0.2258	-0.1132	-0.1701	0.1826	-0.061	-0.800	-9.418	8.618

The calculation shows that *N*(4) with positive charge does not participate to the adsorption phenomenon. Yan et al. [44] revealed that 2-mercaptobenzoxazole (MBO) is the good inhibitor toward copper corrosion in NaCl solution. Their studies show that the inhibition film (MBO-Cu) causes shift of N_{1S} and S_{2p} binding energies. Consequently, it could be inferred that the presence of mercapto group and nitrogen atom in the molecule could have an important role in the formation of the inhibition film.
The computation of some of quantum chemical parameters such as the energies of the molecular orbitals, E_{HOMO} (High Occupied Molecular Orbital Energy) and E_{LUMO} (Lowest Unoccupied Molecular Orbital Energy), has been determined for possible relations with the inhibitor efficiencies of the inhibitors tested (Table 4). HOMO energy is often associated with the electron donating ability of a molecule. The less negative HOMO energy and the smaller energy gap ($\Delta E = E_{LUMO} - E_{HOMO}$) are often interpreted by a stronger chemisorption bond and perhaps greater inhibition efficiency [45, 46]. The plot of the inhibition efficiency of tetrazolic compounds against E_{HOMO} showed a linear correlation of slope equal to unity and regression coefficient $R = 0.99$ (Fig. 7). The similar results were obtained elsewhere [47].
From the results of the comparative study, it's evident that PT and PMT were the excellent corrosion inhibitors for copper in nitric acid medium. Afterwards of this work, we proposed doing a detailed study of PMT in order to better understand its inhibition mechanism.

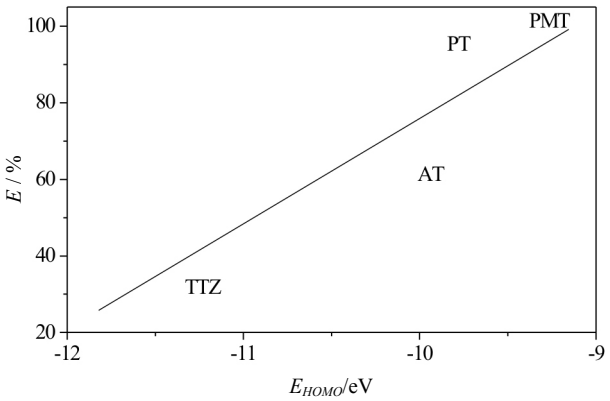

Fig. 7. *Correlation of HOMO energies with percent inhibition efficiency of tetrazole derivatives*

Effect of PMT concentration

Table 5 regroups the gravimetric parameters (W_{corr} and E_G / %) of copper in 0.1M HNO_3 in the presence of PMT at different concentrations after 72 h of period immersion.

Table 5
Corrosion rate of copper in 0.1 M HNO_3 with PMT at different concentration, and the corresponding inhibition efficiencies at T = 25°C

[PMT]	W_{corr} / µg cm^{-2}·h^{-1}	E_G / %
Blank	3.65	-
10^{-9} M	1.83	50
10^{-8} M	1.45	60
10^{-7} M	0.65	82
10^{-6} M	0.50	86
10^{-5} M	0.38	90
10^{-4} M	0.20	94
10^{-3} M	0.09	97

According to this data, it's clear that the corrosion rate of copper in the blank is higher in comparison with the blank containing PMT. The addition of 10^{-9} M PMT into the aggressive medium reduces this corrosion rate by 51 % and reaches 97 % at 10^{-3} M. The inhibition efficiency of PMT increases as function of its concentration and exceeds 90 % from 10^{-5} M.

Fig. 8 presents the evolution of the current densities as function of the over-voltage near of the corrosion potential E_{corr}.

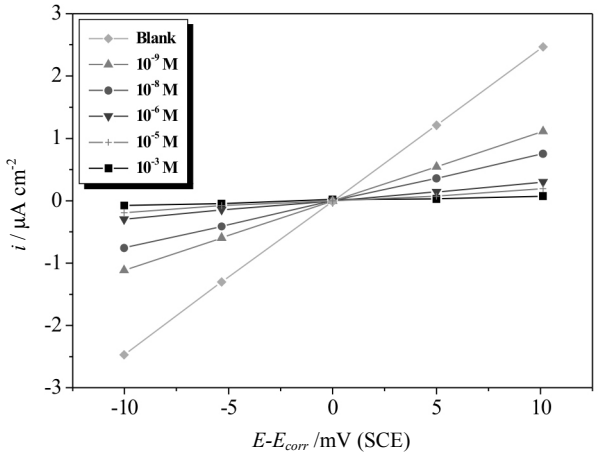

Fig. 8. *Linear polarization curves of copper in 0.1 M HNO_3 with PMT at different concentration*

The corrosion parameters such as the values of polarization resistance R_p and corresponding inhibition efficiencies (E_{R_p} / %) are shown in Table 6.

From the polarization resistance measurement (Fig. 8, Table 6), the polarization resistance R_p related to the copper in 0.1 M HNO_3 is the lower value. However, R_p was found to increase with the rise of PMT concentration. This result was accompanied with an increase of the inhibition efficiencies.

The effect of the addition of PMT at different concentration on the corrosion behaviour of copper in 0.1 M HNO_3 was studied also by the use of electrochemical impedance spectroscopy (EIS) measurements. The impedance diagrams and the corresponding electrochemical parameters are shown, respectively, in Fig. 9 and Table 6.

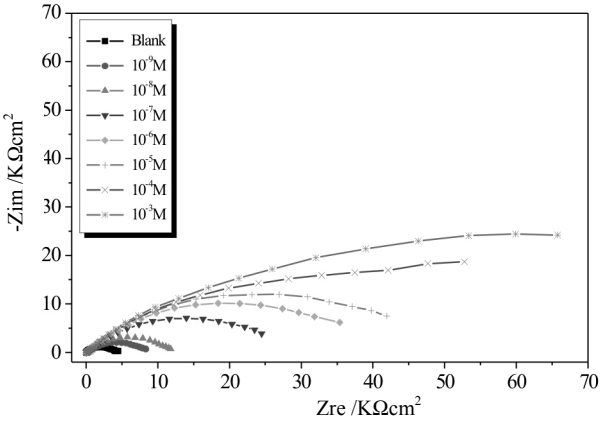

Fig. 9. *Nyquist plots obtained for copper in 0.1 M HNO_3 with PMT at different concentrations*

Table 6
Polarization resistance and impedance parameters of copper in 0.1 M HNO_3 in the presence of PMT at various concentrations, and the corresponding inhibition efficiencies

[PMT]	R_p/Ω cm^2	R_t/Ω cm^2	f_m/Hz	C_{dl}/µF cm^{-2}	E_{Rp}/%	E_{Rt}/%
Blank	4050	4096	0.63	61.7	-	-
10^{-9} M	9010	8340	0.63	30.3	55	51
10^{-8} M	13135	12250	0.63	20.6	69	66
10^{-7} M	20250	26180	0.40	15.2	80	84
10^{-6} M	34033	37990	0.35	12	88	89
10^{-5} M	52600	50070	0.3	10.6	92	92
10^{-4} M	67500	90450	0.2	8.8	94	95
10^{-3} M	132320	135170	0.2	5.9	97	97

The impedance diagrams obtained have, generally, a semicircular appearance. It indicates that the corrosion of copper is mainly controlled by a charge transfer process. The interaction of the tested molecule with the metal surface should be competitive with the interaction of the ions in the solution. In this case, the chemisorption has occurred. The adsorption would have occurred through polar centres as nitrogen and sulphur atoms. As for the shape of the impedance diagrams obtained, more nonperfect semi-circulars were found above 10^{-5}M concentration. This explains that PMT is very efficient at high concentrations. The similar results were found elsewhere [32-36].

From the impedance data, we conclude that increasing of PMT concentration provokes an increase of the value of

R_t and consequently the inhibition efficiency values. This behaviour shows the adsorption of PMT on copper surface which is approved also by the decrease of the values of double-layer capacitance as function of the concentration of PMT. This decrease may be due to the film formation on the copper surface [28, 30, 48-50].

Data were tested graphically by fitting to various isotherms. Fig. 10 shows the dependence of the fraction (θ) as function of the logarithm of the concentration of PMT, where θ is the ratio (*E*/%)/100.

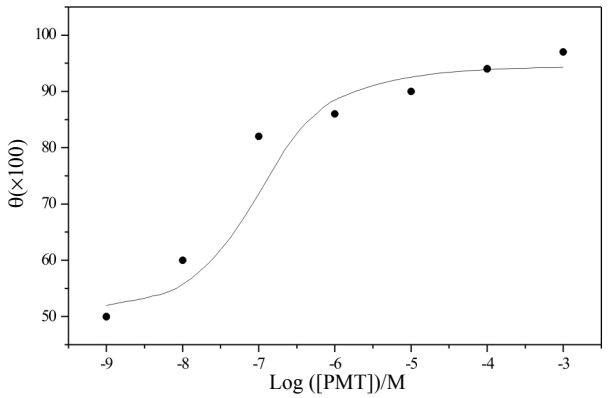

Fig. 10. *Frumkin isotherm adsorption of PMT on the copper surface in 0.1M HNO_3*

The obtained plot is consistent with an S-shape adsorbed isotherm for PMT showing an adsorption on the copper surface according to the Fumkin isotherm.

$$\frac{\theta}{1-\theta}\exp(-f\theta) = KC \qquad (6)$$

with

$$K = \frac{1}{55.5}\exp\left(-\frac{\Delta G^{\circ}_{ads}}{RT}\right), \qquad (7)$$

where ΔG°_{ads} is the free enthalpy of adsorption and f is a function of adsorption energy. The average value of k, f and ΔG°_{ads} calculated from θ = Log ([PMT]) curve are: f = -8.52; K= $13.5 \cdot 10^9$ and $\Delta\,\Delta G^{\circ}_{ads}$ = -67.7 kJ·mol^{-1}.

The negative value of ΔG°_{ads} indicates that strongly adsorbed on the copper surface. Literature shows that more negative than -40 kJ mol^{-1} indicating chemisorption of PMT molecules. Moreover, the inhibition of copper by PMT is often explained by formation of Cu(II)-PMT through its heteroatoms [30].

Conclusion

The inhibiting effect of tetrazolic compounds in 0.1 M HNO_3 on copper was studied by various methods. The results are in good agreement and the main conclusions are as follows.

− The corrosion inhibition efficiency (*E*/%) of tetrazolic compounds follows the sequence: TTZ < AT < PT < < PMT.

− PMT was found to be the best inhibitor for copper.

− The inhibition efficiency of PMT exceeds 90 % above concentration of 10^{-5} M.

− PMT adsorbs on the copper surface according to the Frumkin adsorption isotherm. The value of ΔG°_{ads} indicates that PMT adsorbs strongly and spontaneously.

References

1. Zucchi F., Grassi V., Frignani A., Trabanelli G. Inhibition of copper corrosion by silane coatings // Corrosion Science. 2004. Vol. 46, No. 11. P. 2853-2865.

2. Fouda A.S., Abd El-Aal A., Kandil A.B. The effect of some phthalimide derivatives on corrosion behavior of copper in nitric acid // Desalination. 2006. Vol. 201. No. 1-3. P. 216-223.

3. Dafali A., Hammouti B., Mokhlisse R., Kertit S. Substituted uracils as corrosion inhibitors for copper in 3 % NaCl solution // Corrosion Science. 2003. Vol. 45, No. 8. P. 1619-1630.

4. Otmacic H., Stupnisek-Lisac E. Copper corrosion inhibitors in near neutral media // Electrochim Acta. 2003. Vol. 48, No.8. P. 985-991.

5. Mihit M., El Issami S., Bouklah M et al. The inhibited effect of some tetrazolic compounds towards the corrosion of brass in nitric acid solution // Applied Surface Science. 2006. Vol. 252, No. 6. P. 2389-2395.

6. EL Issami S., Mihit M., Bazzi L et al. 1-phenyl-5-mercapto-tetrazole as an efficient inhibitors for copper corrosion in 0.1M HCl // Transactions of the SAEST. 2005. Vol. 40. P. 24-28.

7. El Issami S., Bazzi L., Hilali M et al. Inhibition of copper corrosion in HCl 0.5 M medium by some triazolic compounds // Annales de Chimie Sciences des Materiaux. 2002. Vol. 27, No. 4. P. 63-72.

8. El Issami S., Bazzi L., Mihit M et al. Some triazolic compounds as corrosion inhibitors for copper in hydrocloric acid // Pigment & Resin Technology. 2007. Vol. 36, No. 3. P. 161-168.

9. Kertit S., Essoufi H., Hammouti B., Benkaddour M. 1-phenyl-5-mercapto-1,2,3,4-tetrazole (PMT): un nouvel inhibiteur de corrosion de l'alliage Cu-Zn efficace a très faible concentration // Journal de Chimie Physique. 1998. Vol. 95, No. 9. P. 2070-2082.

10. Al-Kharafi F.M., Al-Hajjar F.H., Katrib A. Inhibition by heterocyclic compounds of corrosion of copper // Corrosion Science. 1990. Vol. 30, No. 8-9. P. 869-875.

11. Gonzalez S., Laz M.M., Souto R.M. et al. Synergistic effects in the inhibition of copper corrosion // Corrosion.1993. Vol. 49, No. 6. P. 450-456.

12. Carron K.T., Lowis M.L., Dong J. et al. Surface-enhanced Raman scattering and cyclic voltammetry studies of synergetic effects in the corrosion inhibition of copper by polybenzimidazole and mercaptobenzimidazole at high

temperature // Journal of Materials Science. 1993. Vol. 28, No. 15. P. 4099-4103.
13. Samide A., Bibicu I., Rogalski M., Preda M. A study of the corrosion inhibition of carbon-steel in dilluted ammonia media using 2-mercapto-benzothiazol (MBT) // Acta Chimica. Slovenica. 2004. Vol. 51, No. 1. P. 127-136.
14. Jennings G.K., Laibinis P.E. Self-assembled monolayers of alkanethiols on clean copper surfaces // Physicochemical and Engineering Aspects. 1996. Vol. 116, No. 1-2. P. 105-114.
15. Poling G.W. Reflection infra-red studies of films formed by benzotriazole on Cu // Corrosion Science. 1970. Vol. 10, No. 5. P. 359-370.
16. Cotton J.B., Scholes I.R. Benzotriazole and related compounds as corrosion inhibitors for copper // British Corrosion Journal. 1967. Vol. 2. P. 1-7.
17. Zucchi F., Fonsati M., Trabanelli G. 1996. Giornate Nationali Sulla Corrosion e Protezione, 3rd., AIM, Milano 115.
18. Tremont R., Cabrera C.R. Electrochemical and surface analysis study of copper corrosion protection by 1-propanethiol and propyltrimethoxysilane: A comparison with 3-mercaptopropyltrimethoxysilane // J. of Appl. Electrochem. 2002. Vol. 32, No. 7. P. 783-793.
19. Ryu D.Y., Free M.L. The importance of temperature and viscosity effects for surfactant adsorption measurements made using the electrochemical quartz crystal microbalance // J. of Colloid and Interface Sci. 2003. Vol. 264, No. 2. P. 402-406.
20. Wang C.-T., Chen S.-H., Ma H.-Y., Qi C.-S. Protection of copper corrosion by carbazole and N-vinylcarbazole self-assembled films in NaCl solution // J. of Appl. Electrochem. 2003. Vol. 343. P. 179-184.
21. Christy A.G., Lowe A., Otieni-Alegro V., Stoll M., Webster R.D. Voltammetric and Raman micro-spectroscopic studies on artificial copper pits grown in simulated potable water // J. of Appl. Electrochem. 2004. Vol. 34. P. 225-233.
22. Voisey K.T., Liu Z., Stott F.H. Inhibition of metal dusting using thermal spray coatings and laser treatment // Surface and Coatings Technology. 2006. Vol. 201. P. 637-648.
23. Fonsati M., Zucchi F., Trabanelli G. Study of corrosion inhibition of copper in 0.1 M NaCl using the EQCM technique // Electrochim. Acta. 1998. Vol.44. No.2-3. P. 311-322.
24. Zucchi F., Trabanelli G., Fonsati M. Tetrazole derivatives as corrosion inhibitors for copper in chloride solutions // Corrosion Science. 1996. Vol. 38, No. 11. P. 2019-2029.
25. Szocs E., Vastag G., Shaban A, Kalman E. Electrochemical behaviour of an inhibitor film formed on copper surface // Corrosion Science. 2005. Vol. 47. P. 893-908.
26. Blajiev O., Hubin A. Inhibition of copper corrosion in chloride solutions by amino-mercapto-thiadiazol and methyl-mercapto-thiadiazol: an impedance spectroscopy and a quantum-chemical investigation // Electrochim. Acta. 2004. Vol. 49. P. 2761-2770.
27. Ismail K.M. Electrochemical preparation and kinetic study of poly(o-tolidine) in aqueous medium // Electrochem. Acta. 2007. Vol. 58. P. 3883-3888.
28. Kertit S., Hammouti B. Corrosion inhibition of iron in 1M HCl by 1-phenyl-5-mercapto-1,2,3,4-tetrazole // Applied Surface Science. 1996. Vol. 93. P. 59-66.
29. Vastag G., Szocs E., Shaban A., Kalman E. New inhibitors for copper corrosion // Pure Appl. Chem. 2001. Vol. 73, No. 12. P. 1861-1869.
30. Ye X.R., Xin X.Q., Zhu J.J., Xue Z.L. Coordination compound films of 1-phenyl-5-mercaptotetrazole on copper surface // Applied Surface Science. 1998. Vol. 135. P. 307-317.
31. Tsuru T., Haruyama S., Gijutsu B. Corrosion inhibition of iron by amphoteric surfactants in 2M HCl // J. Jpn. Soc. Corros. Eng. 1978. Vol. 27. P. 573-581.
32. Frignani A., Monticelli C., Brunoro G., Trabanelli G. (1985) Proc 6th Eur Symp Corr Inh Ferrara Italy 1519.
33. Sherif E.M., Park S.M. 2-amino-5-ethyl-1,3,4-thiadiazole as a corrosion inhibitor for copper in 3.0 % NaCl solutions // Corrosion Science. 2006. Vol. 48. P. 4065-4079.
34. Ma H., Chen S., Yin B., Zhao S., Liu X. Impedance spectroscopic study of corrosion inhibition of copper by surfactants in the acidic solutions // Corrosion Science. 2003. Vol. 45. P. 867-882.
35. Guo W.J., Chen S.H., Huang B.D., Ma H.Y., Yang X.G. Protection of self-assembled monolayers formed from triethyl phosphate and mixed self-assembled monolayers from triethyl phosphate and cetyltrimethyl ammonium bromide for copper against corrosion // Electrochim. Acta. 2006. Vol. 52, No. 1. P. 108-113.
36. Larabi L., Benali O., Mekelleche S.M., Harek Y. 2-mercapto-1-methylimidazole as corrosion inhibitor for copper in hydrochloric acid // Applied Surface Science. 2006. Vol. 253, No. 3. P. 1371-1378.
37. Zhou G.D., Feng Y., Fujishima A., Loo B.H. Detection of pitting on cast iron with AC impedance spectroscopy // Bull. Chem. Soc. Jpn. 1992. Vol. 65, No. 9. P. 2315-2318.
38. Hladky K., John D.G., Worthington S.E., Herbert D. Corrosion monitoring on stainless steel under condensing nitric acid conditions // Br. Corrosion. J. 1980. Vol. 15. P. 20-33.
39. Walter G.W. A review of impedance plot methods used for corrosion performance analysis of painted metals // Corrosion Science. 1986. Vol. 26, No. 9. P. 681-703.
40. Kertit S., Bekkouch K., Hammouti B. Corrosion inhibition of a carbon steel in 2 M H_3PO_4 medium by tetrazole: type organic compounds // Rev. Metal. Paris. 1998. Vol.95. No.2. P. 251-257.
41. Thomas J.G.N. (1981) in: Proceedings of the Fifth European Symposium on Corrosion Inhibitors, Ann. Univ. Ferrara. 453.
42. Ihlenfeldt W.D., Gasteiger J. Hash codes for the identification and classification of molecular structure elements // J. Comput Chem. 1994. Vol. 8, No.15. P. 793-813.

43. Zhang D.Q., Gao L.X., Zhou G.D. Synergistic effect of 2-mercapto benzimidazole and KI on copper corrosion inhibition in aerated sulfuric acid solution // J. of Appl. Electrochem. 2003. Vol. 33, No. 6. P. 361-366.
44. Yan C.W., Lin H.C., Cao C.N. Investigation of inhibition of 2-mercaptobenzoxazole for copper corrosion // Electrochim. Acta. 2000. Vol. 45, No. 17. P. 2815-2821.
45. Abdallah M., Helal E.A., Fouda A.S. Aminopyrimidine derivatives as inhibitors for corrosion of 1018 carbon steel in nitric acid solution // Corrosion Science. 2006. Vol. 48. P. 1639-1654.
46. Wang H., Wang X., Wang H., Wang L., Liu A. DFT study of new bipyrazole derivatives and their potential activity as corrosion inhibitors // J. Mol. Model. 2007. Vol. 13. P. 147-149.
47. Khaled K.F. The effect of poly(vinyl caprolactone-co-vinyl pyridine) and poly(vinyl imidazol-co-vinyl pyridine) on the corrosion of steel in H_3PO_4 media // Electrochim. Acta. 2003. Vol. 48, No. 17. P. 2493-2503.
48. Bentiss F., Traisnel M., Vezin H., Lagrenée M. Linear resistance model of the inhibition mechanism of steel in HCl by triazole and oxadiazole derivatives: structure-activity correlations // Corrosion Science. 2003. Vol. 45, No. 2. P. 371-380.
49. Lebrini M., Lagrenée M., Vezin H., Traisnel M., Bentis F. Experimental and theoretical study for corrosion inhibition of mild steel in normal hydrochloric acid solution by some new macrocyclic polyether compounds // Corrosion Science. 2007. Vol. 49, No. 5. P. 2254-2269.
50. Bentiss F., Vezin H., Lagrenée M. The inhibition of mild steel corrosion in acidic solutions by 2,5-bis(4-pyridyl)-1,3,4-thiadiazole: Structure–activity correlation // Corrosion Science. 2002. Vol. 48, No. 5. P. 1279-1291.

.

PHYSICAL PROPERTIES OF STABILIZED ICE SLURRY FOR TRANSPORT OF COLD THERMAL ENERGY

L. Royon

Pres Paris Est, Laboratoire MSC, University Paris Denis Diderot, Paris 75013, France
E-mail: laurent.royon@paris7.jussieu.fr

Received: 29 July 2007; accepted: 25 Aug 2007

A dispersion of phase-change materials is proposed as an experimental biphasic refrigerant. The phase change material is water stabilized by a tri-dimensional network of polymer, obtained by using a polymerizing process. The particle contains 90 per cent of water and has the consistency of a viscoelastic solid above the phase-change temperature. The measured values of the physical properties of the biphasic refrigerant, that is, specific heat, latent heat, density are presented for the considered temperature range. Pressure drop measurements are investigated and results show that the pressure drops of the slurry increased over the whole range of measured flow rate, while remaining in suitable values for a practical use. A supercooling phenomena is observed if the size of the particles becomes lower than 1mm, but the degree of supercooling however does not exceed 3 °C. The various advantages of this slurry show that this fluid appears well adapted for a wide variety of schemes where the production involves low temperature intervals, such as the refrigeration industry.

Keywords: cold storage and application of ice energy in homes and industry

Laurent Royon

Organization: Laboratory of Matter and Complex system, CNRS 7057.
Education: Doctor in Science, Paris Est University.
Experience: Scientific research on complex fluid as polymer solution and colloidal suspension.
Main range of scientific interests: rheology and thermodynamics of complex matter, heat transfer with phase change state.
Publications: 15 papers in international scientific journal in Int. Comm. Heat and Mass transfer, Int. J. of Energy Research, Experimental Heat Transfer, Energy Conversion management. 1 French Patent (2001).

Introduction

Restrictions on the use of greenhouse gases e.g. carbon dioxyde (CO_2), methane (CH_4), nitrous oxide (N_2O), hydrofluorocarbons (HCFs) etc, harmful on the layer of ozone, constraint the refrigeration and air-conditioning industry to develop practical solutions for the production and distribution of cold energy. One of them is the use of indirect cooling system which allow a significant reduction of primary refrigerant charge. Nevertheless, these systems currently have a limited efficiency because of the low heat capacity of the secondary fluid. In order to overcome these deficiencies, a promising technique is the application of biphasic fluids in which the dispersed component can undergo a solid-liquid phase transition. Such secondary fluids offer indeed many advantages as high cooling capacity, the possibility of using the same medium for both energy transport and storage (thereby reducing losses during the heat exchange process), a constant temperature during heat exchange, high heat transfer rates to the phase change component due to large surface area to weight ratio, a lower pumping rate, a higher heat transfer coefficient than conventional single-phase working fluid [1-3].

Among different slurries, ice-water slurry is one of the first PCMs suspension used in industrial applications. The fluid consists of mixtures of water (or ethanol/water) and fine ice particles which the size distribution (0.1 to 3 mm) depend on different production methods and the storage method. Several studies have been shown that heat capacity will be increased 2-4 times more than a traditional monophasic fluid and the size of the district cooling machinery can be reduced accordingly [4-6]. The major economical and technical drawback appears though the high cost of icemaking equipment and its maintenance. Actually, new research is focused on fluidized bed heat exchangers as an alternative solution to produce low-cost ice slurry [7].

An alternative form of ice slurry is presented in this paper. The idea is based on the stabilization of water (or ice) by a polymeric matrix. Water or ice is thus kept inside a tri-dimensional network. This form of coating gives the opportunity to use this slurry like a conventional secondary fluid.

The aim of this work is to present some experimental studies on the physical properties of this original slurry. The first part of this paper is devoted to a presentation of this double-phase working fluid and quantitative results concerning its thermophysical properties are presented in the second part in order to point out the potentialities of the material to accumulate and transport a great quantity of thermal energy.

Presentation of the stabilized ice slurry

The making of the particles of the slurry, which was the subject of a patent Anvar (Flaud et al. [8]), is based on a process of mass polymerization. The obtained particle contains a water concentration close to 90 per cent and has the consistency of a viscoelastic gel for a temperature above 0 °C. The phase-change element is thus retained in the network both because of interfacial stress and chemical bonds and no exudation of water occurs during the phase change cycle (Fig. 1). A very small quantity of antifreeze protein (AFP) is introduced in the water mother solution in order, for the final particle, to inhibit agglomeration of particle containing ice. Same additives are used for ice slurry [9, 10].

***Fig. 1**. Schematic representation of a spherical PCM particle*

The final material remains a well shape-defined sample, requiring no coating. It appears white and hard when frozen as opposed to transparent and elastic when unfrozen. Particles are then dispersed in a carrier fluid, which must be selected very carefully because it constitutes the greater fraction of the circulating material and serves as intermediary for heat transfer between the dispersed phase and the heat exchanger surfaces. Syltherm HF manufactured by Dow Chemical Company is chosen as suspending phase. A solid fraction of 25 % is taken for this study.

Physical characteristics of the slurry

The thermal characteristics and the flowability of the slurry, and their variation with weight fraction are reviewed in this section.

Thermal characteristics

Table 1 shows the specific heat capacity and the latent heat of the slurry as a function of the weight fraction of particles. This data are established taking into account that the measured specific heat capacity of a particle is 3.9 kJ·kg^{-1} °C^{-1} (for $T > 0$ °C) and the latent heat is 292 kJ·kg^{-1} and that the measured specific heat capacity of the suspended phase is 1.549 kJ·kg^{-1} °C^{-1}.

Table 1

Latent heat and specific heat capacity of the slurry

Weight fraction (%)	Latent heat (kJ·kg^{-1})	Specific heat capacity (kJ·kg^{-1} °C^{-1})
10	29.2	1.78
20	58.4	2.02
30	87.6	2.25
40	116.8	2.49

The density of the continuous phase oscillates between 906 kg·m^{-3} (at 20 °C) and 912 kg·m^{-3} (at -20 °C). The density of the particle is respectively 1047 kg·m^{-3} for $T >$ 0 °C and 920 kg·m^{-3} for $T < 0$ °C. According to the temperature and the weight fraction considered, the slurry is thus presented in the form of a quasi-homogeneous fluid when $T < 0$ °C. For $T > 0$ °C, the slurry is non-homogeneous because of phenomenon of sedimentation. A separation between the phases can be observed when the flow is stopped.

Pressure drop

A small-scale loop circuit is built for studying the fluid with in steady isothermal conditions. Flow tests were conducted with the carrier fluid and 25 % particle slurry at flow rate Q between 1 and 5 m^3/h. Temperature in the test section is maintained constant at 23 °C and then at -7 °C respectively. In order to validate the reliability of the loop and the results, experimental runs was performed using at first the suspending phase. Experimental runs were then performed with slurry at different flow rates.
Fig. 2 and Fig. 3 show the variation of the pressure loss with the velocity along the test section for two temperatures, 23 °C and -7 °C respectively. For the single phase and the two-phase mixture, one can observed that the pressure drop increases with velocity and decreases with temperature. This measured pressure-drop represents the results of a single quasi-steady test.

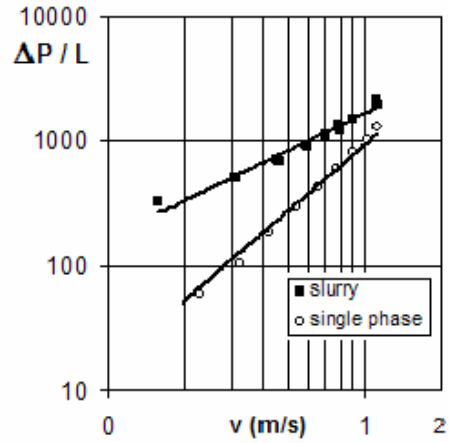

***Fig. 2.** Pressure drops versus velocity at T = -23 °C*

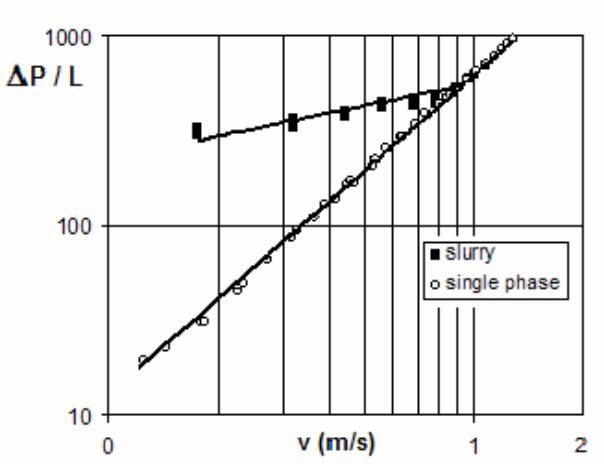

Fig. 3. *Pressure drops versus velocity at T = -7 °C*

Experimental data, presented in logarithmic coordinates, show that, for the carrier fluid, the pressure drop increases as $V^{1,75}$. This result is found in accordance with classical formula of Blasius form for turbulent flow. The maximum deviation of the measured pressure drop from the predicted values of the Blasius equation was 2 %. Therefore, the experimental system can be considered reliable.

For the slurry, on note that i) pressure drops are, for low velocity, always higher than pressure drops of the carrier fluid and ii) pressure loss of the particles flow at solid state (-7 °C) is greater than pressure loss at liquid state (+23 °C). At high velocity (> 1 m/s), pressure drop of the slurry tends to data of the single phase, which is characteristic of a symmetric suspension flow pattern. One note that this effect is very well observed for T = = 23 °C comparatively for T = -7 °C, although particle density is closer to carrier fluid density for T = -7 °C. This result can be interpreted with volume expansion of particles and particle aggregates. At intermediate velocity (< 1 m/s), the divergence of the slurry curves from the suspending fluid increases with decreasing flow rate, which reflects an asymmetric suspension flow pattern.

Aggregation phenomena

Cooling tests, carried out in a thermostated bath, showed that no aggregation appears when the slurry was placed under mixing (even weak). No difficulties are observed if a stagnant slurry is mixed again (for periods up to 60 min). On the other hand, an aggregation of the particles appears when the phase change liquid-solid is carried out without mixing. The phenomenon of aggregation is related to the dendritic form of the ice. Dendrites have the possibility of developing out of the polymeric matrix. Links between particles can thus be established if the slurry is placed without agitation. These links will be all the more easy to break that the size of particles is important.

Supercooling phenomena

Fig. 4 presents examples of recording of the temperature of slurry subjected to a cooling in a very slightly agitated tank. The slurry is characterized by the size from their particle respectively 0.6 mm (Fig. 4, *a)* and 2 mm (Fig. 4, *b*). It can clearly seen that supercooling occurs during the freezing process for slurry which average size of particle is 0.6 mm. The degree of supercooling is about 2 °C for this example.

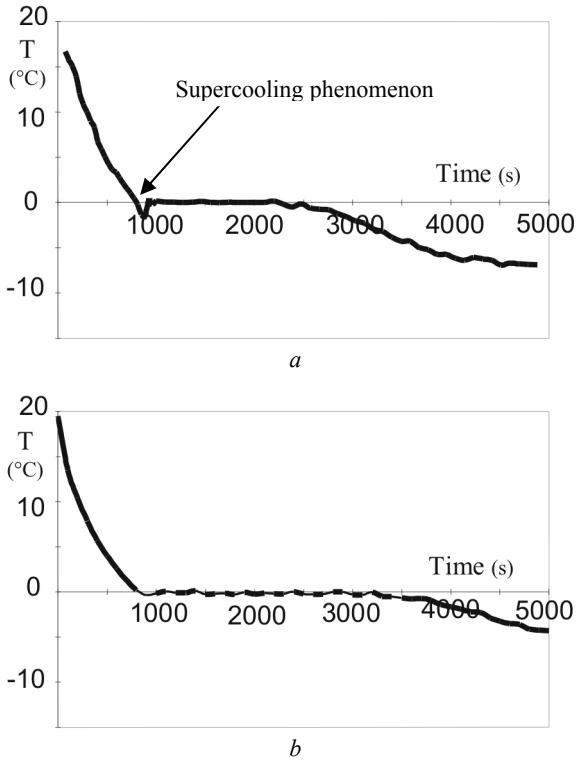

Fig. 4. *Cooling of the slurry in an agitated tank*

This delay with solidification is related mainly to the size of the particles [11, 12]. For an average mean size higher than 1mm, the fluid does not present practically any supercooling when the fluid is mixing.

Principal advantages of the slurry

For the purpose of air-conditioning applications, the use of the slurry instead of conventional chilled water presents several advantages. The principal ones of them are those of ice slurry. One can quote in particular:

1) the quasi-constancy of the temperature in the whole of the circulating pipe;
2) a circulation under a range of pressure close to the atmospheric pressure;
3) high heat transfer coefficient because of the presence of the liquid phase;
4) the possibility of making energy storage.

The other advantages which are specific to this slurry are:

a) a constant weight fraction in the circulating pipe;
b) more significant weight fraction (> 35 per cent) by the polydispersity of the PCM particles;
c) the absence of a generator of ice. A passage though a heat exchanger surface (evaporator) is enough to reload the slurry in "ice".
In addition, these advantages create considerable interest in this slurry-based air conditioning.

Concluding remarks

A prototype of slurry is presented as a potential working fluid for district cooling and air conditioning process. This double-phase fluid consists of particles of a gel containing a water concentration close to 90 per cent, dispersed in a carrier fluid with adjusted density and viscosity. This mixture is presented as a suspension of aqueous gel in oil for the temperature $T > 0$ °C, and as a suspension of gel of ice in oil for the temperature $T < 0$ °C.
The thermal parameters of this slurry are very near of those ice slurry, described in literature (for example [4, 13]). Its originality and its principal advantage is becoming from the classic heat exchanger surface used to store the latent cold heat.
Research is continuing on this slurry in order to determine other properties as heat transfer coefficient, pressure drop and flowability for different configurations.

References

1. Charunyakorn P., Sengupta S., Roy S.K. Forced convection heat transfer in microencapsulated phase change material slurries: flow in circular ducts // Int. J. Heat Mass Transfer. 1991. Vol. 34. P. 819-835.
2. Goel M., Roy S.K., Sengupta S. Laminar forced convection heat transfer in microencapsulated phase change material suspensions // Int. J. Heat Mass Transfer. 1994. Vol. 37. P. 593-604.
3. Roy S.K., Sengupta S. An evaluation of phase change microcapsules for use in enhanced heat transfer fluids' // Int. Comm. Heat Mass Transfer. 1991. Vol. 18. P. 495-506.
4. Ben Lackdhar M. Caractérisation thermohydraulique d'un fluide frigoporteur diphasique: le coulis de glace. Etude théorique et expérimentale. Thesis of physics, Insa de Lyon, No. 98, ISAL 0092, 1998, France.
5. Bellas J., Chaer I., Tassou S.A. Heat transfer and pressure drop of ice slurries in plate heat exchanger // Appl. Therm. Eng. 2002. Vol. 22. P. 721-732.
6. Knodel B.D., France D.M., Choi U.S., Wambsganss M.W. Heat transfer and pressure drop in ice-water slurries // Appl. Therm. Eng. 2000. Vol. 20. P. 671-685.
7. Meewisse J.W., Infante Ferreira C.A. Validation of the use of heat transfer models in liqui/solid fluidized beds for ice slurry generation // Int. J. of Heat & Mass Transf. 2003. Vol. 46. P. 3683-3695.
8. Flaud P., Tardi M., Schwartzman S. Patent Anvar No. 854012929, 1987.
9. Grandum S., Nagagomi K. Characteristics of ice slurry containing antifreeze protein for ice storage applications // J. of Thermophysics and Heat Transfer. 1997. Vol. 11, No. 3. P. 461-466.
10. Grandum S., Yabe A., Nakagomi K., Tanaka M., Takemura F., Kobayashi Y., Frivik P.E. Analysis of ice crystal growth for a crystal surface containing adsorbed antifreeze proteins // J. Cryst. Growth. 1999. Vol. 205. P. 382-390.
11. Clausse D. Caractérisation des propriétés thermophysiques d'une emulsion // Rev. Gén. Therm. Fr. 1985. No. 279. P. 263-268.
12. Clausse D. Germination de Phases // Entropie. 1990. No. 153. P. 33-39.
13. Paul J. La glace biphasique une autre technique de refrigeration // Rev. Gén. Froid. 1993. Vol. 9. P. 12-17.

ОСНОВНЫЕ ПРОБЛЕМЫ ЭНЕРГЕТИКИ
И АЛЬТЕРНАТИВНОЙ ЭНЕРГЕТИКИ

BASIC PROBLEMS OF ENERGY AND RENEWABLE ENERGY

STUDY OF THE MECHANICAL BEHAVIOUR OF CLAY, A NATURAL MATERIAL FOR HOUSE CONSTRUCTION

Y. Gagou, E. Padayodi**, K.-E. Atcholi**, P. Saint-Grégoire****

*LPMC, Université de Picardie Jules Verne, 33 rue Saint-Leu, 80039 Amiens Cedex 01, France
Telephone: +33 (0)3 22 82 78 27; Fax: +33 (0)3 22 82 78 91; E-mail: yaogagou@gmail.com

**LERMPS, UTBM, BP 449, 90010 Belfort Cedex, France
***UNIMES (The University of Nîmes), 30021 Nîmes Cedex 01, France

Received: 15 Dec 2007; accepted: 19 Jan 2008

Experimental results were obtained on four types of clays from various sites in Togo, West Africa (where they are traditionally used in house construction), to understand the rheological behaviour of these materials and the effects of the heat treatment on them, in order to optimize the process of structures manufacture. Four types of clays show very different behaviours, and the observed origin of sample cracking is compatible with the stress distribution in the structures.

Keywords: structural materials

Yaovi Gagou

Organization: Formed initially in the University of Lomé (Togo), Dr Yaovi Gagou has pursued his studies in France, first in Besançon and Belfort to defend his master in Mechanics of structures (in sept.1998). Then he continued at Toulon University where he prepared and defended his PhD on ferroelectrics (in March 2002). He is now assistant professor in Amiens (France), in Picardie Jules Verne University (since 2003).
Education: University of Lome (TOGO), Faculty of Sciences (1991-1996); University of Franche-Comté at Besançon (1997-1998); University of Sud Toulon-Var at Toulon (1999-2002).
Experience: Secondary School (Lycee de Chantilly in France): Teacher (2002-2003). University of Picardie Jules Verne in Amiens: Assistant professor and researcher (from 2003).
Scientific research projects: AI No. MA/07/165 Foreign Affair Ministry (France). Implication in the organization of several scientific meetings.
Main range of scientific interests: PLD, ferroelectrics (mainly Tungsten Bronzes), electrical and dielectric properties, material science, alternative energies for third world countries.
Publications: 16 papers in international scientific journals.

Introduction

Clay-based materials compete today with composite materials and find important applications in various fields of modern industry including civil engineering for the construction of big monuments and buildings, dams, ports, bridges, tarmacs, roads, etc [1, 2, 3]. Clay is also used in industry refractory materials for the manufacture of enameled earthenware, porcelain, and ceramics.
The mechanical behaviour of a clay-based structure depends not only on the chemical composition of the original raw material, i.e. the deposit site and its constituent minerals, but also on experimental conditions of formatting (consistency of the clay paste, external mechanical stresses and drying conditions).

Theoretical frame

Rheological behaviour

Clay pastes studied in this work were modeled by the classical law (see for instance references [4, 5]): $\sigma = k\dot{\varepsilon}^m\varepsilon^n$, where σ is the stress applied on the sample, k the consistency of the dough, $\dot{\varepsilon}$ the rate of deformation, ε – the generalized strain, m – the coefficient of sensitivity on the velocity, n – the coefficient of hardening.
By fitting the experimental curves by the above law, the obtained parameters are consistent with those typically obtained in the literature, namely: $0.02 < k < 0.5$ MPa·S^{-m}; $0.05 < m < 0.8$ and $0.03 < n < 0.60$.
This law is based on the properties of the class of so-called viscometric flows. In this case, for these flows, the stress tensor can be written in the form below, considering the axes in cylindrical coordinates [6, 7].

Besides, the measurement of the strain time rate permits to define three functions: $\tau(\gamma) = \sigma_{12}$, $N_1(\gamma) = \sigma_{11} - \sigma_{22}$, $N_2(\gamma) = \sigma_{22} - \sigma_{33}$, called viscometric functions, which define the behaviour of the fluid (here the clay paste).

As we noted in the preceding paragraph, the problem is treated in cylindrical coordinates. Fig. 1 illustrates the geometrical considerations used. The (cylindrical) symmetry imposes that the non-zero stress components are: σ_{rr}, $\sigma_{\theta\theta}$, σ_{zz}, τ_{rz}.

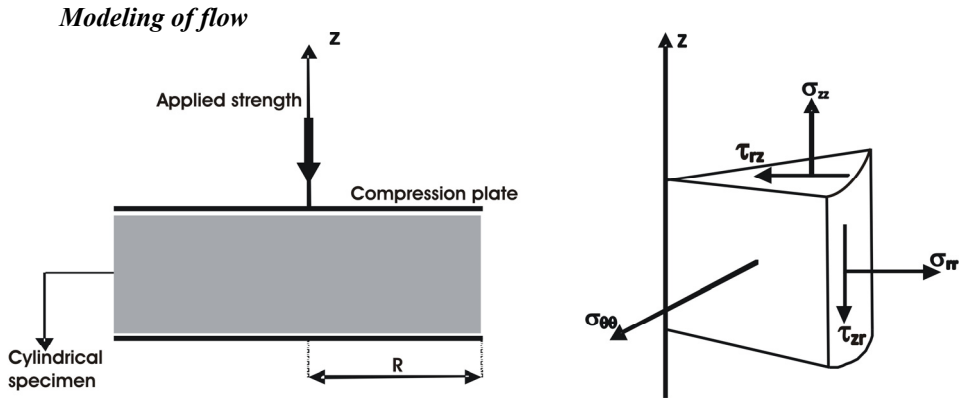

Fig. 1. *Plastometer with parallel plate and the stresses on a cylindrical element*

In our analysis of clay pastes, we neglect the terms related to gravity, because of the high rigidity of the paste, completely filling the inner cylinder.
In the same way we consider only the case of sufficiently slow flows to be able to neglect the inertial terms.
Under these conditions, the balance equations are written as [8, 9, 10]:

$$\begin{cases} \rho\dfrac{\partial u_r}{\partial t} = -\dfrac{\partial p}{\partial r} + \left[\dfrac{1}{r}\dfrac{\partial}{\partial r}\left(r\sigma_{rr}^{(d)} - \dfrac{\sigma_{\theta\theta}^{(d)}}{r} + \dfrac{\partial \tau_{rz}^{(d)}}{\partial z}\right)\right] \\ \rho\dfrac{\partial u_\theta}{\partial t} = -\dfrac{1}{r}\left[\dfrac{\partial p}{\partial \theta} - \dfrac{\partial \sigma_{\theta\theta}^{(d)}}{\partial \theta}\right] \\ \rho\dfrac{\partial u_z}{\partial t} = -\dfrac{\partial p}{\partial z} + \left[\dfrac{1}{r}\dfrac{\partial}{\partial r}\left(r\tau_{rz}^{(d)}\right) + \dfrac{\partial \sigma_{zz}^{(d)}}{\partial z}\right] \end{cases} \quad (1)$$

where u_r, u_θ, u_z are the components of velocity in the radial directions, tangential and axial, respectively, and p is the uniaxial pressure of the piston.
With the approximation that the material is assumed to be incompressible, the continuity equation writes:

$$\frac{1}{r}\frac{\partial}{\partial r}\left(ru_r\right) + \frac{1}{r}\frac{\partial u_\theta}{\partial \theta} + \frac{u_r}{\partial z} = 0. \quad (2)$$

It is assumed that the law governing the fluid behaviour may be written as:

$$\sigma_{ij}^{(d)} = \Psi\varepsilon_{ij}^{(d)}. \quad (3)$$

Ψ is a function of invariants of the strain time rate tensor that is independent of the deformation (strain) history.
The compression tests were also carried out on specimens submitted to drying, in the condition of a low rate of deformation (~ 0.5 mm/min, to avoid an abrupt fracture of the sample) in order to locate and follow the cracking of the material.

Experimental study

Experimental devices

The mold we used is a duralumin block with a cylindrical cavity of diameter 30 mm, with a well polished boundary. It is equipped with a plunger that is used to compress the clay paste manually in the cavity. This equipment is presented in Fig. 2. The set mold and the plunger are placed between two plates of the compression machine that allows to apply a controlled force during the formatting. The removal from the mold is done by slowly moving the plunger across one end of the mold. A plate absorbing shocks allows to retrieve the sample out.

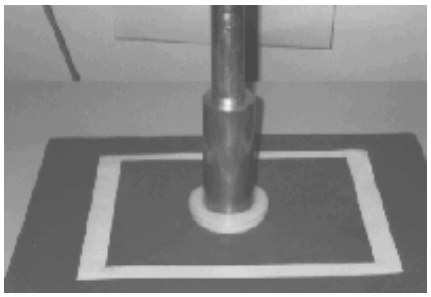

Fig. 2. *Plunger in place in the mold*

The universal tension/compression machine (INSTRON type), consists of a set of two columns equipped with a cross piece whose motion is performed by two ball screws of 1000 mm long with a pitch of 0.01 mm. It offers the possibility of displacements with a rate between 0.5 and 500 mm/min by steps of 0.01 mm/min. It is equipped with two parallel plates for the traction/ compression and the maximum force to be applied is 50 kN. The machine is entirely controlled by computer for the acquisition and processing of experimental results.

Preparation of the clay paste

Clays used in industry are generally a natural mixture of the following three main constituents [11, 12, 13]: kaolin clay (aluminum oxide Al_2O_3, silica $2SiO_2$, water $2H_2O$), feldspar providing sodium (Na) and potassium (K) that allow the formation of the vitreous phase, a neutral constituent ("charge") that reduces the shrinkage but does not act on the reactions during burning.

The different kinds of clays studied in this work are natural ones, coming from four different sites of Togo. They are labelled according to Table 1.

Table 1

The 4 studied clays from Togo (West Africa) and their notation

Clay variety	Notation
Green clay from Kouvé	AVK
Green clay from Togblékopé	AVTK
Red clay from Guérin-kouka	ARGK
White clay from Bandjéli	ABB

Clay powders were placed during 24 hours in an oven at 60 °C for a complete drying. The grading plays an important role in the mechanical properties of the obtained paste. A paste with smaller particles sizes has a more marked plasticity because the particles react more intensively between each other.

For the characterization of samples, we start from a quantity m_0 of anhydrous clay powder, which is then mixed with the quantity m_e of water to get a paste whose water content noted ω writes:

$$\omega = 100\frac{m_e}{m_0}, \text{ with } m_e = m - m_0, \ \omega = 100\frac{m - m_0}{m_0}.$$

The masses were measured using a METTLE PJ 360 Delta Range balance, with an accuracy of 0.01 g.

The water content ω ~ 18 % was deduced from the assessment of fluidity, of the consistency of paste and the external appearance of specimens after removal. The water content of the four varieties of studied clays range from 15 % to 20 %. This region of plasticity for pastes prepared is consistent with the limits set by ATTERBERG [14, 15, 16].

To get a clay paste having satisfying plasticity properties, the powder-water mixture must be kneaded (for about 2 h) until getting a homogeneous paste. The paste is then stored in a hermetically climatic chamber for more than 24 hours, to insure a uniform moisture content while preventing evaporation and increasing the plasticity of the paste under the effect of microorganisms that play an important role in the process.

Preparation and drying test specimens

The conditions used for the preparation of specimens are similar to those used in industrial tile factories (ω ~ 20 %, mass density ρ ~ g/cm^3). All specimens were prepared in the same experimental conditions, from the powder of the 4 varieties of clay. The specimen size (diameter D = 30 mm, height h = 30 mm) is defined to ensure a uniform compaction within the thickness of the specimen.

Compaction is performed by imposing the plunger motion with a low rate of 3 mm/min to avoid resistance due to the viscosity of the paste.

Clay pastes, even though they have good characteristics of cohesion, are subject to adhesion to the metallic walls in industrial processes, and this is also the case for the mold we used. In most cases, friction is below the threshold at which shear occurs. Therefore, pastes slip instead of warping, which promotes good removal without special lubricants [17, 18, 19]. Several samples were elaborated as shown in Fig. 3 where 24 specimens having a cylindrical shape are presented.

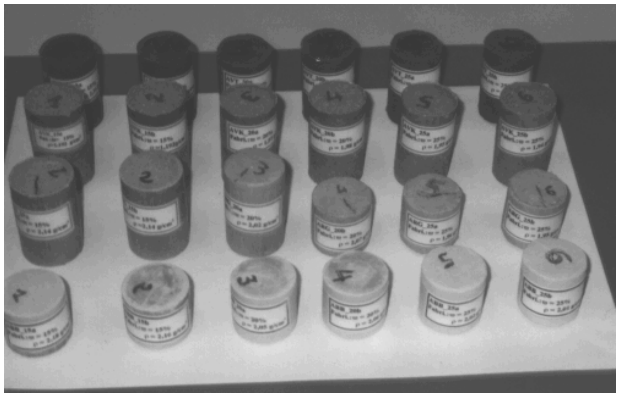

Fig. 3. *Clay specimens with cylindrical shape (from front to the back: ABB, ARGK, AVTK, AVK clays)*

In order to study the influence of the applied force, namely of the stress when compacting the paste, we divided the original clay paste in several samples, and we applied three levels of charge, one per sample: 5, 20 and 35 kN, for each kind of clay. It appears that the mass density ρ ~ 2 g/cm^3 is reached for the four varieties of clay we studied, already at 5 kN.

Experimental results on pastes

Fig. 4 shows the compaction curves for the four clay paste varieties with an applied force up to 35 kN. This representation follows the usual one found in literature, where the applied force is on the ordinate and the induced deformation is on the axis of abscissa (though deformation is a function of the force) because of the simple (parabolic) shape of the curve. We observe that, if all curves have the same general aspect, they differ clearly. The most flat curve corresponds to the AVK clay that presents also the most marked plasticity. We may introduce a parameter to characterize the curves, for instance the spreading W of the curve at a given value of the applied force. We observe that $W_{AVK} > W_{ARG} > W_{AVTK} > W_{ABB}$, namely the W parameter decreases from the most resistant (in dried state) and more plastic (as paste) to the less resistant and less plastic paste.

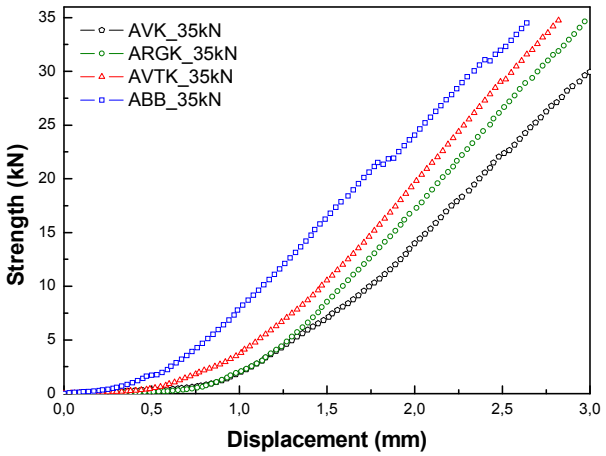

Fig. 4. Compaction curves of the four clay varieties pastes at a strength F = 35 kN

Fig. 5 gives the behaviour of each clay paste for three different levels of compaction. We observe that curves obtained at different force value during the pastes compaction, do not coincide: the reproducibility is difficult to obtain, and this expresses a strong sensitivity of experimental results on tiny experimental uncontrolled differences. We may invoke air bubbles in the bulk of the paste or at the interface with the boundaries, or an inhomogeneity in the original paste ball before its division into the different specimens and the existence of shear strength at the internal wall of the mould when dragging the clay paste.

In spite of this uncertainty as far as the reproducibility is concerned, we shall see in next paragraph that we may draw conclusions concerning the mechanical properties of the obtained dried specimens.

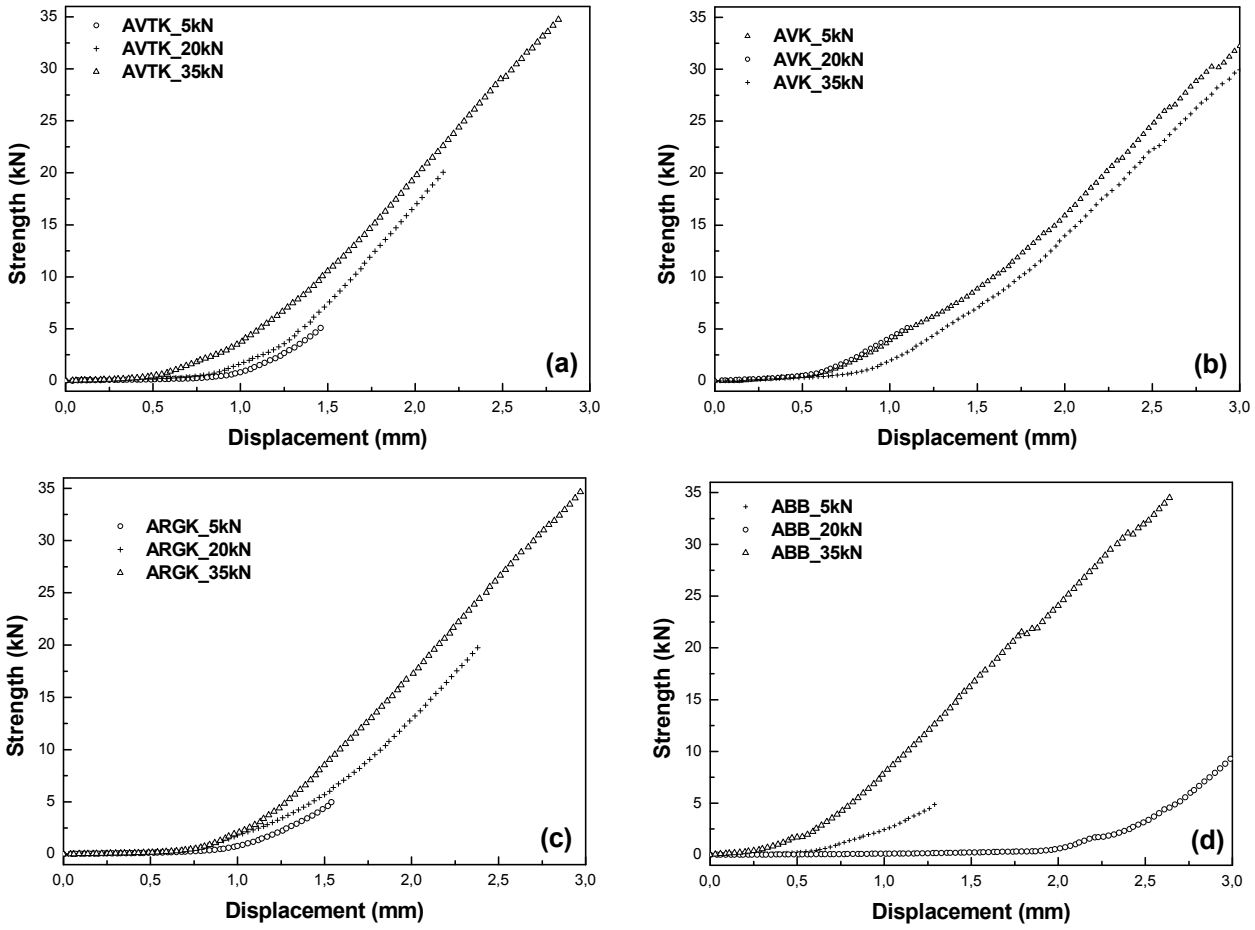

Fig. 5. Compaction curves of the four clay varieties pastes under three different strengths for each specimen (F = 5, 20 and 35 kN)

The characteristics and comments on pastes and prepared specimens are described in Table 2. After compression, the specimens are taken off from the cavity and then confined in a waterproof box at the room temperature. The moisture content of specimens is gradually reduced by a slow drying so as not to disrupt the normal removal of the matrix. Otherwise, it would create localized cracks. During the drying (and the accompanying consolidation of the structure) there always occurs a contraction of the size due to the evaporation of water and the reduction of pores.

Table 2

Characterization of clay pastes and visual observation of test samples

Clay varieties	Water content (%)	Consistency of the paste	External appearance of the wet specimen	Appearance of the dried specimen
Green clay from Kouvé (AVK)	18	Pasty and plastic	Smooth, moist cracks barely visible	Less visible porosity
Green clay Togblékopé (AVTK)	18	Pasty and very plastic	Very wet and deforms easily	Open porosity
Red clay from Guérin-kouka (ARGK)	18	Wet powder	Solid, with very smooth appearance	No cracks or pores
White clay from Bandjéli (ABB)	18	Pasty and less plastic	Smooth and less humid	Good appearance after drying

Experimental results on dried specimens: compression tests

The test results show that the specimens compacted to 20 kN are less subject to damaging than those compacted to 5 kN. Thus, the larger the strength of compaction, the better the dried specimen resists to compression, which is confirmed by a better resistance to damaging of the specimens compacted to 35 kN. Visual observations of dried specimens do not however allow us to mark a notable difference on cracks. Table 3 shows the values of the constraints at the fracture threshold, and resumes visual aspects of the samples tested in compression. These results confirm the key role of compaction in the preparation of clay based materials (removal of air bubbles in the paste, reduction of pore, density increase of the material).

Fig. 6 shows the compression test on the four dried specimens of the clay variety studied. One can observe different Young modulus for each specimen proving different mechanical behaviour of each variety.

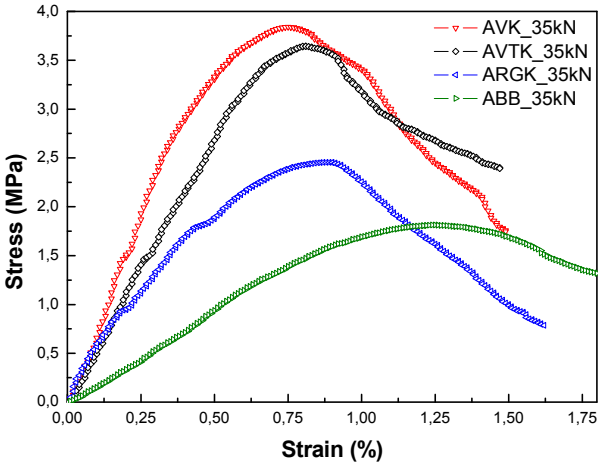

Fig. 6. *Comparative compression test curves for the four different dried specimens initially compacted at 35 kN*

Table 3

Dried specimens characterization

Compacting strengths						
	5 kN		20 kN		30 kN	
Clay varieties	Stress maxi (MPa)	Specimen external observations	Stress maxi (MPa)	Specimen external observations	Stress maxi (MPa)	Specimen external observations
AVTK	4.37	total fracture	6.06	mean fracture	6.35	important fracture
AVK	5.46	total fracture	5.66	lateral fracture	6.42	important fracture
ARGK	2.91	mean fracture	3.76	break less pronounced	3.85	several breaks
ABB	1.90	crash	2.06	erosion	2.72	partial erosion

Fig. 7 presents the compression tests curves on the dried specimens for the four varieties of clay and for three different loads related to the paste initial compacting. These curves show that the elastic modulus and constraints at the fracture threshold increases with the overall load applied during the molding of the paste. The maximum value of the constraint at fracture threshold is of the order of ~ 5 MPa.

Contrary to observations on the paste, we noted that the ABB clay is the least resistant after drying while it was the most reactive during kneading and resistant to compression. The explanation for this behaviour has to be found in the chemical composition of this clay, and in the atomic bonds in the structure. It is relevant at this stage to remember that the pastes are made up of clay particles electrically polarized sheets with opposite charges on both sides. These charges attract in the clay,

water molecules which act as lubricants between sheets and confer plasticity properties to the paste. This may be accounted for by forces between particles of minerals themselves and water molecules: electrostatic forces between particles, dynamic forces between water flows and particles, Van der Waals forces, gravity, and capillary forces [19, 20, 21]. In the paste, the sheets can thus slide over one another, lubricated by water layers, and this so called hydroplasticity and the behaviour during kneading are strongly dependent on the structural configuration involving water whose influence is predominent. It may thus be understood that dried specimens properties that depend only on the structural arrangement in the mineral matter are not related with those of pastes.

The analysis of all data, shows that thermoplastic and less resistant clay is ABB (Young modulus E = 0.8 MPa, and rupture stress $\sigma_{r\text{-max}}$ = 1.90 MPa). The most elastic and resistant clay is AVK (Young modulus E = 2.8 MPa, and rupture stress $\sigma_{r\text{-max}}$ = 6.42 MPa).

The cracking of a structure after its formatting depends on several factors. The most common factors are the nature of the clay, the shrinkage during drying, and the constraints at removal. The samples studied here have the same shrinkage rate.

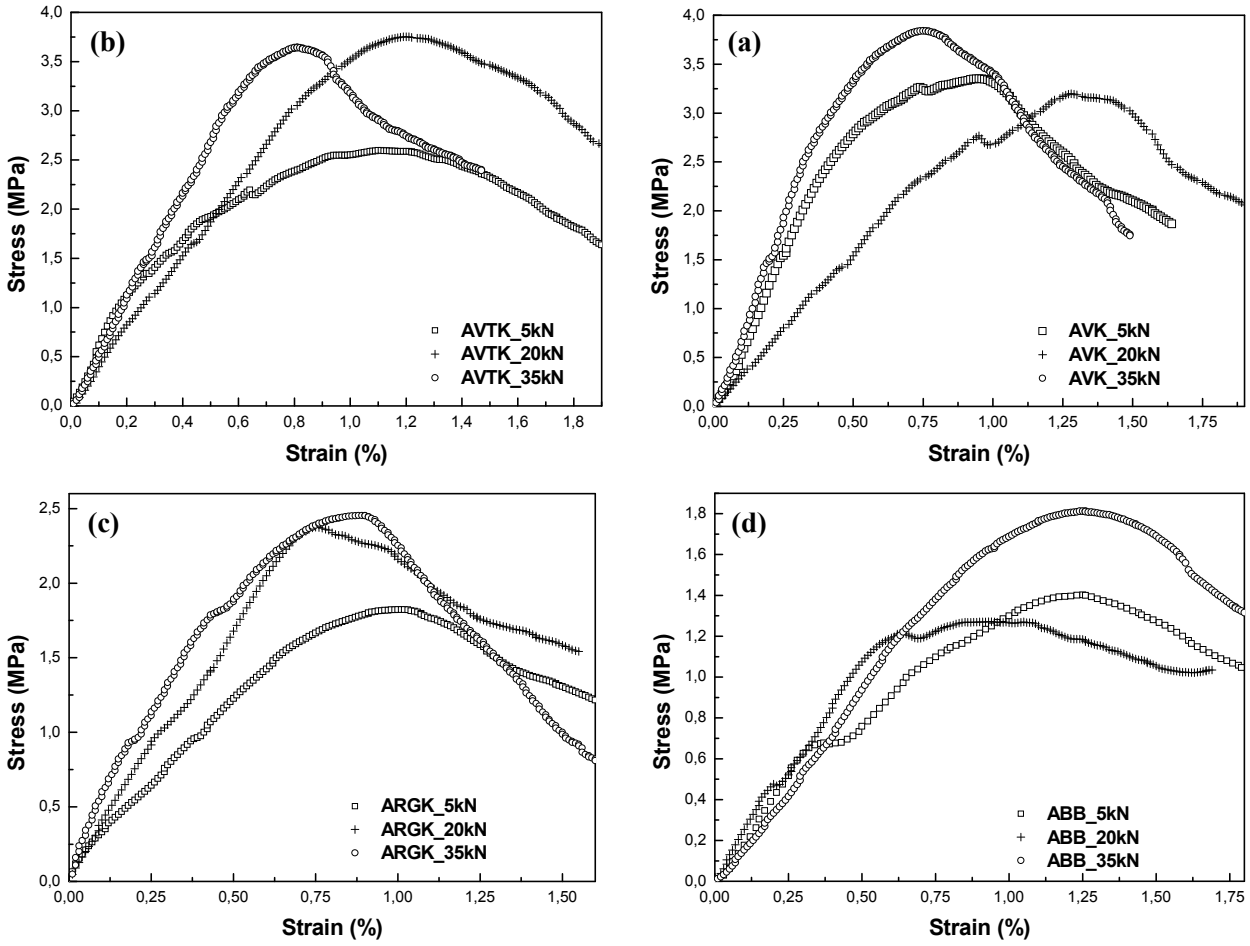

Fig. 7. *Compression test curves on dried specimens of the four clay varieties initially compacted as paste at three different strengths (F= 5, 20 and 35 kN)*

Conclusion

This work has enabled us to understand the problems of the clay paste rheological properties by comparing the behaviour of four varieties of clays, and to show the influence of the compaction load of the clay paste on the resistance of the dried material. The compression tests on the dried structures showed longitudinal cracks on the side faces that are more remarkable on less compacted specimens.

It is likely that the cracks found on the side faces of compressed dried specimens result at least partially from those initiated by the formatting. A numerical approach based on an elasto-viscoplastic model will allow us to better describe the distribution of the stress and displacement fields in the dried material. In addition, observations under microscope should allow us to quantify the problem of matrix cracking in order to deduce the influence of the formatting. Work is underway to clarify these issues. Finally, a more

sophisticated model should take into account details on the microscopic structure of the materials studied, both in the hydrated form (paste) and in the dried one.

References

1. Darve F., Hicher P.-Y., Renouard J.-M. Les géomatériaux. Ed. Hermes, 1995. T. 1. P. 89-100.
2. Charles A.J.F. et al. Physical investigation of surface membrane-water // Carbohydrate Polymers. 2001. 45. P. 189-194.
3. Assal H.H. et al. The role of lime inclusion of the properties of fired clay // Ind. Ceram. 1999. 19. P. 82-92.
4. Ashby M.F., Jones D.R.H. Microstructure et mise en œuvre. Ed. Dunod, 1991. T. 2. P. 149-194.
5. Chiarelli A.-S., Shao J.-F., Hoteit N. Modeling of elastoplastic damage behaviour of a claystone // Int. J. Plasticity. 2003. 19. P. 23-45.
6. Conil N., Djeran-Maigre I., Cabrillac R., Su K. Poroplastic damage model for claystones // Appl. Clay Sci. 2004. 26. P. 473-487.
7. Hirata S., Yao S., Nishida K. Multiple regression analysis between the mechanical and physical properties of cohesive soils // Soils and Foundations. 1990. 30. P. 91-108.
8. Couarraze G., Grossiord J.L. Init. à la Rhéologie. Ed. Lavoisier-Tec & doc. 1991. 5-20. P. 51-91.
9. Carretero M.I. et al. The influence of shaping and firing technologies on ceramic properties… // Appl. Clay Sci. 2002. 20. P. 301-306.
10. Costet J. Cours pratique de mécanique des sols: Plasticité et calcul des tassements; troisième Édition, Ed. Dunod, 1983. Vol. 1.
11. Jouenne C.A. Traité de céramiques et de matériaux minéraux. Ed. Septima, Paris, 1999.
12. Parande A.K. et al. Study on strength and corrosive performance for steel embedded… // Const. and Build. Materials. 2008. 22. P. 125-134.
13. Costet J. Cours pratique de mécanique des sols: Plasticité et calcul des tassements; troisième Édition, Ed. Dunod, 1983. Vol. 1.
14. Lambe T.W., Whitman R.V. Soil Mechanics, SI version // Wiley, New York, 1979.
15. Yalcin A. The effects of clay on landslides: A case study // Appl. Clay Sci. 2007. 38. P. 77–85.
16. Couarraze G., Grossiord J.L. Initiation à la Rhéologie, 5-91, Ed. Lavoisier-Tec & doc, 1991.
17. Barthelemy B. Notions pratiques de la mécanique de la rupture, Ed. Eyrolles, 1980.
18. Druyanov B.A., Nepershin R.I. Problem of technological plasticity, Ed. ElsevieR // Col. Studies in applied Mechanics, 1994. 38. P. 357-389.
19. Laroze S., Barrau J.-J. Mécanique des structures solides élastiques, plaques et coques, Ed. Ensae // Col. Sup'Aéro. 1995. Vol. 1 bis.
20. Derjaguin B.V., Landau L.D. Acta Physicochim. URSS, 1941. 14. P. 633–652.
21. Verwey W., Overbeek J.Th.G. Theory of Stability of… Elsevier, Amsterdam, 1948.

IS INDUSTRIAL DEVELOPMENT INCOMPATIBLE WITH CONSTRAINTS OF INDUSTRIAL ECOLOGY IN CAMEROON?

A. Kemajou, O. Bergossi**, T. Tamo Tatietse***, B.S. Diboma**

* Ecole Normale Supérieure d'Enseignement Technique, ENSET - Université de Douala,
BP 1872 Douala, Cameroon
Mobile phone: (237) 77 76 74 80, e-mail: kemajoualexis@yahoo.fr
Mobile phone: (237) 77 69 96 31 e-mail: benjamin_diboma@yahoo.fr

**CREIDD, Université de technologie de Troyes,
12 rue Marie Curie, BP 2060, 10010 Troyes cedex, France
e-mail: olivier.bergossi@utt.fr

***Ecole Nationale Supérieure Polytechnique, ENSP, Université de Yaoundé I
BP 83902 Yaoundé, Cameroun
Phone: (237) 22 22 45 47, e-mail: thomas_tatietse@hotmail.com

Received: 24 Sept 2007; accepted: 31 Oct 2007

The present industrial development trend in Cameroon does not give the expected results but rather accumulate environmental risks. This article analyzes industrial practices in a number of key sectors from the angle of industrial ecology, showing a non optimized consumption of inputs and energy as well as non-rationally exploited resources. If the increase of input is added to the dilapidated industrial fabric it would give a massive increase of waste which is a considerable pollution source. Examples and suggestions on the possibilities of applications of industrial ecology to Cameroon are presented at the end of this article.

Keywords: ecological problems of industrial megapolises, problems of factory and domestic waste utilization, sustainable development

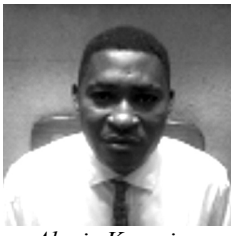

Alexis Kemajou

Organization: Thermal and Environmental Research Laboratory, Teaching Researcher in charge of research within the Energy, Thermal and Environment Research Laboratory at ENSET.
Education: PhD in Energy Engineering Sciences, University of Yaoundé I (UYI) – ENSP (1990-1995), DESS in Energy Management – University of Reims France, Faculty of Sciences (1986-1987) – Engineer in Industrial Thermal Management – French Institute of the Thermal Studies and climate Management of Paris (1982-1986).
Experience: APAVE – Bordeaux France, Engineer (1987-1990). ENSP UYI Cameroon, Assistant Lecturer (1990-1995). ENSET UD, Lecturer (1995-2007).
Main range of scientific interest: thermal and energy studies on buildings, energy efficiency and the environment, air conditioning.
Publications: 4 articles specialised reviews and 8 communications.

Olivier Bergossi

Organization: Center for Research and Interdisciplinary Studies on Sustainable Development (CREIDD), University of technology of Troyes (UTT, France).
Education: Doctorate in Engineering Sciences, 1995, University of Franche-Comté (France), Master degree in Industrial Ecology, 2003, UTT.
Experience: Lecturer (UTT, 1996-2005), Research on near-field optics (1996-2001, UTT), Sustainable development (since 2003, UTT), Technology of Information and Communication in Education (TICE) for engineering (since 2001, UTT) – French cooperation in Cameroon, project "Comètes" (2005-2007).
Main range of scientific interest: physics (optoelectronics and nanotechnologies), TICE, sustainable development (industrial ecology, ecological footprint).
Publications: 11 articles about near-field optics, 2 articles about TICE and 2 articles about sustainable development.

Thomas Tamo Tatietse
Organisation: School of Engineering (Ecole Polytechnique), University of Yaoundé I.
Education: Engineering at Ecole Polytechnique Yaoundé, DEA, Doctorat INSA from Lyon (France), Postdoctorat Université Laval (Canada), HDR Institut National Polytechnique Grenoble (France).
Experience: University Lecturer, Visiting Teacher-Researcher at Université Laval (Canada), at Institut National Polytechnique de Grenoble and at INSA Lyon (France), at Université de Liège (Belgique). Presently Head of the Civil Engineering Department at the School of Engineering UYI, since 2001. Deputy Director of the School of Engineering since 2004.
Main range of scientific interest: applied hydrology, electrical Energy, conception and management of networks, optimisation of combinations, programming of civil engineering constructions, management of productions.
Publications: 12 articles in high reference international scientific reviews, as well as 22 communications during international conferences.

Benjamin S. Diboma

Organization: University of Douala, Temporary Assistant Lecturer in Research within the Energy, Thermal and Environment Research Laboratory of ENSET Douala, PhD student in Energy Engineering Sciences.
Education: DEA in Energy Studies EDSFA (2005-2007), Energy Laboratory. DIPLET in Air-conditioning – ENSET, University of Douala (1994-1997 and 2002-2004).
Experience: Technical high school Obala (Cameroon) (1997-2002) ENSET – University of Douala, Temporary Assistant Lecturer (2002-2007).
Main range of scientific interest: energy, electricity, thermal networks in buildings, energy efficiency and the environment, air-conditioning.
Publications: 1 communication.

Introduction

Developing countries (DC) are confronted with several problems which include delay in technology development, dilapidation of industrial fabric [1], insufficient financial means, use of not optimal transformation and production processes, but also socio-political aspects such as poor governance, general level of education, continuous demographic growth or certain cultural impediments. In this era of globalization, the "classical" manner of economical development used by western countries during the two past centuries does not seem operational in these countries, notably those of the African continent. To the above enumerated constraints should be added that of global warming of the planet and international competitive rush for primary products (oil, ores). Several big-time DC are carrying out original developments activities which put the environment at the heart of development politics. Brazil has been recognized as pioneer in bio fuels for example, but the efforts of China are so enormous in this area, according to the level of challenges that she must face in a bid to modernize her industrial base [2]. China's leadership strives to set up a "cyclical" economy [2], which greatly ties in with the scientific notion of industrial ecology [3]. As such, could this original mode of industrial ecology be applied to another group of DC, given that Sub-Saharan Africa countries are bogged down by development problems for which classical solutions advocated by the western international experts do not seem to have an answer? If yes, which basic principles adaptations of industrial ecology or circular economy, will be required in order to take account of their local constraints and their development priorities? The representative sample country chosen for this study is Cameroon, given its position, size, and development level, often presented as "Africa in miniature". As early as 1999, the Institute for Communication and Analysis of Sciences and Technologies (ICAST) carried out a fact-finding mission to Cameroon on the concrete perspectives of industrial ecology in Africa [4]. We are now using this study as our takeoff point, while directing our research and investigations towards some key sectors of industrial ecology, especially the waste sector. The increase of input and energy flux, added to the current trend of economical growth in DC, have resulted in a massive increase in waste, which in itself is a source of pollution and degradation of the environment.

Furthermore, through inquiry carried out on a representative sample of Cameroonian corporations, this study will examine the treatment of domestic and industrial waste and make an inventory of actions and possibilities of industrial ecology in the informal sector. The ensuing results and discussions will bring out the possible contributions of industrial ecology to the setting up of models that would valorise waste management and optimize the flux of inputs and energies in Cameroon.
Above all else in this sector, industrial operators as well as politicians in charge and all development actors must ask the following question: how could we optimize the flux of input and energy while improving productivity and preserving the environment and available resources? This preoccupation goes beyond pollution problems and delves into the long term evolution of Cameroon's industrial fabric as a whole; it even delves into the sub regional framework of the Economic and Monetary Community of Central Africa (CEMAC) [5].

Context

Presentation of Cameroon

Geographic situation in Africa

Cameroon is often called "Africa in Miniature". This is because it is representative of the continent in several ways and is situated in the centre of Africa (Fig. 1). It covers varied vegetations, climatic and cultural zones, as well as comprising very varied populations. As compared to other African countries, Cameroon appears to be extremely rich in natural resources and in potentialities of all sorts. Farming and husbandry benefit from very favourable climatic conditions and vegetation.

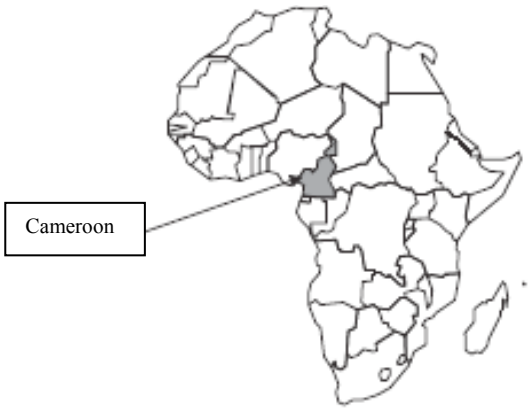

Fig. 1. *Cameroon in Africa*

Exploitation of the equatorial forest here is very lucrative. The subsoil is rich in oil, bauxite, iron and various minerals. In the South of Cameroon, the dense hydrographical network could guarantee water and the electricity for all. Well mastered tourism, currently a neglected domain, could be one of the pillars of development. Unfortunately, the management of the all these resources is not yet optimum and a great majority of the population lives below poverty line.

Some basic data [6]

The Republic of Cameroon is situated in the central region of Africa and extends northwards from the Gulf of Guinea by the ocean Atlantic to Lake Chad. This triangular-shaped country spreads out over a length of 1.200 km between latitudes 2° North and 13° North and a width of 850 km between the longitudes 8° Is and 16° Is.

Surface area: 475 442 km^2.

Population: 16.4 millions of inhabitants (2006).

Density: 34 inhabitants/km^2.

Demographic growth: 1.93 % /year (2005) – for comparison, France: 0.35 %.

Principal resources: precious wood, cocoa, coffee, cotton, rubber, food plants (millet, sorghum, manioc-cassava), husbandry, bovine, aluminium and oil.

GDP: 12.5 billions €/year, representing half of CEMAC zone – GDP/inhabitant: 760 €/year.

Human Development Index: the HDI for Cameroon is 0.506, which ranks Cameroon at 144th out of 177 countries (206) [7]. The Cameroon HDI reached a maximum of 0.514 in 1990.

Industrial ecology and the requirements of industrial development

For Cameroon to attain the main Millennium Development Goals (MDG) [8] there is need to accelerate economic growth based on the industrialization of production sectors.

The main determinants of industrial development that have an impact on the environment is the exploitation of natural resources (primary products), technological processes used in the production of economic goods, as well as energy supply.

To meet with the challenge of sustainable industrial development, industrial ecology must be based on four principles [3]:

− cut down on all sorts of dissipation (energy or inherent to products, at manufacture, usage, and end of life);

− dematerialize products and the services, in order to ensure flux of inputs and energy not correlated with GDP growth and HDI improve;

− decarbonise energy, with as main objective to fight against the greenhouse effect;

− valorise waste management as secondary resources with the intention of attaining an industrial system friendly to the biosphere.

Is it possible to integrate these four principles in a national policy of sustainable economic development that respond in priority to the MDG? In this study we present some data and analysis, as well as propose some avenues for reflection on the possibility and means of integrating industrial ecology to the problematic of development in Cameroon.

The industrial development and the environmental constraints

Industrial evolution of Cameroon

The industrial development of post-independent Cameroon corresponds to three phases marked by a high political determination to progress, but whose implementation suffered from hazardous economical situations: the economy experienced a growth period (1960-1982), then a period of recession (1984-1993) and now one of revival (since 1994). The GDP growth rate is of 4 % per year since 2001, but a great part of this growth is absorbed by high demographic increase [9].

The Industrial fabric is concentrated geographically and covers only a small part of the industrial sectors. Douala is the industrial capital of the country, mostly due to its harbour and industrial zone. The principal businesses of the country are involved in such sectors as:

− agro-industry (Brasseries du Cameroun, SOCAPALM);

− agricultural transformation (SODECOTON);

− forestry exploitation;

− heavy industries (CIMENCAM for cement, ALUCAM for aluminium, etc);

− energy production and distribution (AES-SONEL, SNH: Société Nationale des Hydrocarures, SONARA: Société Nationale de Raffinage);

− distribution (FOKOU group for instance [10]);

− the banking sector;

− transport: CAMAIR (airline), CAMRAIL (railway);

− telecommunications: MTN and Orange companies, etc.

This fabric is on the whole aging. Corruption, slow administrative procedures, tax insecurity, etc, make investment difficult in the country. The informal sector (sector of non declared work and therefore as a rule subject to low income) has been on the increase since the economic crisis of 1983, and now stands at 90 % of urban manpower and becomes therefore essential for all studies or economic forecast.

Energy supply

Energy is one of the essential factors of productions for industrial development, because it is used in transportations and as means to operate equipments producing economic goods and activating these goods themselves. Though it is imperative to have access to necessary and sufficient energy, Cameroon unfortunately experienced since 2001 a considerable energy deficit of 100 MW/per annum. Competent companies, including the principal electric energy distributor AES-SONEL, invested massively in the production of thermal energy to maintain industrial production. An 85 MW heavy-duty fuel plant, with a capacity of 17 tons/hour of fuel, was put in service in 2004, but the production of 11.6 MW·h of electricity by combustion liberates 9.3 tons of Carbon Dioxide.

The thermal production of electricity by AES-SONEL is increasing, as it stood at 156 GW·h in 2004, and this trend is being maintained.

Companies also get involved in energy auto-production by the acquisition of diesel electric generators. A recent study [11] put CO_2 discharges by Cameroonian businesses at 26870 tons. The autonomous production of electricity is estimated in 2005 at 450 GW·h, with an annual growth rate of 2.17 %. That implies that CO_2 emissions will increase over the coming years, the more so as measures taken to reduce national electricity deficit seem to be inefficient [11].

Technology processes

The transformation of raw materials into economic goods is done in production units by implementing various technological processes. This transformation generates wastes that contain polluting substances for the environment. Industrialists are more interested in the increase of profits and competition, rather than in facing the dangers that these production residues represent [11]. The treatment of waste is never well envisaged, and it is thus with despair that one observes the burying of waste without respect of the norms, poorly adapted sites, spillages of toxic substances in the sea environments (the example of the Abidjan lagoon in Ivory Coast is very edifying). Technological processes must be able to reduce waste, cut down on their poisonous effects; but the present dilapidation of industrial fabric in Cameroon does not encourage such environmental policy. There is thus the lack of necessary investments to ensure modernization, in an economic environment marked by weak internal financial means and a general climate of not too attractive for business [12].

Exploitation of natural resources

Industrial performance is conditioned by the supply of raw materials which are basically natural resources. Unfortunately, this non rational exploitation of natural resources led to a degradation of the ecosystems. The surface area of forests reduced by 2.4 % between 1990 and 2000 [8], and as such leading to a dramatic impoverishment of wildlife and big animals due to poaching, while our resources in waters will undergo a reduction of 33 % in average in 20 years. The advance of the desert consecutive to global warming of the planet can affect farming and water resources in the northern zone of the country and especially destabilize neighbouring countries (Chad, Nigeria), with repercussions on Cameroon. The extraction of subsoil resources deeply modified the morphology and sea bed of certain regions of the globe, and Cameroon is part of the exposed countries (exploitation of hydrocarbons in the Guinea gulf, mining projects of breadth in the East and the North).

Environmental constraints

Knowing environmental constraints [13] is a response to the numerous perils that we know: global warming which induces an elevation of the level of seas, climatic disruptions (phenomenon of El Nino, frequency of cyclones, etc.). The United nations through its specialized bodies has organised several summits and lectures elaborating these environmental constraints; there is the "Earth Summit" at Rio (Brazil) some 15 years ago, and that of Johannesburg (South Africa, 2002) [5], specific summits to a special group of countries as the Summit of the Small Insular States in Development held at Mauritius Island (2005) [14].

At the international level, these constraints concern four big themes: the reduction of the transmissions of greenhouse gases, sustainable development, preservation of biodiversity and the rational management of energy resources.

Cameroon did not stay away from the dynamics of the search for solutions; it ratified and signed several conventions and protocols, while law No. 96/12 of August 05 1996 relating to the management of the environment was adopted [15]. Industrial actions must respect certain norms contained in this law, especially as control organisms were set up. Concretely, this will entail the respect of the Montreal protocol and its amendments, the preservation of the regulatory role of forests, the elimination or recycling of industrial waste, the carrying out of environmental impact assessment studies for all project with direct or indirect incidence on the environment (examples: construction project of the Lom-Pangar Dam, the construction of the Chad-Cameroon pipe line), the need to inform the populations on the harmful effects of wastes.

Cameroon signed the adhesion to the Kyoto protocol of July 23 2002 and participates in actively in the activities of the Clean Development Mechanism (MDP) [16].

The perception of changes involved here implies taking into account the protection of the environment and the investments that it generates shall be stretch onto industrial development and respect of the principles of the industrial ecology, which are two incompatible concepts in DC.

Specificity of the countries in the process of development: the weight of the informal sector

The poor inhabitants of DC are usually confronted with the problem of their day-to-day subsistence. The purchasing power of households is very weak, feeding and health care are a daily headache, and this encourages the development of an informal sector alongside the formal sector. So long as these basic questions are not determined, these populations cannot pay themselves the "luxury" of ecological preoccupations. Cameroon is not free from this reality. Her informal sector considerably developed since 1990 following a conjunction of facts: salary cuts of the officials by 60 %, blocking of the recruitments of university graduates into the public service and severity of the of structural adjustment plans [17]. The informal sector actors work in all domains of activity: production, commerce, recuperation, textiles, etc. It is in this wake that the importations of used clothing, whose

noxious effects on health are known, increased to the point where its market parts in this domain are higher than that of Cameroonian Textile Industry (CICAM). The recuperation business developed and concerns all products (scrap iron, used electric and electronic devices, plastic). The production of the consumer goods also developed as well as a variety of manufactured and handicraft products sold in markets (yogurt, fruit juice, dairy products). The advent of the Chinese cheap manufactured motorcycles ("taxi-bikes") that imposed, next to classic public transport and original trends such as common township taxis is an indicator of the dynamism of the informal sector in this activity domain.

From the foregoing, it can be deduced that in Developing Countries safeguard of the environment in the informal sector is not integrated in their vision of the world in the same manner as in the rich countries [4]. The question here is whether the growth of informal sector activities hat puts is itself the one of respects the protection constraints of the environment in Cameroon. Is the industrial ecology capable of help this informal sector in the problematic, and, through its systemic and collaborative approach, to bring back progressively its actors towards the definite sector? An attempted response to these preoccupations is brought by our research described hereafter.

Enquiry on Cameroonian businesses

General framework of the study

This study concerns on the one hand Cameroonian businesses that produce important quantities of industrial waste and on the other hand those that work in the collection and treatment of production residues. This study further covers actors of the informal sector. The geographic framework of this study covers the cities of Douala and Yaounde which, according to the statistics of the Ministry of the Industrial and Commercial Development (MINDIC) contain more than 80 % business in the country. This inquiry was specific to corporations involved in the business of waste treatment such as HYSACAM (Hygiene and Sanitation Corporation Cameroon), BOCAM (group Fokou [10]) and BOCOM, the industrial corporation ALUCAM, and of the domain food processing. These companies were chosen because the responded to certain criteria, such as the nature of the industrial activity, the typology and the mass of the industrial waste products, and the flux of raw materials and energies.

Our findings were based on statistics of the services of customs and taxes, on registers provided by the Chamber of Commerce, Mines and Energy, as well as from the Business Directory; we covered 70 companies. Since the informal sector is not well structured and almost infinite in size, we were not able to extract enterprises-test. Our study thus limited its research to ten big participants of the formal sector whose activities have links with the methods of industrial ecology. Through our study of these corporations, we wanted to analyze two questions:

− What is the weight of the informal sector market and what waste does it produce?

− What means can be used to sensitize and train manufacturers, the informal sector and others stakeholders?

Methodology

This chapter dwells on the methodology that we systematically adopted for our different investigations and analysis.

Inductive method

The inductive method [18] in principle use the estimation of the variables per the whole population statistics collected from the data in the sample. We constituted a sample of 20 corporations that were grouped together in strata and whose results after correction will enable the obtention of reliable indicators on industrial ecology in Cameroon.

Stratification [19]: our assessment base of N broken down in in k strata in which one take off sample, and consider a variable X of which one would want to estimate the average M. One obtains:

− at the sample:

$$m_h = \frac{1}{N_h}\sum_{s=1}^{N_h} X_{hs}\ , \tag{1}$$

$$\overline{X}_h = \frac{1}{n_h}\sum_{i=1}^{n_h} X_{hi}\ ; \tag{2}$$

− at the level of populations:

$$m_h = \sum_{h=1}^{k} \frac{N_h}{N}\ . \tag{3}$$

This average is estimated at

$$\overline{X}' = \sum_{h=1}^{k} \frac{N_h}{N}\overline{X}_h \tag{4}$$

with $\overline{X}'$ being the assessor of average m.

X_{hs} is the value of the variable X for the company U_{hs} having number s inside strata h.

X_{hi} is the value of the variable X for the sample-company U_{hi} pointed out at the number i drawing inside strata h.

N_h/N represent the weight of the different strata in the population, n_h/n their weight in the sample. The estimation of the rate of waste treated is an important indicator which makes us see the management level of production wastes of economic goods in a more global perspective aimed at reducing flux of raw material and energy that will enhance of the matter flows and of energy than recommend the methods of the industrial ecology.

Estimated proportion of treated waste

This estimation is based on data collected in corporations that produce waste and in those specialized in the collection and treatment of industrial and domestic

wastes. By weighing the residues we could determine the percentage of the industrial waste treated. The debits of treated liquid flows were measured in each of the sample companies.

We note:

$Q_{hd_{ti}}$: the mass of waste produced by the corporation U_{hi} and processed;

Q_{hd_i}: the mass of waste produced by the corporation U_{hi};

ψ_{hi}: the rate of waste from corporation U_{hi} which are treated.

$$\Psi_{h_i} = \frac{Q_{hd_{ti}}}{Q_{hd_i}}. \quad (5)$$

Rectified at the population scale, the equation (4) leads to an average $\overline{\Psi'}$:

$$\overline{\Psi'} = \frac{1}{N}\sum_{h=1}^{k}\frac{N_h}{n_h}\sum_{i-1}^{n_h}\Psi_{hi}. \quad (6)$$

Results

This inquiry in companies enabled us, after treatment of the data, to obtain on the one hand quantitative results that were rectified with the assistance of our estimators and on the other hand of quality data that are presented following the two avenues of this study, namely waste and the informal sector.

Domestic and industrial waste

Domestic waste

The company HYSACAM takes care of the collection and treatment of domestic waste [20] in the cities of Douala, Yaoundé, Bafoussam, Limbe and Garoua. The quantity of waste collected represents 40 % of the produced waste and is constantly on the increase as illustrated in the Fig. 2.

Domestic wastes are mostly made up of a fermentable fraction (78.8 %), an inert fraction (10.0 %), and a combustible fraction (11.2 %). HYSACAM exploits several waste dumps of which the main ones are in the neighbourhoods of Makèpe and PK10 in Douala and Nkolfoulou in Yaoundé. The density of waste entering into dump is of 4.5 kN/m^3 and their composition is presented in the Table 1 hereafter.

Table 1

Composition of waste

Fractions	Average (%)
Wood	0.82
Rubber	0.59
Paper	9.86
Gravel	0.91
Metal	1.26
Plastic	8.34
Textiles (leather and cloth)	4.26
Glass and ceramics	1.13
Organic matter	65.79
Finished elements (< 20 mm)	6.95
Hospital waste	0.08

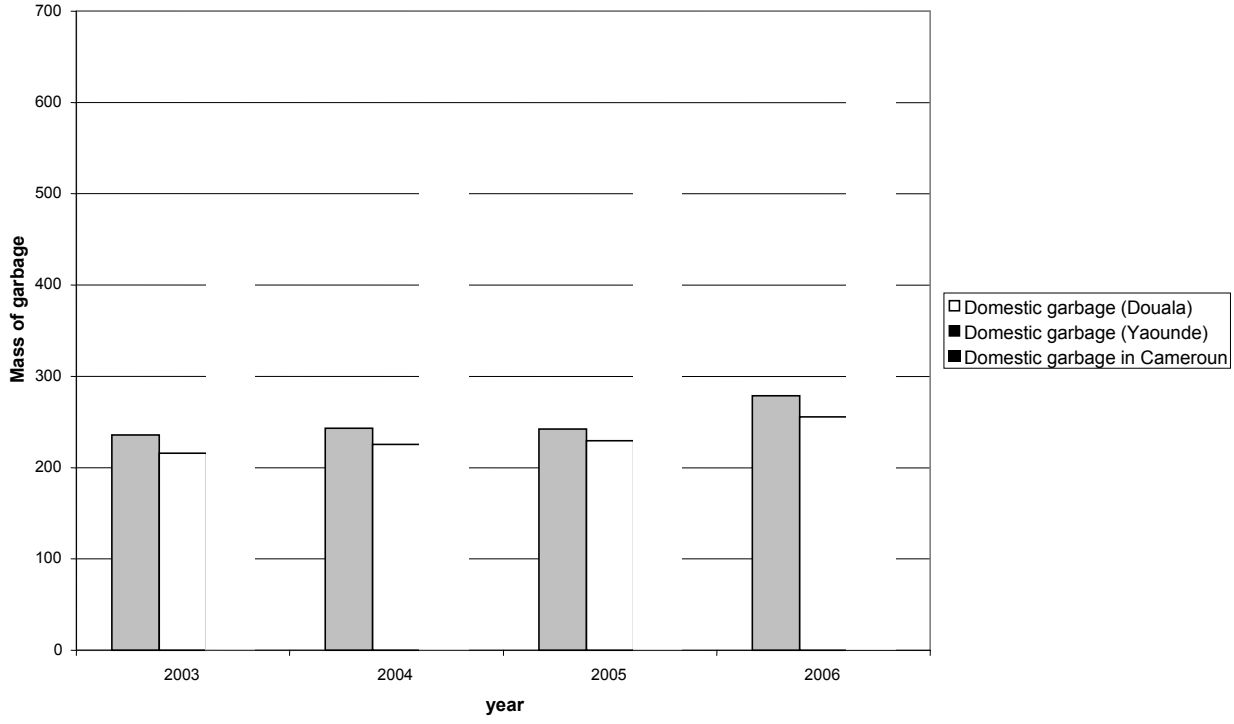

Fig. 2. *Evolution of household waste mass collected by HYSACAM*

Within the framework of environmental protection and development of domestic waste, several initiatives were taken in collaboration with various partners (the National Institute of the Applied Sciences (INSA) of Lyon and the Agency for Environment and Mastery of Energy (ADEME) in France, the Agronomy and Agricultural Sciences Faculty (FASA) of the University of Dschang, and the National Higher School of Engineering ENSP of the University of Yaounde I); this led to the obtention of 25 % of compost matter from household waste [21].

Industrial waste

Most of the industrial waste matter [20] has a high toxicity and their treatment is costly. Two corporations, BOCOM and BOCAM situated in the industrial zone of Bonabéri in Douala, are specialized in the treatment and the recycling of industrial waste which are essentially used oil and waste waters, hydrocarbons slough, used filters, soiled rags, soiled hydrocarbons earths, plastic, lead, cadmium, paint waste and other liquid effluents. Table 2 shows the evolution of the quantities of industrial waste treated by these two corporations during the three last years.

Their main customers are the following national or multinational corporations: ALUCAM, Cameroon Oil Transportation Company (COTCO), MOBIL, TOTAL, CAMRAIL, NESTLE, AES-SONEL, PERENCO, Cameroonian Corporation of oil deposits (SCDP), SAGA, Douala Autonomous Port (PAD).

ALUCAM, in its process for generating electrodes into electrolyzes, produces lead that is toxic and polluting. [20]. This corporation produced 15,000 kg of oily waste, 2,000 kg of oily residues and 500 kg of lead in 2006. It also became involved in a vast program of environmental management that enabled the reduction of its waste by 10 % in three years and disposes henceforth of an underground dump with a technical of a cost of 2.5 million Euros.

Table 2

Evolution of treated industrial waste (2004-2006) [20]

Types of industrial waste (kg)	Year		
	2004	2005	2006
Oily waste	45000	75000	65000
Used Filtres	200000	215000	220000
Used oils and water	90000	125000	105000
Slough	1100	1325	1250
Hydrocarbon waste	1250	1500	1350
Paint waste	7000	7500	9000
Used tyres	6000	6500	7200
Lead from batteries	1000	1300	1700
Plastics	15	25	40

In the domain of agro-industry, this study estimated the proportion of industrial waste produced by activities in this sector and processed by the corporations specialized in recycling and cleanup. This ratio underwent important variations between 2004 and 2006 in each of the companies as shown in Fig. 3. This percentage is situated between 15 and 18 % for main agro-industries in Cameroon after adjustment. The agro-industrial wastes are of several types such as molasses (sugar factory), cotton waste, palm nut shells, and humid effluents (breweries). Table 3 indicates the quantities of waste produced by agro-industries.

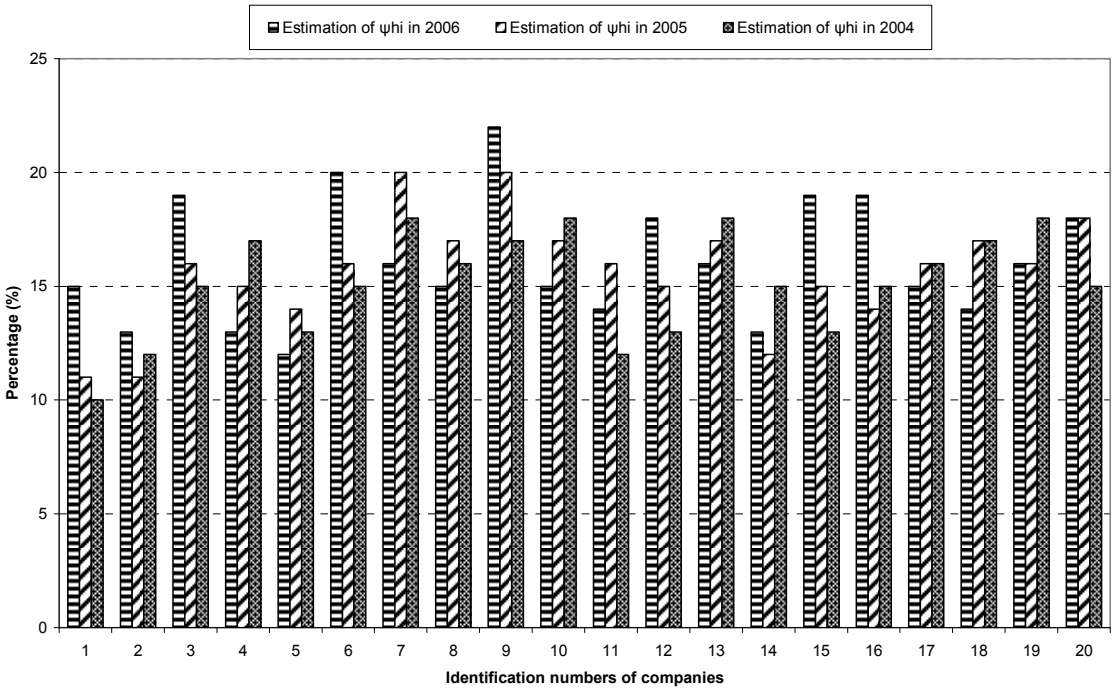

Fig. 3. *Evolution of percentage of treated agro-industry waste (2004-2006)*

Table 3
Weight of agro-industry wastes in thousands of tons

Types of waste	Year		
	2004	2005	2006
Palm nut residue	250	275	260
Molasses	405	412	408
Cotton	700	630	715
Wood	2100	2050	2150
Water	120	132	140
Oil	6	6.3	6.5
Plastic	0.45	0.57	0.65

Gas waste are so high and are a great source of nuisances, and their evaluation is a difficult task and consequently does not feature in this study. Among these residues are those resulting from such activities as transportation, where vehicles are in their majority old and worn out, with poorly regulated engines motors, and where the use of unleaded fuel remains the rule.

Complying to quality norms in agro-industries

Compliance to quality norms that integrate protection of the environment in agro industries is an important preoccupation for both public authorities and the industrialists. Decree No. 98/313 of December 20 1998 to organize the Ministry of Industrial and Commercial Development (MINDIC) created a Normalization and Quality Unit whose missions are: elaboration of the norms, certification and accordance, promotion of quality and assistance to corporations [1]. The adoption of the SME (system of environmental management) enabled the agro-industrial Corporation "GUINESS S.A.-Cameroon" (brewery) to reach certain convincing results, such as: reduction of rejections by 30 % in 2006, reduction of greenhouse gases rejections by the improvement of energy effectiveness, elaboration of an environmental management policy spread out over 13 years, and the construction in 2005 of a wastewater treatment station.

The process to ensure compliance of companies to universal norms, such as the ISO 9001 (ISO 9001:2000 is today the standards universally accepted as giving assurance on the quality of goods and services in supplier-customer relationship) and ISO 14001 (relating to environmental protection and to the promotion of sustainable development) is still on-going, but the question that still stands is whether these constraints will be respected in the long term, the more so as national control organs do not have all the required expertise.

To illustrate local difficulties of implementing quality and environment norms, it should be pointed out that the number of structures having an ISO 9001 certification in Cameroon, all sectors put together, dropped from height in December 2001 to two in December 2003 (for comparison, it rose from 302 to 403 in Tunisia, and the world-wide increase is by 10 % during the same periods). The number of ISO 14001 certificates in Cameroon, all sectors put together, moved form two to only one during this same period, the world-wide growth being of 80 % in the same interval [22].

Informal sectors and waste

Markets of the informal sector are in the increase in all the sectors of activities just as is the number of workers that work in this domain. Fig. 4 indicates the evolution of the percentage of workers in this sector since 1980. Waste produced by the informal sector does not undergo any specific treatment and are dumped in the open or poured in drains. Data in this domain is sparse and imprecise. According to the statistics fro Customs, concerning used clothes, the quantity imported per year is of 120 tons. After sorting, 10 % is of poor quality, giving 12 tons and constitute non-biodegradable waste. In the same vein, the collection of scrap is a rather lucrative informal activity, estimated at almost 500 tons per year of quantities extracted from surrounding environment, representing 30 % of metals wasted rejected by various production chains. Still in this regard, the advent of Chinese low-cost motorcycles gave rise to the multiplication of hand-crafted units for oil change (mechanics) that reject waste in streams and sewers.

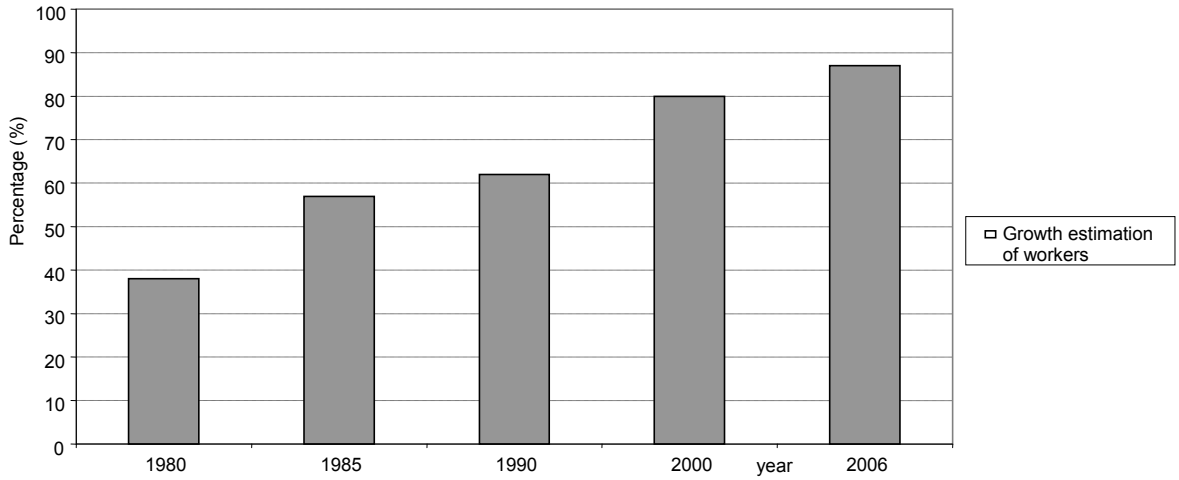

Fig. 4. *Growth estimation of workers*

If we suppose that each "taxi bike" rejects 3 litres of effluents a months and that the cities Douala and Yaoundé dispose altogether of 100,000 motorcycles, that gives up to 3600 m^3 of chemical non-treated substances that contaminate the water table each year.

Analysis and discussions

Treatment of domestic waste

The treatment of domestic waste improved and the last analyses of lixiviates carried out by Centre Pasteur of Cameroon [20] show that the concentration of heavy metals falls below European norms but that such parameters as the DBO5 and the DBO require constant controls; this implies envisaging experimentation of a specific treatment using biological filters for low levels of organic pollution.

Qualitative analysis carried out by ICAST [4] in the sector of waste management broadly revealed that certain unemployed persons create their own activities in the sector of recycling waste ("rag-and-bone men", "plastic waste collectors", "manufacturers of barbecues"). The conditions in which these activities are carried out are variously appreciated, from the viewpoint of work ethics. Nevertheless if recycling was organized activity, it is evident that it would provide a lot of jobs. It is this possibility to create unskilled jobs that explains the boom of this type of activity in most countries of the South; it also explains why several countries of the North maintain such jobs in multinational corporations specialized in the management and treatment of waste. Certain towns or regions, in Asia mostly, are also involved in waste management at global level: dealing with ships at the end of their lifespan, disposal of electrical and electronic waste, etc.

Similar examples of recuperation activities can be described in other Cameroonian industries (Union Allumettière équatoriale (UNALOR), Société des Oléagineux du Cameroun (SOC) for example). An industrial ecology approach, especially in the sector of recycling, can only but enhance the creation of jobs in a country such as Cameroon.

Treatment of the industrial waste

The management of the industrial waste is a global preoccupation because of the ever increasing flux of materials. The poisonous nature of the industrial waste and their potential to degrade environmental quality lead to the need to treat them before any rejection in the nature. The treatment and recycling of industrial production residues requires a know-how and means that are not within reach of all companies, and has as direct consequences a low treatment rate of industrial waste at 15 %, according to the investigation presented above.

The absence of a system for the management of industrial waste leads to spillages of waste in rivers, a source of pollution with disastrous consequences on health and the environment, as well as the liberation of CO_2 due to the dumping of industrial residues without confinement. Lead generated notably in the manufacture of electrodes by the aluminium factory ALUCAM must undergo specific treatment as the stipulated in the Basel Convention [15] but BOCOM, which works locally in the domain of recycling industrial residues, does not have all the required competences. The waste and energy flows going out of their incinerators are not treated but rejected into nature.

With regard to waste production in the agro-industry, mostly liquid waste, they are poured in gutters that drain rainwater and this provokes blockages and consequently frequent and serious floods in the cities during the rains. Compliance to quality norms that integrate protection of the environment in agro industries is an important preoccupation for both public authorities and the industrialists. The flux of material and energy is so important while companies do not dispose the financial and technological means to treat or to recycle industrial waste originating from their different production activities. The application of the principles and methods of industrial ecology led to slowing down the impact of green waste in certain developing countries; this is the case of India [3] or China [2].

What can therefore be the contributions of industrial ecology in the functioning of Cameroonian industries? Industrial ecology can contribute to the optimization of the flux of materials and energy through certain projects such as:

− valorising domestic garbage;
− valorising industrial waste;
− recovering gas produced by oil refineries;
− producing electricity from biomass;
− treating water and protecting the water table;
− ensuring complementarities between industrial production handicraft the informal sector.

Sensitisation of actors of the informal sector is an imperative even to authorities, elected officials, development groups and actors of the industry that must integrate this vision in the definition of national policy orientation on industrial development. Beyond sensitisation, actions aimed at ensuring training of decision-makers would logically complete the setup.

Other steps remain to be met in order to activate an industrial ecology process, such as the collection and sharing of reliable and updated data on industries and groups. It should be noted that a symposium in Cameroon recently treated this complex subject [23]. So too should several laws in Cameroon and the zone CEMAC be analyzed so as to handle imperatives on industrial ecology, especially texts relating to waste management.

At the level of Municipalities, reflections can examine the positioning of industrial zones, which initially are set up at the outskirts of the city (such as in Douala) but which are later surrounded by considerable population densities. The problematic of the environmental management of these Zones can be enlightened by the industrial ecology approach. A global analysis of Industrial Zones and material and energy flux therein

could lead to measures aiming at creating to encouraging the establishment of specific transformation companies that will enable the completion of these flows and consequently a decrease of industrial waste. The idea here is to envisage the transformation of classical industrial zones into eco-parks it of Kalundborg models [3] or Chinese eco-parks [2].

Conclusion

Industrialisation has contributed to an increase of productivity of Cameroonian companies, thus improving the living conditions of populations. But this increase of production activity in corporations was carried out for a long time without the integration of environmental constraints, and they have nevertheless shown their importance of the effects of pollution on populations. Industrial ecology constitutes a privileged approach that must allow the economy and in particular the private sector to play an active and constructive role in sustainable economic development strategies. Nevertheless, the industrial development and the principles of the industrial ecology appear at the present time as incompatible notions within the Cameroonian industries. The investigation conducted in a representative sample of the Cameroonian industries showed that input and energy consumption in the industry is not optimized, while the available resources are not used rationally. In addition, the recent phenomena of explosion of the informal sector and urban population to Cameroon, alongside an economic crisis that slowed down the attraction of investors to the country for international competition, as well as other structural weaknesses, all make it difficult to implement recipes for the deployment of industrial ecology.

Cameroon is a key nation in the attempt to implement an original way of sustainable economic and industrial development south of the Sahara, through industrial ecology and by respecting the Millennium Development Objectives alongside environmental constraints. This method can get inspiration from western and Chinese experiences underway. Several actions were evoked in this article. The idea now is to identify potential blockages to change and to formulate the specific adaptations to Cameroon and Sub-Saharan Africa.

References

1. Nkutchet M. L'énergie au Cameroun. Paris: L'Harmattan, 2004.
2. Fan X., Bourg D., Erkman S., L'économie circulaire en Chine // Futuribles. 2006. No. 234. P. 21-42.
3. Erkman S. Vers une écologie industrielle. Paris: Editions Charles Léopold Mayer, 2004.
4. Schmidlin M. Perspectives concrètes pour l'écologie industrielle en Afrique: l'Exemple du Cameroun. Report on a prospecting mission ICAST in Cameroon. January to May 1999. Geneva/Douala: ICAST, 2000.
5. World Summit on Sustainable Development, Johannesburg, 26th August to 04th September 2002, http://www.sommetjohannesburg.org.
6. Encyclopedia WikiDCia, http://fr.wikiDCia.org/wiki/Cameroun.
7. Statistical data from the Human Development Report, "UNDP", 2006, http://hdr.undp.org/hdr2006/statistics/.
8. Noumsi S., Tekeu J.C. Dimension industrielle du développement durable au Cameroun, ONUDI report, "ONUDI", 2001, http://www.unido.org/userfiles/timminsk/RIO10-IND-cameroon-french.pdf.
9. Kamgnia B., Touna M. Le comportement d'investissement privé au Cameroun: un resserrement de la contrainte fiscale. University of Yaoundé II, 2002.
10. Description of the activities of the group Fokou, including the companies BOCOM and BOCAM, http://www.fokou.com.
11. Diboma B. Offre d'énergie électrique et développement des industries au Cameroun, mémoire DEA, Université de Douala, 2007. P. 17-18, 62-63.
12. Latreille T., Leenhardt B., Massuyeau B. Perspectives économiques et financières des pays de la zone franc, projections Jumbo 2004-2005. Paris: AFD, 2004.
13. Ngnikam E. Energie et Ecodéveloppement au Cameroun // Revue hélio-international. 2006.
14. United Nations conference on Small Islands Developing States – Mauritius, January 2005, http://www.un.org/smallislands2005.
15. Clean Development Mechanism in Cameroon, http://www.cdmcameroon.org.
16. Kyoto Protocol, http://unfccc.int/2860.php.
17. Fohopa R., Garro O., Mortelette J.P. L'emploi et la formation au Cameroun, l'enquête génération 2000. Yaoundé: Edition Proximité, 2006.
18. Baillargeon G. Méthodes statistiques de l'ingénieur, volume I. Trois-Rivières: Les éditions SMG, 2006.
19. Grais B. Méthodes statistiques, tome II. Paris: Dunod, 2001.
20. Ndame M.K. Modélisation de la production de biogaz et conception d'un système d'acquisition de données sur le bio réacteur discontinue du laboratoire d'énergie de l'EDSFA de Douala, Master degree report, University of Douala, 2007.
21. Ngnikam E., Tanawa E. Les villes d'Afrique face à leurs déchets. Belfort-Montbéliard: Editions UTBM, 2006.
22. The ISO survey of ISO 9001:2000 and ISO 14001 Certificates – 2003, International Organisation for Standardization report, www.iso.ch/iso/en/iso9000-14000/pdf/survey2003.pdf.
23. Conference, Les TICE au service de la ville camerounaise, ENSP Yaoundé – January 2007, publication in progress, http://ticetville.projetcometes.org.

ON THE NEW POSITIVE ELECTRODE MATERIALS FOR HIGH ENERGY DENSITY LITHIUM ION BATTERIES

I. Saadoune, M. Dahbi**, M. Yahya***, A. Almaggoussi*****

LP2E2M, Equipe Chimie des Matériaux et de l'Environnement
Avenue A. Khattabi, BP 549, 40000 Marrakech, Morocco
Tel.: 212 24 43 46 88, Fax: 212 24 43 31 70
*E-mail: saadoune1@yahoo.fr
**E-mail: dahbi1979@yahoo.fr

LP2E2M, Equipe Chimie des Matériaux et de l'Environnement and Equipe Matériaux Optoélectroniques
Avenue A. Khattabi, BP 549, 40000 Marrakech, Morocco
Tel.: 212 24 43 46 88, Fax: 212 24 43 31 70
***E-mail: y_m_mustapha@yahoo.fr
****E-mail: maggoussi@menara.ma

Received: 22 Sept 2007; accepted: 30 Oct 2007

The layered $LiCo_{0.8}Ni_{0.1}Mn_{0.1}O_2$ and $LiNi_{0.65}Co_{0.25}Mn_{0.10}O_2$ positive electrode materials were synthesized by the combustion method using sucrose as fuel, and characterized by X-ray diffraction. The powders adopted the α–$NaFeO_2$ structure (R^{-3m} space group). Lithium is located between the transition metal ions slabs made up by edge sharing MO_6 octahedra (M: Ni, Co, Mn). X-ray diffraction data refinement by the Rietveld method shows that both samples present bi-dimensional structure with no Li/Ni cation mixing. Cycling tests revealed a great difference in the electrochemical behaviors. Lithium extraction from $LiNi_{0.65}Co_{0.25}Mn_{0.10}O_2$ involves only one redox process with a continuous evolution of the potential with composition, while they are two domains in the potential vs capacity curve of the $Li//LiCo_{0.8}Ni_{0.1}Mn_{0.1}O_2$ electrochemical cell. The first one at 3.6 V corresponds to the Ni^{4+}/Ni^{2+} redox couple while the second one at 3.9 V corresponds to the Co^{4+}/Co^{3+}. More than 190 mA·h/g could be delivered by $LiCo_{0.8}Ni_{0.1}Mn_{0.1}O_2$ electrode which could be considered as a good electrochemical performance by comparison with the most commercialized cathode $LiCoO_2$.

Keywords: electric energy storage, structural materials, new structural materials for renewable energy

Ismael Saadoune

Organization(s): University Cadi Ayyad, Faculty of Sciences and Technology Marrakesh, Full professor, Director of the Materials and Environmental Chemistry Laboratory.
Education: French PhD (University Bordeaux I, France, 1988-1992), Moroccan PhD (University Cadi Ayyad, Morocco, 1992-1996), Master course (University Casablanca, Morocco, 1984-1988).
Experience: University Bordeaux I, Associate professor (1989-1991). University Cadi Ayyad, Full professor, Tokyo University of Science, Invited professor (2002), Leader of 10 research projects.
Main range of scientific interests: lithium batteries, solid state chemistry, physical properties.
Publications: 32 papers in international scientific journals, 70 communications in international meetings.

Mohammed Dahbi

Organization(s): University Cadi Ayyad, Faculty of Sciences and Technology Marrakesh.
Education: Graduate diploma (2003-2004), Master (2004-2005), PhD (2006-2009).
Experience: Member of 4 research projects.
Main range of scientific interests: structural analysis, lithium batteries.
Publications: 2 papers in international scientific journals, 6 communications in international meetings.

Mustapha Yahya

Organization(s): University Cadi Ayyad, Faculty of Sciences and Technology Marrakesh.
Education: Graduate diploma (2003-2004), Master (2005-2006), PhD (2007-2010).
Experience: Member of 2 research projects.
Main range of scientific interests: physics, lithium batteries.
Publications: 2 posters.

Abdelmajid Almaggoussi

Organization(s): University Cadi Ayyad, Faculty of Sciences and Technology Marrakesh, Full professor, Member of Optoelectronic Materials Team.
Education: French PhD (University Montpellier I, France, 1986-1992), Moroccan PhD (University Cadi Ayyad, Morocco, 1997-2003), Master course (University Marrakech, Morocco, 1981-1985).
Experience: University Cadi Ayyad, Full professor, Member of 4 research projects.
Main range of scientific interests: transport phenomena in semiconductors, low dimensional systems (Quantum Well, quantum Wire and Quantum dot).
Publications: 10 papers in international scientific journals, 20 communications in international meetings.

Introduction

Development of environmentally friendly and renewable energy sources is of great importance for a sustainable future. Fossil fuels and nuclear power are currently the dominating energy sources and will most likely continue to be so for the next generations. However, these power sources have drawbacks; the amount of fossil available is finite and nuclear wast disposal involves well-known problems. Today, as evidence of global warming accumulates [1], researchers from many fields focus on developing alternative energy sources and storage techniques, eg., photoelectrochemical cells [2], fuel cells [3] and batteries. The major advantages of the batteries (especially lithium-ion batteries) is its high energy density compared to others systems. It is therefore, used successively in portable electronics e.g., cellular phones, laptops and camcorders.

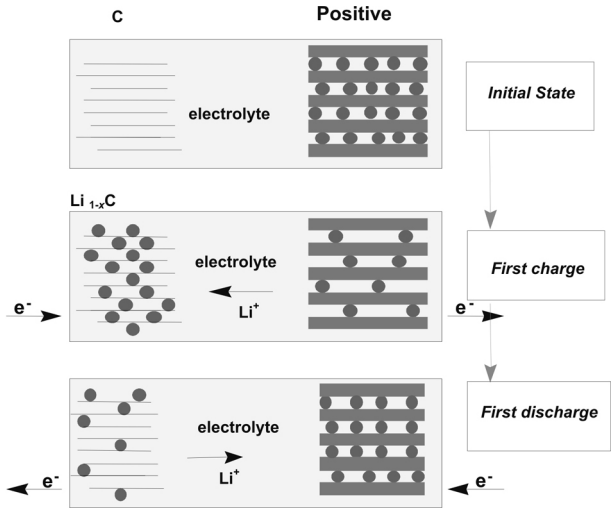

Fig. 1. *Schematic representation of the lithium-ion battery*

As schematically represented in Fig.1, lithium-ion battery consists of carbon as anode, liquid electrolyte and cathode. During the charge process, lithium ions move from the cathode across the electrolyte to the anode and vice versa as the battery is charged. Choosing the positive electrode material is crucial for the battery's overall performance. The most studied materials are $LiCoO_2$ [4], $LiNiO_2$ [5], $LiMn_2O_4$ [6] and $LiFePO_4$ [7]. Since cobalt is expensive, the battery manufacturers are looking for other materials, which can help to reduce the price of the final product without decreased performance.

In the present paper, new positive electrode materials based on Co, Ni and Mn elements were prepared by the combustion method. The electrochemical performances of the studied compounds were discussed in relation with their structural properties.

Experiment

Two compositions for the positive electrode materials were selected: $LiCo_{0.8}Ni_{0.1}Mn_{0.1}O_2$ and $LiNi_{0.65}Co_{0.25}Mn_{0.10}O_2$. Stoichiometric amounts of Li, Co, Ni and Mn nitrates (oxidant) were dissolved simultaneously with the sucrose (fuel) in an aqueous solution. The reaction is extremely violent when using a stoichiometric amount of sucrose. To avoid it, the oxidant/fuel ratio was optimized to 0.67. In this way, the reaction is well controlled. The reagents solution was heated at about 120 °C for 1 h, and then dried; it starts to swell up due to the evaporation of the generated gases leading to a foamy mass. After a few minutes, the mass starts to burn spontaneously without flame. The as prepared material is very light and downy. The final thermal treatments are 900 °C/12 h and 900 °C/1 h for $LiCo_{0.8}Ni_{0.1}Mn_{0.1}O_2$ and $LiNi_{0.65}Co_{0.25}Mn_{0.10}O_2$ respectively.

X-ray diffraction patterns of the powdered samples were obtained with a STOE STADI/P diffractometer (Mo-$K_{\alpha 1}$ radiation, curved Ge (111) monochromator, transmission mode, data step width 0.02° (2θ), linear PSD counter).

Electrochemical properties measurements were performed in lithium cells containing a lithium foil as negative electrode. Positive electrodes were prepared by spreading a mixture of 85 % active material, 10 % carbon black, and 5 % of PVDF [poly(vinylidene fluoride)] in NMP (1-methyl-2pyrrolidinone) onto an aluminum foil. The electrolyte was 1 M $LiPF_6$ (lithium hexafluorophosphate) dissolved in a 2:1 volume ratio solution of EC (ethylene carbonate) and DEC (diethyl carbonate). Cells were cycled galvanostatically using a multi-channel potensiostat (VMP2/Z; Ametek) battery testing system.

Results and discussion

Fig. 2 shows the X-ray diffraction patterns of $LiCo_{0.8}Ni_{0.1}Mn_{0.1}O_2$ and $LiNi_{0.65}Co_{0.25}Mn_{0.10}O_2$.

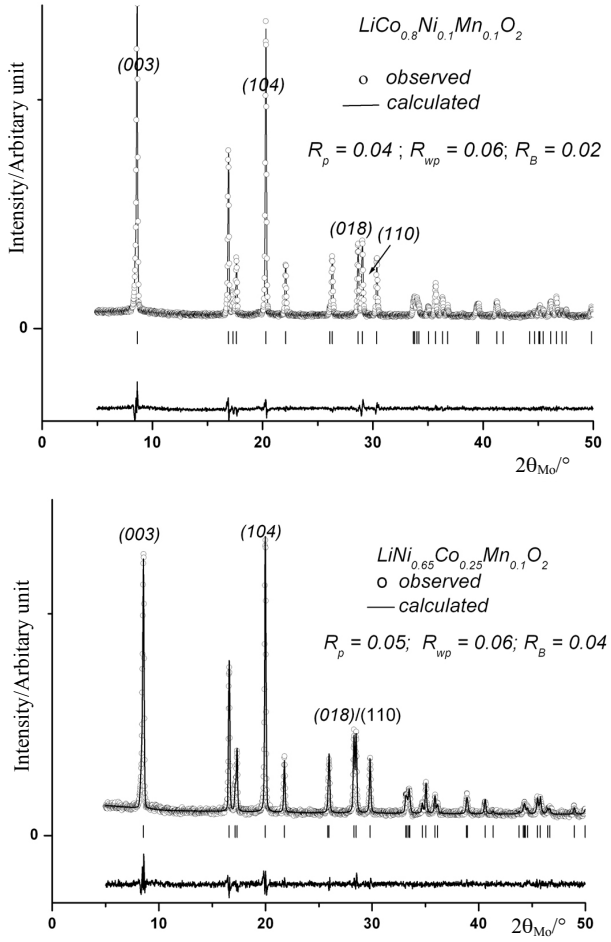

***Fig. 2**. X-ray diffraction patterns of $LiCo_{0.8}Ni_{0.1}Mn_{0.1}O_2$ and $LiNi_{0.65}Co_{0.25}Mn_{0.10}O_2$*

All diffraction peaks can be indexed based on the α-$NaFeO_2$-type structure (Space Group R-3m). The relative intensity of (003) to (104) peaks and the splitting of (018)/(110) diffraction lines clearly indicate a good 2D character of the structure. As shown by Fig. 3, Li and transition metal ions (Ni,Co,Mn) occupying alternate layers with an octahedral environment.

The structural refinement of the X-ray data, using the Rietveld method [8], was done assuming that Li, M (M: Ni,Co,Mn) and O occupy (001/2); (000) and (00z) atomic coordinates. It gives a good reliability between the calculated and observed profiles as demonstrated by the low values of the R_p, R_{wp} and R_B reliability factors. The hexagonal unit cell parameters for the two compounds are: a = 2,8270(1) Å; c = 14,1132(1) Å for the cobalt rich phase ($LiCo_{0.8}Ni_{0.1}Mn_{0.1}O_2$) and a = 2,8459(1) Å; c = 14,0980(3) Å for the nickel rich phase ($LiNi_{0.65}Co_{0.25}Mn_{0.10}O_2$). According to these crystallographic data, we can conclude that within the (Ni,Mn,Co) sheets, a high covalency exists leading to an easy electronic transfer during the electrochemical process. In the same time, lithium ions establishes only a very weak bonding (Van der Waals type) with the oxygen anions. This also leads to an easy lithium diffusion upon lithium extraction or insertion. We could then expect that this kind of compounds exhibit a convenient features to be used as positive electrode materials in lithium-ion batteries.

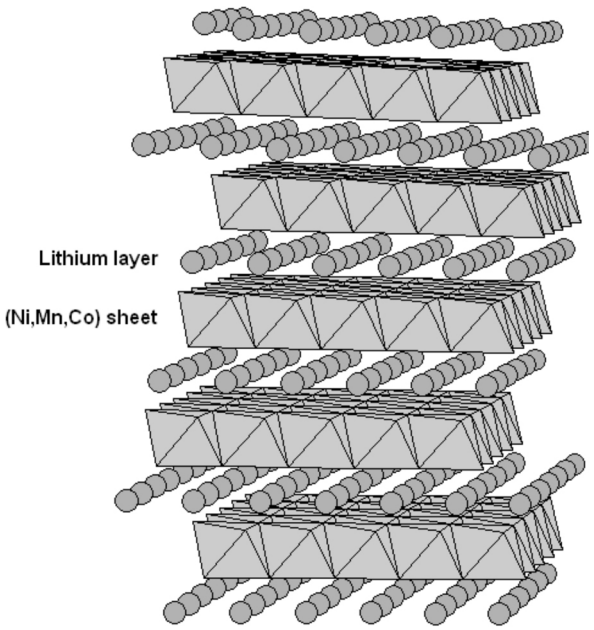

***Fig. 3.** Structure of the $LiCo_{0.8}Ni_{0.1}Mn_{0.1}O_2$ and $LiNi_{0.65}Co_{0.25}Mn_{0.10}O_2$ oxides showing lithium ions between the $(Ni,Co,Mn)O_6$ edge sharing octahedra*

The two materials have been used separately as cathode materials in lithium batteries in order to study their electrochemical behavior. The voltage vs capacity profiles during the first charge are plotted in Fig. 4. For the cobalt rich phase $LiCo_{0.8}Ni_{0.1}Mn_{0.1}O_2$, they are two voltage domains separated by a potential plateau at 3.85 V: the first domain is from 3.6 to 3.8 V, the second from 3.85 to 4.5 V. While for the nickel rich phase $LiNi_{0.65}Co_{0.25}Mn_{0.10}O_2$, a continuous evolution of the potential was evidenced, showing that only one electrochemical process is involved during the lithium extraction from this phase. For the cobalt rich phase, the charge process of the Li//$LiCo_{0.8}Ni_{0.1}Mn_{0.1}O_2$ battery starts by the oxidation of Ni^{3+} to Ni^{4+} ions at about 3.6 V. The oxidation of all 0.1 nickel ion present in the starting phase corresponds to the extraction of 0.1 lithium ions (about 55 mA·h/g). After this redox process, Co^{3+} ions start its oxidation process which corresponds to about 3.9 V. The preferential oxidation of Ni^{3+} compared to Co^{3+} ions was already demonstrated by studying the physical properties (Li NMR spectroscopy, magnetism) of the $Li_xNi_{1-y}Co_yO_2$ system [9-12].

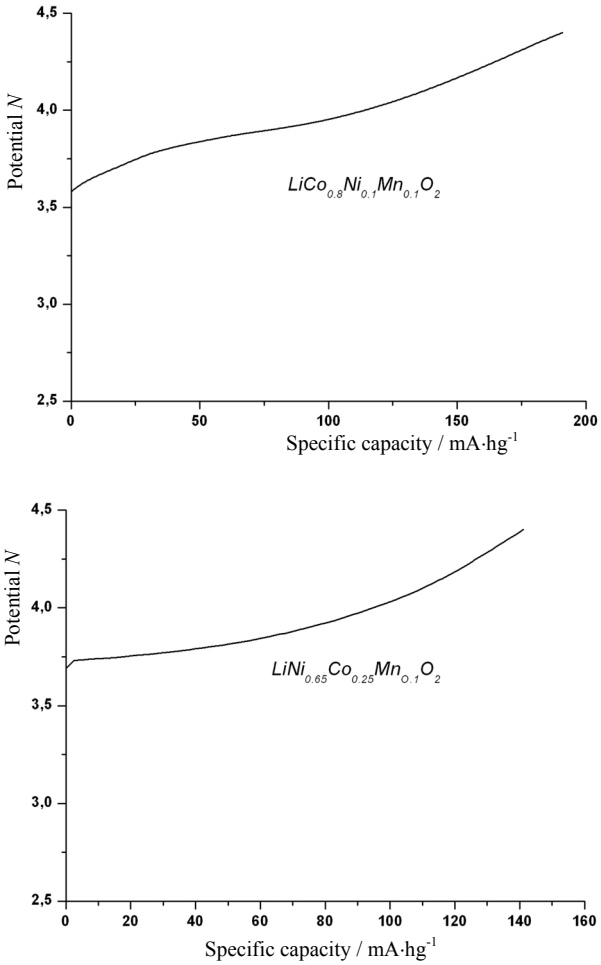

Fig. 4. *The voltage vs capacity profile of the Li// $LiCo_{0.8}Ni_{0.1}Mn_{0.1}O_2$ and Li//$LiNi_{0.65}Co_{0.25}Mn_{0.10}O_2$ electrochemical cells cycled in the same regime C/20 which corresponds to the extraction of one Li ion in 20 hours*

Furthermore, the electrochemical cycling of these two positive electrode materials occurs without structural modifications and with a small variation of the unit cell parameters. This result, which will be published soon, is important from the applications point of view. Indeed, deterioration of the electrochemical performances (long cycle life, cyclability...) is strongly related to the structural stress in the cathode material resulting from the structural changes in the symmetry or/and in the unit cell volume that occur during the cycling [13].

The sample with larger amount of cobalt delivers a charge capacity of 196 mAh/g, which is 35% greater compared to that delivered by the Li//$LiNi_{0.65}Co_{0.25}Mn_{0.10}O_2$ electrochemical cell. Furthermore, the electrochemical cycling (lithium extraction/insertion) of the Li//$LiCo_{0.8}Ni_{0.1}Mn_{0.1}O_2$ occurs without significant modifications in the structural features while lithium extraction from Li_xCoO_2 system (the commercialized cathode) involves many structural changes as reported elsewhere [4]. Thus, $LiCo_{0.8}Ni_{0.1}Mn_{0.1}O_2$ could be considered as much more competitive cathode than $LiNi_{0.65}Co_{0.25}Mn_{0.10}O_2$ for application in the real batteries.

Conclusions

$LiCo_{0.8}Ni_{0.1}Mn_{0.1}O_2$ and $LiNi_{0.65}Co_{0.25}Mn_{0.10}O_2$ were prepared by the simple combustion method using sucrose as fuel. From the results of X-ray diffraction, these two samples were characterized by an α-$NaFeO_2$ type structure with alternating lithium layers with transition metal slabs. In the two-electrode electrochemical cells, $LiNi_{0.65}Co_{0.25}Mn_{0.10}O_2$ shows a smooth charge curve with continuous evolution of the potential versus capacity which suggests less structural transformations with intercalation of lithium. For the cobalt rich phase $LiNi_{0.65}Co_{0.25}Mn_{0.10}O_2$, two electrochemical processes are involved during lithium extraction: the first one corresponds to the oxidation of the Ni ions while the second one corresponds to the Co^{4+}/Co^{3+} redox couple. For this last phase, about 196 mAh/g can be delivered during the electrochemical cycling which makes this positive electrode material competitive from applications point of view.

Acknowledgements

The authors would like to thank the French Ministry of Foreign Affairs, Agence Française de Développement AFD and Institut de Recherche pour le développement IRD for the financial support under the CORUS program (project No. 02 211 121).

References

1. Houghton J.T. Climate change: the scientific basis. New York, Cambridge University Press. 2001.
2. Grätzel M. Photoelectrochemical cells // Nature. 2001. Vol. 414. P. 338-344.
3. Steel B.C.H., Heintzel A. Materials for fuel cell technologies // Nature. 2001. Vol. 414. P. 345-352.
4. Mizushima K., Jones P.C., Wiseman P.J. et al. Li_xCoO_2 ($0 < x < 1.0$): A new cathode material for batteries of high energy densities // Material Research Bulletin. 1980. Vol. 15. P. 783-789.
5. Dahn J.R., Von Sacken U., Juzkow M.W. et al. Rechargeable $LiNiO_2$/carbon cells // Journal of the Electrochemical Society. 1991. Vol. 138. P. 2207-2211.
6. Thackeray M.M., David W.I.F., Bruce P.G. et al. Lithium insertion into manganese spinels // Material Research Bulletin. 1983. Vol. 18. P. 461-472.
7. Padhi A.K., Nanjundaswarmy K.S., Goodenough J.B. Phospho-olivines as positive electrode materials for rechargable lithium batteries // Journal of the Electrochemical Society. 1997. Vol. 144. P. 1188-1194.
8. Roisnel T., Rodriguez-Carjaval J. WinPlotr: A windows tool for powder diffraction pattern analysis // Materials Science Forum. 2001. Vol. 378. P. 118-123.
9. Delmas C., Saadoune I., Rougier A. The cycling properties of the $Li_xNi_{1-y}Co_yO_2$ electrode // Journal of Power Sources. 1993. Vol. 44. P. 595-602.
10. Saadoune I., Delmas C. $LiNi_{1-y}Co_yO_2$ positive electrode materials: relationships between the structure,

physical properties and electrochemical behavior // Journal of Materials Chemistry. 1996. Vol. 6, No. 2. P. 193-199.

11. Saadoune I., Ménétrier M., Delmas C. Redox processes in $Li_xNi_{1-y}Co_yO_2$ cobalt-rich phases // Journal of Materials Chemistry. 1997. Vol. 7, No. 2. P. 2505-2511.

12. Saadoune I., Delmas C. On the $Li_xNi_{0.8}Co_{0.2}O_2$ system // Journal of the Solid State Chemistry. 1998. Vol. 136. P. 8-15.

13. Song M.Y., Lee R., Kwon I. Synthesis by sol-gel method and electrochemical properties of $LiNi_{1-y}Al_yO_2$ cathode materials for lithium secondary battery // Solid State Ionics. 2003. Vol. 156, No. 4. P. 319-328.

STUDY AND CHARACTERIZATION OF THE CONCRETE AND INFLUENCE OF THE TEMPERATURE ON ITS COMPRESSIVE STRENGTH

E. Gourri, M. Ez-Zahery, N. Elalem

Laboratory Materials and Environment (LME)
Faculty of Science, department of chemistry, city ADAKHLA BP 8106 Agadir, Morocco
E-mail: nelalem@gmail.com

Received: 9 Oct 2007; accepted: 10 Jan 2008

The study of the material concrete considered as a composite, constitutes a need which makes it possible to avoid interventions being able to damage or even destroy work. This analysis is intended either for the determination of the elementary composition of materials, or with the potential mineralogical composition or the grain-size distribution, with an aim of envisaging the rational use of materials and of judging the conformity of material.
In this work, one studies on the one hand the general principles of the study of the concrete in order to determine the proportioning of the constituent elements this material and on the other hand, the effect of the temperature on the mixture of cement with the aggregates to have data having a practical interest.

Keywords: structural materials, nanocomposites for application as catalysts

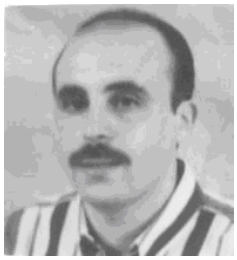
Elhassan Gourri

Organization: Doctorant.
Education: Ibn Zohr University, Faculty of science (2002-2007).
Main range of scientific interests: concrete, cement, compressive strength.

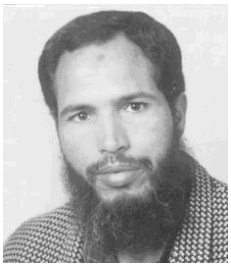
Mohamed Ez-Zahery

Organization: Doctorant.
Education: Ibn Zohr University, Faculty of science (2002-2007).
Main range of scientific interests: infiltration-percolation, sand, waste water.


Nour-Eddine Elalem

Organization: Professor at Ibn Zohr University of Agadir (Morocco).
Education: Maitrise**:** Mohamed V University (Rabat-Morocco) (1978-1982).
Doctorat: NANCY I University (1982-1985).
Doctorat of state: NANCY I University (1985-1988).
Experience: Professor of Chemistry at Faculty of Sciences (Agadir-Morocco) (1988-2007).
Main range of scientific interests: concrete, cement, compressive strength, infiltration-percolation, sand, waste water.
Publications: 13 publications in international journals, 25 communications.

Introduction

The concrete is a relatively recent building material since its employment spread only since the beginning of the XX century [1]. It is the building material today par excellence (meadows of 15 billion tons per year, is approximately 2 tons per human being) [2].
If this material were adopted so universally, it is thanks to the various criteria:
− It is made of primary education natural materials largely distributed to the surface of the ground.
− Its capacities of resistances exceed those of the best natural rocks.
− Its durability can be secular, and it resists corrosive environments, fire, etc…
− Its implementation is rather simple.
− It is castable.
It is thus for economic reasons and techniques that the concrete became irreplaceable in the field of construction.
The study of the composition of the concrete consists in defining the optimal mixture of the various components: aggregates, cement and water. What makes it possible to have a concrete whose quality is that required for the construction of the work in question.

The temperature is also an important parameter of which it is necessary to hold account at the time of the mixture of the various components of the concrete since its variation influences the compressive strength of this last.

Methods and analyses

Analyses were carried out on the various components of the concrete. We undertook a study detailed on cement, sand and the gravels in order to identify the type of our material.

The techniques of investigations used are: gravimetry, potentiometry, photometry with flame, colorimetry, atomic absorption spectrometry (A.A.S), the spectrometry of X-ray fluorescence (X.S.F).

For the study of the composition of the concrete one used method DREUX GORISSE.

This method is a technique which defines in a simple and fast way, a composition with little meadows adopted with the studied concrete. The clothes industry of the test-tubes makes it possible as well as possible to adjust the composition with definitively adopted according to desired qualities and of materials used [3].

Study of the components of the concrete

Identification of cement of Agadir CPJ 45

Chemical composition

The chemical analysis is determined by physical and chemical methods. Table 1 has the results obtained.

Cement of Agadir CPJ 45 is Cement of the Portland type made up of pozzolanas and it is with low contents alkalis.

Table 1

Chemical composition of the initial products of cement of Agadir CPJ 45 in %

	Synopsis chemical analyse												
	Insoluble	SiO_2	Al_2O_3	Fe_2O_3	CaO	MgO	SO_3	K_2O	Na_2O	P_2O_5	PAF*	Cl-	Total
Clinker	0.1	21.6	5.75	3.65	64.4	2	0.9	0.78	0.06	0.17	0.3	-	99.7
Cement	11.8	16.7	5.48	2.80	51.8	3.1	2.7	0.80	0.01	0.28	4.7	0.02	99.8
Cru	0.1	21.2	5.79	3.65	65	1.8	1.1	0.88	0	0.24	0.1	-	99.8
Clay	-	27.8	9.55	3.63	27.7	2.3	0.4	0.35	0.13	0.1	26	-	98.4
Lime stone	-	6.91	0.86	0.39	50.4	0.6	0.1	0.46	0.07	0.11	26.5	-	86

(*) PAF = Loss on the ignition

Potential composition

The mineralogical composition of cement is determined by calculation starting from chemical analysis by using the method of bug. The potential composition of phase is calculated by the equations of bogue [4], in which the chemical formulas represent the percentage in mass of each oxide (Table 2).

Table 2

Potential composition of phase of cement of Agadir CPJ 45

Phase	**Chemical formula**	**Value**
C_3A	$C_3A = 2.65\ Al_2O_3 - 1.69\ Fe_2O_3$	9.07
C_3S	$C_3S = 4.07\ CaO - 7.6\ SiO_2 - 1.43\ Fe_2O_3 - 6.72\ Al_2O_3$	50
C_2S	$C_2S = 88.60\ SiO_2 + 1.08\ Fe_2O_3 + 5.07\ Al_2O_3 - 3.07\ CaO$	24.38
C_4AF	$C_4AF = 3.04\ Fe_2O_3$	11.1

Granulometric analysis

The granulometric analysis is carried out on tamisat with depression of air (sifter alpine). In Table 3 are gathered the results obtained.

The granulometric characteristics of this cement answer largely the usual specifications of cements of quality [5]. That makes it possible to advance that cement of Agadir CPJ 45 presents grains rich in fine elements. Indeed, the granulometry is the dominating factor of the compressive strength at the long limits [6].

Table 3

Results of analysis of the granulometry of cement of Agadir (CPJ 45)

Diametre in µm	**40**	**80**	**160**
% refusal	26	3.8	2
% tamisat	74	96.2	98

Mechanical test: compression and inflection

Normal resistance and the strength to the youth of Portland cement CPJ 45 are the mechanical resistances to compression determined respectively after 28 days and 2 days or 7 days. The results of this mechanical test are deferred in Table 4.

Table 4

Mechanical test: Compression and inflection on cement of Agadir CPJ 45

Resistance to	2 days	7 days	28 days
Compression (MPa)	17.1	29.9	46.1
Inflection (MPa)	4.1	5.8	7.7

According to the results of this mechanical test, one can deduce that cement of Agadir satisfies the mechanical specifications suitably and to the values limit guaranteed according to Moroccan standard NM 10.1.005 [7].

Identification of the aggregates

Granulometric analysis

The grading curves of gravels GI, GII and of the sand of Souss Wadi are represented in Fig. 1.

The grading curve of the aggregates of Souss Wadi is continuous and present a current form, which allows a good implementation.

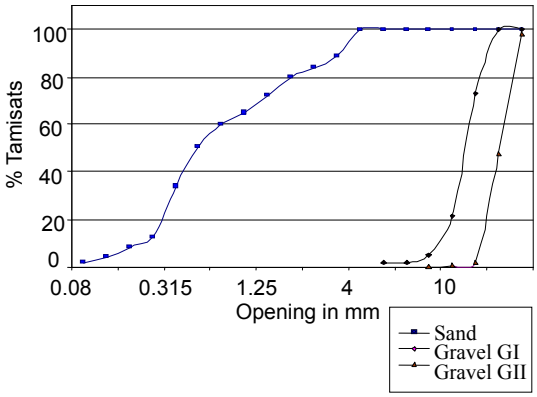

Fig. 1. *Grading curves of the aggregates of Souss Wadi*

Composition of the components by spectrometry of X-ray fluorescence

The spectrometry of X-ray fluorescence makes it possible to determine the centesimal composition in elements (Si, Al, Ca, Fe…) constituting the aggregates. The results obtained are deferred in Table 5.

It arises from the analysis of different constituting concrete which they present largely of the characteristics answering the usual specifications of the concretes of quality.

Table 5

Chemical composition of the aggregates of Souss Wadi

	Synopsis chemical analyse											
	SiO_2	Al_2O_3	Fe_2O_3	CaO	MgO	SO_3	K_2O	Na_2O	P_2O_5	PAF	Total	Moisture
Gravette I	3.84	0.51	0.18	49.8	4	–	0.19	0.02	0.14	42	101	0.026
Gravette II	4.82	0.59	0.20	50.9	2.9	–	0.24	0.01	0.14	41	101	0.045
Sand	64.24	1.14	–	4.87	–	–	–	–	–	1.13	–	–

Study of the composition of the concrete

The method used for the formulation of the concrete is method DREUX GORISSE. It is based on the preliminary knowledge of a grading curve of reference obtained by the rational export of experimental study.

It makes it possible to determine the composition of a sand, cement concrete and gravel, in order to carry out a concrete of satisfactory workability, suitable plasticity and whose mechanical characteristics is those as a preliminary definite.

In this work, we study the formulation of a three-component concrete made up of the sand of Souss Wadi and two gravels of Wadi Souss GI and GII (Fig. 2).

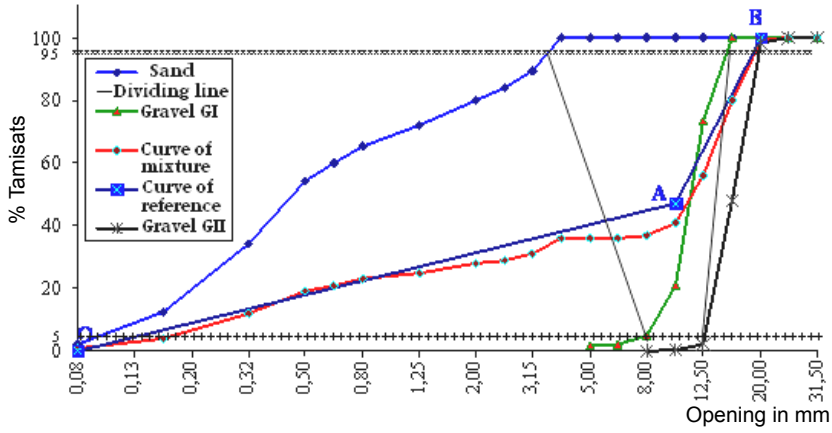

Fig. 2. *Chart of the grading curves of the aggregates, the curve of reference, the dividing lines and the curve of optimal mixture*

The research of the composition of concrete consists in defining the optimal mixture of the various aggregates, the proportioning out of cement and water which makes it possible to have a concrete whose quality is that required for the construction of the work in question.
The curve of mixture is represented on Fig. 2, it presents a continuous form. What allows an easy implementation.
The results of the composition for 1 m^3 of the concrete are gathered in Table 6.

Table 6

Results of the composition of the concrete

Dosage	Sand	Gravel GI	Gravel GII	Cement	Water
Weight (kg)	644	504	715	350	196
Volume in (l)	441	336	473	363	196

Influence temperature on the evolution of the resistance of the concrete in time

After having defined the corrected proportioning of the aggregates, the test-tubes were made according to standard NF P18-422. They were struck after 24 hours in their moulds, then preserved in different temperatures. Three test-tubes are produced per series for each time of conservation. That makes it possible to obtain an acceptable average and to decrease the variation of the results due to problems at the time of the realization of crushing (surfacing for example). The mechanical test consists in placing these test-tubes on a hydraulic press. The results obtained are breaking strengths, expressed in MPa. They are given for various temperatures, and shelf lives of 3.5 and 7 days.
The Fig. 3 shows the evolution of the compressive strength of a proportioned concrete with 350 Kg/m^3 according to the temperature.

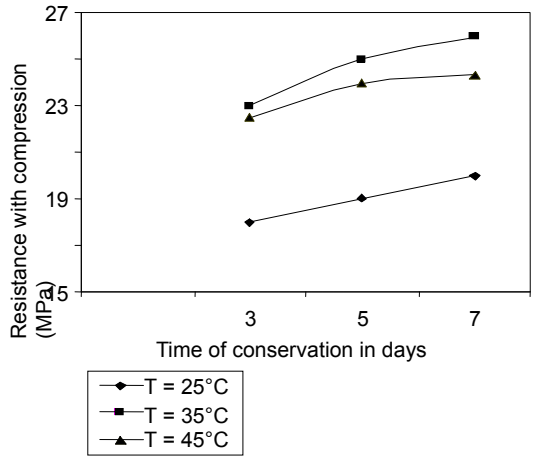

Fig. 3. *Evolution of the compressive strength for various temperatures*

In order to evaluate the impact of the temperature of treatment on long-term resistances (age of at least 28 days), of the test-tubes were preserved during 5 days in various temperatures then maintained in wet room up to 28 days. Fig. 5 has the results obtained.

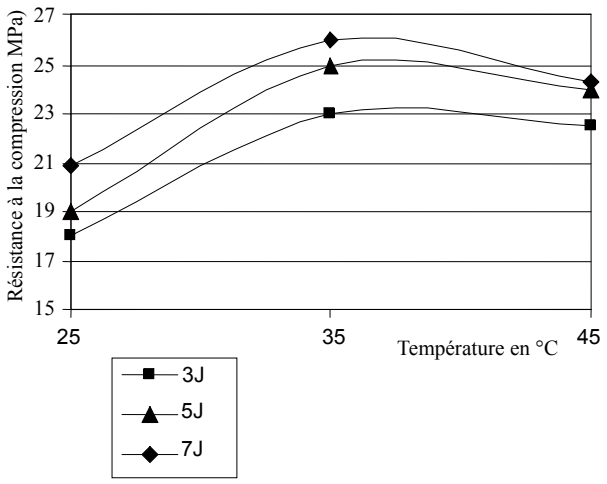

Fig. 4. *Influence of temperature on the evolution of the compressive strength of the concrete in time*

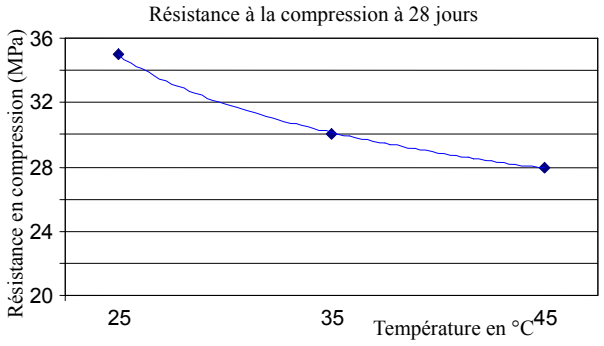

Fig. 5. *Influence of temperature on resistance in long-term compression*

According to Fig. 3, 4 and 5 the strengths to the youth and long-term are influenced by the temperature i.e. the higher the temperature of the concrete is, the more short-term resistance is high. Whereas in the long run the phenomenon is reversed since resistances are worse during rise in the temperature. What makes it possible to advance that heat accelerates the reactions of hydration of the concrete, as it modifies also the speed of hardening. The fall of resistant in the long run comes from important evaporation of the water and with the increase in porosity.

Conclusion

In order to identify the type of material and to lay down the tendencies of the elements which deteriorate the durability of the concrete one carried out a detailed study which consists in carrying out mineralogical and physicochemical tests of analysis on the various components of the concrete: cement, sand and gravels.

Thus, it comes out from these analyses that the latter present physical specifications, chemical, mechanical and geometrical meeting largely the usual characteristics of the concretes of quality. Thereafter, one adopted the method of DREUX GORISSE to determine the formulation of the optimal mixture while making the corrections necessary to the proportioning of cement, the mixing aggregates and water.

The mechanical test consisted in measuring the compressive strengths for various temperatures, and different shelf lives. The concrete matured under conditions of high temperatures develops, in the short run, a strong mechanical resistance. On the other hand, the profit of long-term resistance proves weaker than that of the same concrete preserved at low temperatures. This result is allotted to the important evaporation of water and the increase in porosity. This study enabled us to clear up the behaviour of the concrete under the effect of the temperature.

References

1. Paduari A. La pratique du béton, Edition A. De Boeck, 1969. P. 55.
2. Matériaux de l'ingénieur, Université de Sherbrooke, 2005.
3. Georges D., Jean F. Nouveau guide du béton, édition Eyrolles, 1995.
4. Elaouni B. Contribution à l'hydratation de l'aluminate tricacique, thesis, 1997.
5. Abbas L., Elalem N. // J. Phys. IV France. 2005. Vol. 123. P. 197-201.
6. Sheriff T.C., Sollars C.J., Montgomery D.M., Perry R. Modified clays for organic waste disposal // Environmental Technology Letters, 1987. Vol. 8. P. 501-514.
7. Normes marocaines: NM 10.1.004 et NM 10.1.005 liants hydauliques-caractéristiques des ciments pour tout usage et leur techniques d'essais.

PROMOTING ECOCITIZENSHIP: IN FAVOUR OF BINDING COMMUNICATION

R.-V. Joule, F. Bernard**, S. Halimi-Falkowicz**

*Laboratoire de Psychologie Sociale, Université Aix-Marseille I
29 avenue Robert Schuman, 13090 Aix-en-Provence, France
Phone: 33 (0) 442 953 812; E-mail: joule-rv@up.univ-aix.fr, severinehalimi@free.fr

**Centre de Recherche sur les Pratiques de Médiation et de communication, Université Aix-Marseille I
29 avenue Robert Schuman, 13090 Aix-en-Provence, France
Phone: 33 (0) 442 953 236; E-mail: fbernard@up.univ-mrs.fr

Received: 24 Sept 2007; accepted: 16 Oct 2007

The purpose of this article is to illustrate the way in which the binding communication paradigm (Joule, Girandola, Bernard, in press) can serve to promote environmentally-friendly values and behavior. This paradigm stands at the crossroad of research conducted in both the fields of communication and of commitment. We will be describing 4 recent studies carried out in the south of France. The first study was conducted in a school, the second in a town, the third study aimed at encouraging environmentally-friendly behavior along the seacoast while the purpose of the fourth study was to promote recycling on highway rest areas.

Keywords: philosophy problems, commitment, communication, behavioral change, environment

Robert-Vincent Joule

Organization: Professor of social psychology at University of Provence (France) since 1988. Head of the Laboratory of Social Psychology.
Experience: He was awarded the "Prix de la diffusion scientifique" at the Festival des Sciences et des Technologies in 2002 (President of the Jury: Yves Coppens). Co-director of the International Review of Social Psychology from 2000 to 2006.
Main range of scientific interests: cognitive dissonance and social influence procedures (free will compliance). His most recent research concerns communication and more specifically "committing communication".
Publications: 50 articles in national and international journals. He is the author of several books, and of around thirty chapters in books. In addition he has edited numerous books. His best-known works (written with J.L. Beauvois) are *A Radical dissonance theory* (London and Bristol: Taylor & Francis, 1996), *La soumission librement consentie* (Paris: Presses Universitaires de France, 1998) and also the *Petit traité de manipulation à l'usage des honnêtes gens* (Grenoble: Presses Universitaires de Grenoble, 2002), a best-seller which has been sold at 200,000 copies in France and has been translated in several languages.

Françoise Bernard

Organization: Professor of information sciences and communication at University of Provence (France). Head of the Centre de Recherche sur les Pratiques de Médiation et de communication. President of the Société Française des Sciences de l'Information et de la Communication from 2002 to 2006, and is currently its Honorary Chair.
Main range of scientific interests: communication, change and innovation within organizations. Her most recent research focuses on "committing communication" and is conducted in partnership with Robert-Vincent Joule. She examines, among other things, the relationship between communication and action in the domain of environment.

Séverine Halimi-Falkowicz

Education: Séverine Halimi-Falkowicz did her thesis (2003-2006) under the direction of the professor Robert-Vincent Joule.
Organization: A member of the Laboratory of Social Psychology of the University of Provence (France).
Main range of scientific interests: cognitive dissonance and social influence procedures (free will compliance).

Introduction: the limits of information and persuasion

A prevailing notion about human beings may lead to think that one merely needs to modify the ideas of others to make them behave in the desired way. Information and persuasion are hence widely used to encourage children and adults to adhere to the ideas required for proper social functioning. It seems obvious that, this being done, the proper social behavior will automatically fall into place.

Most major communication campaigns follow this assumption.

But do "good ideas" automatically lead to "proper behavior"? Most likely not. The scientific literature on this topic invites us to be wary as numerous studies have pointed to the gap between good ideas and proper behavior. One of these studies is particularly telling. Peterson, Kealey, Mann, Marek and Sarason (2000) [1] conducted an evaluation of a smoking prevention action (Hutchinson smoking prevention project). From the ages of 8 through 17 years old, the students belonging to an experimental group (about 4000) took part in prevention sessions in class while the students in the control group (also roughly 4000) did not participate in these sessions. The prevention program comprised 65 sessions adapted to each age group and aimed at making the students aware of the negative effects of smoking. As we have already indicated indirectly, the action had no effect on tobacco consumption. Indeed, at the end of the program − when the students were 17 years old − the smoking prevalence was not lower in the experimental group than in the control group despite the fact that the students were fully aware of the negative effects of smoking. Of course, this does not mean that information and persuasion are useless. There is no question that, through time, information and persuasion help to change knowledge, modify attitudes and most certainly induce genuine awareness. Information and persuasion are therefore necessary but not sufficient on their own.

Theoretical option: binding communication

For this reason we have deemed it necessary to connect certain disciplines from the fields of human and social sciences, more specifically we want to bring together researchers from social psychology and researchers from the Sciences of Information and Communication [2, 3].

For the time being, our suggestion is to bring together in a single basic paradigm, on the one hand, studies on communication in general and on persuasive communication, and studies on commitment on the other hand. We call this paradigm binding communication [4].

Studies on commitment [5, 6, 7] show that it does not take much sometimes to go from "good ideas" to "proper behavior".

We do not intend to go over Lewin's studies (1947) [8] and the discovery of the freezing effect, which may be regarded as the starting point of research on commitment. Lewin's famous action-research shows the advantage of securing decisions − commitments − from the people whose behavior one seeks to change. Most of these decisions need to be prepared. A good way of preparing people is to lead them to take a small step in the right direction by making them comply with an innocuous request, which we call a "preparatory action".

The foot-in-the-door procedure

The foot-in-the-door procedure [9] is a good illustration of this. Its principle consists in making a small request (preparatory action) prior to a more substantial one (expected behavior). Results can be spectacular. For instance, Freedman and Fraser managed to multiply by four the likelihood that a person will comply to a costly request (to install a large road sign in their backyard) if this request is preceded by a less costly one likely to be accepted by almost everyone (putting up a small sign promoting safe driving on their window). In research on the foot-in-the-door procedure, the expected behavior can be to put up a big sign in one's backyard as in the aforementioned Freedman et Fraser experiment, but it can also be, for instance, having a person agree to take part in a lengthy survey, stop smoking, make a donation, etc. The range of behaviors obtained with this procedure can be quite wide [7].

Taken as a whole, the foot-in-the-door studies [10, 11] show that the likelihood of securing consent is higher when the points made − or the information given − are preceded by a preparatory action. However, the preparatory action must have certain characteristics for it to produce the expected outcome [12]. Ideally

1) it must actually be carried out (one must not be satisfied with behavioral intentions);
2) there must be a certain cost attached to it;
3) it must involve the same action identification as the final request;
4) no financial compensation should be attached to the action and, generally speaking, no promise of reward should be made.

In short, the preparatory action must be carried out in a context of commitment: free choice, public nature of the action, consequences of the action [6], i.e. in conditions such that subjects are able to explain the action by internal factors (their convictions, their values…), rather than by external factors (pressures inherent to the situation, promises of reward or threat of punishment).

We would like to exemplify how we recently called upon the binding communication paradigm to promote environmentally-friendly values, and more importantly, environmentally-friendly behavior.

Illustrations:
four studies carried out in the south of France

Study 1.
Promoting environmentally-friendly behavior in 9-10-year-old schoolchildren and their parents

The first study [13] was carried out in 11 primary schools within the "Académie des Alpes-Maritimes" (a French regional school authority). It was conducted at the request of the Service of the Environment and Energy of the Provence-Alpes-Côtes d'Azur administrative region within the framework of the European project ALTENER. The aim of this project, which took place during the 2002-2003 school year, was to encourage 9 and 10-year-old schoolchildren and their parents to develop environmentally-friendly behavior. 700 families along with 28 teachers were involved.

Throughout the course of the weeks, the schoolchildren carried out four main preparatory actions. The first preparatory action was to determine what the environmentally-friendly and energy-saving "good practices" and "not so good practices" in their school were. In a second preparatory action the children were asked to do the same at home by taking notes of family habits that could be changed without causing much inconvenience. The third preparatory action involved parents who were asked to help their child fill in a lengthy questionary about energy savings at home (preparatory action for the parents). In the fourth preparatory action, the families were asked to put a sticker in favor of the preservation of the environment on the home fridge.

At the end of the school year, each child and then each family was encouraged to make a public and written commitment to change at least one or two of their habits, for example for the children: to take a shower instead of a bath and for the parents: to leave the car at home when traveling short distances or to switch off the sleep mode on the television set. These commitments were made more official through the signing of two forms: the child signed one in the classroom, and the child and the family jointly signed one at home. A big exhibition was organized at the end of the school year. The exhibition was the opportunity to show the families the projects in favor of the protection of the environment and of energy savings (posters, films, pictures, CD-ROMs…) developed by the children during the school year. A certificate signed by the President of the Region, by the Inspector of Schools and by the teacher was presented to the families during the exhibition.

The conclusions are very positive. A vast majority of children and their parents (100 % in some classes), made a written pledge to carry out specific actions likely to decrease energy consumption (for example always switch off the sleep mode on the television set, etc.). In addition, the dynamic set in motion by this approach led to specific actions such as: switching from ordinary bulbs to low energy bulbs in some schools, or installing paper recycling bins in other schools, etc. Finally, some students sent a letter to local authorities to request, for instance, that light timers be installed in school corridors or that safety be improved along the pedestrian walks leading to the school. These initiatives enabled the school children to experience responsible citizenship first hand and to integrate the desired citizen values.

Study 2. Promoting ecocitizenship in a town

The purpose of the second study [14] was to promote ecocitizenship in the context of a whole town. It was also conducted at the request of the Service of the Environment and Energy of the Provence-Alpes-Côtes d'Azur. The study was carried out in a mid-size town (experimental town). For control purposes, a "classic" communication campaign (posters, brochures, stickers, etc.) was launched in parallel in a comparable town (control town). The same communication support tools were used in both the experimental and the control towns, but in addition, as in study 1, the local residents were asked to carry out preparatory actions and to make commitments. A collective of "relays" was set up on a voluntary basis for this purpose. This group was made up of public authorities, heads of local institutions, teachers, association activity leaders, and shop owners. Each relay was in charge of initiating a specific eco-friendly action involving as many people as possible from his or her close environment (schools, outdoor centers, youth clubs and art centers, sports clubs, tenant and landlord associations, etc.). Their actions, which were in fact preparatory actions, were made public during a Special Events Day − a significant preparatory action − so that everyone could know and see what the others had concretely done for the preservation of the environment. Different events (exhibitions, public debates with local authorities, etc) were organized on this Special Events Day, which took place on a Sunday. But first and foremost, this represented an opportunity of securing concrete commitments from the residents as young students asked them and their families to sign a commitment form. Parents and children could choose from a list of ten possible commitments (for example: take a shower instead of a bath, reduce driving speed by 10 km/h, purchase low energy light bulbs, etc.)

Each signed commitment form was symbolized by a sun icon which was immediately attached to a big net installed on Town Hall Square. A glimpse at the net enabled to follow the progression of the number of commitments made throughout the day. More than 500 commitment forms were signed in that single day. It seems that the action had a real impact on behavior. Indeed, during the year the study took place and compared to the previous year, average consumption per annum for each household increased less (6 %) than in the control town (14 %).

And there is more: other signs point to the fact that a new and – hopefully – sustainable dynamic may be in the making. The collective of "relays" wishes to pursue the operation. They perceive the work accomplished as a starting point rather than a final outcome. And even Town Hall has decided to pitch in by, on the one hand, subsidizing training modules for local artisans (in particular heating

specialists) who want to improve their professional expertise through better control of energy consumption, and on the other hand, making the collective permanent and encouraging its initiatives. Since then, the collective has been setting up events on a yearly basis to develop awareness about energy savings and the protection of the environment. It therefore seems that the operation has triggered off a dynamic most likely to sustain itself.

Study 3. Promoting ecocitizenship along the seacoast

The third study [15] was carried out along the Mediterranean seacost (French Riviera). It was conducted at the request of the Service of the Environment and Energy of the Provence-Alpes-Côtes d'Azur administrative region and of the Environment and Energy Control Agency. This time, the aim was to promote ecocitizenship among sea users (sailors, sea professionals…). The study was carried out within the framework of a collaboration between the Laboratory of Social Psychology of the University of Provence and the "Ecogestes" collective, made up of 16 organizations practicing environment education, that is nearly 50 "sea ambassadors" going to meet users (particularly sailors) directly at sea. The study goal was precisely to improve the intervention plan used by the ambassadors to encourage sea users to modify some of their behaviors so as to preserve the Mediterranean coast.

In practical terms, when they were approached by the ambassadors, the sea users were first led to accept an immediate interview of about twenty minutes on the theme of sea preservation (first preparatory action). Within the framework of this interview, the sea users received information and advices linked to the sea preservation. Their active participation was sought during the whole interview. For example, they were asked for their opinion on the most relevant advices to give to other sea users (second preparatory action). At the end of the interview, the sea users were invited to accept the presentation of a booklet (third preparatory action). This booklet, free, comprised information about sea faun and sea flora and advices to preserve the Mediterranean Sea. As in the first two studies, the sea users were eventually invited to sign a commitment form. They could choose from a list of behaviors those they committed themselves to adopt from now on at sea, for example, to anchor their boat in the sand rather than in the Posidony seagrass bed, to use natural soaps, or to use detergents including an ecolabel. At last, the sea users could put on their boat, if they wanted it, the Ecogeste campaign pennant, so as to serve as an example in terms of environment preservation (reinforcement of commitment via the public characteristic of the action).

During summer, more than 5000 sea users were approached. The intervention procedure used was such that almost all of them accepted, at the end of the interview, to sign the commitment form, thus committing themselves to modify one or more of their behaviors.

In order to assess the intervention impact, the ambassadors got in contact again with some sea users "committed" during the summer season. These ones were easily spotted thanks to the pennant floating on their boat. Within the framework of a new interview, the ambassadors tested their knowledge about the sea environment and about proper behaviors to adopt to work for its preservation. They also collected, by direct observation, pieces of information about actual behaviors on board (anchorage, type of soap or type of cleaning product).

What clearly emerged from this data collection is that committed sea users, compared to those who were not approached for the first interview (control condition), 1) had a better knowledge of the sea environment and the way to preserve it, and 2) had adopted more ecological behaviors on board: for example, they were significantly more numerous to use natural soap (53 % *vs* 39 %) or detergents including an ecolabel (56 % *vs* 24 %), or to anchor in the sand (75 % *vs* 60 %). Thus, the binding-communication plan used on the sea users enabled to result in the expected cognitive and behavioral effects.

In the three studies mentioned above, whether they were geared towards the promotion of ecocitizenship in school children and their families (study 1), in town residents (study 2) or along the seacoast (study 3), the subjects (children and adults) were led to carry out preparatory actions and to sign a commitment form. We must emphasize the fact that in all three instances, the subjects massively agreed to sign the commitment form. Indeed close to 90 % of those approached agreed to sign. There is good reason to be optimistic, bearing in mind the fact that a written commitment is generally kept [16].

The use of binding communication, as it has been conducted in studies 1, 2 and 3, does have however one "practical" drawback: ideally it entails several direct contacts with the people whose behavior one is trying to modify. Indeed it is thanks to these contacts that the canvasser(s) secure(s) preparatory actions first and commitments later on. In a broader sense, these contacts initiate social dynamics (collective ambition, shared values) and promote genuine education on environmental issues (knowledge transfer, distribution of brochures, advice and recommendations, etc.)

Study 4. Promoting litter recycling on a highway rest area

The objective of a fourth study [17] was to determine if it was at all possible to use a binding communication procedure in an efficient way without any contact whatsoever with the subjects (hence without the education phase about the environment), and without having the subject sign a commitment form. The study was carried out on a highway rest area and its purpose was to encourage motorists to recycle their litter. There was no direct interaction with motorists, a media plan (audio messages, posters, etc.) was used instead. The first major decision was to remove the traditional litter bins. The second decision entailed dividing by two the number of spots where motorists could discard their litter so as to secure from them a preparatory action (i.e. to carry their

litter on a distance of several meters) without any contact with them. As recycling was available on each of these spots, the customers who had made the effort of carrying their litter had a decision to make: either recycle (recycle containers were available) or discard without recycling (traditional bins). A sign was placed in full view just above the containers. One could read "I RECYCLE" in bold and "For the planet, for my children and for my children's children" in small print. The motorists were thus encouraged to make the expected eco-friendly choice by conveying the idea that their action has a higher overall purpose [18]. This way of doing things enabled to multiply by almost three the tons of packages recycled in a year on this particular highway rest area.

Conclusion

The four studies presented here have one thing in common: they are based on the securing of preparatory action(s). This is actually quite a feat as it entails changing the "target's" status from mere receiver – as it is often the case in more traditional communication campaigns – to actor. These preparatory actions have a twofold advantage: 1) they will increase the probability of achieving the expected eco-friendly behaviors; 2) they will make the subjects more aware of the educational or persuasive pro-environment messages they may later encounter.

We are, of course, still convinced that the main questions to be answered in the context of an action of communication remain as follows: "What is the right information to convey?", "What are the best arguments to put forth?", "What are the best channels, tools, supports, and media?", "What are the most relevant practices with regard to knowledge transfer?", etc. To these, we would add another question which we deem as important as the others: "What are the preparatory actions that we must obtain from the people whose collaboration we are seeking?" By conferring to the target the status of actor, the answer to this question will therefore separate the "binding" communication approach from a more "traditional" approach.

References

1. Peterson A.V., Kealey K.A., Mann S.L., Marek P.M., Sarason I.G. Hutchinson Smoking Prevention Project: long-term randomized trial in school-based tobacco use prevention-results on smoking // Journal of the National Cancer Institute. 2000. No. 92. P. 1979-1991.

2. Bernard F., Joule R.-V. Lien, sens et action: vers une communication engageante // Communication & Organisation. 2004. No. 24. P. 333-345.

3. Bernard F., Joule R.-V. Le pluralisme méthodologique en Sciences de l'Information et de la Communication à l'épreuve de la communication engageante // Questions de communication. 2005. No. 7. P. 185-207.

4. Joule R.-V., Girandola F., Bernard F. How can people be induced to willingly change their behavior? The path from persuasive communication to committing communication // Social & Personality Psychology Compass. In press.

5. Kiesler C.A. The psychology of commitment. Experiments liking behavior to belief. New York: Academic Press, 1971.

6. Joule R.-V., Beauvois J.L. La soumission librement consentie. Paris: Presses Universitaires de France, 1998.

7. Joule R.-V., Beauvois J.L. Petit traité de manipulation à l'usage des honnêtes gens (nouvelle version). Grenoble: Presses Universitaires de Grenoble, 2002.

8. Lewin K. Group decision and social change. In T.M. Newcomb, E.L. Hartley (Eds.), Readings in social psychology. New York: Henry Holt and Company, 1947. P. 330-344.

9. Freedman J.L., Fraser S.C. Compliance without pressure: the foot-in-the-door technique // Journal of Personality and Social Psychology. 1966. No. 4. P. 195-202.

10. Beaman A.L., Cole C.M., Preston M., Klentz B., Steblay N.M. Fifteen years of foot-in-the-door research: a meta-analysis // Personality and Social Psychology Bulletin. 1983. No. 9. P. 181-196.

11. Dillard J.P., Hunter J.E., Burgoon M. Sequential-request persuasive strategies / Meta-analysis of foot-in-the-door and door-in-the-face // Human Communication Research. 1985. No. 10. P. 461-488.

12. Burger J.M. The foot-in-the-door compliance procedure: a multiple-process analysis and review // Personality and Social Psychology Review. 1999. No. 3. P. 303-325.

13. Joule R.-V. What is the role of energy-education in changing habits? // European congress "Energy education: role, action and tools. European expériences". Bruxelles: 12 March 2004.

14. Joule R.-V., Py J., Bernard F. Qui dit quoi, à qui, en lui faisant faire quoi? Vers une communication engageante. Dans M. Bromberg et A. Trognon (Eds.), Psychologie sociale et communication. Paris: Dunod, 2004. P. 205-218.

15. Joule R.-V., Masclef C., Jarmasson J. Communication engageante et préservation de la méditérranée: Comment promouvoir de nouveaux comportements de la part des plaisanciers? // 2ème Colloque international pluridisciplinaire Eco-citoyenneté: Quels apports des sciences humaines et sociales dans le développement de l'écocitoyenneté et quelles applications dans les domaines touchant à l'environnement. Marseille: 9-10 Novembre 2006.

16. Girandola F., Roussiau N. L'engagement comme source de modifications à long terme // Les Cahiers internationaux de psychologie sociale. 2003. No. 57. P. 83-101.

17. Blanchard G., Joule R.-V. La communication engageante au service du tri des déchets sur les aires d'autoroutes: une expérience-pilote dans le sud de la France // 2ème Colloque international pluridisciplinaire Eco-citoyenneté: Quels apports des sciences humaines et sociales dans le développement de l'écocitoyenneté et quelles applications dans les domaines touchant à l'environnement. Marseille: 9-10 Novembre 2006.

18. Vallacher R.R., Wegner D.M. A theory of action identification. New Jersey: Lawrence Erlbaum, 1985.

ADSORPTION OF DYES YELLOW BEMACID CM-3R AND RED BEMACID CL-BN200 BY A SODIC BENTONITE

N. Ouslimani, M. Maallem

University M'hamed Bougara Boumerdes − Algeria
Faculty of Science of Engineer
E-mail: ouslimanibouberdes@yahoo.fr, maallem_mad@yahoo,fr

Received: 29 Sept 2007; accepted: 31 Oct 2007

The rejections of textile industry are strongly charged in various dyes, which imposes their treatments. The most current method is to adsorb them on solids having specific large surface, for example clays. For our study we retained a local bentonite, available in quantity, which we purified and transformed in sodic form for the adsorption of two acid dyes provided by BEZEMA.
The obtained results show that the output of adsorption is a function of the structure of the dye and of the pH of the medium.

Keywords: ecology of water resources, structural materials, adsorption, bentonite, sodic, dyes

Nassira Ouslimani

Organization: Doctorate.
Education: Teaching to M'Hamed Bougara University of Boumerdes, Facultyof Science of Engineer, Department Genius of the Industrial Processes.
Experience: Scientific research projects, Member of the Laboratory of treatment and working of fibrous polymers.
Main range of scientific interests: textile matters and materials, quality control of finished fabrics, chemistry of the dyes, chemical technology of the textile matters, environment.

Madani Maallem

Organization: Vice-senior in charge with scientific research and the relations foreign with the Faculty of Science of the Engineer of the University of Boumerdes. Lecturer.
Education: Enquiring teacher in Université Me Hamed Bougara of Boumerdes at the Department Genius of the Industrial Processes.
Experience: Framing of Research tasks: Projects of End of Studies, Memories of Magister, Theses of Doctorate of Algerian State, University Research projects.
Main range of scientific interests: textile matters and materials, quality controlfinished fabrics, chemistry of the dyes, chemical technology of the textile matters, physical chemistry of polymers, production of manmade fibers, environment.
Publications: Доклады Академий Наук, Том 313, No. 4, 1990, Доклады Академий Наук, Том 315, No. 5, 1990.

Introduction

The presence of dyes in the effluents of manufacturing industries makes the treatment difficult and expensive [1]. This colouring is caused by the dye which is not fixed on textile fibre [2]. Indeed, the types of dyes used are eliminated with difficulty because of their chemical properties which confer to them a stability with respect to oxidants or make them not easily biodegradable because of their aromatic nucleus [3].
The colour makes water unsuitable to the domestic uses and reduces the transmittance of the light thus limiting the growth of the watery plants [4].

The soluble dyes such as the acid dyes are responsible for delicate problems because the traditional treatments of water having been used in the baths as dyeing do not ensure a satisfactory purification [5].
For this purpose we were interested in the use of a montmorillonite of purified MAGHNIA and transform in sodic form. Because of the large smoothness of the particles, in other words with its useful large surface it is equipped with capacity inflating considerable 5 to 30 times compared to its initial volume.
Not forming part of the structure itself and keeping a certain mobility the sodium ions can be also exchanged. They modify also the distance between the layers and thus the reticular distance.

Matters and materials use

Bentonite

The bentonite used is a local clay which has the advantage of being available and to display after modification adsorbent properties comparable with the products of reputation such as mow activated carbon.

Clay is characterized by its permeability, its thermal properties, and its behavior with respect to the diffusion of the radio operator elements [6].

Clays can acquire new properties by various modifications which can open ways of application above suspicion.

The selected bentonite is light; that can be explained by a concentration raised out of carbonates and alkaline. This is confirmed by the pH of 7.

The dyes

The dyes used are:

– Red BEMACID CL-BN 200;

– Yellow BEMACID CM.3R.

The determination of the concentrations in dyes are determined by the absorptance using a standard spectrophotometer UV UNICAM in the wavelength interval 400 to 700 nm.

Characteristics of bentonite

1 Determination of the chemical composition by fluorescence X. Chemical composition consigned to Table 1 by X-ray fluorescence using a spectrophotometer with x-ray fluorescence (PHILIPS MAGIX PW reveals its character montmoriollonite ($SiO_2/Al_2O_3 = 3.83$).

This characteristic makes it possible to classify it among inflating clays, having properties very important to use it as adsorbent material.

Table 1

The chemical composition of sodic bentonite

Oxides	SiO_2	Al_2O_3	Fe_2O_3	CaO	MgO	SO_3	K_2O	Na_2O	Loss on the ignition
%	67.24	17.53	1.38	0.30	2.74	0.09	0.67	4.8	5.10

Results

Influence of the time of contact

The adsorption of the dyes is rather high: this is because of the hydration of the sodium cation which causes the dispersion of the bentonite [7] thus facilitating the penetration of water in interfoliaceous space and supporting the phenomenon of exchange between bentonite and the coloured solution (Fig. 1).

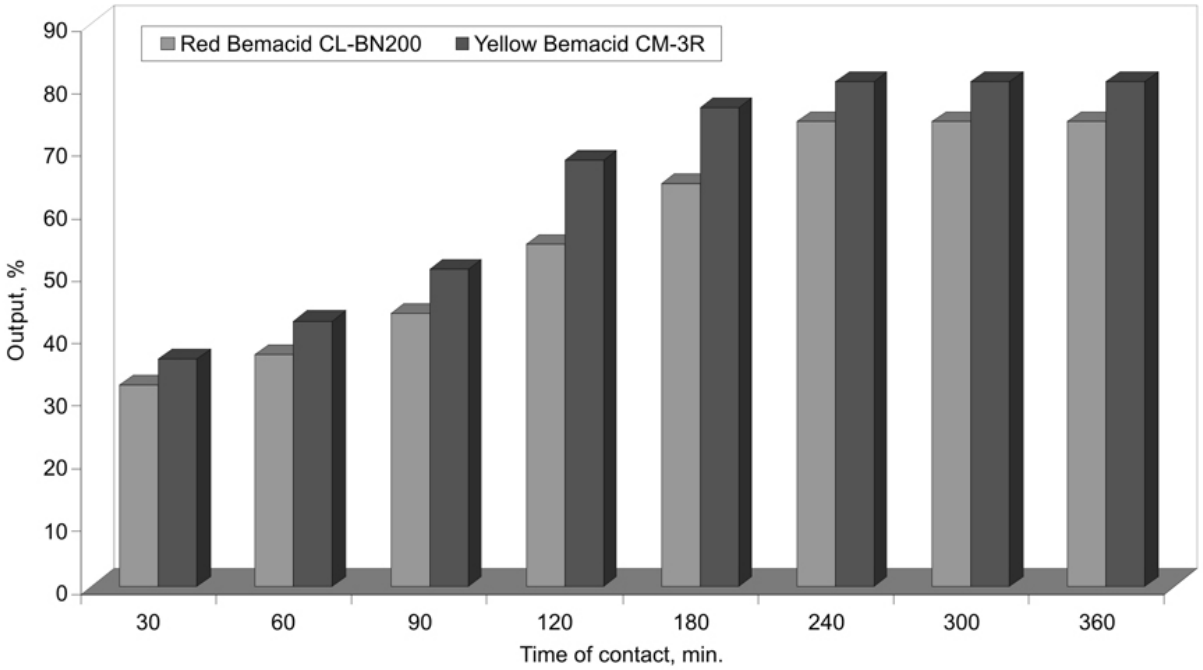

Fig. 1. *Influence of time of contact*

International Scientific Journal for Alternative Energy and Ecology № 6 (62) 2008

Influence of pH

With the pH 2 the quantity of the adsorbed dye is high, a fact due to the influence of the H+ cation on miscelle of the sodic bentonite, which causes the attraction of the dye negatively charged (Fig. 2).

Influence of the temperature

When the temperature increases the quantity of adsorbed dye decreases, which allows us to suppose that one is in the presence of an exothermic phenomenon [8] (Fig. 3).

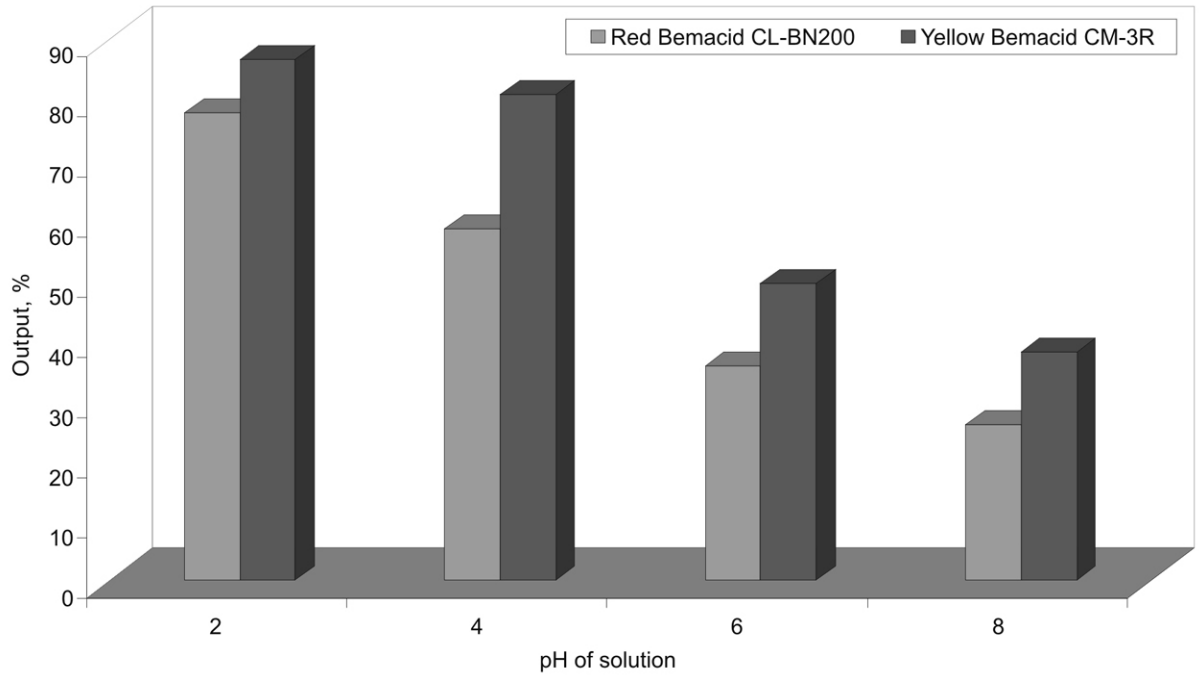

Fig. 2. *Influence of pH*

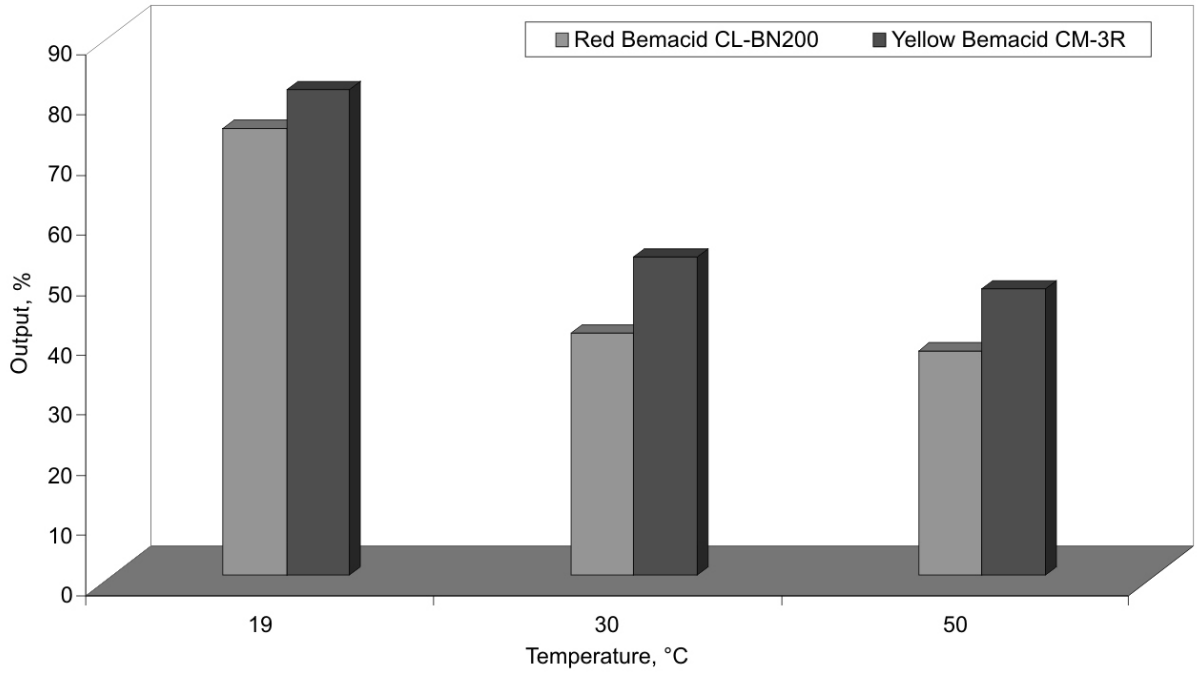

Fig. 3. *Influence of the temperature*

Influence of the concentration *(Fig. 4, 5)*

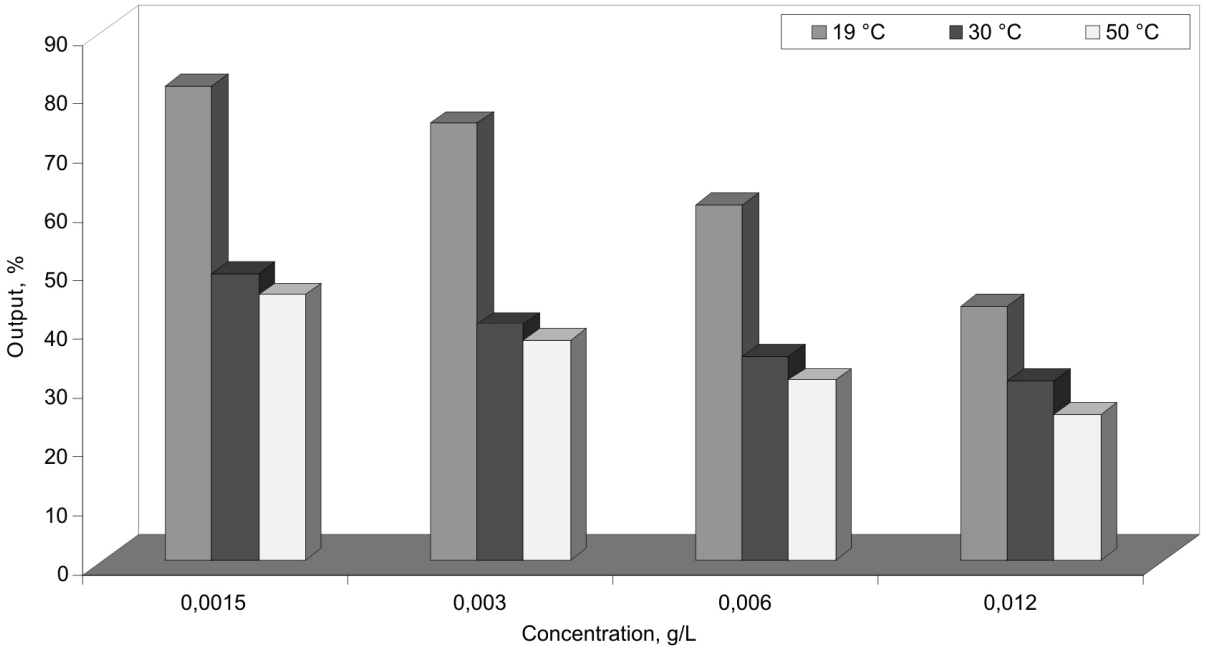

Fig. 4. *Influence of the concentration of red Bemacid CL-BN200*

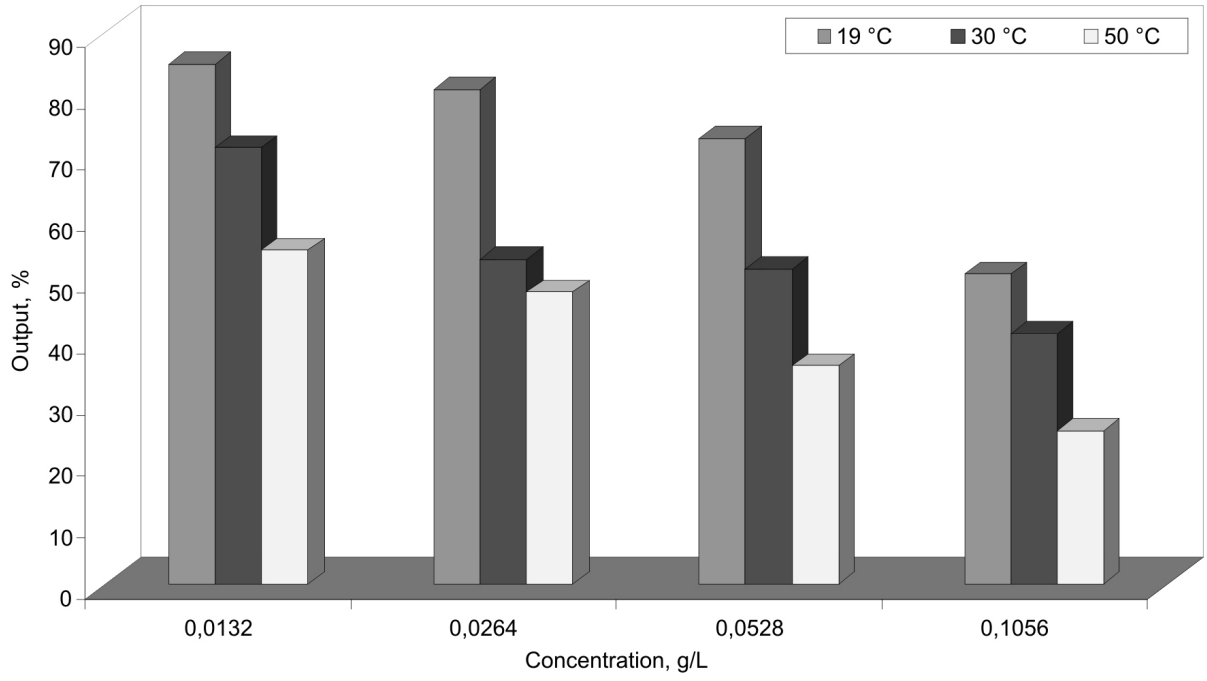

Fig. 5. *Influence of the concentration of red Bemacid CML-3R*

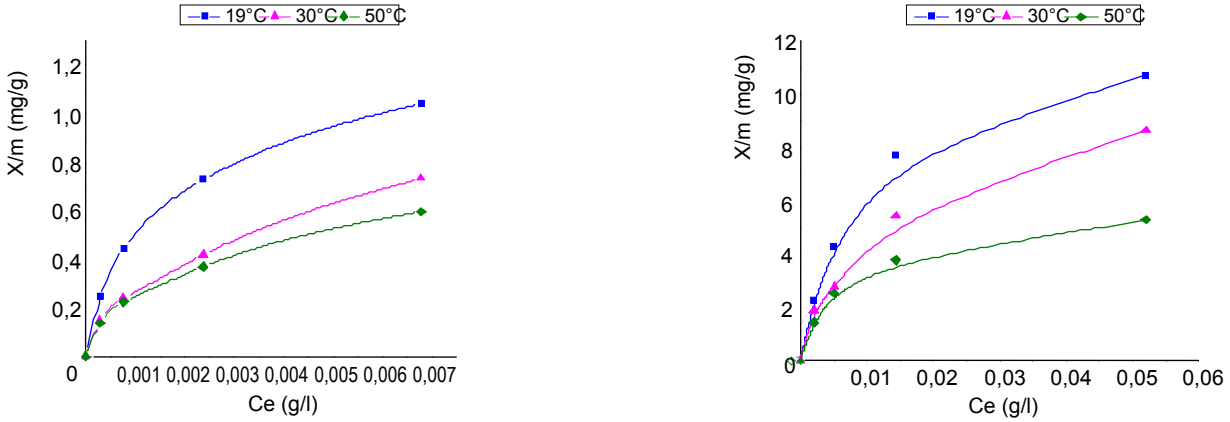

Fig.6. *Isotherms of adsorption of red Bemacid CL-BN200 and Yellow Bemacid CM-3R*

Conclusion

We notice that some parameters giving good performances are:

– temperature 19 °C;

– time 240 min;

– pH 2.

However the yellow dye gives better results; this can be due to the structure of the dye and the difference of solubilities which are of 25 g/l for the red dye and 20 g/l for the yellow dye.

We can say that each dye of the same class can have a different behavior.

This process appears interesting because the treatment by coagulation-floculation gives poor outputs due to the bad quality of the floc which elutriates badly even after addition of coagulant [9].

References

1. Naija A. Action catalytique des argiles type smectite dans le cas des réactions biochimiques,Université de Haute Alsace, 1988.

2. Kramar L. Eviter la pollution de l'eau industrie textile. No. 1266, Juin 1965.

3. Nozet H. Textiles chimiques. Fibres modernes, Eyrolles, Paris, 1976.

4. Malewska K., Nowart T., Winniki J. Effect of flow conditions on ultrafiltration efficieng of dye solutions and texil effluent, 1989.

5. Lemonier M.L., Viguier M. Les textiles et leur entretien, Edition Jaques Lanor , Paris, 1978.

6. Smat A. Contribution à l'étude des transferts de chaleur et de masse dans les matériaux de remplissage d'un stockage de déchets à haute activité, Thèse de doctorat, Université de Paris.

7. Chamely. Clay sedimentolgy, Springer-Verlag, 1989.

8. Avom J., Ketcha J., Badcam M., Matip M.R.L., Gerain P. Adsorption isotherme de l'acide acetique par les charbons d'origine végétale // African Jurnal of Science and technology (AJST) Science and Engineering Series. Vol. 2, No. 2. P. 1-7.

9. Marmagne O., Coste C., Jacquart J.C., Bailli A., Thieblin E. // Industrie textile. No. 1278, Juillet -Aout 1996.

CENTER FOR DEVELOPMENT OF RENEWABLE ENERGY (CDER)

Head: M. Belhamel*
Author: L. Aiche-Hamane**

Route de l'observatoire, BP62 Bouzaréah, 16340, Alger, Algérie.
Tel.: 213 21 90 15 03, 213 21 90 15 60
*E-mail: mbelhamel@cder.dz, ** E-mail: l.aichehamane@cder.dz, Internet site: http://www.cder,dz

Brief presentation

The Centre for Development of Renewable Energy (CDER) was founded in March 1988 by Presidential Decree 88/60. It is a scientific and technological public entity, supervised by the Ministry of higher education and scientific research.
Its main goal is the promotion and the development of renewable energy applications at a national and international level, as well as the protection of the environment and sustainable development.
The organisational structure of CDER is made up of four divisions: Division of Bio-Energy & Environment, Division of Thermal Solar & Geothermal Energy, Division of Wind Energy Systems and Division of Photovoltaic Energy.
Three units are also attached to the CDER: Unit of Development of solar equipment, Unit of Renewable Energy in Sahara desert at Adrar and Unit of Applied Research in Renewable Energy at Ghardaia..
CDER is actively involved in the field of hydrogen as an energy carrier, considering hydrogen as a medium that will enable the storage of excess energy produced from renewable energy sources that will allow an increase of these sources penetration in the electricity and transport sectors.
In this context, CDER is working for the creation of hydrogen research unit.


Pyranomètre


Wind turbine


Solar water heating system


Photovoltaic system

Structure of the Center for Development of Renewable Energy

CDER is composed of four divisions and each division contains 4 groups as following:

− Division of Bio-Energy & Environment carries out applied research for the development of biotechnological processes which are viable and environment-friendly such as hydrogen technologies, production of hydrogen from wind energy, fuel cell...	− Division of Thermal Solar & Geothermal Energy is carries out applied research in the field of thermodynamics, solar thermal and geothermal.
− Division of Wind Energy Systems works on the wind resource assessment, analysis and design of wind system turbines and hybrid wind-diesel systems.	− Division of Photovoltaic Energy is carries out applied research on photovoltaic systems and power electronic devices.

Activities

− In the framework of its mission, CDER organizes and participates in technical and scientific seminars, educational programs, specialized training courses, meetings, etc.
CDER publishes a scientific international journal: **la Revue des Energies Renouvelables** ISSN 1112-2242 and an internal publication, **Le Bulletin des Energies Renouvelables.**
− In the field of hydrogen activities:
− CDER organized the First International Workshop on Hydrogen Energy vector from a renewable origin Algiers, the city of sciences on June 21-23, 2005 (WIH2005).
− CDER is involved in the giant hydrogen exporting project of solar hydrogen from Maghreb to Europe (June 2006)

LABORATOIRE DE PHYSIQUE DU BATIMENT ET DES SYSTEMES - EA4076
FACULTE SCIENCES DE L'HOMME ET DE L'ENVIRONNEMENT
UNIVERSITE DE LA REUNION
(LABORATORY OF BUILDING AND SYSTEMS PHYSICS, UNIVERSITY OF REUNION ISLAND)

Head : François GARDE
Author (*): Jean Philippe PRAENE

117 rue du General Ailleret – 97430 Tampon – REUNION
Tel. +262 692 23 34 11, Fax. +262 262 57 95 41
*E-mail: praene@univ-reunion.fr
http://lpbs.univ-reunion.fr

Brief presentation

LPBS is a French research laboratory specialized in the study of thermal comfort in building. Renewable energy, reduction of energy needs and environmental engineering applied to building are the main lines of research. The activities cover several aspects such as modeling, experiment and validation, fundamental and applied approach is developed.

UNIVERSITE DE LA REUNION
Laboratoire de Physique du Bâtiment et des Systèmes

General description

LPBS exists since the end of 2005. Our initial field of research is modeling and simulation of buildings thermal behavior and the associated components (complex systems, walls etc...). The principal directions taken were those of the development of code and tools for both research and design use.

Through industrial contracts, applications on a large scale of our work were born, in the form of a label of construction applicable to the whole of the DOM (French overseas department). Since its creation, approximately 800 residences were built compared to the regulations enacted following a contract of simulations on residences standard, in partnership with the direction of EDF Departments overseas.

Structure of the laboratory

Head: Professor François Garde (garde@univ-reunion.fr)
Members: 12 (4 Pr., 1 Associate Pr., 7 Lecturers), 3 Researchers, 9 Associate researchers, 13 PhD students.

Research Teams

The laboratory is structured in 4 directions:
− **Pôle PhyBat** "Building Physics"
Dr. Frédéric Miranville (Frederic.Miranville@univ-reunion.fr)
− **Pôle SEERAB** "Renewable Energy and Energetic system applied to Building"
Dr. Franck Lucas (lucas@univ-reunion.fr)
− **Pôle GEAB** "Environnmental engineering applied to building"
Pr. Jean-Claude Gatina (gatina@univ-reunion.fr)
− **Pôle OMAB** "Tools and method applied to building simulation"
Dr. HDR Philippe Lauret (lauret@univ-reunion.fr)

Activities, actions, results, projects

Activities

− System Modeling.
− Building Physics.
− Renewable Energy: Photovoltaic, solar system (cooling, heating...).
− Analysis and control tools development.
− Environmental Science, Biomass.
− System experiment under laboratory and natural conditions.

Results and Projects

− Sustainable building 2002-2005 (330 k€).
− ADIBE² 2006-2009 (200 k€).
− Renewable Energy pilot site (640 k€).
− Positive energy building (2 M€).
− ANR PREBAT 2005: "Photovoltaic" CEA (70 k€).
− ANR PREBAT 2006 ORASOL: Solar cooling system optimization (1351 k€).
− ANR PREBAT 2006 ENERPOS: Development of modeling method and design of positive energy building (533 k€).
− ANR PREBAT 2006 DYNASIMUL: Development of a common simulation platform (1800 k€).
− MEER-TAAF, financement ministère de l'Outre mer: Renewable energy in antarctic austral French territory (30 k€).
− RAFSOL: solar cooling research program (493 k€).
− VEOLIA: solar drying research program (56 k€).
− INCIVOL: Incineration of waste (36 k€).

Experiment Setup

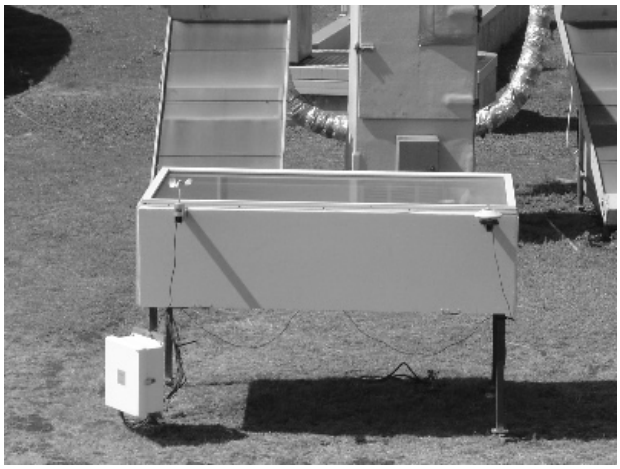

Solar sludge dryer

Mixed solar dryer with air solar collectors

Solar collectors test bench according EN 12975-2

Collaborations, national and international

− LEPTAB, Université de La Rochelle, INSA Lyon, LEMTA Nancy, Université de Cortet, LOCIE Chambéry;
− Ecole Polytechnique de Montréal, Université de Liège;
− Centre for Building Performance Research, Wellington, New Zealand;
− EDF Réunion, Conseil Régional, Agence Régionale de l'Energie Réunion ARER, ADEME, EDF R&D.
− INES (Institut National de l'Energie Solaire), CNRS;
− CEA Cadarache;
− Agence Internationale de l'Energie (IEA);
− Professionnels du Bâtiment, Architectes, Bureaux d'études, Industriels ENR;
− Université de Perpignan;
− Université Malgaches (Antananarivo, Mahajunga, Fianarantsu).

References

1. Tourrand C., Boyer H., Chabriat J.P. Caractérisation thermique de parois de construction par des mesures en site reel. Revue Générale de Thermique, No. 387, mars 1994.
2. Boyer H., Chabriat J.P., Grondin Perez B., Tourrand C., Brau J. Thermal building simulation and computer generation of nodal models // Building and Environment. 1996. Vol. 31, No. 3. P. 207-214.
3. Boyer H., Garde F., Gatina J.C., Brau J. A multi model approach of thermal building simulation for design and research purposes // Energy and Buildings, 28 (1998), 1. P. 71-79.
4. Garde F., Boyer H., Gatina J.C. Demand side management in tropical island buildings. Elaboration of global quality standards for natural and low energy cooling in buildings // Building and Environment, 34 (1998), 1. P. 71-84.
5. Boyer H., Lauret A.P., Adelard L., Mara T.A. Building ventilation: a pressure airflow model computer

generation and elements of validation // Energy and Buildings, 29 (1999). P. 283-292.
6. Adelard L., Boyer H., Garde F., Gatina J.C. A detailled weather data generator for building simulation // Energy and Buildings, 31, 1 (1999). P. 75-88.
7. Lauret A.P., Boyer H., Gatina J.C. Hybrid modelling of the sucrose cristal growth rate // International Journal of Modelling and Simulation, Vol. 21, 1(2001). P. 23-29.
8. Lauret A.P., Boyer H., Gatina J.C. Hybrid modelling of the sugar boiling process // Accepté à Control Engineering Practice, August 1999.
9. Garde F., Boyer H., Celaire R. Conception thermique en climat tropical humide, présentation du label ECODOM // Accepté à Annales du Bâtiment et des Travaux Publics, Nov. 1999.
10. Garde F., Lucas F., Boyer H., Brau J. Multiple model approach of a residential heat pump for integration in building thermal simulation code and comparison with experimental results // ASHRAE Transactions, (American Society of Heating and Refrigeration Engineers), Atlanta Winter meeting, January 2001.
11. Mara T.A., Boyer H., Garde F. 2002. Parametric sensitivity analysis in thermal building using a new method based on spectral analysis. Manuscript accepté à Transactions of ASME (American Society of Mechanical Engineers) // International Journal of Solar Energy Engineering, December 2001.
12. Mara T.A., Garde F., Boyer H., Mamode M. Empirical Validation of the Thermal Model of a Passive Solar Cell test // Accepté à paraître à Energy and Buildings, (2000).
13. Lauret A.J.P., Mara T.A., Boyer H., Adelard L., Garde F. A validation methodology aid for improving a thermal building model: case of diffuse radiation accounting in a tropical climate // Accepté à paraître à Energy and Buildings, (2000).
14. Lucas F., Adelard L., Garde F., Boyer H. Study of moisture in buildings for hot humid climates. Manuscript accepté à Energy and Buildings, September 2001.
15. Lauret A.J.P., Mara T.A., Boyer H., Adelard L., Garde F. A validation methodology aid for improving a thermal building model : how to account for diffuse radiation in a tropical climate // Energy and Buildings 33 (2001). P. 711-718.
16. Garde F., Lauret A.P., Bastide A., Mara T., Lucas F. Development of a nondimensional model for estimating the cooling capacity and electric consumption of single speed split-systems incorporated in a building thermal simulation program. Accepté à ASHRAE Transactions (American Society of Heating Refrigerating and Air Conditioning Engineers), June 2002.
17. Garde-Bentaleb F., Boyer H., Miranville F., Depecker P. Bringing scientific knowledge from research to the professional fields : the case of the thermal and airflow design of buildings under tropical climates // Energy and Buildings, 34 (5): 511-521.
18. Garde F., Boyer H., Célaire R. Bringing simulation to implementation: Presentation of a global approach in the design of passive solar buildings under humid tropical climates // Solar Energy 71 (2): 109-120.
19. Adelard L., Pignolet Tardan F., Lauret P., Mara T., Garde F., Boyer H. Sky temperature modelling for thermal building application // Renewable Energy, 15 (1998). P. 418-430. Présenté au congrès World Renewable Energy Congress, 1998, Italy.
20. Lucas F., Mara T., Garde F., Boyer H. A comparison between CODYRUN and TRNSYS, simulation codes for thermal building behaviour // Renewable Energy, 15 (1998), Part. II. P. 1624-1633. Présenté au congrès World Renewable Energy Congress, 1998, Italy.
21. Mara T.A., Boyer H., Garde F. Parametric Sensitivity Analysis of a Thermal Test Cell Model Using Spectral Analysis // ASME (American Society of Mechanical Engineers) Journal of JSEE (Journal of Solar Energy Engineering).
22. Soubdhan T., Mara T.A., Boyer H., Younes A. Use of BESTEST procedure to improve a building thermal simulation program // Renewable Energy, Part III. P. 1800-1803. Présenté au congrès World Renewable Energy Congress, 2000, U.K.
23. Miranville F., Fock E., Garde F., Herve P. Experimental study of the thermal performances of a composite roof including a reflective insulation material under tropical humid climatic conditions // Renewable Energy, Part I. P. 586-589. Présenté au congrès World Renewable Energy Congress, 2000, U.K.
24. Fock E., Garde F., Lauret P., Gatina J. Artificial neural networks for the prediction of cooling loads of HVAC systems: a case study under tropicale climate // Renewable Energy, Part I. P. 661-664. Présenté au congrès World Renewable Energy Congress, 2000, U.K.

LABORATOIRE D'ENERGETIQUE CARNOT (CARNOT LABORATORY OF ENERGETICS)

Head: Jean M'Boliguipa, PhD
Author: Jean M'Boliguipa

Avenue des Martyrs, Bangui, BP 908, Central African Republic
Phone: +236 75 03 48 43, Fax: +236 21 61 78 90
E-mail: jmboliguipa@yahoo.fr

Brief presentation

The Laboratoire d'Energétique Carnot is a research institution of the Physics Department of Bangui University. It was created in February 2007, and aims at animating a doctoral school in the field of applied physics, with particular interests on renewable energy and environmental problems.

Structure of the laboratory, different groups and their thematic directions

We have three groups in the laboratory:
− Applied Energetics (EA).
− Applied Mechanics (MA).
− Signal and Image Processing (TSI).

Activities, actions, results, projects

Fundamental research

Applied Energetics

− Conception, modeling, simulation and construction of devices for renewable energies (solar dryers, cookers, heaters, etc).
− Physico-chemical studies of african vegetal oils for use as biofuel, and particularly as biodiesel.

Applied Mechanics

− Interaction fluid–structure. Application in the liquid transportation (oil) in tubes.
− Control of solar radiation perturbations by clouds.

Signal and image processing

− Satellite image processing using linear and non-linear filtering methods, neural networks, and Bayes method.
− Comparative study of classical methods for image improvement and of attenuation methods.
− Image compression by attenuation and attenuation correction methods.
− Study of the forest degradation (Centrafrican region) by contours detection, and segmentation methods.

Applied research

Applied Energetics

− Work out of solar radiation map of Central African Republic.
− Conception and construction of solar devices for agriculture, health, mines, and usual life.
− Study of vegetal oils as energy sources.

Signal and image processing

− Restoration of old argentic images.
− Constitution of a bank of satellite images.

Projects

− Several projects in the frame of the improvement of artisanal transformation of food products using renewable energy devices *(submitted to AIRES-SUD/ IRD, TOTAL RCA, UNESCO, World Bank)*.
− Using antennas and network technology to reduce poverty in Central African Republic (with TWAS).

Collaborations, national and international, present and calls for collaborations

National

− French secondary school "Lycée Charles de Gaulle".
− Total Centrafrique.
− Laboratory of Biological Sciences for the Development (University of Bangui).
− Technological Institute of the University.

International

− University of Yaoundé1 (Cameroon).
− Université de Picardie Jules Verne (Amiens, France).
− Commissariat à l'Energie Atomique (France).
− University of Provence (Marseille, France).

Pedagogical activities in related fields

Master on Renewable energies

Head of the preparation: Dr. Luc Bara MARBOUA.

Professional bachelor in solar technology

Head of the preparation: Dr. Jean M'BOLIGUIPA.

CONTACTS

Directeur du Laboratoire d'Energétique Carnot (L.E.C.)
Département de Physique
Faculté des sciences – Université de Bangui, BP 908;
Tel: +236 21 61 50 08
GSM: +236 75 03 48 43
Email: jmboliguipa@yahoo.fr

TEAM OF FLOW AND TRANSFER MODELING (EMET)

Head: Pr. Mohamed NAÏMI

Sultan Moulay Slimane University, Faculty of Sciences and Technologies, Physics Department,
BP 523, Béni-Mellal, Morocco
Phone: (212) 23 48 51 12/22/82, Fax: (212) 23 48 52 01
E-mail: naimi@fstbm.ac.ma, naimima@yahoo.fr
internet site: http://www.fstbm.ac.ma

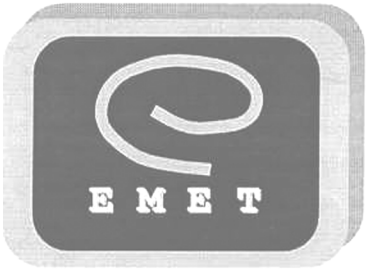

Brief presentation

The Team of Flow and Transfer Modeling (Equipe de Modélisation des Ecoulements et des Transferts, EMET) was created in January 2000 and officially accredited in January 2006. It belongs to the Faculty of Sciences and Technologies (FST) at the Sultan Moulay Slimane University (USMS) of Béni-Mellal (Morocco). 11 members make up the EMET, including 8 teachers researchers (permanent members) and 3 graduate students (nonpermanent members).

Research topics

The topics developed by the EMET are:
− Capillary and natural convections in non-Newtonian fluids;
− Natural, mixed and forced convection heat transfer with or without thermal radiation;
− Flows at low Reynolds number;− Double diffusion with or without Soret effect in porous and clear fluid media;
− Second order modeling of reactive turbulent flows.

Objectives

The industrial systems are often seats of complex flows. For a better optimization of these systems, the fluid mechanics proposes to study and to understand the physical phenomena governing these flows. Thus one is interested in transport of heat or/and mass, turbulence and combustion. These phenomena are not independent each other, but are coupled. In this respect, two approaches can be considered: the experimental approach for the diagnosis and measurements and the numerical calculation approach. This latter offers a double advantage, on the one hand it makes possible the detailed study of these industrial flows and this, by solving the governing equations, which presents a lower cost compared to the former, and on the other hand it informs about the quantities not yet accessible with measurements.
Within this framework, the EMET develops the topics above-mentioned.

Collaborations, national and international

Currently, the EMET is in more or less close collaborations with national (Laboratory of Fluids Mechanics and Energetics, Faculty of Sciences Semlalia, Cadi Ayyad University, Marrakesh, Morocco) and international (Institute for Aerospace Research, National Research Council, Ottawa, Ontario, Canada) scientific organizations. Otherwise, the EMET remains open to any relation with other teams or laboratories concerned with its research area.

Admission terms

To be accepted at the EMET, the candidate for a PhD must have a master's degree in fluid mechanics and transfer phenomena. Moreover, he must have sufficient knowledge of numerical analysis and computer programming.

Opening

The candidate, having obtained his PhD, can be recruited in higher degree teaching or in industrial environments finding interest in his formation.

Some recent scientific contributions

Just below some recent scientific contributions of the EMET.

1. Lamsaadi M., Naïmi M., Hasnaoui M., Bahlaoui A., Raji A. Multiple steady state solutions for natural convection in a tilted rectangular slot containing non-Newtonian power-law fluids and subjected to a transverse thermal gradient // Numerical Heat Transfer Part A. 2007. Vol. 51, No. 3, 4. P. 393-414.
2. Lamsaadi M., Naïmi M., Hasnaoui M., Mamou M., Bahlaoui A., Raji A. Parallel flow convection in a shallow horizontal cavity filled with non-Newtonian

power-law fluids and subjected to horizontal and vertical uniform heat fluxes // under press, Numerical Heat Transfer. Part A. 2007. Vol. 53.
3. Bahlaoui A., Raji A., Hasnaoui M., Lamsaadi M., Naïmi M. Mixed convection in a horizontal channel with emissive walls and partially heated from below // Numerical Heat Transfer. Part A. 2007. Vol. 51. P. 855-875.
4. Bahlaoui A., Raji A., Hasnaoui M., Lamsaadi M., Naïmi M. Coupled natural convection and radiation in a horizontal rectangular enclosure discretely heated from below // Numerical Heat Transfer. Part A. 2007. Vol. 52. P. 1027-1042.
5. Ben Richou A., Ambari A., Lebey M., Khalid Naciri J.K. Drag force on a circular cylinder midway between two parallel plates at *Re* << 1, Part 2: moving uniformly (numerical and experimental) // Chemical Engineering Science. 2004. Vol. 59, No.15, Part 2. P. 3215-3222.
6. Ben Richou A., Ambari A., Lebey M., Khalid Naciri J.K. Drag force on a circular cylinder midway between two parallel plates at Re << 1 Part 2: moving uniformly (numerical and experimental) // Chemical Engineering Science. 2005. Vol. 60, No. 10. P. 2535-2543.

LABORATOIRE D'ENERGETIQUE APPLIQUEE (LABORATORY OF APPLIED ENERGETICS)

M. ADJ (Head)
D. AZILINON (Head Adjoint)
O. SOW (Author)

Laboratoire d'Energétique Appliquée (LEA), Dakar, BP 5085 Dakar Fann, SENEGAL
Phone: 00 221 33 825 34 26, Fax: 00 221 33 825 55 94
E-mail: lea@ucad.sn,
internet site: www.ucad.sn/lea

University Cheih Anta Diop (UCAD)

Laboratoire d'Energétique Appliquée (LEA)

Ecole Supérieure Polytechnique (ESP) de Dakar

Brief presentation

The Laboratory of Applied Energetics was created in 1984 by Professors Souleymane SECK, First Vice-chancellor of University SENGHOR of Alexandria and Bernard CHAPPEY, President of the University of Evry until September 2002 which at that time was respectively Directeur of the University "Ecole Nationale Supérieure Universitaire de Technologie" (ENSUT) and Director of the IUT of Créteil (France). It was directed until September 1991 by Mr. André GIRARDEY, who was detached from the University Paris XII.
The Laboratory of Applied Energetics is invested in the fields of thermodynamics and applied thermics, with for objective the study and the realization of energy systems entering within the framework of the political development of Senegal in particular, and in the sahelian zone in general. Are concerned, the Rational Use of Energy, Thermal Comfort, Saving Renewable Energy and the Energy utilization and other Systems Energy.

PERSONNEL

Direction

− Head: Mamadou Adj
− Head Adjoint: Dorothé Azilinon

Framing

1. Mamadou Adj
2. Dorothé Azilinon
3. Djibril Diaw
4. Mactar Faye
5. Salif Gaye
6. Youssouf Mandiang
7. Vincent Sambou
8. El-Hadji Malick Soumare
9. Ousmane Sow

Researchers in thesis of doctorate 3-rd cycle − 4
Researchers in single thesis of doctorate − 17

General description preface of the head of the laboratory

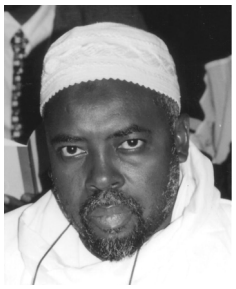

Name: ADJ
First name: Mamadou
Address: LEA, ESP, UCAD BP 5085 Dakar-Fan − Tel.: 33.825 34 26
E-mail: madj@ucad.sn, mhmadj@yahoo.fr,

− Director of studies of ESP.
− Director of the Laboratory of Energy Applied, ESP, UCAD.
− Responsible of the Thermal option, Systems Energy and Environment of Master 2 of Research "Engineerings" of the Polytechnic University.

Formation

− July 1974: A level C
− June 1975: Preparatory year with the Lomonosov Academician of Kiev.
− June 1980: Diploma for the occupation of Electromechanical Engineer of the Polytechnic Institute of Odessa.
− June 1981: BEPA Centers English Improvement of Jules Ferry of Dakar.
− Nov. 1983: Diploma of Thorough Studies Energy, Paris XII.
− Nov. 1987: Doctor-engineer of the ENSUT of Dakar.
− Jan. 1989: Doctor of the University Paris Val de Marne.

Professional activites

Direction of energy ministry for industrial development and the craft industry

− January 1981 − May 1982: Head of the Division of the Great projects.
− May 1982 − March 1983: Responsible for the valorization of renewable energy.
− April 1983 – January1984: Head of the Division of the Secretariat of the National Commission of Energy.

Ecole superieure polytechnique (Ex-ENSUT)
Universite Cheikh Anta Diop de Dakar

Teaching activities

− October 1987 − September 1990: Person in charge of the Laboratory of Electrical engineering.
− October 1990 − September 1991: Person in charge of the Formation HAD of Dpt Electronic engineering.
-October 1991 − September 1996: Chief of the Department Electronic engineering.
− October 1996 − July 2003: Person in charge of the Continuing education of Dpt Electronic engineering.
− Since April 2003: Director of studies of the Polytechnic University.

Research activities − Laboratory of applyed energy

− Researcher at the Laboratory of Applied Energy (LEA) since its creation in Nov. 1984.
− September 1989 − July 1991: Assistant person in charge of the LEA.
− Since October 1991: Director of the Laboratory of Applied Energy.

Coordination of projects

− August 1996 − December 2000: Coordinator for ESP of Project PNUD/FEM RAF/93/G32: Reduction of the gas emissions to greenhouse effect thanks to the improvement of energy efficiency of the buildings in West Africa (Ivory Coast and Senegal) - Senegalese Codes of Energy efficiency and Thermal Comfort of the Building industries.
− October 2000 − December 2004: Person in charge of the Technical Group and Coordinator of the Institutions Sénégalaises (LEA/ESP − ISE (Institute of Sciences of the Environment) and ENEA (National School of Economy Applied)) project PSACD (Sénégalo-German Project of Domestic Fuels), Direction of Energy, GTZ (German Co-operation): Energy planning − Modeling of Under Sector of domestic fuels.

Research orientations of the laboratory

*Rational use of energy (*Dorothé Azilinon, Djibril Diaw)
− energy planning;
− modeling of energy consumption.
Thermal comfort in the habitat and energy saving (Vincent Sambou, El-Hadji M. Soumare)
− numerical modelling of the habitat;
− recovery of solar energy.
*Solar production of cold (*Mamadou Adj, Youssouf Mandiang)
− photovoltaic systems;
− thermoelectric systems;
− thermodynamic systems.
Solar production of warm water (Dorothé Azilinon, Salif Gaye)
− solar-fired heater.
*Materials (*Youssouf Mandiang)
− thermophysical and hydro-thermophysical characteristics of local materials.
Desalination (Mamadou Adj, Ousmane Sow)
− sea water;
− brackish water.
Mechanics of the continuous mediums (Ousmane Sow*)*
− Dynamics of the Structures.
− Mechanics of the continuous media.

Activities

Research tasks

Diplome d'etudes approfondies (diploma of advanced studies) (DEA)

DEA Energy and Dynamics of the Complex systems − University Paris Val de Marne in collaboration with the ENSUT, University Cheik Anta of Dakar.

DEA Sciences Physics for the Engineer − Control and Industrial Process control − University Paris Val de Marne in collaboration with the ENSUT, University Cheik Anta of Dakar.

DEA Engineering sciences − Option Heat transfers & Energy Systems of the Polytechnic University, University Cheik Anta of Dakar.

MASTER Engineerings − Option Heat transfers & Energy Systems of the Polytechnic University, University Cheik Anta of Dakar.

Projects of research and development

Regional project PNUD/FEM/RAF/93/G32

From August 1996 in December 2000 the Laboratory of Applied Energy was implied in the development of the Codes of Energy efficiency and the Thermal Comfort of the Building industries of Senegal within the framework of very important regional project PNUD/FEM/RAF/ 93/G32 on Reduction of the gas emissions to greenhouse effect thanks to the improvement of energy efficiency of the buildings in West Africa Ivory Coast - Senegal). The activities which were developed by the team installation made it possible to produce the principal reports/ratios:

− Total methodological Notes.
− Methodological Notes sectoral (Envelope, Lighting, Electricity, Ventilation & Air-conditioning, Medical Warm water.
− Follow-up of the climatic data.
− Typology of the buildings.
− Complementary Data.
− Development of the input files of the buildings of reference.
− Energy Optimization of the buildings of the Zone of Dakar.
− Energy Optimization of the buildings of the Zones of Kaolack, Tambacounda, Ziguinchor.
− Guides of application for the drafting of the draft standards of the Codes.

Standards Senegalese applicable to the photovoltaic batteries of solar systems

Organizer of the GT3 (Technical Group) Electrochemical Storage of the CT13 (Technical Committee) of Solar energy, the LEA took part in the preparation of standards Senegalese applicable to the photovoltaic solar systems and their components.

The CT13 was created on the initiative of the Project Senegal-German Solar energy. The GT3 worked in the following parts:

− Stationary Batteries with lead: general regulations and testing methods.
− Accumulator Batteries to lead intended for the storage of the photovoltaic electrical energy of origin.
− Auxiliary Electrolyte: physical characteristics, degrees of essential purity, terminals and connections.
− Stationary Batteries with lead intended for the storage of the photovoltaic electrical energy of origin: dimensioning methods, regulations of installation and exploitation.

Work could be done starting from the publications:

− CEI (International Electrotechnical Commission) No. 27, 50, 51, 51, 359, 485, 617, 896-1, 896-2, 1056-1, 1056-2 and 1056-3.
− DIN 43.530 Part 2, 43.530 Part 4.

PSACD (Senegal-German Project of Domestic Fuels)

Since 2000 the Laboratory of Applied Energy is implied in the modeling of the Under-Sector of Domestic Fuels within the framework of the PSACD (Senegal-German Project of Domestic Fuels) in relation to the IER of the University of Stuttgart, the Institute of Sciences of the Environment of and the Techniques Faculty of Science of the UCAD and the Department Town and country planning, Environment and Urban Management of the National school of Economy Applied of the University Sheik Anta Diop.

The objective consists in implementing a model of management and energy valorization of the various types of fuels and technologies used today, in order to allow a provisioning of the Senegalese households of domestic fuels according to their specificity and of the requirements of "sustainable development" in the direction desired by the international community (Brundtland report/ratio, Conference of Rio…).

An Energy System of Reference (S.E.R.) for the production and the consumption of fuels to Senegal was proposed. This SER includes/understands all fuels and technologies used today in Senegal; as well as the socio-economic variables which are associated for them.

Demographic data-gathering and on:

them agricultural and agro-industrial vegetable residues;
them municipal waste;
them technologies of carbonization;
them equipment of cooking;
near the structures concerned allowed to have a base and to carry out simulations to see the evolution of the current location (case of reference) and the impact of the adoption of certain strategies and scenarios (case studies).

THE UNIVERSITY OF DOUALA − CAMEROON
ADVANCED TEACHERS TRAINING COLLEGE FOR TECHNICAL EDUCATION (ENSET)
THERMAL AND ENVIRONMENTAL RESEARCH LABORATORY (LATE)

Head: Alexis Kemajou
Secretary: Koumi Ngoh
Author: Alexis Kemajou

POB 1872 Douala Cameroon
E-mail: kemajoualexis@yahoo.fr
Tel: (327) 77 76 74 80
E-mail : laboenergy@yahoo.fr

Brief presentation of the laboratory

Energy efficiency in buildings and industries while respecting the environment and standards of thermal comfort. Seeking renewable energy sources as to contribute to the reduction of energy crisis in building and industries. Present the realities of industrial ecology in Cameroon and energy in particular.

Staff

− 1 associate professor.
− 4 lecturers.
− 8 doctorate students and 4 Diplome d'Etude Approfondies (DEA) students.

Objectives

1. To further research on the dynamic behaviour of buildings in the hot climate and contribute to putting in place energy standards.
2. To further knowledge in energy production by using renewable energy sources and bio fuels.
3. Diffuse the principles and methods of industrial ecology in developing countries and Cameroon in particular.

Research orientation

− Thermal science for buildings: thermal comfort in buildings.
− Renewable energies: bio fuel, solar energy and bio energy.
− Energy efficiency in buildings and industries.
− Environmental management – waste − Clean Mechanism of Development (CDM) − industrial ecology.
− Commercial and industrial refrigeration.
− Refrigerated preservation of perishable foodstuffs (animal and vegetable).
− Drying and storing of meat, fish and farm crops.
− Study of efficient techniques for the conservation of food stuffs in the hot tropical zone by respecting the cold chain.
− Develop other systems of producing cold noble for the environment.

Articles

− Design of software for cooling load calculation in air-conditioning.
− Design of software for refrigeration load calculation.
− Published two source books in refrigeration and air conditioning system in sub Saharan Africa.
− Research publications: 12 articles published in international research journals.

External scientific collaboration

- 2ie – Département Energie pour le développement Rural – Ouagadougou (Department of Energy for Rural Development).
- ENSP – LAEN Yaoundé Cameroun (National Polytechnics – Energy Laboratory).
- International Institute of Refrigeration (IIR/IIF) – Member of the E1 commission (Air Conditioning) and E2 (Heat pump and energy recuperation) of the I.I.F Paris.
- Calls for collaboration with others laboratories working in the same research orientations.

Source of financing

− Consulting and design engineering for companies and industries by members of the Laboratory: design and realisation of food driers, with heat pump machine.
– Energy Audits in buildings and industries, organization of vocational trainings.
− Design and construction of small and medium bio diesel processors.
− Design and construction of refrigeration systems (commercial and domestic use).

Results obtained

Support for development

− Bio fuels: Production of bio diesel to supply the diesel engines of electricity power generation in rural areas.
− Putting in place of a "Tropical Cooling Well" for the refreshment of buildings in the tropical climate zone through underground air duct.

With industries

− Development of energy efficiency program with industries in Douala.
− Putting in place of an experimental site for the production of biogas with the help of HYSACAM Company.
− Vocational training on recovery, recycling and regeneration of CFC's refrigerants prohibited by the Protocol of Montreal.

Experimental materials

− An experimental (scale model) direct expansion air handling units with a duct system (round and rectangular) in galvanised steel sheets.
− Scale model of reversible heat pumps.
− Direct Digital Control (DDC) unit controller.
− A complete numerical data acquisition system comprising the DAQ card, transmitter, resistance and thermocouple temperature sensors, humidity, pressure and velocity sensors.
− A tool set for fiberglass and galvanised steel sheet duct construction.
− A refrigerant recovery, recycling, regeneration and destruction machine.
− Mercury and digital thermometer, hygrometer, scale balance, manometers.
− A Pitot Tube for dynamic and static pressure measurement.
− Biogas production system from household waste and a digital biogas analyzer.
− A test bench for pressure drop (due to line friction, fitting and valves) in refrigerant lines.
− Test bench of refrigeration cycle and refrigeration troubleshooting.

GROUPE DE RECHERCHE SUR LES ENERGIES RENOUVELABLES (GRER)
RESEARCH GROUP ON RENEWABLE ENERGY

Head: Michel Dupont
E-mail: mdupont@univ-ag.fr, Tel.: 0590590 483 112

Secretary: Rhozelle Louviers
E-mail: rlouvier@univ-ag.fr, Tel.: 0590590 483 306, Fax: 0590590 483 305
Campus de Fouillole
97 157 Pointe a Pitre Cedex
http://www.univ-ag.fr

Brief presentation

The research group on renewable energy has its principal activities on tropical regions: heat transfer in building, particularly on natural convection, wind and solar resource, and energy conversion and storage.
Briefly let us recall that the geographical position of the Guadeloupe and Guyana in tropical and subtropical zone (Fig. 1). Guadeloupe is already equipped with several systems of production of electricity connected to the network: photovoltaic, wind farms, hydroelectric, geothermic. On the contrary, Guyana has more isolated sites off-line to the network.

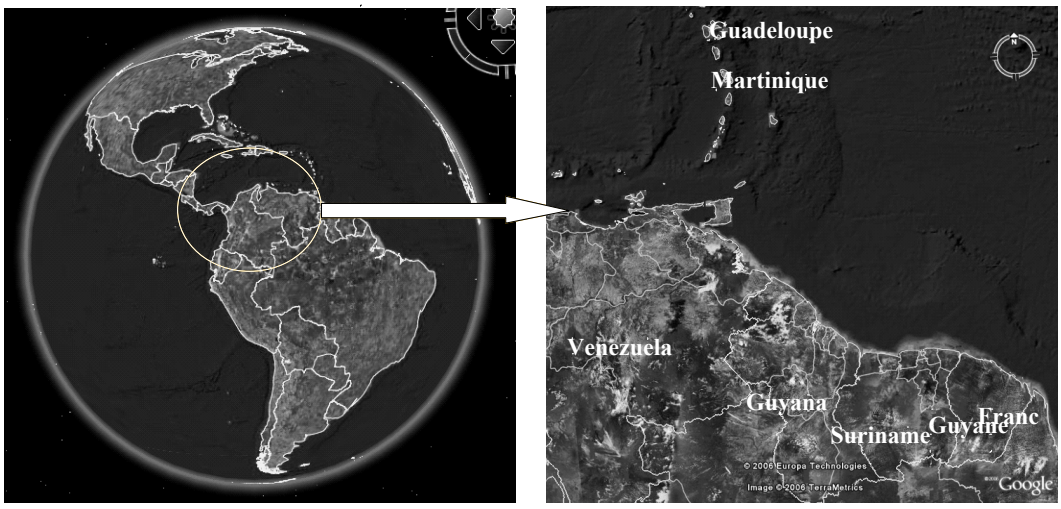

Fig. 1. *Guyana and Guadeloupe location*

Statistical analysis of wind and solar power

Moreover, located in tropical or subtropical zone these areas have a strong sunning (5 kW·h/m^2) and gain advantage of the Trade Wind during all every day. These sites are particularly well adapted to produce energy from the renewable sources. These areas are thus a natural laboratory with regard to use renewable energies. The GRER is thus working on the control and the decentralized production of electricity and on the heat transfer in the habitat in tropical climate.

In Guadeloupe are studied the statistical approach of the wind and the solar resource (Fig. 2) and the natural convection in bioclimatic approach of building.
In Guadeloupe, the electric output from wind farms can currently reach 5 % of the power consumption by the network. The 10 % should be exceeded in the next years. From its fluctuating nature, the power produced by the wind farm, which cannot be for the moment stored, poses an obvious problem of management of the electrical production. The fluctuations on the short scales of time (a few seconds to 1 hour) however pose drastic problems of

management of the network (choice and started means of substitution) as the amplitude of these fluctuations can reach the total potential power of the site.

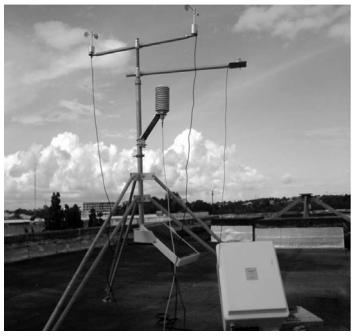

Fig. 2. *Wind velocity and solar radiation measurement apparatus*

It appears necessary to provide the following tools: i) a more exact qualification of the real energy contribution of a wind farm and its dynamics, to test its impact on the network, ii) the forecast, in real-time and on the short scales of time (<1 hour), of the delivered power.
To do that, the aerodynamic measurements and electric output measurements (step: one second) are carried out on the existing production sites in Guadeloupe (Fig. 3).

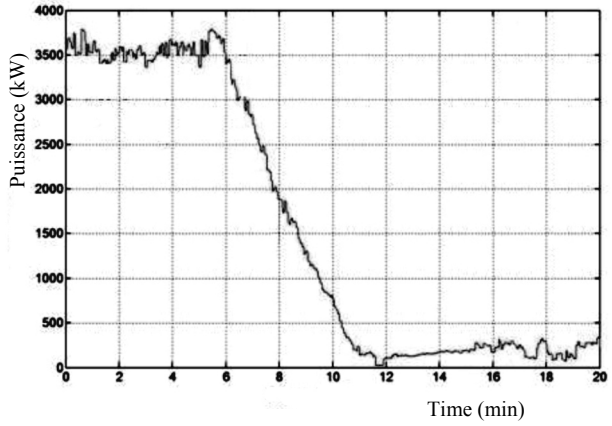

Fig. 3. *Farm power drop following the wind fluctuations*

PV and hydraulic program in French Guyana

Guyana has several sites isolated with centralized or individual photo voltaic installations, dimensioned for villages. The study of the malfunctions of a photo voltaic power station has been done using a method of classification adapted to the measured data. The need for better controlling storage has appeared, particularly because of the variability of a source like solar energy and on the other hand for knowing the statistical and dynamic characteristics solar radiation on the site, but also the dynamic behavior of the accumulators. A dynamic model has been proposed to describe in the most precise possible way the state of load of an accumulator. An experimental device has been set up in the laboratory to follow the dynamic behavior of accumulators in load and in discharge, subjected to constraints. A PhD thesis in joint management with the LEM of Montpelier concerns the validation of the model.
In Guyana, the isolated villages are generally located along the rivers. The weather data highlight a strong seasonal variation of pluviometry complementary to the variations of the sunning (with however a shift: maximum of sunning in October, whereas the low water level is in November). A machine of the hydrokinetic type ("hydrolienne"), using the kinetic energy of the current with a minimum of work of civil engineering, will be an interesting solution to produce electricity for the isolated village. An alternator has been elaborated to compensate the variability of the mechanical renewable energy sources (hydraulics, wind).

Solar protection of building

The solar protection of the building is necessary to reduce the energy consumption. This research topic gave place for three principal subjects of study: i) a study of the not established modes of natural convection in a channel inclined in the field of gravity (thermal boarding in roof), ii) experimental comparative study in condition of real sunning of various types of solid insulators (including reflective thin insulators) for the solar protection of the roofs, iii) thermal response of roof depending of the solar absorptivity (Fig. 4).

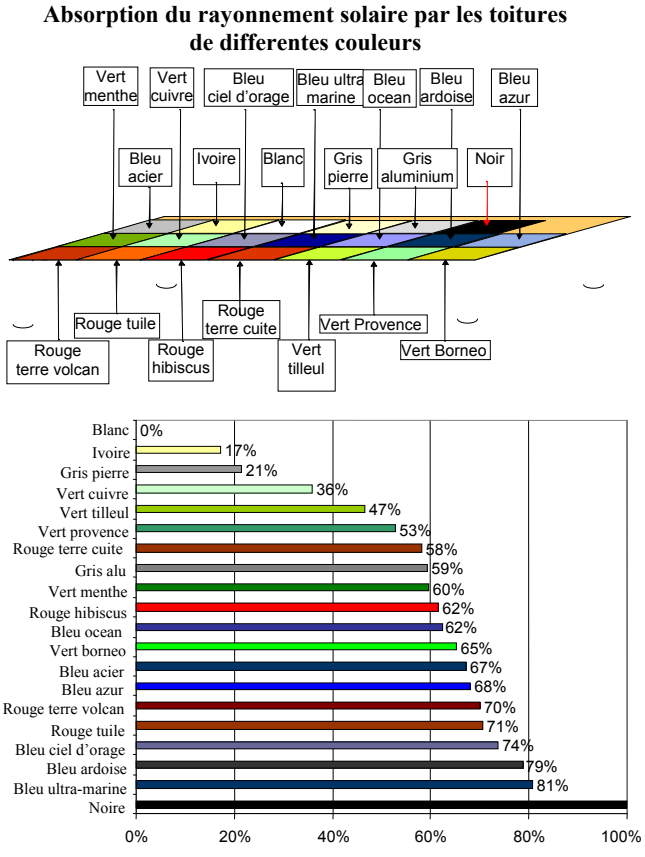

Fig. 4. *Experiment on solar absorption in steel sheet and percentage of temperature increase with the color*

The natural convection air flow resulting from the heating with a constant heat flow of the upper wall of a channel (two-dimensional), opened at each end and inclined in the field of the gravity has been experimented. The lower wall is thermally insulated. This study is directly related to the solar protection of the habitat (roofs and walls) in tropical medium to prevent air conditioning. We thus undertook to make a detailed cartography of the speed and temperature fields of the flow and of the parietal temperatures for a range of number of Grashof corresponding to not established flows. Three goals are pursued: i) to specify the sensitivity of the flow to its boundary conditions and in particular at the entrance of the channel, ii) to specify the conditions of similarity of the flow, iii) to provide the data bases necessary to the comparisons with the numerical studies of this type of open flow. With a laser anemometer device, the non inclusive measurement in the air flow was done simultaneously with the measurement of the temperature profile of the heated wall. The results were analyzed according to the numbers without dimension defining the experimental device: Grashof, Prandlt numbers, depending of the lengthening and slope of the channel. The Fig. 5 shows the experimental device with the laser equipment and a visualization of a reverse air flow which has never been published in the literature before.

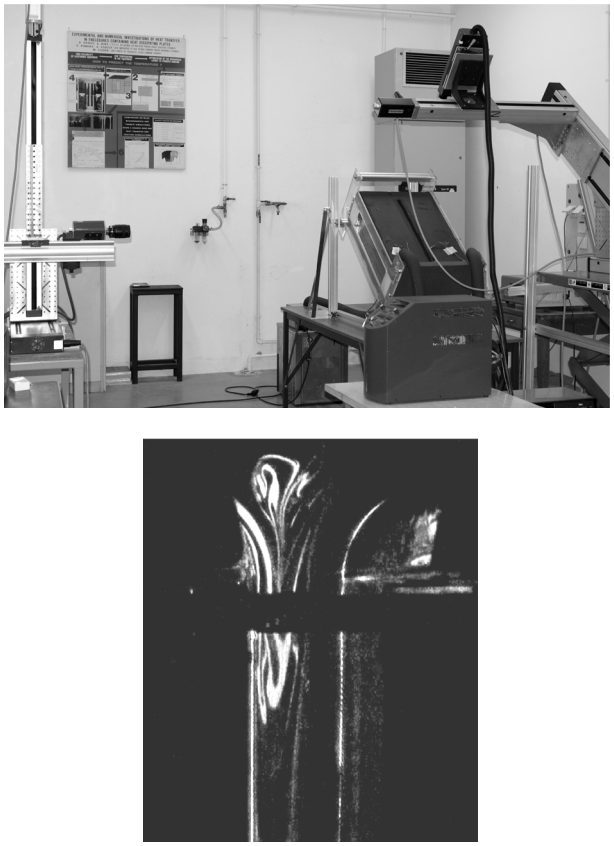

Fig. 5. *Experimental device to generate natural convection flow in an air channel with the laser equipment, reverse flow visualization*

Solar dryer working day and night

In regions where solar energy is abundant, the solar dryer is an adequate solution for the food conservation. However the lack of sun during the night stop the drying process and could be responsible of the degradation of the product. To prevent this damage, a solar dryer has been completed with a solar hot water storage which is used during the night. A patent has been filed in which a solar open cycle air dryer was included at the entrance of the process air flow using a solid desiccant to decrease air moisture. When the air temperature is controlled, the drying process is more reproducible. An experimental device have been experimented in Guadeloupe (FWI) and in French Guyana (Fig. 6). To improve the prototype components size, a dynamic numerical simulation have been done in the electrical analogy scheme. Electrical tools, PSPICE / MATLAB and the thermal transient code TRNSYS have been used. The numerical results has been compared with the experimental data when the air temperature and (or) the air flow was controlled. A good agreement have been obtained.

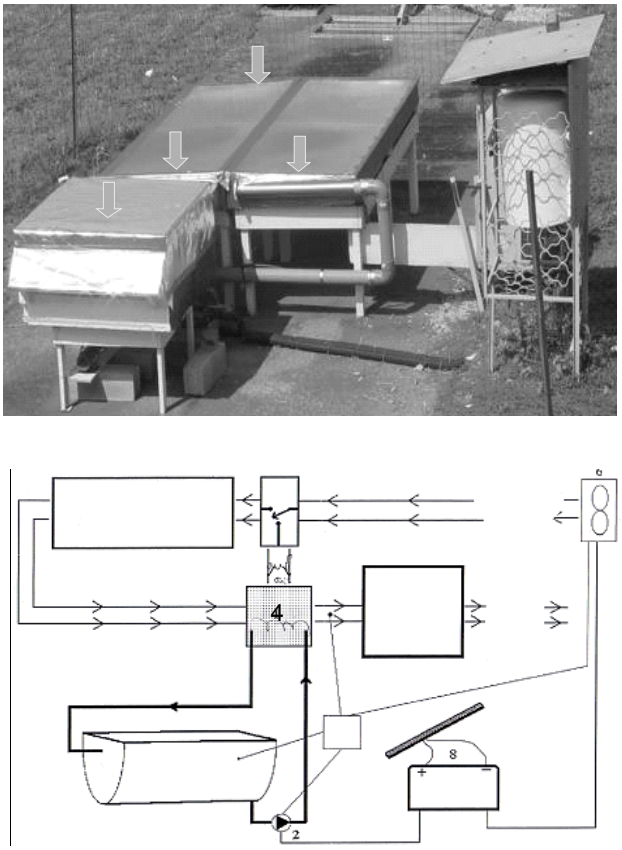

Fig. 6. *Solar dryer with a water tank for night working, view and synoptic diagram*

Joint program on sustainable development monitoring assisted by remote sensing

The GRER is involved in an ambitious project with the French IRD (Institut de Recherche et de Développement) concerning sustainable development in the Amazonian region. It makes use of remote sensing technology, and geographical information cartography. The GRER contributors have an experience in modelling, signal or image processing. This program includes the cartography and physical analysis of renewable energy resources (sun, wind, water, biomass) and the following-up of the environmental impact of biofuels (Fig. 7).

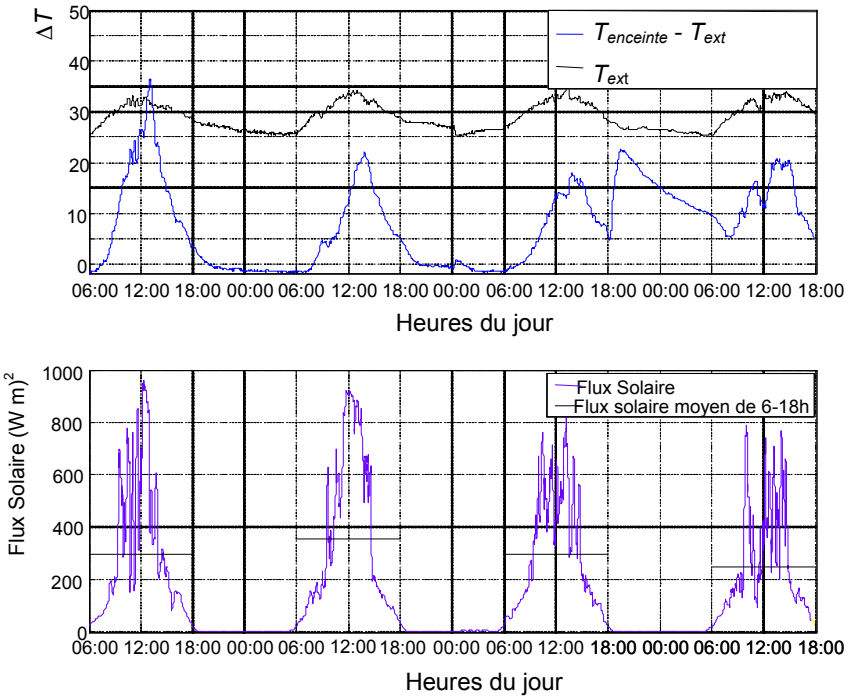

Fig. 7. *Four days drying chamber temperature difference with ambient temperature, opening the hot water tank on the 3-d night*

LABORATOIRE DE MECANIQUE DES FLUIDES (LABORATORY OF THE MECANICS OF THE FLUIDES)

Head (*): Fawaz Massouh
Secretary (**): Martine Portolan
Author (***): Ivan Dobrev, Fawaz Massouh

ENSAM, 151 Bd. de l'Hopital,
75013 PARIS- FRANCE

http://www.paris.ensam.fr
Phone: 33 (0)1 44 24 62 56, Fax: 33 (0)1 44 24 62 66

*E-mail: Fawaz.Massouh@paris.ensam.fr ,

**E-mail: Martine.Portolan@paris.ensam.fr ,

***E-mail: Ivan.Dobrev@paris.ensam.fr,

Brief presentation

ENSAM was founded in 1780 by the duke of La Rochefoucauld-Liancourt, and so far has trained more than 78,000 engineers who have taken part in the industrial development of France. ENSAM is a state institution of scientific, cultural and professional nature placed under the authority of the French Ministry in charge of higher education. ENSAM is composed of 11 Regional Centers and Institutes all over France. As an institution dedicated to teaching technology at the highest levels, ENSAM is involved with theoretical and practical research, and is closely tied to the industrial world. ENSAM now has 22 research groups, either associated or co-associated with the French national organization for scientific research (CNRS), or recognized by the French Ministry of Education or operating under the auspices of ENSAM. The major fields of study research are:

− Mechanics, materials, manufacturing processes.
− Fluid mechanics, energy systems.
− Design, industrialization, risk, decision making.

The Fluid mechanics laboratory at ENSAM-Paris has a wind tunnel equipped with a high precision system for aerodynamic force measurements. The velocity field can be measured by means of particles image velocimetry (PIV) and 3D hot-wire anemometry (HWA). Many research projects are carried out in the fields of automotive and wind turbine aerodynamics.

For several years various investigations on wind turbine wake have been carried out using PIV and HWA. The obtained experimental data makes it possible to validate the wind turbine rotor models developed by the laboratory team.

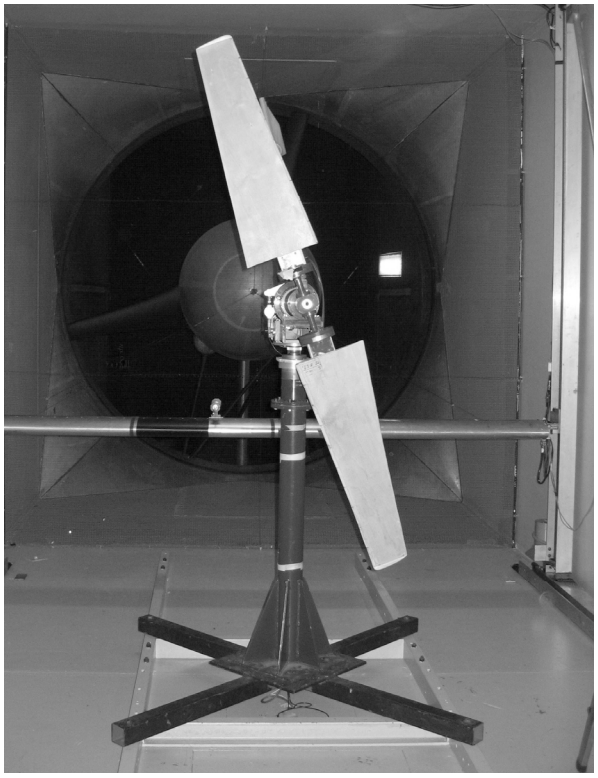

Wind turbine measurement bench

Collaborations, national and international, present and calls for collaborations

Collaboration with: French agency of environment and energy ADEME, ONERA, NREL, Technical University

of Denmark DTU, University of Trondheim NTNU, Technical University of Sofia, Moscow Institute of Energy MPEI, ETSMTL-Montreal, etc.

Acknowledgements

Special thanks are addressed to the French Energy Agency ADEME for their support and funding

References

1. Massouh F., Dobrev I. Exploration of the vortex wake behind of wind turbine rotor // Journal of Physics (IOP) Vol. 75 (2007) 012036, http://www.iop.org/EJ/abstract/1742-6596/75/1/012036
2. Dobrev I., Massouh F., Rapin M. Actuator surface hybrid model // Journal of Physics (IOP) Vol.75 (2007) 012019, http://www.iop.org/EJ/abstract/1742-6596/75/1/012019
3. Dobrev I., Massouh F. Etude du couplage aéroélastique dans le cas d'un rotor éolien, CFM2007-Grenoble, 27-31 Août 2007.
4. Massouh F., Dobrev I., Rapin M. Experimental and Numerical Survey in the Wake of a Wind Turbine // AIAA paper 2007-0423, 45th AIAA Aerospace Sciences Meeting and Exhibit, Reno, NV, Jan. 8-11 2007.
5. Massouh F., Dobrev I. Investigation of Flow Downstream a Horizontal Axis Wind Turbine, 1st International Symposium on Environment, Identities and Mediterranean Area (ISEIM'2006) July 9-13, 2006 - Corte − Ajaccio (France).
6. Jourieh M., Kuszla P., Dobrev I., Massouh F. Hybrid rotor models for the numerical optimisation of wind turbine farms, 1st International Symposium on Environment, Identities and Mediterranean Area (ISEIM'2006) July 9-13, 2006, Corte − Ajaccio (France).
7. Massouh F., Dobrev I., Rapin M. Numerical simulation of wind turbine performance using a hybrid model // AIAA paper 2006-0782, 44th AIAA Aerospace Sciences Meeting and Exhibit, Reno, NV, Jan. 9-12, 2006.
8. Massouh F., Dobrev I. Investigation of wind turbine near wake, Int. Conf. on Jets, Wakes and Separated Flows, ICJWSF-2005. P.513-518. October 5-8, 2005, Toba-shi, Mie, Japan,
9. Dobrev I., Massouh F. Etude d'un modèle hybride pour représenter l'écoulement à travers un rotor éolien, 17 ème Congrès Français de Mécanique, 29/8-2/9/2005, Troyes.
10. Massouh F., Dobrev I., Jourieh M. Etude par PIV du sillage proche d'une éolienne, FLUVISU 11. COLLOQUE de VISUALISATION et de TRAITEMENT D'IMAGES en MECANIQUE des FLUIDES. Ecole Centrale de Lyon 6-9 Juin, 2005.
11. Massouh F., Dobrev I., Dejean F., Laborie A. Etude du sillage d'une éolienne à axe horizontal, 16ème Congrès Français de Mécanique CFM 2003, Nice, 1-5 septembre 2003.

LABORATOIRE DE CHIMIE ORGANIQUE ET PHYSIQUE APPLIQUEE

LABORATORY OF APPLIED ORGANIC CHEMISTRY AND APPLIED PHYSICS
UFR/SEA UNIVERSITY OF OUAGADOUGOU

Head: Pr. M. Nacro**

Authors: Pr. A. Ouedraogo*, Pr. A.D. Samate

UFR/SEA Université de Ouagadougou, BP 7021 Burkina Faso
Phone: (226) 50 30 70 64 ext 50 30 Fax: (226) 50 72 42
Internet site : http://www.univ-ouaga.bf

*e-mail: alioue@univ-ouaga.bf

**e-mail: mnacro@univ-ouaga.bf

Brief presentation

The laboratory is multi-field where work together chemists, physicists and botanists on the following topics:
− tincture plants, rich in aromatic tannins and plants for their essential oils;
− heat transfers, passive air-conditioning by natural convection, study of the physical properties urban waste and environment.

General description

Burkina Faso, is a sahelian and cattle-rearing country where the dyeing and the tanning occupy a significant place on the level of the craftsmen and industry. The aromatic plants are rather known for their medicinal and food properties. The various scientific studies thus allow an adequate use of those while preserving the biodiversity.
The problems of environment are considered in collaboration with the University of Perpignan in France: waste and simulation on the natural convection within the framework of the improvement of thermal comfort in the buildings.
The bibliographical review followed by some analyses in the laboratory (Nacro and Millogo-Rasolodimby [1]) revealed 128 tincture plants and rich in tannins. Kouda [2-3] through its work, led to the results of sifting of 19 species distributed in 12 families according to their content gallic tannin. The species which have a content ranging between 1.4 and 8.7 are most interesting.
One finds nearly 90 aromatic species in Burkina. They are characterized by the fact that they exhale fragrances. The aromates are fresh or dry plants having a sweet-smell or a particularly marked taste. One speaks rather about spices when it is about a seasoning. Oils are required for industry, pharmacy and medicine known as soft.
The chemical composition of oils of 3 species of the *Cymbopogon* kind was analyzed by Djibo [4] et al. That of *Lippia multiflora* is rich in thymol and its acetate should find applications in phytotherapy, as for that of the *Eucalyptus citrodora* which contains the *citronelle* [5].
For 3 years a study of the physical characteristics of oils of *Mentha piperita* [6], *Cymbopogon* [7] and the *Eucalyptus* [8] has been undertaken with measurements of density and optics (optical activity and refractive index) carried out using an interferential method.

Structure of the laboratory and results

One counts various teams with in the laboratory: 5 chemists, 2 physicists and 2 botanists working on the problems of Environment: ecology and energy and having material for the oil extractions, the optical measurements and of computation software [9].
4 students are working in a PhD program in the laboratory (physics and chemistry).
Various results obtained are published. Knowing the properties of the aromatic plants and with tannins, one explains their better uses in traditional pharmacopeia. Some plants of the family of *Verbenacea* in Burkina Faso are used first of all like trees of reafforestation, decorative plants and for the wood of heating (Millogo-Rasolodimby et al [10]), a mean of fighting against the turning into a desert of the Sahel.

References

1. Nacro M., Millogo-Rasolodimby J. Plantes tinctoriales et plantes à tannins du Burkina Faso // Ed. Scientificak A, Amiens.1993.
2. Kouda M., Nacro M. et al. Isolation of Apigeninidin from leaf sheaths of *Sorghum caudatum* // Journal of Chemical Ecology. 1994. Vol. 20, No. 8. P. 2123-2125.
3. Kouda M., Nacro M., Palé E. et al. Composition chimique et utilisation des s*orghos* cultivés au Burkina Faso // Bull. SOACHIM. 1997.
4. Menut C., Djibo A.K., Samaté A.D. et al. Aromatic plants of tropical West Africa // Journal of Essential Oil Research. 2000. Vol. 12. P. 207.
5. Millogo-Rasolodimby J., Samaté D.A. Importance socio-économique des plantes aromatiques, tincoriales et à tannins au Burkina Faso // Etudes flor. Vég. Burkina Faso. 2002. 7. P. 55-58.
6. Ngoya D., Samaté A.D., Ouédraogo A. Composition chimique et caractéristiques physiques de l'huile essentielle de *Mentha Piperita* du Burkina Faso // Annales de l'Université de Ouagadougou. 2005. C. 003. P.175-187.
7. Onadja Y., Ouedraogo A., Samate A.D. Chemical composition and physical characteristics of the essential oil of *Cymbopogon schoenanthus (L.) Spreng* of Burkina Faso // Journal of Applied Sciences. 2007. Vol. 7, No. 4. P. 503-506.
8. Dabiré C., Palé E. et al. Caractéristiques physiques de deux espèces d'*Eucalyptus* acclimatés au Burkina Faso. Submitted to Journal de la SOACHIM.
9. Ouedraogo I., Ouedraogo A., Palm K., Zeghmati B. Modelling of a bioclimatic roof by natural ventilation //submitted to ISJAEE.
10. Millogo-Rasolodimby J. et al. Les *Verbenaceae* introduites au Burkina Faso et leurs utilisations.// AAU reports Ba, Madsen et Sambou. 1998, Vol. 39. P. 302-310.

DEPARTMENT OF PHYSIC'S, LABORATORY OF DOSAGE, ANALYSIS AND CHARACTERIZATION IN HIGH RESOLUTION FERHAT ABBAS UNIVERSITY, SETIF, 19000, ALGERIA

H.Amardjia-Adnani*
A.Merouani**

Department of physics, Laboratory of Dosage, Analysis and Characterization in high Resolution,
Ferhat Abbas University , Sétif , 19000, ALGERIA
Tel/Fax : 00 213 36 92 51 33
*e-mail: adnani2dz@yahoo,fr;
** e-mail: amerouani2001@yahoo,fr

Brief presentation

Our laboratory exists since few years, and it consists of groups of research in optoelectronic materials and renewable energy. It is equipped with devices for synthesis, realisation and characterization, specific to the energizing materials (the simple and mixed oxides).

General description

As it has been underlined before, our laboratory has for vocation, since 2001 researches in the field of renewable energy and related domains, and we wish to acquire news techniques of characterization.

Structure of the laboratory

The structure of the laboratory is defined as follows:

N° Group	Number of researchers	Thematic	Techniques Means	Objective
01	03	Solar cell	− Dip-coating − CVD	Conception of photoanode for dye sensitised solar cell
03	05	Optoelectronic materials	− Résistivimetre	//
04	04	Polymer electrolyte	− Volta lab − Impedencemetre	//

Activities, actions, results, projects

For the different actions, results and projects, we achieved the works of research in progress, as follows:

Period	Results	Project
2001-2004	− Elaboration thin films of SnO_2	Conception of Dye sensitized solar cell (DSSC)
2004-2007	− Elaboration thin films of TiO_2 − Elaboration conductor glass FTO − Characterization of new dyes (organic and inorganic)	Conception of DSSC

Collaborations, national and international, present and calls for collaborations

Our laboratory collaborates with national and international universities as:
− University of Tlemcen (Algeria);
− University of Béjaia (Algeria);
− Unit of development of silicon technology (Algeria);
− Polytechnique Federal Institut of Lausane (Suisse);
− Universite Claude Bernard de Lyon (France).

UNIT OF RESEARCH ON MATERIALS AND RENEWABLE ENERGIES GROUP: PHOTOVOTAIC SYSTEMS

Head: Pr. B. Benyoucef
Authors: R.Maouedj, S.Bousalem*

URMER, Université Abou Bekr Belkaïd, BP 119, Tlemcen, Algérie
Phone: +213 43 21 58 89; Fax: +213 43 2158 90
*E-mail: ra_maouedj@yahoo,fr; Internet site: http://www.univ-tlemcen.dz

Brief presentation

The Unity of research URMER has research interests in the fields of materials and renewable energies. It is composed of 3 laboratories.

Structure of the laboratory, different groups and their thematics, experimental and technical means, etc

There are 3 groups in the unity working in the following topics:
– Renewable energies and materials for energy.
– Modeling and characterization of material for electronic applications.
– Study and prediction of materials.

Activities, actions, results, projects

The activities of research in our Unity are:
1. Renewable energies and materials for energy.
– Renewable energies and development; community and household energy use in less developed countries, biomass energy resources, renewable energy technology transfer especially of photovoltaic, photothermic and wind systems, rural electrification policy in Algeria.
– Preparation and development of material-Applications.
– Energy physics: Thermal transfers and fluid mechanical.
2. Modeling and characterization of material for electronic applications.
– Integers circuits, characterization, modeling.
3. Modeling of materials, amelioration of proprieties, Prediction...
Many articles are published in these fields.

Projects

CMEP
(Prof. N.E. CHABANE SARI)
1999
02 years
Characterization of oxides obtained by thermal and chemical treatments on porous silicon

ANDRU
1st Project ANDRU
(Prof. B. BENYOUCEF)
A partir de 1998
03 years
Autonomous optimization photovoltaic adapted to a site in the Application Hybrid Energy Installation of a Semi-Arid Zone

2nd Project ANDRU
(Prof. N.E. CHABANE SARI)
1999
03 years
Study of Physical Properties of Porous Silicon-Applications

CNEPRU
1st Project CNEPRU
(Prof B. BENYOUCEF)
2000
03 years
Methods for Performance Optimization Conversion Materials Photovoltaics and Photothermiques - Applications Systems Photosolaires

2nd Project CNEPRU
(Prof N. E. CHABANE SARI)
2000
03 years
Using the porous silicon for achieving the display of large surface

3rd Project CNEPRU
(Prof. G. MERAD)
2000
03 years
Survey and Prediction of properties Electronic, Optical, and Thermodynamic Structurales Solid Materials

4th Project CNEPRU
(Prof N. E. CHABANE SARI)
2000
03 years
Characterization of layers D'oxides obtained by Heat Treating Chemicals and Porous silicon-on-Applications for Cell Photovoltaiques

5th Project CNEPRU
(CHERMITTI Ali)
2000
02 years
Integrating a string Articulée with a system analysis of scenes in a system Robotics

6th Project CNEPRU
(Dr SEBBANE Omar)
2000
02 years
Technico-économic study of solar systems and heat thermal models of a solar house

Collaborations, national and international, present and calls for collaborations

The unity URMER is collaboration between various laboratory in France: Metz, Nancy Cedex... As part of these collaborations, foreign dignitaries are regularly invited to present their recent research in the laboratory.

LAPLACE LABORATORY ON PLASMA AND CONVERSION OF ENERGY UNIVERSITY OF TOULOUSE

*Head: Christian Laurent**

Senior researcher at the National Center for Scientific Research (CNRS)

Deputy directors: Professor M. Fadel, Professor G. Zissis

*E-mail: christian.laurent@laplace.univ-tlse.fr
Phone: 33 (0)5 61 55 77 91, Fax: 33 (0)5 61 55 64 52

Université Paul Sabatier
118, route de Narbonne
31062 Toulouse cedex 9, France

Internet site: http://www.laplace.univ-tlse.fr

Brief presentation

Headed by Christian Laurent, Senior Researcher at the National Center for Scientific Research (CNRS), assisted by two Deputy Directors, Professor Maurice Fadel and Professor Georges Zissis, LAPLACE has 11 research groups gathering 266 people including:
− 106 full-time and part time researchers from the CNRS and the University of Toulouse;
− 48 engineers, technicians and administrative staff;
− 112 PhD and trainees.

General description

Scientific domains

Electrical technology, power electronics, plasmas, non equilibrium phenomena, energetics, complex system modelling, renewable energy, durable development, materials for energy, diagnostics, control, design methodology.

Application domains

Generation, transport, management, conversion and utilization of electrical energy, aeronautics and space, embedded systems, transports, health and environment.

Structure of the laboratory

Research groups

Research Group in Energetics, Plasma, and Non-Equilibrium Phenomena

Jean-Pierre Boeuf, CNRS Senior researcher

Non-equilibrium plasma sources, transport phenomena (radiation, plasma, phase transitions), instability and self-organization, diphasic systems, Monte Carlo, PIC, Fluid modelling and experimental validation.

Non-Equilibrium Reactive Plasma

Mohammed Yousfi, CNRS Senior researcher

Basic data for plasma physics and chemistry, particle simulation and fluid modelling, reactive plasma flows, biotechnology and sterilization, air pollution control, dielectric barrier discharges, radiation-matter interactions.

Electric Arc and Thermal Plasma Processes

Jean-Jacques Gonzalez, CNRS Senior researcher

Calculation of the thermo-dynamical properties of pure and mixed gases, study of the phenomena and characterization of the media: within electric arc processes by modelling (fluid/solid), and experiments (optical, inverse methods).

Materials and Plasma Processes

Patrice Raynaud, CNRS Researcher

Low and atmospheric pressure cold plasma, plasma-fluidized bed, dusty plasma, plasma deposition processes, deposits and surface treatments. Diagnostics and physico-chemical studies of plasmas and surfaces.

Light and Matter

Pierre Destruel, Professor

From photon to electron, from electron to photon, the Light and Matter group studies the problems associated with the energy conversion in the electroactive devices: organic photovoltaic cells, discharge lamps, organic electroluminescent diodes.

Solid Dielectrics and Reliability

Gilbert Teyssedre, CNRS Senior researcher

Characterization, understanding and modelling of charge generation phenomena in insulators (under electrical stress or radiation), and identification of the mechanisms leading to ageing and breakdown.

Dielectric Materials in the Energy Conversion

Thierry Lebey, CNRS Senior researcher

Material processing, characterization, modeling, ageing, in view of: 3D hybrid integration in power electronics; high temperature, and high voltage component and electrical systems.

Research Group in Electrodynamics

Bertrand Nogarede, Professor

Study of electromechanical coupling phenomenas in electromagnetic fields and electroactive materials, optimal design, piezoactuators, innovative electrical machines, "intelligent" structures (aerospace, medical…).

Static Converters

Philippe Ladoux, Professor

New topologies of high power converters, 3D integration for power conversion. Safety and reliability of converters, CVD Diamond for power electronics.

Research Group in Energy, Electricity & Systemics

Xavier Roboam, CNRS Senior researcher

Integrated design methods (synthesis, analysis, optimization), transport and embedded networks, alternative energies and new technologies of electrical energy, power converters for electrical discharge.

Electrical System Control and Diagnostics

Pascal Maussion, Assistant professor

Control, performance and reliability of electrical systems improvement , including converters, electrical machines, batteries, embedded actuators, alterno-starters, fuel cells in railways, aviation, automobile and other industries.

Transversal actions

Source – Discharge – Process Optimization

Hubert Piquet, Professor

Design and optimization of a treatment or a process in its overall context, thereby taking into consideration all the source-object interactions.

Reliability and Diagnostics in Energy Conversion

Frédéric Richardeau, CNRS Researcher

Understanding the causes of ageing and failure under functional stresses, managing their effects on the surrounding system and developing methods for the detection and the management of failure.

Electromagnetism, Electrodynamics, Energetics and Plasmas

Jean-Pierre Boeuf, CNRS Senior researcher

Improve the relevance of complex physical models, to develop the synergy between specialists in electromagnetism, electrodynamics, energetics and plasmas, at the interface between the physics and the engineering.

UNIVERSITY OF CORSICA - UMR CNRS 6134: RESEARCH ACTIVITIES IN RENEWABLE ENERGY FIELD

G. Notton, C.Cristofari, J.L. Canaletti, P. Poggi, M. Muselli, N. Heraud*

University of Corsica, Scientific Research Center of Vignola, Route des Sanguinaires, F-20000 Ajaccio, France
Phone: 33.4.95.52.41.52, Fax: 33.4.95.52.41.42
*E-mail: gilles,notton@univ-corse,fr
Internet site: http://spe.univ-corse.fr

Renewable Energy Team

Brief presentation

This research group belongs to the "Physical Systems for Environment" laboratory of the University of Corsica which is a Joint labs partnered with CNRS (National Centre for Scientific Research) of the Department of Information and Engineering Sciences and Technologies. The central theme of our research is the study of the optimal management of energy systems using renewable energy resources.

History of the laboratory

The young Corsican University was created in 1981 but it succeeded to an ephemeral university instituted in 1765 in Corte during Pascal Paoli's government. In the same time, the first research laboratory opened in Ajaccio (after the second oil crisis in 1979) and was dedicated to the study of solar energy systems and more particularly to studies on a 100 kW·e solar thermal electric power plant using solar tracking concentrators installed on the laboratory site (Fig. 1). In 1983, a 44 kW·p photovoltaic pilot plant has been implemented within the solar PV R&D European Economic Community Program (CEE-DG XII) in Paomia-Rondulinu (60 km of our laboratory) (Fig. 2) and the researches, having begun with solar thermal conversion, turned to the photovoltaic conversion and the hybrid systems to provide electricity for remote areas. Today, a large renewable energy research domain is treated and will be presented in the following paragraphs.

Fig. 1. *The research laboratory and 100 kW·e solar power plant*

Fig. 2. *The 44 kWp Photovoltaic power plant*

Research themes

The particularity of solar or wind conversion system comes from the random aspect of the energy sources lied to the no-foreseeable meteorological variation. Thus, even if the system if perfectly known from a mathematical point of view, some physical variables as, efficiency or productivity are lied to the spatio-temporal variations of the source but also of the load. For this reason, the knowledge and the characterisation of the energy source are essential and the solar and wind sources estimation is one of your main research activities.

Each subsystem (wind turbine, photovoltaic collector, battery…) constituting the global energy system is often precisely and individually studied by a lot of laboratories. Our objective is to study all the energy conversion line i.e. the global energy system.

Thus, the methodology used in our work integrates all these particularities and we use a global system approach integrating all the specificities due to the high variability of the energy source.

We can divide our research activities in 6 themes:

− study of the renewable energy resources;

− integration of thermal and/or electrical energy systems in the building and conception of innovating solar collectors;

− hybrid systems for electrical production;

− energy production using large-scale renewable energy systems;

− diagnosis of complex energy production system;

− drinkable water production using water vapour condensation.

Renewable energy sources characterization

As said previously, the study of the energy resources (solar or wind) is necessary to size, optimize and concept the renewable energy systems.

We developed and compared correlation models between various solar radiation components (diffuse, beam, global) on tilted planes because for our behaviour simulations, we need hourly global irradiations (and sometimes diffuse and beam) not easily available [1-2]. A result of this study is shown in Fig. 3.

Some statistical studies have been performed on wind speed or solar radiation data from Markov or ARMA stochastic models. The objective is to develop meteorological simulators used as an input in the simulation process in view to sizing and/or productivity estimation [3-5].

In view to a better estimation of the wind potential and the productivity of a wind turbine, we studied the turbulence phenomena of the wind using a "multi scaling" turbulence model.

The importance of the relief of Corsica introduces striking contrasts from a solar radiation and wind potential point of view; we project to develop a study concerning the solar estimation on all the territory and to analyse the performance of various small PV systems connected to the grid all over Corsica, thus we envisage to connect small PV systems with several meteorological stations disseminated on all the territory taking into account the spatial variability of the energy resource on a small area.

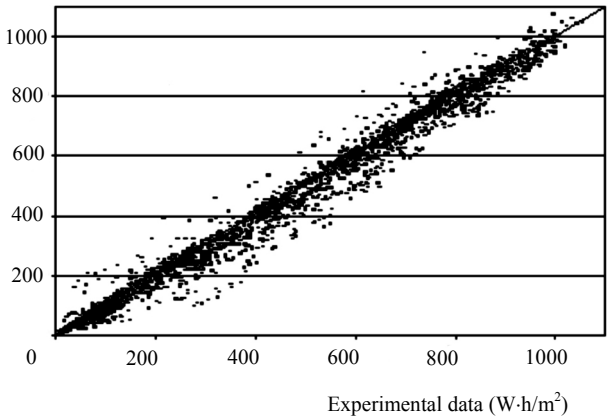

***Fig. 3**. Example of result of correlation to calculate hourly tilted global solar irradiations from horizontal ones*

Development of new solar collector and integration in buildings

We develop solar systems with a high integration level in the building to reduce the electrical or the fossil energy consumption. A copolymer solar water heating collector (MISTHERM® & MISFORCE®) [6-7] for which we modelled the thermal behaviour and optimized the configuration; today, the first one is certified and commercialized and the second one is in the process of being certified. We are working on a hybrid thermal/photovoltaic copolymer solar collector (Fig. 4) based on the previous concept and producing simultaneously electricity and heat. The main advantages of such a solar collectors are: of economical order compared to a combination of separate thermal and PV panels, the area covered with an hybrid solar collector produces more electrical and thermal energy than a corresponding area covered half with standard PV panels and half with conventional thermal collector; the average temperature of operation for the hybrid collector being generally lower than for a standard PV module and its electrical production is increased and at last, a hybrid collector provide architectural uniformity on a roof in contrast to a association of two separate solar collectors. This PV/T collector has been modelled (thermal and electrical behaviour) with its environment (water storage, tub) in low flow conditions with a thermal stratifiA solar or wind system is not only dependent on the individual performance and technical reliability of its components, it depends on the configuration and organization of various subsystems, on the running strategy and on its sizing, without forgetting the energy providing. cation of the tank to improve thermal performances [8].

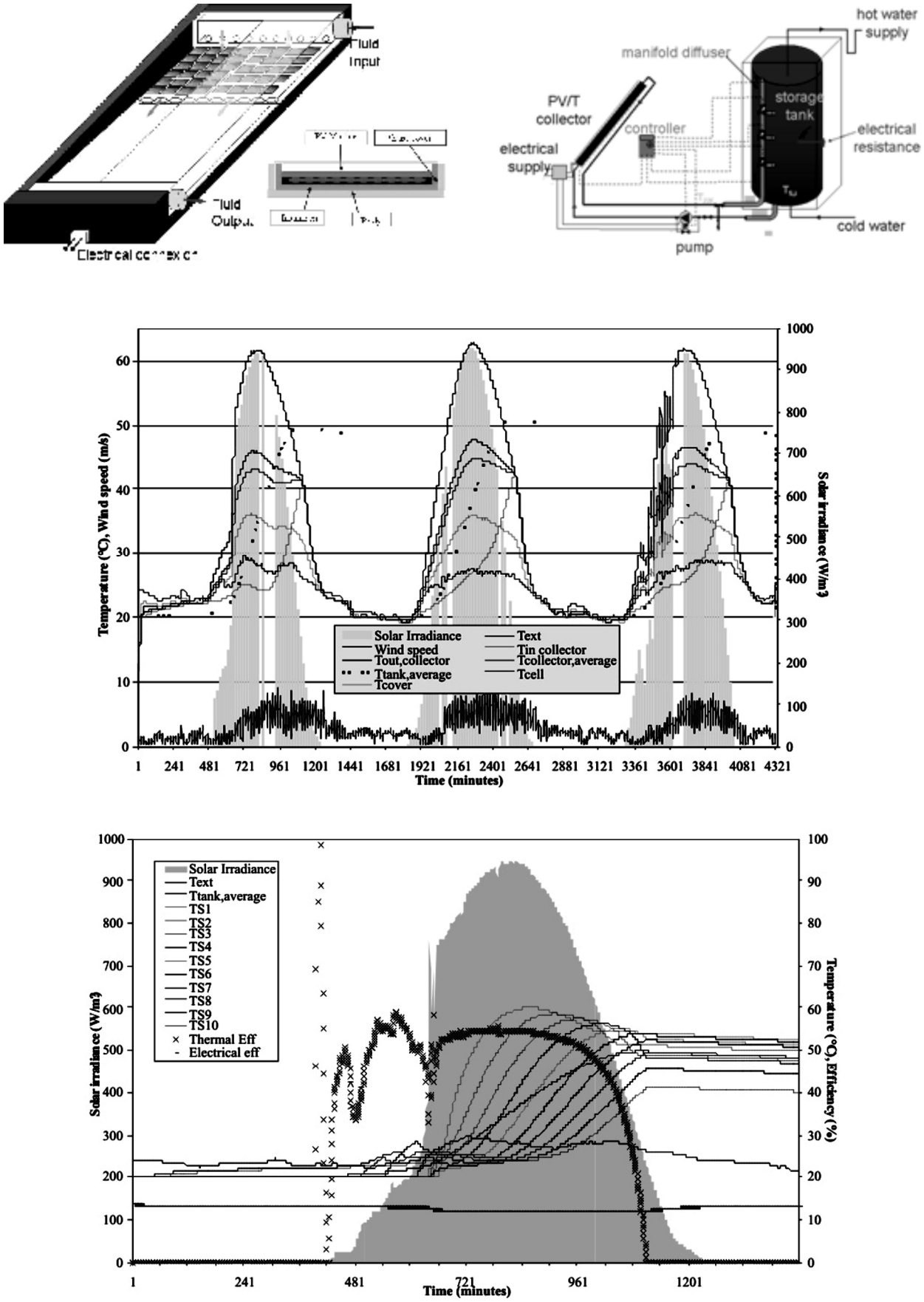

Fig. 4. *The PV solar collector: presentation and results*

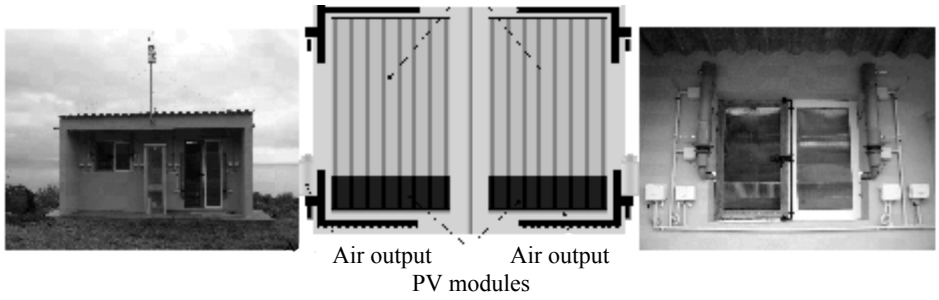

***Fig. 5**. The solar air shutter and the experimental device*

We developed an autonomous air solar collector (CASA® – Capteur à Air Solaire Autonome) with industrial partner SOLARIA SYSTEMS and a new version has been developed with an other local industrial partner (PERI® – Production d'Energie renouvelable Intégrée) about a new concept of air solar collector with high level of integration in the building: a solar air shutter (Fig. 5). The PV modules provide electricity for the air fan into the wall and the air is heated in the shutter before being injected in the house. We are testing, modelling and optimizing this solar air collector totally integrated in the shutter.

Hybrid systems for electrical production

A hybrid system is defined as: a system using more than one energy source and/or producing more than one energy carrier. To couple several energy sources increases the system reliability and the power to provide and to reduce the kW·h production cost. But, it increases too the complexity of the energy system. To produce simultaneous several energy carriers allow to reduce the area of the collector (best integration), to improve the global efficiencies and to reduce the energy losses.

According to this definition, we find:

– hybrid systems for electricity production (this paragraph);

– PV/T solar collector (see previous paragraph).

Hybrid systems are often used to provide electricity in remote areas in coupling various energy production systems as wind turbine, photovoltaic system, engine generator… (Fig. 6). These systems allow a more reliable and less expensive energy production. The problems regarding the design of such a hybrid system are: choosing the correct size of each component, optimizing the system management, optimizing economically the kW·h production cost.

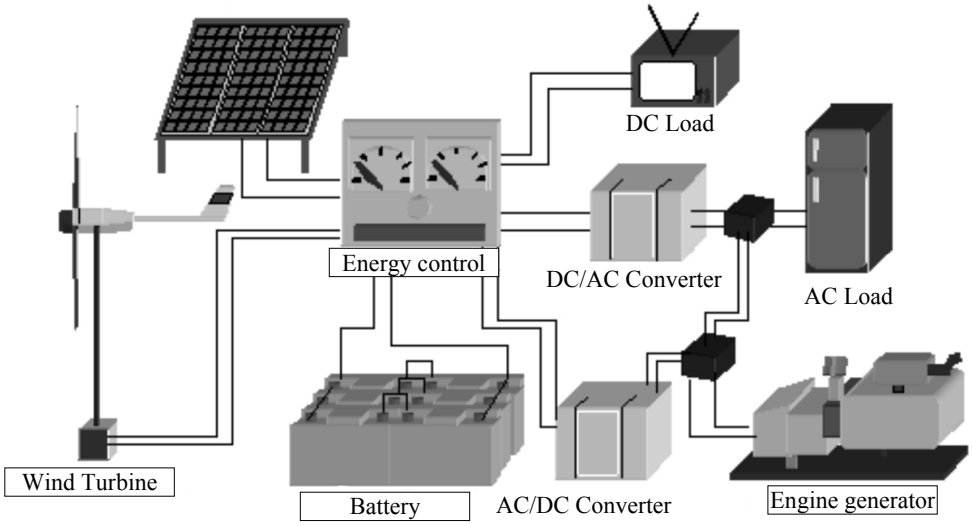

***Fig. 6.** Example of Hybrid system for electrical production*

We developed an optimal sizing methodology [9-12] using energy models for the behaviour of each subsystem. Concerning the behaviour simulation principle, we used a numerical method based on system energy balance and storage continuity equations. At last, a cost optimization is realized and allows to obtain the system producing the lowest kW·h cost.

Large scale renewable systems

It concerns systems directly connected to the grid. This production has some problems due to its high variability which perturbs the electrical network running and limits the integration rate of renewable systems in the electrical network [13-14].

We study the dynamical interactions between the production and the load and analyse the influence of some parameters as: centralisation or distribution of the energy systems, storage energy, electrical network size… to keep the network stability when the renewable production increases. The Corsican electricity network is interesting because it is very small and not connected to the continental network.

We study the influence of dispersed renewable power plant over the territory and the influence of an energy storage to compensate the variations of the renewable power. This storage can be realized by coupling a wind farm with a hydro electrical system as seen in Fig. 7 [15].

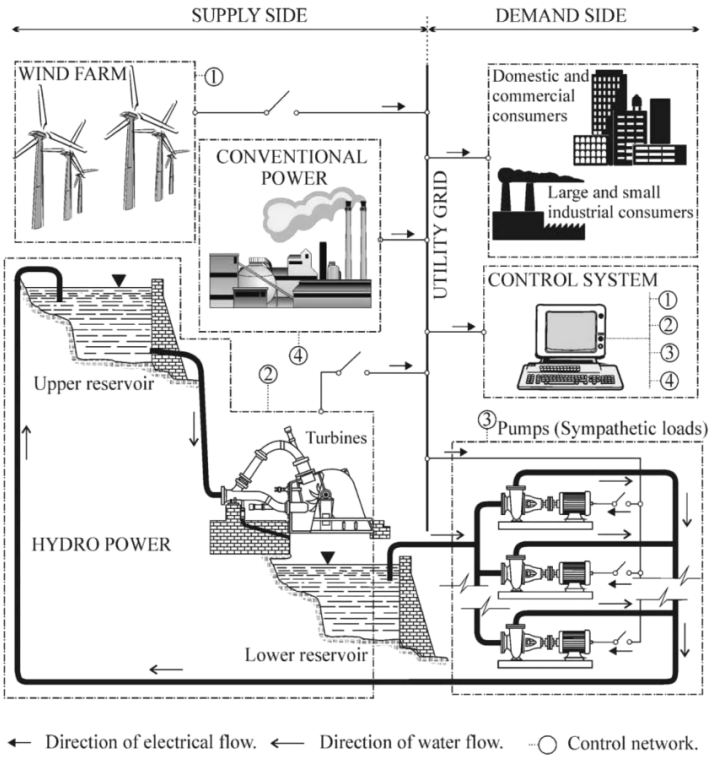

Fig. 7. *Coupling wind turbines with hydro-pumping storage*

Diagnosis of a complex energy system

The renewable energy conversion systems (wind, solar or hybrid) are often very complex. A lot of physical parameters occur in their running. The reliability of such systems is very important and it is necessary to develop methodologies of validations of data (reliability of information coming from automatic process) and of complex systems observability.

We must be sure of the process state or of the energy system state and we develop FDI (Fault Detection and Isolation) methods applied to renewable energy systems to detect the running anomalies of the system or a fault in the measure system or data transmission system [16-17].

This method is applied to a wind turbine to control the good running and looking for the reasons of faults in view to optimize the wind turbine production. A wind turbine model has been developed and the results have been validated on a 40 kW test platform at the University of Mandragon in Spain (Fig. 8). The final objective is to improve the algorithm to detect in real times the working faults and to realize in real time a diagnostic of the system.

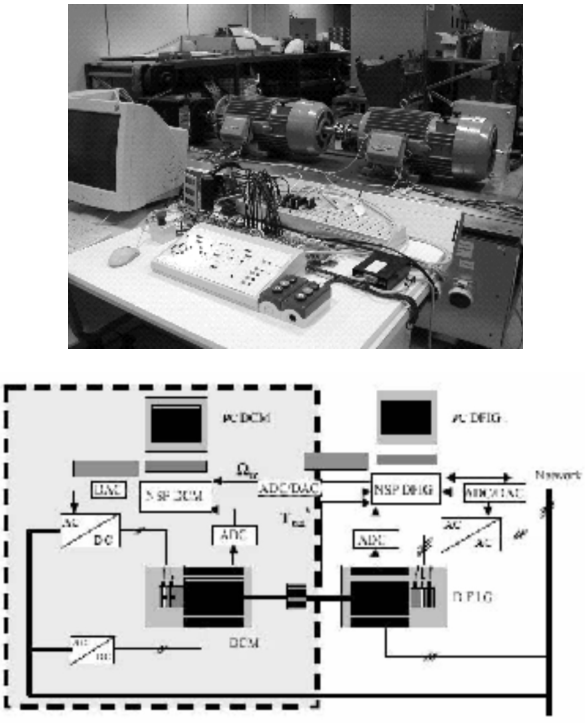

Fig. 8*. Experimental 40 kW platform at the University of Mandragon (Spain)*

Drinkable water production by condensation of atmospheric water vapour

The objective of this research is to develop passive energy systems (without using energy) able to condense the atmospheric water vapour to provide drinkable water for remote populations and to allow air-conditioning in developing countries.

Various prototype condensers have been developed and tested in various meteorological conditions. We defined two new materials for condensation: a plastic film (radiative foil) and a liquid one (painting) more easy to install using some minerals having interesting cooling and emissivity properties (white colour for hot countries allowing air-conditioning in diurnal cycle and dew condensation for night and uncoloured for only water production during nocturnal periods). These materials can cool rapidly and reach the dew temperature. New architectures have been developed too as for example a conic one allowing to increase their performances of 40 % per m^2. Such systems have been implemented and tested [18-20]:

– in Croatia (12 m² condensing roof);

– in French Polynesia in special windy conditions;

– in Israel (Neguev) with an efficiency of 0.6 L/m^2 per night;

– in India, with two plants : the first one at Saraya (850 m^2 of plane condensers) producing 200 L per night and the other one at Kutch with 15000 m² with a production up to 5 m^3 per night (Fig. 9).

a

b

***Fig. 9**. (a) a 850 m² dew plant in Panandhro (India) for bottled fresh water (at the final stage, a surface of 15,000 m² for the production of about 5 m^3/day); (b) a 40 m² dew plant with radiative paint for dew condensation and passive air-conditioning composed by 5 typical rooftop materials encountered in developing countries*

The potability of the water has been verified in a chemical and bacteriologic point of view and allows to conclude that dew water is potable for human use by a low filtering and classical disinfection process from French, European and WHO legislations.

New projects

We described in this paragraph the main research projects for the three next years:

Performance of PV systems

The objectives of this project are: to guarantee the productivity of a PV module, to estimate precisely the energy potential for a photovoltaic production and more particularly in building integration, to predict the production of a PV system connected to the network. Thus, several small meteorological stations will be implemented with 4 standard PV cells measuring solar radiation in various planes. In Corsica, these stations will be coupled with PV systems to study the influence of the grid network quality on the production of the PV systems.

New solar collector H2OSS®

We will study a new concept of water solar collector developed by a collaborating enterprise. It consists to totally integrate a solar water collector into a gutter. A prototype will be available in some months and we will test it, model it and look for optimization of the configuration of the system.

Water vapor condensers

Two objectives:

– development of new materials: less expensive and more efficient. A 30 m² prototype with 4 special substratum applied to developing countries.

– development of new architectures allowing to recuperate not only the condensed vapour but also the rain water. This study will be realized with the Indian Institute of Management.

Hybrid systems: renewable energies and hydrogen

We want to study a new hybrid system using fuel cells as a storage subsystem. Our objective is to develop a simulation model for each element of our system (PV system, fuel cell, electrolyser…) and to build a tool to optimize the configuration of such systems. This tool will be tested on an experimental device installed on the site of our laboratory.

The aim is to realise a modelling, a simulation and a study of the energetic performances of a hybrid system used to feed an electrical typical load for family (4 inhabitants). For instance, this energetic study is not associated to an economic one. The system is constituted by a photovoltaic array (PV), a wind turbine (WT) and a fuel cell used to produce the complementary power, and which is able to satisfy the load alone. The fuel cell used hydrogen produced by an electrolyzer. This electrolyzer

used the PV or WT energy not consumed by the load. At the beginning of the simulation, the hydrogen stock is assumed to be able to satisfy a given number of days of autonomy during winter.

The data used are the typical hourly load, the hourly solar radiation in the plane of the PV array, the hourly wind speed for one year, from our local meteorological station.

The objective is to adjust the peak power of the PV array, the nominal power of the wind turbine, the electrolyzer power, the fuel cell power to obtain the same quantity of hydrogen between the beginning and the end of the yearly simulation. We compute various parameters like the hydrogen volume in the stock at each instant. The configuration of the system and the first results are shown on Fig. 10.

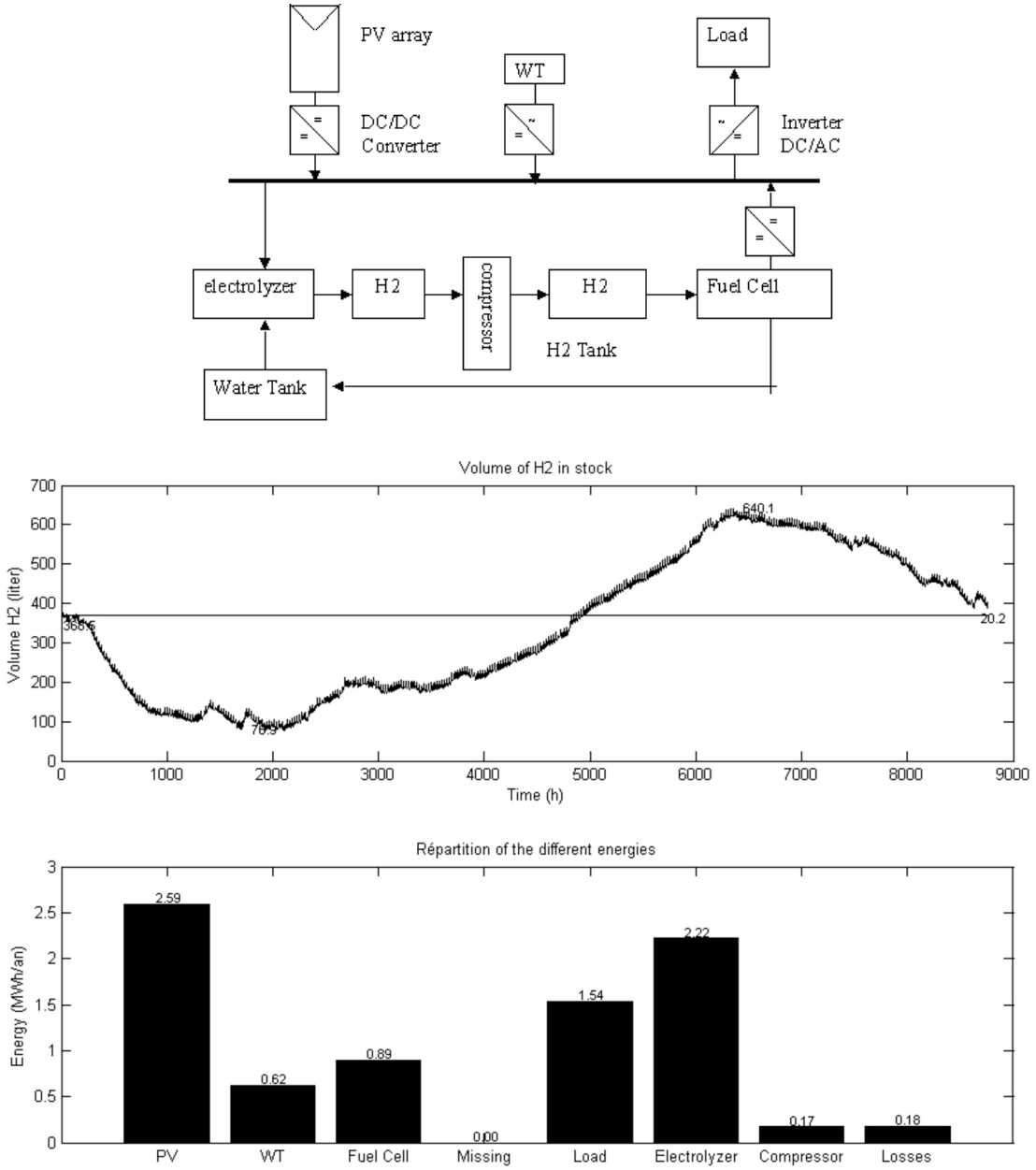

***Fig. 10**. Configuration of the hybrid system and first results*

R&D project: Coupling Renewable energy/H_2/ Fuel cells on an electrical grid

As previously said, the random characteristic of renewable sources limit the integration of renewable systems in an insular electrical grid. One solution to solve this problem consists in introduce an "energy storage". The hydrogen, coupled with renewable energy systems is recognized by scientists as a good solution. We develop with others collaborating organisms an experimental platform with a 3.5 MW PV plant, electrolysers, hydrogen and oxygen storage, and fuel cells (PEMFC) of about 200 kW. The two principal

objectives is, firstly to shave a part of the peak load on the grid, and secondly, after validated the capability of such systems to satisfy this constraint, to disseminate it on specific part of the electrical grid in the island, in view to increase the RES on Corsica.
This project is called MYRTE, and is sponsored by the Corsican Regional Collectivity, the French Governments and the European Community (FEDER).

Scientific collaborations

For three years, numerous collaborations have been developed all over the word.
Our research team is coordinator of a Scientific Exchanges Network between Eastern and Central European Countries and France supported by ADEME (French Environment and Energy Management Agency) and the French Ministry of Foreign Affairs. This network relates to all types of research teams and extends to all the fields from renewable energies. It concerns at the same time scientific and technical projects in Renewable energy. Nowadays, the network is constituted by:
In Eastern and Central European Countries:
- In Bulgaria, Technical University of Sofia, S. Nedeltcheva, V. Lazarov;
- In Romania, Polytechnical University of Bucarest, T. Apostol and Technical University of Construction of Bucarest, I. Colda, A. Damiani;
- In Russia, Moscow Power Engineering Institute and St. Petersburg State Polytechnical University;
- In Serbia, Center for heating, air conditioning and solar energy, University of Kragujevac, M. Bojic;
- In Slovenia, Mechanical Engineering Faculty, University of Ljubljana, V. Butala;
- In Albany, Energy Resources Department, Polytechnic University of Tirana, R. Aleti.

In France:
- Laboratory of Fluid Mechanical, ENSAM Paris, F. Massouh;
- LEG, Electrotechnical Laboratory, INPG Grenoble, C. Schaeffer;
- Electrotechnical Laboratory, Ecole Centrale of Lille, B. François;
- SPE, University of Corsica.

Other scientific partnerships have been developed according to the theme:
- Diagnosis: ENSAM Metz, ENSAM Paris, Mondragon University (Spain);
- Solar Thermal: CSTB (Scientific and Technical Centre for Building), Sophia-Antipolis;
- Radiative condensation: CEA/ESEME; Meteorological Institute of Zagreb (Croatia); The Arid Ecosystems Research Center (Israël); French Polynesian University; Indian Institute of Management (India); Wageningen University (Netherland);
- Renewable energy systems: Building physical Laboratory, University of Reunion; Renewable Energy Group of University of Antilles-Guyana; Physical Laboratory of Genova University (Italy), CEA DTS - INES Chambery and CEA DTH, HELION Fuel Cells Maker.

Teaching activities

In the same "Renewable Energy" field, three formations have been developed:
- a Master called "energy system and renewable energies" with about 30 students on 2 years;
- a Master called "Ecological Engineering" with 40 students on 2 years;
- a professional Licence called "Management of Renewable Energy" opened in the universitary year 2007-2008.

Conclusion

The panel of research activities developed in our laboratory is large but have a common objective which is to optimize the renewable energy systems in taking into account the specific character of these systems lying in the fact that the energy input is a random meteorological data. The large R&D project, 3.5 MW photovoltaic power plant with fuel cell storage, should allow to develop new activities with our partners and increase the potential of the team.

References

1. Notton G., Poggi P., Cristofari C. Predicting hourly solar irradiations on inclined surfaces based on the horizontal measurements: Performances of the association of well-known mathematical models // Energy Conversion and Management. 2006. Vol. 47, No. 13-14. P. 1816-1829.
2. Notton G., Poggi P., Cristofari C. Performance evaluation of various hourly slope irradiation models using Mediterranean experimental data of Ajaccio // Energy Conversion and Management. 2006. Vol. 47, No. 2. P. 147–173.
3. Poggi P., Muselli M., Notton G. et al. Forecasting and simulating wind speed in Corsica by using an autoregressive model // Energy Conversion and Management. 2003. Vol. 44. P. 3177-3196.
4. Muselli M., Poggi P., Notton G. et al. First order Markov chain model for generating synthetic typical days series of global irradiation in order to design PV stand alone systems // Energy Conversion and Management. 2001. Vol. 42, No. 6. P. 675-687.
5. Poggi P., Notton G., Muselli M.et al. Stochastic study of hourly solar radiation in Corsica by using a Markov model // International Journal of Climatology. 2000. Vol. 20, No. 14. P. 1843-1860.
6. Cristofari C., Notton G., Poggi P. et al. Modelling and performance of a copolymer solar water heating collector // Solar Energy. 2002. Vol. 72, No. 2. P. 99-112.
7. Cristofari C., Notton G., Poggi et al. Influence of the flow rate and the tank stratification degree on the

performances of a solar flat-plate collector // International Journal of Thermal Sciences. 2003. Vol. 42, No. 5. P. 455-469.
8. Cristofari C., Notton G., Poggi P. Modelling of a copolymer hybrid PV/T collector // 21th European Photovoltaic Solar Energy Conference and Exhibition, Dresden, Germany, 4-9 September 2006.
9. Notton G., Cristofari C., Poggi P. et al. Wind electrical supply system: behaviour simulation and sizing optimization // Wind Energy. 2001. Vol. 4, No. 2. P. 43-59.
10. Notton G., Muselli M., Poggi P. et al. Decentralized wind energy systems providing small electrical loads in remote area // International Journal of Energy Research. 2001. Vol. 25. P. 141-164.
11. Muselli M., Notton G., Poggi P. et al. PV-Hybrid power systems sizing incorporating battery storage: an analysis via simulation calculations // Renewable Energy. 1999. Vol. 20, No. 1. P. 1-7.
12. Muselli M., Notton G., Poggi P. et al. Computer aided analysis of the integration of renewable energy systems in remote areas using a Geographical Information System // Applied Energy. 1999. Vol. 63, No. 3. P. 141-160.
13. Poggi P., Muselli M., Notton G. et al. Wind farm peak load matching potential in Corsica // 2001 European Wind Energy Conference and Exhibition, ISBN 3-936338-09-4, Copenhaguen, Danemark, 2-6 July 2001. P. 1139-1141.
14. Nedeltcheva S. Poggi P., Notton G. et al. Examination of the influence of the dispersed generation in the distribution networks for medium voltage // IEEE Congress, First International Symposium on Environment, identities in Mediterranean Area, 10-13 July 2006, Corte-Ajaccio.
15. Poggi P., Muselli M., Cristofari C. et al. Coupling hydro and wind electricity production by water-pumping storage // IEEE Congress, First International Symposium on Environment, identities in Mediterranean Area, 10-13 July 2006, Corte-Ajaccio.
16. Bennouna O., Héraud N., Camblong H. et al. Diagnosis of the Doubly Fed Induction Generator of a Wind Turbine // Wind Engineering Journal. 2005. Vol. 29, No. 5. P. 431-448.
17. Bennouna O., Heraud N., Cristofari C. Observability and reliability of a photovoltaic sensor // IEEE International Symposium in Industriel Electronics. Ajaccio, May 4-7, 2004.
18. Muselli M., Beysens D., Milimouk I. A Comparative Study of Two Large Radiative Dew Water Condensers // Journal of Arid Environment. 2006. Vol. 64. P. 54-76.
19. Muselli M., Beysens D., Soyeux E. Is Dew Water Potable? Chemical and Biological Analyses of Dew Water in Ajaccio (Corsica Island, France) // Journal of Environmental Quality. 2006. Vol. 35. P. 1812-1817.
20. Beysens D., Mileta M., Milimouk I. et al. Collecting dew to improve water resources: the D.E.W. project in Biševo (Croatia) // Energy. 2007. Vol. 32, No. 6. P. 1032-1037.

SOCIETE MAROCAINE DES ARGILES - SMA (MOROCCAN SOCIETY OF CLAYS)

Head*: Saad Safrioui
Secretary**: Abdelilah Dekayir
Author: Lahcen Daoudi***

University Moulay Ismail
Faculty of Sciences
BP 11201, Zitoune-Meknès
www.ucam.ac.ma/sma

*E-mail: saad.sefrioui@ghassoul.org, Phone: (212) 35 64 22 52, Fax: (212) 35 64 16 71
** E-mail: dekayir@yahoo.fr, Phone: (212) 35 53 68 08, Fax: (212) 35 53 68 08
*** E-mail: daoudi@fstg-marrakech.ac.ma, Phone: (212) 24 43 34 04, Fax: (212) 24 43 31 70

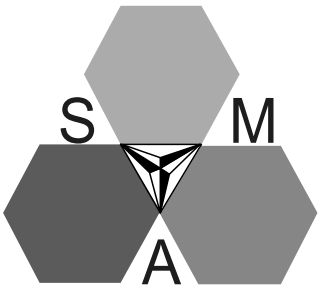

Logo of the group

Brief presentation

During these two last decades, clay minerals have been the subject of many research domains in Morocco; they are used in many industrial applications. Following the example of the international groups of clays, the Moroccan Society of Clays (Société Marocaine de Argiles; SMA), is created with an aim of promoting the sector of clays, by the reinforcement of the bonds between the various actors on the one hand and of the development of the partnership between the University and industrial circle, on the other hand.

Objectives of the Group

The principal objectives of the group are:
− To contribute to the promotion of scientific research, as well fundamental as applied, having milked with clays.
− To create a synergy between the various actors in this field, in the aim for the valorization of this natural resource.
− To contribute to the diffusion of the research tasks at the national and international level by the publishing of a scientific review.
− To organize scientific demonstrations.
− To tie relations of co-operation with other national and international associations, specially with the international groups of clays.
− To organize continuous trainings and all other activities allowing to develop this natural resource.

General description

During these two last decades, a particular interest was granted to the study of moroccan clays. In geology they are used as indicators of environment conditions. In petroleum geology their study provides good ideas about thermal conditions of oil reservoir and specially maturation gradient. Clay minerals have also been used in many industrial applications like building materials; in soil science in front of their absorption properties they are very useful in the conception and production of fertilizers for soils. They are widely used in cosmetics and pharmaceutical products.

With an aim of developing a synergy between the various national actors having milked with these materials, two scientific meetings were organised in Morocco by academics. The First Moroccan Symposium of Clays (SMA1) was held in Marrakech (Cadi Ayyad University) December the 11, and 12 - 2003, with more than one hundred participants. The website of this symposium is (www.ucam.ac.ma/fssm/sma1). The Second Maghrebian Symposium of Clays (SMA2) was held in Meknes (Moulay Ismail University) April the 22, and 23 - 2006, with also about one hundred participants. The website of this symposium is (www.fsmek.ac.ma/sma2). On proposal of the Steering Committee of SMA1, it was adopted, during the meeting of closure first symposium, to create the Moroccan group of study of clays. Thus, a committee was constituted to work out a project of statute. As been appropriate, the statute is written, and then dispatched with the participants for amendment. The organization of SMA2 constituted in fact an opportunity for the outcome of this work.

The emanating committee of the meeting of closure second symposium undertook to call with a meeting to form the Moroccan Company of Clays (SMA). Indeed, a full session was held in Meknes, December the 12 - 2006 at the "Ecole Nationale Supérieure des Arts et Métiers". During this session, the present unanimously adopted the statute and the creation of SMA, and elected a board of directors.

Board of directors

S. Sefrioui, president, director of Société Ghassoul et ses Dérivés – Fès.
A. Bellamlih, vice president, director of Poterie Bellamlih – Meknès.
A. Dekayir, secretary, professor, Faculté des Sciences – Meknès.
M. Hajjaji, vice secretary, professor, Faculté des Sciences – Marrakech.
M. el Maataoui, treasurer, professor, Faculté des Sciences – Meknès.
L. Badra, consilor, professor, Faculté des Sciences – Meknès.
B. Rhouta, consilor, professor, Faculté des Sciences et Techniques – Marrakech.
L. Daoudi, consilor, professor, Faculté des Sciences et Techniques - Marrakech.
N. Tijani, consilor, professor, Faculté des Sciences – Meknès.

Thematics of the group

− Clay Chemistry in weathering and soils.
−- Environment.
− Diagnosis and Hydrothermal alteration.
− Archaeomaterials.
− Industrial Applications.
− Advanced Analytical Technique for Clay Characterization.
− Geomechanics.

Photo of the group after the full session (Meknes, December the 12 – 2006)

ПОДПИСКА-2008

Международный научный журнал
«Альтернативная энергетика и экология»

Уважаемые коллеги! Продолжается подписка на второе полугодие 2008 г.

Наименование:
Международный научный журнал
«Альтернативная энергетика и экология»
Индекс издания: ISSN1608-8298
Периодичность: выходит ежемесячно
Объем издания (страниц): 200–270
Вид рассылки: адресный
Официальный сайт:
http://isjaee.hydrogen.ru
Подписка: через редакцию или по каталогам: Роспечать, МК-Периодика, Интерпочта и др.

Уважаемые читатели!

Вы можете подписаться на Международный научный журнал «Альтернативная энергетика и экология» на 2008 год, заполнив извещение (форма ПД-4) и перечислив на счет НТЦ «ТАТА» сумму в соответствии с таблицами 1 и 2. Копию корешка извещения, пожалуйста, направьте по адресу:

НТЦ «ТАТА»
607183, Нижегородская обл., г. Саров, а/я 687
Генеральному директору А.Л.Гусеву

Пожалуйста, не забудьте в сопроводительном письме указать почтовый адрес получателя подписки.

Оплата осуществляется перечислением денежной суммы на расчетный счет. Юридическим лицам для получения счета необходимо направить запрос по электронной почте gusev@hydrogen.ru или по факсу (83130) 6-31-07 с указанием реквизитов организации.

Извещение

Форма ПД-4

ООО НТЦ «ТАТА»
(наименование получателя платежа)

5254022656 / 525401001
(ИНН получателя платежа)

N 40702810900000001679
(номер счета получателя платежа)

в ОАО «АКБ Саровбизнесбанк» г. Саров
(наименование банка и банковские реквизиты)

к/с 30101810200000000721

042204721
БИК

(*наименование платежа)

Дата_____Сумма платежа:_____руб.___коп.

Кассир

Плательщик (подпись) _____

Форма ПД-4

ООО НТЦ «ТАТА»
(наименование получателя платежа)

5254022656/525401001
(ИНН получателя платежа)

N 40702810900000001679
(номер счета получателя платежа)

в ОАО «АКБ Саровбизнесбанк» г. Саров
(наименование банка и банковские реквизиты)

к/с 30101810200000000721

042204721
БИК

(*наименование платежа)

Дата_____Сумма платежа:_____руб.___коп.

Квитанция

Кассир

Плательщик (подпись) _____

**Внимание! В графе извещения «Наименование платежа» просьба указать Ф.И.О., почтовый адрес получателя, порядковый номер и год выпуска журнала(ов), например: Иванов И.И., 197198, Санкт-Петербург, пр. Добролюбова, 67–14, №1–6 за 2004 г., или №4 за 2002 г.*

Внимание!

Начиная с 31 марта 2007 года всем членам Редколлегии Международного научного журнала «Альтернативная энергетика и экология» предоставляется скидка на подписку:

– членам Редакционного научного комитета — 40% от базовой стоимости*;

– заместителям главного редактора — 30% от базовой стоимости*;

– членам Международного редакционного комитета — 25% от базовой стоимости*;

– членам Международного научно-консультативного совета редакции — 20% от базовой стоимости*;

– членам Совета экспертов — 20% от базовой стоимости*;

– членам Совета рецензентов — 15% от базовой стоимости*.

При осуществлении подписки сразу на весь год базовая стоимость годовой подписки равна удвоенной базовой стоимости на первое полугодие 2008 г. с дополнительной скидкой 5 %.

Заявка на подписку направляется в Редакцию журнала в произвольной форме по адресу: gusev@hydrogen.ru или по факсу: 8-83130-63107.

* При определении базовой стоимости подписки на первое полугодие 2008 г. необходимо руководствоваться Таблицей 1 или Таблицей 2 для различных категорий подписчиков.

Стоимость подписки для различных категорий подписчиков на второе полугодие 2008 года

Таблица 1

Россия

Категория	Стоимость, руб.
Аспиранты	3000
Пенсионеры	3300
Физические лица	4200
Фирмы-распространители	3900
Научные библиотеки организаций	4800
Научно-исследовательские организации	5600
Научно-производственные организации	6000
Российские научные центры	7200
Российские научные ассоциации	7800
Международные научные ассоциации	8700
Национальные и муниципальные научные библиотеки	9000

Таблица 2

Страны СНГ

Категория	Стоимость, руб.
Физические лица	4800
Фирмы-распространители	4200
Научные библиотеки организаций	5400
Научно-исследовательские организации	6000
Научно-производственные организации	6600
Национальные научные центры	7200
Национальные научные ассоциации	8100
Международные научные ассоциации	8400
Национальные и муниципальные научные библиотеки	9000

Информация о плательщике:

(Ф.И.О., адрес плательщика)

(ИНН налогоплательщика)

N

(номер лицевого счета (код) плательщика)

Информация о плательщике:

(Ф.И.О., адрес плательщика)

(ИНН налогоплательщика)

N

(номер лицевого счета (код) плательщика)

ВНИМАНИЕ! По этой квитанции Вы можете оплатить как годовую подписку, так и отдельные номера нашего журнала за 2002–2007 гг.

SUBSCRIPTION-2008

International Scientific Journal for
Alternative Energy and Ecology

Dear Colleagues! Subscription for the year 2008 is available

Issue: International Scientific Journal for Alternative Energy and Ecology (ISJAEE)
ISSN 1608-8298
Periodicity: monthly
Issue volume (pages): 200–270
Distribution: Address

Official site: http://isjaee.hydrogen.ru
Subscription: via editorial board and catalogue

Table 1

Subscription	Physical person	Juridical person	Member of International Association for Hydrogen energy	Member of Editorial board of ISJAEE
Quarter	€110	€235	€75	€60
Half year	€220	€470	€150	€130
Annual	€440	€940	€300	€260

To have an account, juridical persons are to send order by e-mail to **gusev@hydrogen.ru** or by fax **(83130) 6-31-07** mentioning the institution address.

ORDER FORM

To: Scientific Technical Centre «TATA»
P.O.Box 687
Sarov, Nizhnii Novgorod region 607183, Russia
Phone/Fax: +7 (83130) 6-31-07
Phone: +7 (83130) 9-74-72
E-mail: gusev@hydrogen.ru

Please, send me _____ copy/copies of "International Scientific Journal for Alternative Energy and Ecology", ISSN 1608-8298 (_____ issues, 200__ year, _____ € (please, see Table 1), postage included)

Payments options

I've arranged a bank transfer to:

General Director STC «TATA» Limited
SWIFT SABRRUMMNA1
SAVINGS BANK OF THE RUSSIAN FEDERATION
(VOLGO-VYATSKY OFFICE) BRANCH 7695, SAROVSKOE
A/C: 30301840342000604241
STC «TATA» LIMITED INN 5254022656
CORRESP. BANK: Deutsche Bank, Frankfurt am Main,
SWIFT DEUTDEFF
POST BOX 687
607183, SAROV, NIZHNY NOVGOROD REGION, RUSSIA
TRANSIT COUNT 40702978342410200055
Details of payment: «International Scientific Journal for Alternative Energy and Ecology»

Name _____
Organization _____
Mailing Address _____
Number Building_____ Street _____
City_____ State _____
Postal code_____Country _____
E-mail _____ Phone _____
Fax _____
Signed _____ Date _____

SUBSCRIPTION-2008

International Scientific Journal for
Alternative Energy and Ecology

ISJAEE

Dear Colleagues! Subscription for the year 2008 is available

Issue: International Scientific Journal for Alternative Energy and Ecology (ISJAEE)
ISSN 1608-8298
Periodicity: monthly
Issue volume (pages): 200–270
Distribution: Address
Official site: http://isjaee.hydrogen.ru
Subscription: via editorial board and catalogue

Table 2

Subscription	Physical person	Juridical person	Member of International Association for Hydrogen energy	Member of Editorial board of ISJAEE
Quarter	$150	$320	$100	$90
Half year	$300	$640	$200	$180
Annual	$600	$1280	$400	$360

To have an account, juridical persons are to send order by e-mail to **gusev@hydrogen.ru** or by fax **(83130) 6-31-07** mentioning the institution address.

ORDER FORM

ISJAEE

To: Scientific Technical Centre «TATA»
P.O.Box 687
Sarov, Nizhnii Novgorod region 607183, Russia
Phone/Fax: +7 (83130) 6-31-07
Phone: +7 (83130) 9-74-72
E-mail: gusev@hydrogen.ru

Please, send me _____ copy/copies of "International Scientific Journal for Alternative Energy and Ecology", ISSN 1608-8298 (_____ issues, 200__ year, _____ $ (please, see Table 1), postage included)

Payments options

I've arranged a bank transfer to:

STC «TATA» Limited
ACC: 40702840200001001681
BEN. BANK: SAROVBUSINESSBANK
SAROV, RUSSIA
CORR. ACC USD: 30109840300000000142
CORRESP. BANK: ALFA-BANK,
MOSCOW, RUSSIA, SWIFT: ALFARUMM
CORR. ACC USD: 400927098 with «CHASE MANHATTAN BANK», NEW YORK, N.Y.10004, USA. SWIFT: CHASUS33
Details of payment: «International Scientific Journal for Alternative Energy and Ecology»

Name _____
Organization _____
Mailing Address _____
Number Building_____ Street _____
City_____ State _____
Postal code_____Country _____
E-mail _____ Phone _____
Fax _____
Signed _____ Date _____

РЕКЛАМА В МЕЖДУНАРОДНОМ НАУЧНОМ ЖУРНАЛЕ «АЛЬТЕРНАТИВНАЯ ЭНЕРГЕТИКА И ЭКОЛОГИЯ»

Международный научный журнал «Альтернативная энергетика и экология» приглашает научные институты, организации и промышленные предприятия разместить информацию о конференциях, выставках, разрабатываемой и выпускаемой продукции в области альтернативной энергетики и экологии.

Площади рекламного модуля

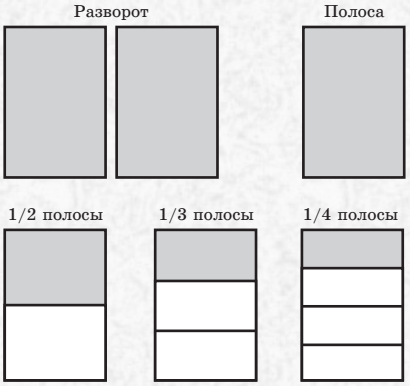

Требования к макетам рекламных модулей, изготовленных заказчиком

Макет рекламного модуля должен иметь размер, соответствующий размеру печатного оттиска. Форматы макетов: растровый — TIFF (см. требования), векторный — Corel Draw (см. требования). Использование редактора Microsoft Word для проектирования макетов рекламных модулей не допускается.

Допускается предоставление макета модуля (кроме обложки) в формате Adobe Pagemaker версий 6.0, 6.5, 7.0. В этом случае должны предоставляться все связанные элементы, а также все используемые шрифты.

Требования к исходным рекламным материалам

Все элементы рекламного модуля (иллюстрации, логотипы, текст и др.) предоставляются в отдельных файлах.

1. Текст

Текст набирается гарнитурой Times New Roman, кегль 14, интервал полуторный. Допускается выделение важной информации полужирным начертанием. Формат Microsoft Word for Windows.

Использование OLE-объектов (графики, слайды презентаций, диаграммы в формате Microsoft Excel, результаты вычислений в математических и иных, в том числе собственных программах) в документах не допускается. Такие объекты присылаются в формате исходной программы и дублируются изображением (см. требования к иллюстрациям).

Использование дополнительных шрифтов (например, логотип выполнен специфической гарнитурой) оговаривается дополнительно. В этом случае предоставляется файл, содержащий начертание букв в формате TTF. Использование PS-шрифтов не допускается.

2. Иллюстрации

Все иллюстрации, находящиеся в рекламном модуле, должны предоставляться в отдельных файлах в форматах TIFF или BMP. Не допускается использование многослойных изображений. Черно-белые изображения должны быть в модели Grayscale. Цветные (обложка) — в модели CMYK. Все ч/б растровые изображения должны иметь разрешение 200 dpi, цветные — 250–400 dpi.

Для векторных изображений предпочтительным является использование формата Corel Draw (*.cdr) до версии 12.0 включительно.

Все встроенные эффекты (линзы, текстурные заливки, тени и т.д.) должны быть переведены в растровое изображение (bitmap). Векторные эффекты (Extrude, Envelope, Contour, Add Perspective, Blend, Distortion, Artistic media) должны быть преобразованы в кривые. Все текстовые объекты должны быть переведены в кривые. Размещение растровых рисунков в документе Corel Draw не допускается.

Стоимость размещения рекламных модулей

Объем рекламного модуля	Технические параметры	Цена публикации в одном номере (руб.)
Обложка (полноцветная)	285x205 мм	300 000
2-я или 3-я страницы обложки (полноцветная)	285x205 мм	50 000
Полный разворот на две полосы*	257x336 мм	25 000
Полная полоса 1/1*	257x168 мм	10 000
1/2 Полосы*	128x168 мм	7 500
1/3 Полосы*	85x168 мм	2 500
1/4 Полосы*	64x168 мм	2 000
СИСТЕМА СКИДОК		
При публикации в 2-3 номерах	10%	
При публикации в 4-6 номерах	15%	
При публикации в 7-9 номерах	20%	
При публикации в 10-12 номерах	50%	

Для заказа рекламной площади и получения счета необходимо заполнить форму заявки и отправить ее по адресу gusev@hydrogen.ru или по факсу (83130) 6-31-07.

Редакция журнала оставляет за собой право отбора поступивших рекламных объявлений.

ADVERTISEMENT IN INTERNATIONAL SCIENTIFIC JOURNAL FOR ALTERNATIVE ENERGY AND ECOLOGY

The International scientific journal "Alternative energy and economy" invites scientific institutes, organizations and industrial enterprises to place advertisements on conferences, exhibitions, designed and production products in the field of alternative energy and ecology.

Spaces for advertisement module

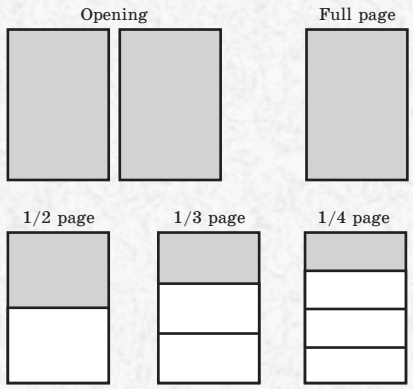

General information on lay-outs of advertisement modules fabricated by a customer

The lay-out of an advertisement module is to have the dimension in accordance with that of a print. Lay-out formats: raster — TIFF (see General information), vector — Corel Draw (see General information). The use of Microsoft Word editor to design lay-outs of advertisement modules is not allowed.

The module lay-out (except the cover) in the format of 6.0, 6.5, 7.0 Adobe Pagemaker versions is allowed to be provided. In this case, all combined elements, and also all available fonts that are not included in the Microsoft Windows structure are to be provided.

Information on original advertisements

All elements of the advertisement module (illustrations, symbols, text, etc.) have to be put in individual files.

1. Text

Text is has to be composed by Times New Roman types, font 14, print interval: one and a half. Important information can be printed in italics. Format — Microsoft Word for Windows.

OLE-objects (graphs, presentation slides, diagrams in Microsoft Excel format, results of computations in mathematical and others including own programmes) are not allowed in documents. The objects as such are required to be sent in original programme format, and are copied by illustrations (see General information on illustrations).

The use of additional fonts (for example, a symbol is given by a specific type) is additionally specified. In this case, a file containing letter design in TTF format. PS-fonts is not allowed.

2. Illustrations

All illustrations available in the advertisement module are to be displayed in TIFF or BMP formats. Multilayer displays are not allowed. Black-and white displays are to be used in Grayscale model. Coloured displays (cover) are in CMYK model. All black-and-white raster displays are to be of resolution of 200 dpi, colour — of 250–400 dpi.

The use of Corel Draw (*.cdr) format to 12 version inclusive is considered to be advantageous for vector display.

All incorporated effects (lenses, texture fillings, shadows, etc.) are to be converted to raster display (bitmap). Vector effects (Extrude, Envelope, Contour, Add Perspective, Blend, Distortion, Artistic media) are to be transformed to curves. All text objects are to be converted to curves. Raster figures are not allowed to be placed in Corel Draw document.

Advertisement space price

Advertisement module space	Technical parameters	Publication price in one issue ($US)
1st page of the cover (full-coloured)	160x145 мм	15000
Full opening in two pages	257x336 мм	2000
2nd or 3d pages of the cover (full-coloured)	257x168 мм	4000
Full page	128x168 мм	1000
1/2 page	85x168 мм	500
1/3 page	64x168 мм	150
1/4 page	64x168 мм	100
Price rebate		
When published in 2-3 issues	5%	
When published in 4-6 issues	7%	
When published in 7-9 issues	10%	
When published in 10-12 issues	15%	

To order an advertisement space and make up a bill, please fill in an order form and send it using the following address: gusev@hydrogen.ru or by fax +7 (83130) 6-31-07.

The editorial board reserves the right to choose advertisements entered.

ПЕРЕЧЕНЬ
НЕОБХОДИМЫХ МАТЕРИАЛОВ ДЛЯ ПУБЛИКАЦИИ В МЕЖДУНАРОДНОМ НАУЧНОМ ЖУРНАЛЕ «АЛЬТЕРНАТИВНАЯ ЭНЕРГЕТИКА И ЭКОЛОГИЯ»

Для своевременного выхода журнала и быстрой публикации работ авторы должны предоставлять в редакцию материалы по перечню, приведенному в таблице ниже. Авторы должны заполнить знаками (+) или (-) графы в столбце «Наличие»

№ п/п	Материал	Наличие
1	Твердая копия рукописи статьи	
2	Электронная версия рукописи статьи	
3	Название статьи на русском языке	
4	Название статьи на английском языке	
5	УДК (PACS)	
6	Автор(ы) статьи	
7	Координаты организаций авторов (включая телефоны и e-mail)	
8	Рисунки (фотографии, схемы)	
9	Подрисуночные подписи на русском языке	
10	Подрисуночные подписи на английском языке	
11	Таблицы	
12	Названия таблиц на русском языке	
13	Названия таблиц на английском языке	
14	Ссылки в тексте на таблицы и рисунки	
15	Список литературы (библиография)	
16	Библиографические ссылки в тексте в соответствии со списком литературы	
17	Структурированность текста, наличие подзаголовков	
18	Аннотация на русском языке	
19	Аннотация на английском языке	
20	Реферат на русском языке	
21	Реферат на английском языке	
22	Резюме на каждого автора (если авторов не более 6) или на главного автора*	
23	Фотография автора (авторов)*	
24	Разрешение на опубликование в открытой печати (экспертное заключение)	
25	Интернет-сообщение на русском языке*	
26	Интернет-сообщение на английском языке*	
27	Соглашение авторов на публикацию статьи в журнале	
28	Рецензии	
29	Сопроводительное письмо руководителя организации (или письмо автора)	
30	Акт проведенных испытаний (если в статье присутствует экспериментальная часть), подписанный участниками испытаний*	

* Материалы, предоставляемые по желанию

CONSENT TO PUBLISH &TRANSFER OF COPYRIGHT

For the mutual benefit and protection of Authors and Publishers it is necessary that Authors provide formal written Consent to Publish and Transfer of Copyright before publication of the Work. The signed Consent ensures that the Publisher has the Author's permission to publish the relevant Contribution. The signed Transfer entitles the Publisher on behalf of the Autor to protect the Contribution against unauthorised use and authorise dissemination by means of offprints, legitimate photocopies, microform editions, reprints, translations, and secondary information sources such as abstracting and indexing services including data bases. The Publisher hereby request the Author to complete and return this form promptly so as to ensure the proper conduct of business.

Title of Contribution:

Author (s):

Title of Work:

Editor(s):

1. The Author hereby assigns to the Publisher the copyright to the Contribution named above whereby the Publisher shall have the exclusive right to publish the said Contribution, and translations of it wholly or in part, throughout the World during the full term of copyright and all renewals and extensions thereof. These rights include without limitation mechanical, electronic and visual reproduction; electronic storage and retrieval; and all other forms of electronic publication or any other types of publication including all subsidiary rigths.

2. The Author retains the right to republich the Contribution in any collection consisting soley of the Author's own Works without charge and subject only to notifying the Publisher of the intent to do so and to ensuring that the publication by the Publisher is properly credited and that the relevant copyright notice is repeated verbatim.

3. In the event of receiving any other request to reprint or translate all or part of the Contribution the Publisher shall endeavour to obtain the approval of the Author prior to giving any such permission.

4. The Author warrants and represents that the Contribution does not infringe upon any copyright or other right(s), and that it does not contain infringing, libellous, obscene or other unlawful matter, that he/she is the sole and exclusive owner of the rights herein conveyed to the Publisher, and that he/she has obtained the customary permission from the copyright owner of his legal representative whenever a passage from copyrighted material is quoted or a table or illustration from such material is used. The Author will indemnify the Publisher for, and hold the Publisher harmless from any breach of the foregoing warranties as a result of publication of the Contribution. The contribution shall be delivered to the Publisher free of copyright charges.

5. The Author quarantees that the Contribution to the Work has not been previosly published elsewhere, or that if it has been published in whole or in part, any permission necessary to publich it in the work has been obtained and provided to Scientific Technical Centre "TATA" Ltd. together with a statement of the original copyright notice.

6. The Author declares that any person named as co-author of the Contribution is aware of the fact and has agreed to being so named.

7. Each first-named author will receive 5 free offprints of his/her article. If additional offprints are required, the editor should be informed upon delivery of the article.

Date _____ Name _____ Date _____ Name _____

Signature* Signature**

*To be signed by the Author, also on behalf of any co-authors, or to be signed by the Employer, where appropriate

** To be signed by the Editor-in-Chief

NAME _____

ADDRESS _____

CITY _____ POSTAL CODE _____

STATE _____ COUNTRY _____

TEL. _____ FAX _____

К сведению авторов.

Редакция Международного научного журнала «Альтернативная энергетика и экология» считает, что авторы, направляя рукопись в Редакцию, согласны передать учредителям и редколлегии Международного научного журнала «Альтернативная энергетика и экология» право опубликовать рукопись на русском языке и в переводе на английском языке. Просим авторов прикладывать к направляемой рукописи Соглашение по форме, приведенной ниже. При этом за авторами сохраняются все остальные права как собственников этой рукописи.

СОГЛАШЕНИЕ О ПЕРЕДАЧЕ АВТОРСКОГО ПРАВА НА ПУБЛИКАЦИЮ

Мы, нижеподписавшиеся, авторы рукописи

_____

_____

_____

_____

передаем учредителям и редколлегии Международного научного журнала «Альтернативная энергетика и экология» право опубликовать эту рукопись на русском языке и в переводе на английском языке. Мы подтверждаем, что эта публикация не нарушает авторского права других лиц или организаций.

Подписи авторов: (ф.и.о., дата, адрес).

_____

_____

_____

_____

Редакция Международного научного журнала «Альтернативная энергетика и экология» принимает статьи как на русском, так и на английском языках. В последнем случае качество языка подвергается дополнительной экспертизе. Кроме того, редакция оставляет за собой право при необходимости запросить русскоязычную версию статьи. Рукописи необходимо направлять по адресу:

Россия,
Нижегородская область, Саров, 607183,
а/я 687,
Редакция АЭЭ,
E-mail: gusev@hydrogen.ru

Подпись Главного редактора _____ /А.Л. Гусев/

ЕЖЕМЕСЯЧНЫЙ РЕЦЕНЗИРУЕМЫЙ И РЕФЕРИРУЕМЫЙ МЕЖДУНАРОДНЫЙ НАУЧНЫЙ ЖУРНАЛ «АЛЬТЕРНАТИВНАЯ ЭНЕРГЕТИКА И ЭКОЛОГИЯ»

Вниманию авторов!

Каждая рукопись подвергается обязательному рецензированию трех рецензентов из числа рецензентов Международного научного журнала «Альтернативная энергетика и экология» и двух рецензентов из числа приглашенных редколлегией. Каждая статья проходит этап предварительного рецензирования и итогового рецензирования. В случае возникновения спорных ситуаций по научным вопросам рукопись передается на рассмотрение в Совет рецензентов Международного научного журнала «Альтернативная энергетика и экология». В случае возникновения спорных ситуаций по возможности технического воплощения идеи, выдвинутой в рукописи, последняя передается в Совет экспертов Международного научного журнала «Альтернативная энергетика и экология».

Срок публикации каждой рукописи не превышает 5 месяцев. В случае наличия рекомендательного письма одного из членов редколлегии Международного научного журнала «Альтернативная энергетика и экология» время рассмотрения рукописи может быть сокращено до 2 месяцев. Срок публикации рукописей, направленных на конкурс, проводимый редколлегией, не превышает 4 месяцев. Срок публикации заказных научных обзоров не превышает 3 месяцев.

В случае необходимости срочной публикации автор (или авторский коллектив) может обратиться в редакцию с мотивированной просьбой опубликовать рукопись в течение трех месяцев.

Редколлегия бескорыстно и оперативно оказывает максимальное содействие всем аспирантам и соискателям ученой степени в качественном представлении их материала в журнале и в Международной научной информационной системе «Водород» в кратчайшие сроки. Все публикации в журнале осуществляются исключительно на бесплатной основе.

В любом случае все рукописи, направляемые в журнал, рецензируются и реферируются в известных международных научных изданиях.

Рукописи в журнале публикуются на русском и на английском языках. Каждой рукописи, поступившей в редакцию, присваивается редакционной номер и дата поступления.

Журнал публикует исключительно оригинальные статьи. Автор несет полную ответственность за соблюдение этого требования.

I. Для своевременного выхода журнала убедительно просим соблюдать следующие правила оформления рукописей.

1. Рукопись представляется как в машинописном, так и в электронном виде. Рукопись на бумажном носителе предоставляется в 2-х экз., второй экземпляр обязательно подписывается авторами на обороте.

Объем рукописей:

- краткие сообщения — до 5 страниц (1800 печатных знаков);
- объем статей, как правило, не должен превышать 9 страниц;
- письма в редакцию — до 3 страниц;
- объем научных обзоров — не более 30 страниц.

2. Рукопись сопровождается:

- сопроводительным письмом руководителя организации, представляющего рукопись, оформленным экспертным заключением или другим документом, разрешающим опубликование в открытой печати (1 экз.), утвержденным руководителем организации и заверенным гербовой печатью. Экспертное разрешение представляют только авторы из России;
- компакт-диском или дискетой, содержащей обязательный пакет электронных файлов, перечисленных ниже **в разделе III**.

3. Текст аннотации на русском и английском языках печатается шрифтом Times New Roman (12 кегль) в одном файле в следующем порядке: наименование статьи, авторы, наименование организации, аннотация на русском языке; далее, через 2 строки, в той же последовательности — на английском языке. В аннотации текст излагается в индикативной форме, объем — не более 600 знаков. Аннотация также публикуется на сайте международного научного информационного портала «Водород» (на русском и английском языках).

4. Текст резюме (15 строк) печатается шрифтом Times New Roman (10 кегль) на русском и английском языках и содержит следующие сведения: место работы, должность, образование, научное звание, ученая степень, награды и научные премии, профессиональный опыт, основной круг научных интересов, количество публикаций автора(ов).

5. Фотографии авторов для резюме представляются в формате TIFF или JPEG.

6. Текст реферата (одна страница) — для опубликования в реферативных журналах (РЖ) ВИНИТИ, «Письма в журнал “Альтернативная энергетика и экология”» (на английском языке).

Параметры страницы:

- формат А4 (210 х 297 мм);
- межстрочный интервал полуторный;
- шрифт Times New Roman (12 кегль) в одном файле в следующем порядке: наименование статьи, автор (авторы), наименование организации, реферат на русском языке; далее, через 2 строки, в той же последовательности — на английском языке.

7. Интернет-сообщение для размещения сигнальной информации на сайтах информационного портала «Водород» и на сайтах информационной сети, посвященной энергетике и экологии. Сообщение размером не более одной страницы излагается в произвольной форме:

- формат А4 (210 х 297 мм);
- межстрочный интервал полуторный;
- шрифт Times New Roman (12 кегль).

Сообщение может включать фотографии и графики.

II. Оформление рукописи:

- редколлегия рекомендует авторам обзоров и статей структурировать представляемый материал, используя подзаголовки (например: «Введение», «Теоретический анализ», «Методика эксперимента», «Результаты и их обсуждение», «Заключение», «Список литературы»);
- текст материала для публикации должен быть тщательно отредактирован автором, следует избегать повторов, не следует без необходимости подробно описывать иллюстративный материал;
- текст должен быть напечатан на белой бумаге:
- формат А4 (210 х 297 мм);
- межстрочный интервал полуторный;
- шрифт Times New Roman (12 кегль).

Рукопись может включать фотографии и графики.

Текст рукописей оформляется в следующей последовательности:

- **индекс универсальной десятичной классификации (УДК или PACS)**;
- **название статьи на русском и на английском языке** (прописными буквами без кавычек, кегль 14 полужирный, выравнивание по центру; переносы не допускаются, точка в конце строки не ставится, подчеркивание не используется);
- **авторы** (инициалы, фамилия, кегль 14 полужирный курсив, выравнивание по центру, точка в конце строки не ставится)
- **название организации, адрес, город, страна, индекс, телефон, факс, e-mail** (кегль 12, выравнивание по центру. В случае, если авторы — представители различных организаций, используется метод надстрочных ссылок, например: А.В.Иванов, Ю.С.Седов*);
- **заголовок раздела** (кегль 14, выравнивание по левому краю, точка не ставится);
- **текст статьи** (шрифт 12, абзацный отступ 1 см, выравнивание по формату);
- **подзаголовок** (шрифт курсивный, кегль 14, выравнивание по левому краю);
- **список литературы** (шрифт обычный, кегль 14, выравнивание по центру).

При написании статьи используются общепринятые термины, единицы измерения и условные обозначения, единообразные по всей статье. **Расшифровка всех (!) используемых авторами обозначений дается при первом употреблении в тексте.**

При наборе статьи на компьютере все латинские обозначения физических величин (*A, I, d, h* и т. п.) набираются курсивом, греческие обозначения, названия функций (β, sin, exp, lim), химических элементов (H_2O) и единиц измерения (МВт/см^2) — прямым (обычным) шрифтом. Символы (ℜ, ℘, ⊗, ∈ и т.п.) оговариваются на полях рукописи.

Таблицы, рисунки, фотографии (желательно черно-белые) размещаются внутри текста и имеют сквозную нумерацию по статье (не по разделам!) и собственные заголовки. Буквенно-цифровая нумерация (1а, 2б) нежелательна. **Названия всех рисунков, фотографий и таблиц приводятся на русском и на английском языках!**

Нумерация обозначений на рисунках дается по порядку номеров по (против) часовой стрелки (для чертежей) или сверху вниз (снизу вверх). Файлы иллюстраций предоставляются в формате TIFF или BMP с разрешением не менее 300 dpi.

Формулы создаются с помощью встроенного редактора формул (Math Type, Microsoft Equation) с нумерацией в круглых скобках (2), выравниваются по центру; расшифровка всех обозначений (букв) в формулах дается в порядке упоминания их в формуле.

Во избежание недоразумений и ошибок редакция рекомендует авторам использовать в формулах буквы латинского, греческого и других (не русских) алфавитов.

Оформление литературных ссылок (списка литературы):

Все литературные ссылки обозначаются порядковой цифрой в квадратных скобках (например, [3]). Литературным ссылкам присваивается порядковый номер по мере их упоминания в тексте.

Библиографические ссылки в списке литературы располагаются в той последовательности, в какой упоминаются в тексте, и оформляются по следующим правилам:

- **для книг**: фамилия и инициалы автора(-ов), название книги, место издания, издательство, год (для трудов конференций — город, страна, год). Например: Ландау Л. Д., Лившиц Е. М. Квантовая механика. М.: Наука, 1988. Или: Elton R. C. X-Ray Lasers. Boston: Academic Press, 1990;
- **для статей** в журнале, сборнике, газете: фамилия и инициалы автора(ов), название статьи, название журнала (сборника), год, том, номер (или номер выпуска), страницы. Например: Полякова А. Л., Васильев Б. М., Купенко И. Н. и др. Изменение зонной структуры полупроводников под давлением // Физика и техника полупроводников. 1976. Т. 9, № 11. С. 2356–2358. Или: Афанасьев А. М. Оптимизация распределения энерговыделения в реакторе с помощью «советов оператору» // Вопросы атомной науки и техники. Сер. Физика и техника ядерных реакторов. 1986. Вып. 2. С. 32–36. Или: Mezain I. H. Rolling circuit boards improves soldering // Electronics. 1977. Vol. 34, No. 16. P. 193–198;
- **для диссертаций и авторефератов диссертаций**: кроме фамилии автора и его инициалов следует указать название диссертации, степень, место защиты (город) и год; для препринтов — название, место издания, год, номер. Например: Горшкова Т. И. Термодинамические свойства и применение некоторых сплавов церия: Автореф. дис. … канд. хим. наук. М., 1976;
- **для патентной документации**: вид патентного документа (авторское свидетельство или патент), номер, название страны, выдавшей документ, индекс международной классификации изобретений, или индекс международной классификации промышленных образцов, или индекс международной классификации товаров и услуг, название патента (а. с.), авторы, название издания, опубликовавшего документ, год и номер издания. Например: А. с. 100970 СССР МКИ^3 В 251 15/00. Устройство для захвата неориентированных деталей типа валов / Ваулин В. С., КенайкинВ.Г. // Открытия. Изобретения. 1983. № 11.

При необходимости в заголовке библиографической ссылки на работу четырех и более авторов могут быть указаны имена всех авторов или первых трех с добавлением слов «и др.».

В списке литературы инициалы авторов должны стоять после фамилий.

III. Правила представления электронной версии материалов для быстрой публикации.

Для максимального ускорения процесса прохождения статьи автор должен направить в адрес главного редактора (e-mail: gusev@hydrogen.ru) обязательный пакет электронных файлов (см. ниже).

Перечень обязательного пакета электронных файлов:

Файлы обозначаются следующим образом (пример):

Article#1_Gusev AL_Hydrogen detectors_(1300).doc,

где: **Article** — рукопись, **#1** — обозначает номер рукописи, присвоенный автором (рукописей может быть несколько на электронном носителе), **Gusev AL** — фамилия первого автора и инициалы, **Hydrogen detectors** — первые два слова из названия рукописи, **(1300)** — номер тематического направления или тематической секции из Тематики журнала (приведена в конце каждого номера журнала).

1. Рукопись — Article#1_Gusev AL_Hydrogen detectors_(1300).doc
2. Аннотация — Summary#1_Gusev AL_Hydrogen detectors_(1300).doc
3. Реферат — Abstract#1_Gusev AL_Hydrogen detectors_(1300).doc
4. Резюме — Resume#1_Gusev AL_Hydrogen detectors_(1300).doc (резюме и фотографии на всех авторов в одном файле)
5. Фотографии и рисунки — Pic-1#1_Gusev AL_Hydrogen detectors_(1300).bmp (Pic-1 — номер рисунка)
6. Разрешение на опубликование в открытой печати — Sanction#1_Gusev AL_Hydrogen detectors_(1300).pdf
7. Интернет-сообщение — Internet#1_Gusev AL_Hydrogen detectors_(1300).doc
8. Соглашение — Agreement#1_Gusev AL_Hydrogen detectors_(1300).pdf
9. Форма передачи рукописи и материалов для публикации — Form#1_Gusev AL_Hydrogen detectors_(1300).doc (MANUSCRIPT TRANSMITTAL FORM)
10. Рецензии — Review-1#1_Gusev AL_Hydrogen detectors_(1300).doc (Review-1 — номер рецензии).
11. Сопроводительное письмо руководителя организации (или письмо автора, если автор — частное лицо) — Letter#1_Gusev AL_Hydrogen detectors_(1300).doc

Внимание!!!

Вместе с электронной версией всех перечисленных документов необходимо направить в редакцию оригиналы всех документов обычной почтой заказным письмом.

Редколлегия обращает внимание авторов на то, что несоблюдение приведенных выше правил может задержать публикацию материала!

Отклоненные редколлегией рукописи (в бумажном и электронном виде) авторам не возвращаются.

АДРЕС РЕДАКЦИИ
607183, Россия, Нижегородская обл., Саров, а/я 687, НТЦ «ТАТА»
Тел.: 8 (83130) 63107, 97472 Факс: 8 (83130) 63107
Моб. тел.: +7-961-63-99-126, +7-962-50-77-914
E-mail: gusev@hydrogen.ru http://isjaee.hydrogen.ru, http://www.hydrogen.ru

MONTHLY REVIEWED AND ABSTRACTED INTERNATIONAL SCIENTIFIC JOURNAL
"ALTERNATIVE ENERGY AND ECOLOGY"

GUIDE TOAUTHORS OF MANUSCRIPTS

To submit manuscripts to be published in the International Scientific Journal for Alternative Energy and Ecology, authors are to follow guides as follows

Each manuscript is compulsory reviewed by 3 referees, two of whom are referees of the International Scientific Journal for Alternative Energy and Ecology, and 1 of those being invited by the Editorial Board. Each article is put through a preliminary and final reviewing. In the event of controversies on scientific problems occur, an article is submitted to the International Reviewers Board of the International Scientific Journal for Alternative Energy and Ecology to be criticized. In the event of controversies on feasible implementation of the idea, presented in the manuscript the latter is submitted to the Experts Board of International Scientific Journal for Alternative Energy and Ecology.

The publication period does not exceed 5 months. Assuming a letter of introduction from a member of the Editorial Board of the International Scientific Journal for Alternative Energy and Ecology, the period for reviewing a manuscript may be kept down to 2 months. The publication period of manuscripts submitted to the competition organized by the Editorial Board does not exceed 4 months. The publication period for registered scientific reviews does not exceed 3 months.

In the event of pressing need for publication, the author or a team of authors may address the Editorial Board to make a justified request to publish a manuscript in the course of 3 months.

The Editorial Board will promptly and without any interest assist all post-graduates and competitors in publishing their materials in the journal and in the International Scientific Information System "Hydrogen" in the shortest possible time. All publications in the journal are issued free of charge.

In any event, all manuscripts submitted to the journal are criticized and abstracted in popular international scientific journals.

Articles are published in Russian and English. Each communication submitted to the Editorial Board is assigned a number and date.

The journal publishes nothing but original articles. The author is responsible for following this guide.

I. For publishing the journal in due time, please follow the guide given below:

1. Manuscript must be submitted either in a typed form or in e-mail: The hard copy of the manuscript must be submitted in 2 copies, the authors must necessarily sign the second copy overleaf.

Manuscripts words:

- brief communications are up to 5 pages (1800 symbols);
- articles, as a rule, are up to 9 pages;
- letters to the Editorial Board are up to 3 pages;
- scientific reviews should not in general be longer than 30 pages.

2. Manuscripts should be accompanied by:

- a letter of the head of the institution who presents the manuscript with the experts' opinion or other document permitting the publication in the press (1 copy) confirmed and affixed by the head of the institution. Authors must present the experts' permission from Russia.
- a CD-disk or diskette containing the essential text of electronic files listed in **Section III.**

3. Abstract text in Russian and English should be typed in normal font Times New Roman in one file as follows: article title, authors, name of an organization, abstract in Russian, and then in 2 lines in the same sequence — in English. The abstract should be given in indicative, and is up to 600 symbols in length. The abstract is also published on site of the International Scientific Information Portal "Hydrogen" (in Russian, and English).

4. The abstract text (15 lines) in Russian and English is printed in font Times New Roman (font size 10) and shall contain the place of organization, title, education, scientific degree, rewards and scientific prizes, experience, main range of scientific interests, number of publications.

5. Authors' photos in TIFF or JPEG format to be published in abstract text.

6. Compact text (one page) to be published in Compact journals (CJ) VINITI, «Letters to the "Alternative energy and ecology"» (in English).

Page format:

- format A4 (210×297 mm)
- print interval: one and a half
- font: Times New Roman (font size 12) in one file as follows: article title, authors, name of an institution, abstract in Russian, and then in 2 lines in the same sequence — in English

7. Internet information for announcing an express-information on sites of the International Scientific Information Portal "Hydrogen", and also on sites of the information network devoted to energy and ecology. Information is given in an arbitrary way:

- format A4 (210×297 mm)
- print interval: one and a half
- font: Times New Roman (font size 12)

The information may include photos and diagrams.

II. Information on manuscript writing

- the Editorial Board recommends authors writing reviews and articles organize their materials using subtitles (for example: "Introduction", "Theoretical Analysis", "Experimental Methods", "Results and Discussion", "Conclusion", "References");
- text for publication must be reviewed carefully by authors; no replica, and one does not need to describe the illustrations in detail;
- text must be typed on white paper:
- format A4 (210×297 mm)
- print interval: one and a half
- font: Times New Roman (font size 12)

A manuscript may contain photos and diagrams.

Text section sequence:

- **universal decimal classification (UDC or PACS);**
- **paper title in Russian and English** (capital letters, font size 14, bold, center-alignment. No division of words is allowed. Do not use quotation marks. Do not use underlining;
- **authors** (initials, surname, font size 14, italic bold, center-alignment, no period in the end);
- **name of organization, address, city, country, postcode, telephone, fax, e-mail** (font size 12, center-alignment. If the authors are from different organizations, the method of superscript references shall be used; for example: A. V. Ivanov, Yu. S. Sedov*);
- **section title** (font size 14, center-alignment, no period in the end);
- **text of the article:** (font size 12, left justification — 1 cm);
- **subtitle:** (italic, font size 14, full justification);
- **references:** (font normal, size 14, full justification).

When drawing up the article one should use generally accepted terms, units and symbols. All designations being used by the authors shall be determined at their first appearance in the text.

When the article is typed on the computer, all Latin designations of physical quantities (*A, I, d, h,* etc.) shall be typed in italic, Greek designations, names of functions (β, sin, exp, lim), chemical elements (H_2O) and units (MW/cm^2) — in upright (normal) font. The symbols ($\Re$, $\wp$, $\otimes$, $\in$, etc.) shall be specified in the manuscript margin.

Tables, figures, photos (black-and-white only) shall be placed inside the text and be consecutive over the article and have own titles. Notation numbering in figures shall be given clockwise

(counter-clockwise) (for drawings) or from top to bottom (from bottom to top) (in numerical order). No figure or diagram plotting by Microsoft Word tools **is allowed.** All figures legends shall be given in Russian and English.

Formulae shall be constructed by means of the integrated formula editor (Math Type, Microsoft Equation) and numbered in parentheses (2), centre-aligned; notation (letters) deciphering in formulae is given as they are mentioned therein. References numbering shall be given in square brackets [3].

It is not allowed to denote different notions by a common letter. Indexes for literal signs in the article text are given in Lation or Russian only (for example, in a Russian-written paper one should use T_m — melting point).

References in the reference list shall be placed in the sequence with which they are mentioned in the text and shall be written according to the following rules:

▪ **for books:** surname and initials of the author(s), title of the book, then the place of publication, publishing house, year (for proceedings of conferences — city, country, year). For example: Landau L. D., Lifshits E. M. Quantum Mechanics. Moscow, "Nauka", 1988. Or: Elton R. C. X-Ray Lasers. Boston: Academic Press, 1990;

▪ **for articles** in a journal, collection, newspaper: initials of the author(s), title of the article, name of the journal (collection), year, volume, No. (or Issue No.), pages. For example: Polyakova A. L., Vassiliev B. M., Kupenko I. N. et al. Variation of the zone structure of semiconductors under pressure // Semiconductor Physics and Technology. 1976. Vol. 9, No. 11. P. 2356–2358. Or: Afanasiev A. M. Optimization of energy release distribution in a reactor by means of "advices of operator" // J. of Nuclear Science and Technology. Physics and Nuclear Reactor Engineering Series. 1986. No. 25. P. 32–36. Or: Mezain I. H. Rolling circuit boards improves soldering // Electronics. 1977. Vol. 34, No. 16. P.193–198;

▪ **for dissertations and dissertation abstracts,** besides the author's surname and initials, one shall indicate the title of the dissertation, degree, place of defence (city) and year, and for preprints — title of the preprint, place of publication, year and number. For example: Gorshkova T. I. Thermodynamic properties and application of certain cerium alloys: Dissertation Abstract. ... Candidate of Chemical Science. Moscow, 1976;

▪ **for patent documentation:** type of the patent document (Authors's certificate or Patent), its number, name of the country issuing the document, index of the international classification of inventions, name of publication where the subject of invention was published, year and number of publication. For example: Author's Certificate 100970 USSR Inc^3 V 251 15/00. Adevice for gripping non-oriented shaft-type parts/Vaulin V. S., Kenaikin B. G. // Discoveries. Inventions. 1983. No. 11.

If the title of a bibliographic reference is to contain four and more authors, all the names can be indicated or only three first names shall be indicated plus the words "et al." The initials in the reference list shall be placed after surnames.

III. Guides to authors presenting e-mail version of materials for express-publication

To foster the process of reviewing the article the author should submit a **required packet of electronic files** to the Editor-in-Chief (e-mail: gusev@hydrogen.ru).

List of required electronic files:

A files is described as follows (example):

Article#1_Gusev AL_Hydrogen detectors_(1300).doc,

where: **Article** is the manuscript, **#1** is the number of the manuscript given by the author (there may be several manuscripts on one electronic file), **Gusev AL** is the name of the first author, **Hydrogen detectors** are first two words from the title of the manuscript, **(1300)** is the number of the topics or topics section in the Journal topics (given in the last page of the journal).

1. **Article** — Article#1_Gusev AL_Hydrogen detectors_(1300).doc
2. **Summary** — Summary#1_Gusev AL_Hydrogen detectors_(1300).doc
3. **Abstract** — Abstract#1_Gusev AL_Hydrogen detectors_(1300).doc
4. **Resume** — Resume#1_Gusev AL_Hydrogen detectors_(1300).doc (resumes and photos of all authors in one file)
5. **Photos and figures** — Fig-1#1_Gusev AL_Hydrogen detectors_(1300).bmp (Fig-1 — number of figure)
6. **Internet information** — Internet#1_Gusev AL_Hydrogen detectors_(1300).doc
8. **Agreement** — Agreement#1_Gusev AL_Hydrogen detectors_(1300).pdf
9. Form to submit manuscripts and materials to be published — Form#1_Gusev AL_Hydrogen detectors_(1300).doc (MANUSCRIPT TRANSMITTAL FORM)
10. **Reviews** — Review-1#1_Gusev AL_Hydrogen detectors_(1300).doc (Review-1 — number of review).
11. **Official letter (or author letter if author is the individual person)** — Letter#1_Gusev AL_Hydrogen detectors_(1300).doc

Attention!

The Editorial Board calls the authors' attention to the fact that the ignorance of the recommendations mentioned above may impede the publication of the material!

Manuscripts (in hard copy and e-mail form) declined by the Editorial Board will not be returned.

ADRESS OF PUBLISHING OFFICE

Scientific Technical Centre «TATA»
P.O.B. 687, Sarov, Nizhni Novgorod region, 607183, Russia
Phone: +7(83130)63107, 97472 Fax: +7(83130) 63107
Cell phones (office): +7-961-63-99-126, +7-962-50-77-914
E-mail: gusev@hydrogen.ru
http://isjaee.hydrogen.ru, http://www.hydrogen.ru

1. Водородная экономика

Ф. Караосманоглу *(Турция, Стамбул, Стамбульский технический университет) (МРК)*
З.Сен *(Турция, Стамбул, Стамбульский технический университет) (МРК)*

1-1-0-0 История водородной энергетики
Т.Н.Везироглу *(США, Майами, МАВЭ, UNIDO-ICHET) (ПГР)*
А. Г. Галеев *(Россия, Сергиев Посад, ФГУП «НИИхиммаш») (МРК)*

1-2-0-0 Безопасность водородной энергетики
А. Г. Галеев *(Россия, Сергиев Посад, ФГУП «НИИхиммаш») (МРК)*
А.Л.Гусев *(Россия, Саров, НТЦ «ТАТА»)*
Я. Клеперис *(Латвия, Рига, Университет Латвии) (МРК)*
Л. Ф. Беловодский *(Россия, Саров, РФЯЦ-ВНИИЭФ) (МНКСР)*

1-2-1-0 Рекомбинаторы водорода
А.Л.Гусев *(Россия, Саров, НТЦ «ТАТА»)*

1-2-2-0 Системы обдува инертными газами

1-2-3-0 Безопасность криогенных систем

1-2-4-0 Технологии безопасного использования водорода на борту транспортных средств

1-3-0-0 Газоаналитические системы и сенсоры водорода
Я. Клеперис *(Латвия, Рига, Университет Латвии) (МРК)*
А. М. Полянский *(Россия, С.-Петербург, ООО «НПК Электронные пучковые технологии») (МРК)*
В.М.Арутюнян, *акад.НАН Армении (Армения, Ереван, Ереванский государственный университет) (РНС)*
Ю.Шунман *(Нидерланды, Делфт, Делфтский технический университет) (МНКСР)*
Л. И. Трахтенберг *(Россия, Москва, Институт химической физики им.Н.Н.Семенова РАН)*

1-4-0-0 Хранение водорода
Я. Клеперис *(Латвия, Рига, Университет Латвии) (МРК)*
О. Н. Сривастава *(Индия, Варанаси, Университет Банарас Хинди) (МРК)*
С.М.Алдошин, *акад.РАН (Россия, ИПХФ РАН, Черноголовка, Россия) (РНС)*
Б.П.Тарасов *(Россия, Черноголовка, ИПХФ РАН) (МРК)*

1-4-1-0 В углеродных наносистемах
О.Н.Ефимов *(Россия, Черноголовка, ИПХФ РАН) (МРК)*
Б. К. Гупта *(Индия, Варанаси, Университет Банарас Хинди) (МРК)*
А. В.Вахрушев *(Россия, Ижевск, Институт прикладной механики УрО РАН) (МРК)*

1-4-2-0 В инкапсулированном газообразном состоянии: в микросферах, пенометаллах, цеолитах и других соединениях
В.С.Коган *(Украина, Харьков, ХФТИ) (МРК)*
Е.Ф.Медведев *(Россия, Саров, РФЯЦ-ВНИИЭФ) (МРК)*
А. Ф.Чабак *(Россия, Москва, Академия перспективных технологий) (МРК)*

1-4-3-0 В газообразном состоянии под давлением
А.С.Коротеев, *акад. РАН (Россия, Москва, ФГУП «Центр Келдыша») (РНС)*

1-4-3-1 В газообразном состоянии в крупных хранилищах

1-4-3-2 В газообразном состоянии в баллонах

1-4-4-0 В жидком состоянии
А.М.Архаров *(Россия, Москва, МГТУ им.Н.Э.Баумана) (МРК)*
А. М.Домашенко *(Россия, Балашиха, ОАО «Криогенмаш») (МРК)*
В.И.Куприянов *(Россия, Балашиха, ОАО «Криогенмаш») (МРК)*
А. А. Макаров *(Россия, Сергиев Посад, ФГУП «НИИхиммаш») (МРК)*
Г. Г. Шевяков *(Россия, Балашиха, ОАО «Криогенмаш») (МРК)*
В. С. Травкин *(США, Лос-Анжелес, Калифорнийский университет) (МРК)*
В. С. Коган *(Украина, Харьков, ХФТИ) (МРК)*
И. Ф. Кузьменко *(Россия, Балашиха, ОАО «Криогенмаш») (МНКСР)*
А. Г. Галеев *(Россия, Сергиев Посад, ФГУП «НИИхиммаш») (МРК)*

1-4-4-1 В криогенном жидком состоянии в стационарных хранилищах

1-4-4-2 В криогенном жидком состоянии на борту транспортных средств
Б.А.Соколов *(Россия, Королев, РКК «Энергия» им.С.П.Королева) (МРК)*

1-4-5-0 В химически связанном состоянии в жидких средах

1-4-6-0 В твердофазном связанном состоянии в металлогидридных системах
М.Д.Хэмптон *(США, Орландо, Университет Центральной Флориды) (ЗГР)*
Б. П. Тарасов *(Россия, Черноголовка, ИПХФ РАН) (МНКСР)*
С. П. Габуда *(Россия, Новосибирск, ИНХ СО РАН) (МРК)*
В. Л. Кожевников *(Россия, Екатеринбург, ИХТТ УрО РАН) (МРК)*
Р. Н. Плетнев *(Россия, Екатеринбург, ИХТТ УрО РАН) (МРК)*

1-4-7-0 В адсорбированном состоянии на криоадсорбентах

1-4-8-0 В комбинированных системах

1-4-9-0 Новые способы хранения водорода

1-5-0-0 Методы получения водорода
И. Ф. Кузьменко *(Россия, Балашиха, ОАО «Криогенмаш») (МНКСР)*
В. В. Лунин, *акад.РАН (Россия, Москва, МГУ) (РНС)*

1-5-1-0 Радиолиз
М. А. Прелас *(США, Коламбия, Университет Миссури-Коламбия) (МРК)*

1-5-2-0 Электролиз

1-5-3-0 Термохимическое разложение воды

1-5-4-0 Разложение аммиака
В. А. Кириллов *(Россия, Новосибирск, Институт катализа им. Г. К. Борескова СО РАН) (МРК)*

1-5-5-0 Каталитическая конверсия (риформинг) газообразных и жидких углеводородов

1-5-6-0 Неполное окисление углеводородов

1-5-7-0 Высокотемпературный метод

1-5-8-0 Гидраты
Р. Н. Плетнев *(Россия, Екатеринбург, ИХТТ УрО РАН) (МРК)*
С. П. Габуда *(Россия, Новосибирск, ИНХ СО РАН) (МРК)*

1-5-9-0 Бортовые конверторные устройства преобразования органических веществ в водород

1-5-10-0 Генерирование водорода на борту в реакции взаимодействия воды с различными металлами (алюминий, магний и т.д.)

1-5-10-1 Механические и электрические способы удаления окисной пленки во время реакции

1-5-10-2 Химические способы удаления окисной пленки во время реакции

1-5-10-3 Ультразвуковые способы удаления окисной пленки во время реакции

1-5-10-4 Способы увеличения удельной поверхности металлов реагентов

1-5-10-5 Термические и барические методы интенсификации реакции генерации водорода

1-5-10-6 Устройства для генерации водорода в реакции взаимодействия воды и металлов для бортового применения

1-5-10-7 Устройства для генерации водорода в реакции взаимодействия воды и металлов для бытового применения

1-5-10-8 Устройства для генерации водорода в реакции взаимодействия воды и металлов для промышленной энергетики

1-5-10-9 Физико-математические модели описания процессов генерации водорода

1-5-10-10 Перспективные направления развития метода для воплощения его на борту транспортных средств

1-5-11-0 Получение водорода из глубинного морского сероводорода
И.М.Неклюдов *(Украина, Харьков, Харьковский физико-технический институт) (МРК)*
Н.А.Азаренков *(Украина, Харьков, Харьковский физико-технический институт) (МРК)*
В.И.Ткаченко *(Украина, Харьков, Харьковский физико-технический институт) (МРК)*

1-5-12-0 Новые способы получения водорода

1-6-0-0 Транспортирование водорода
А. Г. Галеев *(Россия, Сергиев Посад, ФГУП «НИИхиммаш») (МРК)*

1-6-1-0 Транспортирование жидких криогенных продуктов по трубопроводам
А. М. Домашенко *(Россия, Балашиха, ОАО «Криогенмаш») (МРК)*

1-6-2-0 Охлаждение магистралей криогенных систем

1-6-3-0 Неустановившиеся процессы в криогенных системах

1-7-0-0 Топливные элементы
Б. А. Соколов *(Россия, Королев, РКК «Энергия» им.С.П.Королева) (МРК)*
Ю. Н. Шалимов *(Россия, Воронеж, ВГТУ) (МРК)*
В.П. Пахомов *(Россия, Москва, РНЦ «Курчатовский институт») (МРК)*

1-7-1-0 Разработка и производство топливных элементов
1-7-1-1 Мембраны для топливных элементов
1-7-1-2 Компьютерное моделирование функционирования топливных элементов
1-7-2-0 Применение топливных элементов
1-7-2-1 Устройства питания на топливных элементах с конверсией метанола в водород
1-7-3-0 Топливные элементы с предварительной обработкой водородсодержащего топлива
1-8-0-0 Конструкционные материалы
П. Г. Бережко *(Россия, Саров, РФЯЦ-ВНИИЭФ) (МРК)*
А. М. Полянский *(Россия, С.-Петербург, ООО «НПК Электронные пучковые технологии») (МРК)*
В. М. Чертов *(Россия, Москва) (МРК)*
Ю. Н. Шалимов *(Россия, Воронеж, ВГТУ) (МРК)*
П.Сан-Грегуар (*Франция, Тулон-Вар, Университет Тулон-Вара) (ЗГР)*
А. Т. Пономаренко *(Россия, Москва, Институт синтетических полимерных материалов им.Н.С.Ениколопова РАН) (МНКСР)*
Л. В. Спивак *(Россия, Пермь, ПГУ) (МНКСР)*
А. А. Курдюмов *(Россия, С.-Петербург, СПбГУ) (МНКСР)*
М. В. Гольцова *(Украина, Донецк, ДонНТУ) (МНКСР)*
Я. И. Бляшко *(Россия, С.-Петербург, АОЗТ «МНТО ИНСЭТ») (МРК)*
Н. М. Власов *(Россия, Подольск, НИИ НПО «Луч») (МРК)*
И. И. Федик *(Россия, Подольск, НИИ НПО «Луч») (МРК)*
1-8-1-0 Водород в металлах и сплавах
В. А. Гольцов *(Украина, Донецк, ДонНТУ) (МРК)*
Л. Ф. Гольцова *(Украина, Донецк, ДонНТУ) (МРК)*
1-8-2-0 Водородная деградация
1-8-3-0 Системы наводороживания конструкционных материалов
1-8-4-0 Статическая и динамическая прочность материалов
Н. Н. Гердюков *(Россия, Саров, ИФВ РФЯЦ-ВНИИЭФ) (МРК)*
1-8-5-0 Газары. Применение газаров
1-8-6-0 Электропечи для термовакуумных процессов. Вакуумные электропечи сопротивления
Э. Н. Мармер *(Россия, Москва, ОАО «ВНИИЭТО») (МРК)*
1-8-7-0 Новые конструкционные материалы для объектов альтернативной энергетики
1-9-0-0 Методы получения синтез-газа
А. Я. Столяревский *(Россия, Москва, РНЦ «Курчатовский институт») (МРК)*
1-9-1-0 Адиабатическая конверсия природного газа
1-10-0-0 Транспортные средства и приводы на водородном топливе
Т. Гертиг *(Германия, Берлин) (МРК)*
А. Л. Дмитриев *(Россия, С.-Петербург, РНЦ «Прикладная химия») (МРК)*
А. М. Домашенко *(Россия, Балашиха, ОАО «Криогенмаш») (МРК)*
Б. А. Соколов *(Россия, Королев, РКК «Энергия» им.С.П.Королева) (МРК)*
А. Ю. Раменский *(Россия, Москва, «Аудит-Премьер») (МНКСР)*
В. С. Соколов *(Россия, С.-Петербург) (МНКСР)*
1-11-0-0 Водородные автозаправочные станции
1-12-0-0 Водород для энергообеспечения зданий (водородные мини-электростанции на базе топливных элементов)

2. Термодинамический анализ в альтернативной энергетике

В. А. Хуснутдинов *(Россия, Москва, РАО «ЕЭС России») (МРК)*
2-1-0-0 Термодинамический анализ основных энергетических процессов в альтернативной энергетике
2-2-0-0 Эксергетический анализ основных энергетических процессов в альтернативной энергетике

3. Атомная энергетика

Ю.А.Трутнев*, акад. РАН (Россия, Саров, РФЯЦ-ВНИИЭФ) (ПГР)*
А. Я. Столяревский *(Россия, Москва, РНЦ «Курчатовский институт») (МРК)*
А. В. Ивкин *(Россия, Саров, РФЯЦ-ВНИИЭФ) (МНКСР)*
А. Г. Чудин *(Россия, Москва, Федеральное Агентство по атомной энергии РФ) (МНКСР)*
В. А. Афанасьев *(Россия, Саров, РФЯЦ-ВНИИЭФ) (МРК)*
М. А. Прелас *(США, ш.Коламбия, Университет Миссури) (МРК)*
3-1-0-0 Атомно-водородная энергетика
Н. Н. Пономарев-Степной*, акад. РАН (Россия, Москва, РНЦ «Курчатовский институт») (РНС)*
А. Я. Столяревский *(Россия, Москва, РНЦ «Курчатовский институт») (МРК)*
В. Н. Фатеев *(Россия, Москва, РНЦ «Курчатовский институт») (МРК)*
А.Л.Гусев *(Россия, Саров, НТЦ «ТАТА»)*
3-1-1-0 История атомно-водородной энергетики
Н. Н. Пономарев-Степной*, акад. РАН (Россия, Москва, РНЦ «Курчатовский институт») (РНС)*
А.Я.Столяревский *(Россия, Москва, РНЦ «Курчатовский институт») (МРК)*
А.Л.Гусев *(Россия, Саров, НТЦ «ТАТА»)*
3-1-2-0 Высокотемпературные газовые реакторы (ВТГР) для производства водорода высокотемпературными (Т = 1000 °С) методами
3-1-3-0 Быстрые реакторы с натриевым охлаждением (БН) для получения среднетемпературного тепла (Т = 500 °С), производства синтетического газа и водорода
3-1-4-0 Быстрые реакторы со свинцовым охлаждением (БРЕСТ) как реакторы следующего поколения для получения высокотемпературного тепла (Т > 500 °С)
Г. Л. Хорасанов *(Россия, Обнинск, ФГУП «ГНЦ РФ – Физико-энергетический институт им. А. И. Лейпунского») (МРК)*
3-2-0-0 Атомная энергетика для транспортных средств
М. А. Казарян *(Россия, Москва, ФИАН им. П. Н. Лебедева) (МРК)*
И. В. Шаманин *(Россия, Томск, Томский политехнический университет) (МРК)*
3-2-1-0 Радионуклидные источники тепла
3-2-2-0 Радионуклидные термоэлектрические генераторы
3-2-3-0 Термо- и радиационно-стимулированные фазовые превращения в сплавах внедрения (карбидах, нитридах, нитридогидридах, карбогидридах и гидридах переходных металлов, высокотемпературных сверхпроводящих материалах, интерметаллических соединениях)

4. Солнечная энергетика

А. Штейнфелд *(Швейцария, Цюрих, Швейцарский федеральный институт технологий) (МРК)*
Г.И.Исаков *(Азербайджан, Баку, Институт физики НАН) (ЗГР)*
И. Г. Хидиров *(Узбекистан, Ташкент, Институт ядерной физики НАН Узбекистана) (МРК)*
С. Геруни *(Армения, Ереван, Ереванский государственный университет) (МНКСР)*
С. М. Раза *(Пакистан, Кветта, Университет Белуджистана) (МРК)*
С. З. Ильяс *(Пакистан, Кветта, Университет Белуджистана) (МРК)*
А. М. Пенджиев *(Туркменистан, Ашхабат-32, Туркменский политехнический институт) (МРК)*
В. Ф. Гременок *(Белоруссия, Минск, Объединенный институт физики твердого тела и полупроводников) (МНКСР)*
4-1-0-0 История солнечной энергетики
4-2-0-0 Солнечно-водородная энергетика
4-2-1-0 Материалы для солнечно-водородной энергетики
4-3-0-0 Солнечные электростанции
4-3-1-0 Кремниевые солнечные электростанции
4-3-2-0 Космические солнечные станции
4-3-3-0 Фотоэлементы
4-3-4-0 Фотовольтаический эффект в полупроводниковых структурах. Фотоэлектрические модули
4-4-0-0 Наземные солнечные станции
4-4-1-0 Солнечные коллекторы
4-5-0-0 Солнечные города
4-5-1-0 Солнечный дом
4-5-2-0 Солнечные холодильные установки
4-5-3-0 Солнечные водоподъемные системы
4-5-4-0 Гелиоэнергетические установки
4-6-0-0 Солнечный транспорт
4-7-0-0 Концентраторы солнечного излучения

5. Ветроэнергетика

И. З. Богуславский *(Россия, Москва, ОЭЭП РАН) (МРК)*
5-1-0-0 История ветроэнергетики
5-2-0-0 Ветро-водородная энергетика

5-3-0-0 Электрогенераторы для ветроэнергетики
5-4-0-0 Ветроэнергетические установки
5-5-0-0 Ветрогелиоэнергетические установки

6. Приливная энергетика и энергетика морских течений

6-1-0-0 История приливной энергетики
6-2-0-0 Энергетика морских волн
6-3-0-0 Энергетика морских течений

7. Геотермальная энергетика

7-1-0-0 История геотермальной энергетики
7-2-0-0 Фундаментальные исследования в области геотермальной энергетики
7-3-0-0 Проблемы освоения геотермальной энергии
7-4-0-0 Роль моделирования и мониторинга при освоении геотермальной энергии. Оценка геотермального резерва
7-5-0-0 Геотермальные станции
  7-5-1-0 Геотермальные электростанции
  7-5-2-0 Геотермальные тепловые станции
7-6-0-0 Эффективность и надежность геотермальных тепловых и электрических станций
7-7-0-0 Геотермальные ресурсы стран мира и перспективы их освоения

8. Взрывная энергетика

В. Е. Фортов, *акад. РАН (Россия, Москва, Институт теплофизики экстремальных состояний Объединенного института высоких температур РАН) (РНС)*
А. Л. Михайлов *(Россия, Саров, ИФВ РФЯЦ ВНИИЭФ) (МРК)*
Н. Н. Гердюков *(Россия, Саров, ИФВ РФЯЦ-ВНИИЭФ) (МРК)*
А. А. Штерцер *(Россия, Новосибирск, ООО «НПП "МАТЕМ"») (МРК)*
В. Н. Герман *(Россия, Саров, ИФВ РФЯЦ-ВНИИЭФ) (МРК)*
8-1-0-0 Взрывные технологии
8-2-0-0 Компьютерное моделирование задач взрывной энергетики
  8-2-1-0 Постановки задач взрывной энергетики
  8-2-2-0 Подвижные лагранжево-эйлеровы сетки
8-3-0-0 Взрывная дейтериевая энергетика
8-4-0-0 Взрывная энергетика для синтеза новых веществ
  8-4-1-0 Синтез и спекание материалов взрывом
  8-4-2-0 Ударно-волновое спекание материалов
  8-4-3-0 Компьютерное моделирование процессов ударно-волнового спекания материалов
8-5-0-0 Взрывчатые вещества
8-6-0-0 Взрывные камеры
А. А. Штерцер *(Россия, Новосибирск, ООО «НПП "МАТЕМ"») (МРК)*
8-7-0-0 Экстремальные состояния вещества. Детонация. Ударные волны
8-8-0-0 Энергетические материалы и физика детонации
8-9-0-0 Уравнения состояния и фазовые переходы

9. Энергия биомассы

9-1-0-0 Биогазовые установки
9-2-0-0 Термохимические газогенераторы

10. Малые и микрогидроэлектростанции

С. Шатворян *(Армения, Ереван, Энергетический стратегический центр) (МНКСР)*
10-1-0-0 Оборудование малых и микрогидроэлектростанций
10-2-0-0 Деривационные микрогидроэлектростанции

11. Углеродные наноструктуры

А.М.Липанов, *акад. РАН (Россия, Ижевск, Институт прикладной механики УрО РАН) (МРК)*
Ю. М. Шульга *(Россия, Черноголовка, ИПХФ РАН) (МРК)*
В. И. Кодолов *(Россия, Ижевск, Научно-образовательный центр химической физики и мезоскопии УдНЦ УрО РАН) (МНКСР)*
Ю. С. Нечаев *(Россия, Москва, ФГУП «ГНЦ РФ – Центральный институт черной металлургии им.И.П.Бардина») (МНКСР)*
Б. П. Тарасов *(Россия, Черноголовка, ИПХФ РАН) (МНКСР)*
Ю.Д.Третьяков, *акад.РАН (Россия, Москва, ФНМ МГУ) (РНС)*
11-1-0-0 Наносистемы: синтез, свойства, применение
Е. А. Гудилин *(Россия, Москва, ФНМ МГУ) (РНС)*
11-2-0-0 Фуллереновые структуры и углеродные наноматериалы для теплоизоляции
11-3-0-0 Фуллереновые структуры и углеродные наноматериалы для сенсоров водорода
М. В. Воробьева *(Россия, Москва, ГИРЕДМЕТ) (МРК)*
В.М.Арутюнян, *акад.НАН Армении (Армения, Ереван, Ереванский государственный университет) (РНС)*
11-4-0-0 Компьютерное моделирование синтеза углеродных наноматериалов с заданными свойствами
11-5-0-0 Углеродные наноструктуры для автотранспорта

12. Катализ

З. Р. Исмагилов *(Россия, Новосибирск, Институт катализа им. Г. К. Борескова СО РАН) (МРК)*
С.М. Алдошин, *акад.РАН (Россия, ИПХФ РАН, Черноголовка, Россия) (РНС)*
В.Н.Пармон, *акад. РАН (Россия, Новосибирск, Институт катализа им.Г.К.Борескова СО РАН) (РНС)*
В. А. Кириллов *(Россия, Новосибирск, Институт катализа им. Г. К. Борескова СО РАН) (МРК)*
О. Н. Ефимов *(Россия, Черноголовка, ИПХФ РАН) (МРК)*
12-1-0-0 Каталитические методы синтеза альтернативного топлива
12-2-0-0 Катализ в совмещенных схемах «производство энергии и получение полезных продуктов из природного газа»
12-3-0-0 Катализ в генерации рабочего тела в газотурбинных установках
12-4-0-0 Катализ в топливных элементах
12-5-0-0 Катализ в процессах получения синтез-газов и водорода
12-6-0-0 Каталитические методы очистки водорода
12-7-0-0 Катализ в очистке промышленных газовых выбросов энергетических систем
12-8-0-0 Катализ в системах очистки технических вод
12-9-0-0 Фотокаталитические и электрокаталитические методы получения водорода
12-10-0-0 Разработка и исследование свойств материалов для формирования каталитических слоев в топливных элементах
12-11-0-0 О механизмах каталитического действия. Влияние природы металлов и степени их окисления на каталитическую активность
12-12-0-0 Нанокомпозиты для применения в качестве катализаторов. Влияние размерного фактора на каталитическую активность
12-13-0-0 Альтернативные катализаторы без применения платины
12-14-0-0 Проблемы отравления катализаторов
12-15-0-0 Носители катализаторов: дизайн, синтез, свойства
12-16-0-0 Каталитические слои для топливных элементов в планарном исполнении
12-17-0-0 Золь-гель метод для получения катализаторов и носителей катализаторов

13. Термоградиентная энергетика

В. А. Хуснутдинов *(Россия, Москва, РАО «ЕЭС России») (МРК)*

14. Ледниковая энергетика

14-1-0-0 Применение льда в энергетике. Ледяные электростанции
14-2-0-0 Использование холода вечной мерзлоты для термостатирования бытовых и технических объектов

14-3-0-0 Физико-химические свойства льда
14-4-0-0 Теплофизические свойства льда
14-5-0-0 Термодинамические основы получения и применения льда
14-6-0-0 Оборудование для исследования льда
14-7-0-0 Установки для получения льда
14-8-0-0 Способы и механизмы экстренного вскрытия льда для спасения под водой
14-9-0-0 Бинарный лед и его применение
А.Л.Гусев (Россия, Саров, НТЦ «ТАТА»)
14-10-0-0 Применение льда для создания инженерно-технических и архитектурных сооружений
14-11-0-0 Динамика и прочность льда. Динамика хрупкого разрушения. Экспериментальные методы динамической механики разрушения льда
14-12-0-0 Численные и смешанные численно-экспериментальные методы динамической механики разрушения льда
14-13-0-0 Способы удаления ледяных покрытий на водных объектах
14-14-0-0 Аккумулирование холода и применение энергии льда
14-15-0-0 Транспортировка айсбергов и получение пресной воды

15. Термоядерная энергетика

***В. Н. Лобанов** (Россия, Саров, РФЯЦ-ВНИИЭФ) (МРК)*
15-1-0-0 Исследования в области управляемого термоядерного синтеза
15-2-0-0 Рентгеновский термоядерный синтез
15-3-0-0 Пучковый термоядерный синтез
15-4-0-0 Инерциальный термоядерный синтез
15-5-0-0 Изотопный эффект
15-6-0-0 Криогенные тритиевые мишени
15-7-0-0 Мишени высокого давления для исследования процессов мюонного катализа ядерных реакций синтеза
15-8-0-0 Международный проект термоядерного энергетического реактора ИТЭР
15-9-0-0 Радиологическая защита и ядерная безопасность
15-10-0-0 Производство радиоизотопов и их применение
***М. А. Казарян** (Россия, Москва, ФИАН им. Лебедева) (МРК)*
15-11-0-0 Топливный цикл и экология
15-12-0-0 Проектирование, строительство и эксплуатация ядерных исследовательских и энергетических реакторов
15-13-0-0 Промышленное производство компонентов и материалов, необходимых для использования в ядерных реакторах и их топливных циклах
15-14-0-0 Снятие с эксплуатации, дезактивация и обращение с отходами энергетических реакторов
15-15-0-0 Исследования в области технологии производства лазеров и их применения
15-16-0-0 Системы ТОКАМАК
15-17-0-0 Промежуточные системы с магнитным удержанием

16. Криогенные и пневматические транспортные средства

***А.Л.Гусев** (Россия, Саров, НТЦ «ТАТА»)*
16-1-0-0 Криогенный азотный транспорт
16-2-0-0 Автомобили на инертных газах для опасных объектов (пожарные, служебные аэропортов, складов горючесмазочных материалов, для взрывоопасных химических производств и др.)
16-3-0-0 Пневматические транспортные средства

17. Основные проблемы энергетики и альтернативной энергетики

17-1-0-0 Аккумулирование электрической энергии
17-2-0-0 Сверхпроводящие материалы. Сверхпроводимость. Сверхпроводимость в энергетике
17-3-0-0 Новые циклы и схемы термотрансформаторов
17-4-0-0 Проблемы освещения мегаполисов

18. Применение гелия и специальных материалов в транспортных средствах

***Ю.А.Рыжов,** акад.РАН (Россия, Москва, Международный инженерный университет) (РНС)*
18-1-0-0 Дирижабли для перевозки крупногабаритных грузов
18-2-0-0 Дирижабли для контроля за чрезвычайными ситуациями в мегаполисах: автоинспекция, пожарная безопасность, антитерроризм, наблюдение за техническим и экологическим состоянием промышленных зданий и сооружений. Энергонадзор (контроль тепловых утечек зданий в масштабе города)
18-3-0-0 Пожарные, нейтрализационные, полицейские дирижабли

19. Ювенильный водород в процессах геотектоники и геохимии

***С.В.Дигонский** (Россия, Екатеринбург, ФГУП «Урангеологоразведка») (МРК)*
***В.Л.Сывороткин** (Россия, Москва, МГУ им. М. В. Ломоносова)(МРК)*
19-1-0-0 Роль водорода в химическом строении мироздания
19-2-0-0 Движущие силы развития Земли и планет
19-3-0-0 Водород в ядре Земли
19-4-0-0 Геология и геохимия природных газов зон глубинных разломов
19-5-0-0 Транспорт ювенильного водорода через толщу Земли и формирование электрозаряженных зон
19-6-0-0 Природный синтез углеродистых веществ
19-7-0-0 Глубинная дегазация Земли, глобальные катастрофы и аномальные явления

20. Бортовые аккумуляторы энергии

20-1-0-0 Тепловые аккумуляторы энергии
А.Л.Гусев (Россия, Саров, НТЦ «ТАТА»)
20-1-1-0 Температура выше 273 К
20-1-2-0 Температура ниже 273 К
20-1-3-0 Температура ниже 77 К
20-2-0-0 Маховичные аккумуляторы энергии
20-3-0-0 Электрические аккумуляторы энергии
20-4-0-0 Пружинные аккумуляторы энергии
20-5-0-0 Пневматические аккумуляторы энергии
20-6-0-0 Химические аккумуляторы энергии

21. Законодательная база

***П. Б. Шелищ** (Россия, Москва, Государственная Дума РФ, президент НАВЭ) (МНКСР)*
21-1-0-0 Законодательная база альтернативной энергетики в России
21-2-0-0 Законодательное обеспечение инновационного развития водородной энергетики
21-3-0-0 Законодательная база альтернативной энергетики стран СНГ
21-4-0-0 Законодательная база экологии

22. Экономические аспекты

22-1-0-0 Инвестиционная привлекательность различных стран мира и фирм
22-2-0-0 Запасы традиционных энергоресурсов стран экспортеров и мировые запасы
22-3-0-0 Государственные научно-технические программы развития водородной энергетики
22-4-0-0 Экономический анализ
***В. А. Хуснутдинов** (Россия, Москва, РАО «ЕЭС России») (МРК)*
22-5-0-0 Бизнес-планирование

23. Энергетика и экология

О. Л. Фиговский *(Израиль, Мигдал Ха'Емек, Израильский исследовательский центр «Polymate») (МРК)*
М. В. Воробьева *(Россия, Москва, ГИРЕДМЕТ) (МРК)*
23-1-0-0 Парниковый эффект
23-2-0-0 Экологические проблемы мегаполисов
23-3-0-0 Экология воздушной среды и космического пространства
23-4-0-0 Экология водных ресурсов
23-5-0-0 Проблемы вредных выбросов в атмосферу тепловыми электрическими станциями
23-6-0-0 Проблемы загрязнения почвы традиционными энергоносителями
23-7-0-0 Экологический туризм и экокурорты
23-8-0-0 Проблемы переработки промышленных и бытовых отходов

24. Энергоэффективные способы и устройства разделения и очистки агрессивных газовых смесей

А.Л.Гусев *(Россия, Саров, НТЦ «ТАТА»)*
М.А.Казарян *(Россия, Москва, ФИАН им. П. Н. Лебедева) (МРК)*
А.А.Боброва *(Россия, Саров, РФЯЦ-ВНИИЭФ)*

26. Образование и научно-исследовательские центры

Л. А. Илькаева *(Россия, Саров, РФЯЦ-ВНИИЭФ) (МНКСР)*
Б. Ф. Реутов *(Россия, Москва, Федеральное агентство образования и науки РФ) (МРК)*
А. В. Чувиковский *(Россия, Саров, ИПК РФЯЦ-ВНИИЭФ) (МРК)*
Ю.П.Щербак *(Россия, Саров, СарФТИ) (МНКСР)*
Ж.-П. Концен *(Бельгия, Кармановский институт гидрогазодинамики) (МРК)*
26-1-0-0 Образовательные программы в области водородной экономики
26-2-0-0 Водородные технопарки, наукограды
26-3-0-0 Молодежь в науке и технике

27. Информация

А.И. Саликов *(Россия, Москва, ДОР ЦНИИатоминформ) (МНКСР)*
Е. М. Тарараева *(Россия, Москва, ДОР ЦНИИатоминформ) (МНКСР)*
Е.А.Гудилин *(Россия, Москва, ФНМ МГУ им. М.В.Ломоносова) (РНС)*
Т.Н.Кондырина *(Россия, Саров, НТЦ «ТАТА»)*
27-1-0-0 Периодические издания
27-2-0-0 Интернет-ресурсы
27-3-0-0 Научные биографии ученых мира
27-4-0-0 Научные фонды, научные проекты
27-5-0-0 Международные научные конференции
27-6-0-0 Рекламные материалы инвестиционных фирм и фирм-производителей
27-7-0-0 Новые научные книги
27-8-0-0 Патенты
27-9-0-0 Энциклопедия альтернативной энергетики. Термины и определения
27-10-0-0 Отзывы, письма в редакцию, краткие сообщения
27-11-0-0 Обращения членов редакционного научного совета

1. Hydrogen economy

F.Karaosmanoglu *(Turkey, Istanbul, Istanbul Technical University) (IEB)*
Z.Sen *(Turkey, Istanbul, Istanbul Technical University) (IEB)*

1-1-0-0 History of hydrogen economy
T.N.Veziroglu *(USA, Miami, IAHE, UNIDO-ICHET) (HECH)*
A.G.Galeev *(Russia, Sergiev Posad, JSC "NIIHIMMASH") (IEB)*

1-2-0-0 Safety of hydrogen energy
A.G.Galeev *(Russia, Sergiev Posad, JSC "NIIHIMMASH") (IEB)*
A.L.Gusev *(Russia, Sarov, STC "TATA")*
J.Kleperis *(Latvia, Riga, University of Latvia) (IEB)*
L.F.Belovodskiy *(Russia, Sarov, RFNC-VNIIEF) (IEAB)*

1-2-1-0 Hydrogen recombinators
A.L.Gusev *(Russia, Sarov, STC "TATA")*

1-2-2-0 Systems of inert gas blowing off

1-2-3-0 Ensuring of the safe operation of cryogenic systems

1-2-4-0 Safe application of hydrogen on board the vehicle

1-3-0-0 Gas analytical systems and hydrogen sensors
J.Kleperis *(Latvia, Riga, University of Latvia) (IEB)*
A.M.Polyansky *(Russia, S.-Petersburg, OOO "Electronic & Beam Technologies Ltd.") (IEB)*
V.M.Aroutiounian, *Academician NAS of Armenia (Armenia, Yerevan, Yerevan State University) (SEB)*
J.Schoonman *(Netherlands, Delft, Delft University of Technology) (IEAB)*
L.I.Trakhtenberg *(Russia, Moscow, N.N.Semenov Institute of Chemical Physics RAS) (IEB)*

1-4-0-0 Hydrogen storage
J.Kleperis *(Latvia, Riga, University of Latvia) (IEB)*
O.N.Srivastava *(India, Varanasi, Banaras Hindu University) (IEB)*
S.M.Aldoshin, *Academician RAS (Russia, Chernogolovka, IPCP RAS) (SEB)*
B.P.Tarasov *(Russia, Chernogolovka, IPCP RAS) (IEB)*

1-4-1-0 Hydrogen storage in carbon nanosystems
O.N.Efimov *(Russia, Chernogolovka, IPCP RAS) (IEB)*
B.K.Gupta *(India, Varanasi, Banaras Hindu University) (IEB)*
A.V. Vakhroushev *(Russia, Izhevsk, Institute of Applied Mechanics of Ural branch of RAS) (IEB)*

1-4-2-0 Hydrogen storage in an incapsulated gaseous state: in microspheres,in foam metals,in zeolites and others
V.S.Kogan *(Ukraine, Khar'kov, NSC Kharkov Institute of Physics and Technology) (IEB)*
A.F.Chabak *(Russia, Moscow, Academy of perspective technologies) (IEB)*
E.F.Medvedev *(Russia, Sarov, RFNC-VNIIEF) (IEB)*

1-4-3-0 Hydrogen storage in gaseous state under pressure
A.S.Koroteev, *Academician RAS (Russia, Moscow, Keldysh Research Center) (SEB)*

1-4-3-1 Hydrogen storage in gaseous state in large reservoirs

1-4-3-2 Hydrogen storage in gaseous state in tank

1-4-4-0 Hydrogen storage in liquid state
A.M.Arkharov *(Russia, Moscow, Bauman Moscow State Technical University) (IEB)*
A.M.Domashenko *(Russia, Balashikha, JSC "Cryogenmash") (IEB)*
V.I.Kupriyanov *(Russia, Balashikha, JSC "Cryogenmash") (IEB)*
A.A.Makarov *(Russia, Sergiev Posad, JSC "NIIHIMMASH") (IEB)*
G.G.Shevyakov *(Russia, Balashikha, JSC "Cryogenmash") (IEB)*
V.S.Travkin *(USA, Los Angeles, University of California) (IEB)*
V.S.Kogan *(Ukraine, Khar'kov, NSC Kharkov Institute of Physics and Technology) (IEB)*
I.F.Kuz'menko *(Russia, Balashikha, JSC "Cryogenmash") (IEAB)*
A.G.Galeev *(Russia, Sergiev Posad, JSC "NIIHIMMASH") (IEB)*

1-4-4-1 Hydrogen storage in cryogenic liquid state in large reservoirs

1-4-4-2 Hydrogen storage in cryogenic liquid state on board the vehicles
B.A.Sokolov *(Russia, Korolyov, S.P.Korolyov Energia RSC) (IEB)*

1-4-5-0 Hydrogen storage in chemically-bonded state in liquid media

1-4-6-0 Hydrogen storage in solid phase state in metal hydride systems
M.D.Hampton *(USA, Orlando, University of Central Florida) (DECH)*
B.P.Tarasov *(Russia, Chernogolovka, IPCP RAS) (IEB)*
S.P.Gabuda *(Russia, Novosibirsk, IIC SO RAS) (IEB)*
V.L.Kozhevnikov *(Russia, Ekaterinburg, ISSC Ural Branch of RAS) (IEB)*
R.N.Pletnev *(Russia, Ekaterinburg, ISSC Ural Branch of RAS) (IEB)*

1-4-7-0 Hydrogen storage in combined systems

1-4-8-0 Hydrogen storage in adsorbed state in cryogenic adsorbents

1-4-9-0 Novel methods of hydrogen storage

1-5-0-0 Hydrogen production methods
I.F.Kuz'menko *(Russia, Balashikha, JSC "Cryogenmash") (IEAB)*
V.V.Lunin, *Academician RAS (Russia, Moscow, M. V. Lomonosov MSU)*

1-5-1-0 Radiolysis
M.A.Prelas *(USA, Columbia, University of Missouri-Columbia) (IEB)*

1-5-2-0 Electrolysis

1-5-3-0 Hydrogen production via thermochemical dissociation of water

1-5-4-0 Hydrogen production by ammonia decomposition
V.A.Kirillov *(Russia, Novosibirsk, Boreskov Institute of Catalysis) (IEB)*

1-5-5-0 Method of catalytic conversion (reforming) of gaseous and liquid hydrocarbons

1-5-6-0 Hydrogen production by partial oxidation of hydrocarbons

1-5-7-0 High-temperature process for hydrogen production

1-5-8-0 Hydrates
R.N.Pletnev *(Russia, Ekaterinburg, ISSC Ural Branch of RAS) (IEB)*
S.P.Gabuda *(Russia, Novosibirsk, IIC SO RAS) (IEB)*

1-5-9-0 Hydrogen production on board of the vehicle from organic fuels

1-5-10-0 On board hydrogen production via reaction of interaction of water and metals (aluminium,magnesium etc.)

1-5-10-1 Mechanic and electric methods of removal of oxide layer during reaction

1-5-10-2 Chemical methods of removal of oxide layer during reaction

1-5-10-3 Ultrasonic methods of removal of oxide layer during reaction

1-5-10-4 Methods of increase of specific surface of metals

1-5-10-5 Thermal and pressure methods of intensification of hydrogen production

1-5-10-6 Devices for on board hydrogen production via reaction of interaction of water and metals

1-5-10-7 Devices for hydrogen production via reaction of interaction of water and metals for domestic apllications

1-5-10-8 Devices for hydrogen production via reaction of interaction of water and metals for commercial apllications

1-5-10-9 Physico-mathematical model of processes of hydrogen production

1-5-10-10 Novel lines of development of method for on-board application

1-5-11-0 Hydrogen production from deep-sea hydrogen sulphide
I.M.Neklyudov *(Ukraine, Khar'kov, Khar'kov Physical Technical Institute) (IEB)*
N.A.Azarenkov *(Ukraine, Khar'kov, Khar'kov Physical Technical Institute) (IEB)*

***V.I.Tkachenko** (Ukraine, Khar'kov, Khar'kov Physical Technical Institute) (IEB)*

1-5-11-0 Novel hydrogen production methods

1-6-0-0 Hydrogen transport

***A.G.Galeev** (Russia, Sergiev Posad, JSC "NIIHIMMASH") (IEB)*

1-6-1-0 Transport of liquid cryogenic products by pipelines

***A.M.Domashenko** (Russia, Balashikha, JSC "Cryogenmash") (IEB)*

1-6-2-0 Cooling of cryogenic system mains

1-6-3-0 Transient processes in cryogenic systems

1-7-0-0 Fuel cells

***B.A.Sokolov** (Russia, Korolyov, S.P.Korolyov Energia RSC) (IEB)*
***Yu.N.Shalimov** (Russia, Voronezh, VSTU) (IEB)*
***V.P.Pakhomov** (Russia, Moscow, RRC "Kurchatov Institute") (IEB)*

1-7-1-0 Research and production of fuel cells

1-7-1-1 Membanes for fuel cells

1-7-1-2 Computer simulation of fuel cell operation

1-7-2-0 Fuel cells application

1-7-2-1 Power supply on fuel cells with methanol conversion for portable devices

1-7-3-0 Fuel cells with hydrogenous fuel pre-processing

1-8-0-0 Structural materials

***P.G.Berezhko** (Russia, Sarov, RFNC-VNIIEF) (IEB)*
***A.M.Polyansky** (Russia, S.-Petersburg, OOO "Electronic & Beam Technologies Ltd.") (IEB)*
***V.M.Chertov** (Russia, Moscow) (IEB)*
***Yu.N.Shalimov** (Russia, Voronezh, VSTU) (IEB)*
***P.Saint-Gregoire** (France, University de Toulon et du Var) (DECH)*
***F.A.Lewis** (Great Britain, Belfast, The Queen's University of Belfast) (SEB)*
***A.T.Ponomarenko** (Russia, Moscow, Enikolopov Institute of Synthetic Polymer Materials of RAS) (IEAB)*
***L.V.Spivak** (Russia, Perm', Perm' State University) (IEAB)*
***M.V.Gol'tsova** (Ukraine, Donetsk, Donetsk STU) (IEAB)*
***N.M.Vlasov** (Russia, Podol'sk, SRI SIA "Luch") (IEB)*
***I.I.Fedik** (Russia, Podol'sk, SRI SIA "Luch") (IEB)*

1-8-1-0 Hydrogen in metals and alloys

***V.A.Gol'tsov** (Ukraine, Donetsk, DonSTU) (IEB)*
***L.F.Gol'tsova** (Ukraine, Donetsk, DonSTU) (IEB)*

1-8-2-0 Hydrogen degradation

1-8-3-0 Structural materials hydrogenation systems

1-8-4-0 Static and dynamic strength of structural materials

***N.N.Gerdyukov** (Russia, Sarov, Institute of Experimental Gasdynamics and Physics of Explosion RFNC-VNIIEF) (IEB)*

1-8-5-0 Gasars. Application of gasars in marine and air fleet, motor-car construction

1-8-6-0 Electrical furnaces for thermovacuum processes

***E.N.Marmer** (Moscow, VNIIETO)*

1-8-7-0 New structural materials for renewable energy structures

1-9-0-0 Synthesis-gas production methods

***A.Ya.Stolyarevskiy** (Russia, Moscow, RRC "Kurchatov Institute") (IEB)*

1-9-1-0 Adiabatic conversion of the natural gas

1-10-0-0 Hydrogen fuel vehicles and engines

***T.Gaertig** (Germany, Berlin) (IEB)*
***A.L.Dmitriev** (Russia, S.-Petersburg, RSC "Applied Chemistry") (IEB)*
***A.M.Domashenko** (Russia, Balashikha, JSC "Cryogenmash") (IEB)*
***B.A.Sokolov** (Russia, Korolyov, S.P.Korolyov Energia RSC) (IEB)*
***A.Yu.Ramenskiy** (Russia, Moscow, Audit-Premier) (IEAB)*
***V.S.Sokolov** (Russia, S.Petersburg) (IEAB)*

1-11-0-0 Hydrogen filling stations

1-12-0-0 Hydrogen for providing buildings, structures and houses with energy. Micro hydrogen power plants based on fuel cells

2. Thermodynamic analysis in renewable energy

***V. A. Khusnutdinov** (Russia, Moscow, RAO UES of Russia) (IEB)*

2-1-0-0 Thermodynamic analysis of basic energy generation processes in alternative energy

2-2-0-0 Exergetic analysis of basic energy generation processes in alternative energy

3. Atomic energy

***Yu.A.Trutnev**, Academician RAS (Russia, Sarov, RFNC-VNIIEF) (HECH)*
***A.Ya.Stolyarevskiy** (Russia, Moscow, RRC "Kurchatov Institute") (IEB)*
***A.V.Ivkin** (Russia, Sarov, RFNC-VNIIEF) (IEAB)*
***A.G.Chudin** (Russia, Moscow, Federal Agency for Nuclear Energy) (IEAB)*
***V.A.Afanas'ev** (Russia, Sarov, RFNC-VNIIEF) (IEB)*
***M. A. Prelas** (USA, Columbia, University of Missouri) (IEB)*

3-1-0-0 Atomic-hydrogen energy

***N.N.Ponomaryov-Stepnoy**, Academician RAS (Russia, Moscow, RRC "Kurchatov Institute") (SEB)*
***A.Ya.Stolyarevskiy** (Russia, Moscow, RRC "Kurchatov Institute") (IEB)*
***V.N.Fateev** (Russia, Moscow, RRC "Kurchatov Institute") (IEB)*
***A.L.Gusev** (Russia, Sarov, STC "TATA")*

3-1-1-0 History of atomic-hydrogen energy

***N.N.Ponomaryov-Stepnoy**, Academician RAS (Russia, Moscow, RRC "Kurchatov Institute") (SEB)*
***A.Ya.Stolyarevskiy** (Russia, Moscow, RRC "Kurchatov Institute") (IEB)*
***A.L.Gusev** (Russia, Sarov, STC "TATA")*

3-1-2-0 High-temperature gas reactors (HTGR) for hydrogen production via high-temperature processes

3-1-3-0 Fast reactors with sodium cooling (SC) to produce mid-temperature heat,and synthesis gas and hydrogen

3-1-4-0 Fast reactors with lead cooling as reactors of future generation to produce high-temperature heat

***G.L.Khorasanov** (Obninsk, SSC of the RF – Institute for Physics and Power Engineering Named After A.I.Leypunsky) (IEB)*

3-2-0-0 Atomic energy for vehicles

***M. A. Kazaryan** (Russia, Moscow, P.N.Lebedev FIAN) (IEB)*
***I.V. Shamanin** (Russia, Tomsk, Tomsk Polytechnical University) (IEB)*

3-2-1-0 Radionuclide heat sources

3-2-2-0 Radionuclide thermoelectric generators

3-2-3-0 Thermo- and radiation-stimulated phase transformation in alloys incorporated (carbides, nitrides, nitrides-hydrides, carbohydrides and hydrides of transition metals, high-temperature, super-conducting materials, intermetallic composition)

4. Solar energy

***A.Steinfield** (Switzerland, Zurich, ETH-Swiss Federal Institute) (IEB)*
***G.I.Isakov** (Azerbaijan, Baku, Institute of Physics of NAS of Azerbaijan) (DECH)*
***I.G.Khidirov** (Uzbekistan, Tashkent, Institute of Nuclear Physics of NAS of Uzbekistan) (IEB)*
***S.Geruny** (Armenia, Yerevan, Yerevan State University) (IEB)*
***S.M.Raza** (Pakistan, Quetta, University Of Balochistan) (IEB)*
***S.Z.Ilyas** (Pakistan, Quetta, University Of Balochistan) (IEB)*
***A.M.Pendjiev** (Turkmenistan, Ashkhabat-32, Tutkmenian polytechnic institute) (IEB)*
***V. F. Gremenok** (Belorussia, Minsk, Joined Institute of Solid State and Semi-conductor Physics) (IEAB)*

4-1-0-0 History of solar energy

4-2-0-0 Solar-hydrogen energy

4-2-1-0 Materials for solar-hydrogen energy

4-3-0-0 Solar power plants

4-3-1-0 Silicone solar thermal electric plants

4-3-2-0 Space solar stations

4-3-3-0 Photoelectric cell

4-3-4-0 Photovoltaic effect in semiconductor structures. Photoelectric modules

4-4-0-0 Ground solar stations

4-4-1-0 Solar collectors

4-5-0-0 Solar cities

4-5-1-0 Solar buildings

4-5-2-0 Solar refrigerators

4-5-3-0 Solar water-lifting systems

4-5-4-0 Solar energy units

4-6-0-0 Solar transport
4-7-0-0 Solar radiation concentrators

5. Wind energy

I.Z.Boguslavskiy *(Russia, Moscow, DBREPE RAS) (IEB)*
5-1-0-0 History of wind energy
5-2-0-0 Hydrogen-wind energy
5-3-0-0 Electric generators for wind energy
5-4-0-0 Wind energy plants
5-5-0-0 Wind-solar energy plants

6. Tide energy and sea tide energy

6-1-0-0 History of energy of tides
6-2-0-0 Sea waves energy
6-3-0-0 Sea tide energy

7. Geothermal energy

7-1-0-0 History of geothermal energy
7-2-0-0 Basic research into geothermal energy
7-3-0-0 Problems of geothermal energy assimilation
7-4-0-0 Role of modeling and monitoring in geothermal energy assimilation. Appraisal of geothermal resources
7-5-0-0 Geothermal plants
7-5-1-0 Geothermal power plants
7-5-2-0 Geothermal heat plants
7-6-0-0 Efficiency and reliability of geothermal heat and power plants. Major ways to improve the efficiency of geothermal heat and power plants
7-7-0-0 Geothermal resources of world countries and prospects of their development

8. Explosion energy

V.E.Fortov*, Academician RAS (Russia, Moscow, Institute of thermal physics of extremal state RAS) (SEB)*
A.L.Mikhailov *(Russia, Sarov, Institute of Experimental Gasdynamics and Physics of Explosion RFNC-VNIIEF) (IEB)*
N.N.Gerdyukov *(Russia, Sarov, Institute of Experimental Gasdynamics and Physics of Explosion RFNC-VNIIEF) (IEB)*
A.A.Sterzer *(Russia, Novosibirsk, MATEM Co. Ltd) (IEB)*
V.N.German *(Russia, Sarov, Institute of Experimental Gasdynamics and Physics of Explosion RFNC-VNIIEF) (IEB)*
8-1-0-0 Explosion technologies
8-2-0-0 Computer simulation of problems for explosion energy
8-2-1-0 Setting up problems for explosion energy
8-2-2-0 Mobile Lagrangian and Euler grids
8-3-0-0 Explosion deuterium energy
8-4-0-0 Explosion energy for syntheses of new materials
8-4-1-0 Materials synthesis and sticking by the explosion
8-4-2-0 Shock-wave sticking
8-4-3-0 Computer modelling of processes of material shock-wave sticking
8-5-0-0 Explosives
8-6-0-0 Blasting chambers
A.A.Sterzer *(Russia, Novosibirsk, MATEM Co. Ltd) (IEB)*
8-7-0-0 Extremal state of matter. Detonation. Shock waves
8-8-0-0 Energy materials and physics of detonation
8-9-0-0 Equations of the state and phase transition

9. Energy of biomass

S.A.Markov *(USA, Greencastle, DePauw University) (IEB)*
9-1-0-0 Biogas plants
9-2-0-0 Thermochemical gas generators

10. Small and micro hydro-power plants

S.Shatvoryan *(Armenia, Yerevan, Energy Strategy Center) (IEB)*
10-1-0-0 Equipment for small and micro hydro-power plants (HPP)
10-2-0-0 Derivation micro hydro-power plants

11. Carbon nanostructures

A.M.Lipanov*, Academician RAS (Russia, Izhevsk, Institute of Applied Mechanics UB RAS) (IEB)*
Yu.M.Shul'ga *(Russia, Chernogolovka, JSC "Cryogenmash") (IEB)*
V.I.Kodolov *(Russia, Izhevsk, BRHE Centre of Chemical Physics and Mesoscopy) (IEAB)*
Yu.S.Nechaev *(Russia, Moscow, Bardin Research Institute of the Ferrous-Metals Industry) (IEAB)*
B.P.Tarasov *(Chernogolovka, IPCP RAS) (IEAB)*
Yu.D.Tretiakov*, Academician RAS (Russia, Moscow, FMS MSU) (SEB)*
11-1-0-0 Nanosystems: synthesis,properties,and application
E.A.Goodilin*, Member Corresponding RAS (Russia, Moscow, FMS MSU) (SEB)*
11-2-0-0 Fullerene structures and carbon nanomaterials for heat insulation
11-3-0-0 Fullerene structures and carbon nanomaterials for hydrogen sensors
M.V.Vorobiova *(Russia, Moscow, GIREDMET) (IEAB)*
V.M.Aroutiounian*, Academician NAS of Armenia (Armenia, Yerevan, Yerevan State University) (SEB)*
11-4-0-0 Computer simulation of synthesis of carbon nanomaterials with specified properties
11-5-0-0 Carbon nanostructures for vehicles

12. Catalysis for renewable energy

Z.R.Ismagilov *(Russia, Novosibirsk, Boreskov Institute of Catalysis) (IEB)*
S.M.Aldoshin*, Academician RAS (Russia, Chernogolovka, IPCP RAS) (SEB)*
V.N.Parmon*, Academician RAS (Russia, Novosibirsk, Boreskov Institute of Catalysis of SD RAS) (SEB)*
V.A.Kirillov *(Russia, Novosibirsk, Boreskov Institute of Catalysis of SD RAS) (IEB)*
O.N.Efimov *(Russia, Chernogolovka, IPCP RAS) (IEB)*
12-1-0-0 Catalytic methods for synthesis of alternative fuel
12-2-0-0 Catalysis in combined schemes «energy generation and production of useful products from natural gas»
12-3-0-0 Catalysis in generation of working fluid in gas turbines as an effective alternative flare generation method
12-4-0-0 Catalysis of fuel cells
12-5-0-0 Catalysis in processes of production of synthesis gas and hydrogen
12-6-0-0 Catalytic methods of hydrogen treatment
12-7-0-0 Catalysis in treating of power reactor waste gases
12-8-0-0 Catalysis in process water treatment systems
12-9-0-0 Photocatalytic and electrocatalytic methods for hydrogen production
12-10-0-0 Development and study of material properties to form catalytic layers in fuel cells
12-11-0-0 On mechanism of catalytic action. Effect of metal nature and degree of oxidation thereof on catalytic activity
12-12-0-0 Nanocomposites for application as catalysts. Effect of dimension factor on catalytic activity
12-13-0-0 Alternative catalysts with no platinum
12-14-0-0 Problems of catalyst poisoning
12-15-0-0 Catalyst carriers: design,synthesis,and properties
12-16-0-0 Catalytic layers for fuel cells in planar design
12-17-0-0 Sol-gel process for production of catalysts and catalyst carriers

13. Thermogradient energy

***V.A. Khusnutdinov** (Russia, Moscow, RAO UES of Russia) (IEB)*

14. Ice energy

14-1-0-0 Application of ice in energy. Glacial power stations
14-2-0-0 Application of cold of permafrost for thermostatic control of domestic and process structures
14-3-0-0 Physical and chemical properties of ice
14-4-0-0 Thermal properties of ice
14-5-0-0 Thermodynamic basis for production and application of ice
14-6-0-0 Equipment for ice testing
14-7-0-0 Facilities for ice production
14-8-0-0 Methods and machinery for ice emergent break up for safety depth devices and over-land vehicles undergoing disaster
14-9-0-0 Binary ice in science and technique
***A.L.Gusev** (Russia, Sarov, STC "TATA")*
14-10-0-0 Application of ice for construction of engineering and technical,and architecture structures
14-11-0-0 Ice dynamics and strength. Embrittlement dynamics. Experimental methods of ice breaking up dynamic mechanics
14-12-0-0 Numerical and combined numerical and experimental methods of ice breaking up dynamic mechanics
14-13-0-0 Techniques for removing ice from water reservoirs
14-14-0-0 Cold storage and application
14-15-0-0 Transport of icebergs and production of fresh water

15. Thermonuclear energy

***V. N. Lobanov** (Russia, Sarov, RFNC-VNIIEF) (IEB)*
15-1-0-0 Investigations on the controlled thermonuclear fusion
15-2-0-0 X-ray thermonuclear fusion
15-3-0-0 Beam fusion
15-4-0-0 Inertial fusion
15-5-0-0 Isotope effect
15-6-0-0 Cryogenic tritium targets
15-7-0-0 High-pressure targets designed for research of nuon catalysis processes in nuclear fusion
15-8-0-0 International project of thermonuclear fusion reactor,ITER
15-9-0-0 Radiological protection and nuclear security
15-10-0-0 Production of radioisotopes and application
***M. A. Kazaryan** (Russia, Moscow, FIAN Lebedev Institute of Physics of RAS) (IEB)*
15-11-0-0 Fuel cycle and ecology
15-12-0-0 Design, construction and maintenance of nuclear research and power reactors
15-13-0-0 Production of components and materials required for application in nuclear reactors and fuel cycles thereof
15-14-0-0 TOKAMAK systems
15-15-0-0 Auxiliary magnetocumulative systems

16. Cryogenic and pneumatic vehicles

***A.L.Gusev** (Russia, Sarov, STC "TATA")*
16-1-0-0 Cryogenic nitrogen transport
16-2-0-0 Inert gas-based cryogenic vehicles for hazardous structures: fire engines,air port auxiliary vehicles, fuel and lubricant storage,vehicles in dangerously explosive chemical production
16-3-0-0 Pneumatic vehicles

17. Basic problems of energy and renewable energy

17-1-0-0 Electric energy storage
17-2-0-0 Superconductive materials. Superconductivity. Superconductivity of energy
17-3-0-0 New cycles and schemes for thermotransformers
17-4-0-0 Problems of megapolise illumination

18. Application of helium and special materials in vehicles

***Yu.A.Ryjov**, Academician RAS (Russia, Moscow, International University of Engineering) (SEB)*
18-1-0-0 Airships to transfer large-sized cargoes
18-2-0-0 Airships to control states of emergency in megapolises: car inspection, fire safety, terrorism combat, technical and ecological state control of industrial buildings and structures. Energy control (heat leak control in buildings on a city's scale)
18-3-0-0 Fire fighting airships, counteracting, and police airships

19. Juvenile hydrogen in geotectonics and geochemistry processes

***S.V.Digonskiy** (Russia, Ekaterinburg, FGUP "Urangeologorazvedka") (IEB)*
***V.L.Syvorotkin** (Russia, Moscow, M.V.Lomonosov Moscow state university) (IEB)*
19-1-0-0 Role of hydrogen in chemical composition of the universe
19-2-0-0 Diving forces in the evolution of Earth and planets
19-3-0-0 Hydrogen in the Earth's core
19-4-0-0 Geology and geochemistry of natural gases in deep fault areas
19-5-0-0 Transport of juvenile hydrogen through the Earth stratum and formation of electrically charged zones
19-6-0-0 Natural synthesis of carbon-based substances
19-7-0-0 Deep degasifying of the Earth, global disasters and anomalous phenomena

20. On-board energy accumulators

20-1-0-0 Thermal energy accumulators
***A.L.Gusev** (Russia, Sarov, STC "TATA")*
20-1-1-0 Temperature above 273 K
20-1-2-0 Temperature below 273 K
20-1-3-0 Temperature below 77 K
20-2-0-0 Flywheel energy accumulators
20-3-0-0 Electrical energy accumulators
20-4-0-0 Spring energy accumulators
20-5-0-0 Compressed-air energy accumulators
20-6-0-0 Chemical energy accumulators

21. Legislative basis

***P.B.Shelishch** (Russia, Moscow, RF State Duma, President of National Association of Hydrogen Energy) (IEAB)*
21-1-0-0 Legislation basis for renewable energy in Russia
21-2-0-0 Legislation assurance for innovation development of hydrogen energy
21-3-0-0 Legislation basis for renewable energy in CIS
21-4-0-0 Legislation basis for ecology

22. Economical aspects

22-1-0-0 Investment attractiveness of various countries and companies in renewable energy
22-2-0-0 Resources of conventional energy sources in exporting countries and world resources
22-3-0-0 National scientific and technological programmes of the development of hydrogen economy
22-4-0-0 Economical analisys in renewable energy
V. A. Khusnutdinov *(Russia, Moscow, RAO UES of Russia) (IEB)*
22-5-0-0 Business-planning in renewable energy

23. Energy and ecology

O.L.Figovsky *(Israel, Migdal Ha'Emek, Israel Research Center Polymate) (IEB)*
M.V.Vorobiova *(Russia, Moscow, GIREDMET) (IEB)*
23-1-0-0 Greenhouse gas effect
23-2-0-0 Ecological problems of industrial megapolises
23-3-0-0 Ecology of air atmosphere and space
23-4-0-0 Ecology of water resources
23-5-0-0 Problems of unhealthy atmospheric emissions by heat-electric generating plants
23-6-0-0 Problems of groung pollution by energy carriers
23-7-0-0 Ecological tourism and ecological resorts
23-8-0-0 Problems of factory and domestic waste utilization

24. Energy efficiency methods and facilities for agressive gas mixture separation and purification

A.L.Gusev *(Russia, Sarov, STC "TATA")*
M. A. Kazaryan *(Russia, Moscow, P.N.Lebedev FIAN) (IEB)*
A.A.Bobrova *(Russia, Sarov, RFNC-VNIIEF)*

26. Education and scientific research centres

L.A.Il'kaeva *(Russia, Sarov, RFNC-VNIIEF) (IEAB)*
B.F.Reutov *(Russia, Moscow, Federal Agency for Education and Sciences of RF) (IEB)*
A.V.Chuvikovskiy *(Russia, Sarov, RFNC-VNIIEF) (IEB)*
Yu. P. Shcherbak *(Russia, Sarov, Sarov Physicotechnical Institute) (IEB)*
J.-P. Contzen *(Belgium, von Karman Institute for Fluid Dynamics) (IEB)*
26-1-0-0 Educational programmes in hydrogen economy
26-2-0-0 Hydrogen trading estates and science and research cities
26-3-0-0 Young people in alternative energy and ecology science and technology

27. Information

A.I.Salikov *(Russia, Moscow, CNIIATOMINFORM) (IEAB)*
E.M.Tararaeva *(Russia, Moscow, CNIIATOMINFORM) (IEAB)*
E.A.Goodilin*, Member Corresponding RAS (Russia, Moscow, FMS MSU) (SEB)*
T. N. Kondirina *(Russia, Sarov, STC "TATA")*
27-1-0-0 Review of periodicals
27-2-0-0 Review of leading internet-resources
27-3-0-0 Prominent scientists' biographies
27-4-0-0 Scientific funds and scientific projects
27-5-0-0 International scientific conferences
27-6-0-0 Advertising matters of investment companies and manufacturers
27-7-0-0 Review of new scientific books
27-8-0-0 Patents
27-9-0-0 Encyclopedia of renewable energy. Terms and definitions
27-10-0-0 Opinions,letters in publishing office,short articles
27-11-0-0 Messages of members of Scientific editorial board

Аббревиатуры

РНС — Редакционный научный совет
МРК — Международный редакционный комитет
МНКСР — Международный научно-консультативный совет редакции
ЭС — Экспертный совет
МСР — Международный совет рецензентов

Abbreviation

SEB — Scientific Editorial Board
IEB — International Editorial Board
IEAB — International Editorial Advisory Board
EB — Experts Board
IRB — International Reviewers Board

Главному редактору Гусеву Александру Леонидовичу
607183, Россия, Нижегородская обл., Саров, а/я 687, НТЦ «ТАТА»
Тел.: 8 (83130) 63107, 97472; факс: 8 (83130) 63107
Моб. тел.: +7-961-63-99-126, +7-962-50-77-914
E-mail: gusev@hydrogen.ru, http://isjaee.hydrogen.ru, http://www.hydrogen.ru

To Alexander L. Gusev, Editor-in-Chief
Scientific Technical Centre "TATA", P.O.B. 687, Sarov, Nizhni Novgorod region, 607183, Russia
Phone: +7 (83130) 63107, 97472; fax: +7 (83130) 63107
Cell phones (office): +7-961-63-99-126, +7-962-50-77-914
E-mail: gusev@hydrogen.ru, http://isjaee.hydrogen.ru, http://www.hydrogen.ru

Международный научный журнал «Альтернативная энергетика и экология»
Подписано в печать 11.09.2008 г.
Формат 60×84/8 Усл. печ. л. ~33,01 Уч.-изд. л. ~27,8
Отпечатано в типографии ООО НТЦ «ТАТА» г. Саров Нижегородской обл.
Цена договорная

Журнал включен в каталог «Роспечать» (индекс 10337 «Альтернативная энергетика и экология») и Объединенный каталог «Пресса России. Российские и зарубежные газеты и журналы» (индекс 41935 «Альтернативная энергетика и экология»).

Международная конференция
«Водородные технологии: вопросы стандартизации»
посвящена 100-летию со дня рождения Б.И. Шелища
Санкт-Петербург, 26-27 сентября 2008 г.

International Conference
«Hydrogen technologies: issues of standardization»
marking 100 anniversary of Boris Shelisch's birth
Saint-Petersburg, 26-27 September 2008

ОРГКОМИТЕТ

Председатель

Г.И. Элькин (Руководитель Федерального агентства по техническому регулированию и метрологии)

Заместители председателя

Б.Н. Кузык (Генеральный директор Национальной инновационной компании «Новые энергетические проекты», чл.-корр. РАН)
В.В. Окрепилов (Генеральный директор Центра испытаний и сертификации "ТЕСТ-С.-Петербург", член Президиума РАН, чл.-корр.)
П.Б. Шелищ (Президент Национальной ассоциации водородной энергетики, председатель Технического комитета № 29)

Ответственный секретарь

А.Ю. Раменский (Вице-президент НАВЭ)

Члены Оргкомитета

А.Л. Гусев (Главный редактор журнала «Альтернативная энергетика и экология»)
А.Г. Забродский (Директор Физико-технического института им. А.Ф. Иоффе РАН)
А.С. Коротеев (Академик РАН, руководитель ФГУП "Исследовательский центр им. М.В. Келдыша")
С.П. Малышенко (Зам. председателя исполкома международного партнерства по водородной энергетике)
Н.Н. Пономарев-Степной (академик РАН, вице-президент РНЦ "Курчатовский институт")
В.А. Пивнюк (Вице-президент ОАО ГМК "Норильский никель")
Б.Ф. Реутов (Руководитель отдела Федерального агентства по науке и инновациям)
А.С. Сигов (Ректор МИРЭА, чл.-корр. РАН)
В.Л. Туманов (Зам. генерального директора Национальной инновационной компании "Новые энергетические проекты")
В.А. Язев (Зам. Председателя Государственной Думы РФ, член президиума НАВЭ)

****

ПРОГРАММА КОНФЕРЕНЦИИ

10-00 Открытие конференции. Приветствия руководителей Ростехрегулирования, Санкт-Петербурга, Национальной ассоциации водородной энергетики (НАВЭ)
10-30 О национальной системе технического регулирования в высокотехнологичных отраслях промышленности – *В.Ю.Саламатин*, заместитель Министра промышленности и торговли РФ
11-00 Об участии России в развитии международной стандартизации и задачах технических комитетов – *Г.И.Элькин*, руководитель Ростехрегулирования
11-30 О развитии национальной системы стандартизации в области машиностроения и энергетики, включая водородные технологии – *А.В.Зажигалкин*, директор ВНИИНМАШ
12-00 О деятельности ТК 197 "Водородные технологии" ИСО – *представитель ТК*
12-30 О деятельности ТК 105 "Технологии топливных элементов" МЭК – *представитель ТК*
13-00 О деятельности ТК 29 "Водородные технологии" Ростехрегулирования в области стандартизации – *А.Ю.Раменский*, ответственный секретарь ТК 29
14-30 О проекте технического регламента по безопасности водородных систем и перспективах стандартизации в этой области – *П.Б.Шелищ*, председатель ТК 29, президент НАВЭ
15-00 О проекте технического регламента по безопасности топливных элементов и перспективах стандартизации в этой области – *А.Н.Курский*, член ТК 29, заместитель руководителя аппарата комитета Государственной Думы РФ
15-30 О роли стандартизации в инновационных энергетических проектах – *Б.Н.Кузык*, член-корреспондент РАН, генеральный директор Национальной инновационной компании "Новые энергетические проекты"
16-00 Тенденции развития стандартизации и метрологии в инновационной сфере на примере нанотехнологий – *В.В.Окрепилов*, член-корреспондент РАН, генеральный директор ФГУ "Тест-С-Петербург"
16-30 Основные критерии для формирования стандартов в области водородной энергетики – *А.Л. Гусев*, главный редактор журнала «Альтернативная энергетика и экология»
17-00 Обсуждение докладов конференции
17-30 Принятие резолюции

PROGRAM OF CONFERENCE

10-00 Opening of the conference. Greetings of the Head of Russian Technical Regulator, Government of the city of Saint-Petersburg and National Association of Hydrogen Energy
10-30 On the National system of technical regulation in the high-tech sector – *Salamatin V.U.*, Vice-Minister of industry and trade of the Russian Federation
11-00 On the participation of Russia in the development of international standardization and about objectives of technical committees – *Elkin G.I.*, Head of the Federal Agency on Technical Regulating and Metrology
11-30 On the development of National standards system in the machine building industry and energy sector, including hydrogen technologies – *Zazhigalkin A.V.*, Director of the Russian National Research Institute of Machinery (VNIINMASH)
12-00 On the activities of the TC 197 "Hydrogen technologies" ISO – *representative of the TC*
12-30 On the activities of the TC 105 "Fuel cell technologies" IEC – *representative of the TC*
13-00 On the activities of TC 29 "Hydrogen Technologies" of the Russian Technical Regulator in the standardization sector – *Ramensky A.U.*, executive secretary of TC 29
14-30 On the project of technical regulation on the safety of hydrogen systems and perspectives of standardization in this sector – *Shelisch P.B.*, Chairman of TC 29, President of National Association of Hydrogen Energy
15-00 On the project of technical regulation on the safety of fuel cells and perspectives of standardization in this sector – *Kursky A.N.*, member of TC 29, Deputy director of the administration of committee of the State Duma of the RF
15-30 On the role of standardization in innovative energy projects – *Kuzyk B.N.*, Corresponding member of Russian Academy of Sciences, General Director of National innovative company "New energy projects"
16-00 Tendencies of development of standardization and metrology in the sphere of innovations in nanotechnologies sector– *Okrepilov V.V.*, Corresponding member of Russian Academy of Sciences, General Director of the FSI "Trest-St-Petersburg"
16-30 Principal criteria for formation of standards in the Hydrogen Energy – *Gusev A.L.*, Editor-in-Chief of the journal for Alternative Energy and Ecology
17-00 Discussion of reports
17-30 Adoption of a resolution